Analysis of the interactions between *Aspergillus fumigatus*, *Pseudomonas aeruginosa* and a model of the alveolar surface

A thesis submitted to Maynooth University
for the degree of Doctor of Philosophy

Anatte Margalit, B.Sc

October 2019

Supervisor	Co-supervisor	Head of Department
Prof. Kevin Kavanagh	**Dr. James C. Carolan**	**Prof. Paul Moynagh**
Medical Mycology Laboratory Department of Biology Maynooth University	Applied Proteomics Laboratory Department of Biology Maynooth University	Dept. of Biology Maynooth University

List of Figures

Chapter 1

Chapter 2

Chapter 3

Chapter 4

Chapter 5

Chapter 6

Tables

Chapter 2

Chapter 3

Publications

Margalit, A., Carolan, J. C., Kavanagh, K. (2020). Characterization of the Proteomic Response of A549 Cells Following Sequential Exposure to *Aspergillus fumigatus* and *Pseudomonas aeruginosa.* J. Proteome Res. 19 (1):279-291.

Margalit, A., Sheehan, D., Carolan, J. C., Kavanagh, K. (2019). *A. fumigatus* promotes the Growth of *P. aeruginosa* in a nutrient-deficient environment (under review).

Margalit, A., Carolan, J. C., Kavanagh, K. *P. aeruginosa* alters the growth and secondary metabolite production of *A. fumigatus* (manuscript in production).

Margalit, A., Carolan, J. C., Kavanagh, K. An *Aspergillus fumigatus* compound that displays anti-bacterial activity (manuscript in production).

Margalit, A., and Kavanagh K. (2015). The Innate Immune Response to *Aspergillus fumigatus* on the Alveolar Surface FEMS Microbiol Rev. 39(5):670-87. (Not part of this thesis)

Margalit A., Kowalczyk M. J., Żaba R., Kavanagh K. (2016). The role of altered cutaneous immune responses in the induction and persistence of rosacea. J. Dermatol Sci. 82(1):3-8. (Not part of this thesis)

Conferences attended

Irish Mass Spectrometry Society Annual Conference. UCD, Dublin, 2019

The Annual Microbiology Society Conference 2019, ICC Belfast

Microbiology Society Focused Meeting, Microbes and Mucosal Surfaces, University College Dublin, 2018.

Irish Fungal Society Conference, 2018, Maynooth University.

Irish Fungal Society Annual Conference 2016, The Grand Hotel, Malahide, Co. Dublin

Presentations

Poster Presentation

Aspergillus fumigatus alters the growth of *Pseudomonas aeruginosa* in a nutrient-poor environment. **Anatte Margalit**, James. C. Carolan and Kevin Kavanagh. The Annual Microbiology Society Conference 2019, ICC Belfast

Disruption of the apoptotic pathway in A549 cellsfollowing exposure to *Aspergillus fumigatus* conidia. **Anatte Margalit**, James C. Carolan and Kevin Kavanagh. Irish Fungal Society Annual Conference 2016, The Grand Hotel, Malahide, Co. Dublin

Oral Presentations

Characterizing the Response of A549 Cells to *Aspergillus fumigatus* and *Pseudomonas aeruginosa:* A Proteomic Approach. **Anatte Margalit**, James C. Carolan and Kevin Kavanagh. Microbiology Society Focused Meeting, Microbes and Mucosal Surfaces, University College Dublin, 2018.

Characterizing the Response of A549 Cells to *Aspergillus fumigatus* and *Pseudomonas aeruginosa:* A Proteomic Approach. **Anatte Margalit**, James C. Carolan and Kevin Kavanagh. Irish Fungal Society Conference, 2018, Maynooth University.

Disruption of the apoptotic pathway in A549 cellsfollowing exposure to *Aspergillus fumigatus* conidia. **Anatte Margalit**, James C. Carolan and Kevin Kavanagh. Irish Fungal Society Annual Conference 2016, The Grand Hotel, Malahide, Co. Dublin

Departmental Presentations

Aspergillus fumigatus alters the growth of *Pseudomonas aeruginosa* in a nutrient-poor environment. **Anatte Margalit**, James. C. Carolan and Kevin Kavanagh. Maynooth University Annual Biology Research Day, 2019

Characterizing the Response of A549 Cells to *Aspergillus fumigatus* and *Pseudomonas aeruginosa:* A Proteomic Approach. **Anatte Margalit**, James C. Carolan and Kevin Kavanagh. Maynooth University Annual Biology Research Day, 2018.

Disruption of the apoptotic pathway in A549 cellsfollowing exposure to *Aspergillus fumigatus* conidia. **Anatte Margalit**, James C. Carolan and Kevin Kavanagh. Maynooth University Annual Biology Research Day, 2018.

Acknowledgments

I want to express my sincerest gratitude to the two most incredible supervisors any postgraduate student could wish for. To Kevin, I want to thank you for your support, guidance, encouragement, and patience over the past number of years and for having faith and confidence in me and in my work. You helped to make my postgraduate research experience an incredibly positive one and for that, I will always be grateful. Jim, thank you so much for guiding me through the complicated world of proteomics for the brain storming sessions. Thank you for your honesty and for teaching me never to accept standards below what I set for myself. What I have taken from my postgraduate research experience would not have been remotely as fulfilling without your help.

I also want to acknowledge the amazing support, the time and effort gifted to me by Dr. Rebecca Owens and Dr. Trini Velasco-Torrijos in helping me with a large portion of my research. Thank you for imparting your wisdom and for sharing your knowledge, experience, and enthusiasm for science with me. You took time out of your own busy schedule to help me with my work and for that, I am extremely grateful.

I also want to thank Ger, Amie and Ronan, for creating an atmosphere in the lab that made it a brilliant place to work. Thank you for sharing the good times and the not so good times with me and for making me laugh through it all! And to all the people in the lab, Dejana, Magda, Rachel, Ahmad, thank you for continuing to produce the positive vibes in the lab! I am so fortunate to be working alongside such a great crew and to have made so many amazing friends in Callan during my postgraduate research career; Jim's Lab, Sean's Lab, Dean's Lab, Peter's Lab, Ciara's Lab, Eoin's Lab; you make Callan a wonderful place to work. Michelle, Tina, Jean, Terry, Patricia, Frances and all the crew in the Prep Lab, thank you for your support over the last four years. Your efficiency and patience is inspiring!

I would like to acknowledge Dr. Paul Dowling and Dr. Fiona Walsh, for taking your time to attend annual assessment meetings and for providing encouragement, support and advice.

I also want to acknowledge the Irish Research Council for believing in my project and my abilities and for funding my PhD. I would like to thank the Microbiology Society for providing me with funding to travel to Israel in 2017 to do research in the University of Tel Aviv and for providing me with funding to attend their conferences.

Last but certainly not least, I want to acknowledge my amazing family, especially my incredible son Alex, who has provided incredible support, motivation and kind words while I was writing my thesis, and over the past four years. I could not have done this without your help. I want to express my sincerest thanks to my Mam and my sisters, who provided me with a listening ear when I needed it. Thank you Mam and Niamh for providing me with dinners when I was writing my thesis. Those small gestures meant so much. I want to acknowledge my Dad, who provided support from far away and always showed enthusiasm for my research. I want to express my sincere gratitude to my Aunt Ger and Uncle Kieran. I would not be where I am today without your incredible support, your motivation, your kindness and your belief in me. You have all, helped me to learn a lot about myself and for that I am extremely grateful.

DECLARATION

This thesis has not been submitted in whole or part to this or any other university for any degree and is the original work of the author except where stated.

Signed _____

Anatte Margalit, B.Sc.

Date _____

Abbreviations

ABC	ATP-binding cassette
ABPA	Allergic bronchopulmonary aspergillosis
AEC	Airway epithelial cell
ASL	Airway surface liquid
ANOVA	Analysis of variance
APS	Ammonium persulphate
BP	Biological process
CC	Cellular component
CCL	Chemokine ligand
CCR	Chemokine receptor
CuF	Culture filtrate
CF	Cystic fibrosis
CFTR	Cystic fibrosis transmembrane conductance regulator
CFU	Colony forming units
CGD	Chronic granulomatous disease
CH	Carbon hydrogen
COSY	Correlation Spectroscopy
CLR	C-type lectin receptor
CXCL	Chemokine ligand
CXCR	Chemokine receptor
DC	Dendritic cell
DC-SIGN	Dendritic cell-specific ICAM-3-grabbing non-ntegrin
DCM	Dichloromethane
DEPT	Distortionless Enhancement by Polarization Transfer
DMEM	Dulbecco's Modified Eagle Medium
DNA	Deoxyribonucleic acid
DTT	Dithiothreitol
EC	Epithelial cell
ER	Endoplasmic reticulum
ERAD	ER-associated degradation pathway
ETC	Electron transport chain
FcγR	Fc-gamma receptor
FCS	Foetal calf serum
FDR	False Discovery Rates
GM-CSF	Granulocyte Macrophage Colony-Stimulating Factor
GO	Gene Ontology

HBD	Human beta-defensin
HCl	Hydrochloric acid
HMBC	Heteronuclear Multiple Bond Correlation
HSQC	heteronuclear single quantum correlation
HQNO	4-hydroxy-2-heptylquinoline-N-oxide
IA	Invasive aspergillosis
IAA	Iodoacetamide
IDO	Indoleamine 2
IEF	Isoelectric Focusing
IFN	Interferon
IL	Interlukin
IPA	Invasive pulmonary aspergillosis
KEGG	Kyoto Encyclopaedia of Genes and Genomes
LPS	lipopolysaccharide
LFQ	Label-free quantitative
MAPK	Mitogen-activated protein kinase
MeOH	Methanol
MMP12	matrix metalloproteinase 12
MBL	mannan-binding lectin
MBP	Major basic protein
MDR	Multidrug resistant
MF	Molecular function
MIP-1α	Macrophage Inflammatory Protein
NADPH	Nicotinamide adenine dinucleotide phosphate reduced
NAOH	Sodium hydroxide
NE	Neutrophil elastase
NEMO	NF-kappa-B essential modulator
NETs	Neutrophil extracellular traps
NF-κB	Nuclear factor kappa-light-chain-enhancer of activated B cells
NLRP3	NOD-, LRR- and pyrin domain-containing protein 3
NOD2	Nucleotide-binding oligomerization domain-2 NLRP3
NOS	Nitric oxide species
NRP	Non-ribosomal peptide
ns	not significant
OMP	Outer membrane protein
OD	Optical density
OSMAC	One strain-Many compounds approach
OXPHOS	Oxidative phosphorylation
PAMPs	Pathogen-associated molecular pattern
PCA	principal component analysis

PCA	Phenazine-1-carboxylic acid PCN
PCN	Pyocyanin
PMN	Polymorphnuclear cell
PRR	Pattern recognition receptor
PQS	Pseudomonas quinolone signal
PTX3	Pentraxin 3
MS	Mass spectrometry
MM	Minimal Media
MWCO	Molecular weight cut-off
NMR	Nuclear Magnetic Resonance
PCL	periciliary liquid
ppm	parts per million
RP-HPLC	Reverse Phase High Performance Liquid Chromatography
SAB	Sabouraud
SDS PAGE	Sodium Dodecyl Sulphate Gel Electrophoresis-Poly Acrylamide Gel Electrophoresis
SSDA	Statistically significant differentially abundant
STRING	Search Tool for the Retrieval of INteracting Genes
TLR	Toll-like receptor
UPR	Unfolded protein response
TFA	Trifluoroacetic acid
TrxR	Thioredoxin reductase
TOCSY	Total Correlation Spectroscopy
1D	1 Dimensional
1-HP.	1-hydroxyphenazine
2D	2 Dimensional

Abstract

Aspergillus fumigatus and *Pseudomonas aeruginosa* are the most prevalent fungal and bacterial pathogens associated with cystic fibrosis (CF)-related infections, respectively. Co-infection with both pathogens is associated with a deterioration in lung function. Despite the persistence of *A. fumigatus* in the CF airways from an early age, *P. aeruginosa* eventually predominates as the primary pathogen and chronic infection by these bacteria is associated with morbidity and mortality. *P. aeruginosa* has a profound capacity to adapt to the hostile conditions that characterize the CF airways. Nonetheless, several factors are likely to facilitate colonization in the airways, including a compromised host cellular response and alterations to the microbial environment, perhaps generated in part by other microorganisms, such as *A. fumigatus*. *A. fumigatus* is the causative agent of allergic bronchopulmonary aspergillosis (ABPA), a disease characterized by the induction of a hypersensitivity response in host cells. The interactions between *A. fumigatus* and host epithelial cells, such as the alveolar epithelial cell line A549, have been well characterized. The response of A549 cells to exposure by multiple pathogens is less well understood. With this in mind, a proteomic approach was employed to investigate changes to the proteome of A549 cells in response to exposure by *A. fumigatus* and *P. aeruginosa*. Label-free quantitative (LFQ) proteomics revealed distinct changes to the host-cell proteome in response to either or both pathogens. Alterations to the proteome were dependent on the duration and sequence of infection. The results presented in this thesis suggest that *A. fumigatus* render A549 cells unable to internalize bacteria, thus providing an environment in which *P. aeruginosa* can proliferate. Interaction studies between *A. fumigatus* and *P. aeruginosa* identified a key role for *A. fumigatus* in creating a nutrient-rich environment in which *P. aeruginosa* could proliferate. The emergence of antibiotic resistant bacteria, including *P. aeruginosa* has led to an urgency for the need to discover novel antibiotics. Saprophytic fungi inherently produce a range of antimicrobial compounds that enable competition in their ecological niche. Fortuitously for humans, these compounds can be exploited for medicinal purposes. The process of identification of one such potentially novel anti-bacterial compound produced by *A. fumigatus* is described here. The effect of the compound on the *P. aeruginosa* proteome was characterized by LFQ proteomics with a view to gaining insights into the mechanism of action by which the anti-bacterial agent inhibits bacterial growth. Taken together, the findings presented in this thesis offer novel insights into the complex dynamics that exist between the host, *P. aeruginosa* and *A. fumigatus*.

Chapter 1

General Introduction

1.1 Cystic fibrosis

Cystic fibrosis (CF) is an autosomal recessive disorder caused by a mutation in the gene encoding the cystic fibrosis transmembrane conductance regulator (CFTR) (Rommens *et al.*, 1989). Although it affects multiple organs, morbidity and mortality is associated with chronic lung disease caused by numerous factors including abnormal airway surface liquid (ASL), chronic inflammation and microbial infection. CF is the most common life-limiting hereditary disorder amongst Caucasians (O'Sullivan and Freedman, 2009) and affects more than 70,000 individuals worldwide. Ireland has the highest incidence of CF per head of population and as of 2017, 1377 individuals were living with CF in the Republic of Ireland (Farrell *et al.*, 2007; CF Registry of Ireland 2017 Annual Report, 2017). Due to an increase in life expectancy, the population of CF patients is increasing, as is the age for survival thanks to advances in medicine. In 2007, approximately 5 % of CF patients survived till the age of 40 (CF Registry of Ireland Annual Report 2007). In 2017, this number had risen to 10 % of the CF population (CF Registry of Ireland 2017 Annual Report, 2017).

The CFTR protein is a chloride channel that is expressed on epithelial cells and blood cells (Yoshimura *et al.*, 1991; Painter *et al.*, 2006). In addition to its primary role of regulating cellular chloride and bicarbonate levels, CFTR also negatively regulates sodium transport (Stutts *et al.*, 1995). Deletion of phenylalanine at residue 508 (F508del) of the CFTR gene is the most common mutation associated with CF and affects approximately 82% of patients (Lopes-Pacheco, 2020). Defects caused by F508del lead to proteasome-mediated degradation of CFTR, and CFTR that do reach the cell surface do not function optimally (Ward *et al.*, 1995; Vankeerberghen *et al.*, 2002). Other common mutations such as G551D, in which glycine is replaced by aspartic acid at residue 551, account for approximately 5% of the mutations associated with the disease (Lopes-Pacheco, 2020). This mutation affects the gating function of the ion channel (Bompadre *et al.*, 2008). These defects in CFTR result in a ion imbalance leading to viscous secretions that cause ducts to become plugged and atrophic in the affected organs (Vankeerberghen *et al.*, 2002).

In the respiratory system, pulmonary epithelia secrete the ASL, the composition of which is crucial for maintaining homeostasis, including normal ciliary function for the removal of mucus and microbes from the airways. Additionally, the ASL is a source of

antimicrobial peptides and thus plays an important role in the first line of defence against potential pulmonary pathogens. In the CF airways, defective CFTR leads to abnormal ASL characterized by dehydrated, viscous fluid resulting from an imbalance in sodium and chloride ions, and decreased water content (Verkman *et al.*, 2003). The thick sticky nature of the ASL makes oxygen diffusion difficult, causing hypoxia, the cilia are compressed thereby disrupting the mucociliary elevator, and defective bicarbonate transport creates a low pH environment that is unfavourable for antimicrobial peptide activity (Tate *et al.*, 2002; Pezzulo *et al.*, 2012; Tilley *et al.*, 2015; Haq *et al.*, 2016; Ahmad *et al.*, 2019). Dysfunctional mucus clearance and ciliary action, defective antimicrobial activity and an environment, in which microbes can evade antibiotics and cells of the innate immune system, provide a reservoir conducive to the growth and persistence of pathogens.

1.1.1 The microbial environment of the CF airways

The microbial environment of the CF airways is a diverse and evolving ecosystem and from infancy, the lungs of CF patients are subject to colonization by a range of microbial species. Culture independent techniques have revealed a wide variation in the microbiota of the CF airways (Rogers *et al.*, 2003; Coburn *et al.*, 2015; Filkins and O'Toole, 2015). Although there does exist several genera including *Streptococcus, Prevotella, Rothia, Veillonella* and *Actinomyces*, individual species such as *Pseudomonas aeruginosa* and *Burkholderia cepacia* tend to dominated when they are present (Coburn *et al.*, 2015; Zemanick *et al.*, 2017).

The CF airways are characterized by an age-related succession of microbial species; in children under the age of 16, *Staphylococcus aureus, Haemophilus influenza* and *Stenotrophomonas maltophilia* predominate (CF Registry of Ireland Annual Report, 2017; Zemanick *et al.*, 2017). As patients get older, the species diversity decreases and *H. influenza* and *S. aureus* are replaced by *Pseudomonas aeruginosa* which becomes the most dominant pathogen (Coburn *et al.*, 2015; CF Registry of Ireland 2017 Annual Report, 2017; Zemanick *et al.*, 2017) (Fig. 1A). The pathogenic mould, *Aspergillus fumigatus* is detected from early childhood and is persistent in the CF airways throughout the life of the patient (Coburn *et al.*, 2015; CF Registry of Ireland 2017 Annual Report, 2017) (Fig. 1B).

Microbial diversity is greatest in children aged 2 – 10 years but reduces with age until it plateaus at approximately 25 years (Coburn *et al.*, 2015; Zemanick *et al.*, 2017). Age-related reduction in species diversity is strongly correlated with increased colonization by *P. aeruginosa* and *Burkholderia* spp. and with a deterioration in lung function (Coburn *et al.*, 2015; Filkins *et al.*, 2012)**.**

Age-related prevalence rates of bacterial species in Irish CF patients

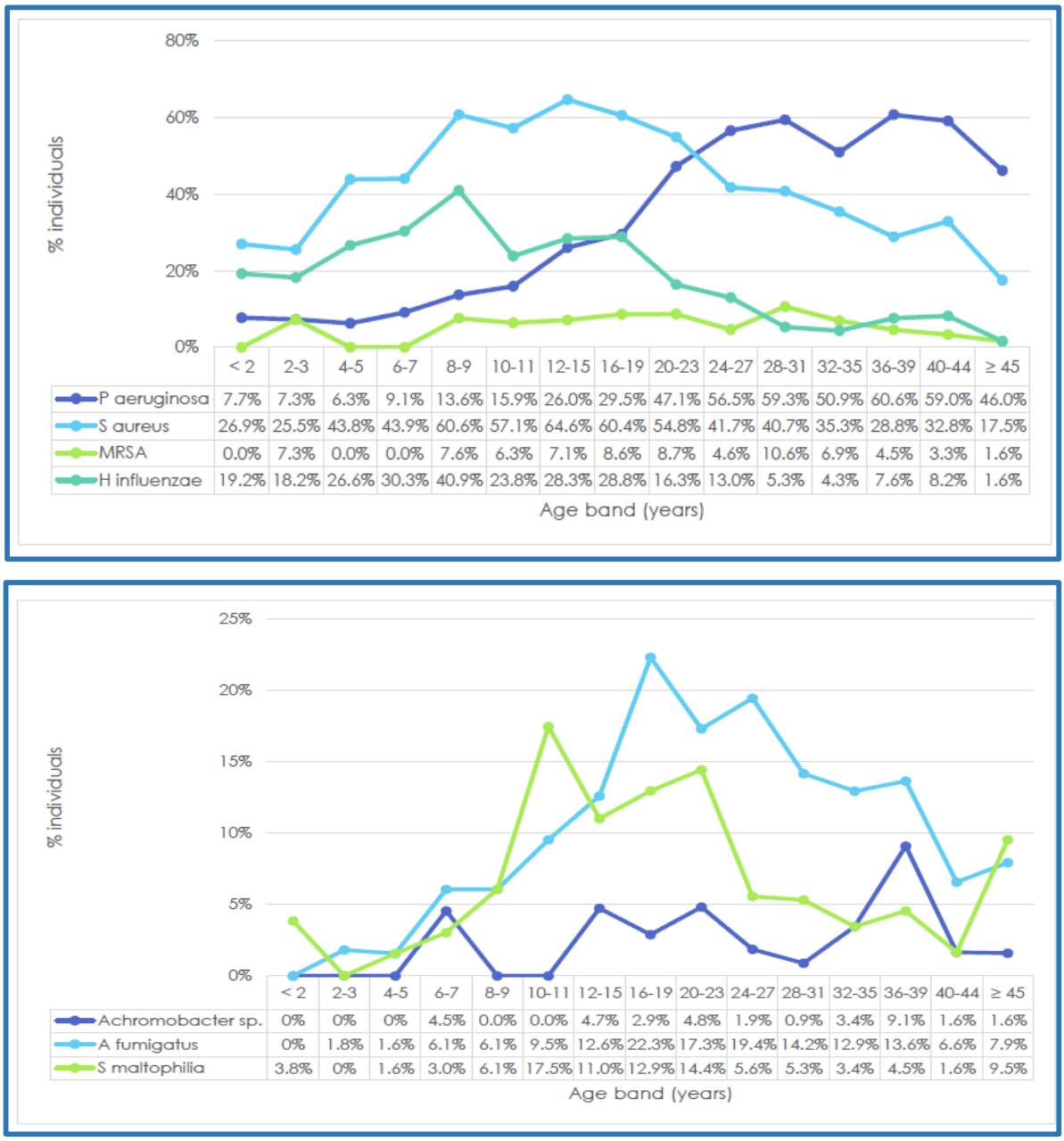

A	< 2	2-3	4-5	6-7	8-9	10-11	12-15	16-19	20-23	24-27	28-31	32-35	36-39	40-44	≥ 45
P aeruginosa	7.7%	7.3%	6.3%	9.1%	13.6%	15.9%	26.0%	29.5%	47.1%	56.5%	59.3%	50.9%	60.6%	59.0%	46.0%
S aureus	26.9%	25.5%	43.8%	43.9%	60.6%	57.1%	64.6%	60.4%	54.8%	41.7%	40.7%	35.3%	28.8%	32.8%	17.5%
MRSA	0.0%	7.3%	0.0%	0.0%	7.6%	6.3%	7.1%	8.6%	8.7%	4.6%	10.6%	6.9%	4.5%	3.3%	1.6%
H influenzae	19.2%	18.2%	26.6%	30.3%	40.9%	23.8%	28.3%	28.8%	16.3%	13.0%	5.3%	4.3%	7.6%	8.2%	1.6%

B	< 2	2-3	4-5	6-7	8-9	10-11	12-15	16-19	20-23	24-27	28-31	32-35	36-39	40-44	≥ 45
Achromobacter sp.	0%	0%	0%	4.5%	0.0%	0.0%	4.7%	2.9%	4.8%	1.9%	0.9%	3.4%	9.1%	1.6%	1.6%
A fumigatus	0%	1.8%	1.6%	6.1%	6.1%	9.5%	12.6%	22.3%	17.3%	19.4%	14.2%	12.9%	13.6%	6.6%	7.9%
S maltophilia	3.8%	0%	1.6%	3.0%	6.1%	17.5%	11.0%	12.9%	14.4%	5.6%	5.3%	3.4%	4.5%	1.6%	9.5%

Fig. 1 The prevalence of microbial pathogens in the CF airways The prevalence of *P. aeruginosa*, *S. aureus*, MRSA and *H. influenza* (A) and non-tuberculous mycobacteria, Achromobacter species, *A. fumigatus*, *S. maltophilia* and *B. cepacia* complex (B) detected in the airways of CF patients registered with Cystic Fibrosis Registry of Ireland. Prevalence was measured as a function of age group and was assessed in 2017. Data and figures adapted from the Annual Report of the Cystic Fibrosis Registry of Ireland, 2017.

1.1.2 Impact of polymicrobial infections in CF

Chronic infection in the CF airways drives cycles of inflammation mediated by pro-inflammatory cytokines, continuous recruitment of proinflammatory white blood cells to the lungs and downregulation of the regulatory cytokine, IL-10 (Bonfield et al., 1995; Courtney et al., 2004; Wagner et al., 2016; Zhou et al., 2016). In the immunocompetent lung, neutrophils account for approximately 1 % of the inflammatory cell population however this increases to 70 % in the CF lung (Kelly *et al.*, 2008). The excessive influx of neutrophils to the lungs is in part due to higher than normal levels of IL-8, the neutrophil chemotactic chemokine produced by pulmonary epithelial cells and macrophages in response to inhaled microbes (Jundi and Greene, 2015). Neutrophils play a pivotal role in the cellular innate immune response and their capacity to phagocytose and kill pathogens means they are indispensable in the clearance of microorganisms (Rosales *et al.*, 2017). However, prolonged neutrophil activity is correlated with deteriorating lung function in CF patients (Dittrich *et al.*, 2018). During phagocytosis, oxygen consumption by neutrophils is increased through the action of NADPH oxidase, which is required for superoxide production. Superoxide is converted to hydrogen peroxide, which is used by myeloperoxidase to produce bactericidal reactive oxygen species (ROS). This process is called oxidative burst and contributes to the hypoxic environment in the CF airways resulting from high levels of oxygen consumption. Neutrophils also kill pathogens by non-oxidative mechanisms through the release of antimicrobial components contained within granules. These enzymes include neutrophil elastase (NE), Proteinase 3 and cathepsin-G that are released upon neutrophil activation in a process called degranulation (Hahn *et al.*, 2011; Twigg *et al.*, 2015). Although degranulation is essential for microbial killing, degranulation events caused by continuous neutrophil stimulation contribute to inflammation and structural damage in the airways (Downey *et al.*, 2009; Hahn *et al.*, 2011). Excessive protease activity by NE has several consequences, which exacerbate inflammation in the CF lung. These include the inhibition of neutrophil activity through cleavage of the IL-8 receptor CXCR1 (Hartl *et al.*, 2007) and promoting mucin production thereby increasing mucus content (Voynow et al., 2004). NE degradation of the CFTR protein (Le Gars *et al.*, 2013) and activation of sodium channels further exacerbates the ionic imbalance that already exists in the CF airways (Caldwell *et al.*, 2005).

In addition to neutrophils, pulmonary macrophages are central to the cellular innate immune response against inhaled microbes. Macrophages phagocytose and digest pathogens, and release pro-inflammatory cytokines, which recruit neutrophils and other components of the immune response to the infection site (Byrne *et al.*, 2015). Macrophage matrix metalloproteinase 12 (MMP12) is secreted by activated macrophages. It has a number of functions including structural remodelling and proinflammatory properties (Wagner *et al.*, 2016). Along with NE, MMP12 contributes to pulmonary epithelial damage and compromises airway structural integrity (Trojanek *et al.*, 2014; Twigg *et al.*, 2015; Wagner *et al.*, 2016). Chronic cycles of inflammation, infection, and constant remodelling of the pulmonary surface result in dysfunctional airway epithelium and progressive loss of lung function. These pulmonary defects are exploited by certain pathogens, which ultimately contribute to respiratory failure and mortality.

1.1.3 Advances in therapy for cystic fibrosis

Individuals with CF are living longer and have a better quality of life thanks to advances in medicine. However, current therapeutic regimes are limited to treating the symptoms of the disease such as dehydrated mucus, microbial infection and inflammation rather than targeting the underlying molecular cause of CF (De Boeck and Amaral, 2016). The most recent breakthrough therapies target the defects in the CFTR protein and include a group of small molecules known an CFTR modulators (Ramsey *et al.*, 2019). These drugs can be categorized by their function as potentiators, which target and enhance the activity of the CFTR gated ion channel or correctors that facilitate processing and transport of the CFTR protein to the cell surface (Ramsey *et al.*, 2019). Drugs such as ivacaftor (a potentiator) may be used in isolation to treat disease caused by the *G551D-CFTR* mutation, or in combination with drugs such as lumacaftor and tezacaftor (correctors) which, together with ivacaftor are commonly used to treat disease caused by the homozygous *F508del-CFTR* mutation (Sermet-Gaudelus, 2013; Lopes-Pacheco, 2020).

Mucolytics are a class of mucoactive agents, which may be prescribed for the treatment of the thick sticky mucus arising from defects in CFTR. Mucolytics are characterized based on their ability to degrade various components of mucus thereby decreasing the viscosity and elasticity to enable mucus clearance from the airways (Henke

and Ratjen, 2007). Dornase alpha (deoxyribonuclease I) is the mucoactive agent of choice for treating mucus-associated complications in CF (Yang and Montgomery, 2018). Dornase alpha is a proteolytic enzyme which targets DNA that exists in the CF airways in large quantities due to disintegrating lymphocytes and microbial biofilms (Henke and Ratjen, 2007; Hall-Stoodley *et al.*, 2008). It is administered as an aerosol and designed for long term use by CF patients (Balsamo *et al.*, 2010). Another mucoactive agent, mannitol, is administered in powder form and has beneficial effects on mucociliary clearance in the CF airways (Nevitt *et al.*, 2018). Mannitol is an osmotic agent thought to improve the hydration of airway secretions by increasing the influx of water into the airways (Reeves *et al.*, 2012; Bilton *et al.*, 2013).

Despite the efficacy of CFTR modulators and mucoactive agents in treating CF symptoms, microbial infection is an ongoing challenge for individuals living with CF. Because of the propensity for pulmonary infection to occur in the CF airways, antibiotics are frequently used to treat such infections. In the context of CF, antibiotic therapy aims to eradicate acute infections and control chronic infections. The choice of antibiotic and treatment schedule is determined by the cause(s) of infection, resistance to antibiotics, and whether the infection is chronic or acute. Antibiotics can be administered by intravenously, orally or by inhalation (Smith *et al.*, 2017). The latter is beneficial for chronic infections such as those caused by *P. aeruginosa* (Chmiel *et al.*, 2014). For example, aztreonam aerosol or tobramycin inhalation powder is recommended for the treatment of chronic *P. aeruginosa* infections, which are often complicated by antibacterial resistance (Hamed and Debonnett, 2017; Bassetti *et al.*, 2018a). For acute infections caused by *P. aeruginosa*, therapy may aggressive and often relies on the use of two different antibiotic classes until the resistance to one is determined and the patient can be prescribed the most effective treatment (Bassetti *et al.*, 2018b). Aminoglycosides such as tobramycin or amikacin or colistin (polymyxin) may be combined with fluoroquinolone (e.g. ciprofloxacin), cephalosporin (e.g. ceftazidime) or carbapenem (e.g. meropenem) antibiotics (Chmiel *et al.*, 2014). Vancomycin and linezolid are used to treat infections caused by Gram positive bacteria such as MRSA.

Until a therapy targeting the underlying cause of CF, (i.e. the defects in CFTR) is provided, symptomatic treatments will remain exclusive as the choice of treatment for CF. Significant progress in gene therapy approaches have been made in the past decade, and provide some hope that a "cure" for CF may yet be possible. (Yan *et al.*, 2019). A

number of challenges exist, not least ensuring the delivery of therapy to the primary target location, the lungs. The pulmonary immune system is efficient and complex and provides an obstacle for the entry of viral vectors, the preferred choice for gene therapy (Yan *et al.*, 2019). This is complicated further by defective mucus in the CF airways. Non-viral vectors such a liposomes have been trialled but have shown little efficacy due to difficulties concerned with transport to the cell (Cooney *et al.*, 2018). With the advent of CRISPR-Cas9 gene editing techniques in the past decade, comes a potential solution that will alleviate the symptoms associated with CF (Hodges and Conlon, 2019). However, this approach is in its infant days of research and many challenges remain to be addressed before this therapy reaches the clinic (Colemeadow *et al.*, 2016).

1.1.4 The microbial environment in non-cystic fibrosis-related conditions

Individuals that live with non-cystic fibrosis-related respiratory diseases are also susceptible to infection with *A. fumigatus* and *P. aeruginosa*. Such pulmonary disorders include chronic obstructive pulmonary disorder (COPD) and chronic bronchiectasis, which are characterized by the permanent dilation of bronchial airways due to muscle and elastic tissue destruction mediated by consistent inflammation in the lungs. Chronic cough, increase in sputum production and difficulty in mucus clearance are features of COPD and bronchiectasis (McShane *et al.*, 2013). The development of COPD is largely associated with cigarette smoking although there is also a genetic element involved in a small percentage of cases (Athanazio, 2012). Bronchiectasis may arise as a complication of COPD and approximately 30 – 60% of individuals with COPD develop bronchiectasis (Everaerts *et al.*, 2018). The symptoms of bronchiectasis result from cycles of infection and inflammation caused by existing immunodeficiency disorders, infection by non-tuberculosis mycobacteria or by primary ciliary dyskinesia, a disorder that effects the mucociliary elevator, which is responsible for removing pathogens from the airways (Bilton, 2008). The prevalence of bronchiectasis in the US approximately five times that of cystic fibrosis and is a major cause of hospitalization due to increased rates of infection (McDonnell *et al.*, 2015; Knapp *et al.*, 2016; Weycker *et al.*, 2017).

The prevalence of *P. aeruginosa* in adults with COPD is estimated to be between 4-15% and higher for individuals with severe COPD and bronchiectasis as part of the diagnosis (Murphy *et al.*, 2008; Gallego *et al.*, 2014). In contrast, the frequency of

chronic *P. aeruginosa* infection for individuals with bronchiectasis as the primary conditions is between 9-31% (Araújo *et al.*, 2018). Compared to infection by other pathogens, *P. aeruginosa* is associated with disease progression, recurrent pulmonary exacerbations and poorer clinical outcomes, including a higher rate of mortality in patients with bronchiectasis (McDonnell *et al.*, 2015; Chai and Xu, 2020). The incidence of poly-microbial infections are also greater where *P. aeruginosa* is detected (McDonnell *et al.*, 2015). Co-infection with *P. aeruginosa* and *A. fumigatus* have been detected in severe cases of COPD and the presence of *P. aeruginosa* in the airways is considered a risk factor for *A. fumigatus* infection (Huerta *et al.*, 2014). *A. fumigatus* is frequently isolated from the airways of individuals with COPD and bronchiectasis and infection with *A. fumigatus* is a risk factor for the onset of bronchiectasis in COPD (Moss, 2015; Everaerts *et al.*, 2017; Máiz *et al.*, 2018; Everaerts *et al.*, 2018). ABPA is employed as a diagnostic feature of bronchiectasis and can inform treatment programmes (Bilton, 2008).

Symptomatic treatment schedules for bronchiectasis depend on the cause and the severity of the disease. Inhaled corticosteroids are standard in the treatment of bronchiectasis (De Soyza and Aliberti, 2016). Macrolides such as azithromycin are commonly used to treat bacterial infections as this class of antibiotics are active against *P. aeruginosa* and have the added benefit of possessing anti-inflammatory properties (Chalmers *et al.*, 2015). However, the emergence of antimicrobial resistance, and the changes that occur to the lung microbiota caused by the long-term use of these macrolides are a cause for concern (Rogers *et al.*, 2014; Chalmers *et al.*, 2015). Inhaled amikacin is also recommended for treatment of bronchiectasis and is associated with reduced pulmonary exacerbations (Ailiyaer *et al.*, 2018). Treatment options for ABPA are not as clear as those for bacterial infections (De Soyza and Aliberti, 2016). In general, corticosteroids are used for the symptomatic treatment of ABPA. Itraconazole has shown some efficacy in relieving the symptoms of ABPA, particularly when used in conjunction with corticosteroids (Wark *et al.*, 2003; Wark *et al.*, 2004).

1.2 Study of polymicrobial interactions

The microbial diversity that exists in the CF lung inevitably gives rise to species-species interactions. Such interactions can have negative consequences for the host as the outcome eventually favours either or both pathogens (Peters *et al.*, 2012; Nguyen and Oglesby-sherrouse, 2016). In the context of infection, polymicrobial interactions may be synergistic, where the cooperation between two or more microbes leads to a worse outcome for the host in comparison to when either of the microbes are present alone (Murray *et al.*, 2014). In contrast, antagonism occurs when two or more species hinder or inhibit the growth of another. This may confer protection to the host, but may also promote the growth of the antagonist, which may be detrimental to host health (Nguyen and Oglesby-sherrouse, 2016).

In the CF airways, pathogens must compete with each other for nutrients and space against a backdrop of inflammation and the possible use of antibiotics. The perception of, and response to signals from these challenges is regulated by quorum sensing, a method of communication using chemical signals that enables bacteria to regulate gene expression in a cell-density dependent manner (Schuster *et al.*, 2013). Competition is mediated, in part, by quorum sensing (Hibbing *et al.*, 2010). Given its predominant pathogenic role in the CF airways, quorum sensing in *P. aeruginosa* has been studied extensively in the context of nutrient depletion and competition with other microbial species.

In vivo and *in vitro* co-culture studies have revealed a complex synergistic – antagonistic relationship that exists between *P. aeruginosa* and *S. aureus*. *P. aeruginosa* sequesters iron from *S. aureus* by lysing its competitor – a process mediated by *Pseudomonas* quinolone signal (PQS) (Mashburn *et al.*, 2005). Quinolones are small signalling molecules involved in quorum sensing. Iron is an essential nutrient for bacterial growth and virulence and in iron-depleted environments *P. aeruginosa* upregulates a number of genes encoding iron uptake systems which facilitate the sequestration of iron from its surroundings (Nguyen *et al.*, 2015). Amongst these iron sequestration mechanisms is the increase in PQS biosynthesis (Oglesby *et al.*, 2008). Thus, *P. aeruginosa* exploits *S. aureus* as a source of iron under iron-limiting conditions. On the other hand, *P. aeruginosa* was shown to confer resistance to *S. aureus* against aminoglycoside antibiotics by supressing *S. aureus* respiration through the production of

4-hydroxy-2-heptylquinoline-N-oxide (HQNO), which, paradoxically, is an anti-staphylococcal growth suppressor (Hoffman *et al.*, 2006). Longitudinal studies have established that co-infection with *P. aeruginosa* and *S. aureus* is more detrimental to lung function than infection with *P. aeruginosa* alone (Maliniak *et al.*, 2016).

Interaction studies between *P. aeruginosa* and the oropharyngeal flora isolated from the sputum of CF patients identified an increase in the number of upregulated genes associated with pathogenesis in *P. aeruginosa* (Duan *et al.*, 2003). In the same study, lung damage was more severe in rats exposed to *P. aeruginosa* and a representative of oropharyngeal flora (a *Streptococcus* strain) than in rats exposed to either species alone (Duan *et al.*, 2003).

In other co-culture studies, the presence of peptidoglycan, a major cell-wall component of Gram-positive bacteria, was found to induce a number of virulence factors in *P. aeruginosa*, including the expression of PQS, which regulates the synthesis not only of HQNO but also other antimicrobials including pyocyanin and elastases (Korgaonkar *et al.*, 2013). *In vivo* studies using *Drosophila* demonstrated that upon the introduction of *P. aeruginosa* into the infection model, the abundance of Gram-positive bacteria decreased substantially. Similar results were found in a murine wound model (Korgaonkar *et al.*, 2013).

Despite the persistence of fungal pathogens in the CF airways, their interactions with bacteria are just beginning to be explored (Briard *et al.*, 2019). Numerous studies have focused on the interactions between *P. aeruginosa* and the commensal yeast, *Candida albicans*. *In vitro* studies show that *P. aeruginosa* inhibits the *C. albicans* yeast to filament transition, biofilm formation and intracellular adherence through the production of phenazines (Holcombe *et al.*, 2010; Morales *et al.*, 2013). Chen et al., (2014) demonstrated that *P. aeruginosa* phenazines stimulate ethanol production in *C. albicans* which in turn stimulates bacterial biofilm formation (Chen *et al.*, 2014). *In vivo* studies tell a somewhat different story as demonstrated by Lopez-Medina et al., (2015) who used a murine co-infection model, to show that *C. albicans* suppresses expression of *P. aeruginosa* virulence factors pyoverdine and pyochelin to reduce virulence (but not colonization) of the bacteria in mice (Lopez-Medina *et al.*, 2015). Studies using zebra fish as an *in vivo* model of the mucosal surface have shown synergism between *C. albicans*

and *P. aeruginosa* and in this infection model, virulence in both pathogens, and host mortality was increased (Bergeron *et al.*, 2017).

These studies demonstrate that polymicrobial interactions are difficult to dissect and the results are largely dependent upon the model system used to analyse these interactions. Nonetheless, the findings arising from such studies contribute to our understanding of microbial interactions and help in detecting potential therapeutic targets.

1.3 *In vitro* models for the study of pathogen host interactions of the lung

The airway epithelium is the first point of contact with inhaled microorganisms and is central in the innate immune responses to potential pathogens. *In vivo*, airway epithelial cells (AECs) provide a physical defense by providing a structural barrier against incoming microbes and maintaing the mucociliary elavator. AECs also provide molecular and cellular defenses through the production of antimicrobial peptides, reactive oxygen and nitrogen species, and cytokines and chemokines which orchestrate the cellular arm of the innate immune response and eventually the adaptive immune response. The morphology and function of ECs is determined by their location in the respiratory tract. Therefore, *in vitro* models have been developed to mimic specific systems within the tract, including laryngeal, bronciolar and alveolar.

As with all model systems, advantages and disadvantages exist regardless of the cell line chosen. Immortal cell lines derived from carcinomas or virus-transformed cells offer several advantages; they are easy to handle, grow quickly and provide reproducible results. Additionally, they bypass ethical concerns associated with the use of human tissue. On the other hand, these cell lines provide only a 2D monolayer, whereas *in vivo* cells exist as complex, differentiated 3D structures. However, this aspect of *in vitro* cell culture has somewhat been addressed with the development of novel protocols allowing for 3D structure of immortal cell lines (Carterson *et al.*, 2005a; Chandorkar *et al.*, 2017). Serial passage of immortal cell lines can cause genotypic and phenotypic variation, which may cause heterogeneity in cultures (Kaur and Dufour, 2012). Because of this, immortal cell lines may not adequately represent primary cells. Nonetheless, immortal cell lines have proven extremely useful in understanding how pathogens interact with the host to initiate pulmonary infection and have provided insights into the host response to pathogen invasion.

Because primary cell lines most closely represent the tissue of origin, they are excellent model systems for studying the physiology of a particular tissue (Pezzulo *et al.*, 2011). However, they have a limited life span and are associated with variability because they are taken directly from donor tissue. Growing conditions must be customized to the specific cell type and it is more difficult to achieve a large sample size, thereby limiting research opportunities.

In the context of airway infections, several *in vitro* infection models derived from humans have been developed to study host interactions with pulmonary pathogens. The most commonly used cell lines employed for these studies include A549, a type II pneumocyte derived from an alveolar carcinoma (Lieber *et al.*, 1976), 16HBE cells derived from bronchial epithelial cells and transformed with SV40, and CFBE cells derived from bronchial epithelial cells of CF patients and transformed with SV40/adenovirus (Zeitlin *et al.*, 1991; Cozens *et al.*, 1994). Since their development, these cell lines have been used for many studies investigating the interactions between CF-associated pathogens and the host (Chi *et al.*, 1991; Daly *et al.*, 1999; Wasylnka and Moore, 2002; Wasylnka, 2003; Berkova *et al.*, 2006; Osherov, 2012; David *et al.*, 2015; Surmann *et al.*, 2015; Golovkine *et al.*, 2016; Bertuzzi *et al.*, 2018).

1.4 The A549 cell line as a model for infection at the alveolar surface

The alveolar epithelium is composed primarily of type I alveolar epithelial (AE) cells, which account for 95 % of the alveolar surface, and type II AE cells, which account for 5 % of the alveolar surface (Mason, 2006). Type I AE cells function as the air-blood barrier. Type II AE cells are type I progenitor cells that are involved in epithelial repair through proliferation, surfactant production and play a role in the innate immune response through pathogen recognition, phagocytosis, pathogen killing, cytokine production and surfactant production (SP-A and SP-D) (McElroy and Kasper, 2004; Mason, 2006; Mao *et al.*, 2015)

The A549 cell line is composed of type II-like alveolar epithelial cells (pneumocyte) that originates from a human lung carcinoma. Since their development in 1976 by Lieber *et al.*, they have been used in many studies investigating pathogen-host interactions. With the exception of surfactant production, these cells provide several features performed by primary Type II AE cells, including pathogen recognition, uptake and killing and cytokine

production (Wasylnka and Moore, 2002; Mao *et al.*, 2015; Chen *et al.*, 2015). Ease of handling, reproducibility and innate immune functions, have made A549 cells an attractive *in vitro* model of the alveolar surface and for the study of pulmonary pathogen-host interactions with fungal pathogens such as; *A. fumigatus* (Croft *et al.*, 2016; Bertuzzi *et al.*, 2018), bacteria such as *P. aeruginosa, S. aureus* and *B. cepacia* (McClean and Callaghan, 2009; Surmann *et al.*, 2015; Hall *et al.*, 2016), and viral pathogens such as influenza and HRSV (Munday *et al.*, 2010; Cao *et al.*, 2017).

1.5 *Aspergillus fumigatus;* an opportunistic human pathogen

Aspergillus fumigatus belongs to the genus *Aspergillus*, which also includes *A. flavus*, *A. niger*, *A. terreus* and *A. nidulans*. Aspergilli are saprophytic filamentous, moulds that release airborne hydrophobic spores called conidia, which are approximately 2 – 3 µm in diameter and blue-green in colour. Although its natural ecological niche is the soil, *A. fumigatus* is ubiquitous, existing indoors and outdoors (Latgé, 1999). Because of this, inhalation of conidia is a daily occurrence. *A. fumigatus* is an opportunistic pathogen and the most pathogenic out of its genus (Kosmidis and Denning, 2015). For immunocompetent individuals, inhaled conidia are swiftly cleared by cells of the pulmonary immune system (Dagenais and Keller, 2009). However, in immunocompromised individuals, *A. fumigatus* can cause a mycosis called aspergillosis, the severity of which is determined by the immune status of the host. Aspergillosis can manifest in one of three forms; allergic aspergillosis, the most common form of which is known as allergic bronchopulmonary aspergillosis (ABPA) is characterized by the induction of an immune response triggered by the secretion of toxins and allergens from the developing fungus. Saprophytic aspergillosis is characterized by the development of aspergilloma (fungal ball) in chronic lung cavities of the pulmonary tissue, such as those caused by tuberculosis (Chabi *et al.*, 2015). Invasive aspergillosis (IA) is the most devastating form of aspergillosis and is characterized by the dissemination of fungal hyphae throughout the tissues of the affected area. This occurs in the lungs in more than 90 % of cases and is called invasive pulmonary aspergillosis (IPA) (Hope *et al.*, 2005). Although a number of *Aspergillus* species have been associated with invasive aspergillosis, *A. fumigatus* accounts for approximately 90% of these cases (Denning, 1998). IA targets severely immunocompromised individuals including individuals with

neutropenia, organ transplant recipients and chemotherapy patients (Kosmidis and Denning, 2015).

1.5.1 *A. fumigatus* pathogenesis and host – from inhalation to germination

A. fumigatus is a versatile microorganism that is equipped to survive and propagate in a variety of environments (Paulussen *et al.*, 2017). The fungus possesses a number of features that make it an excellent human pathogen, including the ability to grow at high temperatures and varying pH. *A. fumigatus* can sustain growth above 42°C, which in the context of human infection is beneficial for maintaining infection under high temperature conditions (Chang *et al.*, 2004). Additionally, it can adapt to the changing pH of the mammalian host by activating a set of pH-responsive genes regulated by the transcription factor, PacC (Bignell *et al.*, 2005; Bertuzzi *et al.*, 2014).

The physical size and hydrophobic nature enables *A. fumigatus* conidia to enter the respiratory tract through inhalation, bypass mucocilary clearance, and reach the alveoli. Within 30 minutes, resting conidia become metabolically active and begin to swell (Fig 2A and 2B).

If left unchallenged by cells of the immune system, conidia begin to germinate within approximately three hours and by eight hours, hypha being to form (Fig. 2C and 2D).

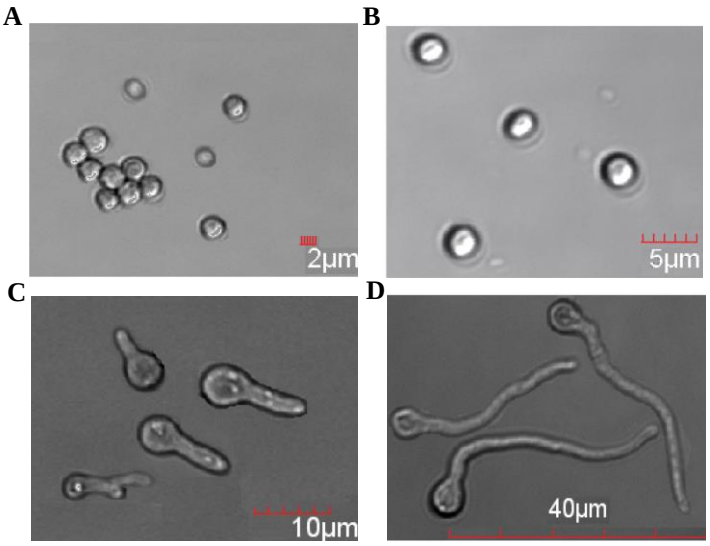

Fig. 1.2. The morphology of *A. fumigatus* The differing morphological stages of *A. fumigatus* growth in Sabouraud dextrose liquid medium; as time proceeds, resting conidia at zero hours (A) begin to swell after two hours (B) and germinate after 6 hours (C), eventually producing hypha by 24 hours (D).

1.5.1.1 Host cell recognition of *A. fumigatus*

Cells of the immune system and pulmonary epithelia possess pathogen recognition receptors (PRRs) which detect pathogen associated molecular patterns (PAMPs) on pathogens. A range of PRRs have been implicated in the recognition of *A. fumigatus* including Toll-like receptors (TLR) 2, 3, 4 and 9, NOD2 and NLRP3 (Meier *et al.*, 2003; Ramirez-Ortiz *et al.*, 2008; Saïd-Sadier *et al.*, 2010; Li *et al.*, 2012; Beisswenger *et al.*, 2012). The C-type lectin receptors (CLRs) dectin-1, dectin-2, DC-SGIN, Mincle and mannose receptors are the primary receptors for β(1,3)-glucan residues that coat the *A. fumigatus* conidia cell (Brown and Gordon, 2001; Serrano-Gómez *et al.*, 2005; Sun *et al.*, 2013; Bertuzzi *et al.*, 2014; Goyal *et al.*, 2018).

A. fumigatus conidia may evade initial host-cell recognition by masking β(1,3)-glucan residues with a thin proteinaceous hydrophobic layer called RodA hydrophobin (Carrion *et al.*, 2013). As conidia germinate, the RodA layer is shed and β(1,3)-glucan residues are revealed, allowing for recognition by cells expressing dectin-1.

Until recently, little was known about the recognition of non-germinating conidia by host cells. A role for a pulmonary and hepatic murine endothelial cell CLR called MelLec in the detection of Dihydroxynapthalene (DHN)-melanin was described by Stappers and colleagues (Stappers *et al.*, 2018). DHN-melanin is a secondary metabolite found in the conidial cell wall. In the environment, it confers resistance against desiccation and damage from UV radiation, and in the host it plays an important role in virulence by scavenging ROS and protecting conidia against phagocytosis by professional phagocytes (Jahn *et al.*, 2002; Heinekamp *et al.*, 2013; Pal *et al.*, 2013). Interestingly, recognition of this PAMP by MelLec was lost as conidia began to swell and germinate, thus indicating a role for this receptor during the very early stages of fungal infection (Stappers *et al.*, 2018). Moreover, DHN-melanin is masked by RodA, thus until conidia shed this hydrophobin, the cellular immune-recognition response is limited.

1.5.1.2 The humoral response to *A. fumigatus*

The early host response against inhaled conidia is mediated by the cellular and humoral arm of the innate immune system. The humoral component of innate immunity augments the cellular response in various ways and is comprised of several soluble recognition receptors including Pentraxins, complement proteins, ficolins and collectins such as SP-A and SP-D (Bottazzi *et al.*, 2010; Carreto-Binaghi *et al.*, 2016). Pentraxin 3 (PTX3) is a soluble recognition receptor expressed by activated epithelial cells, endothelial cells and myeloid cells and is constitutively expressed as part of the neutrophil arsenal of antimicrobial peptides (Jaillon *et al.*, 2007; Moalli *et al.*, 2010). PTX3 binds to conidia, but not to hyphae and its role in host defence against *A. fumigatus* has been described as indispensable (Garlanda *et al.*, 2002). This was supported with *in vivo* studies which demonstrated that PTX3-deficient mice were unable to survive conidial infection and PTX3-deficient mice that were supplemented with exogenous PTX3 had increased survival rates and decreased fungal burdens in the lungs (Garlanda *et al.*, 2002). PTX3 promotes the interaction with and uptake of conidia by macrophages *in vitro* and *in vivo* (Garlanda *et al.*, 2002). Interestingly, the levels of PTX3 was lower in the sputum of CF patients than that of individuals with chronic obstructive pulmonary disorder (COPD) (Hamon *et al.*, 2013). The low levels of PTX3 was attributed to N-terminal proteolytic cleavage of PTX3 by serine proteases derived from *A. fumigatus* and neutrophil elastases – both of which are frequent in the CF airways (Hamon *et al.*, 2013).

Some soluble recognition receptors interact together to enhance fungal killing. For example, PTX3 interacts with several components of the complement system to activate the three complement pathways (classical, alternative and lectin pathway) (Garlanda *et al.*, 2016). However, the killing power of the complement system on conidia is questionable, as studies have identified *A. fumigatus* defence mechanisms that have evolved to evade or degrade several components of the complement system. The *alb1* and *arp1* genes belong to a gene cluster that regulates the DHN-melanin pathway in *A. fumigatus* conidia (Heinekamp *et al.*, 2013). Mutants deficient in these proteins were more susceptible to deposition by the complement protein, C3 on the conidial cell wall, thus indicating a role for DHN-melanin in early evasion of the complement system (Tsai *et al.*, 1997; Tsai *et al.*, 1998). The *A. fumigatus* metalloprotease Mep1p cleaves several complement proteins including C3, C4 and C5, MBL and Ficolin-1 (Shende *et al.*, 2018). Since Mep1p is produced by conidia, the authors proposed that *A. fumigatus* could

inactivate the complement during the very early stages of infection. A serine protease, Alp1, secreted by *A. fumigatus* hyphae was also found to degrade the C1q, C3, C4 and C5 members of the complement system, thereby indicating that the complement cascade could be inactivated by *A. fumigatus* that has evaded earlier detection by the innate immune system (Behnsen *et al.*, 2010).

Ficolins are recognition molecules that specifically target N-acetyl compounds such as N-acetylglucosamine components on fungal cell walls and activate the lectin complement pathway (Endo *et al.*, 2011). Although their role in fungal immunity is not well established, these lectins do appear to have a protective role against *A. fumigatus* (Genster *et al.*, 2016). Interaction with PTX3 enhanced binding of both ficolin-2 and PTX3 to conidia and ficolin-2 mediated complement protein deposition on the surface of conidia, a process that was enhanced by the presence of PTX3 (Ma *et al.*, 2009). *In vivo*, ficolin knock-out mice exposed to sub-lethal doses of *A. fumigatus* conidia displayed delayed fungal clearance and impaired production of proinflammatory cytokines IL-1β and IL-6, indicating a role for ficolins in modulating inflammation as a response to *A. fumigatus* (Genster *et al.*, 2016).

Lastly, SP-A and SP-D are surfactant proteins that belong to the C-type lectin family of recognition receptors and as such, they bind various carbohydrate structures on the outer surface of incoming airway pathogens. *In vitro*, SP-A and SP-D opsonize conidia, resulting in agglutination of the spores and enhanced phagocytosis by alveolar macrophages and neutrophils (Madan *et al.*, 1997). SP-A and SP-D are also though to play a role in regulating a hypersensitivity response and murine models of ABPA treated with exogenous SP-A and SP-D displayed lower levels of eosinophilia than untreated mice (Madan *et al.*, 1997; Madan *et al.*, 2001).

1.5.1.3 Manipulation of host epithelial cells by *A. fumigatus*

Inhaled *A. fumigatus* conidia that reach the alveoli can be internalized by AE cells. Endocytosis is, in part, dectin-1-dependent and is mediated by PacC-regulated genes in the fungus (Bertuzzi *et al.*, 2014). These interactions are actin-dependent and damaging to host-cell integrity (Kogan *et al.*, 2004; Bertuzzi *et al.*, 2014). Once internalized, conidia are trafficked to late endosomes where a proportion of them are killed within the acidic compartments (Wasylnka and Moore, 2002). However, the killing ability of AE cells is

inferior to that of professional phagocytes such as macrophages, neutrophils and dendritic cells and a small number of conidia can survive and germinate within the cells (Wasylnka, 2003).

Interestingly however, the DHN-melanin is reported to promote the uptake of conidia into AE cells, inhibit phagolysosmal acidification and caspase-3-dependent apoptosis in A549 cells (Amin *et al.*, 2014). The inhibition of host cell apoptosis by conidia has been reported previously in several studies and thus, it is plausible that *A. fumigatus* exploits epithelial cells as mechanisms of evasion from the immune system (Daly *et al.*, 1999; Berkova *et al.*, 2006; Féménia *et al.*, 2009).

1.5.1.4 The innate immune cell response to *A. fumigatus*

Alveolar macrophages are resident phagocytes of the pulmonary innate immune system and play a major role in clearing inhaled pathogens from the lung (Cheung *et al.*, 2000; Philippe *et al.*, 2003). When *A. fumigatus* conidia are deposited in the lung, the role of macrophages is to limit germination (Tanaka *et al.*, 2015; Rosowski *et al.*, 2018). In this way, the host is protected from the effects of hyphae and from the potential tissue damage cause by excessive neutrophil influx required to kill germinating conidia (Fig. 1.3).

Inhaled conidia that reach the lower airways are engulfed by macrophages in an actin-dependent manner and internalized conidia are contained within a phagosome which undergoes maturation by fusing with a lysosome, forming a phagolysosome (Ibrahim-Granet *et al.*, 2003). Vacuolar ATPases induce phagolysosome acidification and activate hydrolytic enzymes such as cathepsin-D and chitinases, which initiate degradation of the fungal cell wall (Ibrahim-Granet et al., 2003). *A. fumigatus* conidia begin to swell approximately three hours after engulfment and the resulting exposure of β-(1, 3) glucans initiates fungal detection by intracellular PRRs dectin-1 and TLR9 which associate with the phagolysosome (Ibrahim-Granet *et al.*, 2003; Kasperkovitz *et al.*, 2010; Faro-Trindade *et al.*, 2012). Coinciding with this event is the generation of ROS, the production of which correlates directly to elevated levels of fungal killing, and the production of proinflammatory cytokines including TNF-α and IL-6 (Philippe *et al.*, 2003; Dubourdeau *et al.*, 2006).

The orchestration of a macrophage-mediated proinflammatory response is important for the clearance of germinated conidia, which is a neutrophil-dependent process (Philippe *et al.*, 2003; Rosowski *et al.*, 2018)**.**

Neutrophils are indispensable for the control of *A. fumigatus* infection. This is highlighted by prevalence of IA in individuals with chronic granulomatous disease (CGD), a disease characterized by defective NADPH oxidase (King *et al.*, 2016b). The critical role for neutrophils in innate defence against *A. fumigatus* has been highlighted in several *in vivo* studies, which have demonstrated high mortality rates and ease of fungal colonization in neutropenic murine models of aspergillosis (Stephens-Romero *et al.*, 2005; Mircescu *et al.*, 2009). Neutrophils employ a range of oxidative and non-oxidative mechanisms to destroy developing hyphae, including phagocytosis, NADPH oxidase-mediated ROS production and the discharge of a range of antimicrobial proteases from granules such as histones H2A, H2B, and H3.1, neutrophil elastase (NE), myeloperoxidase (MPO), cathepsin G, azurocidin, and defensin 1 (Shlezinger *et al.*, 2017; Shopova *et al.*, 2019).

The formation of neutrophil extracellular traps (NETs) was described by Brinkmann et al. (2004) as a novel form of neutrophil-mediated antimicrobial defense and has since been implicated in the host defense against *A. fumigatus* (Bruns et al.,2010; McCormick et al. 2010; Röhm et al. 2014). NETs are networks of extracellular fibers composed of decondensed nuclear chromatin that bind histones and antimicrobial granular proteins (Brinkmann et al. 2004). NET formation (NETosis) is induced by a variety of microbes or proinflammatory mediators such as IL-8 and is particularly important for defense against pathogens that are too large to be phagocytosed, such as *A. fumigatus* hyphae (Brinkmann et al. 2004; Urban et al., 2006). NETs inhibit the growth of, but do not kill hyphae, thereby indicating a role for NETs during the latter stages of *A. fumigatus* infection (McCormick et al. 2010). Calprotectin, a NET-associated protein chelates zinc ions thereby starving the fungus of an essential nutrient (McCormick et al. 2010; Bianchi et al. 2011). Lactoferrin, a glycoprotein released during neutrophil degranulation, also contributes to fungal nutrient depletion by sequestering iron from *A. fumigatus* (Zarember *et al.*, 2007) (Fig. 1.3).

1.5.1.5 The adaptive immune response to *A. fumigatus*

The role of Dendritic cells (DC) in the immune system is to bridge innate and adaptive immune responses. Immature DCs (iDC) phagocytose resting conidia, swollen conidia and germinating conidia causing them to become activated and mature (Bozza *et al.*, 2002; Gafa *et al.*, 2006; Hsieh *et al.*, 2017). Mature DC express CCR7, which direct the cells to lymphoid tissues where they interact with their cognate naïve helper T-cells (Th) to activate an adaptive immune response (Riol-Blanco *et al.*, 2005). *A. fumigatus*-infected DC produce cytokines that drive specific T-cell responses. As well as TNF-α and IL-1β, DC secrete IL-12, IL-23 and IL-27 cytokines that are associated with stimulating Th1-mediated adaptive immune responses. IFN-γ is a cytokine with particular importance in fungal clearance and its production by Th1 cells in response to IL-23 stimulation, demonstrates an important role for DCs in providing defence against *A. fumigatus* (Smits *et al.*, 2004; Gafa *et al.*, 2006). Another IFN-γ-producing cell is the Natural Killer (NK) cell, whose role in anti-*A. fumigatus* defence has been shown *in vivo* and *in vitro* to be significantly important (Park *et al.*, 2009; Bouzani *et al.*, 2011). Infected DC produce IL-10 during the later stages of *A. fumigatus* infection (Bozza *et al.*, 2002; Gafa *et al.*, 2006). This is a crucial immunoregulatory cytokine required to downregulate inflammation when an infection has cleared.

The upregulation of IL-10 and IL-4 are associated with the switch from a Th1-mediate response to a Th2-mediated response, commonly observed in asthma and ABPA (Stevens, 2006). Th2 responses are characterized by an increase in IL-5 and IL-4 which drive eosinophil maturation, IL-13, which is responsible for mucus hypersecretion and activate IgE and IgG1 antibody production in B cells (Stevens *et al.*, 2003; Allard *et al.*, 2006; Chaudhary and Marr, 2011; Murdock *et al.*, 2011). Defects in the CFTR gene are heavily linked with the dysregulation of the T-cell-mediated immune response and the intrinsic bias for Th2 responses (Allard *et al.*, 2006; Ratner and Mueller, 2012).

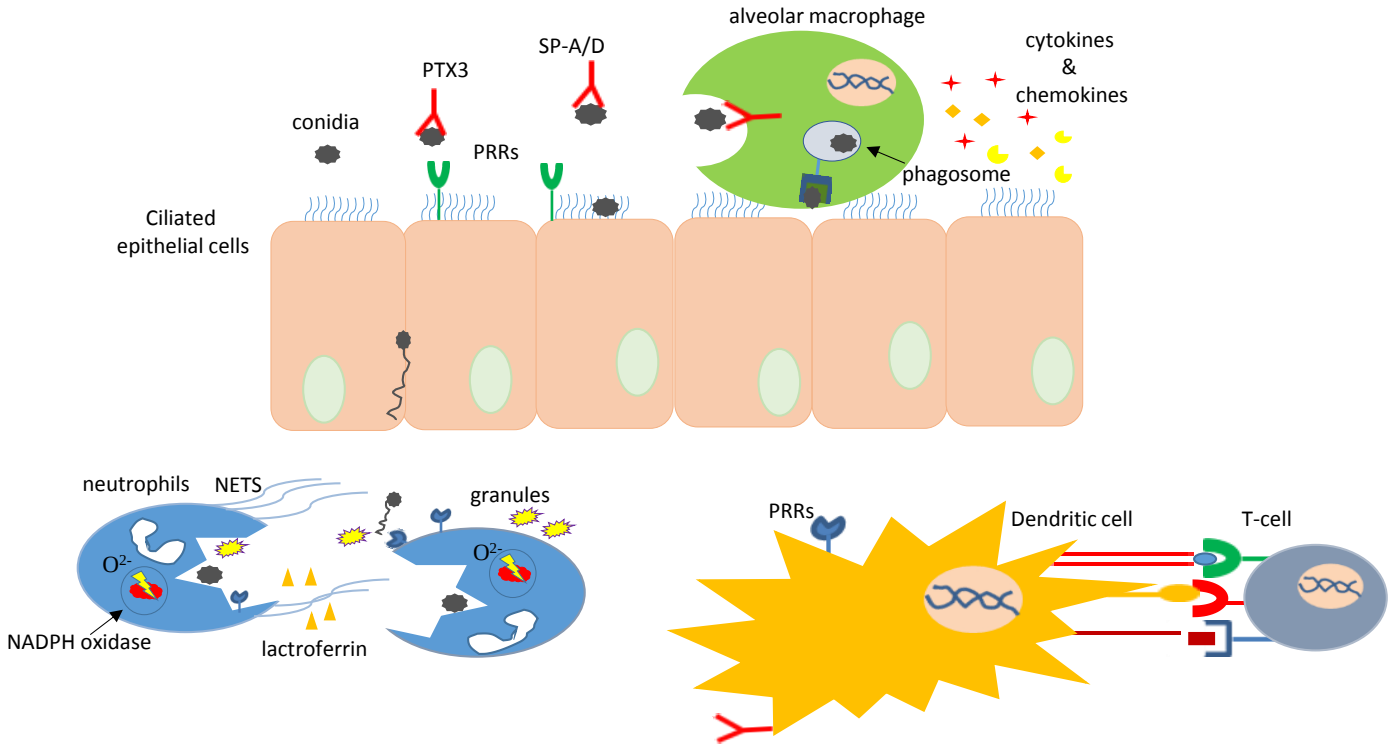

Fig. 1.3 The innate immune response to *A. fumigatus*. Immunocompetent lung, conidia are immediately met by a host of soluble recognition receptors including PTX3 and SP-D which bind to and enhance conidial phagocytosis by AM. AM recognition and uptake of conidia is mediated by Dectin-1 and TLRs and leads to the induction of a proinflammatory response. Conidia that have escaped attack by AM, germinate and penetrate through the alveolar surface. AM- and EC-derived proinflammatory mediators recruit neutrophils to the site of infection. Neutrophils employ oxidative-dependent (ROS generation) and oxidative-independent (NET formation, degranulation and lactoferrin production) mechanisms to inactivate germinating conidia and hyphae. At the site of infection, DCs phagocytose and process germinated conidia for subsequent antigen presentation to naïve T cells, which in turn activate an adaptive immune response to *A. fumigatus*.

1.5.2 The role of *A. fumigatus* secondary metabolites in establishing infection

A. fumigatus conidia that escape killing by the host immune system begin to germinate and produce hyphae. Fungal hyphae secrete secondary metabolites that have immunosuppressant properties, such as gliotoxin and fumagillin and secrete a range of lytic enzymes such as lipases and proteases that enable fungal expansion and dissemination through pulmonary tissue (Kogan *et al.*, 2004; Tsunawaki *et al.*, 2004; Farnell *et al.*, 2012; Guruceaga *et al.*, 2018; Raffa and Keller, 2019).

One of the features that make *A. fumigatus* a successful human pathogen is the ability to modulate disease progression through the production of numerous secondary metabolites. As previously discussed in section 1.5.1, DHN melanin limits the effects of ROS and interferes with the phagocytic properties and phagosome acidification in phagocytic cells (Amin *et al.*, 2014).

Gliotoxin belongs to the epipolythiodioxopiperazine class of fungal toxins and is characterized by a disulphide bridge across the piperazine ring (Dolan *et al.*, 2015). The disulphide bridge is a reactive functional group to which toxicity is attributed. *A. fumigatus* is protected from the toxic effects of gliotoxin through the upregulation of *gliT*, a gene encoding GliT, a gliotoxin reductase which oxidizes free thiol groups on the molecule and reduces oxygen to hydrogen peroxide (Schrettl *et al.*, 2010; Scharf *et al.*, 2016). ROS is generated through the reduction and oxidation of the disulphide bonds, thereby interfering with redox homeostasis in the host (Scharf *et al.*, 2016).

It is well established that gliotoxin interferes with the host immune response in numerous ways. Gliotoxin inhibits activation of the transcription factor nuclear factor κB (NFκB) by preventing proteasome-dependent degradation of the NFκB inhibitor, IκBα through interference with the proteasome (Kroll *et al.*, 1999). NFκB is a major immune-regulatory transcription factor and is involved in upregulating proinflammatory cytokines. Thus, through inhibition of NFκB, gliotoxin downregulates the host immune response. Gliotoxin targets the pro-apoptotic protein Bak to induce apoptosis *in vitro* and *in vivo* (Pardo *et al.*, 2006). Gliotoxin is in part, responsible for the suppression of angiogenesis was inhibited in mice exposed to *A. fumigatus*, although a role for other secondary metabolites was attributed to this inhibition also (Ben-Ami *et al.*, 2009). Gliotoxin suppresses the cellular arm of the immune system in a number of ways. Gliotoxin interferes with NADPH oxidase activity thereby inhibiting the production of ROS (Tsunawaki *et al.*, 2004). Gliotoxin targets phosphatidylinositol 3,4,5-trisphosphate, which impairs actin dynamics, hence phagocytosis, as was shown to be the case in murine macrophages (Schlam *et al.*, 2016a). Gliotoixin has also been implicated in interfering with the ciliary beat in human respiratory cells *in vitro* (Amitani *et al.*, 1995). The *in vivo* effects of gliotoxin were demonstrated in an immunosuppressed (non-neutropenic) murine model of IPA (Sugui *et al.*, 2007). Mice were exposed to a mutant strain of *A. fumigatus* in which the The *gliP* gene encoding GliP, a nonribosomal peptide synthase that catalyzes the first step in the gliotoxin biosynthesis pathway was deleted. Mutant

strains were unable to trigger ROS in neutrophils, induce apoptosis in mouse endothelial fibroblasts and showed reduced ability to induce mortality in immunosuppressed mice (Sugui *et al.*, 2007).

Fumagillin displays similar immunosuppressant properties to gliotoxin. Although to a lesser extent than gliotoxin, fumagillin retards ciliary beating in epithelial cells (Amitani *et al.*, 1995; Fallon *et al.*, 2010). It is internalized by A549 cells and induces cellular damage as measured by the amount of chromium released in a ^{51}Cr release assay (Guruceaga *et al.*, 2018). Fumagillin has exceptional anti-angiogenic properties and covalently binds to methionine aminopeptidase-2 (MetAP-2) via its epoxide ring thereby inhibiting endothelial cell proliferation (Sin *et al.*, 1997; Griffith *et al.*, 1998). Fumagillin affects neutrophil phagocytosis by interfering with f-actin assembly (Fallon *et al.*, 2010). Additionally, NADPH oxidase assembly and neutrophil degranulation is reduced in cells exposed to fumagillin, thus inhibiting the ability of these cells to kill internalized pathogens (Fallon *et al.*, 2010).

1.5.3 Impact of *A. fumigatus* on cystic fibrosis patients

A. fumigatus is the causative agent of allergic bronchopulmonary aspergillosis, (ABPA). It is estimated that 1 – 2 % of asthma patients and 1 – 15 % of CF patients are affected by ABPA (Stevens *et al.*, 2003). Clinical manifestations of ABPA include wheezing and bronchospasms and for individuals with CF, decline in lung function may occur (Janahi *et al.*, 2017). For non-CF patients, ABPA diagnostic criteria include asthma, elevated serum levels of *Aspergillus*-specific IgG antibodies, elevated serum levels of IgE and eosinophilia (Tanner and Judson, 2008; Patterson and Strek, 2010). Several of the diagnostic criteria for ABPA are common manifestations of CF, for example, elevated IgG and IgE anti-*A. fumigatus* antibodies are not uncommon in CF serum due to sensitization to *A. fumigatus* in CF (Knutsen *et al.*, 2004). For this reason diagnosis of ABPA in a CF patient may present certain challenges (Tanner and Judson, 2008). Nonetheless, *A. fumigatus*-specific IgE levels are recognized as the most useful diagnostic tool (Knutsen *et al.*, 2004; Agarwal *et al.*, 2013).

ABPA is described as a hypersensitivity lung disease in response to bronchial colonization by *A. fumigatus* (Knutsen and Slavin, 2011). It occurs when conidia deposited in the airways begin to germinated and release metabolites such as gliotoxin,

fumagillin, and allergens such as Asp f family of allergens (Daly and Kavanagh, 2001; Farnell *et al.*, 2012). These toxins disturb the epithelial barrier and impede mucociliary clearance (Amitani *et al.*, 1995; Kogan *et al.*, 2004). An influx of pulmonary macrophages and neutrophils mediate a proinflammatory cytokine cascade that promote a Th2-type adaptive immune response involving the release of IL-4, IL-5, IL-9 and IL-13 (Caminati *et al.*, 2018). IL-4 induces IgE production, which binds to and sensitizes basophils and mast cells. IL-5 and IL-9 recruit eosinophils and mast cells to the infection site and IL-13 induces mucus hypersecretion, airway fibrosis and eotaxin production, thus contributing to the eosinophilic inflammatory response (Zhu *et al.*, 1999; Fahy, 2015). These factors contribute to the chronic inflammation that feature heavily in the CF airways (Fig. 1.4).

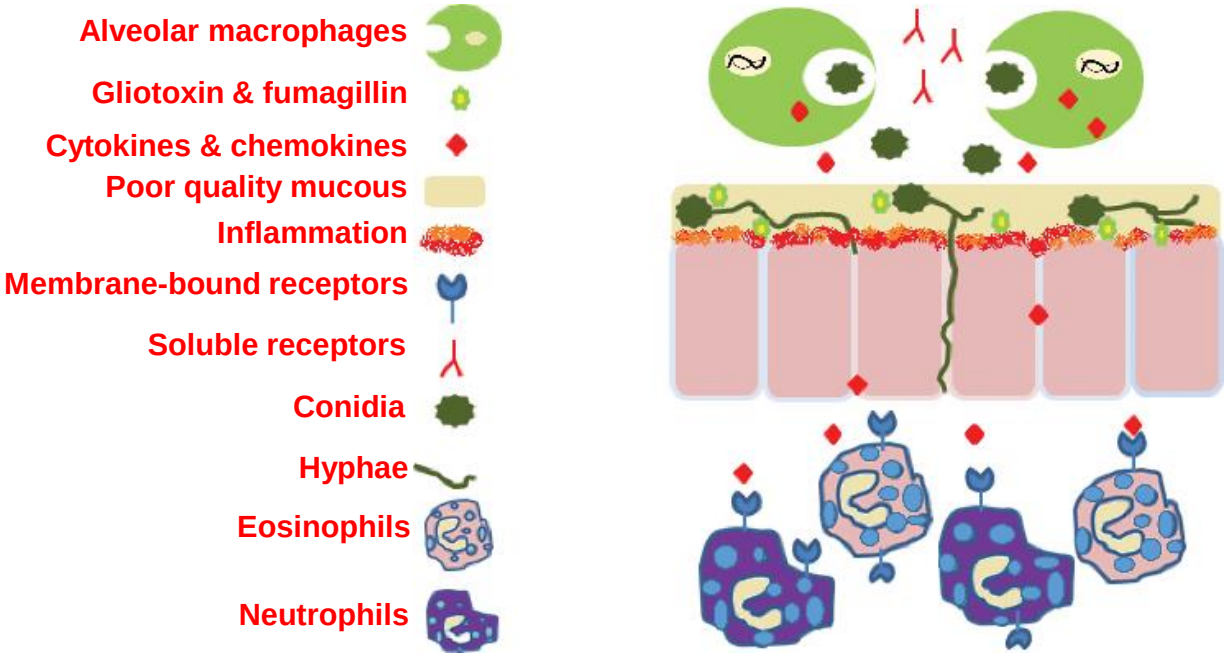

Fig. 1.4 The effect of *A. fumigatus* on the immunocompromised lung. The immunocompromised lung, or the asthmatic and CF lung, provides an environment that is conducive to conidial growth. Poor quality mucus inhibits access to conidia by immunological mediators, thus conidia germinate and penetrate through the alveolar surface. Hyphae produce gliotoxin and fumagillin, which deactivate the mucociliary elevator and inhibit neutrophil activity. An overexaggerated inflammatory response to *A. fumigatus* mediated by eosinophiles and neutrophils contributes to tissue necrosis and severe pulmonary damage.

1.5.4 Microbial interactions involving *A. fumigatus*

Inhaled *A. fumigatus* conidia form part of the diverse evolving microbial community that influence the disease progression in the CF airways. The way in which *A. fumigatus* interacts with other members of this community is fundamental to understanding how this pathogen competes with others to establish infection or facilitates the establishment of other pathogens in the lung. A better understanding of these dynamics may help predict the treatment regimens necessary to ameliorate the disease. With the exception of *P. aeruginosa*, the interactions between *A. fumigatus* and other pulmonary pathogens remain relatively unexplored, although this is changing as the recognition for the impact of polymicrobial interactions on disease progression is beginning to surface (Filkins and O'Toole, 2015).

While bacteria such as *S. aureus* are associated with chronic colonization in juvenile CF patients, *A. fumigatus* persists throughout the lifetime of individuals with CF but rarely establishes chronic infection (CF Registry of Ireland 2017 Annual Report, 2017; Hurley, 2018; Delfino *et al.*, 2019). Co-cultures of *S. aureus* and *A. fumigatus* conidia revealed antagonistic interactions resulting in the bacteria outcompeting the fungus (Ramírez Granillo *et al.*, 2015). In this study, *S. aureus* cells adhered to conidia and fungal-bound bacteria served as a chemoattractant for other bacterial cells. Fungal inhibition by *S. aureus* was most effective where bacteria adhered to the surface first. Bacteria induced lysis of the conidia and interfered with hyphal development (Ramírez Granillo *et al.*, 2015).

Although *Klebsiella pneumoniae* is not typically associated with CF infections, it is nonetheless a common cause of pulmonary disease (LiPuma, 2010; Leão *et al.*, 2011). *In vitro,* in mixed biofilms, *K. pneumoniae* suppressed *A. fumigatus* conidial germination, hyphal development and biofilm formation without killing the fungus (Nogueira *et al.*, 2019). On the contrary, *K. pneumonia* biofilm increased in the presence of *A. fumigatus*. These effects were dependent on direct contact between the fungal and bacterial pathogens in which *K. pneumoniae* induced oxidative stress and upregulation of cell wall synthesis genes in *A. fumigatus* (Nogueira *et al.*, 2019).

Stenotrophomonas maltophilia is an emerging CF-associated pathogen (Esposito *et al.*, 2017). Interactions between *S. maltophilia* and *A. fumigatus* were analysed in mixed biofilms and, similar to the previous *S. aureus* and *K. pneumoniae*, the results showed

that *S. maltophilia* interacted directly with fungal biofilm and in the presence of bacteria, *A. fumigatus* hyphal formation was delayed, conidiation was abrogated and and biofilm formation was reduced. Moreover, the conidial cell wall was thicker in the presence of S. maltophilia.

These interaction studies indicate that while bacteria outcompete *A. fumigatus* in terms of growth, these encounters do not kill the fungus, rather subdue their ability to become invasive. In the context of CF and asthma, this may be clinically relevant, as although *A. fumigatus* does not become invasive, it does persist and induce prolonged inflammation (Hartl, 2009; Ghosh *et al.*, 2015).

The most common interaction studies involving *A. fumigatus* and another airway pathogen are those that occur with *P. aeruginosa*. The importance of understanding how *A. fumigatus* and *P. aeruginosa* interact is underpinned by the negative impact of co-infection with these pathogens in CF. Thus, understanding the dynamics of the relationship between these pathogens is fundamental for the development of targeted therapeutics that may disturb these interactions and improve patient health.

1.6 *Pseudomonas aeruginosa*: an opportunistic human pathogen

P. aeruginosa is a Gram-negative, rod-shaped bacterium and is ubiquitous in nature, particularly in aquatic and soil environments. Its ubiquitous nature is due to its ability to thrive in environmental niches that are intolerable to other microorganisms and its nutritional versatility. The genome of *P. aeruginosa* is large (~6.3 kbp) (Stover *et al.*, 2000) and approximately 8-10 % of these genes are predicted to be regulators of gene expression (Greenberg, 2000). This confers *P. aeruginosa* with an incredible capacity to adapt rapidly to environmental changes such as nutritional availability (Greenberg, 2000). Additionally, *P. aeruginosa* possess several efflux pumps which can expel toxic compounds, such as antibiotics, from the cell faster than they can accumulate (Greenberg, 2000; Pang *et al.*, 2019). These attributes give *P. aeruginosa* a competitive advantage over other microbes and make this a remarkable opportunistic pathogen of humans.

Most infections caused by *P. aeruginosa* arise from the immunocompromised condition of the host. *P. aeruginosa* is a common cause of nosocomial infections, e.g. neonatal infections and hospital-acquired urinary tract infections, infections in

neutropenic patients undergoing chemotherapy and infections associated with general immunosuppression such as AIDS (Lyczak *et al.*, 2000; de Bentzmann and Plésiat, 2011). However, a number of human diseases exist in which *P. aeruginosa* is characterized as the primary pathogen including chronic respiratory disease in CF patients, bacteraemia that manifests in severe burn victims and the occurrence of ulcerative keratitis in individuals who wear contact lenses for extended periods (Lyczak *et al.*, 2000).

Respiratory infections caused by *P. aeruginosa* can be categorized as acute or chronic. Acute infections are caused by direct trauma to pulmonary tissue such as that which may occur when endotracheal tubes (ETTs) are inserted into the airway for ventilation. ETTs are reservoirs for bacterial biofilms and *P. aeruginosa*-biofilm formation on ETTs is a common cause of hospital-acquired infection (Gibbs and Holzman, 2012; Guillon *et al.*, 2018). Chronic *P. aeruginosa* infections are caused by intrinsic defects in the host immune system, such as those observed in CF. *P. aeruginosa* colonizes the airways from adolescence and persists chronically and intermittently for the lifetime of the individual (Govan and Deretic, 1996; Surette, 2014). The unique relationship that exists between *P. aeruginosa* and the CF airways is best described by Govan and Deretic (1996), who highlighted the inherent ability of *P. aeruginosa* to adapt to the CF pulmonary environment.

"In microbial pathogenesis, there are few more striking examples of *in vivo* microbial adaptation than the asymptomatic colonization of CF lungs by typical nonmucoid *P. aeruginosa* strains and the subsequent emergence of mucoid forms during chronic debilitating pulmonary infection" (Govan and Deretic, 1996).

1.6.1 The host immune response to *P. aeruginosa*

1.6.1.1 The mucociliary elevator

In the immunocompetent host, many of the host immune responses to *P. aeruginosa* are applicable to Gram-negative bacteria in general (Williams *et al.*, 2010). Variations in the host response to particular pathogens are usually observed according to the immunosuppression status of the host and as such, many of the interaction studies analysing the host immune response and *P. aeruginosa* have been performed in the context of CF infection (Lovewell *et al.*, 2014).

To establish infection, *P. aeruginosa* is required to attach to epithelial cells and remain for a period of time, which allows it to secrete its toxic contents into the host. The ASL contains soluble antimicrobial agents (e.g. lactoferrin, lysozyme, human β-defensins and secretory phospholipase A2), which play an integral role in suppressing microbial colonization however the rapid doubling time of bacteria (every 20 minutes under optimal conditions) have shown (*in vitro*) that these peptides alone do not clear bacterial infection from the mucus (Cole *et al.*, 1999). Thus, clearance of bacteria from the airways is also reliant on a functional mucociliary elevator to physically remove bacteria (Knowles and Boucher, 2002).

Defective mucociliary clearance of pathogens in individuals with CF highlight the importance of functional mechanical defence mechanisms in the immune response against *P. aeruginosa* and for this reason, the mucociliary elevator has been characterized as the most important defence mechanism against this bacteria (Wiliiams *et al.*, 2010). The ASL consists of a thick viscous mucus layer and a low-viscosity liquid layer, which rests above ciliated epithelial cells. Mucus consists of varying concentrations of mucins, water and ions. Mucins are glycosylated macromolecules with diverse oligosaccharide side chains and can be tethered to epithelial cells, forming a physical defence barrier against incoming pathogens and other particles (Whitsett and Alenghat, 2015). Pathogens become trapped in the mucus, which is released from host cells by pathogen or host-generated proteases and dispensed from the airways by the mucociliary elevator (Fig. 1.5). Secreted mucins bind to pathogens upon entering the airways and form part of mucus that removes pathogens by the mucociliary elevator. The diversity of the oligosaccharide chains of tethered mucins (encoded by MUC4, MUC13, MUC16 and MUC21) and

secreted mucins (encoded by MUC5AC, MUC5B, MUC1 and MUC2) enable mucins to bind to, and trap most particles that land in the airways (Knowles and Boucher, 2002; Whitsett and Alenghat, 2015). Adequate hydration is required for mucins to unfold its carbohydrate chains, which are required for binding to particles that are deposited into the airway epithelia (Williams *et al.*, 2010).

The low-viscosity of the periciliary liquid (PCL) enables the cilia of the epithelial cells to beat, thereby elevating the mucus layer to the central airways and into the throat where the mucus is swallowed or expectorated (Williams *et al.*, 2010). It is estimated that clearance of bacteria from the airways by the mechanisms described can take up to six hours from the point of bacterial deposition in the peripheral airways (Knowles and Boucher, 2002). Within this time, other components of the innate immune system are activated to facilitate complete clearance of bacteria.

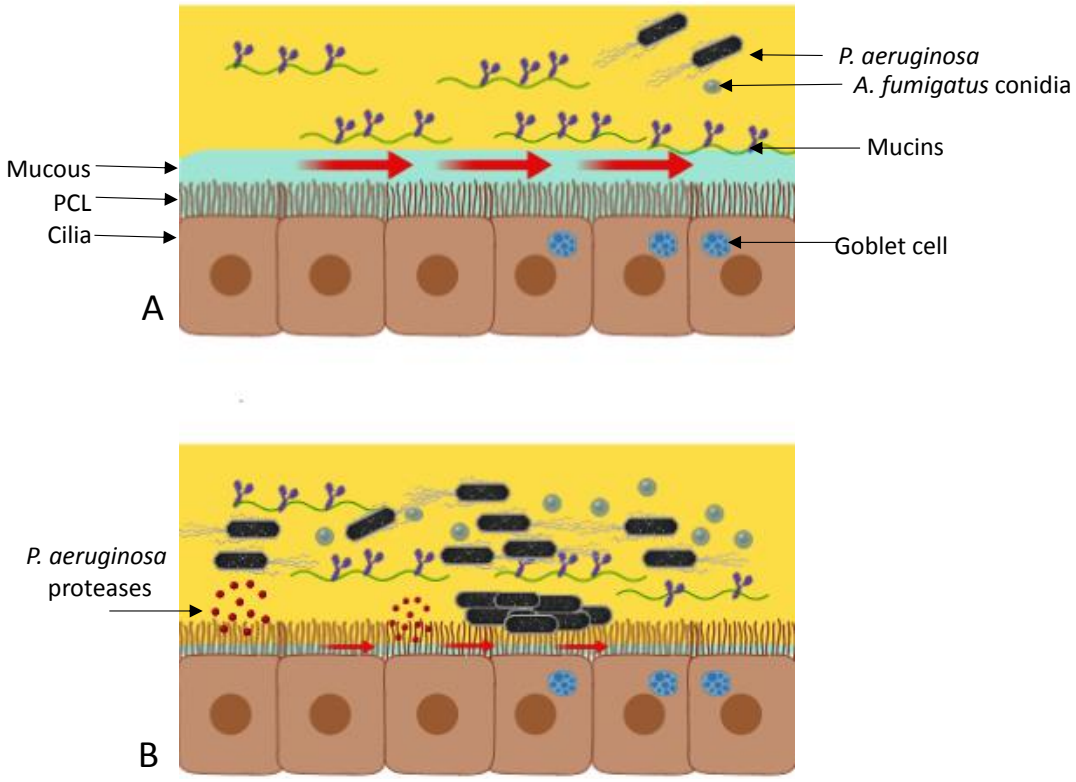

Fig. 1.5 Bacteria in the CF lung (A) Bacteria and conidia that enter the lugs become trapped in mucus and are cleared from the airways by the mucociliary elevator (denoted by large red arrows). (B) Bacteria and conidia that enter the CF lung escape clearance due to defects in the mucociliary elevator (denoted by small red arrows) and alterations in the composition of ASL.

1.6.1.2 Soluble recognition receptors

Host-cell recognition of *P. aeruginosa* is mediated by soluble receptors and cell-surface receptors. The soluble receptor PTX3, is important in defence against *P. aeruginosa* and PTX3-deficient murine model of *P. aeruginosa* infection showed increased rates of mortality than wild-type mice (Garlanda *et al.*, 2002). The surfactant protein SP-A appears to play an important role in defence against *P. aeruginosa* by binding flagellin to enhance phagocytosis by macrophages (Ketko *et al.*, 2013). SP-A induces IL-1β production via activation of the inflammasome and *in vivo*, SP-A-deficient mice infected with *P. aeruginosa* produced less IL-1β than wild-type mice (Ketko *et al.*, 2013). However, motile *P. aeruginosa* strains that possess intact flagella appear to be resistant to SP-A-mediated permeabilization (Zhang *et al.*, 2007). Flagella-deficient mutants lack the same levels of LPS as wild-type *P. aeruginosa*, making the bacterial cell wall more susceptible to membrane permeabilization (Zhang *et al.*, 2007). Furthermore, flagella-deficient mutants produce less exoprotease than wild-type *P. aeruginosa* due to defects in quorum sensing genes, and are thus less able to degrade SP-A (Kuang *et al.*, 2011a). These studies present an important role for flagella beyond motility and demonstrate strategies employed by *P. aeruginosa* to evade the effects of SP-A.

1.6.1.3 Host cellular receptors to detect *P. aeruginosa*

Cell-surface receptor-mediated recognition of *P. aeruginosa* occurs by TLRs and Nod-like receptors (NLRs), which are expressed on airway epithelial cells and phagocytes (Lavoie *et al.*, 2011). TLR2 and TLR4 recognize lipopolysaccharides (LPS) on the outer membrane of the bacterial cell, TLR5 recognizes flagellin proteins located on the flagella of the bacterium and TLR9 recognizes unmethylated CpG motifs on bacterial DNA (Zhang *et al.*, 2005b; Raoust *et al.*, 2009; McIsaac *et al.*, 2012). Binding of bacterial ligands to host receptors activates NF-κB –mediated cytokine expression resulting in the production and release of TNF-α, IL-6, IL-8, granulocyte-colony stimulating factor (GCSF) from epithelial cells and phagocytes (Raoust *et al.*, 2009; Shanks *et al.*, 2010).

P. aeruginosa effectors (ExoS, ExoU, ExoT and ExoY) are introduced into the host cell by Type-3 secretion systems (T3SS) needle-like mechanisms that span the surface of the bacterial cell surface. The insertion of T3SS into host cells create pores, which together with T3SS rod proteins (PscI) and flagellin introduced into the cell by

T3SS activate the NLRC4 inflammasome (Sutterwala *et al.*, 2007; Miao *et al.*, 2010). Activation of the inflammasome induces the proteolytic cleavage of pro-caspase-1 to caspase-1, which converts pro-IL-1β and pro-IL-18 to the biological active forms, IL-1β and IL-18 (He *et al.*, 2016). Pilin, a component of Type IV pili which are used by *P. aeruginosa* for attachment to the host cell also activate IL-1β production when they are introduced into the cell via T3SS or when bacteria escape from vacuoles within the host cell (Arlehamn and Evans, 2011). *P. aeruginosa* escapes activation of NLRC4 via quorum sensing mechanisms. QS-mediated production of pyocyanin and the QS autoinducer 3-oxo-C12-HSL inhibit NLRC4 and NLRP3-meidated inflammasome activation. Furthermore, proteases, produced through QS signals, degrade inflammasome components ASC and caspase-1 in addition to inflammatory cytokines (Yang *et al.*, 2017).

1.6.1.4 Cellular response to *P. aeruginosa*

The term "double edged sword" is often used to neutrophil-mediated inflammation because their role in the innate immune response to pulmonary pathogens is indispensable yet they can cause immense tissue damage in some cases, such as CF (Parkos, 2016). The role of neutrophils in host defence and clearance of *P. aeruginosa* infection is crucial (Koh *et al.*, 2009; Williams *et al.*, 2010; Lavoie *et al.*, 2011). As with *A. fumigatus* killing, neutrophils employ both oxidative (ROS-mediated) and non-oxidative (degranulation) mechanisms to kill *P. aeruginosa*.

The products of neutrophil degranulation are important for bacterial killing, particularly neutrophil elastase (NE) and NE-deficient murine models of acute *P. aeruginosa* infection succumbed to infection by *P. aeruginosa* while wild-type counterparts did not. The role of NE in killing *P. aeruginosa* appears to be dependent on the degradation of bacterial outer membrane protein, OprF (Hirche *et al.*, 2008).

Upon degranulation, neutrophils also release cathelicidin (hCAP-18), or LL-37 in mice, an antimicrobial which has chemotactic activity for neutrophils, monocytes and T cells (Yang *et al.*, 2000). In an *in vivo* model of acute *P. aeruginosa* infection, LL-37 was upregulated in response to bacterial infection and was shown to promote neutrophil-mediated *P. aeruginosa* clearance. The efficacy of LL-37 in neutrophil-mediated bacterial

clearance was demonstrated in *P. aeruginosa*-infected LL-37-deficient mice who when treated with exogenous LL-37 were able to clear the infection (Beaumont *et al.*, 2014).

Neutrophil phagocytosis and the release of NETs are stimulated upon recognition of motile *P. aeruginosa* flagella, resulting in the killing of motile forms of the bacteria (Lovewell *et al.*, 2014; Floyd *et al.*, 2016). The proteolytic enzymes associated with NETs degrade *P. aeruginosa* flagellin and promote downregulation of its expression (López-Boado *et al.*, 2004; Sonawane *et al.*, 2006). This has prompted the suggestion that NETs may promote the downregulation of flagellin and induce the switch from motile to nonmotile *P. aeruginosa*, a process associated with the evolution of *P. aeruginosa* in the CF lung (Mahenthiralingam *et al.*, 1994; Floyd *et al.*, 2016).

The role of macrophages in *P. aeruginosa* clearance appears useful, though dispensable for *P. aeruginosa* clearance (Cheung *et al.*, 2000). The ability to clear *P. aeruginosa* from the airways of macrophage-deficient mice and macrophage-sufficient mice was similar and in both models of acute infection, neutrophils were required to clear bacteria (Cheung *et al.*, 2000). Other studies have shown that the absence of macrophages increased the bacterial clearance time in murine airways and that the level of neutrophilia was reduced in mice where the macrophage population was higher than macrophage-deficient mice (Manicone *et al.*, 2009). Thus, the role of macrophages in clearing *P. aeruginosa* infection, albeit less clear than that of neutrophils, appears to be important in controlling neutrophil activity in response to *P. aeruginosa*.

The T-cell mediated response against *P. aeruginosa* is less well studied than the innate immune response. Nonetheless, the role of these cells in terms of the cytokines they produce is important to the clinical outcome of *P. aeruginosa* infection (Wojnarowski *et al.*, 1999; Moser *et al.*, 2002). It is well established that anti-flammatory cytokine producing Th2 cells are the main T lymphocytes associated with chronic *P. aeruginosa* infections (Hartl *et al.*, 2006). However, Th1-mediated responses are associated with better lung function (Moser *et al.*, 2002).

1.6.2 *P. aeruginosa* virulence factors

The genotypic and phenotypic characteristics of *P. aeruginosa* differ in acute and chronic infections with virulence factors required to establish infection being silenced during chronic infection (Smith *et al.*, 2006).

1.6.2.1 Flagella and Type IV Pili

Flagella are required for motility and binding to heparin sulphates on epithelial cells (Bucior *et al.*, 2012). However, due to its immunogenic characteristic, *fliC*, the gene encoding flagellin protein, is repressed during the establishment of biofilm during chronic infection such as CF (Wolfgang *et al.*, 2004; Guttenplan and Kearns, 2013).

Type IV pili enable a flagella-independent mode of motility through twitching and allow *P. aeruginosa* to adhere to pulmonary epithelial cells via N-glycan residues which are subject to sialylation (Bucior *et al.*, 2012; Burrows, 2012; Martins *et al.*, 2019). Cells with defective CFTR have abnormal sialylation resulting in increased binding sites for *P. aeruginosa*, and thus increase the propensity of *P. aeruginosa* to establish connection with host cells (Saiman and Prince, 1993; Bryan et al., 1998). Binding of pili to host cells upregulates the level of cAMP in bacterial cells, which in turn activates the virulence factor regulator (Vfr) and the expression of multiple virulence factors including T3SS (Wolfgang *et al.*, 2003).

1.6.2.2 Type III secretion systems

The T3SS induces host-cell damage by injecting bacterial effector proteins into the cell. To date, four effector proteins have been characterized (ExoS, ExoU, ExoT and ExoY) although it is possible that more exist (Burstein *et al.*, 2015). These proteins are highly toxic and facilitate dissemination of *P. aeruginosa* during acute infection. In murine models of *P. aeruginosa* pneumonia, the translocation of ExoS occurred predominantly in neutrophils although ExoS secretion into Type I pneumocytes was observed and caused distruption between the pulmonary-vascular barrier, allowing bacteria to disseminate (Rangel *et al.*, 2015). ExoS and ExoT interfere with neutrophil activity through the inhibition of ROS production and inhibit macrophage and epithelial cell phagocytosis by interfering with the actin cytoskeleton (Garrity-Ryan *et al.*, 2000;

Vareechon *et al.*, 2017). Unlike ExoS, which is associated with gradual cell death, ExoU, the most cytotoxic of the effectors induces rapid host-cell death, by cleaving phospholipids and resulting in cell lysis (Finck-Barbançon *et al.*, 1997; Hauser, 2009). ExoU is expressed during the early stages of acute infection and delay in expression is associated with an inability to establish infection due to increased bacterial clearance by the host (Howell *et al.*, 2013).

Although T3SS from CF *P. aeruginosa* isolates have been shown *ex vivo*, to mediate killing of neutrophils, the T3SS-positive phenotype and its secretion profile changes as *P. aeruginosa* established chronic infection in the CF lung, eventually becoming a T3SS-negative phenotype (Dacheux *et al.*, 1999; Jain *et al.*, 2004). T3SS proteins upregulate an antibody-mediated response against these proteins and translocation of bacterial antigens into the host cell stimulates a proinflammatory immune response, which threatens bacterial survival in the lung (Jain *et al.*, 2004). Thus, selection for the T3SS-negative form is likely to benefit *P. aeruginosa* persistence in the CF airways.

1.6.2.3 *P. aeruginosa* Biofilms and Quorum sensing

Repression of T3SS coincides with increased exopolysaccharide production and the emergence of biofilms, which are a classic feature of chronic infection. Biofilms confer a layer of protection against phagocytes and antibiotics. Although neutrophils migrate to biofilms, they become immobilized and surrounded by bacteria that escape from biofilms. Neutrophil degranulation is compromised and oxygen consumption by both neutrophils and the biofilm is increased (Jesaitis *et al.*, 2003)

Biofilm formation is dependent on quorum sensing (QS) in *P. aeruginosa* (Parsek and Greenberg, 2005). QS is the mechanism by which bacteria communicate in cell density-dependent manner and is necessary for the biosynthesis of secondary metabolites such as pyocyanin and rhamnolipids, which induce neutrophil apoptosis and necrosis respectively (Jensen *et al.*, 2007; Managò *et al.*, 2015). Biofilms are unable to form in the absence of iron and under iron-limiting conditions, QS regulates iron acquisition systems by inducing the production of siderophores such as pyoverdin (Stintzi *et al.*, 1998; Singh *et al.*, 2002).

1.6.3 *P. aeruginosa* acute airway pathogenesis

P. aeruginosa is the most common Gram-negative bacteria associated with nosocomial respiratory infections (Curran *et al.*, 2017). Pneumonia is an acute respiratory condition caused by *P. aeruginosa* and is described according to the source of infection, i.e. that acquired in a healthcare setting; Hospital- acquired pneumonia (HAP), Ventilator-acquired pneumonia (VAP) and health care-associated pneumonia (HCAP) and that acquired elsewhere; community-acquired pneumonia (CAP). *P. aeruginosa* strains that are associated with HAP are typically more lethal than those associated with CAP (Williams *et al.*, 2010)

The main contributors to the prevalence of *P. aeruginosa* in hospitals is the close proximity of a large cohort of immunocompromised individuals and the high incidence of multi-drug resistant (MDR) *P. aeruginosa* strains carried by patients (Otter *et al.*, 2014). The most common nosocomial infection occurring in intensive care is VAP, with a global incidence estimated to by 15.6 % (Ramírez-Estrada *et al.*, 2016). The prevalence of MDR strains of *P. aeruginosa* associated the high mortality rates observed in this cohort of patients (Ramírez-Estrada *et al.*, 2016).

1.6.4 Pathogenesis of *P. aeruginosa* in chronic airway conditions

Chronic infection arises where acute infection has not resolved (Gellatly and Hancock, 2013). If left unchallenged by the immune response or effective antibiotics, *P. aeruginosa* form biofilm in the airways. Owing to the difficulties associated with biofilm clearance by a defective host immune system and ineffective antibiotic therapy caused by resistance strains, bacterial infection becomes chronic (Gellatly and Hancock, 2013). Individuals that live with chronic pulmonary disorders such as COPD and chronic bronchiectasis are vulnerable to *P. aeruginosa* infection and although persistent infection is frequent, acute exacerbations also exist (Murphy *et al.*, 2008).

On the contrary, CF patients are plagued by chronic *P. aeruginosa* infection throughout adulthood. The adaptation of *P. aeruginosa* in the CF lung is characterized by a change in morphology from the nonmucoid form to the alginate-producing mucoid form during the process of colonization (Govan and Deretic, 1996).

1.6.5 Adaptation and colonization of *P. aeruginosa* in the CF lung

Several mechanisms owing to defects in CFTR, confer susceptibility to *P. aeruginosa* infection in the CF lung. These include physiologically abnormal ASL, impaired mucociliary clearance and enhanced sialylated receptors to which bacteria bind (Govan and Deretic, 1996). *P. aeruginosa* exploit these defects in host immunity by diversifying genetically and phenotypically into distinct strains that facilitate the persistence of this pathogen in the CF airways (Govan and Deretic, 1996; Winstanley *et al.*, 2016).

The switch from non-mucoid to the over-producing alginate mucoid strain is probably the most pronounced phenotypic change that *P. aeruginosa* adopts as it establishes chronic infection (Marvi*g et al*., 2014). Alginate plays an important role in the maturation and structural stability of *P. aeruginosa* biofilm and increases bacterial evasion of host immune cells and antibiotics (Mauch *et al.*, 2018). Alginate is a major antigenic determinant and induces intense antibody production, specifically IgG and IgA (Pedersen *et al.*, 1990). The role of antibodies in the CF airways is poorly understood, however, reports have suggested defects in the antibody-mediated immune response, such as low avidity of antibodies to *P. aeruginosa* antigens, result opsonic deficiency in the CF immune system, thereby reduced antibody-mediated phagocytosis by macrophages (Moss *et al.*, 1986; Polanec *et al.*, 1997; Mauch *et al.*, 2018). Several loss-of-function mutations that occur during adaptation in the CF lung are characteristic of the establishment of chronic infection, including loss of motility, repression of T3SS and downregulation of QS regulatory genes such as *lasR* (Wolfgang *et al.*, 2004; Jain *et al.*, 2004; Hoffman *et al.*, 2009).

1.6.6 Microbial interactions involving *P. aeruginosa*

In the CF airways, microbial diversity decreases with patient age and this loss of diversity correlates with the onset of chronic *P. aeruginosa* infection and deterioration of lung function (Rogers *et al.*, 2013; Zemanick *et al.*, 2017). The interactions that occur between *P. aeruginosa* and other pulmonary pathogens have a profound impact on bacterial survival, persistence and antibiotic resistance.

S. aureus precedes *P. aeruginosa* as the primary colonizer of the CF airways in the first decade of life (Coutinho *et al.*, 2008). Thus, the interactions that occur between these pathogens forms the basis for which *P. aeruginosa* becomes the successor. Co-colonization is associated with poor clinical outcome (Limoli *et al.*, 2016). *In vitro* and *in vivo* studies using early and late isolates of *P. aeruginosa* from a number of CF patients, have demonstrated that early isolates have a greater capacity to outcompete *S. aureus* than late isolates (Baldan *et al.*, 2014).

The outcome of co-culture studies have shown that *P. aeruginosa* outcompetes *S. aureus* through the upregulation of genes that enable the former to benefit from fermentation products, namely lactate, which *S. aureus* produces when it is forced into fermentation by *P. aeruginosa* (Filkins *et al.*, 2015; Orazi and O'Toole, 2017; Tognon *et al.*, 2019). Oxygen levels decrease and nitrogen levels increase during the early stages of co-culture between these pathogens (Tognon *et al.*, 2019). While this in itself has implications for the CF airways in terms of oxygen depletion, it also benefits the growth of *P. aeruginosa* which has a remarkable ability to switch from aerobic to anaerobic respiration (Van Alst *et al.*, 2009; Hogardt and Heesemann, 2010; Tognon *et al.*, 2019).

Clinical isolates of *P. aeruginosa* have been shown to stimulate *S. aureus* biofilm formation, a process that appears to be regulated, in part, by specific *P. aeruginosa* QS molecules (Fugère *et al.*, 2014). Biofilms play an integral role in conferring resistance to antibiotics in these pathogens. Exposure of *S. aureus* biofilms to *P. aeruginosa* supernatants can decrease susceptibility of *S. aureus* to vancomycin and oxacillin. This "protection" mechanism is dependent on the *P. aeruginosa* QS molecule 2-n-heptyl-4-hydroxyquinoline N-oxide (HQNO), siderophores, pyoverdine and pyochelin and anoxia, all of which induce a decrease the growth of *S. aureus*, which coincides with reduced susceptibility to cell-wall and protein synthesis inhibitors (Orazi and O'Toole, 2017). Conversely, the exoproducts of *S. aureus* have been shown to influence *P. aeruginosa* biofilm formation, making it more resistant to tobramycin, a commonly prescribed antibiotic for CF patients (Beaudoin *et al.*, 2017).

The *Streptococcus milleri* group (SGM) (consisting of *S. anginosus*, *S. constellatus*, and *S. intermedius*) is a clinically relevant CF pathogen associated with pulmonary exacerbations (Parkins *et al.*, 2008). *P. aeruginosa*, particular the mucoid form, has been shown *in vitro*, to promote the growth of SGM (Scott *et al.*, 2019).

However, siderophore overproduction caused by defects in the QS system biosynthetic pathway attenuated SGM growth. The downregulation in QS is associated with the switch to the mucoid form of *P. aeruginosa* (Price *et al.*, 2019). This suggests that during the earlier stages of infection, *P. aeruginosa* siderophore-production via QS inhibits growth of SGM by outcompeting these bacteria for iron resources. However as chronic infection is established, mucoid forms emerge and QS is downregulated, allowing SGM to co-exist with *P. aeruginosa*. Similarly the ability of *S. aureus* to co-exist with mucoid *P. aeruginosa* has been attributed to the downregulation of siderophores and other QS mechanisms otherwise associated with anti-Staphylococcal properties (Limoli *et al.*, 2017; Price *et al.*, 2019). These findings show that synergistic or antagonistic interactions between *P. aeruginosa* and other microbes in the CF environment are *P. aeruginosa*-strain-dependent and can change, as disease progression emergence of several *P. aeruginosa* strains coincide (Scott *et al.*, 2019).

1.7 Interactions between *A. fumigatus* and *P. aeruginosa*

The immunocompromised airways are susceptible to infection by a range of fungal pathogens and several of these, including *Candida* spp., *Cryptococcus* spp. and *Scedosporium aurantiacum* have been studied in the context of co-infection with *P. aeruginosa* (Bandara *et al.*, 2010; Rella *et al.*, 2012; Kaur *et al.*, 2015). In all cases, *P. aeruginosa* inhibits fungal growth and/or biofilm formation. Longitudinal studies have shown that colonization with *A. fumigatus* is associated with an increased risk of *P. aeruginosa* colonization in CF (Paugam *et al.*, 2010; Hector *et al.*, 2016). The prevalence of co-colonization with *P. aeruginosa* and *A. fumigatus* in the CF airways is estimated to be between 3.1 and 15.8 % although this occurrence may be higher (Paugam *et al.*, 2010; Reece *et al.*, 2017a; Zhao *et al.*, 2018a). Disease prognosis is poor when both pathogens are present (Reece *et al.*, 2017a; Zhao *et al.*, 2018a). The number of studies that have begun to investigate *A. fumigatus*-*P. aeruginosa* interactions in the past decade is a reflection on the clinical importance and the negative impact on the CF airways of co-colonization with these pathogens. In general, the results of these studies show that *P. aeruginosa* outcompetes *A. fumigatus*, a finding supported by the predominance of the bacteria in the CF lung.

1.7.1 Antagonistic interactions between *A. fumigatus* and *P. aeruginosa*

P. aeruginosa secretes a range of compounds that inhibit *A. fumigatus* development and biofilm formation (Mowat *et al.*, 2010; Briard *et al.*, 2015; Sass *et al.*, 2018). *P. aeruginosa* phenazines (pyocyanin, phenazine-1-carboxamide, 1-HP and phenazine-1-carboxylic acid) are QS-regulated redox-active molecules that are important in bacterial respiration and energy production in oxygen-limiting environments (Price-Whelan *et al.*, 2006). Phenazines are ROS producing compounds and in the host, changes in the redox balance caused by ROS result in host-cell damage and death (Price-Whelan *et al.*, 2006). The production of ROS by phenazines also has implications for *A. fumigatus* survival (Briard *et al.*, 2015). Phenazines can enter into swollen, but not resting conidia and target the mitochondria, inducing ROS production (Briard *et al.*, 2015). The accumulation of ROS may interfere with *A. fumigatus* growth and biofilms by inducing fungal apoptosis (Briard *et al.*, 2015; Shirazi *et al.*, 2016). Exposure of *A. fumigatus* biofilms to culture supernatants from non-mucoid and mucoid *P. aeruginosa* CuF isolates resulted in a greater increase of ROS in fungal biofilms exposed to the non-mucoid strain (Shirazi *et al.*, 2016). In the CF airways, mucoid strains are associated with the downregulation of QS-regulated molecules including phenazines (Price *et al.*, 2019). This suggests that these antagonistic interactions may occur prior to the switch from non-mucoid to mucoid and the establishment of chronic infection in the CF lung.

The definitive role of phenzaines as a fungicidal agent is uncertain however as phenazine-mutants have also been shown to inhibit fungal growth, although the authors of this study acknowledge the possible anti-fungal role of an unknown molecule upregulated as a result of phenazine depletion (Sass *et al.*, 2018). The *P. aeruginosa* siderophores pyoverdin and 1-hydroxyphenazine (1-HP), chelate iron in the environment, depriving *A. fumigatus* from a necessary nutrient, thereby supressing fungal growth and biofilm formation (Briard et al., 2015; Sass et al., 2018). Pyoverdin is thought to be the key component involved in outcompeting *A. fumigatus* and mutants deficient in pyoverdin biosynthesis were unable to inhibit fungal growth (Sass *et al.*, 2018).

Another class of *P. aeruginosa* QS-regulated molecules are dirhamnolipids. These molecules alter *A. fumigatus* cell-wall phenotype by interfering with the extracellular matrix enabling enhanced bacterial binding to the fungus, increasing melanin production

and inhibiting β 1,3-glucan synthase, causing the hyphal cell-wall to thicken, thereby suppressing fungal growth development (Briard *et al.*, 2017). In co-cultures, *A. fumigatus* stimulates *P. aeruginosa* elastase production, which inhibits the growth of fungus and is also cytotoxic to A549 cells (Smith *et al.*, 2015). These findings are of clinical relevance because although the arsenal of secondary metabolites secreted by *P. aeruginosa* in the presence of *A. fumigatus* may have anti-fungal properties, these bacterial compounds and the consequences arising from their interactions with *A. fumigatus*, have negative implications for the host. For example, *in vivo*, melanin enables fungal evasion of phagocytic activity and scavenges ROS (Eisenman and Casadevall, 2012). *P. aeruginosa* elastases can degrade SP-A and SP-D and disrupt tight junctions between epithelial cells (Mariencheck *et al.*, 2003; Kuang *et al.*, 2011b; Nomura *et al.*, 2014). Phenazines contribute to cytokine-mediated damage to host cells by induce proinflammatory cytokines (Denning *et al.*, 2003; Rada and Leto, 2013)

Despite the demonstrable ability of *P. aeruginosa* to subdue *A. fumigatus* growth (Mowat *et al.*, 2010; Manavathu *et al.*, 2014; Briard *et al.*, 2015; Briard *et al.*, 2017; Sass *et al.*, 2018), several studies reported the capacity of *A. fumigatus* to compete with *P. aeruginosa* (Reece *et al.*, 2018; Sass *et al.*, 2019). This supports the notion that *A. fumigatus* can persist in the CF airways, despite not being the dominant pathogen. *P. aeruginosa* inhibits the growth of *A. fumigatus* conidia but not of hyphae (Manavathu *et al.*, 2014). This may be attributed to the ability of hyphae, but not conidia to produce gliotoxin which has anti-*Pseudomonas* activity (Reece *et al.*, 2018). *A. fumigatus* produce hydroxamate-containing siderophores (ferricrocin, hydroxyferricrocin, fusarinine C, triacetylfusarinine C) in response to iron limitation. The production of these siderophores can mitigate the effect of *P. aeruginosa* pyoverdin and, in part, protect *A. fumigatus* biofilm, as shown in *A. fumigatus* siderophore-deficient mutants, which are more susceptible to the effects of pyoverdin than the wild-type (Sass *et al.*, 2019).

1.7.2 Synergistic interactions between *A. fumigatus* and *P. aeruginosa*

While the relationship between *P. aeruginosa – A. fumigatus* is antagonistic for the most part, some *P. aeruginosa* volatile organic compounds (VOC) have been shown to stimulate the growth of *A. fumigatus* without direct contact between the pathogens (Briard *et al.*, 2016).

Ultimately, whether they are synergistic or antagonistic, the interactions that occur between *A. fumigatus* and *P. aeruginosa* lead to severe damage to the host and, for the CF patient this contributes to a poor prognosis.

1.8 Antimicrobial resistance in *P. aeruginosa*

A hallmark characteristic of *P. aeruginosa* is its tolerance to a vast range of antibiotics. The emergence of multidrug-resistant (MDR) *P. aeruginosa* strains is a significant concern in hospital-acquired infections and is a major cause of morbidity and mortality among the CF community. In general, bacteria adopt one or more of four mechanisms to resist antibiotics. These include i) restricted outer-membrane permeability, ii) biosynthesis of antibiotic inactivating enzymes, iii) modifications of antibiotic-directed targets and iv) efflux pumps (Bassetti *et al.*, 2018a). While some resistance mechanisms are intrinsic, i.e. chromosomally encoded, others are acquired via horizontal transfer or by gene mutations, which can cause changes to antibiotic targets, over expression of efflux pumps and antibiotic inactivating enzymes or reduced antibiotic uptake mechanisms (Pang *et al.*, 2019).

Different *P. aeruginosa* isolates can tolerate various antibiotics by combining numerous resistance mechanisms, including: biosynthesis of β-lactam and aminoglycoside inactivating enzymes (Labby and Garneau-Tsodikova, 2013; Berrazeg *et al.*, 2015), reduced outer-membrane permeability by downregulation or loss of OprD (Li *et al.*, 2012a), fluoroquinolone resistance caused by mutations in gyrases and topoisomerases (Cambau *et al.*, 1995; Akasaka *et al.*, 2001), and over expression of efflux pumps such as resistance-nodular-cell division (RND) family type, which actively pump antibiotics out the of cell (Koo, 2015).

The emergence of MDR pathogenic bacteria poses a major global threat to society and the necessity to develop novel anti-microbial therapeutics is urgent (Aslam *et al.*, 2018). Vaccines, nanoparticles, phage therapy, iron chelators, antimicrobial peptides and lectin inhibitors are currently being explored and show promise (Pang *et al.*, 2019). Novel next generation semi-synthetic derivatives of antibiotics such as plazomicin, an aminoglycoside derivative, have shown some activity against *P. aeruginosa* while carbapenem derivative doripenem can be used for the clearance of *P. aeruginosa* in CF patients (Castanheira *et al.*, 2018; Eljaaly *et al.*, 2019). Combination therapies, which

involve the use of two antibiotics, (e.g. cephalosporin with β-lactamase inhibitors such as Ceftolozane-tazobactam) are now commonly used in the treatment of *P. aeruginosa* infections (Bassetti *et al.*, 2018a).

1.9 Novel antimicrobial drug discovery; approaches and challenges

The "Golden Age" of antibiotic discovery began in 1928 with the identification of penicillin by Alexander Fleming, and lasted until 1987, when acid lipopeptides such as daptomycin emerged (Debono *et al.*, 1987; Silver, 2011; Gould, 2016). During this period, most registered classes of antibiotics were discovered (e.g. β-lactams, aminoglycosides, tetracyclines, macrolides, and chloramphenicol). These antibiotics originated from soil bacteria and moulds, although several novel classes of chemically synthesized antibiotics also emerged at this time (e.g. quinolones and sulphonamide). As screening for natural bioactive products became less fruitful and repeat discoveries were becoming more common, the pharmaceutical companies backing the search for novel antibiotics, withdrew support for such research (Silver, 2011).

With the advent of bacterial genomics in the early 1990s, came the potential for target-based antibacterial drug discovery and a renewed interest by pharmaceuticals to develop novel antibiotics. Intense efforts to discover new antimicrobial compounds were performed using high-throughput screens (HTSs) hundreds of novel bacterial targets were identified, however no successful drug candidates materialized from these screens and the mission to discover novel antibacterial compounds was abandoned by the larger companies (Baker *et al.*, 2018).

Several significant challenges exist which delay the development of novel antibacterial candidates, most notably the balance between ensuring effective antibacterial activity and minimizing toxicity for the patient. Thus, pharmaceutical companies have turned their attention to modifying established classes of antibiotics, and while these next generation antibiotics meet the needs of today's patients, their limitations often mimic that of the preceding generation and resistance to these antibiotics is inevitable (Baker *et al.*, 2018).

It is estimated that two-thirds of the antibiotics prescribed today are derived from natural products and the majority of natural antibiotics have been discovered by screening

microbial isolates obtained from natural habitats such as soil (Newman and Cragg, 2012; Wohlleben *et al.*, 2016). Bacteria and fungi provide an abundance of bioactive metabolites, which can be exploited for the treatment of infectious diseases. These bioactive compounds are bacterial, fungal and plant-derived secondary metabolites such as polyketides (e.g. erythromycin and tetracycline), non-ribosomal peptides (e.g. penicillin G and vancomycin) or polypeptides, terpenes or sterols and are widely used in the modern clinic (Herrmann *et al.*, 2016).

Methods for antibiotic discovery are diverse and several approaches can be employed. These include phenotypic assay systems, targeted drug discovery, chemical screening, genome mining and investigating unexplored strains (Lee *et al.*, 2012; Wohlleben *et al.*, 2016). Although each method is not without its drawbacks, combining bioinformatics, molecular biology, proteomics, analytical and synthetic chemistry will lead to more success in the search for novel antibacterial therapeutics (Coates and Hu, 2007; Lee *et al.*, 2012; Wohlleben *et al.*, 2016).

1.10 Choosing proteomics to investigate inter-species interactions

The host-pathogen and poly-microbial interactions that drive progression of diseases such as CF and ABPA are dynamic and extremely complex. To gain a better insight into the factors that contribute to disease progression, an in-depth understanding of the host and microbe(s) cellular and molecular response is required. Where more than one organism is involved, delineating these interactions poses many challenges. Genomic technologies such as next generation sequencing and gene editing have led the way in addressing some of these challenges by enabling the detection of mutations that may be responsible for microbial virulence, antibiotic resistance or host susceptibilities to certain pathogens (Bertelli and Greub, 2013; Starr *et al.*, 2018).

Without doubt, whole-genome sequencing has provided the foundation for greater insights into biological systems. However, the study of genes alone is insufficient to elucidate the dynamic and responsive biological processes that contribute to disease onset, progression and outcome. Such physiological processes are largely regulated by proteins, their abundance, function and interactions (Graves and Haystead, 2002). It is well established that the level of gene expression and mRNA transcript do not necessarily correlate with protein abundance (Graves and Haystead, 2002). Post-transcriptional and

post-translational modifications ultimately determine the fate of proteins, their function and abundance, which in turn dictates the phenotype of an organism (Graves and Haystead, 2002; Lippolis and De Angelis, 2016).

The proteome, a term coined in 1994 by Marc Wilkins, refers to the "entire protein complement expressed by a genome, or by a cell or tissue type" (Wilkins *et al.*, 1996). Proteomics is the global analysis of the proteome or the study of proteins within the proteome, and incorporates several technological approaches for the separation and identification and quantification of proteins. In conjunction with bioinformatics, proteomics aims to close the knowledge gap between genotype and phenotype so that a greater understanding of biological processes, systems and interactions may be gained (Wilkins *et al.*, 1996; Abbott, 1999; Graves and Haystead, 2002).

1.10.1 Label-free quantitative proteomics

Traditionally, protein identification and quantitation was performed using gel-based techniques, such as 2-dimensional polyacrylamide gel electrophoresis. This involves the separation of complex protein mixtures according to their net molecular charge on immobilized pH gradients (first dimension), and according to their molecular mass by gel electrophoresis (second dimension). Protein alignment software is used to detect changes in protein abundance and protein "spots" of interest are cut out of gels prior to in-gel enzymatic digestion and identification by mass spectrometry (MS). The main limitations with this approach is obtaining reproducible gels and the amount of proteins that can be detected on a single gel (Abbott, 1999). Nonetheless, until more advanced technological solutions were developed, this was the primary method used to separate and quantitatively compare complex protein mixtures.

In the past decade, advancements in technology have allowed for the development of more sensitive methods for proteomic analysis. These MS-based methods usually involve one of two approaches referred to as "top down and "bottom up" proteomics (Lin *et al.*, 2003; Graham *et al.*, 2007). The former involves the analysis of intact proteins by MS. This approach is particularly useful for the study of proteoforms (i.e. different forms of a protein arising from genetic variation, alternative splicing of RNA transcripts and PTMs) (Smith *et al.*, 2013c; Toby *et al.*, 2016).

Bottom-up proteomics is the most common approach for studying complex mixtures of proteins and involves the in-solution digestion of proteins to peptides prior to analysis by MS (Breuker *et al.*, 2008). Shotgun proteomics describes a frequently used "bottom-up" approach for proteomic analysis. This method involves the enzymatic digestion of a complex protein mixture into peptides, which are then fractionated on a reverse phase C18 column prior to analysis by MS (LC–MS) with tandem mass spectrometry (LC–MS/MS) (Gundry *et al.*, 2010). Protein quantification can be performed with a label (i.e. by the addition of metabolic or isobaric chemical labels prior to MS analysis) or without a label (i.e. label-free quantitative proteomics/LFQ) (Li *et al.*, 2012b). LFQ proteomics offers a means of characterizing changes to protein composition in a dynamic environment and by not focusing on specific proteins, it can offer a bias-free analysis of complex proteins mixtures (Graham *et al.*, 2007; Meissner and Mann, 2014). Considering this, LFQ proteomics is a powerful approach for addressing host-pathogen and poly-microbial interactions.

1.10.2 The application of LFQ proteomics for investigating inter-species interactions

In the context of microbial pathogenesis, quantitative proteomics is an important tool for investigating mechanisms of virulence and antimicrobial resistance in pathogens, and offers novel insights into mutualistic, synergistic or antagonistic interactions that occur between different species and the host (Pérez-Llarena and Bou, 2016). The ability to search databases with multiple reference proteomes allows for the simultaneous analysis of several species, such as those which occur in biofilms (Herschend *et al.*, 2017).

The global analysis of the proteome using LFQ proteomics is particularly important in identifying the changes to bacterial proteomes which enable pathogens to recover from antibiotic challenge and acquire resistance (Giddey *et al.*, 2017; Hashemi *et al.*, 2019). Furthermore, LFQ proteomics has provided insights into the mechanisms by which pathogens adapt to the host environment (Surmann *et al.*, 2014; Surmann *et al.*, 2015; Surmann *et al.*, 2016) and the response of the host to pathogen invasion (Surmann *et al.*, 2016; Qu *et al.*, 2017). Understanding the pathways and processes by which pathogens initiate disease, resist antibiotics, and evade the host immune response is important for the identification of potential therapeutic targets.

1.11 Overview of thesis objectives

The emergence of antimicrobial drug resistance necessitates new approaches to challenge fungal and bacterial pathogens and novel therapeutic strategies are required to compensate for the diminishing availability of effective antibiotics. To address these concerns, a better understanding of the mechanisms by which pathogens interact with each other and with the host is needed, so that pathogen vulnerabilities may be identified and targeted accordingly.

The study of polymicrobial interactions presents many challenges although recent advances in bioinformatic and proteomic technologies such as detailed reference genomes, high-resolution mass spectrometry and comprehensive computational tools for data analysis, have made it possible to overcome some of these obstacles.

To this end, the goal of this project was to address the knowledge gap that exists in the area of polymicrobial-host interactions. LFQ proteomics was used to elucidate the biological mechanisms that modulate the interactions between *A. fumigatus*, *P. aeruginosa* and A549 cells (model of the alveolar surface) by providing a global analysis of the changes in protein composition arising from interactions between these organisms. This approach was chosen because of its capacity to support a bias-free analysis of the interactions between different species based on changes to the proteome of the organism being interrogated.

The first objective of this project was to investigate the proteomic response of A549 cells to sequential-infection with *A. fumigatus* and *P. aeruginosa* and to compare this with the host response to infection by either pathogen. By exploring the pathways and processes that are upregulated or downregulated in response to *A. fumigatus* and *P. aeruginosa*, this project sought to gain novel insights into how host cells respond during the early stages of polymicrobial infection and to investigate how one pathogen may eventually predominate over the other in the presence of the host.

The second objective was to examine the relationship between *A. fumigatus* and *P. aeruginosa*, and to measure how synergistic and/or antagonistic interactions could alter the virulence and improve the pathogenicity of these microorganisms. Although *P. aeruginosa* predominates in the CF airways, *A. fumigatus* exists there intermittently throughout the lifetime of a CF patient. This project sought to investigate the phenotypic attributes that enable *P. aeruginosa* to have a competitive advantage over *A. fumigatus*,

and to understand the mechanisms adopted by *A. fumigatus* that allow the fungus to persist in the airways despite the presence of *P. aeruginosa*.

The final objective of this project was to investigate the effect of culture filtrates produced by *A. fumigatus* cultured in media of different compositions. During a classical screening test for fungal-derived antibacterial compounds, the inhibitory effect on *P. aeruginosa* by *A. fumigatus*-derived culture filtrates produced in a nutrient-rich medium was observed. To assess the mechanism by which this compound suppressed bacterial growth, the effect on the *P. aeruginosa* proteome when exposed to a sub-inhibitory dose of the culture filtrate was investigated by LFQ proteomics. Efforts to isolate purify and identify the active compound was performed by reversed-phase high-performance liquid chromatography (RP-HPLC), nuclear magnetic resonance (NMR) and high-resolution mass spectrometry (MS).

The findings obtained during this project provide a solid foundation for which future hypotheses can be formed and tested.

Chapter 2

Material and Methods

2.1 General Chemicals and Reagents

All chemicals were analytical or molecular grade unless otherwise stated, and were obtained from Sigma-Aldrich Co. Ltd. (Arklow, Ireland). Solvents (chloroform, acetonitrile, acetone and methanol) were purchased from Fisher Scientific (Dublin, Ireland). Buffers were prepared using distilled H_2O (dH_2O) or deionized H_2O (ddH_2O). dH_2O was purified with the Millipore Milli-Q apparatus to obtain milli-Q water (de-ionized water; ddH_2O) (18 MΩ).

2.1.1 Phosphate Buffered Saline (PBS)

One PBS tablet (Oxoid, Cambridge, UK) was added to 100 ml dH_2O and autoclaved at 121°C for 15 minutes. PBS was stored at room temperature.

2.1.1.2 PBS-Tween 80 (PBST)

Tween-80 (50 µl) was added to 100 ml sterile PBS and stored at room temperature.

2.1.2 Solutions for pH Adjustment

2.1.2.1 Hydrochloric Acid (HCl) (5 M)

Hydrochloric Acid (43.64 ml) was added slowly to ddH_2O (40 ml) in a glass duran. The final volume was adjusted to 100 ml with ddH_2O. The solution was stored at room temperature.

2.1.2.2 Sodium Hydroxide (NaOH) (5 M)

NaOH pellets (20 g) were added to ddH_2O (80 ml) and dissolved using a magnetic stirrer. The final volume was adjusted to 100 ml with ddH_2O. The solution was stored at room temperature.

2.2 Maintenance and preparation of *P. aeruginosa*

Table 2.1 Bacterial species and strains. The species name, strain and source of bacteria used in experiments.

Species	Strain	Source
Pseudomonas aeruginosa	PAO1	Medical Mycology Laboratory, MU
**Escherichia coli*	PEK499	Antimicrobial resistance and microbiome laboratory, MU
**Staphylococcus aureus*	ATCC-33591	Medical Mycology Laboratory, MU
**Klebsiella pneumoniae*	Clinical Strain	Medical Mycology Unit, MU

*****Bacteria used in Chapter 6 only

2.2.1 Bacterial culture media

Nutrient Agar (Scharlau, Barcelona, Spain) (28 g) was dissolved in 1 L dH_2O. The solution was autoclaved (121°C, 15 minutes), and allowed to cool to ~50 °C. Agar (25 ml) was poured into 90 mm petri dishes, aseptically. The plates were allowed to set and stored at 4 °C. Nutrient Broth (13 g) (Oxoid, Cambridge, UK) was dissolved in 1L dH_2O and autoclaved (121°C, 15 minutes). Liquid media were stored on the bench at room temperature.

2.2.2 Super Optimal Broth with catabolite repression (SOC medium); SOC agar (0.3%)

Tryptone (10 g), Yeast extract (2.5 g), Dextrose (1.8 g), agar (0.75 g), 5 ml $MgSO_4$ 1 M, 1.25 ml KCl 1 M was added to 300 ml dH_2O and dissolved. The solution was brought up to 500 ml with dH_2O and autoclaved (121°C, 15 minutes). The agar was poured into 90 mm petri dishes and stored at 4°C.

2.2.3 Synthetic Cystic Fibrosis Medium (SCFM)

SCFM was prepared according the the protocol in Palmer *et al.* (2007). All amino acids were maintained as 100-mM stocks in and stored at 4°C. Tyrosine, aspartate, and tryptophan were dissolved in 1.0 M, 0.5 M, and 0.2 M NaOH, respectively. All other amino acids were dissolved in ddH_2O. Amino acids (from the 100-mM stocks) were added to a buffered base (6.5 ml 0.2 M NaH_2PO4, 6.25 ml 0.2 M Na_2HPO_4, 0.35 ml 1 M KNO_3, 0.122 g NH_4Cl, 1.11 g KCl, 3.03 g NaCl, 10 mM MOPS, 779.6 ml ddH_2O) in the following volumes: L-aspartate, 8.27 ml; L-threonine, 10.72 ml; L-serine, 14.46 ml; L-glutamate·HCl, 15.49 ml; L-proline, 16.61 ml; L-glycine, 12.03 ml; Lalanine, 17.8 ml; L-cysteine·HCl, 1.6 ml; L-valine, 11.17 ml; L-methionine, 6.33 ml; L-isoleucine, 11.2 ml; L-leucine, 16.09 ml; L-tyrosine, 8.02 ml; L-phenylalanine, 5.3 ml; L-ornithine·HCl, 6.76 ml; L-lysine·HCl, 21.28 ml; L-histidine·HCl, 5.19 ml; L-tryptophan, 0.13 ml; and L-arginine·HCl, 3.06 ml. The pH of the medium was adjusted to 6.8 and filter sterilized through a 0.2 µm membrane filters (Filtropur S, Sarstedt, Germany). The following components were sterilized and added to 1L of the medium; 1.75 ml 1 M CaCl2, 0.61 ml 1 M MgCl2, and 1 ml 3.6 mM $FeSO_4$·7H2O. The medium was stored at 4°C.

2.2.4 Maintenance of *P. aeruginosa*

Pseudomonas aeruginosa (PAO1) was cultivated on Nutrient Agar plates (section 2.2.1) at 37°C and maintained at room temperature. A sterile loop was used to inoculate Nutrient Broth. Bacterial cultures were grown overnight in a shaker at 200 rpm at 37°C to the early stationary phase. Liquid cultures were maintained at room temperature and sub-cultured monthly. The concentration of the bacteria in suspension was measured by obtaining the optical density at 600 nm (OD_{600}), where OD1 represents approximately 3 x 10^8 CFU/ml.

2.2.4.1 Preparation of *P. aeruginosa* in cell culture medium

P. aeruginosa suspension (5 ml, OD 1) was centrifuged at 2000 x *g* for 15 minutes. The bacterial pellet was resuspended in sterile PBS. This step was repeated. Bacterial cells were resuspended in 5 ml cell culture medium (section 2.4.1).

2.2.5 Bacterial toxicity assays

The OD_{600} of bacterial suspensions were measured to 0.1. Bacterial suspension (100 µl) was added to the wells of 96-well plates. Medium (100 µl) was added into the respective wells. The 96-well plates were incubated at 37°C and the absorbance (600 nm) was measured in a microplate reader (Synergy HT Bio-Tek).

2.3 Maintenance and preparation of *A. fumigatus*

Table 2.2 *Aspergillus* species and strains. The species name, strain and source of *Aspergillus* used in experiments.

Species	Strain	Source
Aspergillus fumigatus	ATCC 26933	Medical Mycology Laboratory, MU
Aspergillus flavus	TJES19.1	Fungal genome and secondary metabolism Laboratory, MU
Aspergillus nidulans	AGB551	Fungal genome and secondary metabolism Laboratory, MU

2.3.1 *Aspergillus* culture media (Czapek-Dox)

Czapek-Dox Broth (Duchefa Biochemie B.V., Haarlem, Netherlands) (35 g) was dissolved in 1L dH_2O and autoclaved (121°C, 15 minutes).

2.3.2 *Aspergillus* culture media (Sabouraud)

Sabouraud Dextrose Agar (Oxoid, Cambridge, UK) (65 g) was dissolved in 1 L dH_2O. The solution was autoclaved (121°C, 15 minutes). Agar (25 ml) was poured into 90 mm petri dishes, aseptically. The plates were allowed to set and stored at 4°C. Sabouraud Liquid Medium (SAB) (Oxoid, Cambridge, UK) (30 g) was dissolved in 1 L dH_2O and autoclaved (121°C, 15 minutes). Liquid media was stored on the bench at room temperature.

2.3.3 Minimal Medium Broth

Glucose (2% wt/vol), yeast nitrogen base (without amino acids or ammonium sulfate) (Difco^{TM}) (0.5% wt/vol) and ammonium sulfate (0.5% wt/vol) was added to dH_2O and autoclaved (121°C, 15 minutes).

2.3.4 Culture and maintenance of *A. fumigatus*

A. fumigatus (ATCC 26933, obtained from the American Type Culture Collection) conidia were maintained on Sabouraud Dextrose Agar at room temperature. To sub-culture the stock, a sterile loop was used to streak conidia onto agar plates. The plates were incubated at 37 °C until the conidia had turned blue-green and were covering the entire surface of the agar. For liquid cultures, conidia were harvested from the plate by adding sterile PBST (5 ml), and using a Pasteur pipette to dislodge the conidia and transfer the suspension into a falcon tube. The conidial suspension was centrifuged at 2000 x *g* for 5 minutes in a Beckman GS-6 Centrifuge. The supernatant was discarded and the pellet was resuspended in sterile PBS (5 ml) and centrifuged again. This step was repeated. Conidia were counted using a haemocytometer to determine the conidial density (conidia/ml).

2.3.4.1 Preparation of *A. fumigatus* conidia in mammalian cell culture medium

Conidia were harvested as described in section 2.3.4. Conidia were washed twice with PBS and resuspended in mammalian cell culture medium Dulbecco's Modified Eagle Medium (DMEM) (95 % v/v) was supplemented with foetal calf serum (FCS) (Gibco) (5 % v/v), L-glutamine (2 % v/v) (Gibco).

2.3.5 Culture and maintenance of *A. flavus* and *A. nidulans*

2.3.5.1 Media preparation

Uracil powder (100mg) was added to SAB (100 ml) prior to sterilization by autoclave (121°C). Uridine solution (5 %) was prepared by dissolving 0.5 g uridine into 10 ml ddH_2O and filter sterilized through 0.2 µm membrane filters (Filtropur S, Sarstedt, Germany). When the media had cooled to room temperature 500 µl uridine solution was added to SAB. Agar plates were prepared as described using Sabouraud Dextrose Agar instead of SAB liquid medium (section 2.3.2).

2.3.6 Culture and maintenance of *A. flavus*

A. flavus spores were harvested as described in section 2.3.4 and added to each flask of SAB containing uracil and uridine (section 2.3.5.1) (5×10^5/ml). Cultures were incubated at 30°C, shaking at 200 *rpm.*

2.3.7 Culture and maintenance of *A. nidulans*

SAB was prepared as described in section 2.3.5.1. Pyroxidine (0.1 %) was prepared by dissolving 0.1 g proxidine in 10 ml ddH_2O. Prior to inoculating spores, pyroxidine solution (100 µl) was added to each flask. *A. nidulans* spores were harvested as described in (section 2.3.5.1) and added to each flask ($5 \times 10^{5/}$ml). Cultures were incubated at 37°C shaking at 200 *rpm.*

2.3.8 *A. fumigatus* culture filtrate and *P. aeruginosa* culture filtrates

A. fumigatus conidia (5×10^5 conidia/ml) were cultured in Czapek-Dox for 48 hours. *P. aeruginosa* (a loopful) was cultured in Czapek-Dox for 48 hours. Both cultures were incubated at 37 °C shaking at 200 *rpm*. The fungus and bacteria were removed from the culture using Miracloth and centrifugation, Culture filtrates were filter sterilized through 0.22 µm membrane filters.

2.3.8.1 *A. fumigatus* and *P. aeruginosa* co-culture culture filtrates

A. fumigatus conidia (5 x 10^5 conidia/ml) were cultured in Czapek-Dox for 24 hours. *P. aeruginosa* (a loopful) was cultured in Czapek-Dox for 24 hours. Both cultures were incubated at 37 °C shaking at 200 *rpm*. After 24 hours, the cultures were combined into a sterile 250 ml flask and incubated for a further 24 hours. The fungus and bacteria were removed from the culture using Miracloth and centrifugation, Culture filtrates were filter sterilized through 0.22 µm membrane filters.

2.3.8.2 Exposure of *A. fumigatus* to culture filtrates

A. fumigatus conidia (5 x 10^5 conidia/ml) were cultured for four hours in Czapek-Dox (25 ml) in 125 ml Erlenmeyer flasks. Culture filtrates produced in Czapek-Dox (section 2.3.8 and 2.3.9) (50 ml) were added to the flasks and incubated at 37°C shaking at 200 rpm for 24 hours prior to protein extraction.

2.3.8.3 Exposure of *P. aeruginosa* to culture filtrates

P. aeruginosa was cultured for 24 hours in Czapek-Dox (25 ml) in 125 ml Erlenmeyer flasks. Culture filtrates produced in Czapek-Dox (section 2.3.8 and 2.3.9) (50 ml) were added to the flasks and incubated at 37°C shaking at 200 rpm for 24 hours prior to protein extraction.

2.4 A549 Cell culture medium and maintenance

2.4.1 Cell culture medium

Dulbecco's Modified Eagle Medium (DMEM) (95 % v/v) was supplemented with foetal calf serum (FCS) (Gibco) (5 % v/v), L-glutamine (2 % v/v) (Gibco) and stored at 4 °C.

2.4.2 Cryporeservation buffer

DMEM (40 % v/v) was supplemented with FCS (40 % v/v) and dimethyl sulfoxide (DMSO) (10 % v/v). Cryopreservation buffer was prepared on the day of use, filter-sterilized through 0.2 µm membrane filters and stored on ice.

2.4.3 Maintenance and sub-culturing

The Type II alveolar epithelial cell line A549, ATCC CCL 185 (derived from a human lung carcinoma) was grown in 25 cm^2 tissue culture flasks (Sarstedt) containing 5 ml cell culture medium (section 2.4.1) and incubated at 37ºC in a humidified atmosphere containing 5% CO2. When the flasks were 80 - 90 % confluent, cells were subcultured by trypsinisation (approximately every 3 - 5 days); cell culture medium was removed from the flasks. Trypsin EDTA (Gibco) (1 ml) (diluted with sterile PBS to give a final concentration of 10 % v/v), was added to the flask and removed immediately. Trypsin/PBS solution (4 ml) was added to the flask. The flasks were incubated until the cells began to detach (3 – 5 minutes). The trypsin solution was neutralized with 4 ml cell culture medium. Cells were transferred into a sterile tube and harvested by centrifugation (200 x *g*). The medium was removed and the cell pellet was resuspended with fresh, pre-heated cell culture medium. Cells (1 ml) were seeded into fresh, sterile 25 cm^2 flasks to give an approximate confluency of 25 %. Fresh, pre-heated cell culture medium (4 ml) was added to each flask.

2.4.4 Cryopreservation of A549 cells in Liquid Nitrogen

Cells were cultured to approximately 80 % confluency. Cells were trypsinized and centrifuged (200 x *g*) (section 2.4.3). The cell pellet was resuspended in 1ml cell culture medium (section 2.4.1). 1 ml cryopreservation buffer (section 2.4.2) was added slowly, dropwise. The cell suspension was transferred into two cryo-vials (Thermo Scientific) and stored at -80ºC overnight before being placed into a liquid nitrogen tank for long-term storage.

2.4.5 Recovery of A549 cells from Liquid Nitrogen

A549 cells were recovered from liquid nitrogen and cryo-vials were held in hot water to speed up the thawing processes in order to maintain cell viability. The cell suspension (1 ml) was transferred into a 25 cm^2 flask containing 4 ml pre-heated cell culture medium (section 2.4.1). When cells had attached (6 – 24 hours), the medium was removed and replaced with fresh pre-heated medium.

2.4.6 Exposure of A549 cells to *A. fumigatus* and/or *P. aeruginosa* for 12 hours

Immediately prior to exposure with *A. fumigatus* or *P. aeruginosa*, the cell culture medium in which pre-treated A549 cells were contained, was exchanged with freshly made cell culture medium. *A. fumigatus* conidia and *P. aeruginosa* suspensions were prepared in cell culture medium (section 2.3.4.1 and 2.2.4.1 respectively) and added to each of three sub-confluent flasks of A549 cells to give a final concentration of 2 x 10^4 conidia/ml and 1 x 10^6 CFU/ml, respectively. To co-expose the A549 cells, *A. fumigatus* conidia (2 x 10^4 conidia/ml) and *P. aeruginosa* (2 x 10^5 CFU/ml) were added to flasks. To each of the controls, the medium in which cells were cultured was replaced by fresh cell culture medium. Unexposed cells and pathogen-exposed A549 cells were incubated for 12 hours as described in section 2.4.3, after which the medium was decanted. A549 cells were subjected to protein extraction as described in section 2.5.5 and prepared for LFQ proteomic analysis (section 2.7).

2.4.7 Sequential Exposure of A549 cells to *A. fumigatus* and *P. aeruginosa*

A549 cells were incubated with *A. fumigatus* conidia (2×10^4 conidia/ml, prepared in cell culture medium) for eight hours, after which *P. aeruginosa* (2×10^5 CFU/ml, prepared in cell culture medium) was added to each of the flasks and incubated for a further four hours to give a total incubation period of 12 hours. Separately, *A. fumigatus* and *P. aeruginosa* were cultured with A549 cells also at these densities, for eight and four hours, respectively. Unexposed A549 cells were incubated for 12 hours. Proteins were extracted from the A549 cells after each time-point (section 2.5.5) and prepared for LFQ proteomic analysis (section 2.7).

2.5 Protein extraction

2.5.1 Lysis buffer/Resuspension buffer

Urea (6 M), thiourea (2 M), and tris-HCl (0.1 M) was dissolved in 50 ml ddH_2O, (table 2.3) adjusted to pH 8 and filter sterilized through a 0.2 µm membrane filters. The buffer was stored at 4°C.

2.5.2 Protein quantification by Bradford protein assay

Bio-Rad protein assay dye (Bio-Rad Laboratories) (1 ml) was diluted in PBS (5 ml) prior to use. Sample (20 µl) was added to 980 µl of the diluted Bio-Rad protein assay dye and mixed thoroughly. The final sample (1 ml) was transferred to a 1 ml plastic cuvette and incubated for 5 min at room temperature. Samples were measured by spectrophotometry (Eppendorf Biophotometer) at 595 nm to determine protein quantity.

2.5.3 Protein quantification by Qubit

Protein quantification using the Qubit® Quant-IT™ protein assay kit (Invitrogen) was performed on a Qubit® fluorometer version 2.0 following the manufacturers operating guidelines. For all protein samples quantified by this method, 2 µl of each sample was used for quantification. Sample was added to 198 µl of working buffer (199 µl of Qubit buffer Component B and 1 µl of Qubit dye reagent Component A), gently mixed and incubated (in the dark at room temperature) for 15 minutes before measuring the protein concentration.

2.5.4 Protein precipitation by acetone

Ice-cold acetone (100 %) was added to quantified protein samples in a ratio of five parts acetone to one part protein sample, to concentrate the protein and to remove contaminants. Protein was stored at -20ºC overnight. Precipitated protein was centrifuged at 13,000 x *g* for 10 minutes at 4 °C. Taking care not to disturb the pellet, the acetone was removed and allowed evaporate before preparation of proteins for mass spectrometry.

2.5.5 Protein extraction from A549 cells

A549 cells were harvested by trypsinization as described in section 2.4.3. After centrifugation (200 x *g* for five minutes), the supernatant was discarded. The cell pellet was resuspended in 3 ml sterile PBS and the centrifugation step was repeated. The cell pellet was resuspended in 500 µl lysis buffer (section 2.5.1) supplemented with protease inhibitors (10 µg/ml) (aprotinin, leupeptin, pepstatin A, and *N*α-p-tosyl-L-lysine chloromethyl ketone (TLCK)), and phosphatase inhibitors (phosphatase inhibitor cocktail 2) (1 % v/v). Cell lysates were incubated for two hours at room temperature on a rotary wheel (Stuart Rotator SB2, Bibby Scientific Limited, Staffordshire, UK). The lysate was centrifuged at 8000 x *g* for 10 minutes at 4 °C (Eppendorf Centrifuge 5418). The supernatant containing the protein was transferred into fresh, 1.5 ml Eppendorf tubes. The extracted protein lysates were quantified by Bradford protein assay (section 2.5.2). Acetone was added to the protein as described in section 2.5.4.

2.5.6 Protein extraction from *P. aeruginosa*

P. aeruginosa cells were harvested by centrifugation (3000 x g) for 15 minutes. The supernatant was decanted. The bacterial pellet was resuspended in 20 ml PBS. This wash step was repeated twice. The pellet was resuspended in 1 ml lysis buffer (section 2.5.1) supplemented with protease inhibitors (10 µg/ml) (aprotinin (1 mg/ml), pepstatin A (1mg/ml), and TLCK (1mg/ml)), and phenylmethylsulfonyl fluoride (PMSF) (1 µl/ml, 100 mM) (Table 2.1) on the day of use. The bacteria suspension was sonicated with a sonication probe (Bandelin Sonopuls, Bandelin electronic, Berlin) at 40% power, cycle 3 for 10 seconds. This was repeated twice more with the sample being cooled on ice between each sonication. The sample was centrifuged at 10000 x *g* for 10 min at 4 °C and the supernatant was transferred into fresh 1.5 ml Eppendorf tubes. Protein quantification

was carried out using the Bradford protein assay (section 2.5.2) and acetone precipitated (section 2.5.4).

2.5.7 Protein extraction from *A. fumigatus*

A. fumigatus hyphae were separated from the culture filtrate through miracloth (Merk). Hyphae were weighed prior to protein extraction and transferred into a mortar. Liquid nitrogen was used to snap freeze the hyphae, which were crushed into a fine dust using a pestle. Lysis buffer (4 ml/g hyphae) (section 2.5.1) supplemented with protease inhibitors (10 µg/ml) (aprotinin, pepstatin A, and TLCK), and PMSF (1 µl/ml, 100mM) on the day of use, was added to the crushed hyphae and mixed to make a thick paste. The mixture was transferred into a sterile tube using a Pasteur pipet and sonicated (section 2.5.6). The lysate was centrifuged at 10000 x *g* for 10 min at 4 °C. The supernatant was transferred into fresh 1.5 ml Eppendorf tubes. Protein quantification was carried out using the Bradford protein assay (section 2.5.2) and acetone precipitated (section 2.5.4).

2.5.8 Protein extraction from *A. fumigatus* culture filtrates

A. fumigatus (5×10^5 conidia/ml) was cultured in Czapek-Dox broth (section 2.3.1) or SAB for 48 hours or 72 hours respectively (section 2.3.2) at 200 *rpm* at 37°C. Hyphae were removed using Miracloth and weighed. Culture filtrates were filter sterilized through 0.2 µm membrane filters. The filtered culture filtrate (*A. fumigatus* CuF) were concentrated by centrifugation (Vivaspin 20, 3kDa MWCO PES, Sartorius). Proteins (> 3kDa) were precipitated overnight with acetone prior to digestion and preparation for mass spectrometry.

Table 2.3 Components for lysis/resuspension buffer

Urea (6 M)	18 g	50 ml ddH_2O
Thiourea (2 M)	7.6 g	50 ml ddH_2O
Tris HCl (0.1 M)	0.79 g	50 ml ddH_2O
PMSF (100 mM)	0.87 g	50 ml Ethanol

2.6 Sodium Dodecyl Sulphate Gel Electrophoresis-Poly Acrylamide Gel Electrophoresis (SDS-PAGE)

2.6.1 Stock solutions

2.6.1.1 Tris–HCl (1.5 M)

Tris-HCl (1.5 M) was prepared by dissolving 36.3g Trizma Base (Tris Base) in 200 ml ddH_2O and adjusted to pH 8.8 using HCl. The buffer was filter sterilized with 0.2 µm membrane filters and stored at 4ºC.

2.6.1.2 Tris-HCl (0.5 M)

Tris-HCl (0.5 M) was prepared by dissolving 12.1g Trizma Base in 200 ml deionised water and adjusted to pH 6.8 using HCl. Following pH adjustment 0.5 M Tris-HCl was filter sterilised through a 0.2 µm membrane filter and stored at 4 ºC.

2.6.1.3 Sodium Dodecyl Sulphate (SDS) (10 %)

Sodium dodecyl sulphate (10% w/v) was prepared by dissolving 5 g SDS in 50 ml ddH_2O. The solution was stored at room temperature.

2.6.1.4 Ammonium Persulphate (APS) (10%)

APS (10% w/v) was prepared by dissolving 0.1 g APS in 1 ml ddH_2O and stored at -20°C.

2.6.1.5 10X Electrode Running Buffer

Electrode Running buffer (10X), was prepared by dissolving Tris Base (30g), Glycine (144g) and SDS (10g) in 800 ml distilled water. The volume was adjusted to 1L and stored at room temperature.

2.6.1.6 10X Electrode Running Buffer

10X running buffer was diluted to a 1X running buffer by adding 100 ml to 900 ml dH_2O.

2.6.1.7 Separating gel stock solution (12.5 %)

SDS-PAGE gels were made of acrylamide with 12% (v/v) Bis-acrylamide and cast using Mini-Protean II gel casting apparatus. Two SDS PAGE gels required 12 ml stock solution (Table 2.4.1). To 12 ml separating stock solution, 75 µl APS (10 % v/v) and 6 µl TEMED was added. A Pasteur pipet was used to transfer stock solution into glass plates (1.0mm, Bio-rad), supported by casting apparatus. The gels were sprayed with 0.01 % SDS stock solution (0.1 ml 10 % SDS stock into 9.9 ml dH_2O) to ensure evenness, and were left to solidify at room temperature.

2.6.1.8 Stacking gel stock solution (5 %)

Table 2.4.2 lists the volumes sufficient to make 500 ml stacking solution stock. Two 1D SDS PAGE gels required 5 ml stock solution. To 5 ml stocking stock solution, 50 µl APS (10 % v/v) and 5 µl TEMED was added. A Pasteur pipet was used to transfer stock solution on top of solidified separating gel plates. Combs (10 rows, 1 mm, Bio-rad) were inserted into the gel immediately and were left to solidify at room temperature.

Table 2.4.1 Separating stock solution (12.5 %)

1.5 M Tris-HCl (pH 8.8)	120 ml
ddH_2O	156 ml
30% v/v Bis-Acrylamide (Protogel, National Diagnostics	200 ml
10% v/v SDS	4.8 ml

Table 2.4.2 Stacking stock solution (5 %)

0.5 M Tris-HCl (pH 6.8)	63 ml
ddH_2O	340 ml
30% v/v Bis-Acrylamide (Protogel, National Diagnostics)	83 ml
10% v/v SDS	5 ml

2.6.1.9 Coomassie Brilliant Blue solution and destain

Coomassie Brilliant Blue stain solution (Table 2.4.3) and destain solution (Table 2.4.4) was prepared to a 1L volume and stored at room temperature. Stain was poured over the gel and incubated on a rocker at room temperature for a minimum of 12 hours before being removed and replaced with destain. Gels were rinsed thoroughly with dH_2O prior to scanning. The stain and destain could be reused.

2.6.1.10 Colloidal Coomassie stain and fixing solution

Fixing solution (Table 2.4.5) and Colloidal Coomassie stain solution (Table 2.4.6) were stored at room temperature. Gels were placed in fixing solution for a minimum of 12 hours. The fixing solution was removed and replaced with ddH_2O. After rehydration for approximately 20-30 minutes, ddH_2O was replaced with staining solution and Serva blue (approximately 10 mg). Gels were stained at room temperature on a rocker for 24 – 48 hours. Prior to scanning, stain was discarded and gels were rinsed thoroughly with dH_2O.

Table 2.4.3 Coomassie Brilliant Blue staining solution

Methanol (45 % v/v)	450 ml
Acetic Acid (10 % v/v)	100 ml
Brilliant Blue R (0.1 % w/v)	1 g
dH_2O (45 % v/v)	450 ml

Table 2.4.4 Coomassie destaining solution

Methanol (20 % v/v)	200 ml
Acetic Acid (10 % v/v)	100 ml
dH_2O (70 % v/v)	700 ml

Table 2.4.5 Colloidal Coomassie fixing solution

Ethanol (50 % v/v)	500 ml
Phosphoric acid (3 % v/v)	30 ml
ddH_2O (47 % v/v)	470 ml

Table 2.4.6 Colloidal Coomassie staining solution

Methanol (34 % v/v)	450 ml
Phosphoric acid (3 % v/v)	30 ml
Ammonium sulphate (17 % v/v)	170 g
ddH_2O (46 % v/v)	460 ml

2.6.2 1D SDS-PAGE gel sample loading

Laemmli sample buffer (2X) (7 µl) was added to 3 µl digested protein sample (section 2.7.1) and 10 µl ddH_2O. The final volume (20 µl) was loaded into each well of a 1D SDS gel (2.6.1). Broad Range (10-250 kDa) protein standard (5 µl) (New England Biolabs, UK) was added to the first lane of every gel.

2.6.3 Gel Electrophoresis running parameters

SDS-PAGE gels were immersed in 1X running buffer. The gels were electrophoresed at 60V until the proteins had left the stacking gel (indicated by the position of the blue tracking dye). When the tracking dye had moved to within 0.5 cm from the bottom of the gel, the gels were transferred to a clean staining dish containing 50 ml Coomassie Brilliant Blue stain (section 2.6.1.8) or Colloidal Coomassie fixing solution (section 2.6.1.9.)

2.6.4 Gel visualization and scanning

When they were ready to be visualized and scanned, gels were rinsed thoroughly with dH_2O. Scanning was performed on an Epson scanner (LabScan™ 6.0, Epson Scanner 10000XL software). Images were saved as 8 bit Tiff and 16 bit Tiff for further analysis.

2.6.5 2D SDS PAGE Preparation

2.6.5.1 Isoelectric focusing (IEF) – first dimension protein separation

Isoelectric Focusing (IEF) buffer was prepared to give a final volume of 50 ml (described in Table 2.5.1) and stored in 1ml aliquots at -20ºC. Ampholytes (0.8%, v/v; 2 µl/ml) and DTT (65 mM; 0.02 g/ml) were added to the defrosted aliquots on the day of use and stored at room temperature. Precipitated protein samples (100 µg) in acetone were centrifuged for 10 minutes at 14,000 *g*. Acetone was removed from pelleted protein samples. When the acetone had completely evaporated, samples were resuspended 50µl IEF buffer and placed in a sonication bath (Fisher Scientific) for five minutes. Bromophenol blue was added to the remaining IEF buffer using a pipet tip. IEF buffer/bromophenol blue solution (50 µl) was added to the IEF buffer/protein sample to give a final concentration of 100 µg/100 µl. Protein samples were loaded into the positive end of 7 cm ceramic IPG strip holders. The IPG strip (7 cm) (Immobiline DryStrip pH 4-7; G.E. Healthcare) was added, gel-side down, using a forceps, while the holder was tilted slightly to ensure distribution of sample along the holder. Care was taken to prevent the trapping of air bubbles underneath the strip. The strips were overlaid with Plus One Drystrip Coverfluid (Amersham) (0.5 ml) and subjected to IEF on an IPGphor II IEF Unit using the following programme outlined in Table 2.5.2.

Table 2.5.1 IEF focusing buffer

Urea (8 M)	24 g
Thiourea (2M)	7.6 g
Tris Base (10 mM)	0.079 g
CHAPS (4 % w/v)	2 g
Triton-x 100	0.5 ml
ddH_2O	bring up to final volume 50 ml

Table 2.5.2 Programme used for focusing IEF strips (22.15 hours total)

Time	Volts	Mode
8 hours	50	Gradient
15 minutes	250	Gradient
2 hours	1000	Gradient
4 hours	4000	Gradient
4 hours	8000	Gradient
4 hours	8000	Hold

Table 2.5.3 Equilibration buffer for IEF strips (pH 8.0) (add glycerol last)

Urea (6 M)	180 g
Tris HCl (30 mM)	3.94 g
SDS (2 % w/v)	10 g
ddH_2O	200 ml initially
Glycerol (30% v/v)	150 ml
ddH_2O	bring to 500 ml

Table 2.5.4 Sealing solution (heated for 1 minute in microwave before first use)

Agarose 1% (w/v)	1 g
Bromophenol Blue (0.5 % w/v)	0.5 g
1 X Running buffer	100 ml

2.6.5.2 Equilibration and second dimension protein separation

Equilibration buffer was prepared as described in table 2.5.3. Buffer was separated into 7.5 ml aliquots to ensure full coverage of the strips. Into each aliquot, DTT (DTT; 0.01 g/ml) was added. After focusing, IPG strips were transferred immediately to equilibration buffer/DTT solution and placed on a rotating wheel for 15 minutes. Following reduction by DTT, strips were then transferred to tubes covered in tinfoil containing 7.5ml of equilibration buffer with IAA (0.025 g/ml) and placed on a rotating wheel for 15 min. Following alkylation, IPG strips were rinsed briefly in 1X electrode running buffer (2.6.1.6). Strips were placed on top of homogenous 12.5% SDS-PAGE gels (section 2.6.1.7) and sealed with 1% (w/v) agarose sealing solution (Table 2.5.4) once hand hot. Gels were subjected to electrophoresis (section 2.6.3). When the tracking

dye had reached approximately 0.5 cm from the bottom of the plate, the gels were placed in Colloidal Coomassie fixing solution followed by Colloidal Coomassie stain solution (section 2.6.1.9).

2.6.6 Analysis of protein in 2D SDS PAGE gels

2.6.6.1 Statistical analysis of 2D SDS PAGE gels

2D-PAGE Colloidal Coomassie stained gels were aligned using Progenesis™ SameSpot Software (Nonlinear Dynamics Ltd, UK), to assess the fold change in protein abundance between two groups. The level of differential expression was analysed by ANOVA with p-values of ≤ 0.05 considered statistically significant for changes in protein abundance.

2.6.6.2 Trypsin reconstitution buffer

Sequencing grade trypsin (Promega) (20 µg) was dissolved in 100 µl trypsin resuspension buffer. Trypsin was transferred in 20 µl aliquots and stored at -20 °C until required. To 20 µl trypsin, 980 µl trypsin reconstitution buffer (1ml 10 mM Ammonium bicarbonate, (Table. 2.6), 1 ml acetonitrile and 8 ml ddH_2O) was added to give a final volume of 10 ng/µl.

Table 2.6 Trypsin reconstitution buffer

Ammonium bicarbonate (100 mM)	395 mg dissolved in 50 ml ddH_2O
Ammonium Bicarbonate (10 mM)	1 ml Ammonium bicarbonate (100 mM) in 9 ml ddH_2O

2.6.6.3 In-gel digestion and analysis of SDS-PAGE samples

In-gel digestion of SDS-PAGE samples was carried out according to the protocol of Shevchenko *et al.* (Shevchenko *et al.*, 2007). Briefly, selected bands or spots from SDS-PAGE gels were excised using a needle soaked in acetonitrile and placed in individual labelled 1.5 ml Eppendorf tubes. Gel pieces were destained by addition of 100 µl of 100 mM ammonium bicarbonate (Table 2.3) acetonitrile (1:1 v/v). Samples were vortexed periodically for 30 min. Acetonitrile (500µl) was added to samples, followed by vortexing until the gel pieces became white and shrunk. Acetonitrile was removed and replaced with trypsin in reconstitution buffer (~ 30 µl or more to ensure full coverage of gel piece) (section 2.6.6.2), Samples were incubated at 37 °C overnight. The tryptic digest supernatant was transferred to Eppendorf tubes. Samples were dried to completion using a speedy vac (DNA Speedy Vac Concentrator, Thermo Scientific) and resuspended in ddH_2O containing 0.1% formic acid (20 µl). The samples were filtered through 0.22 µm Cellulose Spin-filters (Costar) before transfer to polypropylene vials. Care was taken to ensure there was no air trapped in the vials. Peptide mixtures generated from in-gel digestion of protein spots were analysed using a 6340 Model Ion Trap LC-Mass Spectrometer (Agilent Technologies, Ireland) using electrospray ionisation with an acetonitrile elution gradient.

2.7 Protein preparation for Label Free Mass Spectrometry

2.7.1 Protein sample digestion

Precipitated protein samples in acetone were centrifuged for 10 minutes at 14,000 *g* and acetone was removed from pelleted protein samples. When the acetone had completely evaporated, resuspension buffer (section 2.5.1) (25 µl) was added to each sample. The sample was resuspended by vortexing and with the aid of a pipette. Sample (5 µl) was removed; 2 µl was reserved for quantification by Qubit (section 2.5.3) and 3 µl was reserved for 1D SDS PAGE (section 2.6). Ammonium bicarbonate (50 mM) (105 µl) (Table 2.7.1) was added to the remaining 20 µl. The protein sample was reduced by adding 1 µl dithiothreitol (DTT) (Table 2.7.1) and incubating on hotplate at 56 °C for 20 minutes. Samples were cooled to room temperature, and alkylated by the addition of 2.7 µl iodoacetamide (IAA) (0.55 M) (Table 2.7.1) and incubated at room temperature in the dark for 15 minutes. Following reduction and alkylation, 1 µl ProteaseMAX™ Surfactant Trypsin Enhancer stock (Promega) (1%, w/v stock) (Table 2.7.1), and 1 µl sequencing grade trypsin (Promega) (0.5 µg/µl) (Table 2.7.1) was added to each protein sample, and incubated at 37°C overnight.

Table 2.7.1 Components for protein sample digestion

Ammonium bicarbonate (50 mM)	0.099g	25 ml ddH_2O
DTT (0.5 M)	0.039 g	0.5 ml Ammonium Bicarbonte (50 mM)
IAA (0.55 M)	0.102 g	0.25 ml Ammonium Bicarbonte (50 mM)
ProteaseMAX	1 mg	0.1 ml ddH_2O
Sequencing Grade Trypsin	20 µg	40 µl trypsin resuspension buffer

Table 2.7.2 Solvents for C18 Spin column clean-up

Sample Buffer 1	Acetonitrile (20 %) TFA (2 %) ddH_2O (78 %)	200 µl 20 µl 780 µl
Activation Solution	Acetonitrile (50 %) ddH_2O (50 %)	2.5 ml 2.5 ml
Equilibration Buffer & Wash Buffer	TFA (0.5 %) Acetonitrile (5 %) ddH_2O (94.5 %)	25 µl 250 µl 4.725 ml
Elution Buffer	Acetonitrile (70 %) ddH_2O (30 %)	700 µl 300 µl

2.7.2 C-18 Spin Column Clean Up

Trifluoroacetic acid (TFA) (1 µl) was added to each tryptic digest sample, and incubated at room temperature for 5 minutes. The samples were centrifuged at 10,000 x *g* for 10 minutes, and the supernatant was aliquoted into sterile Eppendorf tubes. Tryptic digested peptide samples were mixed with sample buffer 1 (Table 2.7.2) at ratio of three: one (peptide sample: sample buffer 1). Pierce® C-18 spin columns (Thermo Scientific, Life Technologies, Rockford, IL, USA) containing C-18 reverse-phase resin were used for the recovery, and purification of tryptic digested peptides.

The C-18 spin columns were placed in receiver tube (1.5 ml Eppendorf tube) and first activated with the addition of 200 µl activation solution (Table 2.7.2) to each column to rinse the walls of the column, and wet the resin, followed by centrifugation at 1500 x g for 1 minute. The flow-through was discarded and the column activation step was repeated. The flow-through was discarded, 200 µl equilibration solution (Table 2.7.2) was added to the C-18 column, and the columns were centrifuged at 1500 x g for 1 minute. The flow-through was discarded, and the equilibration step was repeated.

Tryptic digest sample/sample buffer 1 solution (3:1) was loaded to the top of the C-18 resin bed, and the column was transferred to a new receiver tube. The samples in the column were centrifuged at 1500 x g for 1 minute. The flow-through was collected, re-applied to the C-18 resin bed, and the columns were centrifuged at 1500 x g for 1 minute twice more, to ensure complete sample binding to the C-18 resin. The columns were transferred to new sterile receiver tubes, and 200 µl wash buffer (Table 2.7.2) was added,

and the columns were centrifuged at 1500 x g for 1 minute. The flow-through was discarded, and the wash step was repeated to remove contaminants.

The columns were transferred to new receiver tubes, and 25 µl elution buffer (Table 2.7.2) was added, and the columns were centrifuged at 1500 x g for 1 minute. The elution step was repeated twice more and the eluent (75 µl) was transferred to a new Eppendorf tube. The samples were lyophilised using a vacuum centrifuge (Savant DNA120 SpeedVac Concentrator, Thermo Fisher Scientific Inc., Dublin, Ireland) for approximately two hours at medium drying rate setting or until complete lyophilisation of the peptides had occurred. Dried peptide extracts were stored at -20°C.

2.7.2.1 Peptide preparation for analysis by mass spectrometry

Protein samples resuspended in acetonitrile (2% v/v) and TFA (0.05% v/v). To aid resuspension, samples were sonicated for 5 min and centrifuged at 13,000 x *g*. The supernatant (10 µl) was transferred into vials (VWR) and used for mass spectrometry. The remaining supernatant was stored at -20 °C.

2.8 Mass Spectrometry Analysis

2.8.1 Mass Spectrometry parameters for A549 protein analysis

Digested sample (1 µg) was loaded onto a QExactive (ThermoFisher Scientific) high-resolution accurate mass spectrometer connected to a Dionex Ultimate 3000 (RSLCnano) chromatography system. Peptides were separated by an increasing acetonitrile gradient on a BioBasic™ C18 Picofrit™ column (100 mm length, 75 mm inner diameter), using a 180-minute reverse phase gradient at a flow rate of 250 nL/min^{-1}. All data were acquired with the mass spectrometer operating in an automatic dependent switching mode. A full MS scan at 140,000 resolution and a range of 300 – 1700 *m/z*, was followed by an MS/MS scan at 17,500 resolution, with a range of 200-2000 *m/z* to select the 15 most intense ions prior to MS/MS. Quality control measures were taken before, and after each sample group was analysed by MS. HeLa cell lysate(250 ng/µl) was analysed to ensure that MS paramters were maintained throughout the MS run time.

2.8.1.1 MS/MS Data analysis for A549 cell study

Protein quantification and LFQ normalization of the MS/MS data was performed using MaxQuant version 1.5.3.3 (http://www.maxquant.org). The Andromeda search algorithm incorporated in the MaxQuant software was used to correlate MS/MS data against the Uniprot-SWISS-PROT database for *Homo sapiens* (55651 entries), *A. fumigatus Af293* (9647 entries) and *P. aeruginosa* PAO1 (5564 entries) (downloaded 16/09/2016).

2.8.1.2 Search Parameters

The following search parameters were used: first search peptide tolerance of 20 ppm, second search peptide tolerance 4.5 ppm with cysteine carbamidomethylation as a fixed modification and N-acetylation of protein and oxidation of methionine as variable modifications and a maximum of two missed cleavage sites allowed. False discovery rate (FDR) was set to 1 % for both peptides and proteins, and the FDR was estimated following searches against a target-decoy database. Peptides with minimum length of seven amino acid length were considered for identification and proteins were only considered identified when observed in three replicates of one sample group.

2.8.2 Mass Spectrometry parameters for *P. aeruginosa* and *A. fumigatus* protein analysis

Digested *P. aeruginosa* protein samples (750 ng) was loaded onto a Q Exactive as described in 2.8.1. A 133-minute reverse phase gradient at a flow rate of 300 nL/min^{-1} was applied. All data were acquired with the mass spectrometer operating in an automatic dependent switching mode. A full MS scan at 70,000 resolution and a range of 400 – 1600 *m/z*, was followed by an MS/MS scan at 17,500 resolution, with a range of 200-2000 *m/z* to select the 15 most intense ions prior to MS/MS.

2.8.2.1 MS/MS Data analysis for the *P. aeruginosa* and *A. fumigatus* studies

Protein quantification and LFQ normalization of the MS/MS data was performed using MaxQuant version 1.5.3.3 (http://www.maxquant.org). The Andromeda search algorithm incorporated in the MaxQuant software was used to correlate MS/MS data against the Uniprot-SWISS-PROT database for *P. aeruginosa* PAO1 (5564 entries) or *A. fumigatus* Af293 (9647 entries) respectively (downloaded 11/09/2018). Search parameters applied are described in section 2.8.1.2.

2.8.3 Proteomic analysis

Perseus v.1.5.5.3 (www.maxquant.org/) was used for data analysis, processing and visualisation for all studies. Normalised LFQ intensity values were used as the quantitative measurement of protein abundance for subsequent analysis. The data matrix was first filtered for the removal of contaminants and peptides identified by site. This step involves searching the raw data against a fasta file incorporated in MaxQuant that contains hundreds of contaminant proteins commonly found in laboratory-processed samples. Contaminant proteins are highlighted in the results file and were removed from the analysis. LFQ intensity values were $\log_2$ transformed and each sample was assigned to its corresponding group. Proteins not found in three out of three (in chapter 3, 5 and 6), or four out of four samples (chapter 4) in at least one group were omitted from the analysis. A data-imputation step was conducted to replace missing values with values that simulate signals of low abundant proteins chosen randomly from a distribution of log2 transformed LFQ intensities for all proteins. Imputated values were specified by a downshift of 2 times the standard deviation (SD) of the mean LFQ intensity of all measured values and a width of 0.3 times this SD. The replacement of missing intensities permitted principal component analysis and hierarchical clustering.

Normalised intensity values were used for a principal component analysis (PCA). Exclusively expressed proteins (those that were uniquely expressed or completely absent in one group) were identified from the pre-imputation dataset and included in subsequent analyses, i.e. the statistically significant set of proteins. This was permitted because the mean values and variance of these proteins were assessed to be significantly different to

the low abundant values that replaced the missing values in other samples during the imputation step.

Gene ontology (GO) mapping was also performed in Perseus using the UniProt gene ID for all identified proteins to query the Perseus annotation file and extract terms for biological process, molecular function and Kyoto Encyclopaedia of Genes and Genomes (KEGG) names. Perseus annotation files for *H. sapiens* were downloaded in October 2016. Perseus annotation files for *P. aeruginosa* PAO1 and *A. fumigatus* Af293 were downloaded in October 2018.

To visualise differences between two samples, pairwise Student's t-tests were performed for all using a cut-off of $p<0.05$ on the post-imputated dataset. Volcano plots were generated in Perseus by plotting negative log p-values on the y-axis and $\log_2$ fold-change values on the x-axis for each pairwise comparison. The 'categories' function in Perseus was utilized to highlight and visualise the distribution of various pathways and processes on selected volcano plots. Statistically significant (ANOVA, $p<0.05$) and differentially abundant proteins (SSDA), i.e. with fold change of plus or minus 1.5 were chosen for further analysis. The $\log_2$ transformed LFQ intensities for all SSDA proteins were Z-score normalised and used for hierarchical clustering of samples and SSDA proteins using Euclidean distance and average linkage. GO and KEGG term enrichment analysis was performed on the major protein clusters identified by hierarchical clustering using a Fisher's exact test (a Benjamini-Hochberg corrected FDR of 4%) for enrichment in Uniprot Keywords, gene ontology biological process (GOBP), gene ontology cellular component (GOCC) and KEGG (FDR < 4 %).

2.8.3.1 Parameters for analysis on multi-sample tests

Prior to hierarchical clustering on sequentially exposed groups (described in section 2.4.7) an analysis of variance (ANOVA) was performed for multiple-samples across all four groups using a permutation based false discovery rate of 5 % and below to indicate statistically significant differentially abundant (SSDA) proteins to be included for Z-score normalization and hierarchical clustering.

2.8.3.2 STRING and KEGG analysis

The Search Tool for the Retrieval of INteracting Genes/Proteins (STRING) (Jensen *et al.*, 2009) v11 (http://string-db.org/) was used to map known and predicted protein:protein interactions. UniProt gene lists (extracted from Perseus) were inputted and analysed in STRING using the high confidence (0.700) setting to produce interactive protein networks for each group in all comparisons. GO term enrichment analyses for biological process, molecular function and cellular compartment were conducted to identify potential pathways and processes that warranted further analysis. Such pathways were examined using the KEGG pathways analysis (https://www.genome.jp/kegg/tool/map_pathway2.html) using the 'KEGG Mapper—SearchandColor Pathway' tool. The equivalent KEGG identifiers were obtained using the UniProt 'Retrieve/ID mapping' function (http://www.uniprot.org/uploadlists/) with the organism set to "has" (*H. sapiens*) for the A549 cell protein analysis, "pae" (*P. aeruginosa*) for the *P. aeruginosa* protein analysis and "afm" (*A. fumigatus*) for the *A. fumigatus* protein analysis. Retrieved KEGG IDs were used to identify the most represented pathways.

2.8.4 Mass Spectrometry analysis of *A. fumigatus* culture filtrate protein

2.8.4.1 Mass Spectrometry parameters

Digested proteins samples (500 ng) collected from *A. fumigatus* CuF (section 2.5.8) was loaded onto the Q Exactive (as described in section 2.7). A 65-minute reverse phase gradient at a flow rate of 300 nL/min^{-1} was applied. The remaining parameters are described in section 2.8.2).

2.8.4.2 Protein analysis of *A. fumigatus* culture filtrate

Proteins present in *A. fumigatus* CuF were identified using Proteome Discoverer 1.4 and Sequest HT (SEQUEST HT algorithm, Thermo Scientific) and searched against the UniProtKB database (taxonomy: *Neosartorya fumigata*). Search parameters applied for protein identification were as follows (i) peptide mass tolerance set to 10 ppm, (ii)

MS/MS mass tolerance set to 0.02 Da, (iii) an allowance of up to two missed cleavages, (iv) carbamidomethylation set as a fixed modification and (v) methionine oxidation set as a variable modification. Peptide probability was set to high confidence and peptides with minimum (Xcor) score of two and fewer than three unique peptides were excluded from further analysis.

2.9 Gliotoxin analysis

2.9.1 Gliotoxin extraction from *A. fumigatus* culture filtrates

A. fumigatus hyphae were separated from culture filtrates with miracloth. The wet weight of the hyphae was obtained. The culture filtrate was filter-sterilized using 0.45 µm membrane filters followed by 0.2 µm membrane filters (Filtropur S, Sarstedt, Germany). The culture filtrate (20 ml) was mixed with equal volumes of chloroform (20 ml) and placed on a rocker for two hours at room temperature.

The chloroform (organic layer containing the gliotoxin), was separated from the aqueous layer using a Pasteur pipette. Care was taken not to collect lipids or aqueous solution with the pipet. The chloroform fraction was collected and dried by rotary evaporation in a Büchi rotor evaporator (Brinkmann Instruments; Westbury, NY). Dried extracts were dissolved in 500 µl methanol. The resuspended extract was centrifuged at 14,000 x *g* for 5 min. The supernatant was transferred to a fresh 1.5 ml Eppendorf tube and stored at –20 °C.

2.9.2 Quantification of gliotoxin by RP-HPLC

Gliotoxin was detected by Reversed Phase-HPLC (Shimadzu) with UV detection. The mobile phase (solvent A) was ddH_2O and 0.1% (v/v) TFA and (solvent B) acetonitrile and 0.1% (v/v) (Table 2.8.1). Gliotoxin extract (20 µl) was injected onto a Lunar Omega, 5 µm polar C18, LC column (Phenomenex) at a flow rate of 1 ml/min. Gradient conditions are described in Table 2.8.2 Analysis was performed at an absorbance of 254 nm. A standard curve of peak area versus gliotoxin concentration was constructed using gliotoxin standards (0.1, 0.25, 0.5, 1.0 µg/10 µl) dissolved in methanol (Fig. 2.1).

Table 2.8.1 RP-HPLC mobile phase solvents

Solvent A	1 ml TFA / 1L ddH_2O
Solvent B	1 ml TFA/ 1L Acetonitrile

Table 2.8.2 RP-HPLC gradient conditions for gliotoxin analysis

Time (min)	% Solvent B
0	5
5	5
20	100
30	100
40	5
50	5

2.10 Detection of amino acids by ninhydrin

Culture filtrates from *A. fumigatus*, *P. aeruginosa* and Co-cultures were filter sterilized and analysed for free amino acids using 2 % ninhydrin (Sigma) dissolved in ethanol (Yemm *et al.*, 1955). A standard curve of absorbance (OD_{570}) versus concentration was constructed using amino acid standards (glycine and serine) (Fig. 2.2).

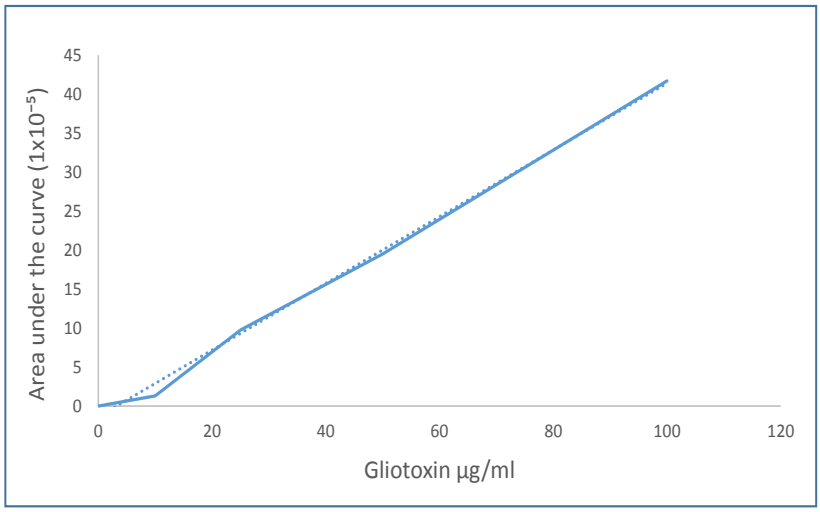

Fig. 2.1 Gliotoxin standard curve Gliotoxin concentrations (µg/ml) were measured against the area under the curve. Analysis of gliotoxin was performed in the absorbance mode at 254 nm.

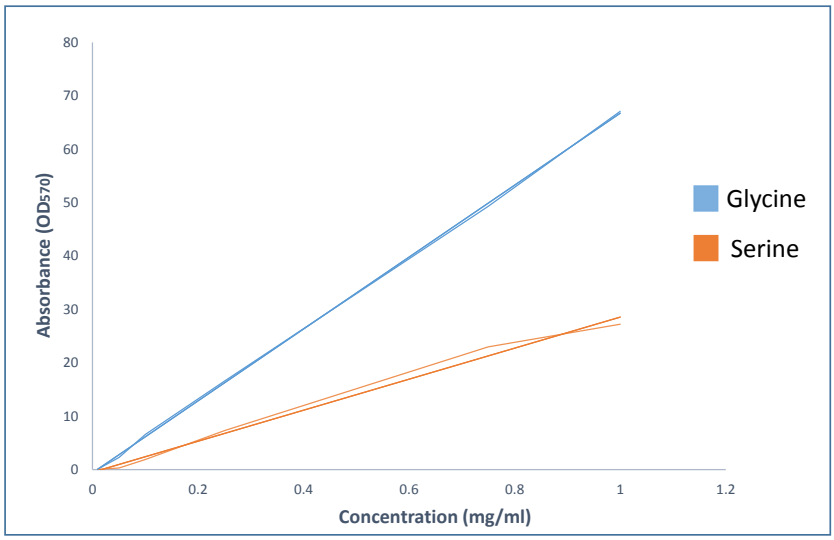

Fig. 2.2 Amino acid standard curve. Concentration (mg/ml) of glycine (blue) and concentration of serine (orange) were measured against the absorbance (570 nm).

2.11 Preparation of *A. fumigatus* antibacterial compound

2.11.1 Culture conditions

A. fumigatus (5 x 10^5 conidia/ml) was cultured in Sabouraud Liquid Medium (SAB) (section 2.3.1) for between 48 and 72 hours in a shaker at 200 rpm at 37°C. The hyphae and the culture filtrate was separated through miracloth. The culture filtrate was filter sterilized using 0.45 µm membrane filters followed by 0.2 µm membrane filters. The filtrates were stored in 40 ml aliquots at -20°C.

2.11.2 Culture filtrate-processing method

2.11.2.1 Freeze drying culture filtrates

Frozen filtrates were placed in liquid nitrogen for five minutes (with the lids of the tubes slightly open) prior to being placed on the freeze dryer to be lyophilized. Dried samples were removed from the freeze dryer after about four days or when the moisture was completely gone. The powder was stored in the fridge at 4°C.

2.11.2.2 Separation of compound by RP-HPLC

Dried material (40 ml starting) was resuspended in 2 ml of ddH_2O and filtered through 0.22 µm cellulose acetate spin filter tubes (Spin-X®, Costar) and transferred to 250 µl vials (Agilent). Samples were detected and fractions were collected by HPLC (Shimadzu). Samples (50 µl) were injected onto a Lunar Omega, 5 µm polar C18, LC column (Phenomenex) at a flow rate of 0.5 ml/minute. Gradient conditions are described in Table 2.9. Fractions (250 µl) were collected between 4.5 and 5.5 minutes. Fractions were pooled together and stored at -20°C.

Table 2.9 RP-HPLC gradient conditions for *A. fumigatus* compound analysis

Time (min)	% Solvent B
0	0
5	0
15	100
18	100
20	0
28	0

2.11.2.3 Separation of compound by size

Pooled fractions were separated by size through centrifugal filters (Vivaspin 20, 3kDa MWCO PES, Sartorius). Sample were centrifuged at 4000 x *g*. The filtrate and the retentate were collected and stored at - 20°C.

2.11.2.4 Separation of compound by polarity

C18 Sep-Pak cartridges (Sep-Pak Vac 3cc 200 mg, Waters) were prepared by passing through methanol (2 x 3 ml aliquots). ddH_2O (3 x 3 ml aliquots) was passed through the column to remove methanol before the filtered sample was applied. Samples were pulled through the column manually with a syringe and were applied to the column twice in total. The flow through (polar component) was collected.

Clean Screen DAU C8 columns (UCT) was prepared by passing through methanol (2 x 5 ml aliquots) followed by ddH_2O (3 x 5 ml aliquots) before loading sample onto the column. The sample was pulled through manually with a syringe and applied to the column twice in total. The flow through (hydrophilic, anionic component) was collected. The samples were stored at -20 °C. Processed samples were lyophilized as described in section 2.11.2.1, and separated by HPLC (section 2.11.2.2) two more times. After the final fractionation, samples were lyophilized and analysed by mass spectrometry and NMR.

2.11.3 Mass Spectrometry analysis of *A. fumigatus* antibacterial compound

Fractions collected from separation by RP-HPLC (section 2.11.2.2) were lyophilized and resuspended in ddH_2O/1 % formic acid. Samples were analysed on a Dionex Ultimate 3000 (RSLCnano) chromatography system coupled to a QExactive (ThermoFisher Scientific) high-resolution accurate mass spectrometer. Peptides were separated by an increasing acetonitrile gradient on a Hypersil Gold aQ C18 polar endcapped column (100 mm length, 2.1 mm inner diameter, 1.9 µm particles), using a 10-minute reverse phase gradient of acetonitrile/0.1% formic acid (5 – 70 % gradient). Samples were analysed in positive mode and negative mode using a top 3 MS/MS method.

2.12 NMR analysis of *A. fumigatus* antibacterial compound

Nuclear Magnetic Resonance (NMR) spectroscopy was performed on fractions collected by RP-HPLC (described in section 2.11.2.2)

NMR spectra were obtained on a Bruker Ascend 500 MHz spectrometer operated at 500 MHz. The samples were found to be fully soluble in deuterium oxide (or mixtures of deuterium oxide:water 10:90) and spectra were recorded at ambient temperature. The signal at 4.7 from HOD was used as reference peak for calibration. Chemical shifts (δ) were reported in ppm.

A series of 1D (1H NMR, 13C NMR and 31P NMR) and 2D experiments, including Correlation Spectroscopy; COSY, Total Correlation Spectroscopy; TOCSY, heteronuclear single quantum correlation; HSQC, Heteronuclear Multiple Bond Correlation; HMBC and Distortionless Enhancement by Polarization Transfer; DEPT) were performed on the samples in order to attempt signal assignation and structure identification**.**

Chapter 3

Characterization of the proteomic response of A549 cells to *Aspergillus fumigatus* and *Pseudomonas aeruginosa*

3.1 Introduction

The average healthy (resting) adult inhales in excess of 7,000 litres of air daily and with this, airborne fungal spores and bacteria are taken into the respiratory tract (Dickson *et al.*, 2016). For immunocompetent individuals, inhaled microbes are swiftly cleared by the pulmonary immune system. Microorganisms become trapped in the mucus secreted by goblet cells and are propelled towards the oropharyngeal junction by ciliary beating and either swallowed or exporated. Those that evade the effects of the mucociliary elevator are phagocytosed and killed by cells of the immune system such as macrophages and neutrophils (Balloy and Chignard, 2009).

The lungs of individuals with cystic fibrosis (CF) are lined with a thick sticky mucus layer and a dehydrated airway surface liquid (ASL) caused by an ion imbalance arising from defects in the CFTR protein (Verkman *et al.*, 2003). These conditions compromise the actions of the mucociliary elevator and thus provide an environment conducive to microbial growth. As a result, the CF airways are colonised by a variety of bacterial and fungal pathogens, which severely affect pulmonary function and contribute to mortality (Tang *et al.*, 2014). The cells of the pulmonary epithelium are the first point of contact with pathogens as they enter the lungs. Understanding how host cells respond to these pathogens and how these microorganisms interact with each other is key to understanding how pulmonary infection develops in the lung (Harriott and Noverr, 2011; Filkins and O'Toole, 2015; Reece *et al.*, 2017a).

The microbial ecology of the CF airways displays an age-related profile that is characterized by colonization with a range of pathogens from infancy, and reduced microbial diversity in adulthood (Coburn *et al.*, 2015). In the first decade of life, the most common detectable pathogens are *Staphylococcus aureus, Haemophilus influenza, Streptococcus spp.* and *Stenotrophomonas maltophilia*. The mould, *Aspergillus fumigatus* is also detected in the airways from childhood and remains the most prominent fungal pathogen in the CF airways (Reece *et al.*, 2019).

In the second decade of life, the Gram-negative bacterium, *Pseudomonas aeruginosa,* succeeds as the predominant pathogen and alongside members of the *Burkholderia cepacia* complex, these bacteria are most associated with poor clinical

outcome (Govan and Deretic, 1996; Koch, 2002). *P. aeruginosa* is recognized as the primary cause of morbidity and mortality within the CF community and it is estimated that 80% of CF sufferers are chronically infected with *P. aeruginosa* by the age of 20 years (Goldberg and Pier, 2000; Koch, 2002; Parkins *et al.*, 2018). Its ability to survive in the CF environment give *P. aeruginosa* a distinct advantage over other microbial species within the lung and once established, chronic infection by this pathogen is rarely eradicated (Govan and Deretic, 1996; Goodman *et al.*, 2004; Winstanley *et al.*, 2016). To survive in the CF lung, *P. aeruginosa* must overcome several challenges from the host immune response including evasion of pulmonary immune cells, oxidative stress, osmotic stress due to an abnormal airway surface liquid (ASL) and exposure to antibiotics (Breidenstein *et al.*, 2011). A consequence of long-term exposure to antibiotics is the emergence of antibiotic resistant strains of *P. aeruginosa* (Breidenstein *et al.*, 2011). These factors, combined with the arsenal of secreted virulent exoproducts such as pyocyanin, rhamnolipids, hemolysin, proteases and elastase, mediate *P. aeruginosa* pathogenesis in the CF airway (Caldwell *et al.*, 2009; Moradali *et al.*, 2017).

The most prevalent fungal pathogen associated with the CF lung is *Aspergillus fumigatus,* which is detected in up to 57% of CF patients (Stevens *et al.*, 2003b; Pihet *et al.*, 2009). *A. fumigatus* is ubiquitous in the environment where it forms and releases airborne conidia which measure 2-3μm in diameter and are thus easily transported through the respiratory tract when inhaled. In the immunocompromised airways, conidia that avoid elimination can germinate and provoke a proinflammatory immune response triggered by the secretion of toxins and allergens from the developing fungus. This can result in the manifestation of a hypersensitivity disorder, allergic bronchopulmonary aspergillosis (ABPA), which affects up to 13% of asthmatics and CF patients (Daly and Kavanagh, 2001; Kraemer *et al.*, 2006; Agarwal *et al.*, 2014). *A. fumigatus* is a versatile pathogen and several factors contribute to persistent infection within the CF lung including its ability to adapt to the hypoxic environment and to acquire nutrients from the host (Dagenais and Keller, 2009). The production of *A. fumigatus* secondary metabolites such as gliotoxin and fumagillin impede the mucociliary elevator and inhibit macrophage and neutrophil activity thereby impairing the primary immune response (Amitani *et al.*, 1995; Fallon *et al.*, 2010; Schlam *et al.*, 2016a). *A. fumigatus* is reported to be the only species associated with increased risk of *P. aeruginosa* colonization in CF and co-infection with these microorganisms is more detrimental to the host than infection by

either pathogen alone (Amin *et al.*, 2010; Leclair and Hogan, 2010; Hector *et al.*, 2016; Reece *et al.*, 2017a). This may be due in part, to an increase in the secretion of toxic compounds resulting from pathogen-host and inter-species interactions (Smith *et al.*, 2015; Sass *et al.*, 2019).

The aim of the work presented in this chapter was to investigate the cellular response to a co-infection of *A. fumigatus* and *P. aeruginosa*, with a view to understanding why *P. aeruginosa* eventually becomes the predominant pathogen. The A549 cell line is a well-established *in vitro* model system for studying pathogen-host interactions on the alveolar cell surface of the lung, particularly in the context of *A. fumigatus* and *P. aeruginosa* infection (Ichikawa *et al.*, 2000; Wasylnka, 2003; Hawdon *et al.*, 2010; Wang *et al.*, 2013; Amin *et al.*, 2014; Chen *et al.*, 2015). Research to date has focused on the response of A549 cells to either *A. fumigatus* or *P. aeruginosa* exposure, however, a better understanding of the cellular response to co-infection is required, as this may inform future therapeutic strategies.

To address this knowledge gap, label-free quantitative (LFQ) proteomics was chosen to explore the response of A549 cells to exposure with *A. fumigatus* or *P. aeruginosa* and to co-exposure with both pathogens. The proteomic data presented here provides an explanation as to why, in the context of co-infection, *P. aeruginosa* predominates over *A. fumigatus* and reveals an important role for A549 cells in facilitating bacterial survival and proliferation. This whole-system approach provides novel insights into the cellular response to poly-microbial challenges and the potential strategies employed by pathogens to modulate and manipulate their hosts.

The primary objective in this study was to investigate the effect that co-exposure to *A. fumigatus* and *P. aeruginosa* had on A549 cells and to compare this with exposure to each pathogen alone. The goal was to understand why *P. aeruginosa*, and not *A. fumigatus*, predominates as the primary pathogen and what role if any, A549 cells have to play in this outcome by analysing their response to different types of pathogen-exposure.

3.2 Results

3.2.1 Part one - Analysis of the proteomic response of A549 cells to exposure by *A. fumigatus* and *P. aeruginosa* for 12 hours

To compare the proteomic response of A549 cells to *A. fumigatus* or *P. aeruginosa*, shotgun proteomics was performed on A549 cells that had been exposed to either *A. fumigatus* (2×10^4 conidia/ml) or *P. aeruginosa* (1×10^6 CFU/ml) for 12 hours (n = 3). The control groups were left unexposed to pathogens. LFQ proteomic analysis (as described in section 2.8.3) identified 2036 proteins post-imputation of the dataset (Table A3.1A). Proteins identified in Perseus as being of non-human origin (i.e. with Uniprot IDs for *A. fumigatus* or *P. aeruginosa*), were considered contaminants and removed from further analysis. Statistically significant ($p<0.05$) proteins arising from pairwise Student's t-tests performed on the different comparisons were determined to be differentially abundant if the fold change was greater than 1.5 and are referred to as statistically significant differentially abundant (SSDA). All SSDA proteins identified in A549 cells following exposure to *A. fumigatus* are listed in Table A3.1B. Of these, 199 SSDA proteins were identified in the *A. fumigatus*-exposed group, of which 142 proteins were increased and 57 proteins were decreased in abundance. All SSDA proteins identified in A549 cells following exposure to *P. aeruginosa* are listed in Table A3.1C. In these groups, 159 SSDA proteins were identified, of which 95 were increased, and 64 were decreased in abundance. All SSDA proteins were searched against the STRING and KEGG databases and used to identify biological pathways and processes over-represented in a particular group.

A principal component analysis (PCA) of all identified proteins resolved distinct differences between the proteomes of each groups (Fig. 3.1A). Components 1 and 2 accounted for 47.6% of the total variance within the data, and all replicates resolved into their corresponding samples. The control sample displayed a clear divergence to those that were challenged with *A. fumigatus* or *P. aeruginosa*.

Hierarchical clustering was performed on the z-scored normalised LFQ intensity values for the 625 SSDA proteins arising from pairwise Student's t-tests ($p < 0.05$). All three biological replicates resolved into their respective sample and six protein clusters (A-F) based on protein-abundance profile similarities (Fig. 3.1B) were resolved. Similarities and distinct differences in the response of the host to each pathogen were

identified (Fig. 3.1B). GO and KEGG term enrichment analysis was performed on all protein clusters with five clusters having enriched terms (Fig. 3.1B; Cluster A and C-F), with each cluster having a representative process or pathway characteristic to that group (Fig. 3.1C). These include processes associated with the endoplasmic reticulum (ER) and Golgi apparatus (Cluster A), processes involving lysosome, mitochondrial membrane and transmembrane transporter activity (Cluster C), processes involving ribonucleotide binding (Cluster D), transcription post-transcriptional regulation (Cluster E) and translation and cellular adhesion (Cluster F). Details of all clusters are included in Table A3.2A and Table A3.2B.

A

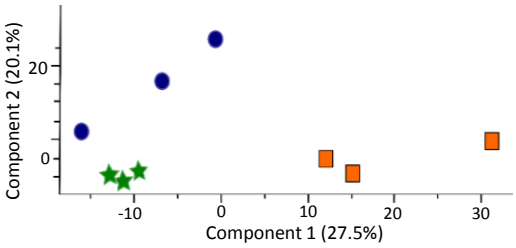

B

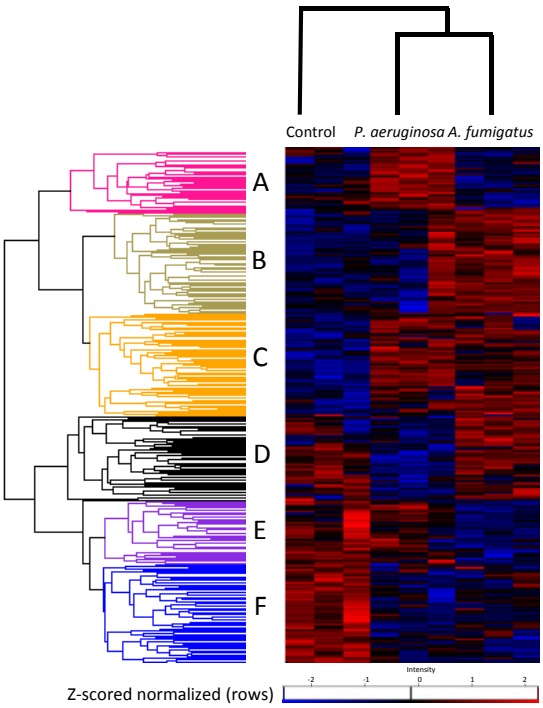

C

Cluster ID	Gene Ontology Term	P-value	Enrichment
A	Endoplasmic reticulum membrane Golgi membrane	1.95E-09 8.15E-06	3.97 3.85
C	lytic vacuole Mitochondria membrane Transmembrane transporter activity	1.46E-05 6.14E-05 6.89E-05	4.9 2.24 2.71
D	microtubule ribonucleotide binding	3.61E-05 1.17E-04	3.51 1.9
E	transcription, DNA-dependent RNA metabolic process mRNA processing	1.29E-07 8.18E-07 4.37E-05	2.82 1.91 2.60
F	Ribosome translation cell junction cell-substrate adherens junction	1.41E-10 7.32E-07 7.33E-07 2.41E-05	4.1 2.53 2.11 2.2

Fig. 3.1 PCA, hierarchical clustering and enrichment analysis of A549 cell proteins display distinct differences between the three infection groups (A) Principal component analysis (PCA) of untreated A549 cells (squares), A549 cells treated with *P. aeruginosa* (circles) or *A. fumigatus* (stars). A clear distinction can be observed between each of the treated groups and the control. (B) Clusters based on protein-abundance profile similarities were resolved by hierarchical clustering on t-test significant ($p<0.05$) and exclusively expressed proteins from comparisons between the three sample groups of A549 cells. Six clusters (A-F) were resolved comprising proteins that display similar expression profiles across treatments. Of these, five clusters (A, C-F) had statistically enriched gene ontology and KEGG terms associated with them (Table A3.2B) and the main terms are summarised for each in Fig. 3.1C

Within Cluster A, 75 proteins with the GOCC term "endoplasmic reticulum" and "Golgi Apparatus" were resolved. Compared to the control, the abundance of these proteins were increased in the *P. aeruginosa*-exposed cells but not in the *A. fumigatus*-exposed cells. The major protein groups included in Cluster B, in which 124 proteins were detected, were associated with the mitochondria and the lysosome. The relative abundance of the proteins included in this cluster were increased in *A. fumigatus*- and *P. aeruginosa*-exposed cells compared to control groups. In Cluster D, which contained 98 proteins, terms associated with ATP binding, ribonucleotide binding and microtubules were identified. The relative abundance of proteins in this cluster were increased primarily in *P. aeruginosa*-exposed A549 cells compared to the control and *A. fumigatus*-exposed cells.

In Cluster E, 77 proteins were identified and were involved in transcriptional and post-transcriptional processes. GOBP terms including "DNA binding, transcription, RNA processing, RNA splicing, mRNA processing" and were associated in this cluster. The greatest decrease in the relative abundance of the proteins included in this cluster was observed in *A. fumigatus*-exposed cells compared to *P. aeruginosa*-exposed cells and the control.

In the final enriched cluster, Cluster F, 121 proteins were resolved. Protein groups involved in this cluster were associated with the KEGG and GOCC term "Ribosome". Numerous GOBP and GOCC terms were identified relating to ribosomal activity (e.g. large ribosomal subunit, small ribosomal subunit and protein complex disassembly), translation (e.g. translational initiation, translational elongation and translational termination) and post-translational activity (e.g. co-translational protein targeting to membrane and protein targeting to ER). Proteins associated with the actin cytoskeleton, cytoskeleton organization, adherens junction and anchoring junction were also identified within this cluster. Proteins groups included in Cluster F were decreased in both pathogen-exposed cells compared to the control.

Volcano plots were produced to show the differences in protein expression between two samples and to depict the changes in pathways and processes that those proteins are involved in (Fig. 3.2A and 3.2B). Proteins involved in the processes and pathways of interest (identified in the "categories function" in Perseus) were displayed

on the volcano plots. In general, the relative abundance of proteins associated with the terms “stress response, metal ion binding and mitochondrial activity” were significantly increased in A549 cells exposed to *A. fumigatus* and *P. aeruginosa* (Fig. 3.2A and 3.2B). A greater number of proteins associated with the term “immune system process” were identified in A549 cells exposed to *P. aeruginosa* compared to *A. fumigatus*-exposed cells. Although the relative abundance of proteins associated with an immune response were upregulated upon exposure to both pathogens, the relative abundance of a significant number of proteins involved in this pathway were decreased in cells exposed to *P. aeruginosa* (Fig. 3.2B).

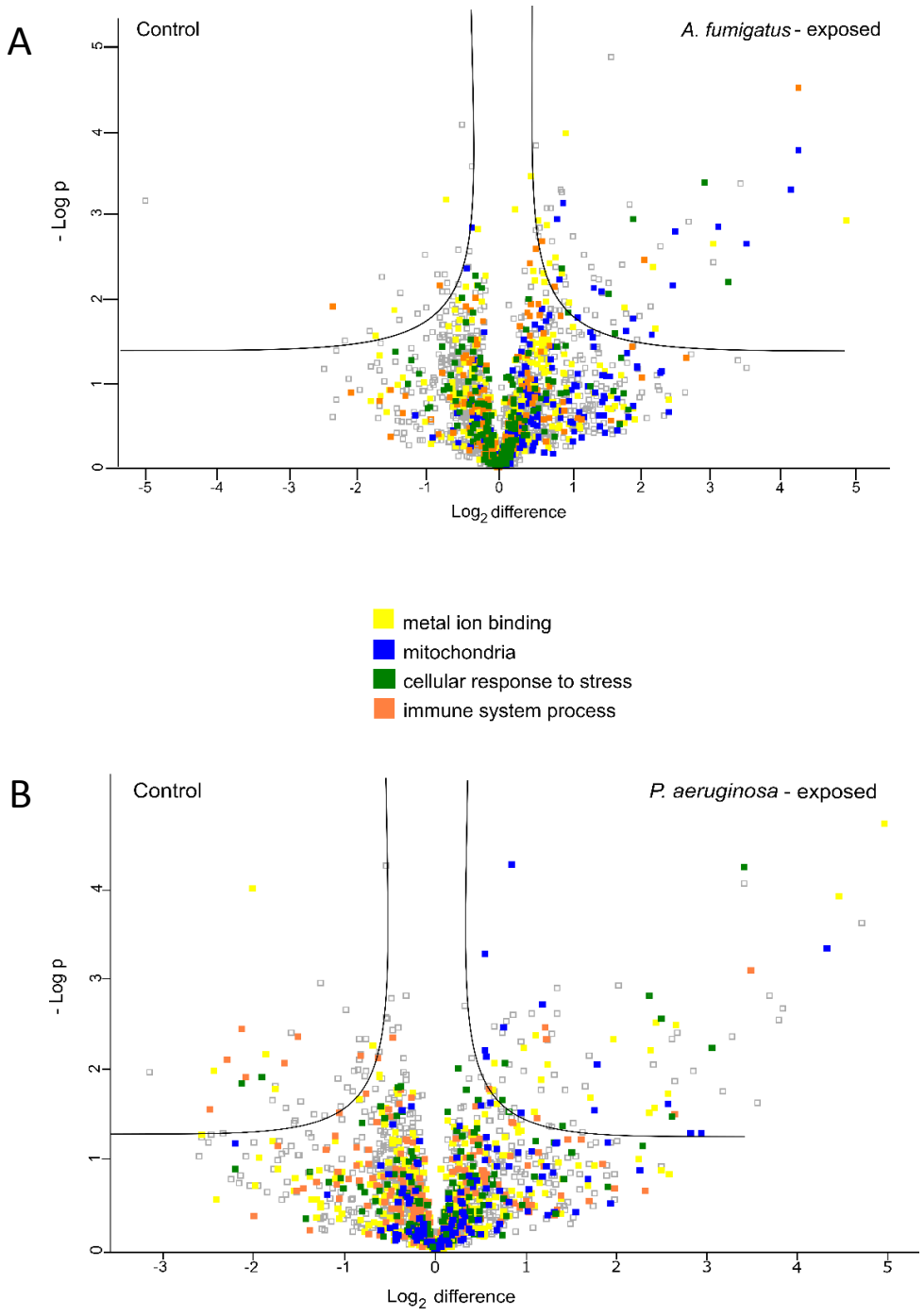

Fig. 3.2 Differential abundance of proteins identified in A549 cells exposed to *A. fumigatus* or *P. aeruginosa* Volcano plots derived from pairwise comparisons between A549 cells and *A. fumigatus*-exposed A549 cells (A) and *P. aeruginosa*-exposed A549 cells (B). The distribution of quantified proteins according to p value (−log10 p-value) and fold change (log_2 mean LFQ intensity difference) are shown. Proteins above the line are considered statistically significant (p-value <0.05). Protein components involved in metal ion binding (yellow), mitochondrial activity (blue) and a cellular stress response were most abundant in both pathogen-exposed groups compared to the control. The abundance of proteins involved in an immune response (orange) was slightly lower in *P. aeruginosa*-exposed groups compared to the *A. fumigatus*-exposed groups.

Copper transport protein ATOX was the most SSDA protein with the greatest fold increase in both *A. fumigatus*-exposed and *P. aeruginosa*-exposed A549 cells and had a fold-change of 36.09 and 26.10 respectively. Half of the top ten most differentially abundant proteins with a fold increase between the two groups were the same, although the fold changes were different (Table. 3.1). These results indicate a similar host cell response is upregulated when exposed to either *A. fumigatus* or *P. aeruginosa*, suggesting a general pathogen-mediated response by A549 cells. On the other hand, none of the top ten SSDA proteins that had reduced abundance were the same in the fungal-exposed cells as the bacterial-exposed cells (Table 3.2). In the *A. fumigatus*-exposed group, the greatest decrease in abundance was observed in catenin alpha (26.62-fold decrease) and in the *P. aeruginosa*-exposed group, the greatest decrease was detected in Ubiquitin-like modifier-activating enzyme 5 (11.57-fold decrease). These results indicate that the attenuation or downregulation of host biological pathways caused by *A. fumigatus* or *P. aeruginosa*, are pathogen-dependent.

Table 3.1 Top ten most increased SSDA proteins identified in A549 cell exposed to *A. fumigatus* or *P. aeruginosa*. Top ten most increased SSDA proteins in A549 cells exposed to *A. fumigatus* or *P. aeruginosa* arising from Student's t-tests on comparisons between the unexposed groups and the *A. fumigatus* – or *P. aeruginosa*-exposed groups.

Pathogen-exposure	Gene	Proteins	Fold change
A. fumigatus	ATOX1	Copper transport protein ATOX1	36.09
	CPLX2	Complexin-2	21.53
	UFM1	Ubiquitin-fold modifier 1	17.24
	SCO1	Protein SCO1 homolog, mitochondrial	12.46
	ACADSB	Acyl-CoA dehydrogenase, mitochondrial	11.06
	DOHH	Deoxyhypusine hydroxylase	11.04
	CREG1	Protein CREG1	9.40
	GCN1L1	Translational activator GCN1	9.27
	COX6A1	Cytochrome c oxidase subunit 6A1	7.39
	ENSA	Alpha-endosulfine	7.00
P. aeruginosa	ATOX1	Copper transport protein ATOX1	26.10
	SCO1	Protein SCO1 homolog, mitochondrial	20.22
	GCN1L1	Translational activator GCN1	15.12
	KTN1	Kinectin	13.90
	EMC1	ER membrane protein complex subunit 1	13.87
	CPLX2	Complexin-2	12.62
	UFM1	Ubiquitin-fold modifier 1	11.10
	SCARB2	Lysosome membrane protein 2	10.11
	ACOX1	Peroxisomal acyl-coenzyme A oxidase 1	8.58
	COX6A1	Cytochrome c oxidase subunit 6A1	8.40

Table 3.2 Top ten most decreased SSDA proteins identified in A549 cell exposed to *A. fumigatus* or *P. aeruginosa*.Top ten most decreased SSDA proteins in A549 cells exposed to *A. fumigatus* or *P. aeruginosa* arising from Student's t-tests on comparisons between the unexposed groups and the *A. fumigatus* – or *P. aeruginosa*-exposed groups.

Pathogen-exposure	Gene	Proteins	Fold change
A. fumigatus	CTNNA2	Catenin alpha-2	-26.62
	PPL	Periplakin	-5.58
	RPAP3	RNA polymerase II-associated protein 3	-3.78
	RPRD2	Regulation of nuclear pre-mRNA domain-containing protein 2	-3.67
	HDGFRP2	Hepatoma-derived growth factor-related protein 2	-3.31
	DDX23	Probable ATP-dependent RNA helicase DDX23	-3.13
	SCAF4	Splicing factor, arginine/serine-rich 15	-2.79
	ABCF3	ATP-binding cassette sub-family F member 3	-2.61
	PARD3	Partitioning defective 3 homolog	-2.60
	MYLK	Myosin light chain kinase, smooth muscle	-2.58
P. aeruginosa	UBA5	Ubiquitin-like modifier-activating enzyme 5	-11.57
	IMP3	U3 small nucleolar ribonucleoprotein protein IMP3	-6.41
	IFI16	Gamma-interferon-inducible protein 16	-5.47
	BAIAP2	BAI1-associated protein 2	-5.31
	ERI1	3-5 exoribonuclease 1	-5.06
	PPP4C	Serine/threonine-protein phosphatase 4	-4.76
	SCCPDH	Saccharopine dehydrogenase-like oxidoreductase	-4.49
	COMMD3	COMM domain-containing protein 3	-4.10
	KIAA0020	Pumilio domain-containing protein KIAA0020	-3.96
	VAMP3;2	Vesicle-associated membrane protein 2;3	-3.95

Enrichment analysis was performed, using STRING on SSDA proteins arising from comparisons between pathogen-exposed and unexposed A549 cells using Student's t-tests ($p<0.05$). The protein networks generated by STRING identified a number of upregulated and downregulated pathways and processes in A549 cells resulting from exposure to *A. fumigatus* (Fig. 3.3A and 3.3B) and *P. aeruginosa* (Fig. 3.3C and 3.3D). Compared to the control, the relative abundance of proteins associated with oxidative stress, the mitochondria, protein folding, lysosomes and mRNA metabolism was increased in *A. fumigatus*-exposed cells (Fig. 3.3A) while proteins involved in RNA processing and the ribosome made up the vast majority of proteins that were decreased in abundance (Fig. 3.3B)

In the *P. aeruginosa*-exposed group, there was an increase in the relative abundance of proteins associated with the immune system, detoxification and protein transport (Fig. 3.3C) and a decrease in RNA processing, translation and endocytosis (Fig. 3.3D. Thus, while some responses appear to be a generalized response to pathogens, *A. fumigatus* and *P. aeruginosa* also illicit a pathogen-specific response in A549 cells.

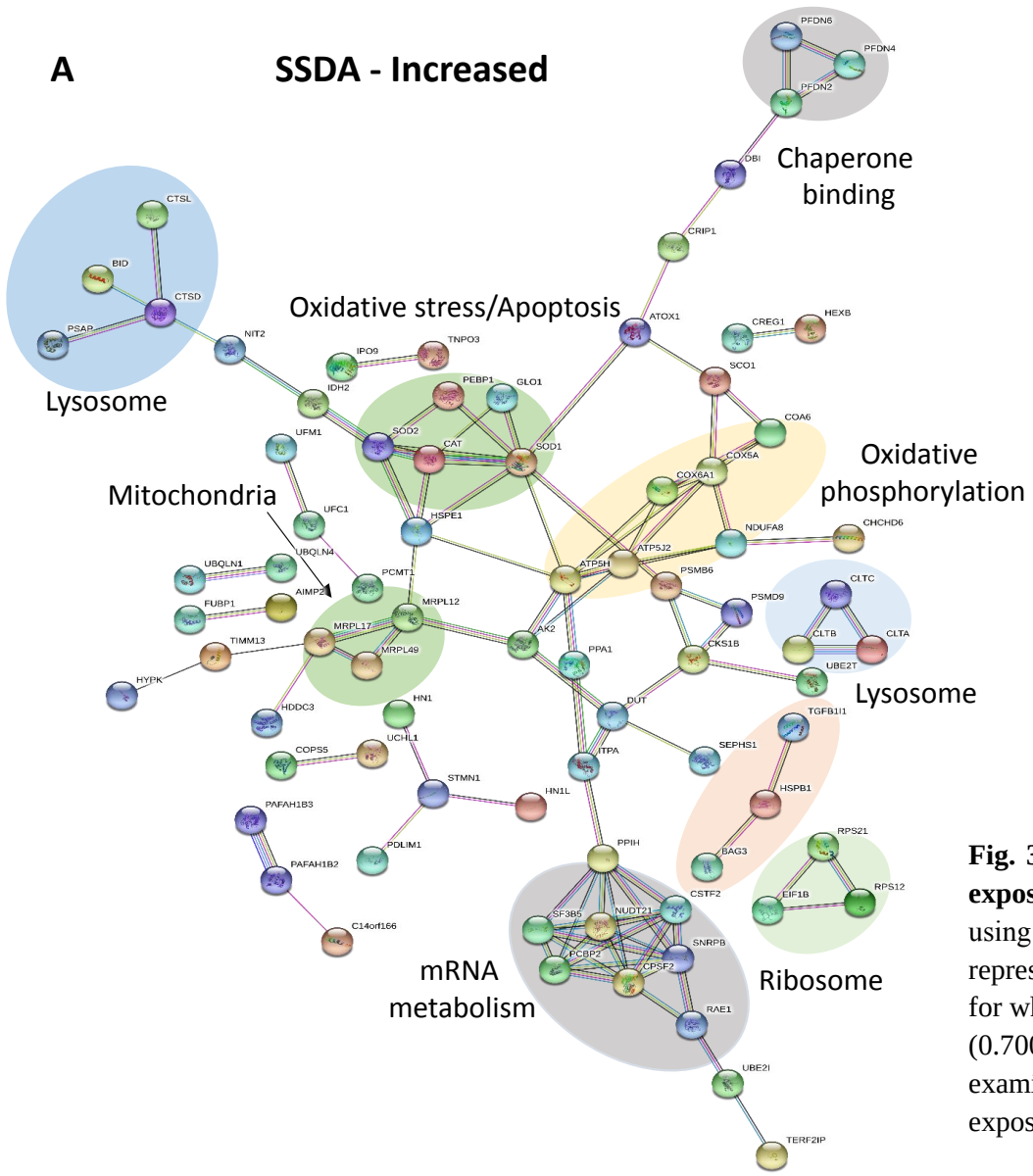

Fig. 3.3 Interaction network analysis of proteins identified in unexposed and pathogen-exposed A549 cells. Protein interaction information was obtained from the STRING database using gene lists extracted from SSDA proteins from Student's t tests ($p < 0.05$). Each node represents a protein and each connecting line represents an interaction, the extent of evidence for which is represented by the width of the line. A high confidence minimum interaction score (0.700) was applied. Statistically enriched KEGG and Gene Ontology (GO) descriptors were examined to identify clusters of proteins enriched between unexposed A549 cells and A549 cells exposed to *A. fumigatus* (A and B) and *P. aeruginosa* (C and D).

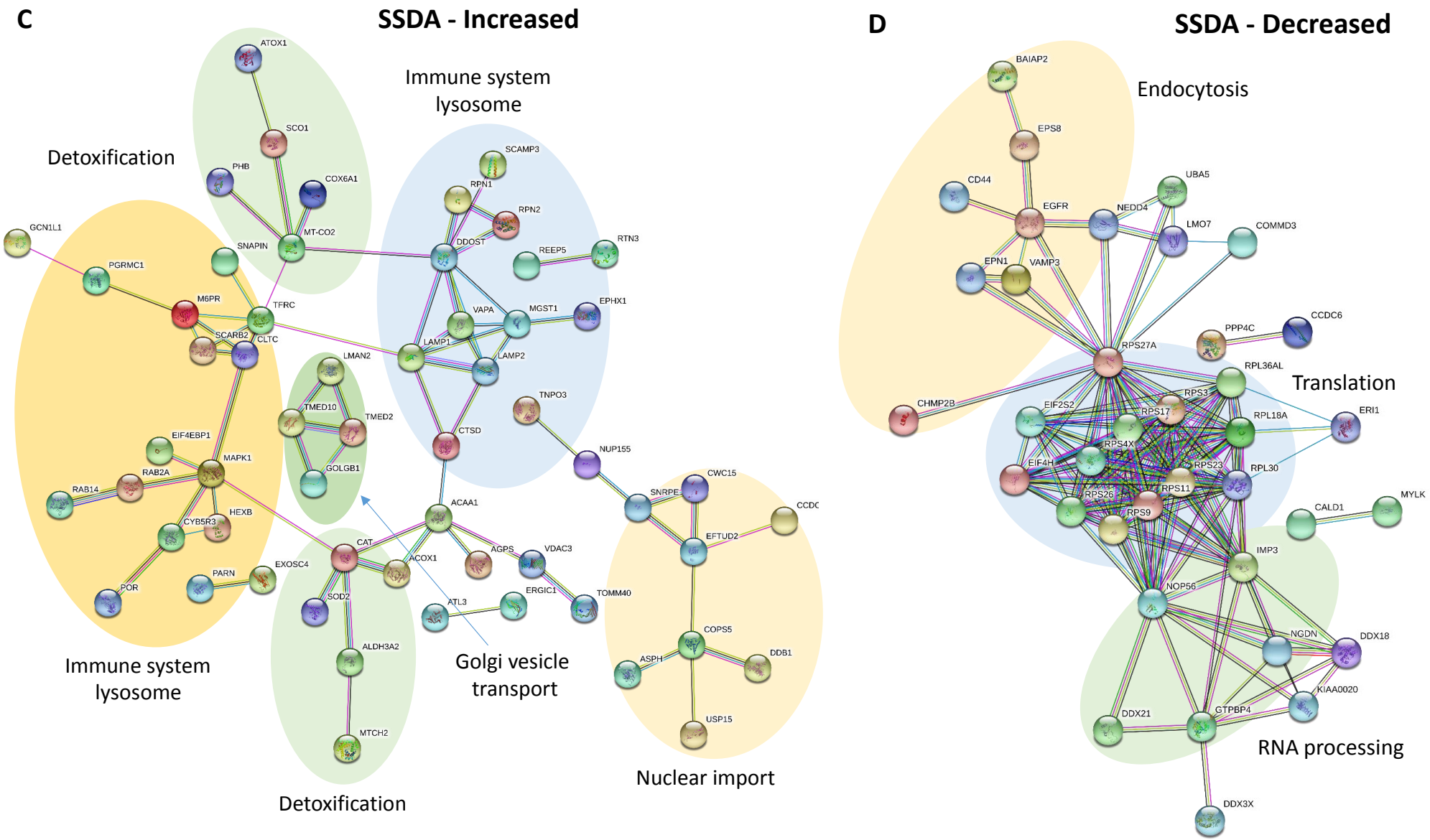
C
SSDA - Increased
Detoxification
Immune system lysosome
Immune system lysosome
Golgi vesicle transport
Nuclear import
Detoxification
ATOX1
SCO1
PHB
COX6A1
MT-CO2
GCN1L1
PGRMC1
SNAPIN
M6PR
TFRC
SCARB2
CLTC
SCAMP3
RPN1
RPN2
DDOST
REEP5
RTN3
VAPA
MGST1
EPHX1
LAMP1
LAMP2
LMAN2
TMED10
TMED2
GOLGB1
CTSD
TNPO3
NUP155
CWC15
SNRPE
CCDC
EFTUD2
ACAA1
CAT
ACOX1
AGPS
VDAC3
ERGIC1
TOMM40
ATL3
SOD2
ALDH3A2
MTCH2
COPS5
ASPH
DDB1
USP15
EIF4EBP1
MAPK1
RAB2A
RAB14
CYB5R3
HEXB
POR
PARN
EXOSC4
D
SSDA - Decreased
Endocytosis
Translation
RNA processing
BAIAP2
EPS8
CD44
EGFR
NEDD4
UBA5
LMO7
COMMD3
EPN1
VAMP3
PPP4C
CCDC6
RPS27A
RPL36AL
CHMP2B
EIF2S2
RPS3
RPS17
RPL18A
ERI1
RPS4X
EIF4H
RPS23
RPL30
RPS26
RPS11
RPS9
CALD1
MYLK
IMP3
NOP56
NGDN
DDX18
KIAA0020
DDX21
GTPBP4
DDX3X

Enrichment analysis on SSDA proteins between *A. fumigatus*-exposed or *P. aeruginosa*-exposed groups and unexposed groups identified changes in several pathways and processes. These pathways are depicted in KEGG maps (Fig. 3.4A-3.5D) and the names of proteins affected in the processes and included in the KEGG maps are listed in Table 3.3A-3.4D Changes in the differential abundance of these proteins are included in Table A 3.3B-D. The "Huntington's disease" pathway, which represents mitochondrial stress, and the lysosome pathway were upregulated in both pathogen-exposed groups compared to the control (Fig. 3.4A and 3.4B, Tabe 3.3A and 3.3B and Fig. 3.5A and 3.5B, Table 3.4A and 3.4B). A decrease in the relative abundance of proteins associated with the "ribosome" pathway was evident in both pathogen-exposed groups compared to the controls (Fig. 3.4C and 3.5C, Table 3.3C and Table 3.5C). In the *P. aeruginosa*-exposed groups, but not the *A. fumigatus*-exposed groups, the relative abundance of several proteins involved in the "endocytosis" pathway were increased (Fig. 3.5D, Table 3.4D). The networks and pathways generated in STRING and KEGG respectively highlight the similarities and differences that occur in A549 cells in response to the fungus and the bacteria.

Fig. 3.4A

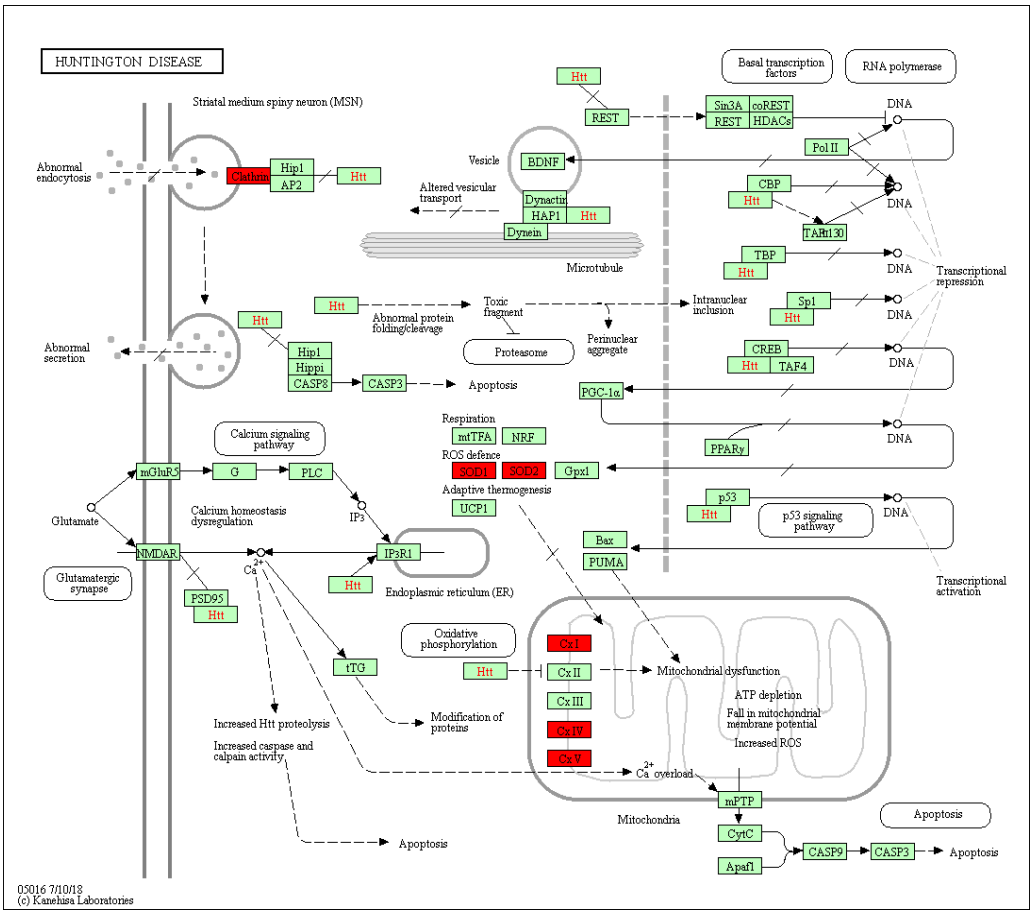

Fig. 3.4B

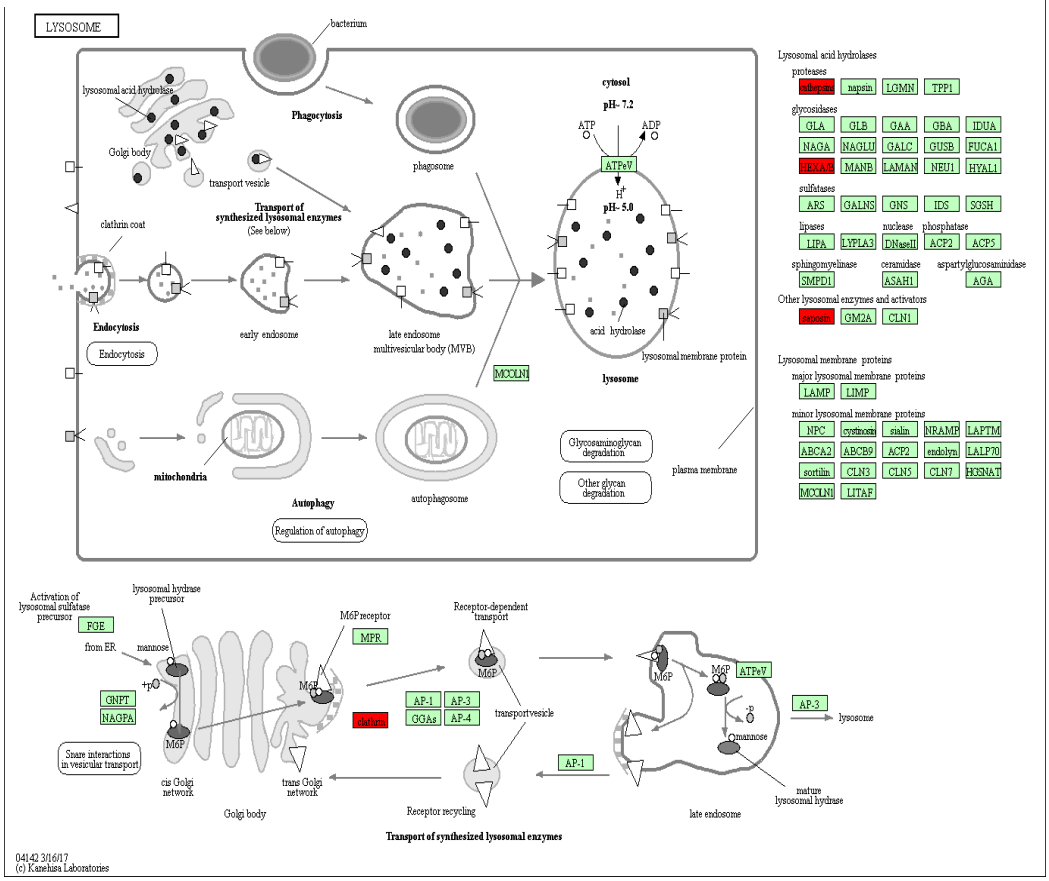

Fig. 3.4C

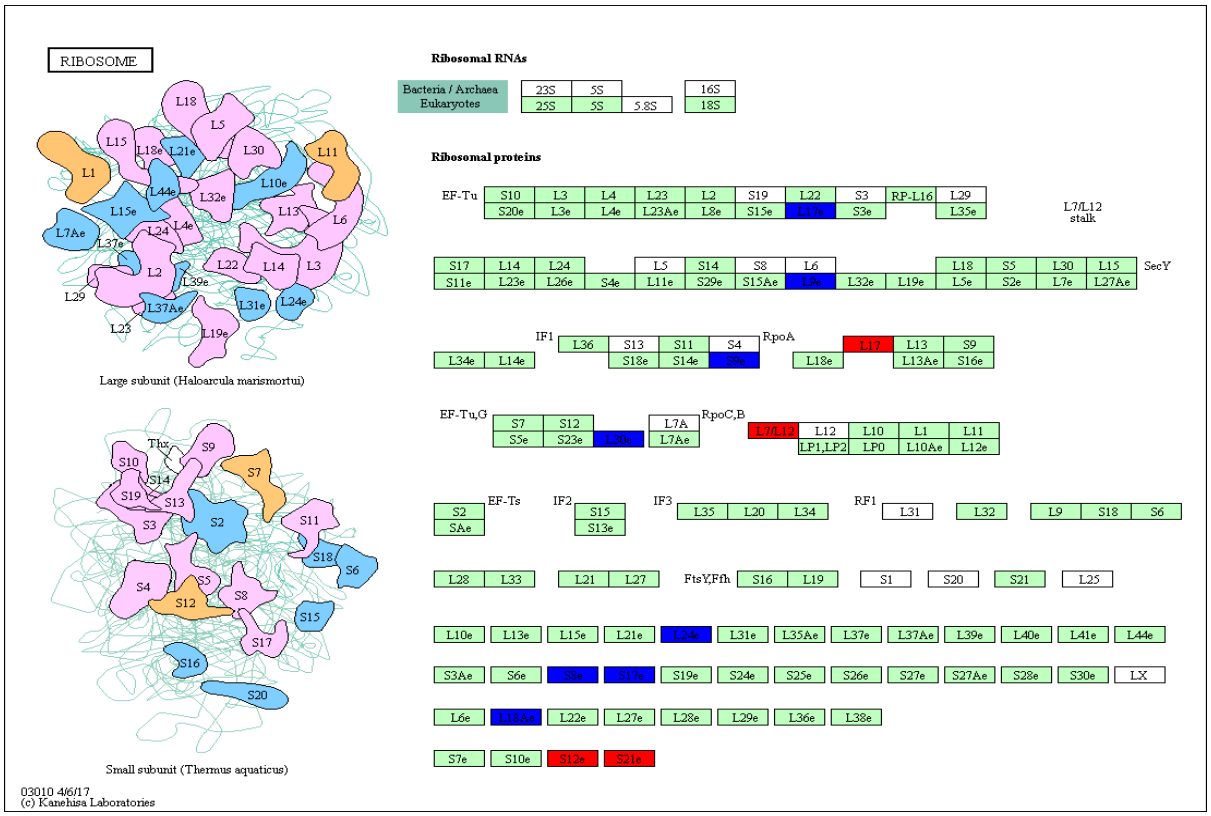

Fig. 3.4 KEGG mapping depicting proteins associated with Huntington's disease, the lysosome pathway and the ribosome. A distinct increase (red) in levels of SSDA proteins involved in the Huntington's disease pathway (A) and the lysosome pathway (B) in *A. fumigatus*-exposed A549 cells compared unexposed A549 cells was observed. The relative abundance of proteins associated with the ribosome was decreased (blue) (C).

Table 3.3A List of proteins involved in Huntington's disease. SSDA proteins arising from comparisons between *A. fumigatus*-exposed A549 cells and unexposed cells and highlighted in the KEGG map depicting Huntington's disease are listed.

Gene name	Protein name
ACTR1A	actin related protein 1A
ATP5PD	ATP synthase peripheral stalk subunit d
CLTA	clathrin light chain A
CLTB	clathrin light chain B
CLTC	clathrin heavy chain
COX6A1	cytochrome c oxidase subunit 6A1
NDUFA8	NADH:ubiquinone oxidoreductase subunit A8
NDUFV2	NADH:ubiquinone oxidoreductase core subunit V2
SOD1	superoxide dismutase 1
SOD2	superoxide dismutase 2
COX5A	cytochrome c oxidase subunit 5A

Table 3.3B List of proteins involved in lysosomes. SSDS proteins arising from comparisons between *A. fumigatus*-exposed A549 cells and unexposed cells and highlighted in the KEGG map depicting the lysosome are listed.

Gene name	Protein name
CLTA	clathrin light chain A
CLTB	clathrin light chain B
CLTC	clathrin heavy chain
CTSD	cathepsin D
CTSL	cathepsin L
HEXB	hexosaminidase subunit beta
PSAP	prosaposin

Table 3.3C List of proteins involved in Ribosomes. SSDS proteins arising from comparisons between *A. fumigatus*-exposed a549 cells and unexposed cells and highlighted in the KEGG map depicting ribosomes are listed.

Gene name	Protein name
RPL9	ribosomal protein L9
RPL17	ribosomal protein L17
RPL18A	ribosomal protein L18a
RPL24	ribosomal protein L24
RPL30	ribosomal protein L30
MRPL12	mitochondrial ribosomal protein L12
RPS8	ribosomal protein S8
RPS9	ribosomal protein S9
RPS12	ribosomal protein S12
RPS17	ribosomal protein S17
RPS21	ribosomal protein S21
RPS26	ribosomal protein S26
RPS27A	ribosomal protein S27a
RPS28	ribosomal protein S28
MRPL17	mitochondrial ribosomal protein L17

Fig. 3.5A

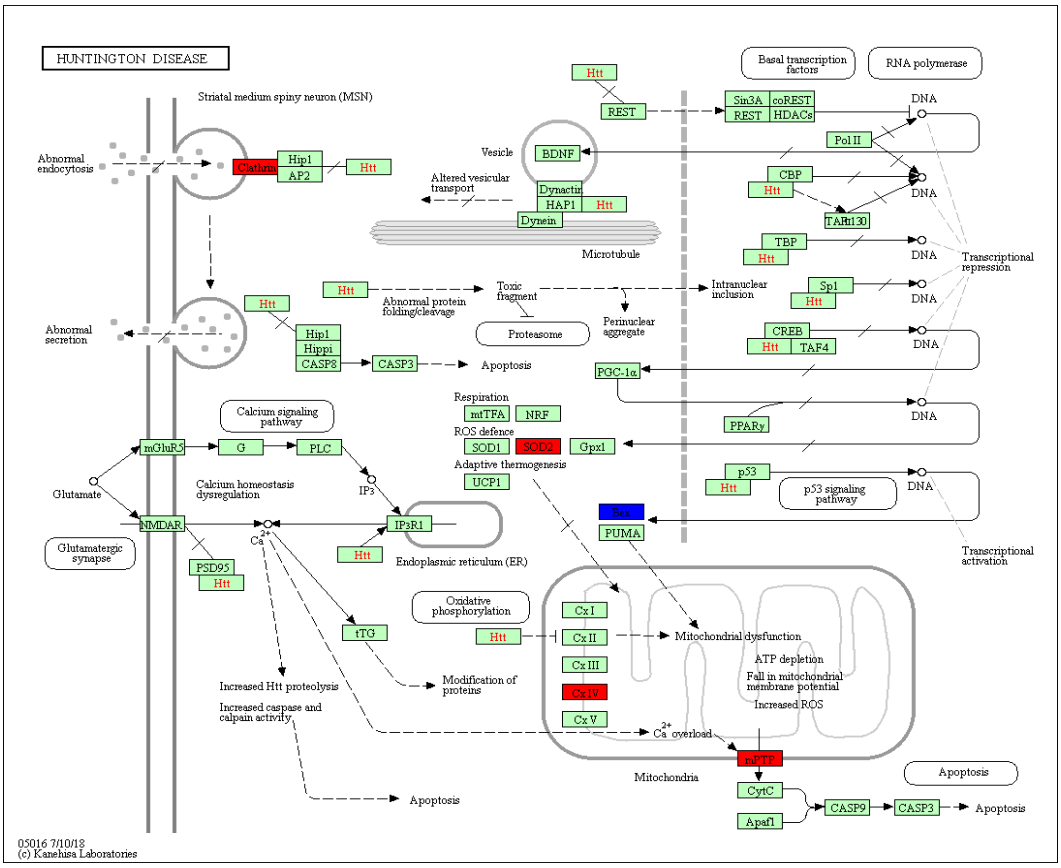

Fig. 3.5B

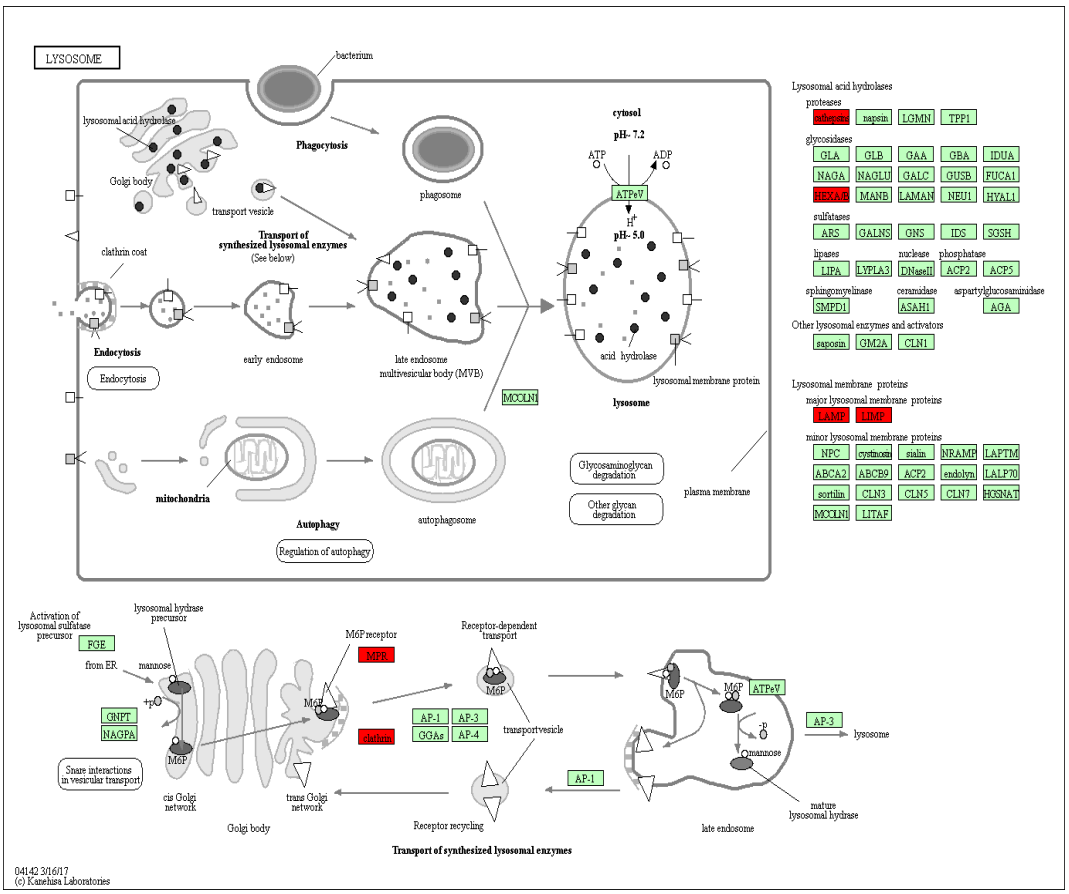

Fig. 3.5C

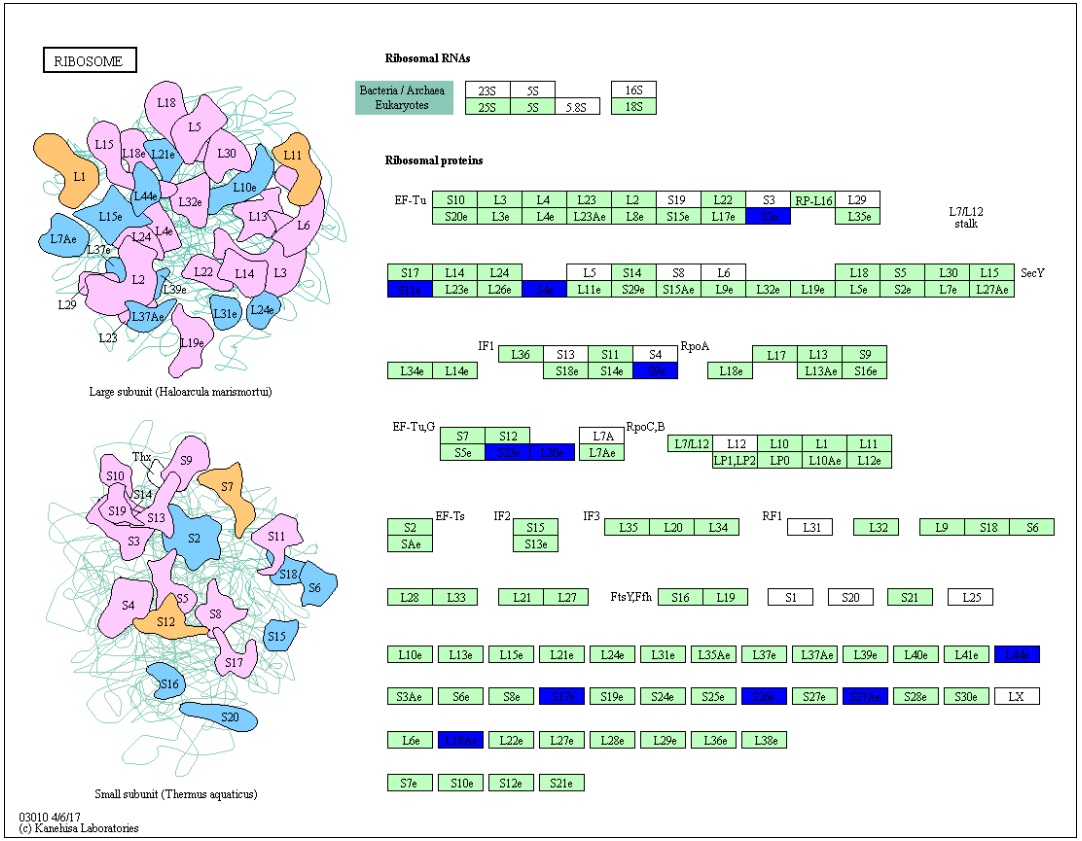

Fig. 3.5D

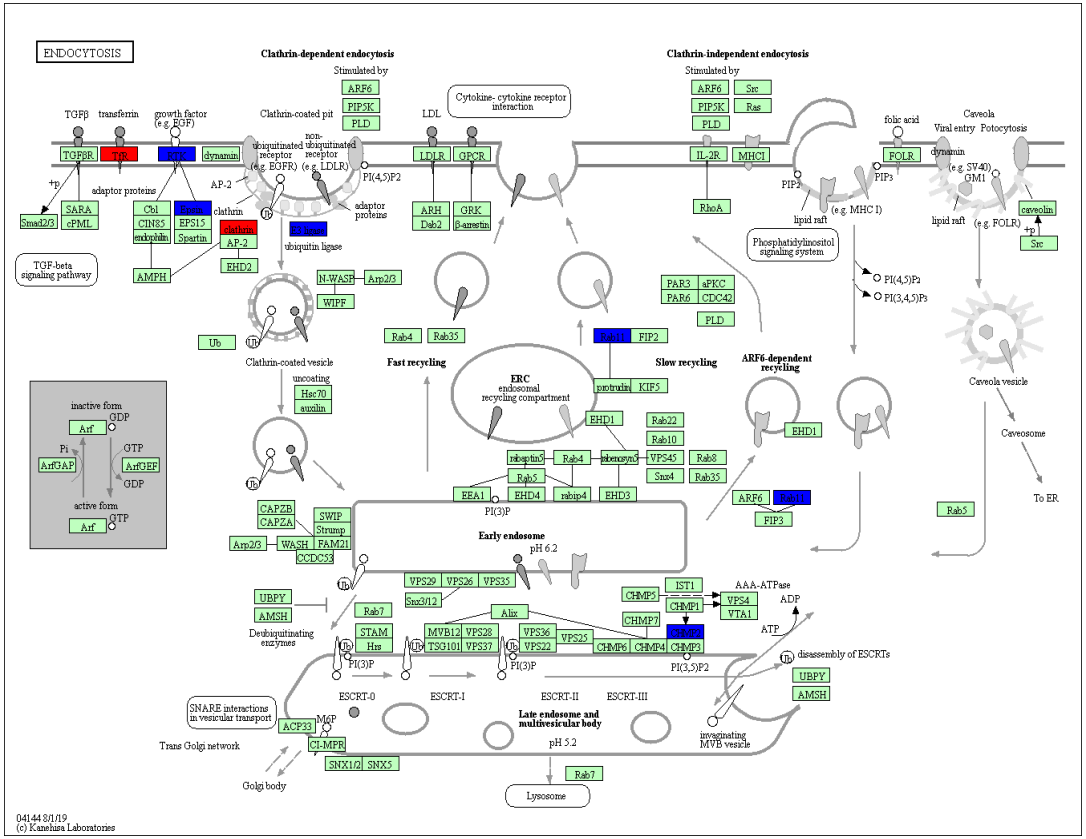

Fig. 3.5 KEGG mapping depicting proteins associated with Huntington's disease, the lysosome pathway, the ribosome and endocytosis A distinct increase (red) in levels of SSDA proteins involved in the Huntington's disease pathway (A) and the lysosome pathway (B) in *P. aeruginosa*-exposed A549 cells compared unexposed A549 cells was observed. The relative abundance of proteins associated with the ribosome were decreased (C) and the endocytosis pathway (D) were decreased (blue).

Table 3.4A List of proteins involved in Huntington's disease. SSDA proteins arising from comparisons between *P. aeruginosa*-exposed A549 cells and unexposed cells and highlighted in the KEGG map depicting Huntington's disease are listed.

Gene name	Protein name
CLTC	clathrin heavy chain
COX6A1	cytochrome c oxidase subunit 6A1
COX2	cytochrome c oxidase subunit II
BAX	BCL2 associated X, apoptosis regulator
SOD2	superoxide dismutase 2
VDAC3	voltage dependent anion channel 3

Table 3.4B List of proteins involved in the Lysosome. SSDA proteins arising from comparisons between *P. aeruginosa*-exposed A549 cells and unexposed cells and highlighted in the KEGG map depicting the lysosome are listed.

Gene name	Protein name
CLTC	clathrin heavy chain
CTSD	cathepsin D
HEXB	hexosaminidase subunit beta
LAMP1	lysosomal associated membrane protein 1
LAMP2	lysosomal associated membrane protein 2
M6PR	mannose-6-phosphate receptor, cation dependent
SCARB2	scavenger receptor class B member 2

Table 3.4C List of proteins involved in the Ribosome. SSDA proteins arising from comparisons between *P. aeruginosa*-exposed A549 cells and unexposed cells and highlighted in the KEGG map depicting the ribosome are listed.

Gene name	Protein name
RPL18A	ribosomal protein L18a
RPL30	ribosomal protein L30
RPL36AL	ribosomal protein L36a like
RPS3	ribosomal protein S3
RPS4X	ribosomal protein S4 X-linked
RPS9	ribosomal protein S9
RPS11	ribosomal protein S11
RPS17	ribosomal protein S17
RPS23	ribosomal protein S23
RPS26	ribosomal protein S26
RPS27A	ribosomal protein S27a

Table 3.4D List of proteins involved in Endocytosis. SSDA proteins arising from comparisons between *P. aeruginosa*-exposed A549 cells and unexposed cells and highlighted in the KEGG map depicting endocytosis are listed.

Gene name	Protein name
CLTC	clathrin heavy chain
EGFR	epidermal growth factor receptor
CHMP2B	charged multivesicular body protein 2B
EPN1	epsin 1
NEDD4	NEDD4 E3 ubiquitin protein ligase
TFRC	transferrin receptor
RAB11B	RAB11B, member RAS oncogene family

A distinct change in the morphology of cells exposed to *A. fumigatus* or *P. aeruginosa* for 12 hours was observed using an inverted microscope (Fig 3.6A-C). The typical morphology of A549 cells under normal conditions is characterized by flat, spread-out, cobble stone-like shaped cell, adhered to the surface of the flask. Unexposed A549 cells displayed this morphology (Fig. 3.6A). Cells exposed to *A. fumigatus* for 12 hours (Fig. 3.6B), appear to retain their shape, many had begun to contract, but remained adhered to the surface of the flask. Cells exposed to *P. aeruginosa* for 12 hours (Fig. 3.6C) had contracted, become rounded and were beginning to detatch from the surface of the flask.

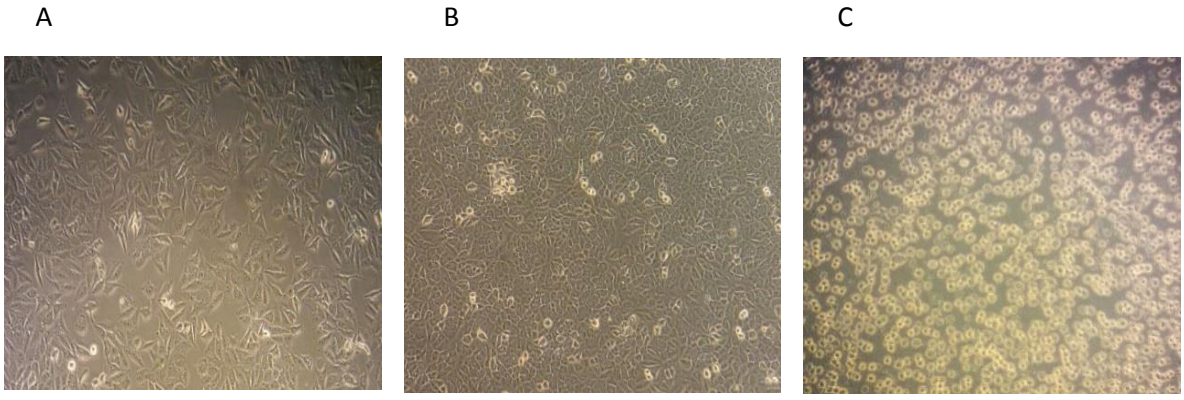

Fig. 3.6 The morphological response of A549 cells to pathogen exposure The morphology of unexposed A549 cells **(A)** and post (12 hours) - exposure to *A. fumigatus* **(B)** and *P. aeruginosa* (C) show distinct differences in the way host cells respond to each pathogen. Unexposed cells are large and spread out in comparison to pathogen-exposed cells. Many of the cells exposed to *A. fumigatus* were beginning to contract but remained adhered to the surface. Most cells exposed to *P. aeruginosa* had contracted and were beginning to detach from the surface. (Magnification power 40X).

3.3.2 Part two - Analysis of the proteomic response of A549 cells to sequential exposure by *A. fumigatus* and *P. aeruginosa*

With a view to comparing the proteomic response between A549 cells exposed to *A. fumigatus* or *P. aeruginosa* with that of exposure to both pathogens simultaneously, A549 cells were co-exposed to *A. fumigatus* and *P. aeruginosa* and incubated for 12 hours (n = 3). LFQ proteomics performed on A549 cells exposed to the co-culture revealed that a significant proportion (40.7 %) of the protein identified in co-culture samples were of bacterial origin. In total, 2824 proteins were identified, 1,720 were of *H. sapiens* origin, 1163 were of *P. aeruginosa* origin and one was of *A. fumigatus* origin. The abundance of bacterial proteins detected in the samples treated with *P. aeruginosa* only for 12 hours was 3.1% (63 bacterial proteins out of 2099 proteins detected).

Histograms were generated based on $\log_2$ transformed LFQ intensity values for all identified proteins in Perseus to determine the distribution of the data. The high frequency of bacterial protein abundance observed in the co-culture samples (Fig. 3.7A ii), compared to that of the samples treated with *P. aeruginosa* only (Fig. 3.7A iii), suggest an increase in replication occurs when *P. aeruginosa* is co-cultured with *A. fumigatus*. To validate this finding, colony forming unit (CFU) counts were performed on samples taken from the A549 cell cultures, in the presence or absence of *A. fumigatus*. There was a 78-fold increase in bacterial burden when *P. aeruginosa* was incubated with *A. fumigatus* and A549 cells compared to that found when *P. aeruginosa* was incubated with A549 cells alone (Fig. 3.7B).

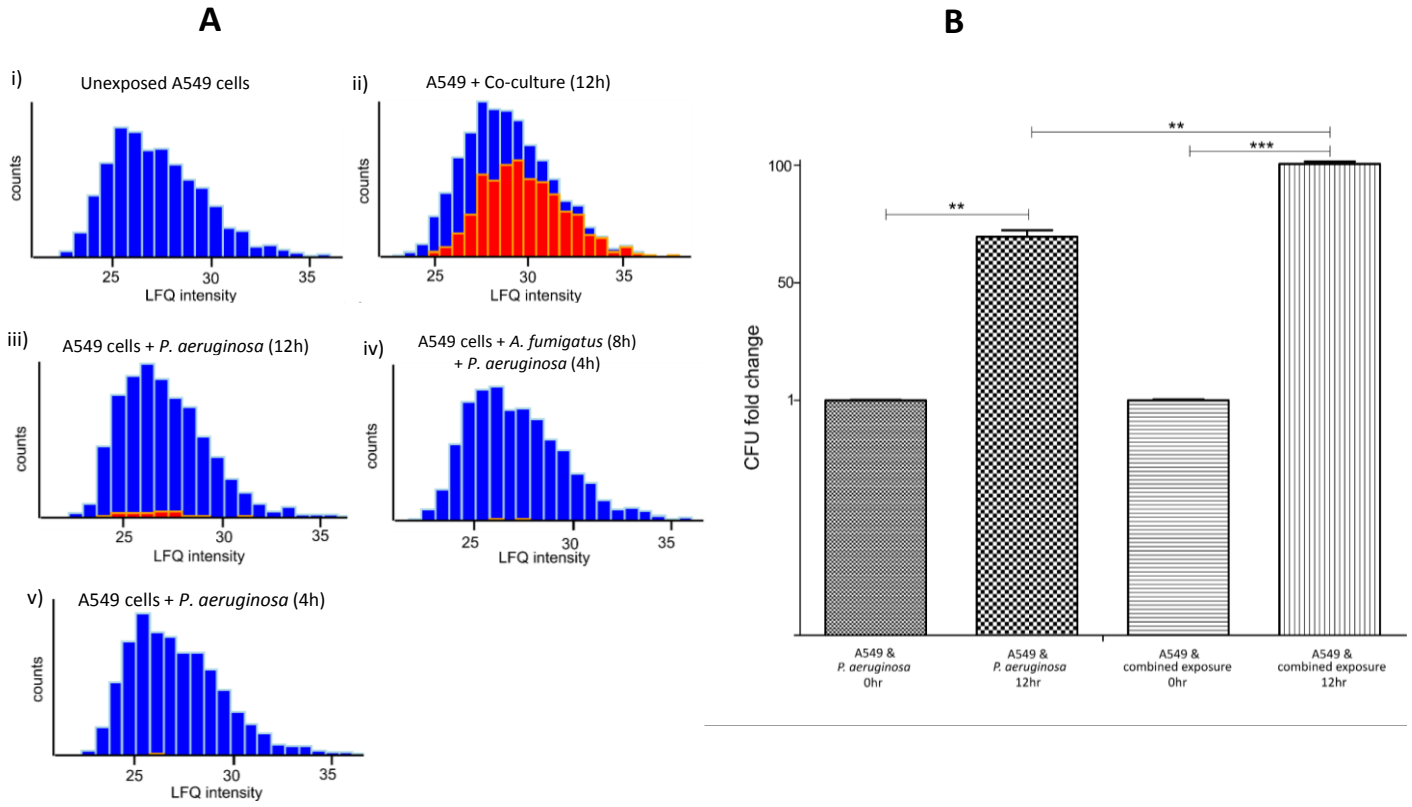

Fig. 3.7 Histograms displaying proportion of *P. aeruginosa* proteins and increases in bacterial burden Histograms (i-v) of log_2 transformed LFQ intensity values displaying the proportion of *P. aeruginosa* proteins (red) present in representative samples comprising A549 proteins (blue) **(A).** Bacterial proteins were not present in unexposed A549 cells (i). Of the total number of proteins identified, 41 % were of bacterial origin after A549 cells were exposed to *P. aeruginosa* and *A. fumigatus* for 12 hours (ii). Of the total number of proteins identified, 3.1 % were of bacterial origin where A549 cells were exposed to *P. aeruginosa* for 12 hours (iii). Of the total number of proteins identified, 0.26 % were of bacterial origin where A549 cells were exposed *A. fumigatus* for 8 hours and *P. aeruginosa* for 4 hours, respectively (iv) or *P. aeruginosa* for 4 hours (v). A549 cells were incubated with *P. aeruginosa* or with *P. aeruginosa* and *A. fumigatus* for 12 hours **(B).** A CFU count performed on aliquots taken from the cultures at zero hours and 12 hours revealed a 78-fold increase in the rate of bacterial replication where *P. aeruginosa* was co-cultured with *A. fumigatus* than on its own.

To investigate whether the increase in bacterial density observed in the co-culture was a growth-promoting effect mediated by the fungus or due to lack of killing by the A549 cells, *P. aeruginosa* was cultured in cell culture medium for 12 hours without the presence of A549 cells or *A. fumigatus*, and separately, in co-culture with *A. fumigatus* conidia (n = 4). There was a five-fold increase in the replication of *P. aeruginosa* when *A. fumigatus* was present (Fig. 3.8A). To determine if the physical presence of *A. fumigatus* conidia, or the secretome of the fungus post-contact with *P. aeruginosa*, was responsible for inducing bacterial-growth proliferation, *P. aeruginosa* was incubated for 12 hours in the supernatant from a 12-hour co-culture of *A. fumigatus* and *P. aeruginosa* and in the supernatant from a 12-hour *P. aeruginosa* culture (n = 4). CFU counts performed after 12 hours revealed no growth-promoting effect on the bacteria incubated with the supernatant from the co-culture and a slight increase in bacteria cultured in its own supernatant (Fig. 3.8B). These findings suggest that *A. fumigatus* conidia promote bacterial growth under these conditions and that their presence is necessary to mediate this growth-promoting effect.

In order to examine the proteomic effect of *P. aeruginosa* and *A. fumigatus* on A549 cells, it was imperative to determine the time-point at which *P. aeruginosa* begins to grow exponentially in co-culture so that the impact of bacterial proliferation would not influence the proteomic analysis of the A549 cells. CFU counts were performed at two-hour time intervals from cultures of *P. aeruginosa* in the absence and presence of *A. fumigatus* (n = 4). By four hours, the rate of bacterial replication had begun to increase rapidly when co-cultured in the presence of *A. fumigatus* (Fig. 3.8C). Based on these findings, an alternative experimental protocol was designed, which took into consideration the point at which *P. aeruginosa* begins to proliferate in the presence of *A. fumigatus*. Because the negative impact of *A. fumigatus* conidia on A549 cells was far less drastic than that of *P. aeruginosa* after 12 hours (Fig. 3.6C), the length of time in which the A549 cells could be exposed to conidia while maintaining cellular integrity was longer than that of *P. aeruginosa*.

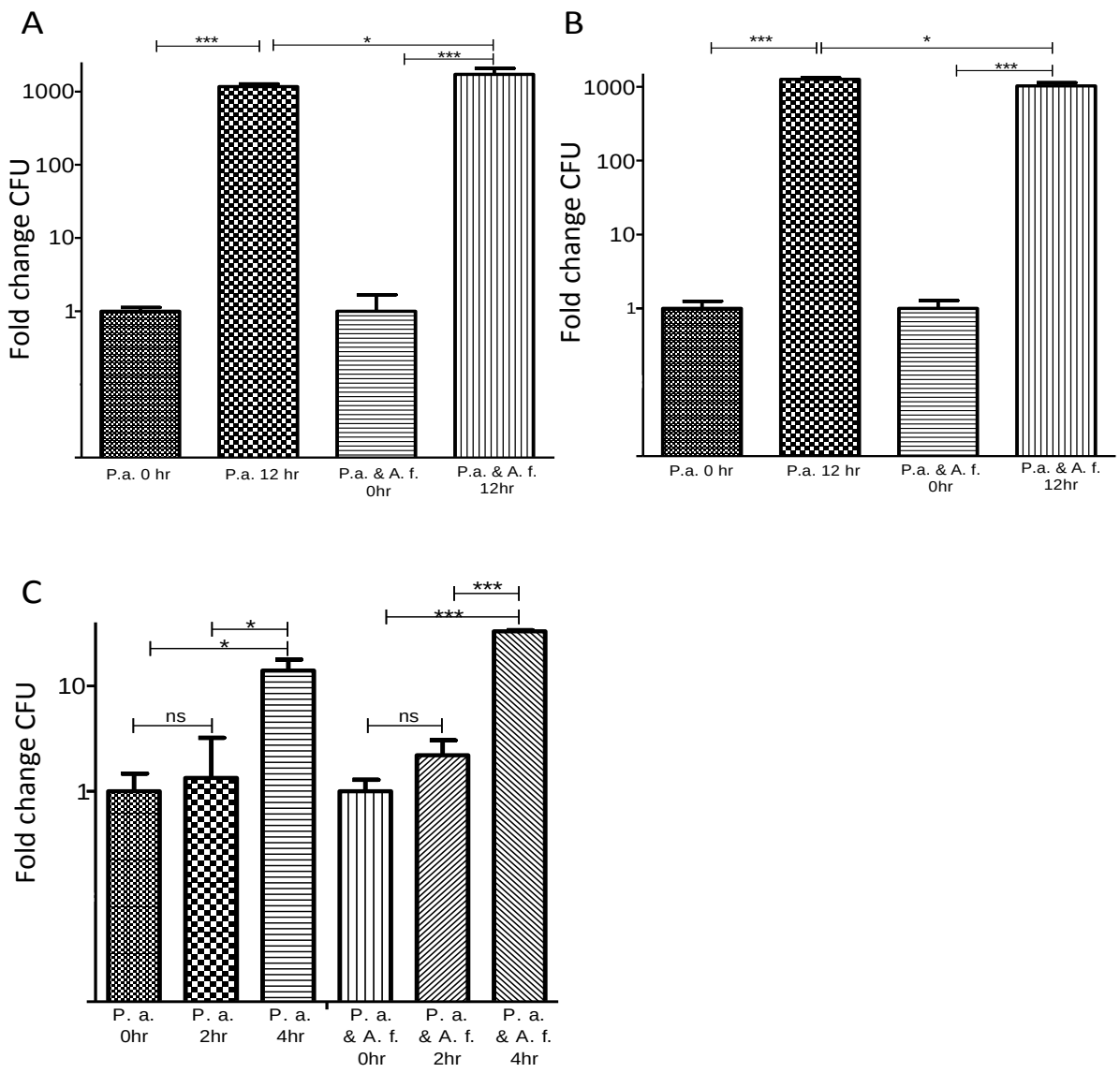

Fig. 3.8 *P. aeruginosa* CFU counts. *P. aeruginosa* (P. a.) was cultured with and without *A. fumigatus* (A. f.) for 12 hours in the absence of A549 cells. CFU counts performed at zero and 12 hours revealed a five-fold increase in the replication of *P. aeruginosa* cultured in the presence of *A. fumigatus* than alone **(A)**. *P. aeruginosa* was cultured in supernatant produced in a 12-hour *P. aeruginosa* culture or a in co-culture with *A. fumigatus*. Compared to that cultured in the co-culture supernatant, bacterial growth rate increased two-fold when cultured in its own supernatant **(B).** *P. aeruginosa* was cultured with and without *A. fumigatus* for 4 hours in the absence of A549 cells. CFU counts were performed at zero, two and four hours. By four hours, the growth of *P. aeruginosa* had increased by 15-fold when cultured with *A. fumigatus* compared to that when cultured alone **(C).** * $p < 0.05$ **$p < 0.01$ *** $p < 0.00$ ns: not significant

With this in mind, A549 cells were incubated with *A. fumigatus* conidia for eight hours, at which time *P. aeruginosa* was added to the culture and incubated for a further four hours (n = 3). LFQ proteomics was performed on A549 cells following the sequential exposure to *A. fumigatus* and *P. aeruginosa*. The proteomic profile was compared with that of cells exposed to *A. fumigatus* for eight hours and *P. aeruginosa* for four hours and unexposed cells (control) (n = 3). The proportion of bacterial proteins detected on this occasion was 0.26% (Fig. 3.5 iv and v).

Proteomic analysis was performed as described in section 2.8.3. In total, 4048 proteins were identified initially, of which 2264 remained after filtering and processing (Table A3.3A). Proteins identified in Perseus as being of non-human origin (i.e. with Uniprot IDs for *A. fumigatus* or *P. aeruginosa*), were considered contaminants and removed from further analysis. Of the 2264 proteins identified post-imputation, 285 proteins in the *A. fumigatus*-exposed group (Table A 3.3B), 497 proteins in the *P. aeruginosa*-exposed group (Table A 3.3C) and 254 proteins in sequentially exposed group (Table A3.3D) were determined to be statistically significant ($p<0.05$) differentially abundant (SSDA) with a fold change of +/- 1.5. SSDA protein identified from the pair wise Student's t-tests were searched against the STRING and KEGG databases and used to identify biological pathways and processes over-represented in a particular group.

A principal component analysis (PCA) of all identified proteins resolved distinct differences between the proteomes of each groups (Fig. 3.9A). Components 1 and 2 accounted for 48.2% of the total variance within the data, and all replicates resolved into their corresponding samples. The control sample displayed a clear divergence to those that were challenged with *A. fumigatus* and/or *P. aeruginosa*. A distinct difference was also observed between the sequentially exposed A549 cells and cells exposed to *A. fumigatus* or *P. aeruginosa*.

Hierarchical clustering was performed on the z-scored normalised LFQ intensity values for the 618 SSDA proteins identified as described in section 2.8.3.1 (ANOVA; Benjamini Hochberg procedure, FDR cut-off value of ≤ 0.05). All three biological replicates resolved into their respective sample. Nine (A-I) protein clusters based on protein abundance profile similarities (Fig. 3.9B) were also resolved. GO and KEGG term

enrichment analysis was performed on all protein clusters with five clusters having enriched terms (Cluster B, F-I), with each cluster having a representative process or pathway characteristic to that group (Fig. 3.9C). These include RNA metabolic processing (Cluster B), protein processing (Cluster F), carbon metabolism (Cluster G), mitochondrial processes (Cluster H), pathogen uptake and processing (Cluster I). Details of all clusters are included in Table A3.4A and Table A3.4B.

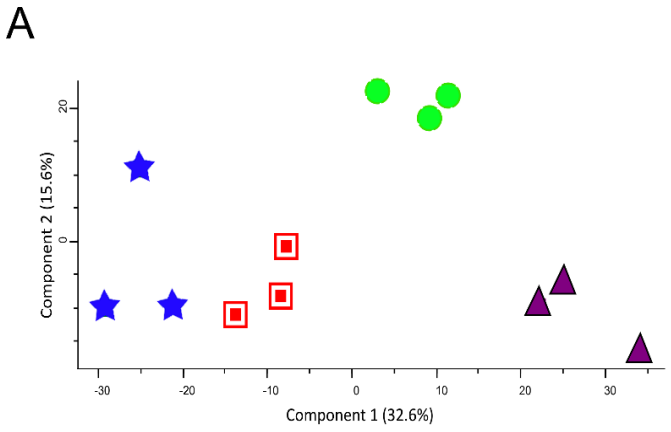

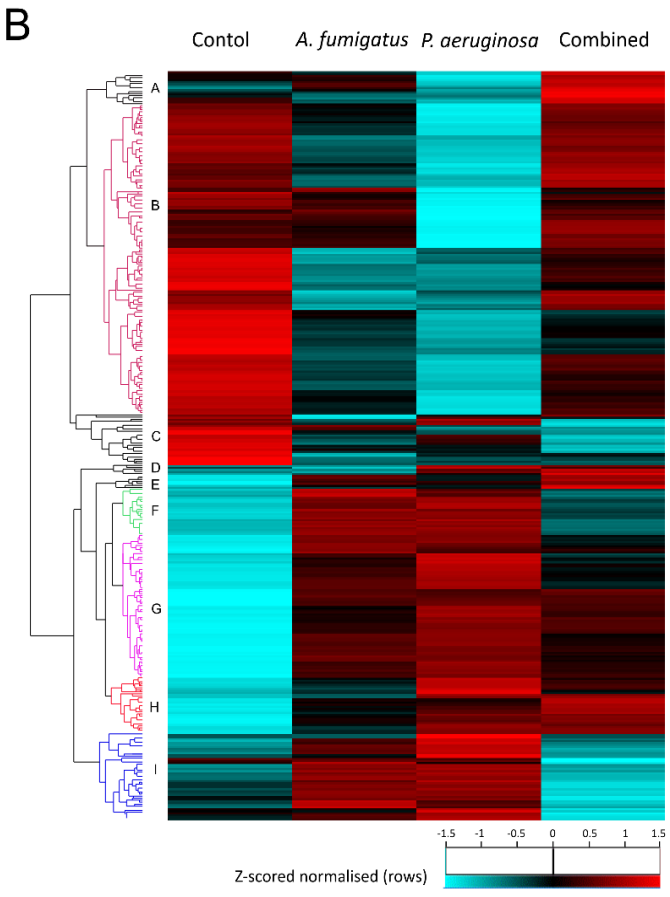

C

Cluster ID	Term	P-value	Enrichment
B	Nucleic acid metabolic process	2.52E-15	1.3229
	Regulation of gene expression	3.90E-08	1.4516
F	Endoplasmic reticulum part	3.37E-05	3.8063
	Catalytic activity	2.01E-05	1.8528
G	Small molecule metabolic process	3.51E-06	1.6233
	Vesicle coat	0.000192	4.0734
	Glycolysis / Gluconeogenesis	4.38E-05	4.1898
H	Oxidation-reduction process	2.20E-09	4.4783
	Mitochondrial part	2.53E-09	3.3956
I	Cell projection	1.72E-08	3.3129
	Hydrolase activity	7.88E-07	2.3333
	Phagosome	1.60E-06	7.5104

Fig. 3.9 PCA, hierarchical clustering and enrichment analysis of A549 cell proteins display distinct differences between the three infection groups Principal component analysis (PCA) of untreated A549 cells (triangles), A549 cells treated with *P. aeruginosa* (stars), *A. fumigatus* (squares) or sequential exposure to both pathogens (circles) (A). A clear distinction can be observed between each of the treated groups and the control. Clusters based on protein-abundance profile similarities were resolved by hierarchical clustering of multi-sample comparisons between the four sample groups of A549 cells (B). Nine clusters (A-I) were resolved comprising proteins that display similar expression profiles across treatments. Of these, five clusters (B, F-I) had statistically enriched gene ontology and KEGG terms associated with them (Table A3.4) and the main terms are summarised for each in Fig. 3.9C.

Within cluster B, GO terms and KEGG pathway analysis resolved 256 proteins with terms associated with RNA processes including gene expression, post-transcriptional regulation, mRNA splicing, translation initiation, ribosomes and transport. Proteins involved in these processes were distinctly less abundant in *P. aeruginosa*-exposed A549 cells as compared to the other groups, indicating attenuation of mRNA processing and translational machinery in A549 cells treated with the bacteria only. Proteins present in cluster F were primarily involved with protein modifications, protein folding, protein degradation and export from the endoplasmic reticulum (ER). The relative abundance of proteins associated with protein processing in the ER was greater in *A. fumigatus*- and *P. aeruginosa*-exposed A549 cells compared to the sequentially infected group and the controls. This trend is reflected in the KEGG pathway analysis. The relative abundance of proteins involved in protein trafficking and vesicle-mediated transport, was higher in all infection groups compared to the control (Cluster G). These processes are depicted in KEGG pathways (Fig. 3.10A-M). The names of proteins affected in the processes included in the KEGG maps are listed in Table 3.5A-3.3M. Changes in the differential abundance of these proteins are included in Table A 3.3B-D.

The relative abundance of proteins associated with energy production by carbohydrate and fatty acid metabolism, and energy derivation by oxidation was increased in the three infected groups compared to the control (Fig. 3.10A-D, Table 3.5A-D). These pathways were most prominent in the *P. aeruginosa*-exposed group (Fig. 3.9B, Cluster G). Amongst the GO terms included in this cluster was oxoacid, cellular ketone and carbohydrate metabolic process and the KEGG glycolysis/gluconeogenesis pathway.

A.1

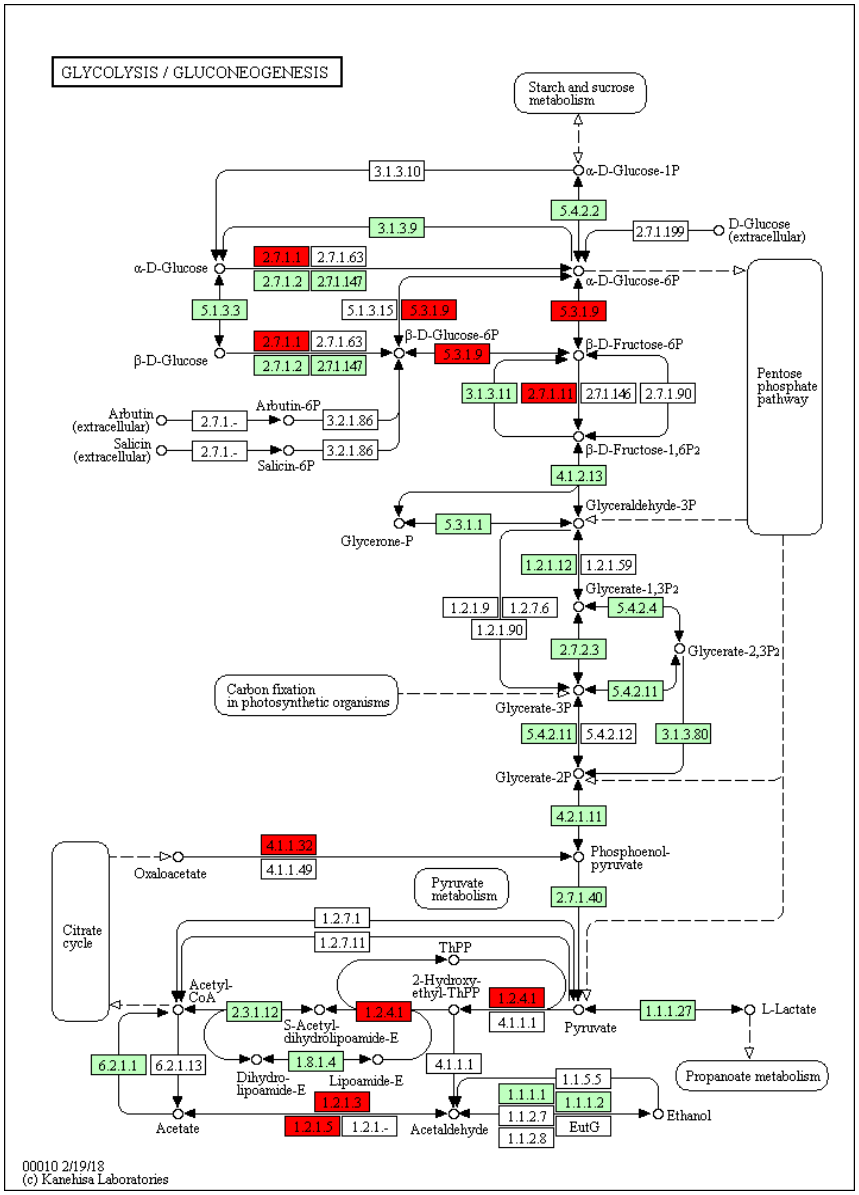
GLYCOLYSIS / GLUCONEOGENESIS
Starch and sucrose metabolism
α-D-Glucose-1P
D-Glucose (extracellular)
α-D-Glucose
α-D-Glucose-6P
β-D-Glucose
β-D-Glucose-6P
β-D-Fructose-6P
Pentose phosphate pathway
Arbutin (extracellular)
Arbutin-6P
Salicin (extracellular)
Salicin-6P
β-D-Fructose-1,6P2
Glyceraldehyde-3P
Glycerone-P
Glycerate-1,3P2
Glycerate-2,3P2
Carbon fixation in photosynthetic organisms
Glycerate-3P
Glycerate-2P
Phosphoenol-pyruvate
Oxaloacetate
Pyruvate metabolism
Citrate cycle
ThPP
Acetyl-CoA
2-Hydroxy-ethyl-ThPP
S-Acetyl-dihydrolipoamide-E
Pyruvate
L-Lactate
Propanoate metabolism
Dihydro-lipoamide-E
Lipoamide-E
Acetate
Acetaldehyde
Ethanol
EutG
00010 2/19/18
(c) Kanehisa Laboratories

A.2

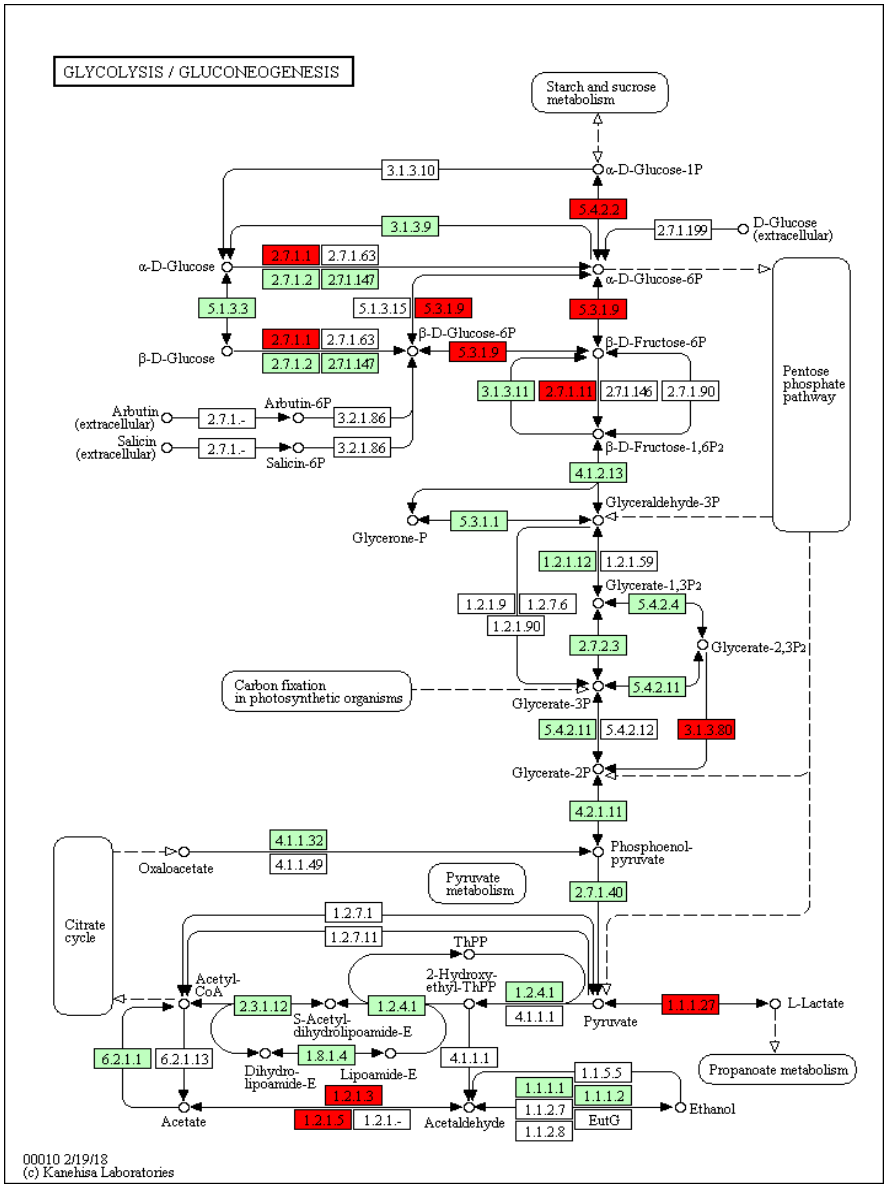
GLYCOLYSIS / GLUCONEOGENESIS
Starch and sucrose metabolism
α-D-Glucose-1P
D-Glucose (extracellular)
α-D-Glucose
α-D-Glucose-6P
β-D-Glucose
β-D-Glucose-6P
β-D-Fructose-6P
Pentose phosphate pathway
Arbutin (extracellular)
Arbutin-6P
Salicin (extracellular)
Salicin-6P
β-D-Fructose-1,6P2
Glyceraldehyde-3P
Glycerone-P
Glycerate-1,3P2
Glycerate-2,3P2
Carbon fixation in photosynthetic organisms
Glycerate-3P
Glycerate-2P
Phosphoenol-pyruvate
Oxaloacetate
Pyruvate metabolism
Citrate cycle
ThPP
Acetyl-CoA
2-Hydroxy-ethyl-ThPP
S-Acetyl-dihydrolipoamide-E
Pyruvate
L-Lactate
Propanoate metabolism
Dihydro-lipoamide-E
Lipoamide-E
Acetate
Acetaldehyde
Ethanol
EutG
00010 2/19/18
(c) Kanehisa Laboratories

A.3

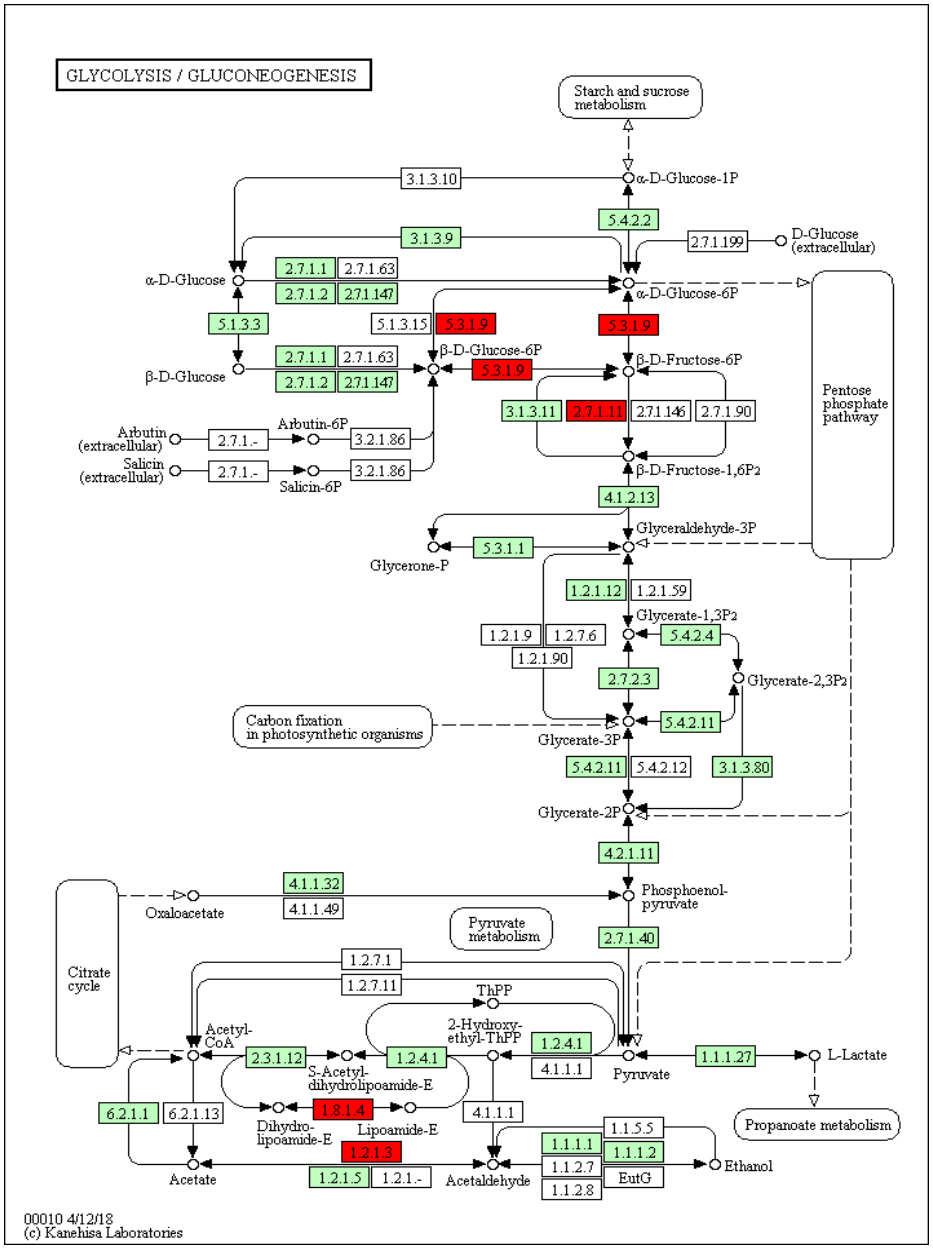

Fig. 3.10A KEGG maps depicting to changes to glycolysis and gluconeogenesis in A549 cells exposed to *A. fumigatus, P. aeruginosa* and sequential exposure to *A. fumigatus* and *P. aeruginosa*. Similarities in the increased levels of SSDA proteins involved in glycolysis and gluconeogenesis pathways between (1) *A. fumigatus*-, (2*) P. aeruginosa*-, and (3) sequentially-exposed A549 cells and the control are identified. Changes to the relative abundance of proteins between the three infected groups of A549 cells were not significant and are thus not depicted here.

Table 3.5A List of proteins involved in glycolysis & gluconeogenesis. SSDA proteins arising from comparisons between the different infection groups of A549 cells and highlighted in the KEGG map depicting glycolysis and gluconeogenesis are listed.

Gene name	Protein name
DLD	dihydrolipoamide dehydrogenase
ALDH2	aldehyde dehydrogenase 2 family member
ALDH1B1	aldehyde dehydrogenase 1 family member B1
ALDH3B1	aldehyde dehydrogenase 3 family member B1
ALDH9A1	aldehyde dehydrogenase 9 family member A1
ALDH3A2	aldehyde dehydrogenase 3 family member A2
GPI	glucose-6-phosphate isomerase
HK1	hexokinase 1
LDHA	lactate dehydrogenase A
PCK2	phosphoenolpyruvate carboxykinase 2, mitochondrial
PDHA1	pyruvate dehydrogenase E1 subunit alpha 1
PFKL	phosphofructokinase, liver type
PGM1	phosphoglucomutase 1
MINPP1	multiple inositol-polyphosphate phosphatase 1

Table 3.5B List of proteins involved in fatty acid degradation. SSDA proteins arising from comparisons between the different infection groups of A549 cells and highlighted in the KEGG map depicting fatty acid degradation are listed.

Gene name	Protein name
ACAA2	acetyl-CoA acyltransferase 2
ECI1	enoyl-CoA delta isomerase 1
ALDH2	aldehyde dehydrogenase 2 family member
ACSL3	acyl-CoA synthetase long chain family member 3
ACSL4	acyl-CoA synthetase long chain family member 4
ALDH1B1	aldehyde dehydrogenase 1 family member B1
ALDH9A1	aldehyde dehydrogenase 9 family member A1
ALDH3A2	aldehyde dehydrogenase 3 family member A2
HADHA	hydroxyacyl-CoA dehydrogenase complex subunit alpha
HADHB	hydroxyacyl-CoA dehydrogenase complex subunit beta
HADH	hydroxyacyl-CoA dehydrogenase
ACADSB	acyl-CoA dehydrogenase short/branched chain
ACADVL	acyl-CoA dehydrogenase very long chain
ACAT1	acetyl-CoA acetyltransferase 1

B.1

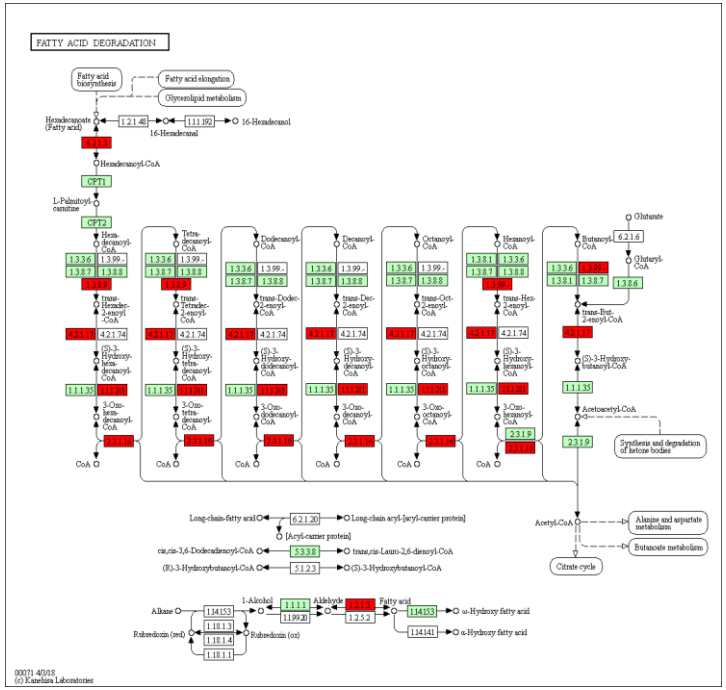

B.2

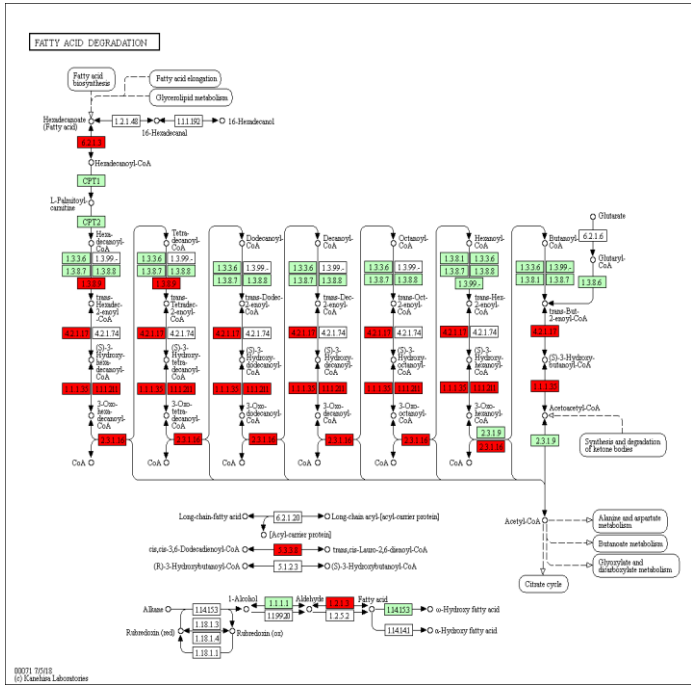

B.3

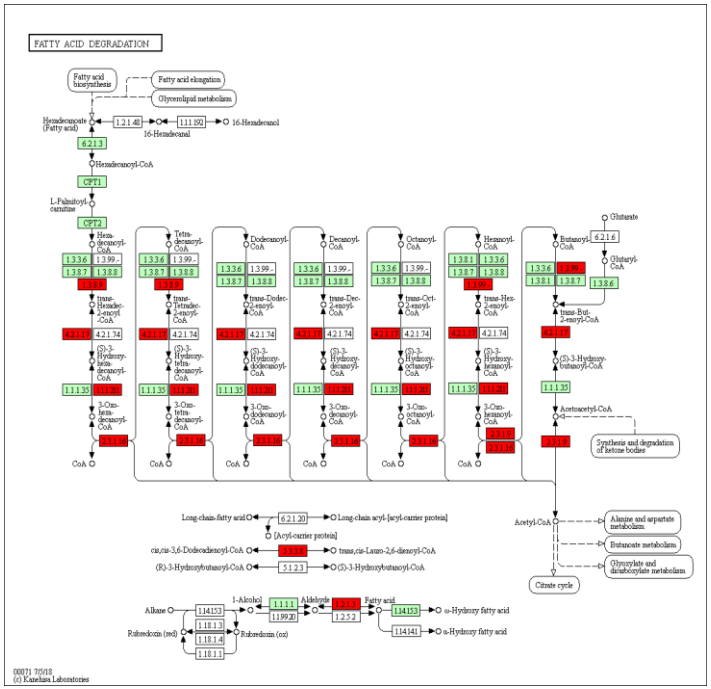

Fig. 3.10B KEGG maps depicting changes to fatty acid degradation in A549 cells exposed to *A. fumigatus, P. aeruginosa* and sequential exposure to *A. fumigatus* and *P. aeruginosa*. Similarities in the increased levels of SSDA proteins involved in the fatty acid degradation pathways between (1) *A. fumigatus*-, (2) *P. aeruginosa*-, and (3) sequentially exposed A549 cells and the control were identified. Changes in the abundance of proteins between the three infected groups of A549 cells were not significant and are thus not depicted here.

C.1

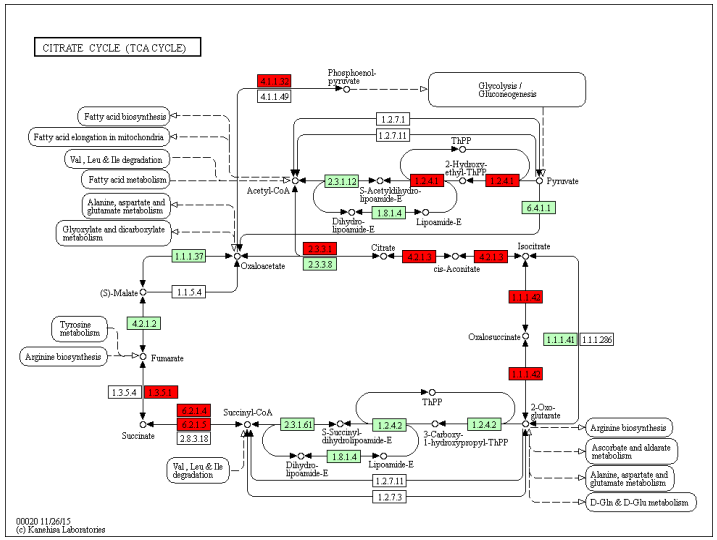

C.2

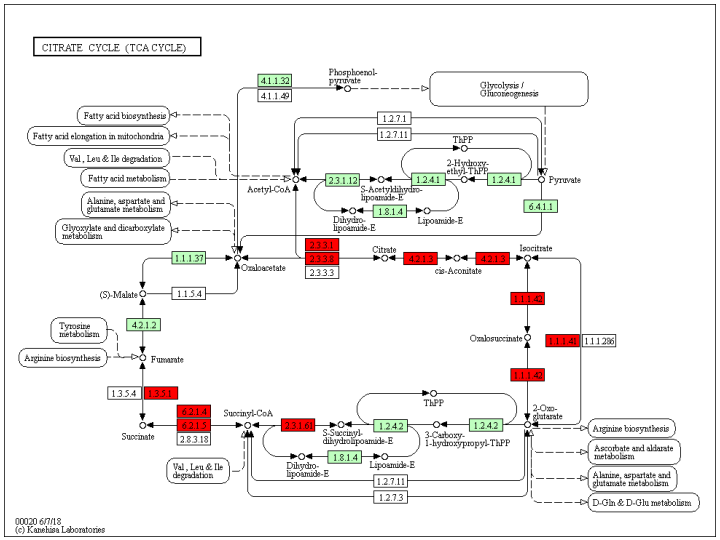

C.3

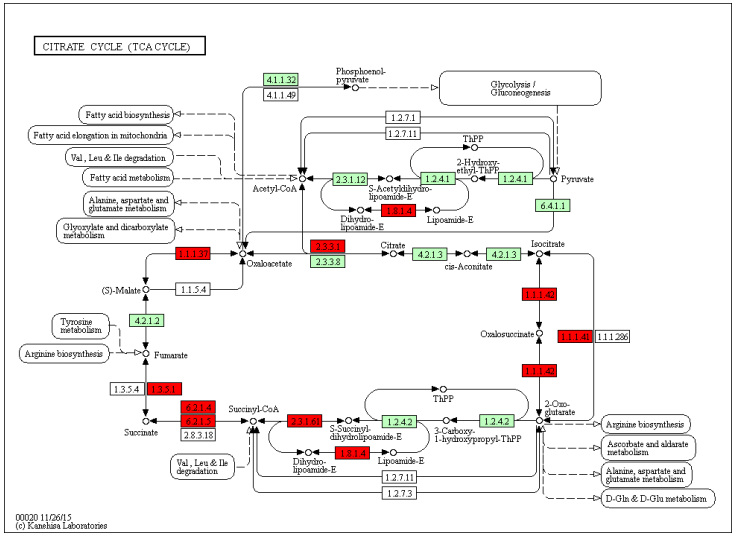

Fig. 3.10C KEGG maps depicting changes to the TCA cycle between A549 cells exposed to *A. fumigatus, P. aeruginosa* and sequential exposure to *A. fumigatus* and *P. aeruginosa*. Similarities in the increased levels of SSDA proteins involved in the Citric Acid (TCA) cycle pathways between (1) *A. fumigatus*-, (2) *P. aeruginosa*-, and (3) sequentially-exposed A549 cells and the control were identified. Changes in the relative abundance of proteins between the three infected groups of A549 cells were not significant and are thus not depicted here.

Table 3.5C List of proteins involved in the TCA cycle. SSDA proteins arising from comparisons between the different infection groups of A549 cells and highlighted in the KEGG map depicting the TCA cycle are listed.

Gene name	Protein name
CS	citrate synthase
DLD	dihydrolipoamide dehydrogenase
DLST	dihydrolipoamide S-succinyltransferase
IDH2	isocitrate dehydrogenase (NADP(+)) 2
IDH3A	isocitrate dehydrogenase (NAD(+)) 3 catalytic subunit alpha
IDH3B	isocitrate dehydrogenase (NAD(+)) 3 non-catalytic subunit beta
MDH2	malate dehydrogenase 2
ACLY	ATP citrate lyase
ACO1	aconitase 1
ACO2	aconitase 2
PCK2	phosphoenolpyruvate carboxykinase 2, mitochondrial
PDHA1	pyruvate dehydrogenase E1 subunit alpha 1
SDHA	succinate dehydrogenase complex flavoprotein subunit A
SUCLG2	succinate-CoA ligase GDP-forming subunit beta
SUCLG1	succinate-CoA ligase GDP/ADP-forming subunit alpha
SUCLA2	succinate-CoA ligase ADP-forming subunit beta

The relative abundance of mitochondrial proteins and mitochondria-related processes were increased across all three infected groups of A549 cells compared to the control (Cluster H). This is reflected in the KEGG pathways (Fig. 3.10D and 3.10E, Table 3.5D and 3.3E). GO terms for the mitochondria and associated processes included mitochondrion, oxidoreductase activity, oxidative phosphorylation and the respiratory electron transport chain (ETC) were included in this cluster. Proteins associated with these GO terms were most abundant in the *P. aeruginosa*-exposed group, and sequentially infected group respectively, compared to the *A. fumigatus*-exposed group and the control. Differential changes in the relative abundance of proteins associated with protein processing pathways was detected between the A549 cells exposed to *A. fumigatus* or *P. aeruginosa* compared to sequentially exposed groups and the control. The relative abundance of proteins involved in protein processing in the ER were increased in the groups exposed to *A. fumigatus* or *P. aeruginosa* compared to sequentially exposed cells and the control (Fig. 3.10F, Table 3.5F). The relative abundance of proteins involved in ubiquitin-mediated proteolysis was significantly decreased in cells exposed to *P. aeruginosa* compared to the other groups (Fig.3.10G, Table 3.10G).

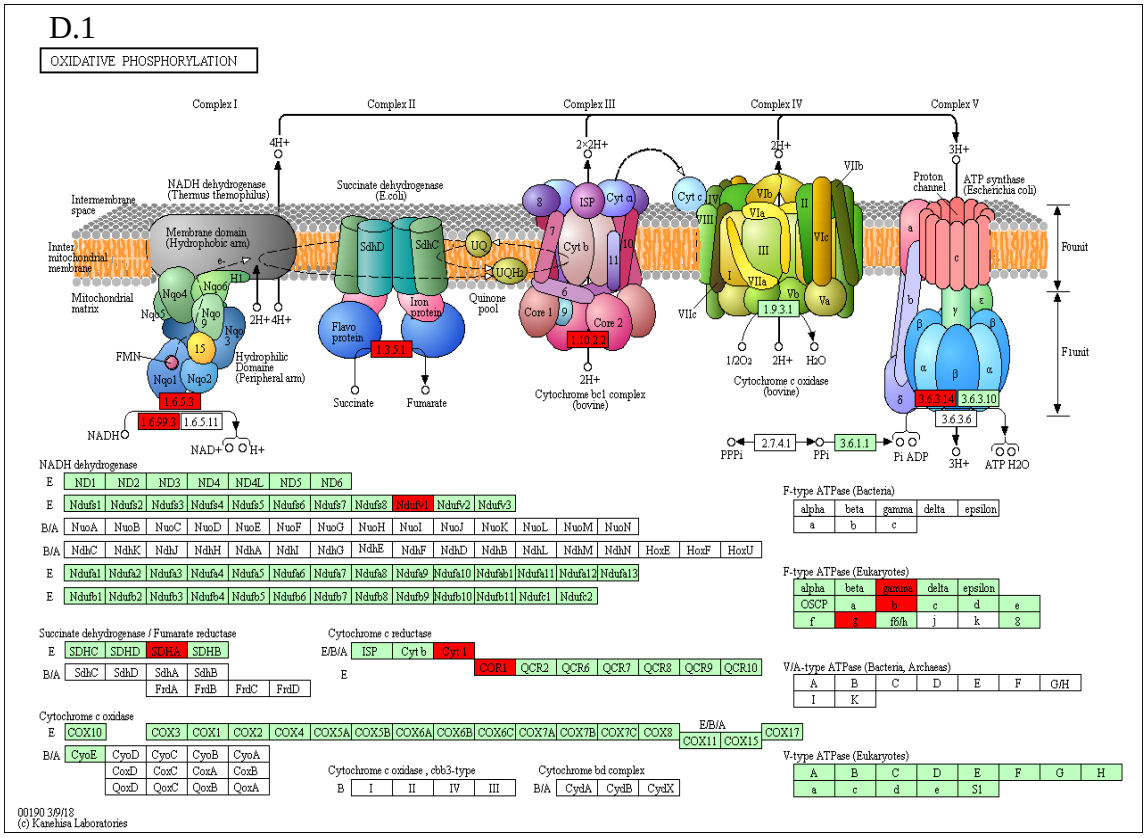
D.1
OXIDATIVE PHOSPHORYLATION
Complex I
Complex II
Complex III
Complex IV
Complex V
NADH dehydrogenase (Thermus thermophilus)
Succinate dehydrogenase (E.coli)
Intermembrane space
Inner mitochondrial membrane
Mitochondrial matrix
Membrane domain (Hydrophobic arm)
Hydrophilic Domain (Peripheral arm)
Flavo protein
Iron protein
Quinone pool
Cytochrome bc1 complex (bovine)
Cytochrome c oxidase (bovine)
Proton channel
ATP synthase (Escherichia coli)
Fo unit
F1 unit
NADH dehydrogenase
Succinate dehydrogenase / Fumarate reductase
Cytochrome c reductase
Cytochrome c oxidase
Cytochrome c oxidase , cbb3-type
Cytochrome bd complex
F-type ATPase (Bacteria)
F-type ATPase (Eukaryotes)
V/A-type ATPase (Bacteria, Archaeas)
V-type ATPase (Eukaryotes)
00190 3/9/18
(c) Kanehisa Laboratories

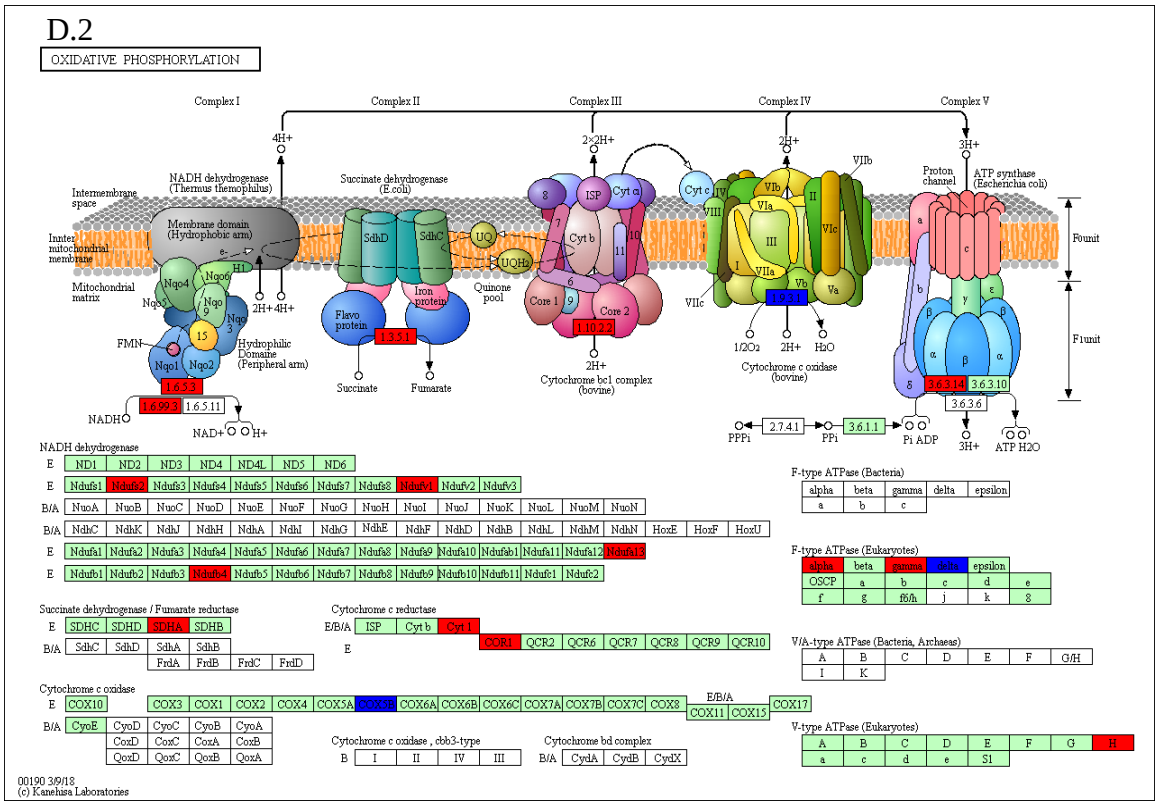
D.2
OXIDATIVE PHOSPHORYLATION
Complex I
Complex II
Complex III
Complex IV
Complex V
NADH dehydrogenase (Thermus thermophilus)
Succinate dehydrogenase (E.coli)
Intermembrane space
Inner mitochondrial membrane
Mitochondrial matrix
Membrane domain (Hydrophobic arm)
Hydrophilic Domain (Peripheral arm)
Flavo protein
Iron protein
Quinone pool
Cytochrome bc1 complex (bovine)
Cytochrome c oxidase (bovine)
Proton channel
ATP synthase (Escherichia coli)
Fo unit
F1 unit
NADH dehydrogenase
Succinate dehydrogenase / Fumarate reductase
Cytochrome c reductase
Cytochrome c oxidase
Cytochrome c oxidase , cbb3-type
Cytochrome bd complex
F-type ATPase (Bacteria)
F-type ATPase (Eukaryotes)
V/A-type ATPase (Bacteria, Archaeas)
V-type ATPase (Eukaryotes)
00190 3/9/18
(c) Kanehisa Laboratories

D.3

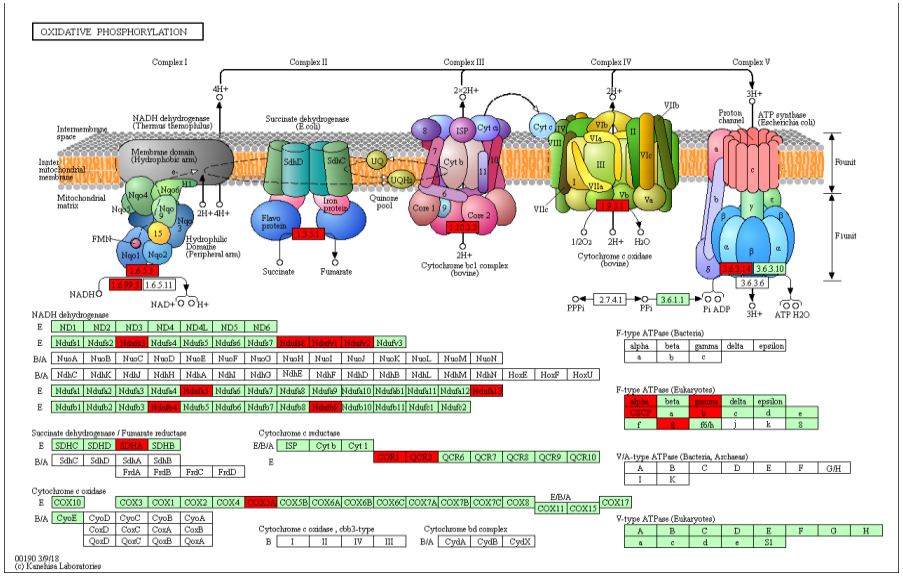

D.4

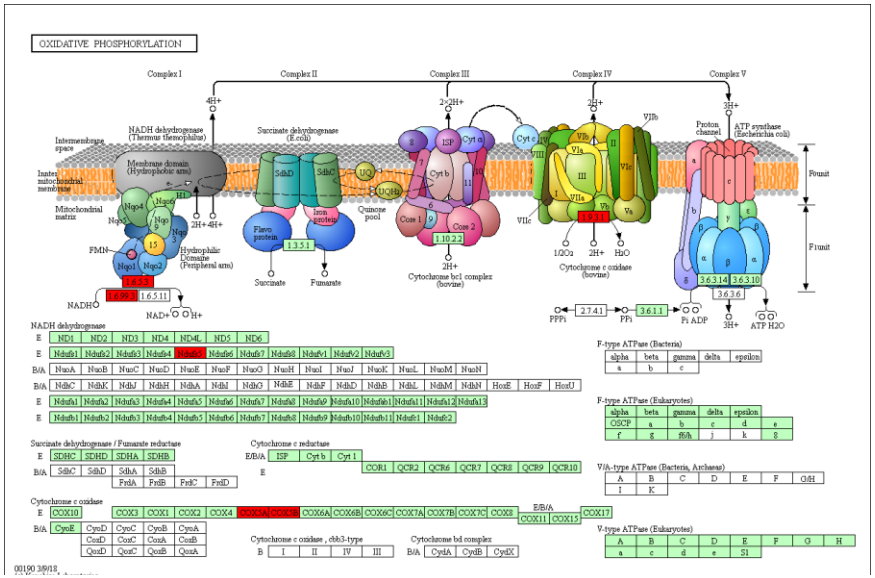

D.5

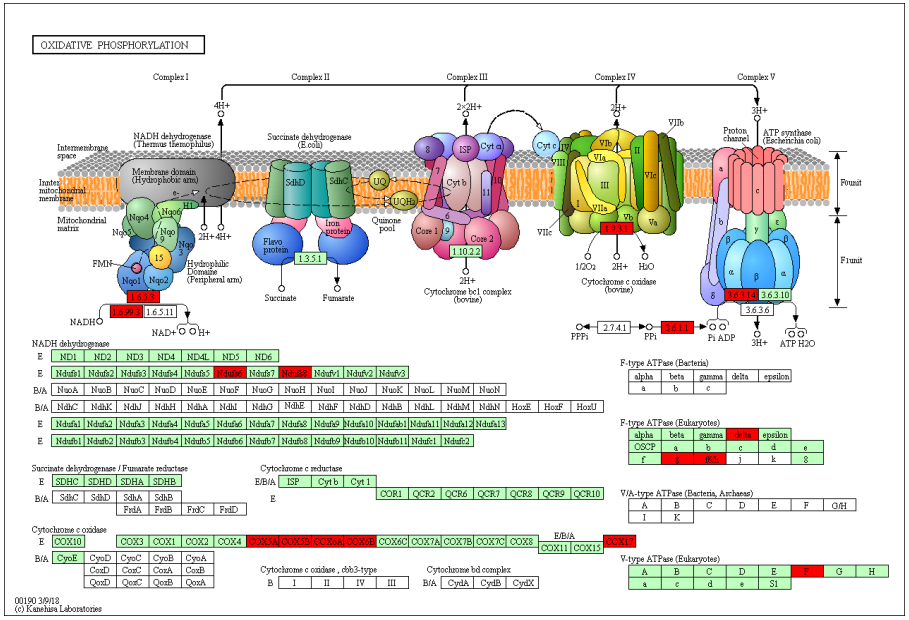

Fig. 3.10D KEGG maps depicting changes to the OXPHOS pathway in A549 cells exposed to *A. fumigatus, P. aeruginosa* and sequential exposure to *A. fumigatus* and *P. aeruginosa*. Similarities in the the increased levels of SSDA proteins involved in the oxidative phosphorylation pathways between (1) *A. fumigatus*-, (2) *P. aeruginosa*-, and (3) sequentially-exposed A549 cells and the control are identified. Compared to (5) *A. fumigatus*-, and (4) *P. aeruginosa*-exposed A549 cells, the abundance of proteins associated with oxidative phosphorylation was higher in sequentially exposed cells.

E.1

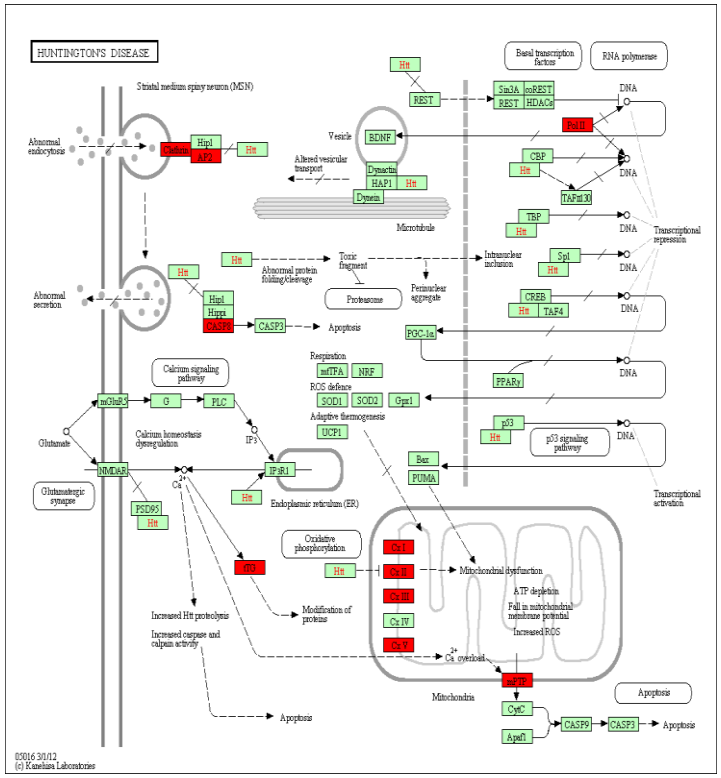
HUNTINGTON'S DISEASE
Striatal medium spiny neuron (MSN)
Basal transcription factors
RNA polymerase
Abnormal endocytosis
Vesicle
Altered vesicular transport
Microtubule
Abnormal secretion
Abnormal protein folding/cleavage
Toxic fragment
Proteasome
Perinuclear aggregate
Intranuclear inclusion
Transcriptional repression
Transcriptional activation
Apoptosis
Respiration
ROS defence
Adaptive thermogenesis
Calcium signaling pathway
Calcium homeostasis dysregulation
Glutamatergic synapse
Glutamate
Endoplasmic reticulum (ER)
Oxidative phosphorylation
Mitochondrial dysfunction
ATP depletion
Fall in mitochondrial membrane potential
Increased ROS
Increased Htt proteolysis
Increased caspase and calpain activity
Modification of proteins
Mitochondria
p53 signaling pathway
REST
Sin3A
coREST
REST
HDACs
Pol II
BDNF
CBP
TAFII130
TBP
Dynactin
HAP1
Dynein
Cleform
Hip1
AP2
Spl
CREB
TAF4
Hip1
Hippi
CASP8
CASP3
PGC-1α
PPARγ
p53
Bax
PUMA
mGluR5
G
PLC
IP3
NMDAR
IP3R1
PSD95
SOD1
SOD2
Gpx1
UCP1
mHTT
NRF
Htt
Cx I
Cx II
Cx III
Cx IV
Cx V
Ca overload
mPTP
CytC
Apaf1
CASP9
05016 30/12
(c) Kanehisa Laboratories

E.2

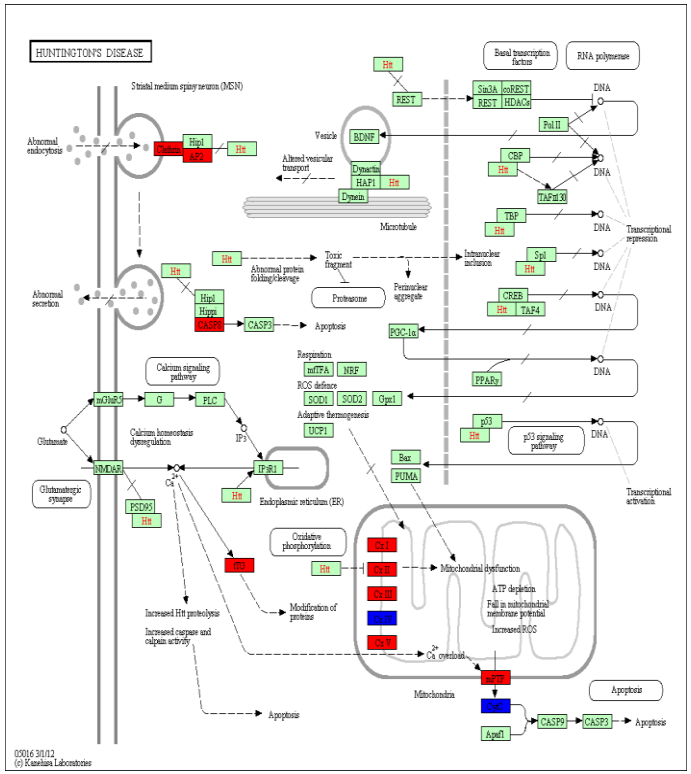
HUNTINGTON'S DISEASE
Striatal medium spiny neuron (MSN)
Basal transcription factors
RNA polymerase
Abnormal endocytosis
Vesicle
Altered vesicular transport
Microtubule
Abnormal secretion
Abnormal protein folding/cleavage
Toxic fragment
Proteasome
Perinuclear aggregate
Intranuclear inclusion
Transcriptional repression
Transcriptional activation
Apoptosis
Respiration
ROS defence
Adaptive thermogenesis
Calcium signaling pathway
Calcium homeostasis dysregulation
Glutamatergic synapse
Glutamate
Endoplasmic reticulum (ER)
Oxidative phosphorylation
Mitochondrial dysfunction
ATP depletion
Fall in mitochondrial membrane potential
Increased ROS
Increased Htt proteolysis
Increased caspase and calpain activity
Modification of proteins
Mitochondria
p53 signaling pathway
REST
Sin3A
coREST
REST
HDACs
Pol II
BDNF
CBP
TAFII130
TBP
Dynactin
HAP1
Dynein
Cleform
Hip1
AP2
Spl
CREB
TAF4
Hip1
Hippi
CASP8
CASP3
PGC-1α
PPARγ
p53
Bax
PUMA
mGluR5
G
PLC
IP3
NMDAR
IP3R1
PSD95
SOD1
SOD2
Gpx1
UCP1
mHTT
NRF
Htt
Cx I
Cx II
Cx III
Cx IV
Cx V
Ca overload
mPTP
CytC
Apaf1
CASP9
05016 30/12
(c) Kanehisa Laboratories

E.3

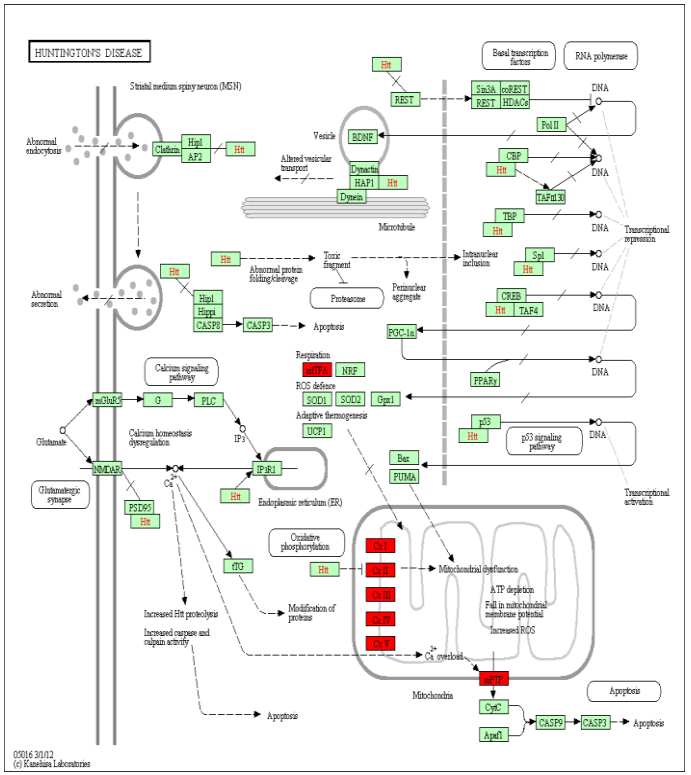
HUNTINGTON'S DISEASE
Striatal medium spiny neuron (MSN)
Basal transcription factors
RNA polymerase
Abnormal endocytosis
Vesicle
Altered vesicular transport
Microtubule
Abnormal secretion
Abnormal protein folding/cleavage
Toxic fragment
Proteasome
Perinuclear aggregate
Intranuclear inclusion
Transcriptional repression
Transcriptional activation
Apoptosis
Respiration
ROS defence
Adaptive thermogenesis
Calcium signaling pathway
Calcium homeostasis dysregulation
Glutamatergic synapse
Glutamate
Endoplasmic reticulum (ER)
Oxidative phosphorylation
Mitochondrial dysfunction
ATP depletion
Fall in mitochondrial membrane potential
Increased ROS
Increased Htt proteolysis
Increased caspase and calpain activity
Modification of proteins
Mitochondria
p53 signaling pathway
REST
Sin3A
coREST
REST
HDACs
Pol II
BDNF
CBP
TAFII130
TBP
Dynactin
HAP1
Dynein
Cleform
Hip1
AP2
Spl
CREB
TAF4
Hip1
Hippi
CASP8
CASP3
PGC-1α
PPARγ
p53
Bax
PUMA
mGluR5
G
PLC
IP3
NMDAR
IP3R1
PSD95
SOD1
SOD2
Gpx1
UCP1
mHTT
NRF
Htt
Cx I
Cx II
Cx III
Cx IV
Cx V
Ca overload
mPTP
CytC
Apaf1
CASP9
05016 30/12
(c) Kanehisa Laboratories

E.4

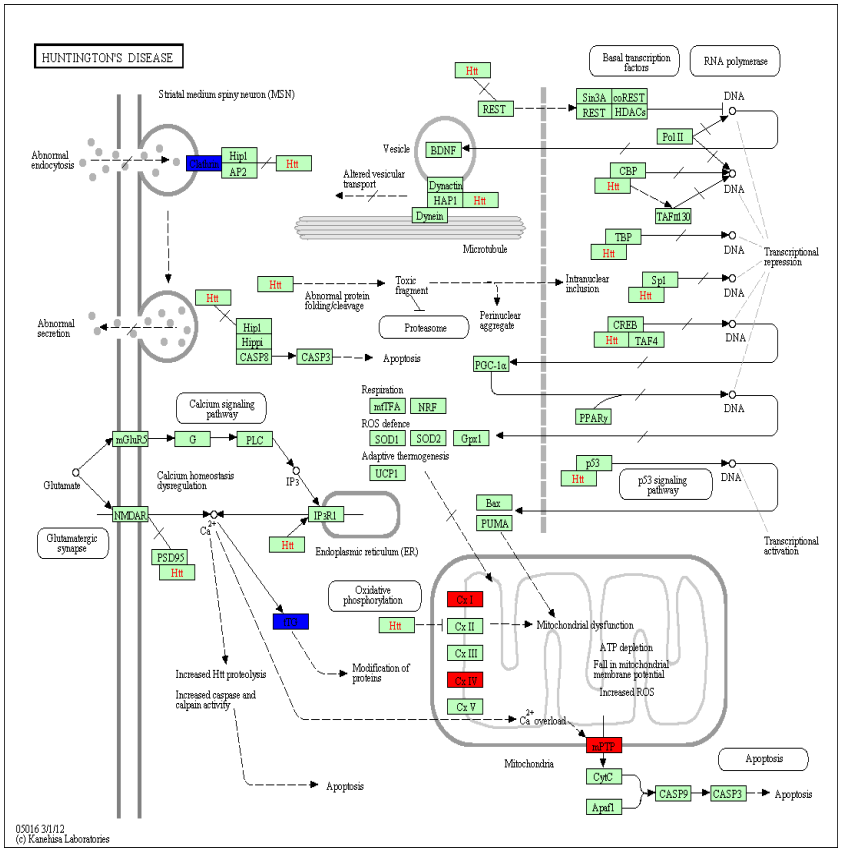

E.5

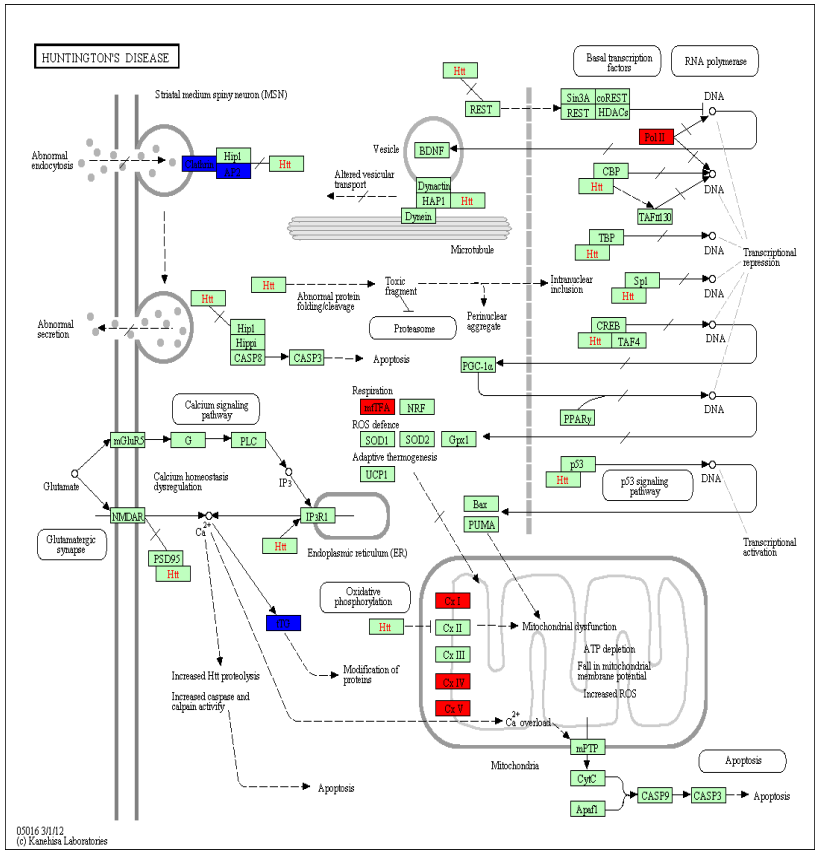

Fig. 3.10E KEGG maps depicting changes to the Huntington's disease pathway between A549 cells exposed to *A. fumigatus, P. aeruginosa* and sequential exposure to *A. fumigatus* and *P. aeruginosa*. Increased (red) and decreased (blue) levels of SSDA proteins involved in the Huntington's Disease pathway (ultimately resulting in apoptosis) were identified between (1) *A. fumigatus*, (2) *P. aeruginosa*, and (3) sequentially exposed A549 cells and the control. The abundance of proteins associated with complex I – V of the mitochondrial respiratory transport chain was greater in the sequentially infected A549 cells compared to the other pathogen-exposed groups (4, 5).

Table 3.5D List of proteins involved in the oxidative phosphorylatin pathway. SSDA proteins arising from comparisons between the different infection groups of A549 cells and highlighted in the KEGG map depicting the oxidative phosphorylation are listed.

Gene name	Protein name
ATP5MG	ATP synthase membrane subunit g
COX5B	cytochrome c oxidase subunit 5B
CYC1	cytochrome c1
NDUFA5	NADH:ubiquinone oxidoreductase subunit A5
NDUFB4	NADH:ubiquinone oxidoreductase subunit B4
NDUFB9	NADH:ubiquinone oxidoreductase subunit B9
NDUFS2	NADH:ubiquinone oxidoreductase core subunit S2
NDUFS3	NADH:ubiquinone oxidoreductase core subunit S3
NDUFV1	NADH:ubiquinone oxidoreductase core subunit V1
NDUFS8	NADH:ubiquinone oxidoreductase core subunit S8
NDUFV2	NADH:ubiquinone oxidoreductase core subunit V2
ATP5F1A	ATP synthase F1 subunit alpha
ATP5F1C	ATP synthase F1 subunit gamma
NDUFA13	NADH:ubiquinone oxidoreductase subunit A13
ATP5F1D	ATP synthase F1 subunit delta
ATP5PB	ATP synthase peripheral stalk-membrane subunit b
ATP6V1H	ATPase H+ transporting V1 subunit H
ATP5PO	ATP synthase peripheral stalk subunit OSCP
SDHA	succinate dehydrogenase complex flavoprotein
UQCRC1	ubiquinol-cytochrome c reductase core protein 1
UQCRC2	ubiquinol-cytochrome c reductase core protein 2
COX5A	cytochrome c oxidase subunit 5A

Table 3.5E List of proteins involved in the Huntigton's Disease pathway. SSDA proteins arising from comparisons between the different infection groups of A549 cells and highlighted in the KEGG map depicting the Huntington's disease pathway are listed.

Gene name	Protein name
CLTC	clathrin heavy chain
COX5B	cytochrome c oxidase subunit 5B
CYC1	cytochrome c1
AP2B1	adaptor related protein complex 2 subunit beta 1
SLC25A5	solute carrier family 25 member 5
SLC25A6	solute carrier family 25 member 6
NDUFA5	NADH:ubiquinone oxidoreductase subunit A5
NDUFB4	NADH:ubiquinone oxidoreductase subunit B4
NDUFB9	NADH:ubiquinone oxidoreductase subunit B9
NDUFS2	NADH:ubiquinone oxidoreductase core subunit S2
NDUFS3	NADH:ubiquinone oxidoreductase core subunit S3
NDUFV1	NADH:ubiquinone oxidoreductase core subunit V1
NDUFS8	NADH:ubiquinone oxidoreductase core subunit S8
NDUFV2	NADH:ubiquinone oxidoreductase core subunit V2
ATP5F1A	ATP synthase F1 subunit alpha
ATP5F1C	ATP synthase F1 subunit gamma
NDUFA13	NADH:ubiquinone oxidoreductase subunit A13
ATP5F1D	ATP synthase F1 subunit delta
ATP5PB	ATP synthase peripheral stalk-membrane subunit b
ATP5PO	ATP synthase peripheral stalk subunit OSCP
CYCS	cytochrome c, somatic
POLR2A	RNA polymerase II subunit A
SDHA	succinate dehydrogenase complex flavoprotein subunit A
TFAM	transcription factor A, mitochondrial
TGM2	transglutaminase 2
UQCRC1	ubiquinol-cytochrome c reductase core protein 1
UQCRC2	ubiquinol-cytochrome c reductase core protein 2
VDAC3	voltage dependent anion channel 3
TUBA1A	tubulin alpha 1a
CASP8	caspase 8
COX5A	cytochrome c oxidase subunit 5A

F.1

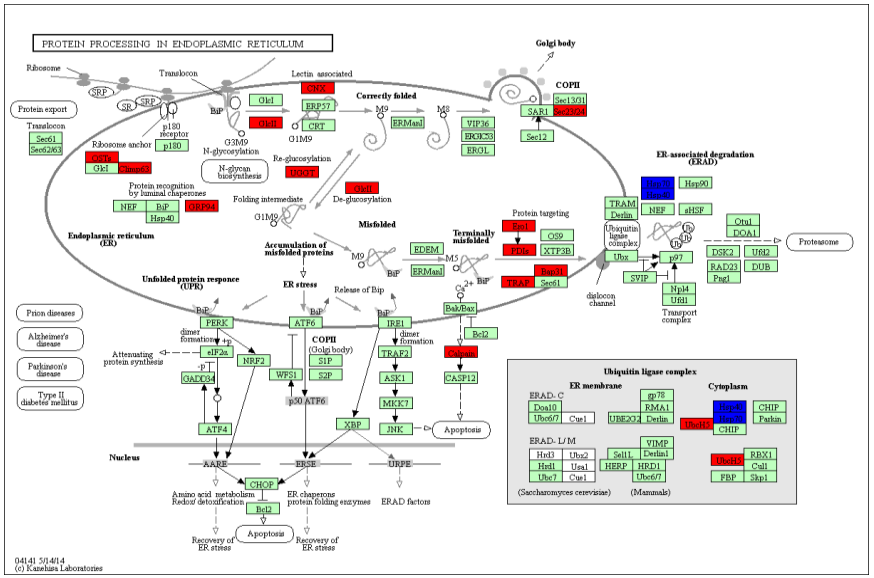
PROTEIN PROCESSING IN ENDOPLASMIC RETICULUM
Golgi body
Ribosome
Translocon
Lectin associated
Protein export
Correctly folded
COPII
Endoplasmic reticulum (ER)
Misfolded
Terminally misfolded
Protein targeting
ER-associated degradation (ERAD)
Proteasome
Accumulation of misfolded proteins
Unfolded protein responce (UPR)
ER stress
Release of Bip
Prion diseases
Alzheimer's disease
Parkinson's disease
Type II diabetes mellitus
Attenuating protein synthesis
COPII (Golgi body)
Nucleus
Amino acid metabolism Redox/ detoxification
ER chaperone protein folding enzymes
ERAD factors
Apoptosis
Recovery of ER stress
Ubiquitin ligase complex
ER membrane
Cytoplasm
(Saccharomyces cerevisiae)
(Mammals)
04141 5/14/14
(c) Kanehisa Laboratories

F.2

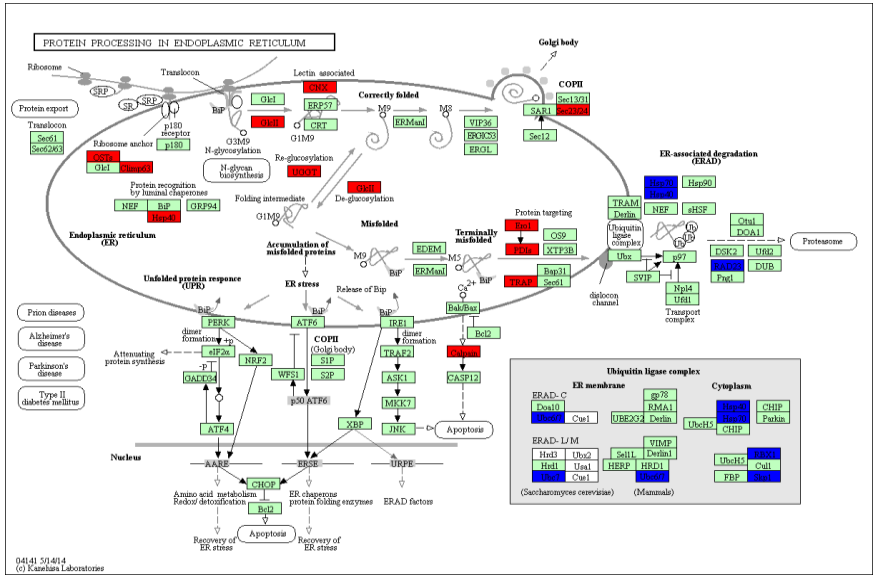
PROTEIN PROCESSING IN ENDOPLASMIC RETICULUM
Golgi body
Ribosome
Translocon
Lectin associated
Protein export
Correctly folded
COPII
Endoplasmic reticulum (ER)
Misfolded
Terminally misfolded
Protein targeting
ER-associated degradation (ERAD)
Proteasome
Accumulation of misfolded proteins
Unfolded protein responce (UPR)
ER stress
Release of Bip
Prion diseases
Alzheimer's disease
Parkinson's disease
Type II diabetes mellitus
Attenuating protein synthesis
COPII (Golgi body)
Nucleus
Amino acid metabolism Redox/ detoxification
ER chaperone protein folding enzymes
ERAD factors
Apoptosis
Recovery of ER stress
Ubiquitin ligase complex
ER membrane
Cytoplasm
(Saccharomyces cerevisiae)
(Mammals)
04141 5/14/14
(c) Kanehisa Laboratories

F.3

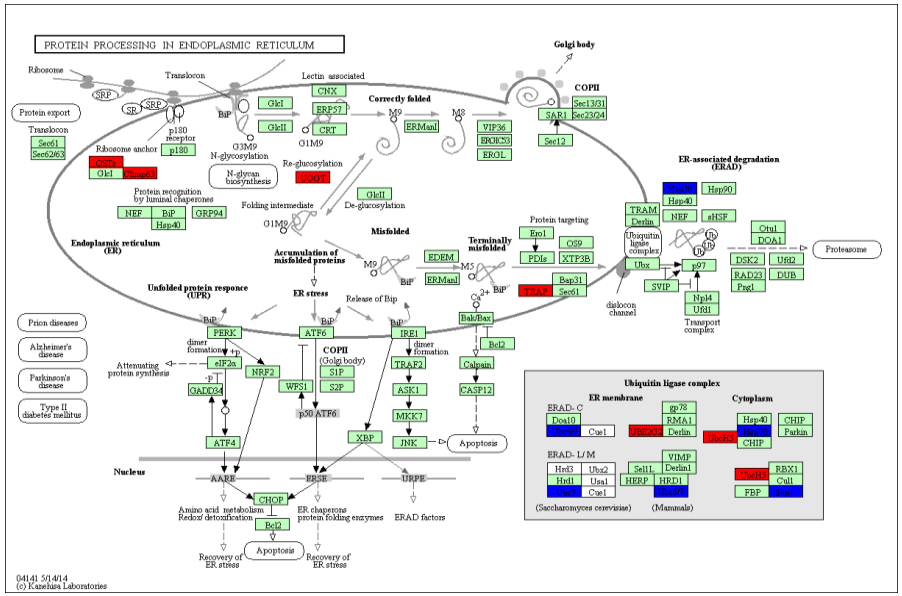
PROTEIN PROCESSING IN ENDOPLASMIC RETICULUM
Golgi body
Ribosome
Translocon
Lectin associated
Protein export
Correctly folded
COPII
Endoplasmic reticulum (ER)
Misfolded
Terminally misfolded
Protein targeting
ER-associated degradation (ERAD)
Proteasome
Accumulation of misfolded proteins
Unfolded protein responce (UPR)
ER stress
Release of Bip
Prion diseases
Alzheimer's disease
Parkinson's disease
Type II diabetes mellitus
Attenuating protein synthesis
COPII (Golgi body)
Nucleus
Amino acid metabolism Redox/ detoxification
ER chaperone protein folding enzymes
ERAD factors
Apoptosis
Recovery of ER stress
Ubiquitin ligase complex
ER membrane
Cytoplasm
(Saccharomyces cerevisiae)
(Mammals)
04141 5/14/14
(c) Kanehisa Laboratories

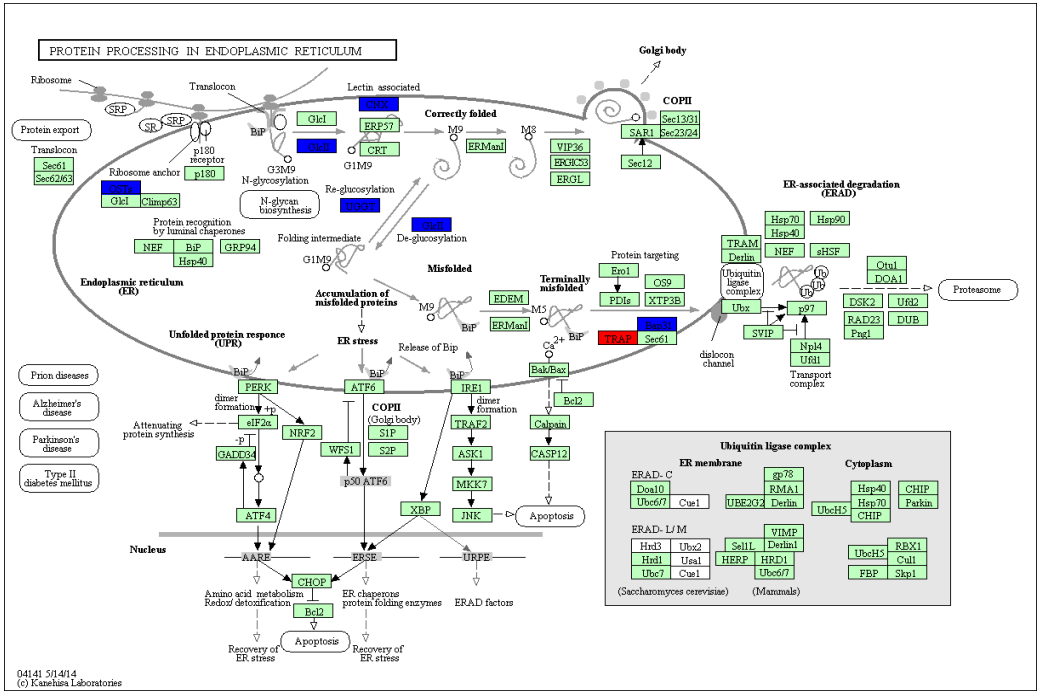

F.4

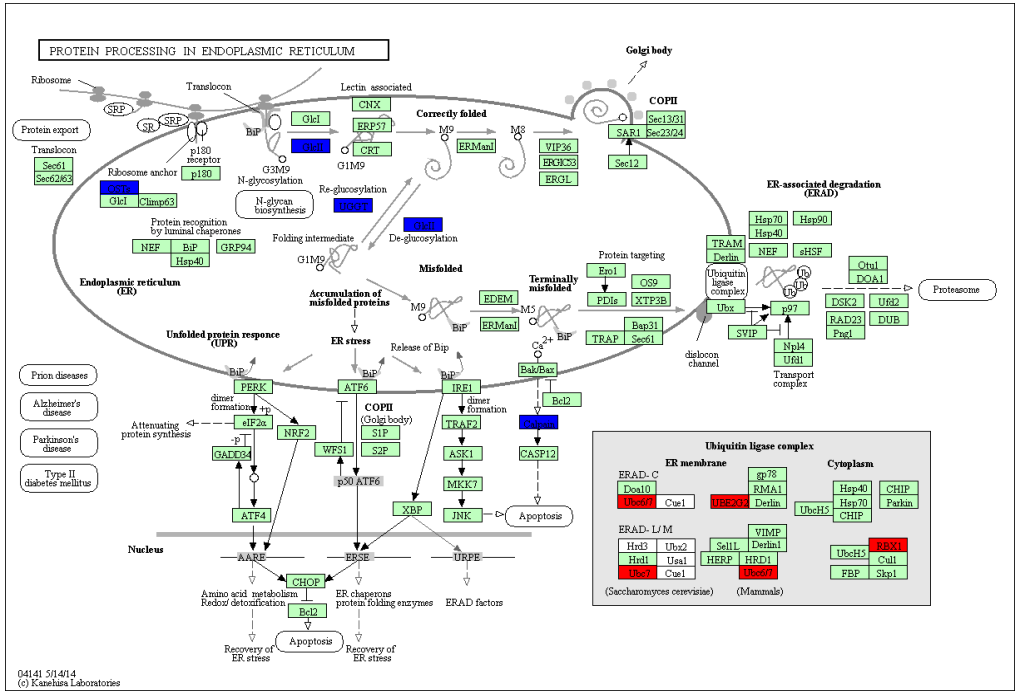

F.5

Fig. 3.10F KEGG maps depicting changes in the protein-processing pathway in the ER between A549 cells exposed to *A. fumigatus, P. aeruginosa* and sequential exposure to *A. fumigatus* and *P. aeruginosa*. Compared to the control, the abundance of proteins acting within the ER was increased (red) in (1) *A. fumigatus*-, (2) *P. aeruginosa* and (3) sequentially-exposed A549 cells. The protein abundance in this pathway was lower (blue) in sequentially exposed cells compared to the (4) *A. fumigatus*- and (5) *P. aeruginosa*-exposed A549 cells. The levels of proteins associated with the ubiquitin ligase complex were decreased in all pathogen-exposed groups compared to the control (1-3) and increased in the sequentially exposed A549 cells compared to *P. aeruginosa*-exposed cells (5).

G.1

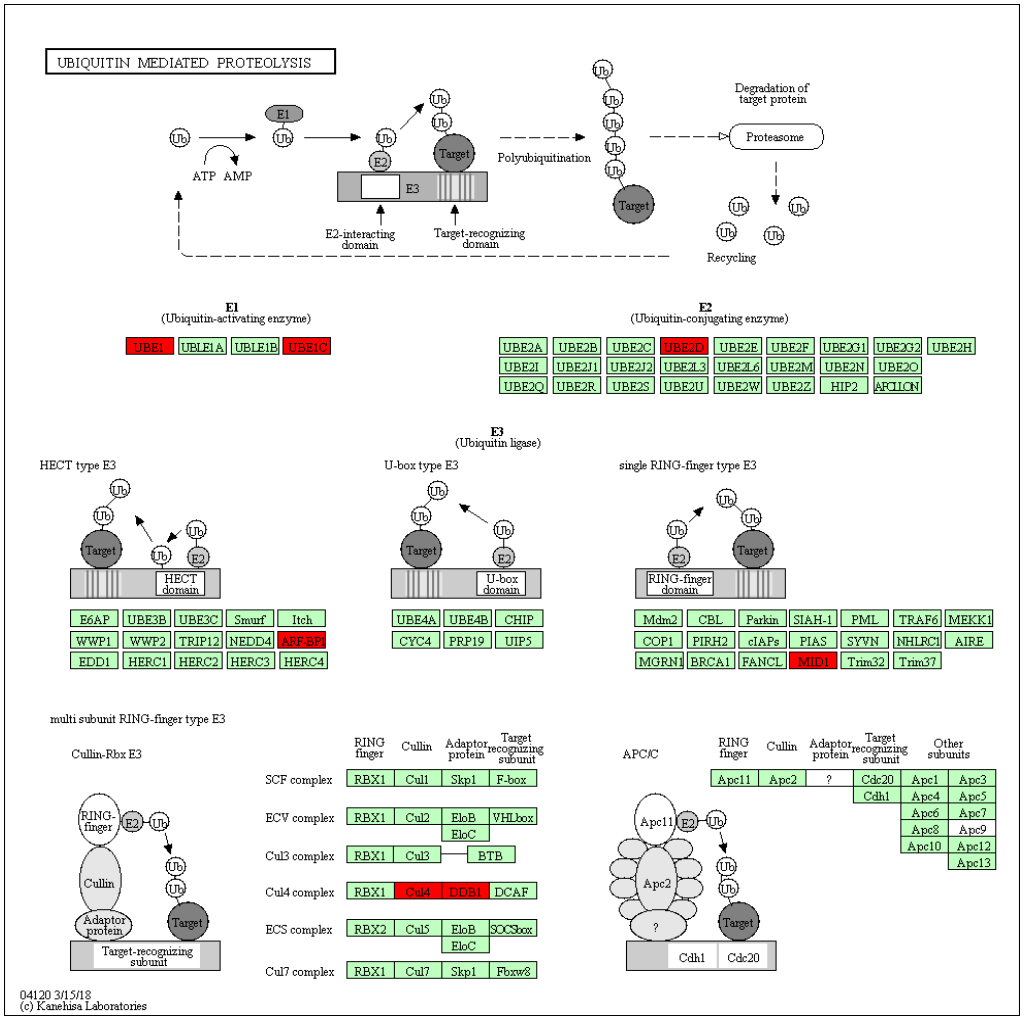
UBIQUITIN MEDIATED PROTEOLYSIS
E1
ATP AMP
E2
E3
Target
Polyubiquitination
Degradation of target protein
Proteasome
E2-interacting domain
Target-recognizing domain
Recycling
E1 (Ubiquitin-activating enzyme)
UBE1 UBLE1A UBLE1B UBE1C
E2 (Ubiquitin-conjugating enzyme)
UBE2A UBE2B UBE2C UBE2D UBE2E UBE2F UBE2G1 UBE2G2 UBE2H
UBE2I UBE2J1 UBE2J2 UBE2L3 UBE2L6 UBE2M UBE2N UBE2O
UBE2Q UBE2R UBE2S UBE2U UBE2W UBE2Z HIP2 ARCUCN
E3 (Ubiquitin ligase)
HECT type E3
HECT domain
E6AP UBE3B UBE3C Smurf Itch
WWP1 WWP2 TRIP12 NEDD4 ARF-BP1
EDD1 HERC1 HERC2 HERC3 HERC4
U-box type E3
U-box domain
UBE4A UBE4B CHIP
CYC4 PRP19 UIP5
single RING-finger type E3
RING-finger domain
Mdm2 CBL Parkin SIAH-1 PML TRAF6 MEKK1
COP1 PIRH2 cIAPs PIAS SYVN NHLRC1 AIRE
MGRN1 BRCA1 FANCL MID1 Trim32 Trim37
multi subunit RING-finger type E3
Cullin-Rbx E3
RING-finger
Cullin
Adaptor protein
Target-recognizing subunit
RING finger
Cullin
Adaptor protein
Target recognizing subunit
SCF complex RBX1 Cul1 Skp1 F-box
ECV complex RBX1 Cul2 EloB VHLbox EloC
Cul3 complex RBX1 Cul3 BTB
Cul4 complex RBX1 Cul4 DDB1 DCAF
ECS complex RBX2 Cul5 EloB SOCSbox EloC
Cul7 complex RBX1 Cul7 Skp1 Fbxw8
APC/C
Other subunits
Apc11 Apc2 ? Cdc20 Apc1 Apc3
Cdh1 Apc4 Apc5
Apc6 Apc7
Apc8 Apc9
Apc10 Apc12
Apc13
Cdh1 Cdc20
04120 3/15/18
(c) Kanehisa Laboratories

G.2

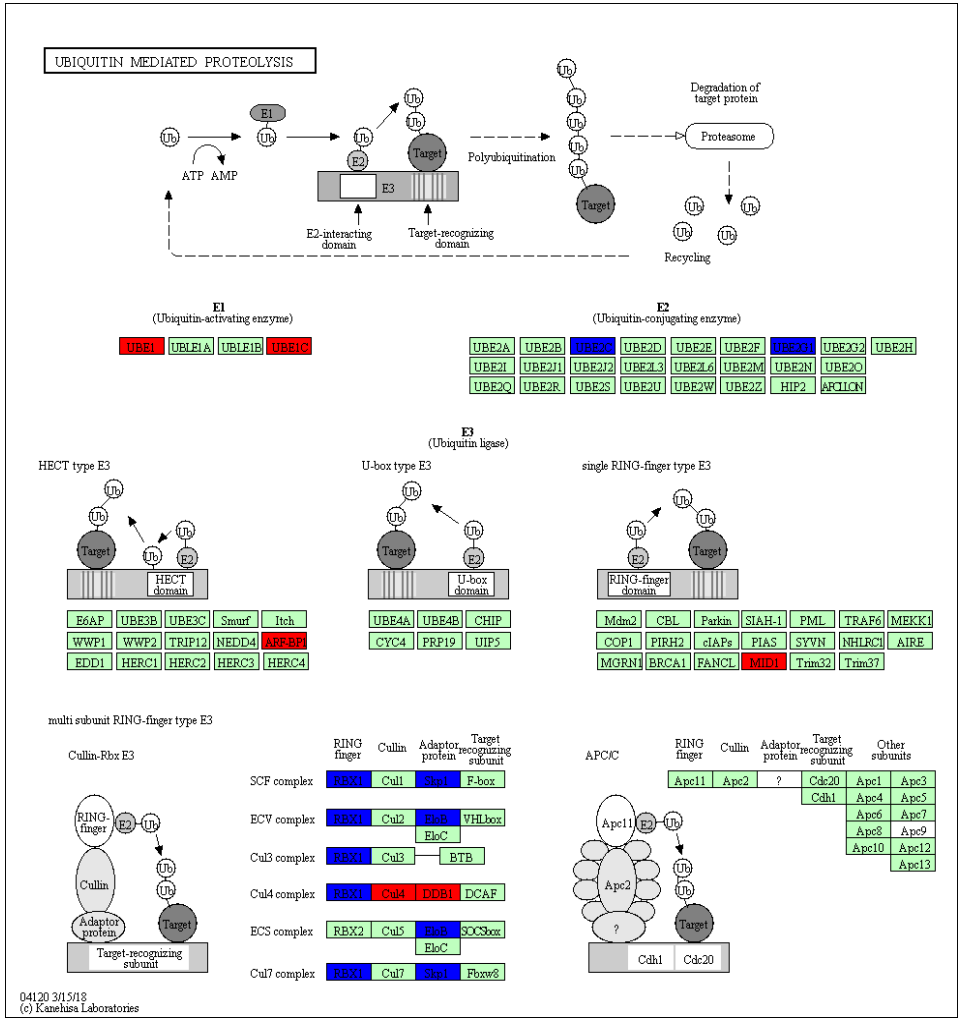
UBIQUITIN MEDIATED PROTEOLYSIS
E1
ATP AMP
E2
E3
Target
Polyubiquitination
Degradation of target protein
Proteasome
E2-interacting domain
Target-recognizing domain
Recycling
E1 (Ubiquitin-activating enzyme)
UBE1 UBLE1A UBLE1B UBE1C
E2 (Ubiquitin-conjugating enzyme)
UBE2A UBE2B UBE2C UBE2D UBE2E UBE2F UBE2G1 UBE2G2 UBE2H
UBE2I UBE2J1 UBE2J2 UBE2L3 UBE2L6 UBE2M UBE2N UBE2O
UBE2Q UBE2R UBE2S UBE2U UBE2W UBE2Z HIP2 ARCUCN
E3 (Ubiquitin ligase)
HECT type E3
HECT domain
E6AP UBE3B UBE3C Smurf Itch
WWP1 WWP2 TRIP12 NEDD4 ARF-BP1
EDD1 HERC1 HERC2 HERC3 HERC4
U-box type E3
U-box domain
UBE4A UBE4B CHIP
CYC4 PRP19 UIP5
single RING-finger type E3
RING-finger domain
Mdm2 CBL Parkin SIAH-1 PML TRAF6 MEKK1
COP1 PIRH2 cIAPs PIAS SYVN NHLRC1 AIRE
MGRN1 BRCA1 FANCL MID1 Trim32 Trim37
multi subunit RING-finger type E3
Cullin-Rbx E3
RING-finger
Cullin
Adaptor protein
Target-recognizing subunit
RING finger
Cullin
Adaptor protein
Target recognizing subunit
SCF complex RBX1 Cul1 Skp1 F-box
ECV complex RBX1 Cul2 EloB VHLbox EloC
Cul3 complex RBX1 Cul3 BTB
Cul4 complex RBX1 Cul4 DDB1 DCAF
ECS complex RBX2 Cul5 EloB SOCSbox EloC
Cul7 complex RBX1 Cul7 Skp1 Fbxw8
APC/C
Other subunits
Apc11 Apc2 ? Cdc20 Apc1 Apc3
Cdh1 Apc4 Apc5
Apc6 Apc7
Apc8 Apc9
Apc10 Apc12
Apc13
Cdh1 Cdc20
04120 3/15/18
(c) Kanehisa Laboratories

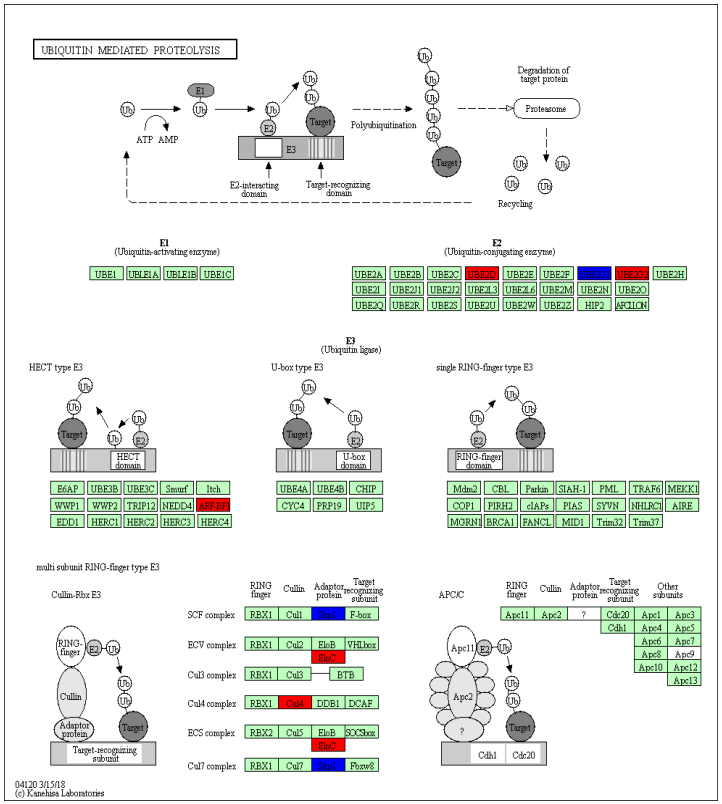

G.3

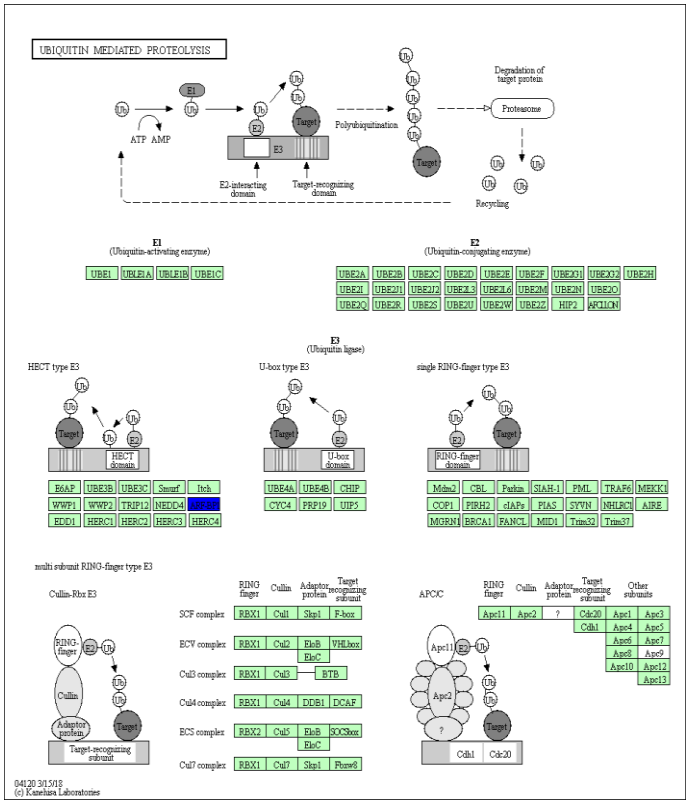

G.4

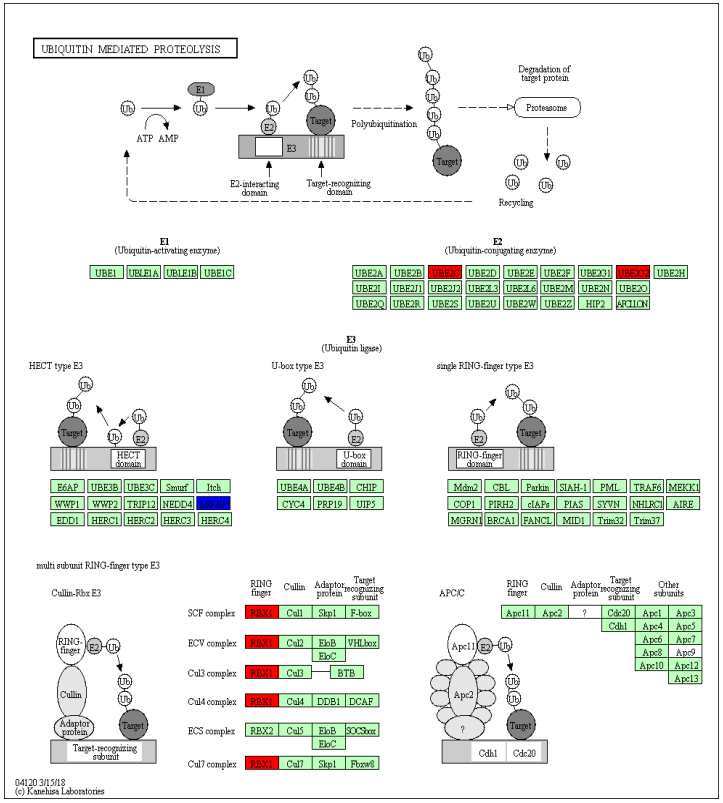

G.5

Fig.3.10G KEGG maps depicting changes in the ubiquitin-mediated proteolysis pathway between A549 cells exposed to *A. fumigatus, P. aeruginosa* and sequential exposure to *A. fumigatus* and *P. aeruginosa*. A distinct increase (red) in levels of SSDA proteins involved in the ubiquitin-mediated proteolytic pathway in (1) *A. fumigatus* were detected. This response is decreased in *P. aeruginosa*- exposed A549 cells compared to the control (2). The response of sequentially exposed cells (3) compared to the control resembled that of the *P. aeruginosa* exposed group. There were few significant differences between sequentially exposed cells and *A. fumigatus*-exposed cells (4). Comparison between sequentially exposed cells and *P. aeruginosa*-exposed cells indicated a higher abundance in proteins associated with this pathway in sequentially exposed cells (5).

Table 3.5F List of proteins involved in protein processing in the ER. SSDA proteins arising from comparisons between the different infection groups of A549 cells and highlighted in the KEGG map depicting protein processing in the ER are listed.

Gene name	Protein name
BCAP31	B cell receptor associated protein 31
DNAJA2	DnaJ heat shock protein family (Hsp40) member A2
SEC23B	SEC23 homolog B, COPII coat complex component
SEC23A	Sec23 homolog A, COPII coat complex component
CKAP4	cytoskeleton associated protein 4
DDOST	dolichyl-diphosphooligosaccharide
GANAB	glucosidase II alpha subunit
ERO1A	endoplasmic reticulum oxidoreductase 1 alpha
DNAJA1	DnaJ heat shock protein family (Hsp40) member A1
HSPA6	heat shock protein family A (Hsp70) member 6
P4HB	prolyl 4-hydroxylase subunit beta
DNAJC3	DnaJ heat shock protein family (Hsp40) member C3
UGGT1	UDP-glucose glycoprotein glucosyltransferase 1
RAD23B	RAD23 homolog B, nucleotide excision repair protein
RPN1	ribophorin I
RPN2	ribophorin II
SKP1	S-phase kinase associated protein 1
SSR1	signal sequence receptor subunit 1
SSR4	signal sequence receptor subunit 4
HSP90B1	heat shock protein 90 beta family member 1
UBE2D1	ubiquitin conjugating enzyme E2 D1
UBE2G1	ubiquitin conjugating enzyme E2 G1
UBE2G2	ubiquitin conjugating enzyme E2 G2
CANX	calnexin
CAPN1	calpain 1
PDIA4	protein disulfide isomerase family A member 4
SEC24C	SEC24 homolog C, COPII coat complex component
RBX1	ring-box 1

Table 3.5G List of proteins involved in ubiquitin-meidated proteolysis. SSDA proteins arising from comparisons between the different infection groups of A549 cells and highlighted in the KEGG map depicting ubiquitin-mediated proteolysis are listed.

Gene name	Protein name
HUWE1	HECT, UBA and WWE domain containing E3 ubiquitin protein ligase 1
UBE2C	ubiquitin conjugating enzyme E2 C
DDB1	damage specific DNA binding protein 1
MID1	midline 1
SKP1	S-phase kinase associated protein 1
ELOC	elongin C
ELOB	elongin B
UBA1	ubiquitin like modifier activating enzyme 1
UBE2D1	ubiquitin conjugating enzyme E2 D1
UBE2G1	ubiquitin conjugating enzyme E2 G1
UBE2G2	ubiquitin conjugating enzyme E2 G2
CUL4B	cullin 4B
UBA3	ubiquitin like modifier activating enzyme 3
RBX1	ring-box 1

GO term enrichment analysis within Cluster I, identified key biological processes, molecular functions and cellular components involved with the uptake and processing of pathogens and activation of an immune response. The protein abundance profile of the sequentially exposed groups was comparable to that of the control but distinctly different to that of the *A. fumigatus* and *P. aeruginosa* exposed groups in which the relative abundance of proteins was greater compared to the sequentially exposed A549 cells. Biological processes included cellular response to stimuli, cell motility, vesicle-mediated transport and signal transduction. Catalytic activity involving hydrolases, pyrophosphatases and nucleoside-triphosphatase were among the molecular functions included in this cluster. Proteins involved in parts of the cell that form cell projections, endosome, lysosome and receptor complexes formed a significant proportion of the proteins found in this cluster. This trend was reflected in the KEGG maps (Fig. 3.10H-M), where the levels of proteins in several pathways associated with pathogen uptake and processing including endocytosis, phagosome and lysosome activity were reduced in the sequentially exposed groups.

H.1

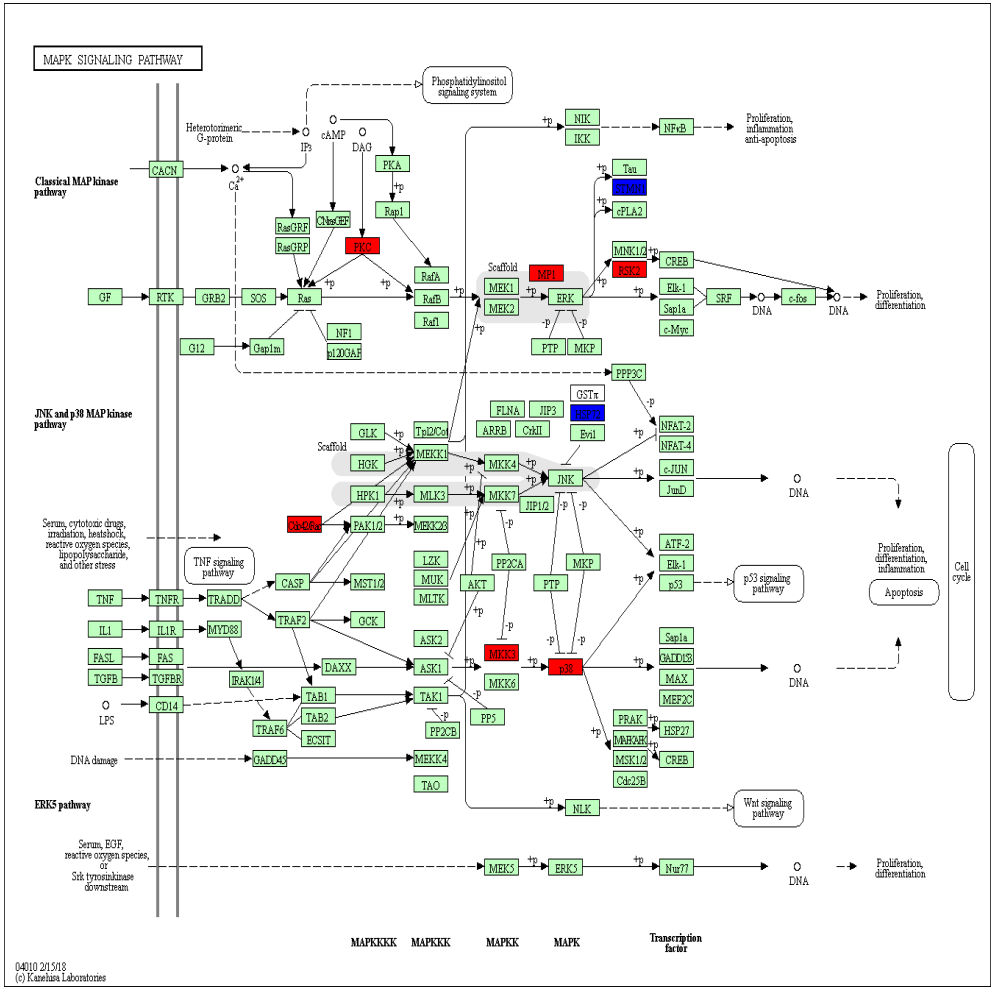
MAPK SIGNALING PATHWAY
Classical MAP kinase pathway
JNK and p38 MAP kinase pathway
ERK5 pathway
MAPKKKK
MAPKKK
MAPKK
MAPK
Transcription factor
04010 2/15/18
(c) Kanehisa Laboratories

H.2

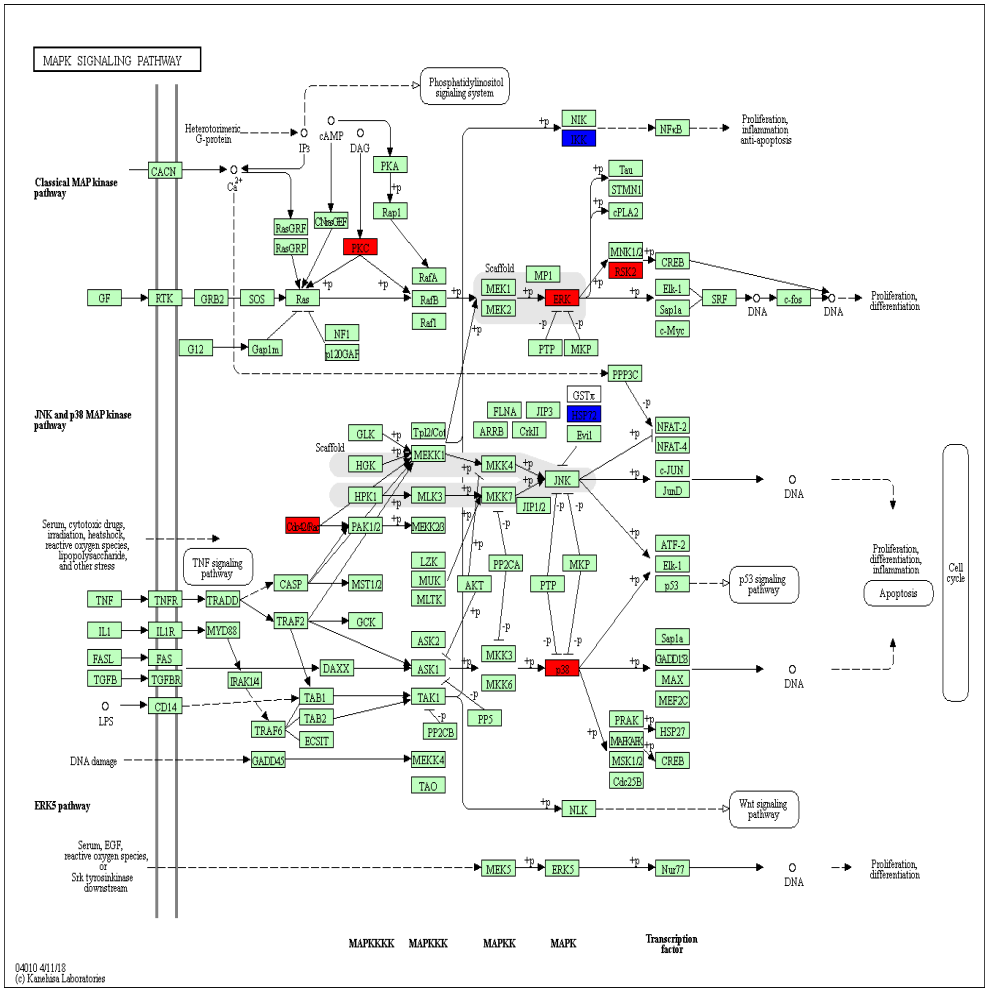
MAPK SIGNALING PATHWAY
Classical MAP kinase pathway
JNK and p38 MAP kinase pathway
ERK5 pathway
MAPKKKK
MAPKKK
MAPKK
MAPK
Transcription factor
04010 4/11/18
(c) Kanehisa Laboratories

H.3

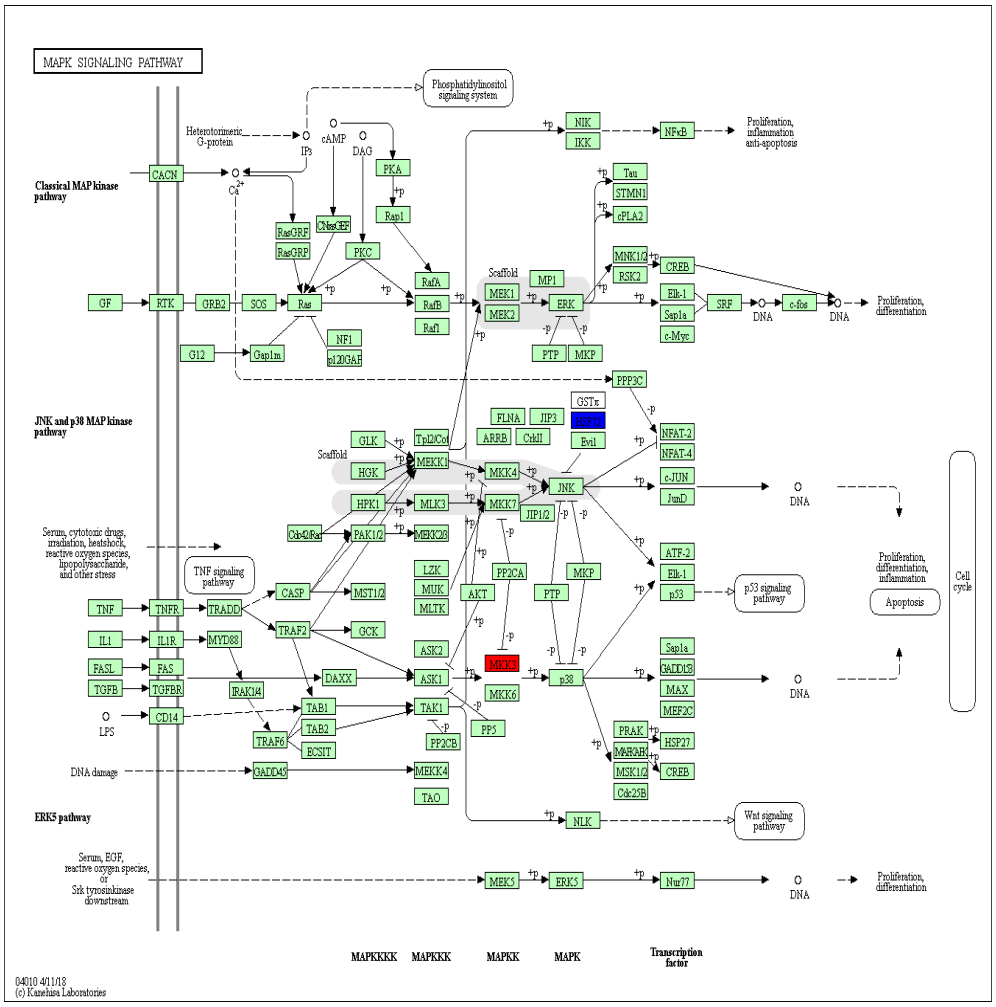

Fig. 3.10H KEGG maps depicting changes to the classical MAPK pathways and JNK and p38 MAPK pathways between A549 cells exposed to *A. fumigatus, P. aeruginosa* and sequential exposure to *A. fumigatus* and *P. aeruginosa*. An increase (red) and decrease (blue) in levels of proteins associated with the MAPK pathway was identified. The level of protein abundance is mostly increased in (1) *A. fumigatus*- and (2) *P. aeruginosa*, and (3) sequentially exposed A549 cells compared to the control. Changes to the relative abundance of proteins between the three infected groups of A549 cells were not significant and are thus not depicted here.

I.1

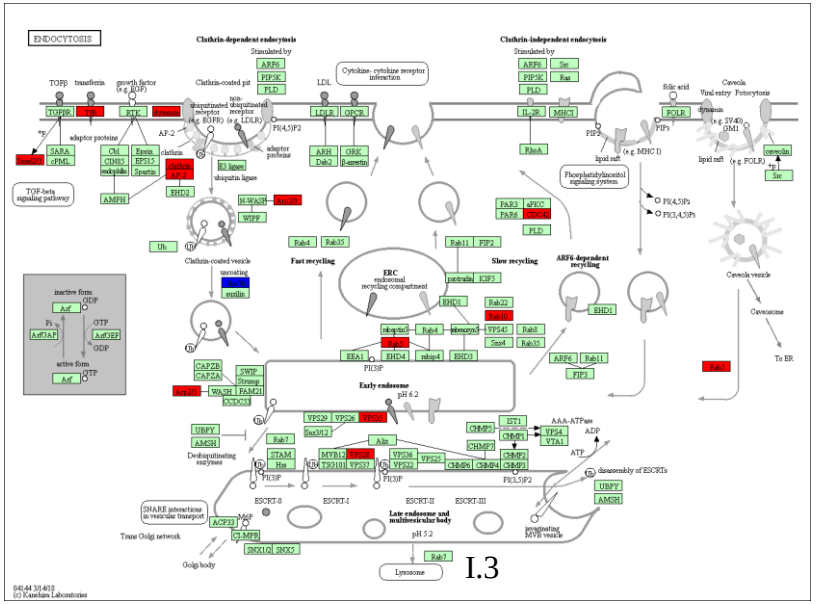
ENDOCYTOSIS
Clathrin-dependent endocytosis
Clathrin-independent endocytosis
Cytokine- cytokine receptor interaction
Fast recycling
Slow recycling
ARF6-dependent recycling
Early endosome
Late endosome and multivesicular body
Lysosome
Golgi body
Trans Golgi network
Caveosome
Caveola vesicle
Clathrin-coated vesicle
Phosphatidylinositol signaling system
TGF-beta signaling pathway
SNARE interactions in vesicular transport
ESCRT-0
ESCRT-I
ESCRT-II
ESCRT-III
disassembly of ESCRTs
(c) Kanehisa Laboratories

I.3

I.2

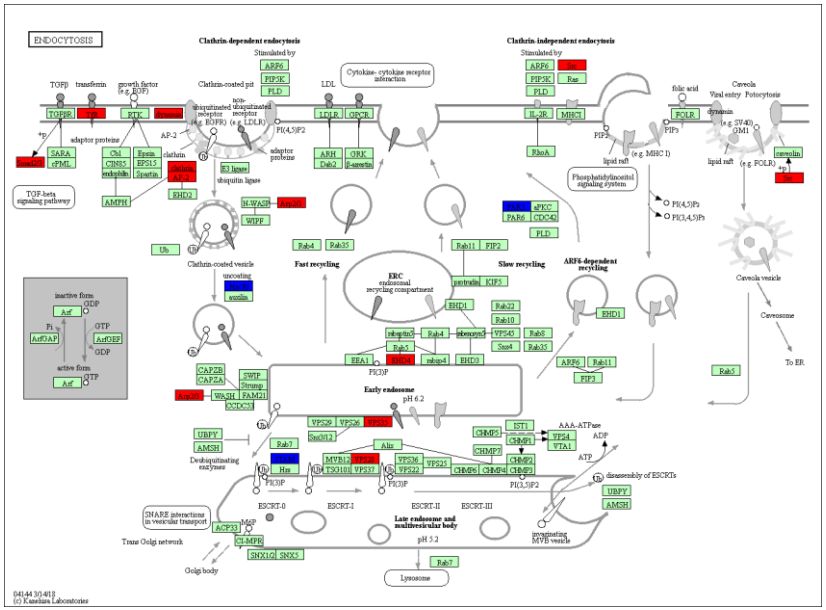
ENDOCYTOSIS
Clathrin-dependent endocytosis
Clathrin-independent endocytosis
Cytokine- cytokine receptor interaction
Fast recycling
Slow recycling
ARF6-dependent recycling
Early endosome
Late endosome and multivesicular body
Lysosome
Golgi body
Trans Golgi network
Caveosome
Caveola vesicle
Clathrin-coated vesicle
Phosphatidylinositol signaling system
TGF-beta signaling pathway
SNARE interactions in vesicular transport
ESCRT-0
ESCRT-I
ESCRT-II
ESCRT-III
disassembly of ESCRTs
(c) Kanehisa Laboratories

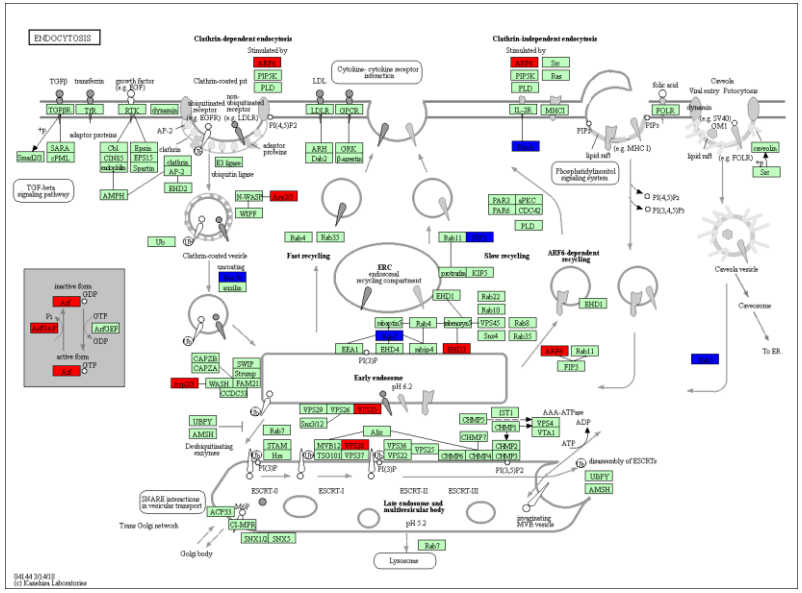
ENDOCYTOSIS
Clathrin-dependent endocytosis
Clathrin-independent endocytosis
Cytokine- cytokine receptor interaction
Fast recycling
Slow recycling
ARF6-dependent recycling
Early endosome
Late endosome and multivesicular body
Lysosome
Golgi body
Trans Golgi network
Caveosome
Caveola vesicle
Clathrin-coated vesicle
Phosphatidylinositol signaling system
TGF-beta signaling pathway
SNARE interactions in vesicular transport
ESCRT-0
ESCRT-I
ESCRT-II
ESCRT-III
disassembly of ESCRTs
(c) Kanehisa Laboratories

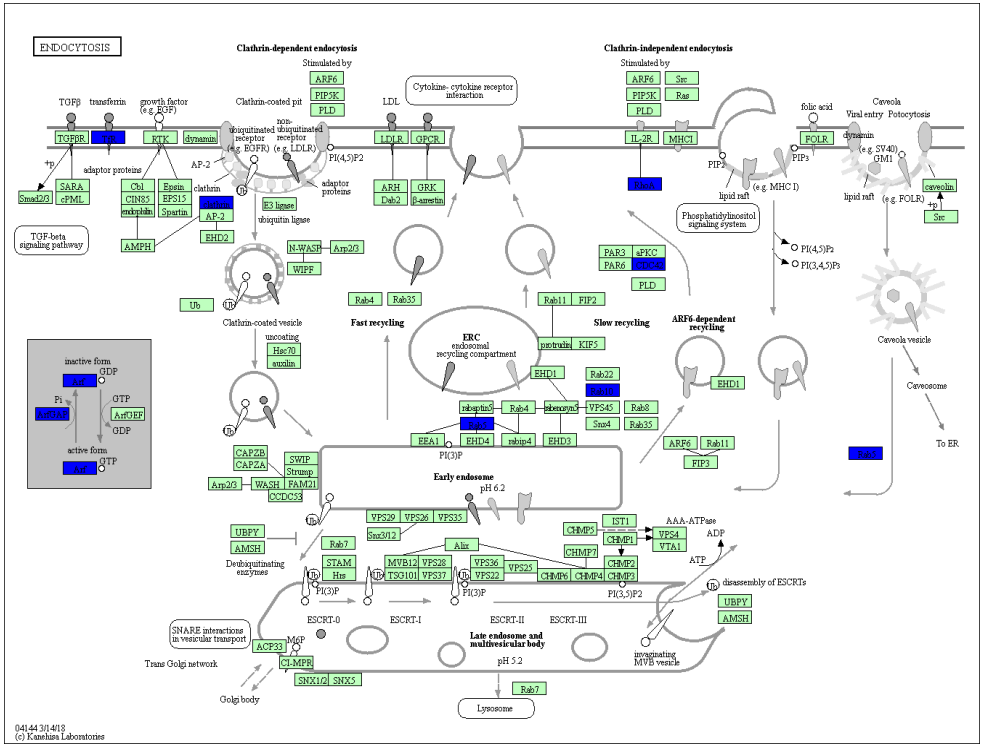

I.4

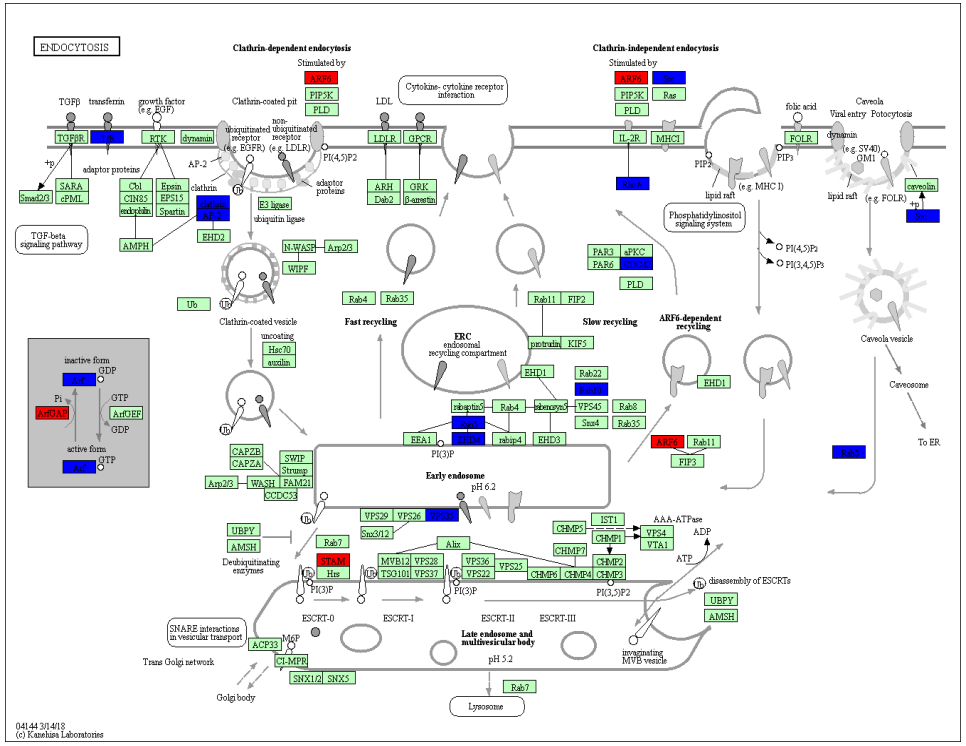

I.5

Fig. 3.10I KEGG maps depicting changes to the endocytosis pathway between A549 cells exposed to *A. fumigatus, P. aeruginosa* and sequential exposure to *A. fumigatus* and *P. aeruginosa*. An increase (red) and decrease (blue) in levels of proteins associated was identified. The level of protein abundance is mostly increased in (1) *A. fumigatus*- and (2) *P. aeruginosa*, and (3) sequentially-exposed A549 cells compared to the control. Compared to (4) *A. fumigatus*- and (5) *P. aeruginosa*-exposed cells, the level of proteins associated with endocytosis are reduced sequentially exposed cells.

Table 3.5H List of proteins involved in the MAPK pathway. SSDA proteins arising from comparisons between the different infection groups of A549 cells and highlighted in the KEGG map depicting the MAPK pathway are listed.

Gene name	Protein name
MAPK14	mitogen-activated protein kinase 14
HSPA6	heat shock protein family A (Hsp70) member 6
STMN1	stathmin 1
PRKCA	protein kinase C alpha
MAPK1	mitogen-activated protein kinase 1
MAPK3	mitogen-activated protein kinase 3
MAP2K3	mitogen-activated protein kinase kinase 3
RAC1	Rac family small GTPase 1
RPS6KA3	ribosomal protein S6 kinase A3
IKBKG	inhibitor of nuclear factor kappa B kinase regulatory subunit gamma
LAMTOR3	late endosomal/lysosomal adaptor, MAPK and MTOR activator 3
CDC42	cell division cycle 42

Table 3.5I list of proteins involved in the endocytosis pathway. SSDA proteins arising from comparisons between the different infection groups of A549 cells and highlighted in the KEGG map depicting the endocytosis pathway are listed.

GENE NAME	Protein name
ARPC4	actin related protein 2/3 complex subunit 4
ARPC1B	actin related protein 2/3 complex subunit 1B
RAB10	RAB10, member RAS oncogene family
CLTC	clathrin heavy chain
AP2B1	adaptor related protein complex 2 subunit beta 1
DNM2	dynamin 2
EHD4	EH domain containing 4
EHD3	EH domain containing 3
HSPA6	heat shock protein family A (Hsp70) member 6
ARF6	ADP ribosylation factor 6
RHOA	ras homolog family member A
SMAD3	SMAD family member 3
VPS28	VPS28 subunit of ESCRT-I
VPS35	VPS35 retromer complex component
PARD3	par-3 family cell polarity regulator
RAB5C	RAB5C, member RAS oncogene family
SRC	SRC proto-oncogene, non-receptor tyrosine kinase
TFRC	transferrin receptor
RAB11FIP1	RAB11 family interacting protein 1
STAM	signal transducing adaptor molecule
ACAP1	ArfGAP with coiled-coil, ankyrin repeat and PH domains 1
CDC42	cell division cycle 42

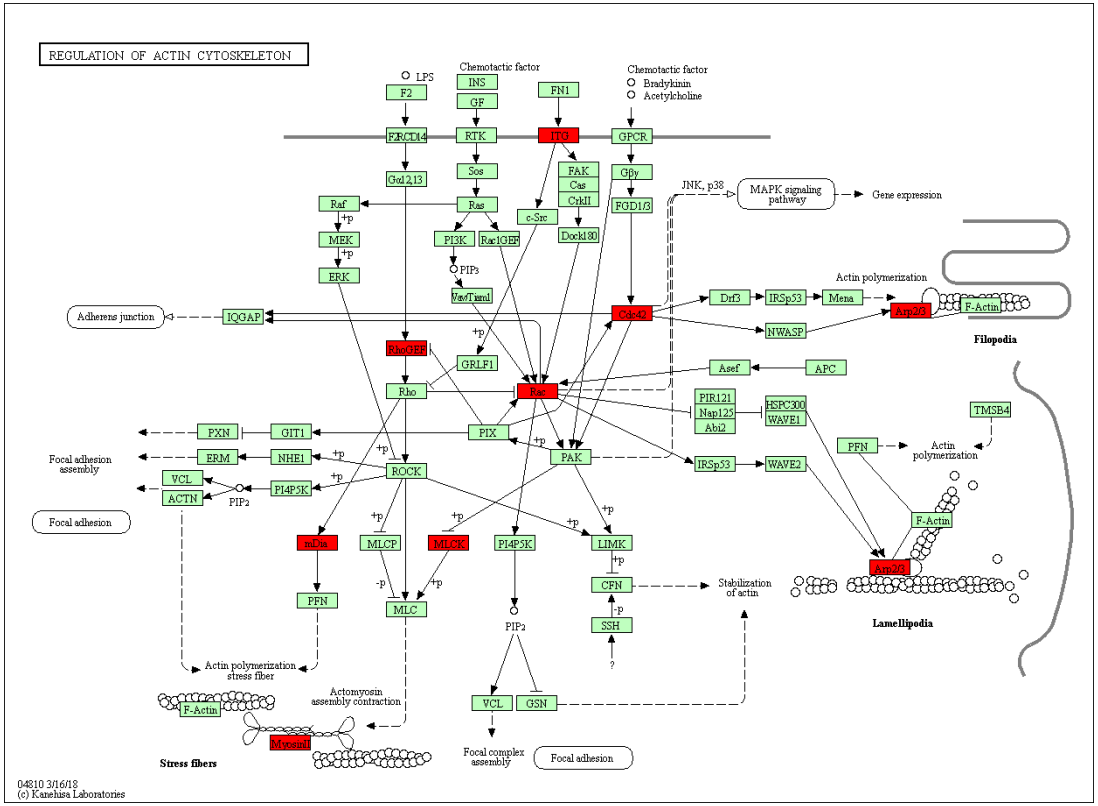
REGULATION OF ACTIN CYTOSKELETON
LPS
Chemotactic factor
Chemotactic factor
Bradykinin
Acetylcholine
F2
INS
GF
FN1
F2RCL14
RTK
ITG
GPCR
Gαi2,i3
Sos
FAK
Cas
CrkII
Gβγ
JNK, p38
MAPK signaling pathway
Gene expression
Raf
Ras
c-Src
FGD1/3
MEK
PI3K
Rac1GEF
Dock180
ERK
PIP3
WaveTiam1
Actin polymerization
Adherens junction
IQGAP
Cdc42
Drf3
IRSp53
Mena
Arp2/3
F-Actin
NWASP
Filopodia
RhoGEF
GRLF1
Asef
APC
Rho
Rac
PIR121
Nap125
Abi2
HSPC300
WAVE1
TMSB4
PXN
GIT1
PIX
PAK
PFN
Actin polymerization
Focal adhesion assembly
ERM
NHE1
IRSp53
WAVE2
VCL
ACTN
PI4P5K
PIP2
Focal adhesion
mDia
MLCP
MLCK
PI4P5K
LIMK
F-Actin
Arp2/3
CFN
Stabilization of actin
PFN
MLC
PIP2
SSH
Lamellipodia
Actin polymerization stress fiber
Actomyosin assembly contraction
F-Actin
VCL
GSN
Myosin
Focal complex assembly
Focal adhesion
Stress fibers
04810 3/16/18
(c) Kanehisa Laboratories

J.1

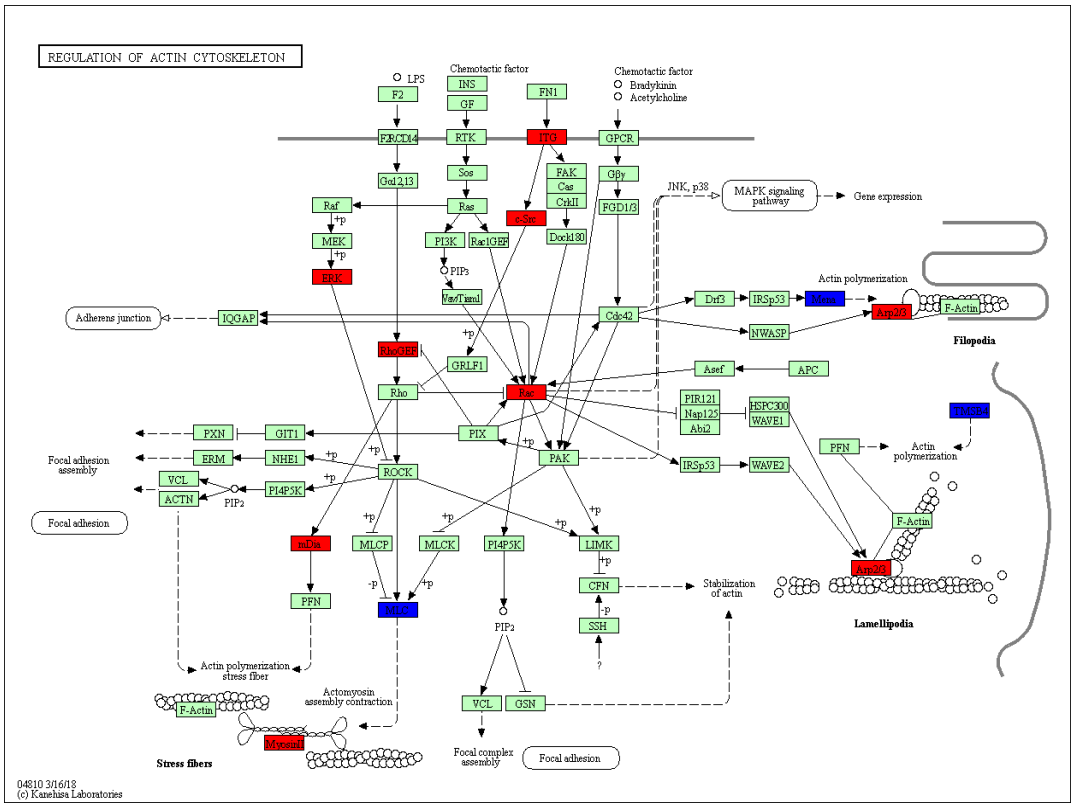
REGULATION OF ACTIN CYTOSKELETON
LPS
Chemotactic factor
Chemotactic factor
Bradykinin
Acetylcholine
F2
INS
GF
FN1
F2RCL14
RTK
ITG
GPCR
Gαi2,i3
Sos
FAK
Cas
CrkII
Gβγ
JNK, p38
MAPK signaling pathway
Gene expression
Raf
Ras
c-Src
FGD1/3
MEK
PI3K
Rac1GEF
Dock180
ERK
PIP3
WaveTiam1
Actin polymerization
Adherens junction
IQGAP
Cdc42
Drf3
IRSp53
Mena
Arp2/3
F-Actin
NWASP
Filopodia
RhoGEF
GRLF1
Asef
APC
Rho
Rac
PIR121
Nap125
Abi2
HSPC300
WAVE1
TMSB4
PXN
GIT1
PIX
PAK
PFN
Actin polymerization
Focal adhesion assembly
ERM
NHE1
IRSp53
WAVE2
VCL
ACTN
PI4P5K
PIP2
Focal adhesion
mDia
MLCP
MLCK
PI4P5K
LIMK
F-Actin
Arp2/3
CFN
Stabilization of actin
PFN
MLC
PIP2
SSH
Lamellipodia
Actin polymerization stress fiber
Actomyosin assembly contraction
F-Actin
VCL
GSN
Myosin
Focal complex assembly
Focal adhesion
Stress fibers
04810 3/16/18
(c) Kanehisa Laboratories

J.2

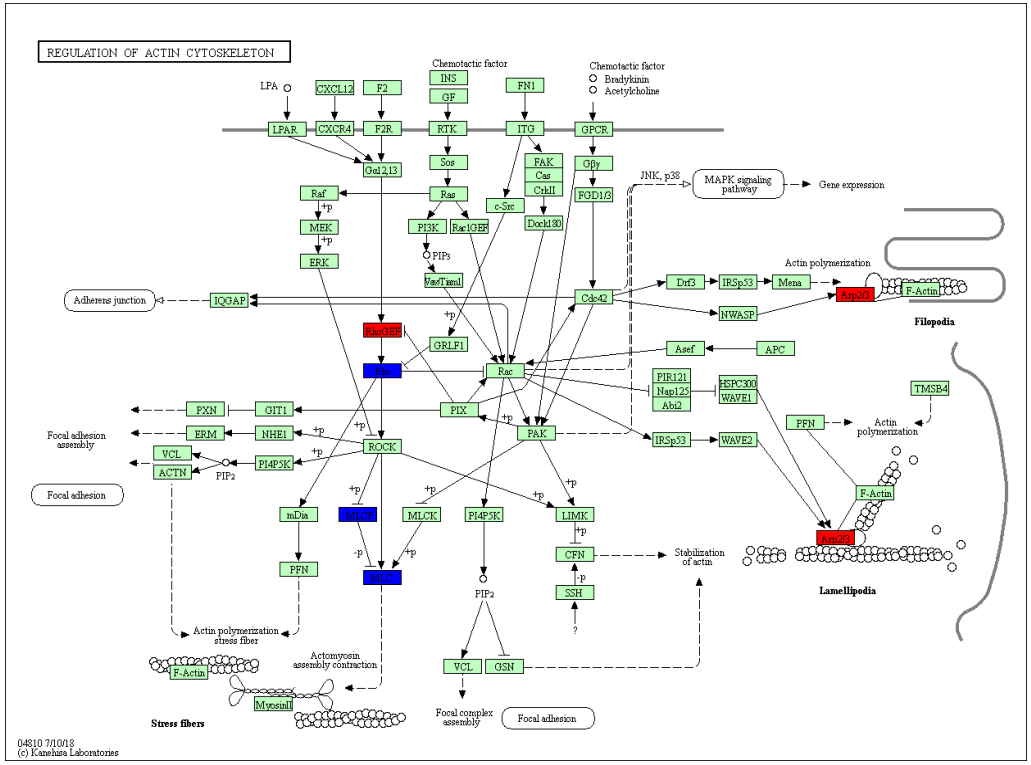
REGULATION OF ACTIN CYTOSKELETON
Chemotactic factor
Chemotactic factor
Bradykinin
Acetylcholine
LPA
CXCL12
F2
INS
GF
FN1
LPAR
CXCR4
F2R
RTK
ITG
GPCR
Gαi2,i3
Sos
FAK
Cas
CrkII
Gβγ
JNK, p38
MAPK signaling pathway
Gene expression
Raf
Ras
c-Src
FGD1/3
MEK
PI3K
Rac1GEF
Dock180
ERK
PIP3
Vav/Tiam1
Actin polymerization
Adherens junction
IQGAP
Cdc42
Drf3
IRSp53
Mena
Arp2/3
F-Actin
NWASP
Filopodia
RhoGEF
GRLF1
Rac
Asef
APC
Rho
PIR121
Nap125
Abi2
HSPC300
WAVE1
TMSB4
PXN
GIT1
PIX
PAK
PFN
Actin polymerization
Focal adhesion assembly
ERM
NHE1
VCL
ACTN
ROCK
PIP2
PI4P5K
Focal adhesion
mDia
MLCP
MLCK
LIMK
CFN
Stabilization of actin
MLC
SSH
Lamellipodia
Actin polymerization stress fiber
Actomyosin assembly contraction
F-Actin
Myosin
VCL
GSN
Stress fibers
Focal complex assembly
Focal adhesion
04810 7/10/18
(c) Kanehisa Laboratories

J.3

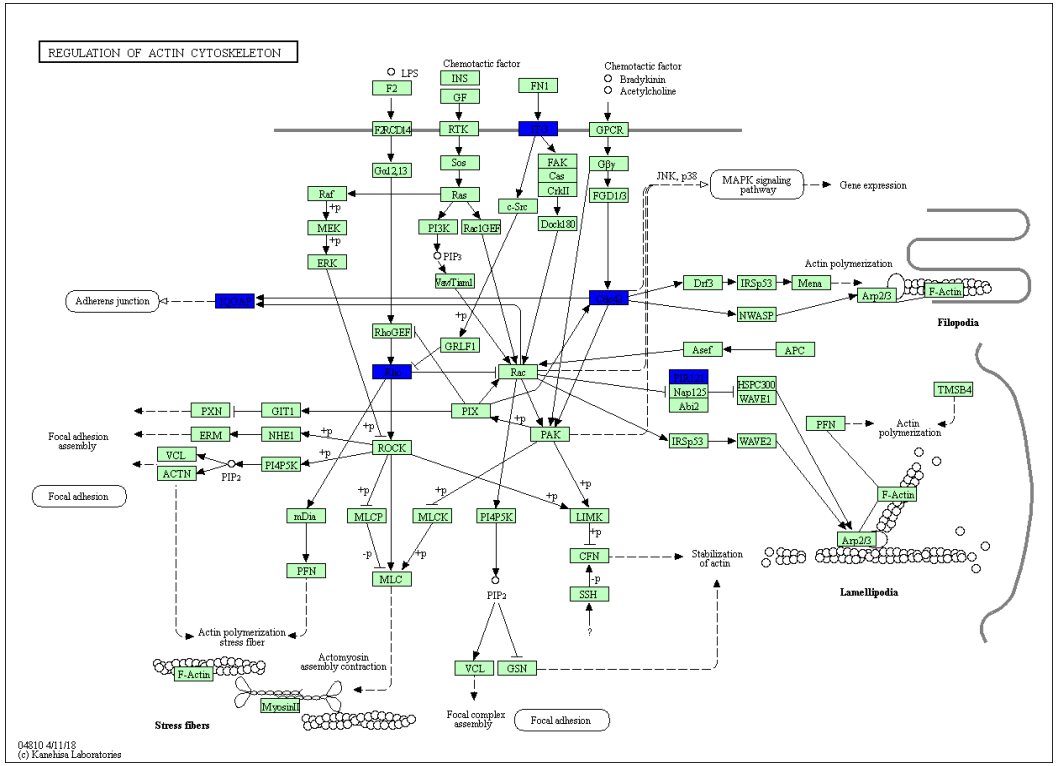
REGULATION OF ACTIN CYTOSKELETON
LPS
Chemotactic factor
Chemotactic factor
Bradykinin
Acetylcholine
F2
INS
GF
FN1
F2R/CD14
RTK
ITG
GPCR
Gαi2,i3
Sos
FAK
Cas
CrkII
Gβγ
JNK, p38
MAPK signaling pathway
Gene expression
Raf
Ras
c-Src
FGD1/3
MEK
PI3K
Rac1GEF
Dock180
ERK
PIP3
Vav/Tiam1
Actin polymerization
Adherens junction
IQGAP
Cdc42
Drf3
IRSp53
Mena
Arp2/3
F-Actin
NWASP
Filopodia
RhoGEF
GRLF1
Rac
Asef
APC
Rho
PIR121
Nap125
Abi2
HSPC300
WAVE1
TMSB4
PXN
GIT1
PIX
PAK
PFN
Actin polymerization
Focal adhesion assembly
ERM
NHE1
VCL
ACTN
ROCK
PIP2
PI4P5K
Focal adhesion
mDia
MLCP
MLCK
LIMK
CFN
Stabilization of actin
MLC
SSH
Lamellipodia
Actin polymerization stress fiber
Actomyosin assembly contraction
F-Actin
Myosin
VCL
GSN
Stress fibers
Focal complex assembly
Focal adhesion
04810 4/11/18
(c) Kanehisa Laboratories

J.4

J.5

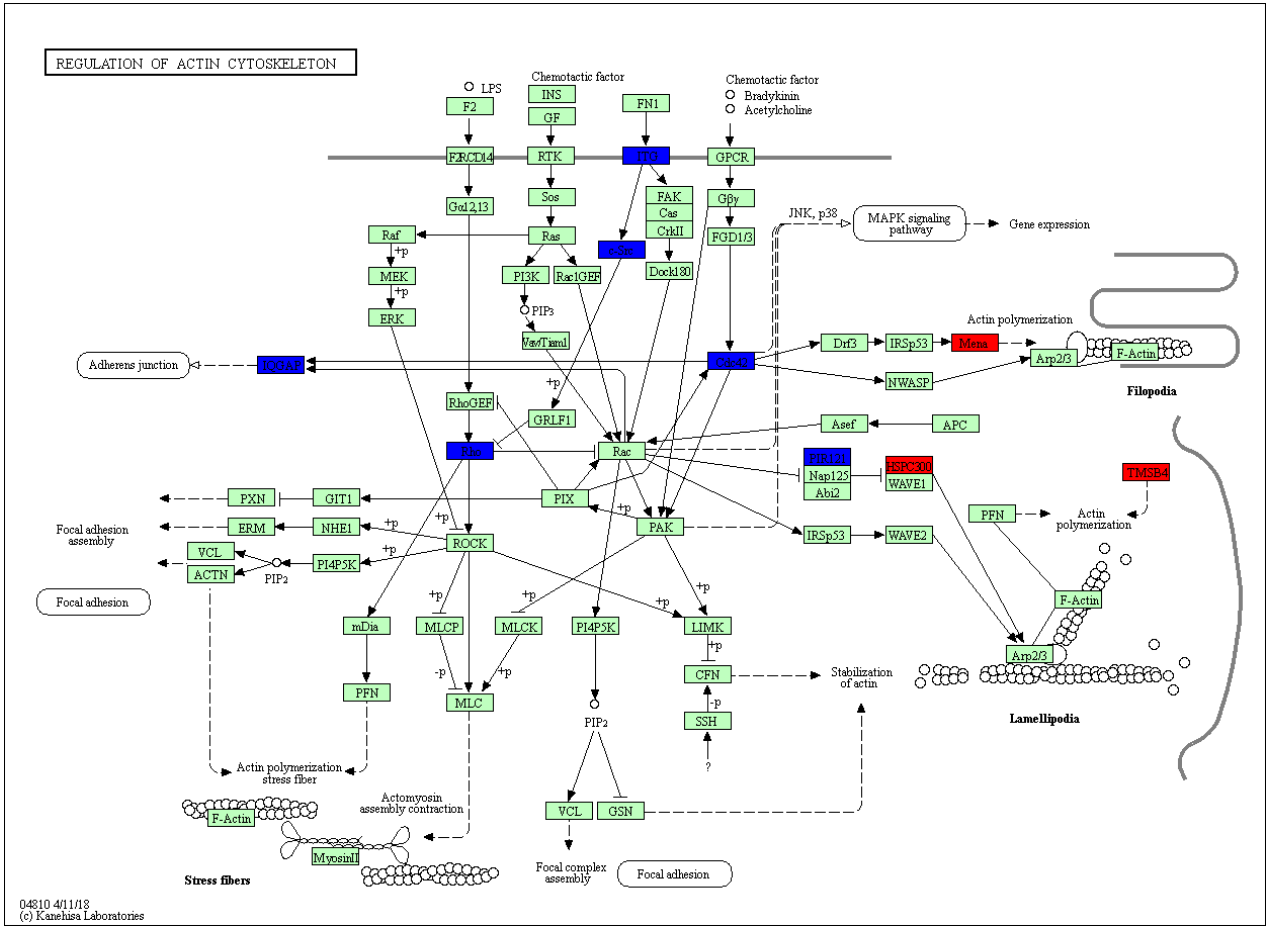

Fig. 3.10J KEGG map depicting changes to the actin cytoskeleton between A549 cells exposed to *A. fumigatus, P. aeruginosa* and sequential exposure to *A. fumigatus* and *P. aeruginosa*. Increased (red) and decreased (blue) levels of SSDA proteins involved in the regulation of actin cytoskeleton between (1) *A. fumigatus*, (2) *P. aeruginosa*, and (3) sequentially exposed A549 cells and the control were identified. Compared to the *A. fumigatus*- (4), and *P. aeruginosa*-exposed cells (5), this pathway was downregulated in the sequentially exposed group of A549 cells as indicated by the number of proteins highlighted in blue.

Table 3.5J List of proteins involved in the regulation of the actin cytoskeleton. SSDA proteins arising from comparisons between the different infection groups of A549 cells and highlighted in the KEGG map depicting the regulation of the actin cystoskeleton are listed

Gene name	Protein name
ARPC4	actin related protein 2/3 complex subunit 4
ARPC1B	actin related protein 2/3 complex subunit 1B
MYL12A	myosin light chain 12A
DIAPH1	diaphanous related formin 1
ITGB1	integrin subunit beta 1
RHOA	ras homolog family member A
MYH9	myosin heavy chain 9
MYH10	myosin heavy chain 10
MYLK	myosin light chain kinase
PPP1R12C	protein phosphatase 1 regulatory subunit 12C
ENAH	ENAH actin regulator
MAPK1	mitogen-activated protein kinase 1
MAPK3	mitogen-activated protein kinase 3
RAC1	Rac family small GTPase 1
SRC	SRC proto-oncogene, non-receptor tyrosine kinase
TMSB4X	thymosin beta 4 X-linked
ARHGEF1	Rho guanine nucleotide exchange factor 1
CDC42	cell division cycle 42

Table 3.5K List of proteins involved in bacterial invasion of epithelial cells. SSDA proteins arising from comparisons between the different infection groups of A549 cells and highlighted in the kegg map depicting bacterial invasion of epithelial cells are listed

Gene name	Protein name
ARPC4	actin related protein 2/3 complex subunit 4
ARPC1B	actin related protein 2/3 complex subunit 1B
CLTC	clathrin heavy chain
CTNNA2	catenin alpha 2
DNM2	dynamin 2
CTTN	cortactin
ITGB1	integrin subunit beta 1
RHOA	ras homolog family member A
RAC1	Rac family small GTPase 1
SRC	SRC proto-oncogene, non-receptor tyrosine kinase
CDC42	cell division cycle 42

K.1

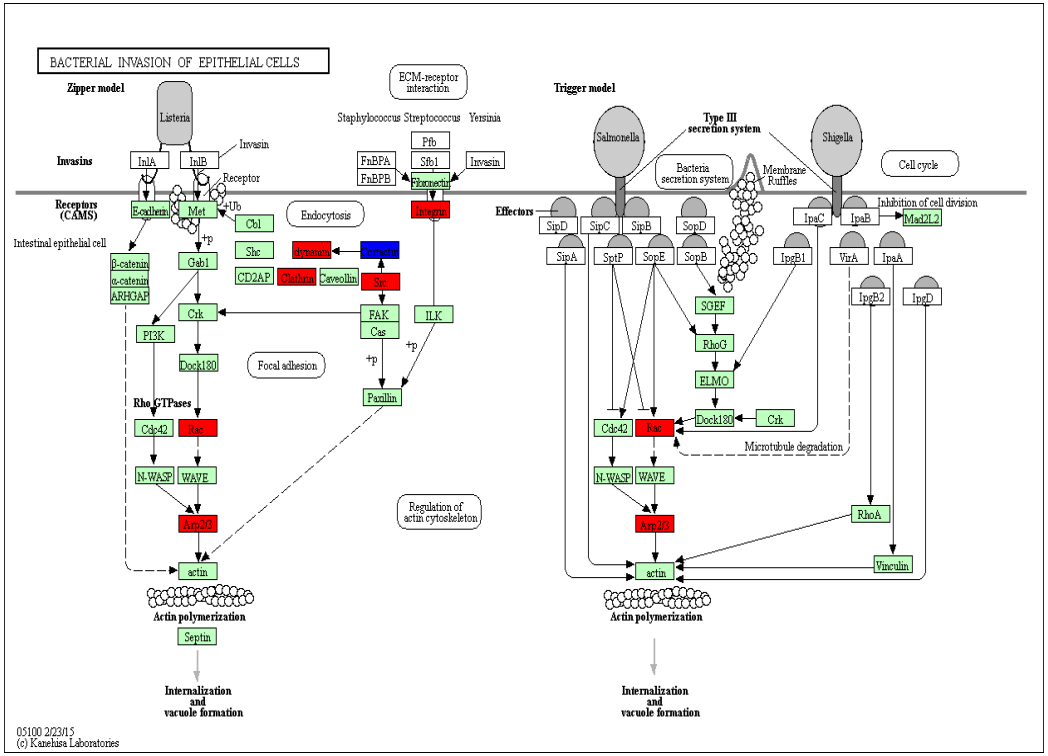
BACTERIAL INVASION OF EPITHELIAL CELLS
Zipper model
Trigger model
ECM-receptor interaction
Staphylococcus Streptococcus Yersinia
Listeria
Salmonella
Shigella
Type III secretion system
Bacteria secretion system
Membrane Ruffles
Cell cycle
Invasins
InlA
InlB
Invasin
Receptor
Pfb
FnBPA
FnBPB
Sfb1
Fibronectin
Receptors (CAMs)
E-cadherin
Met
+Ub
Cbl
Endocytosis
Integrin
Effectors
SipD
SipC
SipB
SopD
IpaC
IpaB
Msd2L2
Inhibition of cell division
Intestinal epithelial cell
SipA
SptP
SopE
SopB
IpgB1
VirA
IpaA
IpgB2
IpgD
β-catenin
α-catenin
ARHGAP
Gab1
Shc
dynamin
Cortactin
CD2AP
Clathrin
Caveolin
Src
Crk
FAK
Cas
ILK
PI3K
Dock180
Focal adhesion
+p
Paxillin
Rho GTPases
Cdc42
Rac
SGEF
RhoG
ELMO
Microtubule degradation
N-WASP
WAVE
Arp2/3
RhoA
Regulation of actin cytoskeleton
actin
Vinculin
Actin polymerization
Septin
Internalization and vacuole formation
05100 2/23/15
(c) Kanehisa Laboratories

K.2

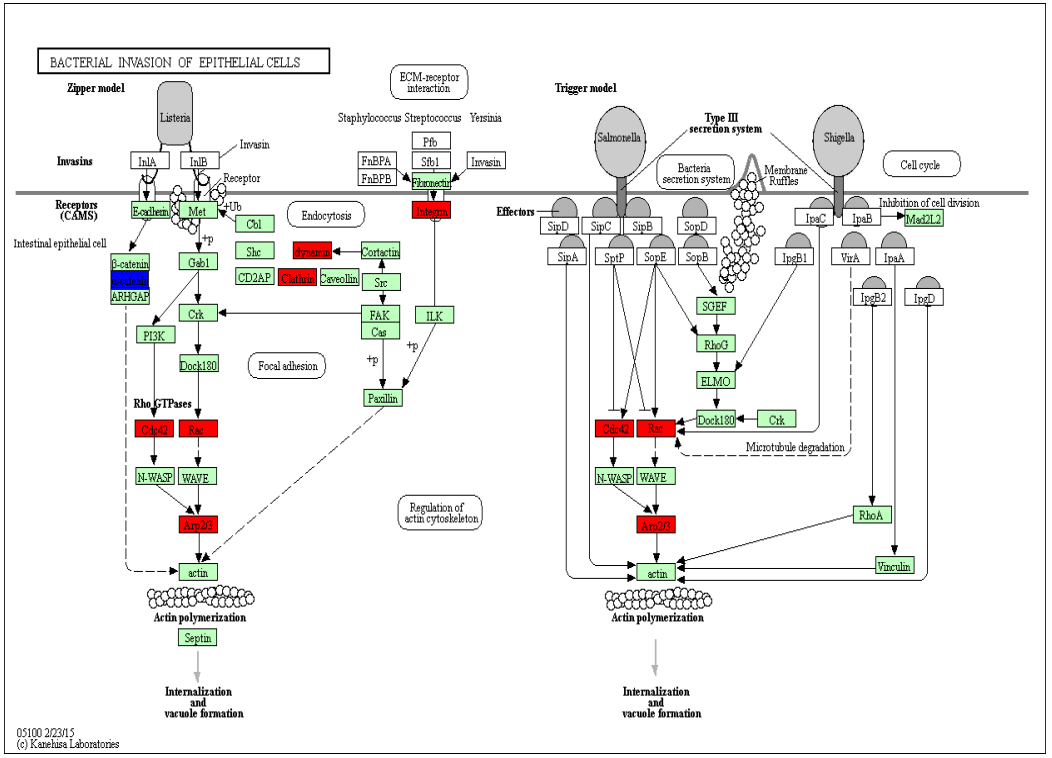
BACTERIAL INVASION OF EPITHELIAL CELLS
Zipper model
Trigger model
ECM-receptor interaction
Staphylococcus Streptococcus Yersinia
Listeria
Salmonella
Shigella
Type III secretion system
Bacteria secretion system
Membrane Ruffles
Cell cycle
Invasins
InlA
InlB
Invasin
Receptor
Pfb
FnBPA
FnBPB
Sfb1
Fibronectin
Receptors (CAMs)
E-cadherin
Met
+Ub
Cbl
Endocytosis
Integrin
Effectors
SipD
SipC
SipB
SopD
IpaC
IpaB
Msd2L2
Inhibition of cell division
Intestinal epithelial cell
SipA
SptP
SopE
SopB
IpgB1
VirA
IpaA
IpgB2
IpgD
β-catenin
α-catenin
ARHGAP
Gab1
Shc
dynamin
Cortactin
CD2AP
Clathrin
Caveolin
Src
Crk
FAK
Cas
ILK
PI3K
Dock180
Focal adhesion
+p
Paxillin
Rho GTPases
Cdc42
Rac
SGEF
RhoG
ELMO
Microtubule degradation
N-WASP
WAVE
Arp2/3
RhoA
Regulation of actin cytoskeleton
actin
Vinculin
Actin polymerization
Septin
Internalization and vacuole formation
05100 2/23/15
(c) Kanehisa Laboratories

K.3

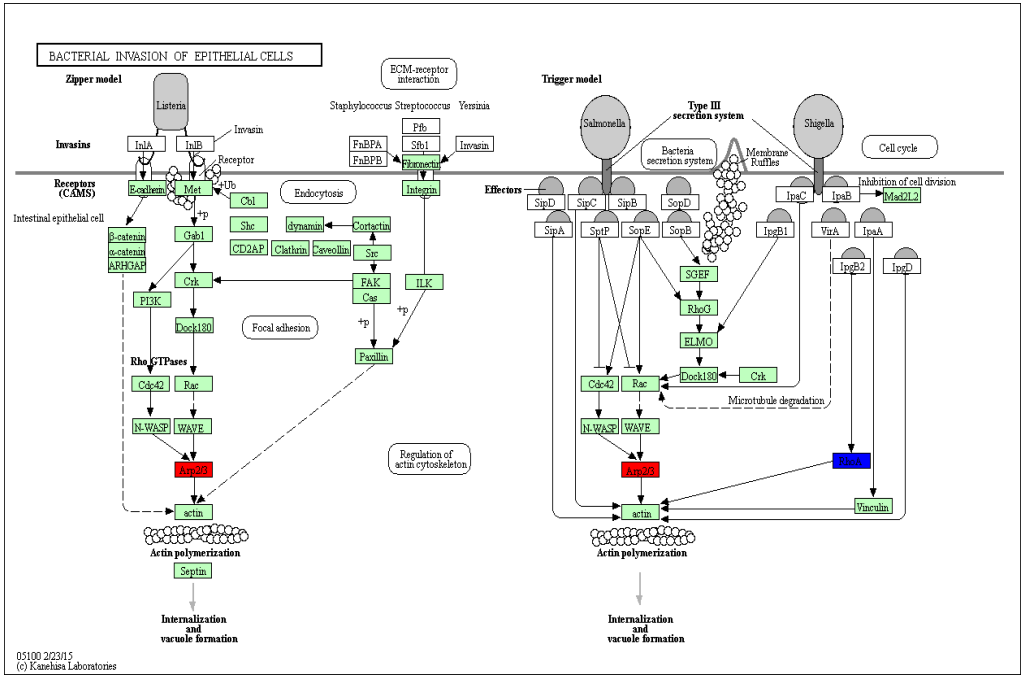

K.4

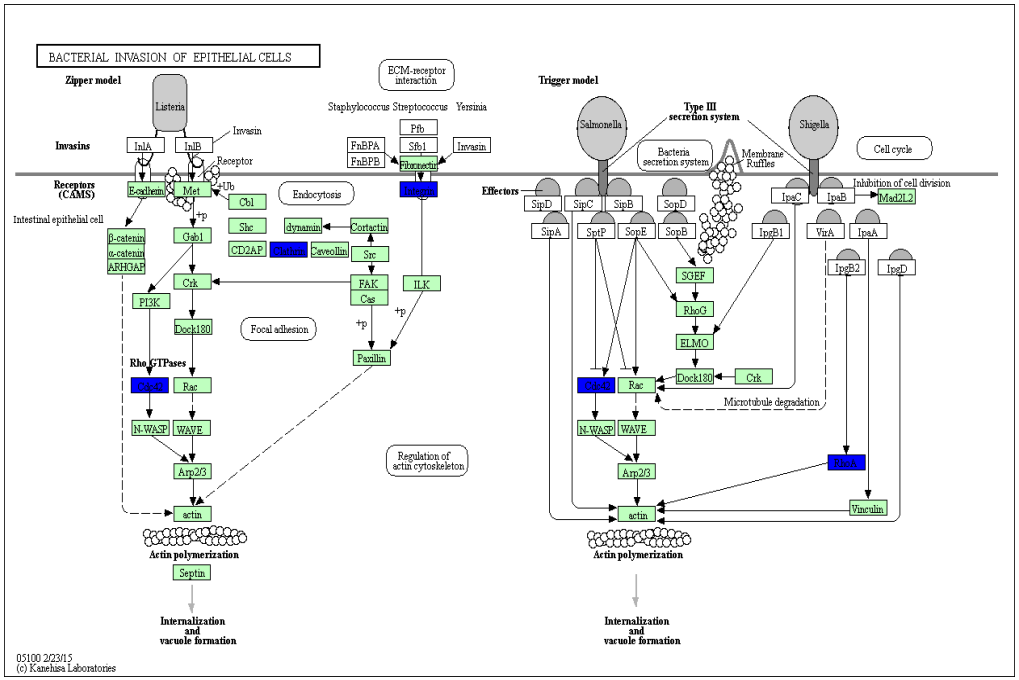

K.5

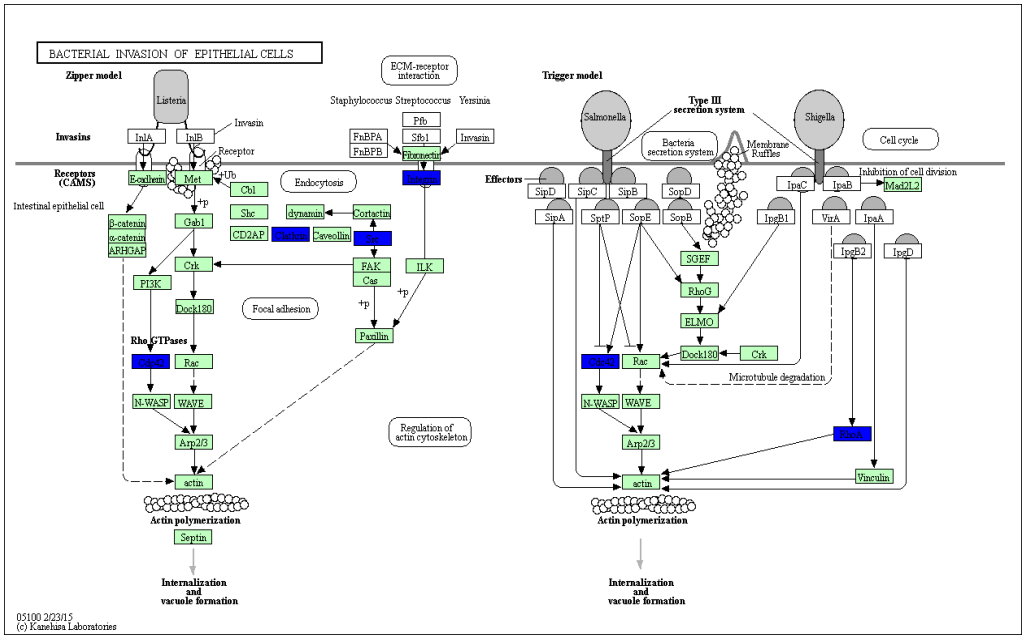

Fig.3.10K KEGG maps depicting a pathway of bacterial invasion of epithelial cells in A549 cells exposed to *A. fumigatus*, *P. aeruginosa* and sequential exposure to *A. fumigatus* and *P. aeruginosa*. Increased (red) and decreased (blue) levels of SSDA proteins involved in the bacterial invasion pathway between (1) *A. fumigatus*, (2) *P. aeruginosa*, and (3) sequentially exposed A549 cells and the control were identified . Compared to *A. fumigatus*- (4) and *P. aeruginosa* exposed cells (5), this pathway was clearly downregulated in the sequentially exposed A549 cells as indicated by the number of proteins highlighted in blue.

L.1

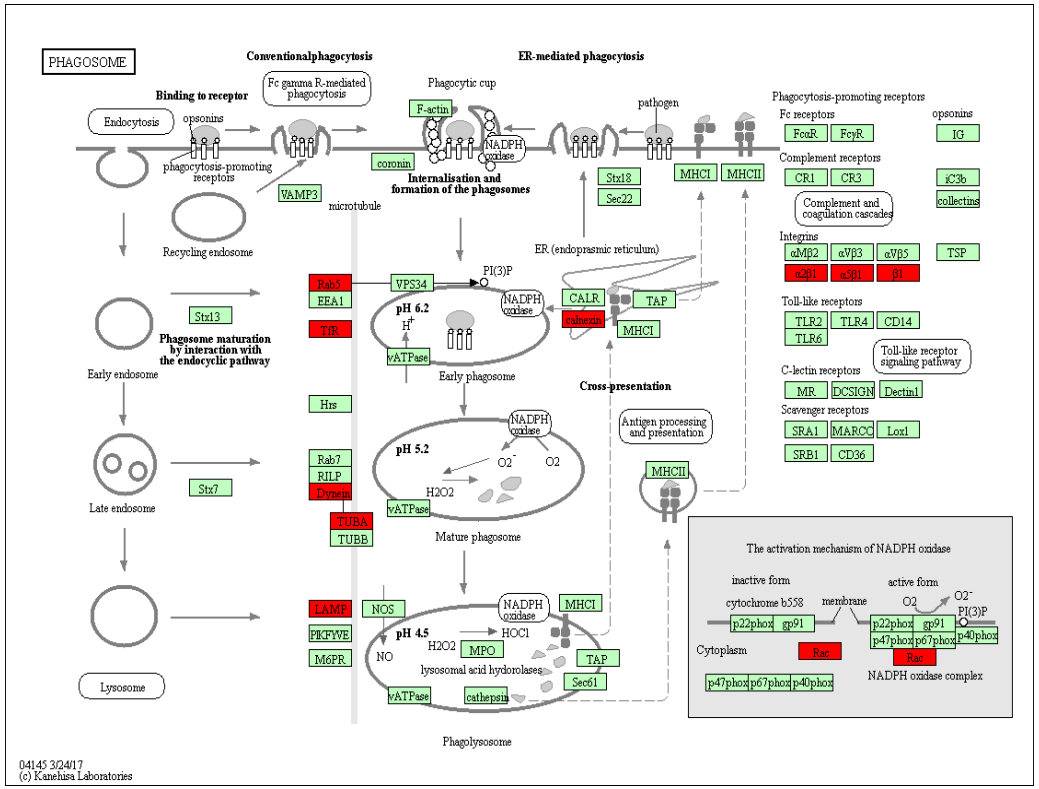
PHAGOSOME
Conventionalphagocytosis
ER-mediated phagocytosis
Binding to receptor
Fc gamma R-mediated phagocytosis
Phagocytic cup
F-actin
pathogen
Endocytosis
opsonins
phagocytosis-promoting receptors
VAMP3
microtubule
coronin
NADPH oxidase
Internalisation and formation of the phagosomes
Stx18
Sec22
MHCI
MHCII
Phagocytosis-promoting receptors
Fc receptors
FcαR
FcγR
opsonins
IG
Complement receptors
CR1
CR3
iC3b
collectins
Complement and coagulation cascades
Integrins
αMβ2
αVβ3
αVβ5
TSP
α2β1
α5β1
β1
Toll-like receptors
TLR2
TLR4
CD14
TLR6
Toll-like receptor signaling pathway
C-lectin receptors
MR
DCSIGN
Dectin1
Scavenger receptors
SRA1
MARCO
Lox1
SRB1
CD36
Recycling endosome
ER (endoprasmic reticulum)
Rab5
EEA1
VPS34
PI(3)P
CALR
calnexin
TAP
TfR
vATPase
pH 6.2
Early endosome
Early phagosome
Cross-presentation
Stx13
Phagosome maturation by interaction with the endocytic pathway
Hrs
Rab7
RILP
Dynein
pH 5.2
O2-
O2
H2O2
Antigen processing and presentation
Late endosome
Stx7
TUBA
TUBB
Mature phagosome
LAMP
NOS
PIKFYVE
M6PR
pH 4.5
HOCl
NO
MPO
lysosomal acid hydrolases
Sec61
cathepsin
Lysosome
Phagolysosome
The activation mechanism of NADPH oxidase
inactive form
active form
cytochrome b558
membrane
p22phox
gp91
p47phox
p67phox
p40phox
Cytoplasm
Rac
NADPH oxidase complex
04145 3/24/17
(c) Kanehisa Laboratories

L.2

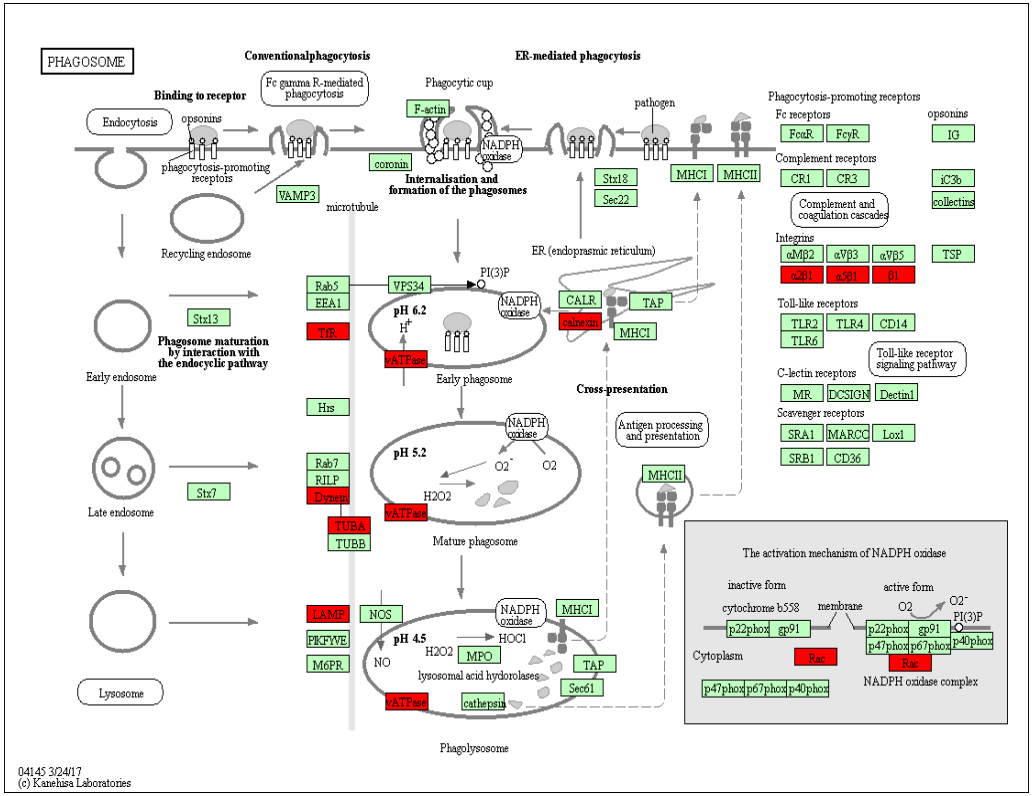
PHAGOSOME
Conventionalphagocytosis
ER-mediated phagocytosis
Binding to receptor
Fc gamma R-mediated phagocytosis
Phagocytic cup
F-actin
pathogen
Endocytosis
opsonins
phagocytosis-promoting receptors
VAMP3
microtubule
coronin
NADPH oxidase
Internalisation and formation of the phagosomes
Stx18
Sec22
MHCI
MHCII
Phagocytosis-promoting receptors
Fc receptors
FcαR
FcγR
opsonins
IG
Complement receptors
CR1
CR3
iC3b
collectins
Complement and coagulation cascades
Integrins
αMβ2
αVβ3
αVβ5
TSP
α2β1
α5β1
β1
Toll-like receptors
TLR2
TLR4
CD14
TLR6
Toll-like receptor signaling pathway
C-lectin receptors
MR
DCSIGN
Dectin1
Scavenger receptors
SRA1
MARCO
Lox1
SRB1
CD36
Recycling endosome
ER (endoprasmic reticulum)
Rab5
EEA1
VPS34
PI(3)P
CALR
calnexin
TAP
TfR
vATPase
pH 6.2
Early endosome
Early phagosome
Cross-presentation
Stx13
Phagosome maturation by interaction with the endocytic pathway
Hrs
Rab7
RILP
Dynein
pH 5.2
O2-
O2
H2O2
Antigen processing and presentation
Late endosome
Stx7
TUBA
TUBB
Mature phagosome
LAMP
NOS
PIKFYVE
M6PR
pH 4.5
HOCl
NO
MPO
lysosomal acid hydrolases
Sec61
cathepsin
Lysosome
Phagolysosome
The activation mechanism of NADPH oxidase
inactive form
active form
cytochrome b558
membrane
p22phox
gp91
p47phox
p67phox
p40phox
Cytoplasm
Rac
NADPH oxidase complex
04145 3/24/17
(c) Kanehisa Laboratories

L.3

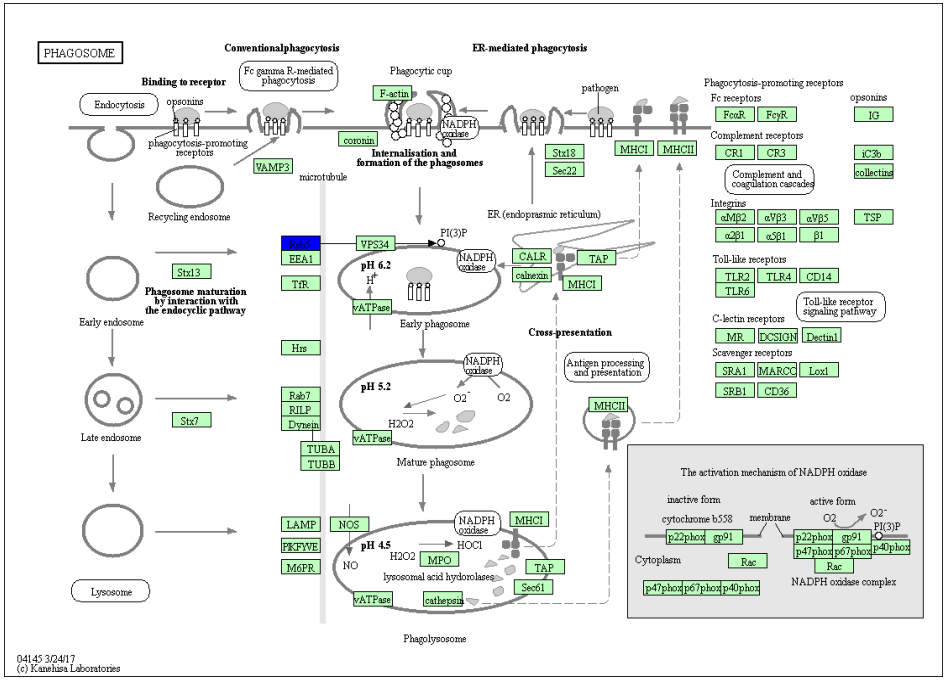

L.4

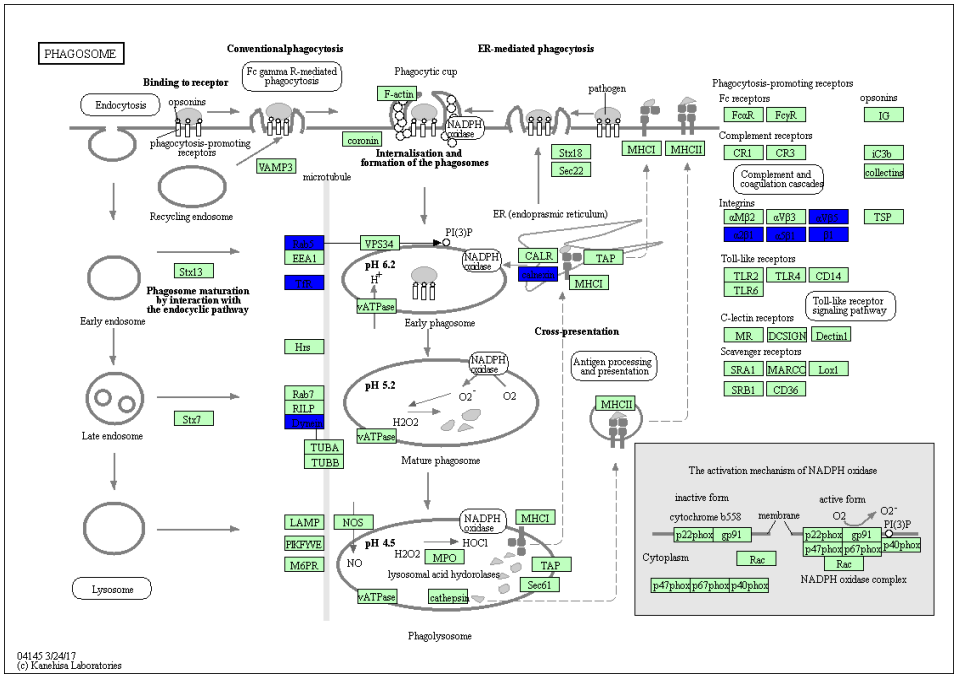

L.5

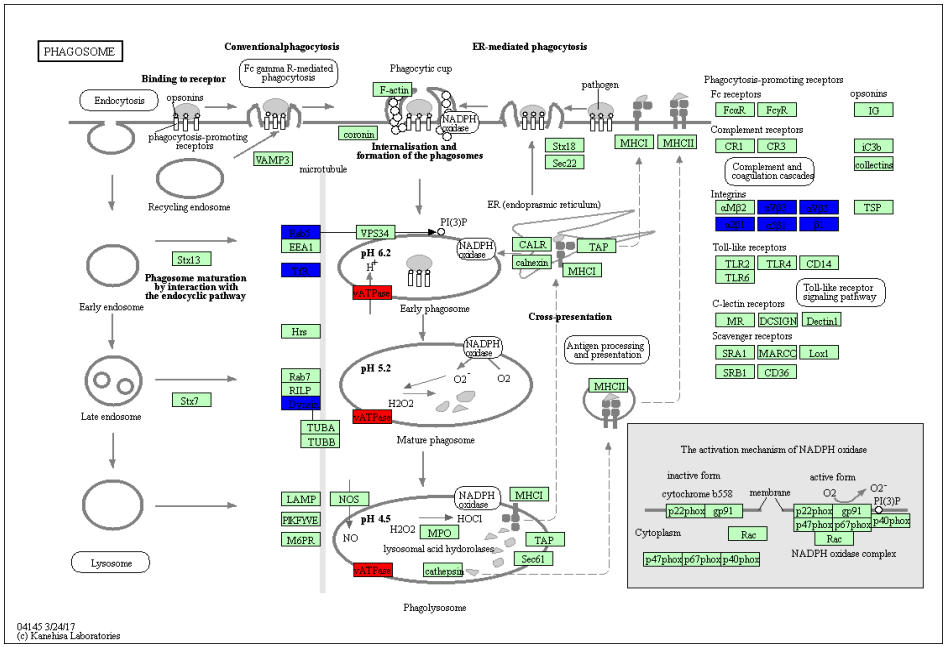

Fig. 3.10L KEGG maps depicting changes in phagosome-associated proteins between A549 cells exposed to *A. fumigatus, P. aeruginosa* and sequential exposure to *A. fumigatus* and *P. aeruginosa*. A distinct increase (red) in levels of SSDA proteins involved in the phagosome pathway in (1) *A. fumigatus*, (2) *P. aeruginosa*- exposed A549 cells and the control was identified. The response of sequentially exposed cells and the control were similar with the exception of one protein, Rab5, which was decreased in abundance (3). Compared to *A. fumigatus*- (4) and *P. aeruginosa* exposed cells (5), this pathway was clearly downregulated in the sequentially exposed A549 cells as indicated by the number of proteins highlighted in blue.

M.1

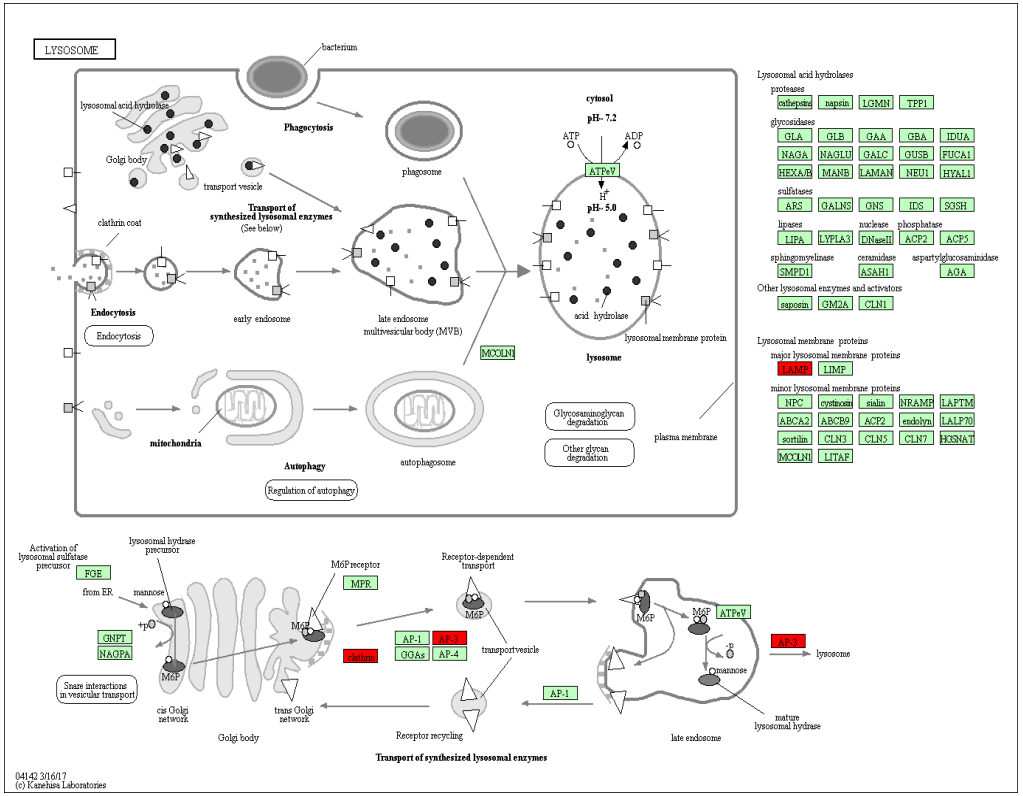
LYSOSOME
bacterium
lysosomal acid hydrolase
Phagocytosis
Golgi body
transport vesicle
phagosome
cytosol
pH- 7.2
ATP
ADP
ATPeV
H+
pH- 5.0
Transport of synthesized lysosomal enzymes (See below)
clathrin coat
Endocytosis
Endocytosis
early endosome
late endosome
multivesicular body (MVB)
MCOLN1
lysosome
acid hydrolase
lysosomal membrane protein
mitochondria
Autophagy
autophagosome
Regulation of autophagy
Glycosaminoglycan degradation
Other glycan degradation
plasma membrane
Lysosomal acid hydrolases
proteases
cathepsins napsin LGMN TPP1
glycosidases
GLA GLB GAA GBA IDUA
NAGA NAGLU GALC GUSB FUCA1
HEXA/B MANB LAMAN NEU1 HYAL1
sulfatases
ARS GALNS GNS IDS SGSH
lipases nuclease phosphatase
LIPA LYPLA3 DNaseII ACP2 ACP5
sphingomyelinase ceramidase aspartylglucosaminidase
SMPD1 ASAH1 AGA
Other lysosomal enzymes and activators
saposin GM2A CLN1
Lysosomal membrane proteins
major lysosomal membrane proteins
LAMP LIMP
minor lysosomal membrane proteins
NPC cystinosin sialin NRAMP LAPTM
ABCA2 ABCB9 ACP2 endolyn LALP70
sortilin CLN3 CLN5 CLN7 HGSNAT
MCOLN1 LITAF
Activation of lysosomal sulfatase precursor
FGE
lysosomal hydrase precursor
from ER
mannose
M6P receptor
MPR
Receptor-dependent transport
GNPT
NAGPA
M6P
clathrin
transportvesicle
AP-1 AP-3
GGAs AP-4
ATPeV
AP-3
lysosome
Snare interactions in vesicular transport
cis Golgi network
trans Golgi network
Golgi body
Receptor recycling
late endosome
mannose
mature lysosomal hydrase
Transport of synthesized lysosomal enzymes
04142 3/16/17
(c) Kanehisa Laboratories

M.2

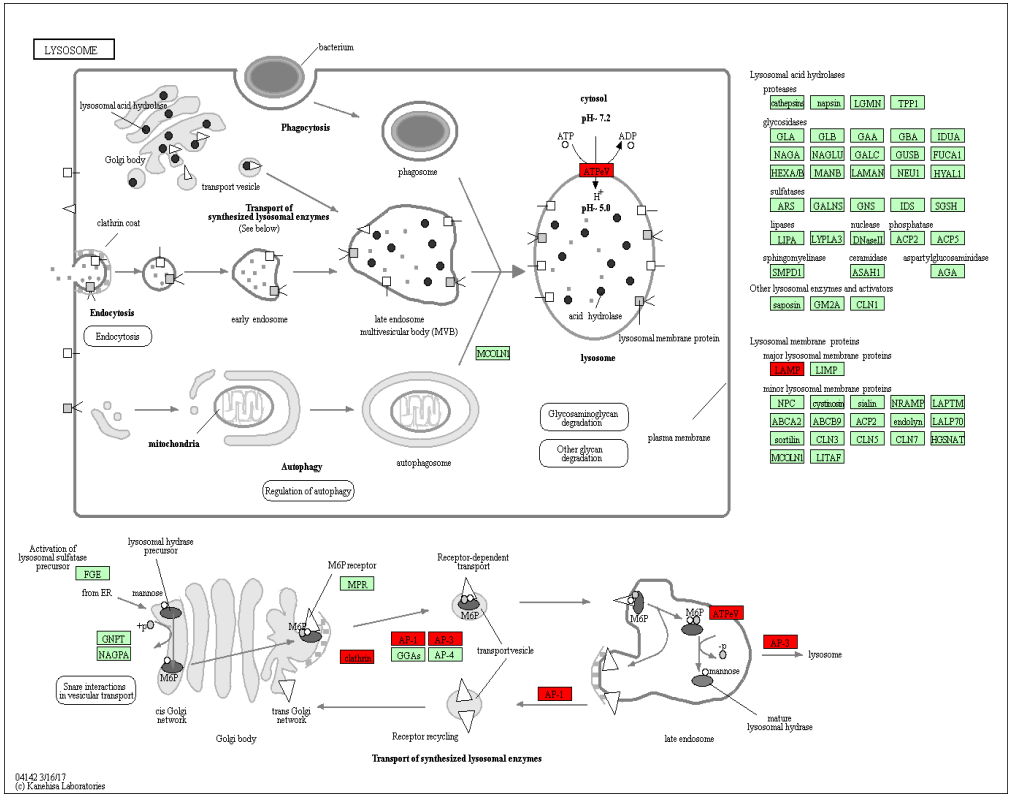
LYSOSOME
bacterium
lysosomal acid hydrolase
Phagocytosis
Golgi body
transport vesicle
phagosome
cytosol
pH- 7.2
ATP
ADP
ATPeV
H+
pH- 5.0
Transport of synthesized lysosomal enzymes (See below)
clathrin coat
Endocytosis
Endocytosis
early endosome
late endosome
multivesicular body (MVB)
MCOLN1
lysosome
acid hydrolase
lysosomal membrane protein
mitochondria
Autophagy
autophagosome
Regulation of autophagy
Glycosaminoglycan degradation
Other glycan degradation
plasma membrane
Lysosomal acid hydrolases
proteases
cathepsins napsin LGMN TPP1
glycosidases
GLA GLB GAA GBA IDUA
NAGA NAGLU GALC GUSB FUCA1
HEXA/B MANB LAMAN NEU1 HYAL1
sulfatases
ARS GALNS GNS IDS SGSH
lipases nuclease phosphatase
LIPA LYPLA3 DNaseII ACP2 ACP5
sphingomyelinase ceramidase aspartylglucosaminidase
SMPD1 ASAH1 AGA
Other lysosomal enzymes and activators
saposin GM2A CLN1
Lysosomal membrane proteins
major lysosomal membrane proteins
LAMP LIMP
minor lysosomal membrane proteins
NPC cystinosin sialin NRAMP LAPTM
ABCA2 ABCB9 ACP2 endolyn LALP70
sortilin CLN3 CLN5 CLN7 HGSNAT
MCOLN1 LITAF
Activation of lysosomal sulfatase precursor
FGE
lysosomal hydrase precursor
from ER
mannose
M6P receptor
MPR
Receptor-dependent transport
GNPT
NAGPA
M6P
clathrin
transportvesicle
AP-1 AP-3
GGAs AP-4
ATPeV
AP-3
lysosome
Snare interactions in vesicular transport
cis Golgi network
trans Golgi network
Golgi body
Receptor recycling
late endosome
mannose
mature lysosomal hydrase
Transport of synthesized lysosomal enzymes
04142 3/16/17
(c) Kanehisa Laboratories

M.3

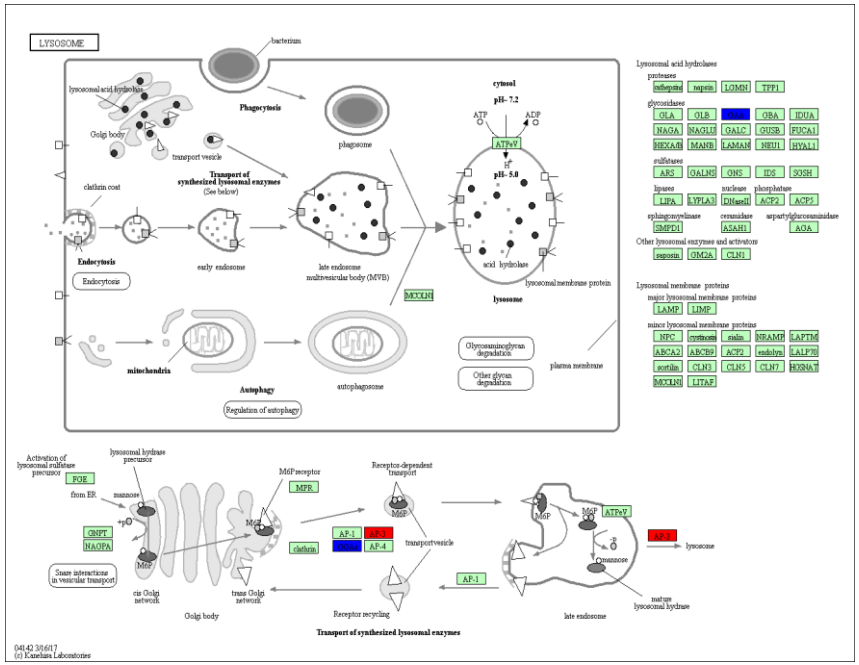

M.4

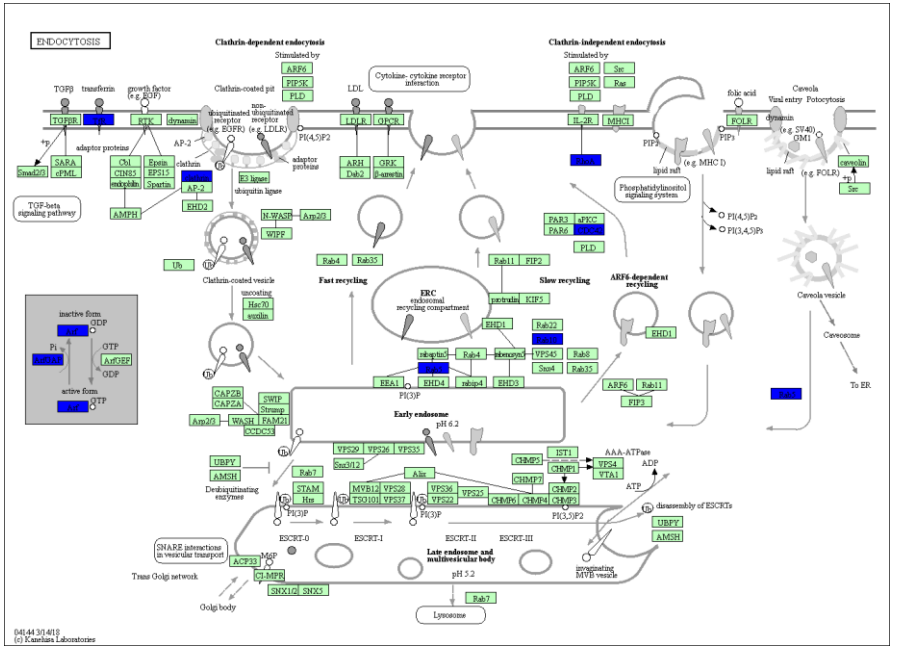

M.5

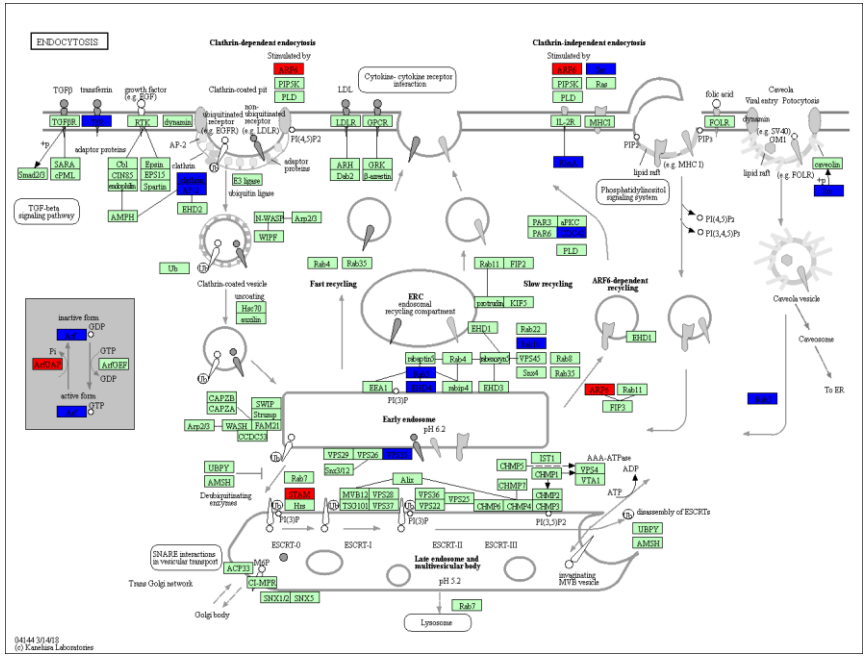

Fig. 3.10M KEGG maps depicting changes to the lysosome pathways between A549 cells exposed to *A. fumigatus*, *P. aeruginosa* and sequential exposure to *A. fumigatus* and *P. aeruginosa*. Increased (red) and decreased (blue) levels of SSDA proteins involved in the lysosome between (1) *A. fumigatus*, (2) *P. aeruginosa*, and (3) sequentially exposed A549 cells and the control were identified. Compared to *A. fumigatus*- (4) and *P. aeruginosa* exposed cells (5), this pathway was clearly downregulated in the sequentially exposed A549 cells as indicated by the number of proteins highlighted in blue.

Table 3.5L list of proteins involved in lysosomes. SSDA proteins arising from comparisons between the different infection groups of A549 cells and highlighted in the KEGG map depicting processes associated with the lysosome are listed.

Gene name	Protein name
CLTC	clathrin heavy chain
AP1B1	adaptor related protein complex 1 subunit beta 1
GAA	glucosidase alpha, acid
GGA1	golgi associated, gamma adaptin ear containing, ARF binding protein 1
AP3M1	adaptor related protein complex 3 subunit mu 1
LAMP1	lysosomal associated membrane protein 1
ATP6V1H	ATPase H+ transporting V1 subunit H
AP3B1	adaptor related protein complex 3 subunit beta 1
AP1M1	adaptor related protein complex 1 subunit mu 1
AP3D1	adaptor related protein complex 3 subunit delta 1

Table 3.5M List of proteins involved in phagosomes. SSDA proteins arising from comparisons between the different infection groups of A549 cells and highlighted in the kegg map depicting proteins associated with phagosomes are listed.

Gene name	Protein name
DYNC1H1	dynein cytoplasmic 1 heavy chain 1
ITGB1	integrin subunit beta 1
LAMP1	lysosomal associated membrane protein 1
ATP6V1H	ATPase H+ transporting V1 subunit H
RAB5C	RAB5C, member RAS oncogene family
RAC1	Rac family small GTPase 1
TFRC	transferrin receptor
TUBA1A	tubulin alpha 1a
CANX	calnexin

Volcano plots were produced to determine the differences in protein abundance between two samples and to depict the changes in pathways and processes those proteins are involved in (Fig. 3.11A-E). Increases in the relative abundance of proteins associated with mitochondrial-related processes including, oxidative phosphorylation and the TCA cycle, were observed in all pathogen-exposed groups, which supports the profile observed in the heatmap (Fig. 3.9B, Cluster H). Immune system processes and protein transport were increased in *A. fumigatus*- and *P. aeruginosa*- exposed groups to a greater extent than sequentially exposed cells (Fig. 3.11B). A decrease in the relative abundance of proteins associated with RNA metabolic processes was most evident in *P. aeruginosa*-exposed cells although this process was also observed to a lesser extent in *A. fumigatus*- and sequentially exposed cells (Fig. 3.11A-C; Fig. 3.12A-C). A similar trend in the downregulation of this pathway was observed in Fig. 2B, Cluster B.

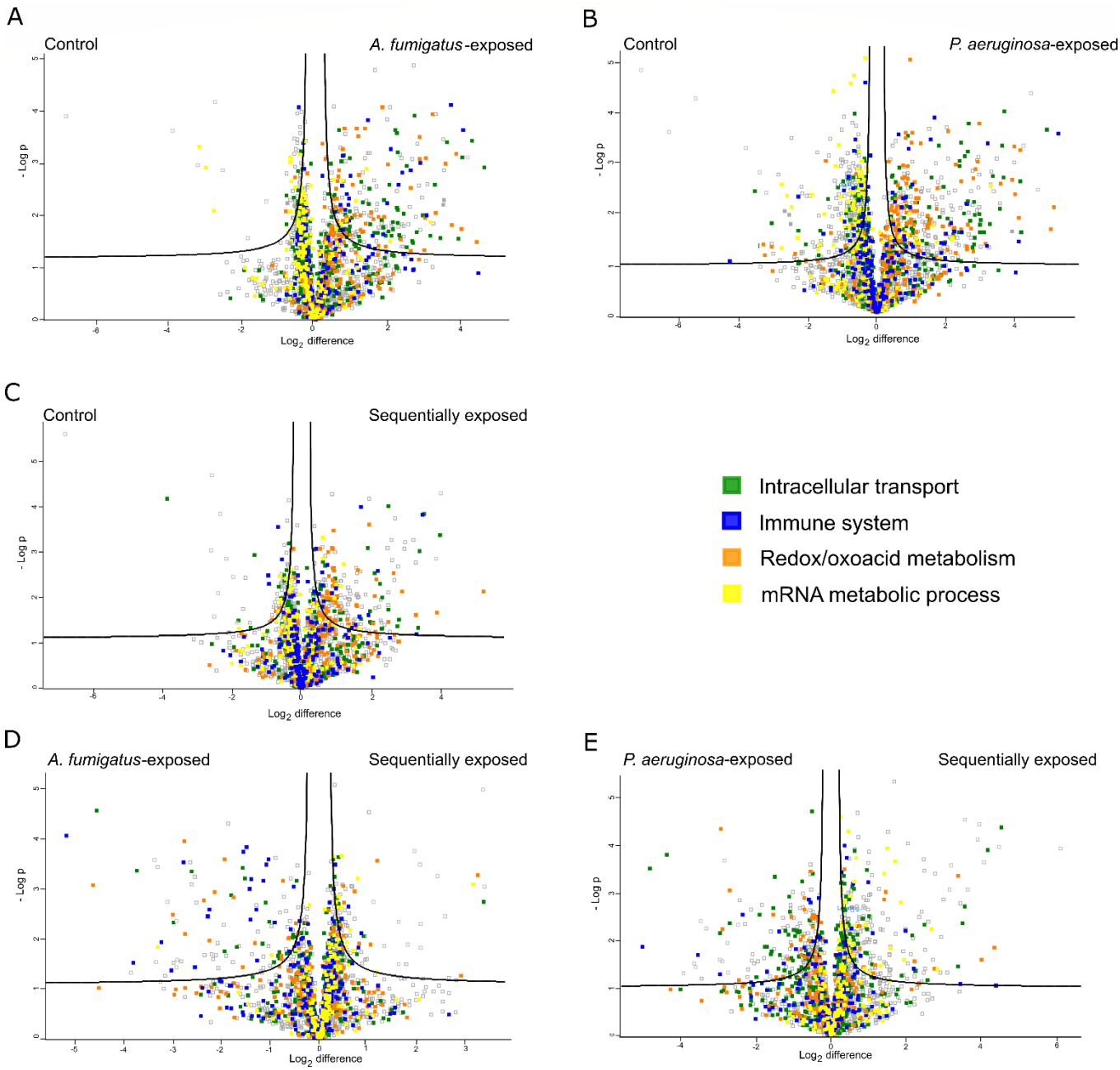

Fig. 3.11 Differential abundance of proteins identified in A549 cells exposed to *A. fumigatus* or *P. aeruginosa* Volcano plots derived from pairwise comparisons between unexposed A549 cells and cells exposed to *A.fumigatus* for 8 hours (A), A549 cells exposed to *P. aeruginosa* for 4 hours (B), and (C) sequentially exposed A549 cells (8 hour exposure to *A. fumigatus* followed by 4 hour exposure to *P. aeruginosa* for 4 hours). Pairwise comparisons were also made between sequentially exposed A549 cells and *A. fumigatus*-exposed A549 cells (D) and *P. aeruginosa*-exposed A549 cells (E). The distribution of quantified proteins according to p value (−log10 p-value) and fold change (log_2 mean LFQ intensity difference) are shown. Proteins above the line are considered statistically significant (p-value <0.05). Protein components of the immune system (blue) and of intracellular transport (green) are most abundant in all pathogen-exposed groups compared to the control.

A greater immune response is observed in *A. fumigatus*- and *P. aeruginosa*-exposed groups than in sequentially exposed groups. Proteins associated with mitochondrial activity including redox reaction and oxacid metabolic processes (orange) are more abundant in pathogen exposed-groups compared to the control, but less abundant in sequentially exposed groups when compared to *A. fumigatus*- and *P. aeruginosa*-exposed cells. A decrease in the relative abundance of proteins associated with RNA metabolic processes (yellow) was most evident in *P. aeruginosa*-exposed cells although also observed to a lesser extent in *A. fumigatus*- and sequentially exposed cells.

Enrichment analysis was performed using STRING on SSDA proteins arising from comparisons between pathogen-exposed and unexposed A549 cells using Student's t-tests ($p<0.05$) (Fig. 3.12). The protein networks generated by STRING identified a number of upregulated and downregulated pathways and processes in A549 cells, which supported the findings identified in the volcano plots in Fig. 3.11 and the dataset arising from hierarchical clustering (Fig. 3.9B). Compared to the control, the relative abundance of proteins associated with oxidative stress, the mitochondria increased in all pathogen-exposed groups (SSDA Increase, Fig. 3.12A-C) while proteins involved in RNA processing and the ribosome made up the vast majority of proteins that were decreased in abundance (SSDA Decrease, Fig. 3.12A-C). Increases in immune system processes were detected in *A. fumigatus*-exposed and *P. aeruginosa*-exposed groups compared to sequentially exposed cells and the controls (Fig. 3.12A and B). Pathways associated with transcription and translation were most affected in *P. aeruginosa*-exposed groups compared to the other groups (3.12B). Pathways involved with intracellular protein transport were more affected in *A. fumigatus*-exposed and sequentially exposed groups compared to *P. aeruginosa*- exposed groups and the control (Fig. 3.12A and C).

Fig. 3.12 A SSDA Increase

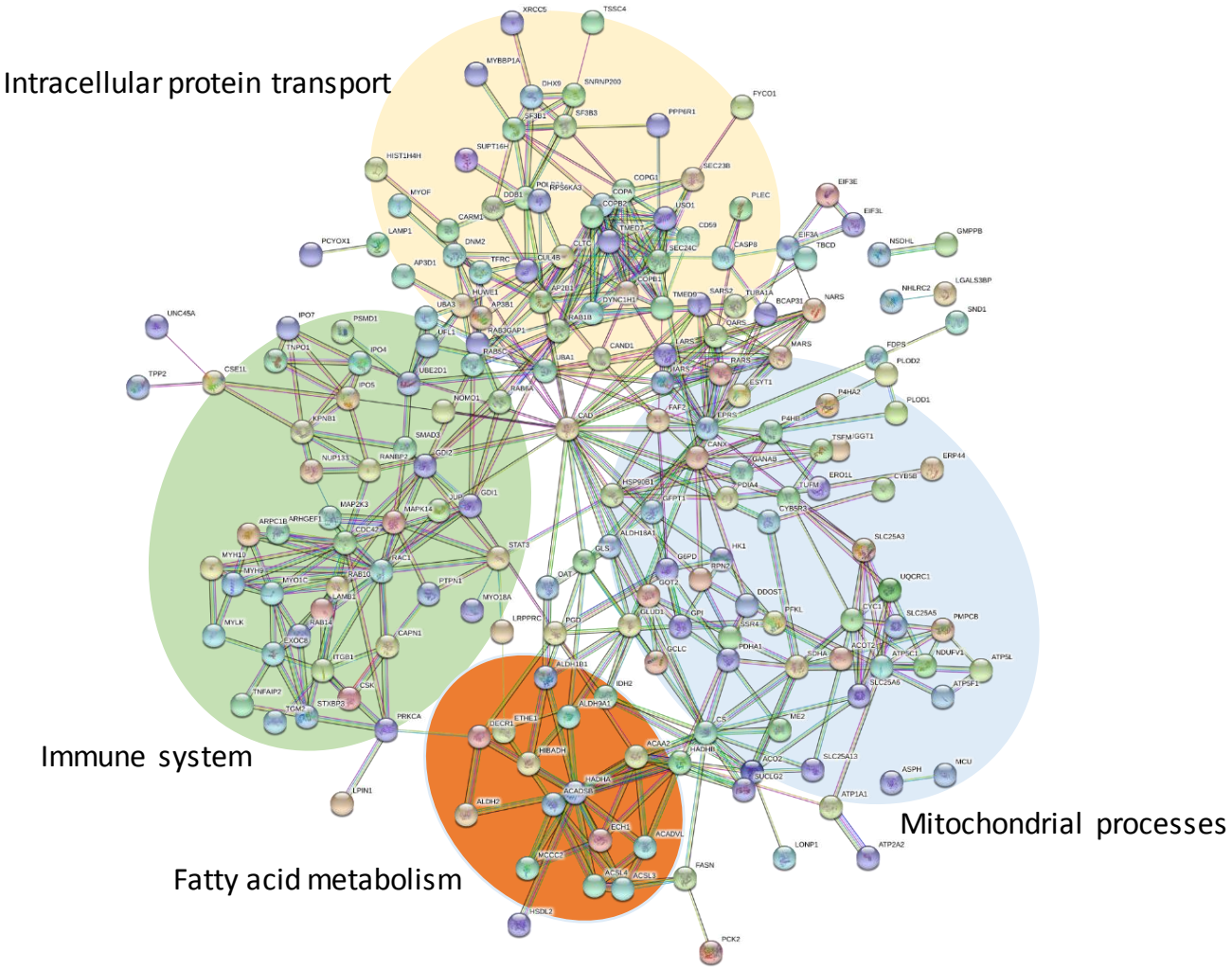

SSDA Decrease

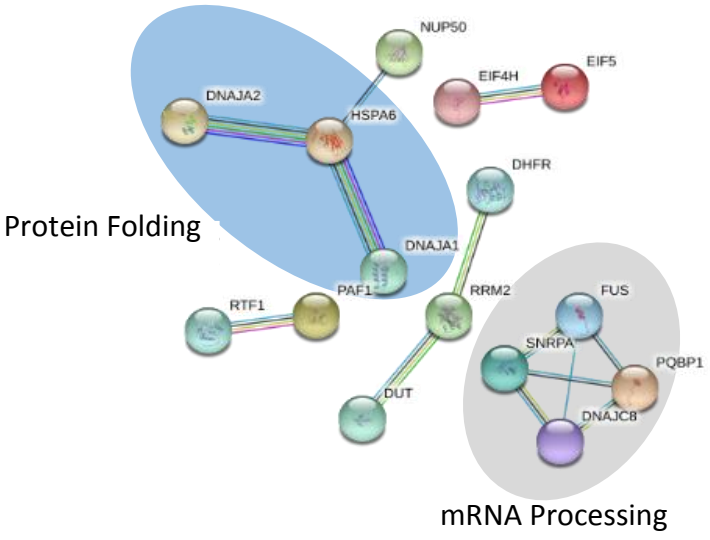

Fig. 3.12 B

SSDA Increase

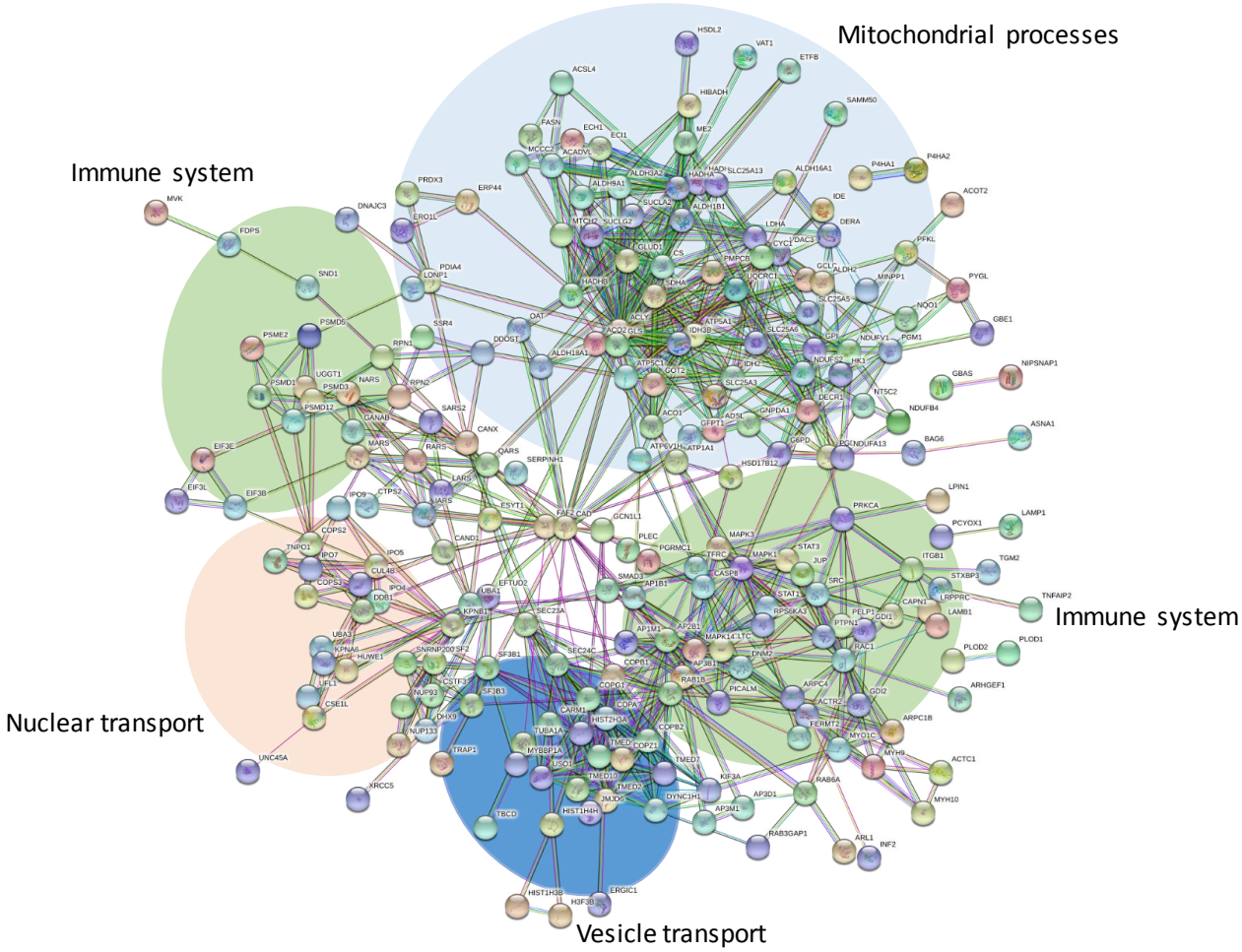

SSDA Decrease

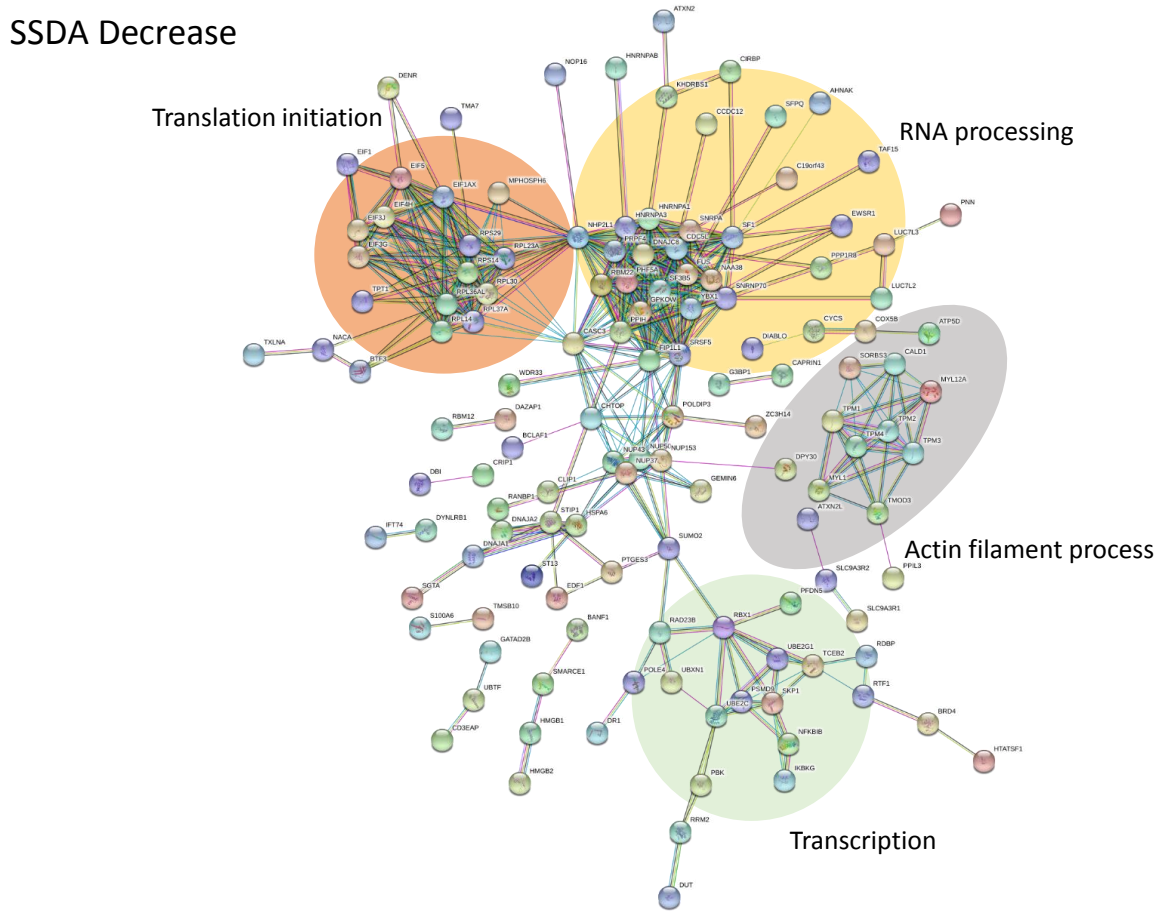

Fig. 3.12 C

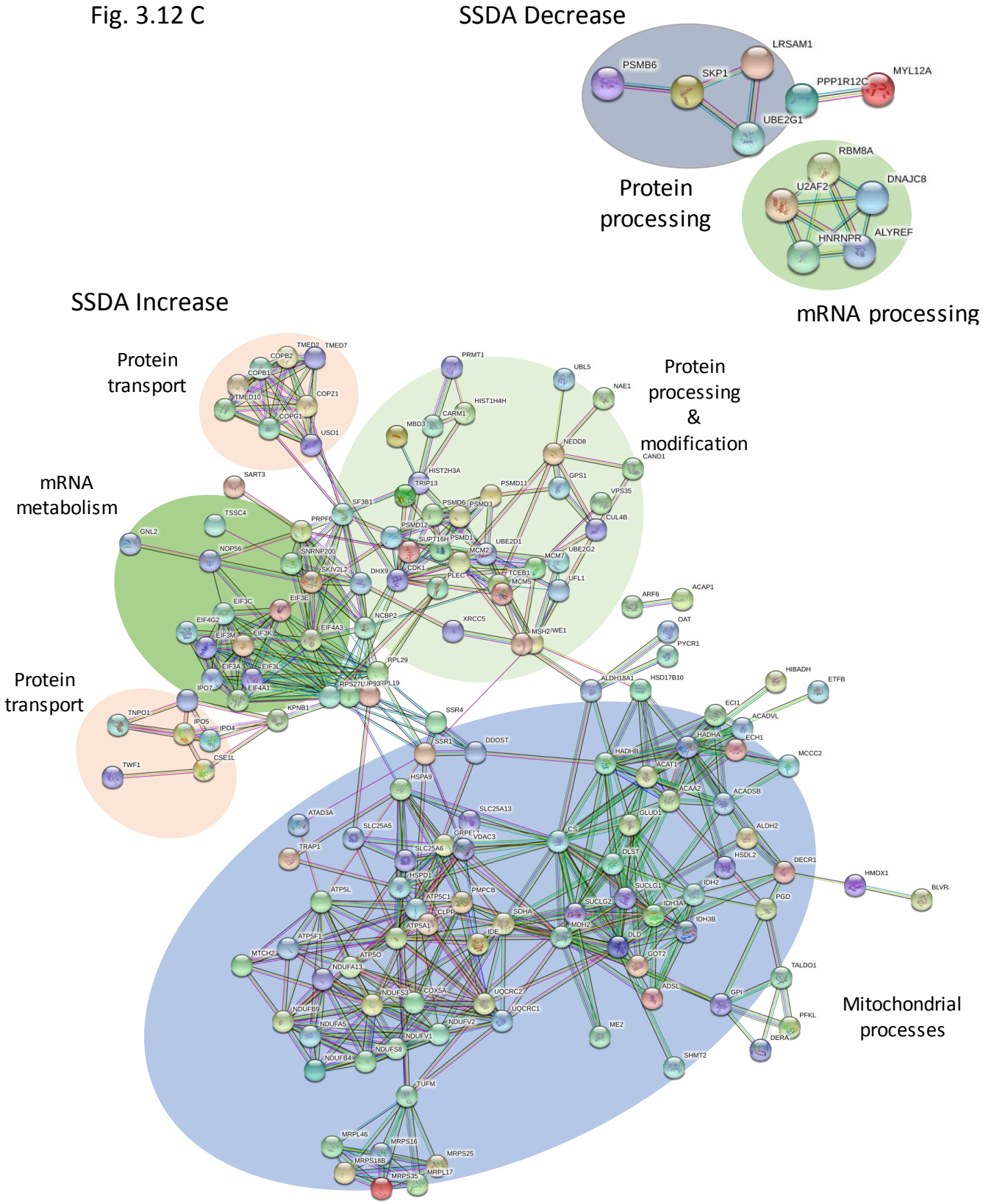

Fig. 3.12 Interaction network analysis of proteins identified in unexposed and pathogen-exposed A549 cells. Protein interaction information was obtained from the STRING database using gene lists extracted for statistically significant differentially abundant (SSDA) proteins from pair wise t-tests ($p < 0.05$). Each node represents a protein and each connecting line represents an interaction, the extent of evidence for which is represented by the width of the line. A high confidence minimum interaction score (0.700) was applied. Statistically enriched KEGG and Gene Ontology (GO) descriptors were examined to identify clusters of proteins enriched between untreated A549 cells and A549 cells treated with A) *A. fumigatus*, B) *P. aeruginosa*, C) a sequential infection with *A. fumigatus* and *P. aeruginosa.*

Taken together, the results from this study demonstrate a role for *A.fumigtaus* in promoting the growth of *P. aeruginosa*. The impact of this interaction on A549 cells is reflected by the proteomic analysis, which reveal deficient pathogen-uptake and killing mechanisms in the host cells. These results are summarized in Fig. 3.13.

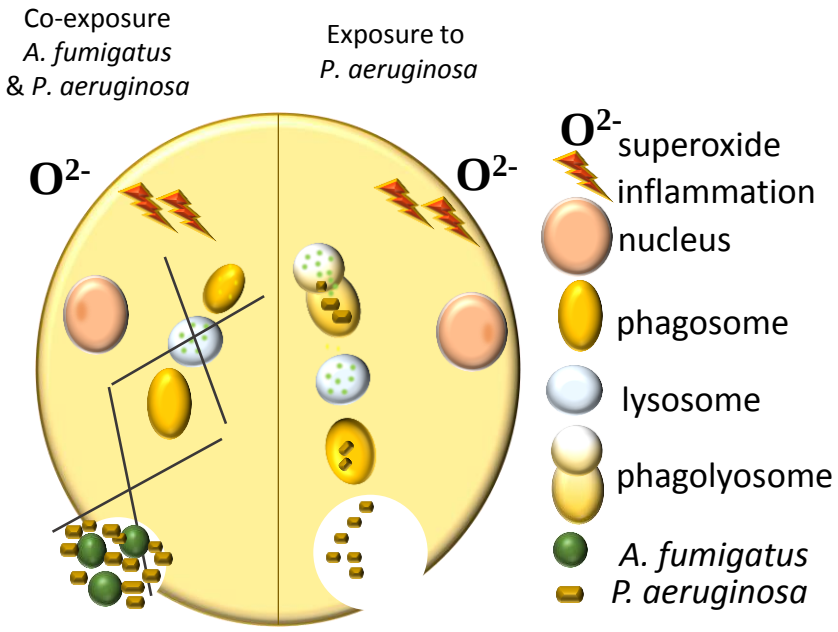

Fig. 3.13. **Response of A549 cells to exposure by *A. fumigatus* and *P. aeruginosa*.** Increased phagocytosis and pathogen killing via lysosomes are characteristic of A549 cells when exposed to *P. aeruginosa*. In contrast, the pathogen-uptake and killing ability of A549 cells exposed to *A. fumigatus* and *P aeruginosa* simultaneously are inhibited, leading to greater bacterial burden.

Unexposed A549 cells retained their typical morphology (flat, cobblestone shaped) (Fig. 3.14A). A549 cells exposed to *A. fumigatus* for eight hours retained their shape and remained adhered to the surface of the flask as expected given the maintenance of morphology after exposure to conidia for 12 hours (Fig. 3.14B). Cells exposed to *P. aeruginosa* for four hours also retained their shape although some cells were beginning to contract slightly although this may be due to the initiation of cell division (Fig. 3.14C). In general, cells exposed to *A. fumigatus* for eight hours and *P. aeruginosa* for four hours, retained their shape and were remained adhered to the flask prior to trypsinization, although some cells were beginning to become isolated from other cells (Fig. 3.14D). The morphology of dividing A549 cells (A) and dying A549 cells (B) is also depicted in fig. 3.15

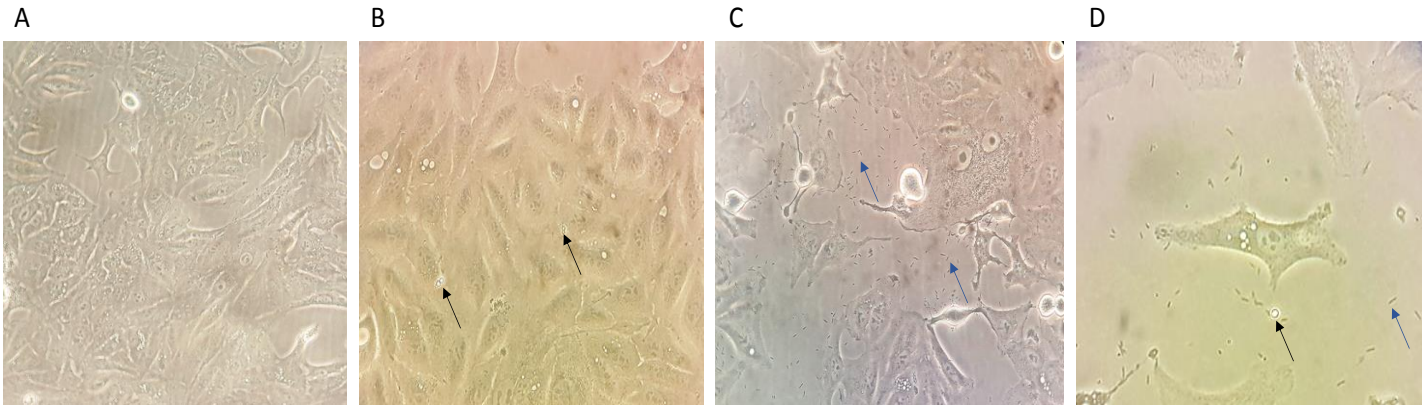

Fig. 3.14 Changes in morphology of A549 cells in response to *A. fumigatus* and/or *P. aeruginosa*. Unexposed A549 cells (A) and cells exposed to *A. fumigatus* conidia (black arrows) for eight hours (B) retained their shape. Some cells exposed to *P. aeruginosa* (blue arrows) for four hours (C) began contract and adopt a rounded shape while others maintained their regular shape. Some cells separated and became isolated. Cells exposed to *A. fumigatus* followed by *P. aeruginosa* (D) retained their shape although some cells began to adopt a rounded shape and became isolated from other cells.

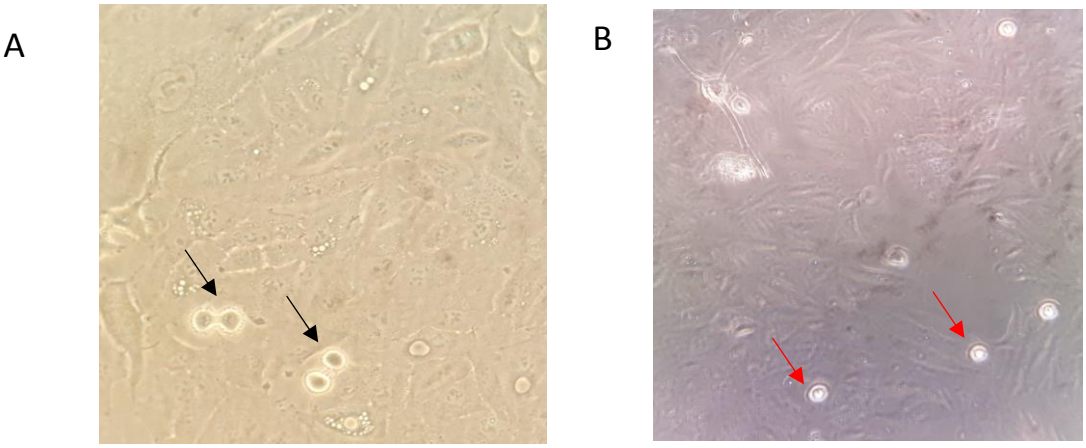

Fig. 3.15 A549 cell morphology. Non-dividing or "resting" A549 cells take on a "squashed cobblestone" type shape. Mitotic cells (black arrows) contract before they begin to divide (Fig. A). Cells become rounded as they divide before adopting the typical "resting" shape again. Cells undergoing oxidative stress, dead or dying cells (red arrows) contract, become rounded and detach from the surface (B) (Magnification 40X).

3.3 Discussion – Part one

3.3.1 Characterizing the response of A549 cells to a 12 hours exposure of *A. fumigatus* or *P. aeruginosa*

While many studies have investigated the proteomic response of a host to a single pathogen, few have examined the response of the host to co-infection by more than one pathogen. The reason for this, at least in part, lies in the complexity of multi-organism systems and the significant challenges that arise when analysing the resulting datasets. This study aimed to address some of these challenges so that the cellular response of a model system to infection by two pathogens could be characterized. The experiment was designed with a view to characterizing the proteomic response of A549 cells to exposure to *A. fumigatus* or *P. aeruginosa* for 12 hours, and to compare the resulting proteomic profile with the one created when co-exposed to both pathogens. The response of A549 cells to exposure by *A. fumigatus* for greater than 12 hours while maintaining cell viability has been reported (Wasylnka, 2003). However, it was not possible to expose A549 cells to *P. aeruginosa* for more than 12 hours while retaining cell viability. As the purpose of the study was to compare how active A549 cells respond to each pathogen, it was important to expose the cells for the greatest, but also a similar length of time while ensuring maintenance of cell viability. LFQ proteomics revealed similarities and differences in the proteomic response of A549 cells to exposure with either pathogen for 12 hours.

3.3.2 *A. fumigatus* and *P. aeruginosa* infections alter ribosome activity in A549 cells

Ribosome activity was severely impacted by exposure to by either *A. fumigatus* or *P. aeruginosa* with a decrease in the relative abundance of proteins associated with the ribosome, RNA processing and translation (Fig. 3.1B; Fig. 3.2A-D; Fig. 3.4C and 3.5C). Thus, this appears to be a general response to infection rather than a pathogen-specific response. Downregulation of translation is a protective mechanism by which host epithelia alert surrounding cells to danger (Mohr and Sonenberg, 2012). However, pathogens may also influence and manipulate the host environment by targeting host

translational machinery in an attempt to limit the translation of mRNAs that code for immune effectors (Mohr and Sonenberg, 2012). The host may respond by increasing activity of posttranscriptional mediators including eukaryotic translation initiation factors (eIFs), elongation factors and their respective regulators that are required to meet the demands of orchestrating an appropriate immune response or, by activating other elements of immune signalling such as the MAPK signalling cascade (Mohr and Sonenberg, 2012; Fontana *et al.*, 2012). It has been well documented that the *P. aeruginosa* exotoxin A, ExoA, is an inhibitor of host protein synthesis and inhibits translation by ADP-ribosylation of elongation factor 2 (eEF2) (Pollack, 1983; Fontana *et al.*, 2011). Translation inhibition by ExoA alerts the host to infection, which responds by activating an immune response (Fontana *et al.*, 2012).

RNA splicing of host transcripts encoding immune mediators is integral in orchestrating an appropriate immune response to pathogens (Chauhan *et al.*, 2019). The synergistic effect of translation inhibition and activation of an immune response has been demonstrated in a number of model organisms including mice, macrophages and *Caenorhabditis elegans* (Fontana *et al.*, 2011; Dunbar *et al.*, 2012; Fontana *et al.*, 2012; McEwan *et al.*, 2012). Some pathogens may interfere with host RNA splicing machinery thereby derailing the immune response to evade killing (Kalam *et al.*, 2017; Chauhan *et al.*, 2019). In this study, the abundance of several proteins involved with RNA splicing was altered (e.g. Peptidyl-prolyl cis-trans isomerase H and Spliceosome-associated protein CWC15 homolog increased in *A. fumigatus*- and *P. aeruginosa*-exposed cells respectively) (Table A 3.1 and Table A 3.1B).

3.3.3 *A. fumigatus* and *P. aeruginosa* infection upregulate oxidative stress and detoxification pathways in A549 cells

Cellular energy can be produced through glycolysis and through the degradation of fatty acids by β-oxidation in the mitochondria and peroxisomes. The latter is a high energy yielding process in which long, medium and short chain fatty acids are converted to acetyl-CoA, which then feeds into the tricarboxylic acid cycle (TCA cycle) in the mitochondria or used for lipid metabolism in peroxisomes (Quijano *et al.*, 2016). Reactive oxygen species (ROS) are by-products of energy metabolism and β-oxidation of

fatty acids that occur in the mitochondria. ROS such as superoxide anion (O_2^-) or hydrogen peroxide (H_2O_2) are produced during a series of redox reactions when oxygen is converted to superoxide radicals resulting from oxidative phosphorylation (OXPHOS) that occurs during the TCA cycle. ROS regulate a vast range of intracellular signalling networks and play a critical role in modulating physiological behaviours induced by pathogens including apoptosis and innate immune responses. Excessive levels of ROS induce oxidative stress. This is an indicator of mitochondrial dysfunction, often associated with diseases such as Huntington's disease (Ott *et al.*, 2007). ROS are key components of the innate immune response and production is intensified during microbial infection whereby it is directly and indirectly, involved in combating infectious agents through direct killing of the pathogen and by activating inflammatory pathways, respectively (Ivanov *et al.*, 2017).

In this study, the relative abundance of mitochondrial proteins was increased in A549 cells exposed to *A. fumigatus* or *P. aeruginosa* compared to unexposed cells. Oxidative stress and metal ion binding pathways were upregulated, indicating a detoxification response (Fig. 3.1B; Fig. 3.2A and 3.2B; Fig. 3.3A, C). Copper transport protein ATOX1 and Protein SCO1 were two of the most differentially abundant proteins in A549 cells treated with *A. fumigatus* and *P. aeruginosa* (post-imputation) (Table 3.1 and 3.2). These proteins play a major role in copper homeostasis and are involved in energy production and removal of superoxides (Hatori and Lutsenko, 2016). Copper is an essential co-factor of Superoxide dismutase (SOD1), a ROS scavenging enzyme that converts superoxide anions into oxygen and hydrogen peroxide in a process termed "dismutation" (Banks and Andersen, 2019). The relative abundance of SOD1 and SOD2 was increased in *A. fumigatus*-exposed cells, but only SOD2 was statistically SSDA in *P. aeruginosa*-exposed cells compared to unexposed cells. The levels of catalase were increased in both pathogen-exposed groups (Table A 3.1A and A3.B).

3.3.4 *A. fumigatus* and *P. aeruginosa* infection induce an immune response in A549 cells

The immune response of the pulmonary epithelia has been well described in the context of *A. fumigatus* and *P. aeruginosa* infection, both *in vivo* and *in vitro* (Vos *et al.*, 2005; Dagenais and Keller, 2009; Hawdon *et al.*, 2010; Lavoie *et al.*, 2011). Previous studies have employed gene expression techniques, RNA-Seq and immunoassays to demonstrate the immune response of A549 cells to *A. fumigatus* and *P. aeruginosa*. A549 cells respond to these pathogens by upregulating an immune response through the production of inflammatory mediators such as IL-1β, TNF-α, IL-6 and IL-8 (Carterson *et al.*, 2005b; Bellanger *et al.*, 2009; Hawdon *et al.*, 2010; Cigana *et al.*, 2011; Chen *et al.*, 2015).

The proteomic results from this study demonstrate that *A. fumigatus* and *P. aeruginosa* induce a pro-inflammatory response in A549 cells mediated in part through NLR signalling via PYCARD, which was exclusive to the pathogen-exposed groups only (Table A 3.1A and Table A 3.1B). PYCARD is a component of the inflammasome and acts as an adaptor for caspase-1, which when activated has multiple functions including the cleavage of pro-IL1β into its mature form (Martinon *et al.*, 2002). Caspase-1 is also a key mediator of apoptosis (Tsuchiya *et al.*, 2019). Thus, activation of this enzyme in pathogen-exposed groups indicates A549 cells may upregulate an inflammasome-mediated pro-inflammatory response and/or apoptosis.

In general, the immune response was more profound in cells exposed to *P. aeruginosa* (Fig. 3.2B; Fig.3.3C). This was reflected in the number of proteins detected and their relative increase in abundance in *P. aeruginosa*-exposed A549 cells. The relative abundance of Gamma-interferon-inducible protein 16 (IFI16) showed the greatest decrease in abundance in *P. aeruginosa*-exposed cells. This protein is a negative-regulator of the inflammasome (Veeranki *et al.*, 2011), thus its downregulation increases inflammasome-mediated immune response or apoptosis in these cells.

Pathogens that enter host cells are trafficked to lysosomes, vesicles in which the acidic environment creates unfavourable conditions for pathogen survival (Escoll *et al.*, 2015). Lysosomes also play an important role in cellular proteostasis by degrading misfolded proteins, including those unable to be degraded by the proteasome (Jackson and Hewitt, 2016). A consequence of infection is an increase the demand for protein folding as peptide biosynthesis is upregulated to mount defence against the pathogen (van

't Wout *et al.*, 2015). In this study, there was an increase in the relative abundance of proteins associated with lysosomes in both pathogen-exposed groups compared to the controls, which is indicative of a cellular stress response (Fig. 3.3A and 3.3C; Fig. 3.4B and 3.5B).

3.3.5 *P. aeruginosa* infection alters the proteome in the endoplasmic reticulum of A549 cells

The endoplasmic reticulum (ER) is a large membrane bound organelle responsible for protein synthesis, folding and posttranslational modification (PTM). When the protein folding capacity of the ER is exceeded, the accumulation of unfolded or misfolded polypeptides induce ER stress, thereby activating the unfolded protein response (UPR). The UPR is cyto-protective mechanism that functions in the restoration of ER homeostasis through a series of signalling pathways (So, 2018). Activation of the UPR can be triggered by multiple stimuli including oxidative stress, imbalance in calcium and iron content, nutrient depletion, and viral infection (So, 2018). Microbial infection increases demand for the biosynthesis and folding of inflammatory proteins, thereby contributing to ER stress and activation of UPR resulting from a build-up of unfolded proteins in the ER lumen (van 't Wout *et al.*, 2015).

Induction of the UPR pathway results in attenuation of mRNA translation, increasing the protein folding capacity by upregulating gene expression of molecular chaperones and enzymes involved in PTM and ensuring the degradation of permanently misfolded proteins by the proteasome via the ER-associated degradation pathway (ERAD) (Celli and Tsolis, 2015). In the event that ER homeostasis cannot be restored, the cell can initiate autophagy and undergo a programme of apoptosis (Ron and Walter, 2007).

A number of bacterial pathogens including *Listeria monocytogenes*, *Brucella melitensis* and *Mycobacterium tuberculosis* activate the UPR through various organism-dependent mechanisms (Seimon *et al.*, 2010; Pillich *et al.*, 2012; Smith *et al.*, 2013b). *P. aeruginosa* possess multiple mechanisms that induce ER stress and activate the UPR pathway (van 't Wout *et al.*, 2015; Jiang *et al.*, 2016; Kim *et al.*, 2018). The *P. aeruginosa* exotoxin pyocyanin, and a phospholipase effector protein TpIE, induce splicing of XBP-1 mRNA, whose protein product is involved in positively regulating expression of UPR-

associated genes including chaperones BiP/GRP78 and Hsp90/GRP94 (Uemura *et al.*, 2009; van 't Wout *et al.*, 2015; Jiang *et al.*, 2016).

The proteomic data in this study revealed an increase in the relative abundance of proteins associated with the ER and Golgi apparatus in *P. aeruginosa*-exposed cells compared with *A. fumigatus*-exposed cells and the control groups (Fig. 3.1B). A number of proteins in this group were associated with the UPR including Vesicle-associated membrane protein-associated protein B/C and Reticulon 3, indicating an ER stress response to bacterial exposure (Kanekura *et al.*, 2006; Wan *et al.*, 2007). This stress response may have in part, triggered apoptotic events as evidenced by the increase in a number of pro-apoptotic proteins including DnaJ homolog subfamily C member 10 and Apoptosis-inducing factor 1 (Kim *et al.*, 2006; Thomas and Spyrou, 2009).

3.3.6 *A. fumigatus* and *P. aeruginosa* infection alter A549 cell morphology

In this study, A549 cells were cultured as a monolayer. The morphology of these "resting" (i.e. non-dividing) cells under such conditions are typically characterized by a flattened, "squashed cobblestone" type shape (Fig. 3.15A). Changes from this morphology to a contracted rounded shape indicates stress (Smit-de Vries *et al.*, 2007). Cells contract before dividing and take a more rounded shape. However, cells undergoing apoptosis also contract and become rounded. These cells eventually detach from the flasks as they die. Unexposed A549 cells and cells exposed to *A. fumigatus* for 12 hours did not appear stressed. However, cells exposed to *P. aeruginosa* for 12 hours had contracted, become rounded and were beginning to detach from the surface. These results are somewhat reflective of what occurs in the CF airways whereby *A. fumigatus* can persist in the airways without inducing the same acute inflammatory response and cellular damage as *P. aeruginosa*.

3.3.7 *P. aeruginosa* growth rate is increased in the presence of *A. fumigatus*.

Co-infection with *A. fumigatus* and *P. aeruginosa* is not uncommon (Zhao *et al.*, 2018a), thus, a better understanding of the host cellular response is important for making decisions as how to treat such infection. In this study, LFQ proteomics was used to investigate the proteomic response of A549 cells to co-infection with *A. fumigatus* and *P. aeruginosa*. The proteomic data revealed that the rate of bacterial replication increased when *A. fumigatus* conidia were co-cultured with *P. aeruginosa* for 12 hours. This was reflected in the high abundance of bacterial proteins detected by the mass spectrometer where *A. fumigatus* was present compared to when *P. aeruginosa* was cultured with A549 cells alone for the same length of time (Fig. 3.5A, i and ii). CFU counts confirmed the finding observed in the proteomics data, and determined that *A. fumigatus* conidia must be present for bacterial replication to escalate, as the secretome from a co-culture of *A. fumigatus* and *P. aeruginosa* did not induce the same growth effect (Fig. 3.5B). For this reason, further experiments were performed to determine the point at which *P. aeruginosa* began to proliferate exponentially so that the pathogens could be removed from the A549 cell culture and protein extraction could be performed before this began to occur.

Several studies have reported antagonism between *A. fumigatus* and *P. aeruginosa* (Shirazi *et al.*, 2016; Briard *et al.*, 2017; Sass *et al.*, 2018; Briard *et al.*, 2019). In general, these studies report that *P. aeruginosa* outcompetes *A. fumigatus* by affecting the growth and development of the fungus by the secretion of a range of secondary metabolites. In this study, *A. fumigatus* conidia appeared to induce the replication rate of *P. aeruginosa*, potentially by altering the environment, thereby making it more conducive to bacterial replication. This of course has implications *in vivo*, where co-infection occurs.

3.4 Discussion – Part two

3.4.1 The proteomic response of A549 cells to sequential exposure by *A. fumigatus* and *P. aeruginosa*

The presence of *A. fumigatus* conidia were determined influence the increase in bacterial growth rate when in culture with *P. aeruginosa* and A549 cells. Where conidia were present, bacterial density was greater compared to that which occurred in the absence of the fungus after the same incubation time (12 hours). Having determined the point at which *P. aeruginosa* began to replicate exponentially in the presence of *A. fumigatus*, the experimental design in part one of this chapter was revisited so that the proteomic response of A549 cells to sequential exposure by *A. fumigatus* and *P. aeruginosa* could be investigated. Cells were exposed to *A. fumigatus* and *P. aeruginosa* sequentially, for eight hours and four hours respectively. The resulting proteome was compared with the proteomic profile of cells exposed to *A. fumigatus* (for eight hours) or *P. aeruginosa* (for four hours). LFQ proteomics was used to compare the individual proteins and pathways, which contribute to the response of A549 cells when exposed to *A. fumigatus* or *P. aeruginosa* with those observed in the sequentially exposed A549 cells. Based on the analysis of the proteomic profile, distinct similarities and differences were observed between the three infection groups. These findings may explain why *P. aeruginosa* predominates in the presence of *A. fumigatus*.

3.4.2 *A. fumigatus* and/or *P. aeruginosa* infection alter the abundance of proteins associated with energy output in A549 cells

It is well established that host cells respond to the presence of pathogens by altering their metabolic processes (Eisenreich *et al.*, 2013) A clear signature of microbial infection is an alteration in carbohydrate and amino acid metabolism by the host (Eisenreich *et al.*, 2017). In this study, comparative analysis between the untreated group and the three infection models demonstrated a clear increase in the relative abundance of proteins associated with carbohydrate and amino acid metabolism in the three pathogen-exposed groups of A549 cells compared to the unexposed cells. An increase in host metabolic processes was greatest in *P. aeruginosa*-exposed A549 cells suggesting that *P.*

aeruginosa induce a more drastic alteration to host cell energy metabolism than *A. fumigatus* (Fig. 3.9B, Cluster G). Compared to the fungal and bacterial-exposed groups, these same metabolic changes were not detected in sequentially exposed cells, as reflected by the fewer number of proteins associated with this pathoway in this group. Thus, it is possible that prior exposure to fungal conidia has a debilitating effect on the host cells such that they are unable to alter their metabolism in a way the meets the demands of countering a bacterial infection.

3.4.3 *A. fumigatus* and/or *P. aeruginosa* infection alter the abundance of proteins associated with mitochondrial stress in A549 cells

An increase in the relative abundance of proteins associated with mitochondrial activity and oxidative stress were indicative of a mitochondrial stress response pathway across all pathogen-exposed groups. Processes relating to oxidative stress including fatty acid degradation and the TCA cycle (Fig. 3.10B and C), the OXPHOS pathway (Fig. 3.10D) and Huntington's Disease pathway (Fig. 3.10E), were enriched across all treated groups of A549 cells (Fig. 3.9B, Cluster H; Figure 3A-C). The abundance of proteins associated with mitochondrial activity, as determined by hierarchical clustering (Fig. 3.9B, Cluster H), was greatest in the *P. aeruginosa*- and sequentially treated cells compared to the *A. fumigatus*-treated cells. These results indicate that *P. aeruginosa* are the cause of the heightened oxidative stress response observed in the sequentially exposed A549 cells.

Several protein groups identified in the A549 cells analysed in part one and part two of this chapter, include terms associated with "mitochondria". Although there was an increase in the relative abundance of proteins associated with mitochondrial activity in both groups, the profile of these proteins was somewhat different (Table A 3.1-3.4). For example, ATOX1, which was the most differentially abundant protein in the 12-hour pathogen –exposed groups were not SSDA in any of the groups in part two. SCO1 was present in all pathogen-exposed groups but with a three-fold decrease compared to the 12-hour pathogen exposures. The relative abundance of superoxide dismutase was increased in the 12-hour pathogen exposure but were not SSDA in the pathogen-exposed groups in part two. These results indicate temporal changes in the cellular stress response mediated by different proteins as exposure to the pathogen persists.

Pyocyanin (PCN) is a cytotoxic, redox-reactive phenazine produced by most strains of *P. aeruginosa*, including PAO1, the strain used in this study (Mavrodi *et al.*, 2001). PCN is a known inducer of oxidative stress in epithelial cells (Liu *et al.*, 2013; Rada and Leto, 2013), and its effect on the decline of respiratory health and lung function is well-documented (Hunter *et al.*, 2012; Rada and Leto, 2013). Therefore, it is probably not surprising that an increase in the relative abundance of proteins and pathways associated with oxidative activity in the mitochondria of *P. aeruginosa*-exposed and sequentially challenged A549 cells were detected in the proteomic data. Further studies to establish the presence of, and quantify the amount of pyocyanin produced in this infection model are required to determine the role of pyocyanin in affecting the A549 cell proteome.

Aside from the immune response, few studies have focused on the effect of *A. fumigatus* on mammalian cells, and in the context of infection, more is known about the host response to *P. aeruginosa*. In this chapter, an increase in the relative abundance of proteins and pathways associated with the mitochondria in *A. fumigatus*-exposed A549 cells for eight hours, indicate that *A. fumigatus* induce mitochondrial stress in the host. This response is less intense than that caused by the four-hour exposure to *P. aeruginosa*.

One consequence of mitochondrial stress is apoptosis. This can be activated in response to stress-induced danger signals, such as microbial infection (Galluzzi *et al.*, 2012). Several studies have demonstrated that *A. fumigatus* can inhibit apoptosis in epithelial cells and thus survive and germinate in the host, evading detection by the immune system (Daly *et al.*, 1999; Berkova *et al.*, 2006; Heinekamp *et al.*, 2013; Amin *et al.*, 2014). The ability to survive in the host while inhibiting apoptosis has been attributed to the pigment, DHN melanin, a pigment found in conidia (Amin *et al.*, 2014). The results here show that a number of pathways associated with mitochondrial stress are not as significantly increased in *A. fumigatus*-exposed A549 cells compared to *P. aeruginosa*- and sequentially exposed cells. This may be due to the ability of conidia to evade host detection, or modulate or the signals required for host cells to carry out a program of apoptosis (Berkova *et al.*, 2006; Féménia *et al.*, 2009; Amin *et al.*, 2014). Furthermore, this may be the reason that the A549 cells in this study retained their shape and appeared "less stressed" in comparison to *P. aeruginosa* exposed cells (Fig. 3.4 and 3.10).

3.4.4 Exposure to *A. fumigatus* or *P. aeruginosa* results in a decrease in the abundance of ribosomal proteins in A549 cells

The mRNA processing pathways were significantly decreased in *P. aeruginosa*-exposed A549 cells and less so in *A. fumigatus*-exposed cells compared to the control and the sequential infection groups. Reductions in the relative abundance of proteins associated with transcription, the ribosome and translation were identified (Fig. 3.9B, Cluster B, Table A 3.2). The synergistic effect of translation inhibition and activation of an immune response has been demonstrated in a number of model organisms including mice, macrophages and *Caenorhabditis elegans* (Fontana *et al.*, 2011; Dunbar *et al.*, 2012; McEwan *et al.*, 2012; Fontana *et al.*, 2012). This may explain the findings in our results, whereby the decrease in the relative abundance of proteins involved in translation correlate with an increase in the relative abundance of proteins associated with immune system processes (Fig. 3.11, Fig. 3.9B, Cluster A).

Compared to bacteria, very little is known about the relationship between fungal pathogens and host translational machinery (Alves, 2014; Bignell *et al.*, 2018). Interestingly, exposure of A549 cells to *P. aeruginosa*, subsequent to *A. fumigatus*, did not appear to affect translational processing despite the additional four-hour incubation with *P. aeruginosa* (Fig. 3.9B). By not interfering with protein synthesis in the host, it is possible that *A. fumigatus* creates an environment in which *P. aeruginosa* can also avoid triggering an immune response, allowing the pathogen time to establish infection. These findings may provide one explanation as to why the proteomic response of A549 cells to sequential exposure of *A. fumigatus* and *P. aeruginosa* resemble that of the fungal infection and not of the bacterial infection both in the context of the proteomic profile and morphology (Fig. 3.9B and Fig. 3.10H-M)

3.4.5 *A. fumigatus* and *P. aeruginosa* infection alter the abundance of proteins associated with protein processing in the ER of A549 cells

The relative abundance of multiple proteins associated with protein processing in the ER was increased in *A. fumigatus*- and *P. aeruginosa*-exposed groups compared to the controls and sequentially exposed A549 cells (Fig. 3.9B, Cluster F; Fig. 3.10F). These included proteins involved in co-translational and post-translational modifications (ptm),

protein folding (e.g. ER oxidoreductin 1 and protein disulphide isomerase), protein transport from the ER, (DNAJC3, glycoprotein glucosyltransferase, calnexin, members of the TRAP complex and regulators of ER-stress induced apoptosis. On the other hand, Hsp70, a chaperone that plays a central role in detecting, refolding, or destroying misfolded proteins, was decreased in abundance by 6.8 fold (post-imputation) in all infection groups (Table A 3.2B-D). The role of Hsp70 in cell survival and division has been well studied and its downregulation is associated with apoptosis in cancer cells and bacterial infection models (Frese *et al.*, 2003; Gurbuxani *et al.*, 2003; Liu *et al.*, 2011). This suggests a generic response to infection in which the cell attempts to undergo a programme of apoptosis, possibly resulting from the ER stress imposed by the fungus and bacteria.

The role of the ER is not limited to protein processing, and this organelle is becoming more recognized as key modulator of the host immune response (Zhang and Kaufman, 2008; Blohmke *et al.*, 2012; van ‘t Wout *et al.*, 2015; Lee *et al.*, 2016; So, 2018; Jeong *et al.*, 2018; Kim *et al.*, 2018). *In vivo* and *in vitro* studies have demonstrated an increase in ER stress markers in murine lungs and tracheal epithelial cells challenged with *A. fumigatus* antigens, respectively and it has recently been suggested that ABPA-related symptoms may be attributed to *A. fumigatus*-induced ER stress (Lee *et al.*, 2016; Jeong *et al.*, 2018). *P. aeruginosa* secretes virulence factors including pyocyanin and TpIE that are known to induce ER stress and activate UPR via the p38 MAPK pathway (van ‘t Wout *et al.*, 2015; Jiang *et al.*, 2016; Kim *et al.*, 2018). The p38 MAPK signalling pathway is central to integrating the ER stress response and the immune response to *P. aeruginosa* infection, as has been demonstrated in several studies (Balloy *et al.*, 2008; Sharon *et al.*, 2011; Lee *et al.*, 2016). The data in this study revealed a significant increase in the levels of multiple proteins associated with the MAPK pathway in both *A. fumigatus* and *P. aeruginosa*-exposed A549 cells compared to un-exposed cells (Fig. 3.10H). Specifically, MAPK14, one of four p38 MAPKs for which the ER stress response is largely dependent (van ‘t Wout *et al.*, 2015) increased four-fold in A549 cells exposed to each pathogen. In contrast, fewer significant differences in the MAPK pathway were observed between sequentially exposed cells and the control.

ROS are by-products of the intra- and intermolecular disulphide bond formation, which takes place in the ER under oxidizing conditions. The transport of electrons required for disulphide-bond formation is mediated by ER oxidoreductin 1 (ERO1), and protein disulphide isomerase (PDI). In addition to these enzymes, the antioxidant,

glutathione reduces disulphide bonds, an important step to ensuring correct folding of some proteins. During infection, the accumulation of misfolded proteins in the ER can result in the depletion of reduced glutathione as it is consumed during the reduction of misfolded proteins (Zhang & Kaufman, 2008). Consequently, oxidative stress is induced and this can in turn promote inflammation (Mytilineou *et al.*, 2002). In this study, the abundance of ERO1 and PDI were significantly increased in *A. fumigatus*- and *P. aeruginosa*-exposed cells but not in sequentially exposed cells. This finding suggests increased oxidation-reduction activity in the ER of cells exposed to *A. fumigatus* or *P. aeruginosa*, which in turn indicates increased levels of ROS formation within these cells (Fig. 3.9B, Cluster B; Fig. 3.10F). However, the response of sequentially exposed cells was distinctly different and resembled the control more-so than the other infection groups despite experiencing a greater microbial load.

Based on these observations, *A. fumigatus* and *P. aeruginosa* are more likely to induce ER stress and consequently ER-stress induced inflammation in A549 cells exposed to the cells separately than sequentially. This response, or lack thereof, in sequentially exposed cells may influence the way in which the host challenges the pathogen.

3.4.6 *P. aeruginosa* but not *A. fumigatus* downregulate the ubiquitination pathway in A549 cells

Ubiquitin-dependent proteasomal degradation and ubiquitin-associated autophagy play a central role during and post pathogen-induced infection by eliminating misfolded, damaged or short-lived regulatory proteins (Lapaquette *et al.*, 2015; Li *et al.*, 2016). These pathways are crucial in maintaining protein homeostasis, as sustained inflammation has detrimental outcomes for host tissue. Some pathogens have evolved mechanisms to deliver virulence factors into the host. These effector proteins can hijack elements of the ubiquitination system, causing alterations to the host proteome, and allowing the pathogen to evade the immune system (Bomberger *et al.*, 2011; Bomberger *et al.*, 2014; Li *et al.*, 2016; Maculins *et al.*, 2016; Malet *et al.*, 2018).

In this chapter, one of the most noticeable differences in the ubiquitination pathway was a decrease in the relative abundance of several proteins in *P. aeruginosa*-exposed cells compared to the controls and the other infection groups (Fig 3.10G). Key components of E2 ubiquitin conjugating enzymes (e.g. UBE2C and UBE2G) and ubiquitin ligase complexes (SKP1 and RBX1) were decreased in *P. aeruginosa*-exposed A549 cells and to a lesser extent, in sequentially exposed cells. These results indicate an alteration in the protein degradation pathway in sequentially exposed A549 cells mediated by *P. aeruginosa*. Given the central role of the ubiquitination pathway in regulating inflammation, this may have significant consequences for the outcome of the cellular response to infection by this pathogen.

3.4.7 *A. fumigatus* or *P. aeruginosa* infection induce increases in the abundance of proteins associated with an immune response in A549 cells

In general, the whole-cell proteomic analysis in this study showed that *A. fumigatus*- and *P. aeruginosa*, separately and sequentially, activated an immune response in A549 cells (Figure 3.8A-C). Compared to *A. fumigatus*-exposed cells, the relative abundance of many immune system proteins in the sequentially exposed group was decreased (Figure 3.8D). This suggests that certain elements of the immune response are downregulated by *P. aeruginosa* but not by *A. fumigatus*. Thus, the immune response of A549 cells when exposed to *A. fumigatus* or *P. aeruginosa* is distinctly different to that when cells are exposed to these pathogens sequentially. This may be due to initial activation of the immune system caused by *A. fumigatus*, which is subsequently attenuated by the presence of *P. aeruginosa*.

Despite the heightened immune response observed in cells exposed to *P. aeruginosa*, the relative abundance of several proteins associated with an inflammatory response were decreased in bacterial-treated A549 cells, including NF-kappa-B essential modulator (NEMO), HMG-1 and HMG-2. This is not entirely surprising as there is evidence to show that virulence factors secreted by some pathogenic bacteria, including *P. aeruginosa*, can inhibit elements of the immune system from activating a pro-inflammatory response (Zhou *et al.*, 2005; Ashida *et al.*, 2010; Zhao *et al.*, 2019). For example, *Yersinia* YopJ effector protein de-ubiquitinates TRAF6, thereby blocking the

activating signal for NF-κB activity (Zhou *et al.*, 2005). *Shigella* IpaH9.8, an E3 ubiquitin ligase-like protein, targets NEMO, a regulator of NF-κB inhibtors, for degradation, thereby inhibiting NF-κB activity (Ashida *et al.*, 2010). More recently, a *P. aeruginosa* secreted virulence factor, TesG was found to target and inhibit the activity of small GTPases including RhoA, Rac2 and Rap1 (Zhao *et al.*, 2019). Since these GTPases play an important role in regulating the immune response to infection, it is possible that *P. aeruginosa* suppresses the immune system through the secretion of TesG (Zhao *et al.*, 2019).

3.4.8 Sequential exposure to *A. fumigatus* and *P. aeruginosa* alter the abundance of proteins associated with actin formation and pathogen processing in A549 cells

Many studies have demonstrated that *A. fumigatus* and *P. aeruginosa* can be internalized by, and trafficked within A549 cells in an actin-dependent process (Chi *et al.*, 1991; May and Machesky, 2001; Wasylnka and Moore, 2002; Wasylnka, 2003; Zhang *et al.*, 2005a; Hawdon *et al.*, 2010; Amin *et al.*, 2014; Zhao *et al.*, 2019). In this study, the relative abundance of proteins associated with endocytosis and the actin cytoskeleton, including the small GTPases Rab, Rho Rac and Cdc42, were increased in *A. fumigatus*- and *P. aeruginosa*-exposed A549 cells in comparison to the control groups and sequentially exposed cells (Fig. 3.10J-L). This indicates that A549 cells are capable of initiating phagocytosis when exposed to *A. fumigatus* or *P. aeruginosa*, however sequential exposure to both pathogens appears to interfere with this process. There is evidence to show that *A. fumigatus* and *P. aeruginosa* can inhibit phagocytosis through various mechanisms (Bertout *et al.*, 2002; Krall *et al.*, 2002; Deng and Barbieri, 2008; Akoumianaki *et al.*, 2016). The data here suggest a greater interference with the process of phagocytosis in cells that were sequentially exposed to the fungus and bacteria, respectively (Fig. 3.10I-K). The inability to take up bacteria may explain in part, why so many bacterial proteins were present in the initial co-infection model. Because bacteria replicate every 20 minutes under optimal conditions (Cole *et al.*, 1999), the inability of host cells to phagocytose and digest bacterial cells would enable the pathogen population to expand rapidly.

Once internalized pathogens become engulfed in phagosomes. These vacuoles become progressively more acidified by vATPase activity until they fuse with a lysosome to form phagolysosomes, which are characterized by degradative enzyme activity and the production of ROS (Uribe-Quero and Rosales, 2017). *A. fumigatus* and *P. aeruginosa* can survive and replicate within A549 cells by interfering with phagosome acidification and hijacking proteins involved in vesicle trafficking, respectively (Chi *et al.*, 1991; Wasylnka *et al.*, 2005; Angus *et al.*, 2008; Hawdon *et al.*, 2010; Amin *et al.*, 2014). The proteomic data in this study show that the relative abundance of proteins involved in the phagosomal and lysosomal pathways was greater in the fungal- and bacterial-exposed A549 cells compared to the control and sequentially exposed cells. The relative abundance of vATPases was increased in *P. aeruginosa*-exposed and sequentially exposed A549 cells, suggesting that bacteria induced lysosomal acidification in host cells (Fig. 3.9B, Cluster I; Fig. 3.10L and Fig. 3.10M).

Taken together, these results indicate that A549 cells respond to infection by *A. fumigatus* or *P. aeruginosa* by initiating a pathway of phagocytosis and pathogen degradation. In contrast, sequentially challenged cells were unable to upregulate a similar process of pathogen elimination. This inability to clear microbial infection could be detrimental to the host and favour pathogen survival and proliferation. The data described here should form the basis for future studies, which may include an analysis of the effect on phagocytosis in epithelial cells such as A549, and alveolar epithelial cells lines (e.g PAEpiC) when sequentially exposed to *A. fumigatus* and *P. aeruginosa*. Alternative model organisms to human epithelial cells include haemocytes derived from the larvae of the Greater Wax Moth, *Galleria mellonella*. These phagocytic cells have many similarities to human granulocytes such as neutrophils and thus may prove useful for *in vitro* studies such as phagocytosis assays (Bergin *et al.*, 2005; Tomiotto-Pellissier *et al.*, 2016; Maguire *et al.*, 2017).

3.5 Conclusion

In this chapter, the proteomic response of A549 cells to *A. fumigatus* and *P. aeruginosa* was characterised and revealed novel insights into the molecular responses to infection and co-infection of host cells. The results highlight a specific series of proteomic responses when cells were exposed to a single pathogen including inhibition of translation, infection-mediated protein processing in the ER and upregulation of the immune response. In contrast, initially exposing cells to *A. fumigatus* and then to *P. aeruginosa* lead to an intrinsically different response characterised by inhibition of phagocytosis and the pathogen degradation pathway involving the phagosome and lysosome. These results suggest that pre-exposure to *A. fumigatus* render the A549 cells unable to destroy *P. aeruginosa* and thus become more susceptible to colonisation by bacteria.

In the CF airways, pathogens such as *A. fumigatus* and *Staphylococcus aureus* predominate in the early years of life, but *P. aeruginosa* and *Burkholderia cepacia* become the dominant pathogens in the later years of life and contribute to death. The results presented here suggest that pre-exposure to *A. fumigatus* alters the response of cells to *P. aeruginosa* exposure and thus lead to increased development of disease symptoms *in vivo***.** This indicates that in the lungs of CF patients, *A. fumigatus* colonisation may cause the cells of the alveolar surface to become more susceptible to subsequent colonisation and infection by *P. aeruginosa* thus leading to increased morbidity and mortality.

Chapter 4

Analysis of the interactions between *Pseudomonas aeruginosa* and *Aspergillus fumigatus*: A proteomic perspective

4.1 Introduction

With the advent of high throughput technologies such as mass spectrometry based proteomics, RNA-seq and next generation sequencing, our understanding of polymicrobial interactions has been greatly improved over the past decade (Short *et al.*, 2014). Although the microbial ecology of the cystic fibrosis airways is diverse, *P. aeruginosa* predominates as the primary opportunistic pathogen and is the main cause for morbidity and mortality among cystic fibrosis patients (Harrison, 2007; Filkins and O'Toole, 2015; Reece *et al.*, 2017a; Zhao and Yu, 2018).

A. fumigatus is detected with *P. aeruginosa* in the cystic fibrosis airways from early childhood and begins to peak during adolescence (Cystic Fibrosis Trust, 2017; CF Registry of Ireland 2017 Annual Report, 2017). Where co-colonization exists, disease prognosis is poor (Reece *et al.*, 2017a; Zhao *et al.*, 2018a). Despite the prevalence and persistence of *A. fumigatus* throughout childhood and into adulthood, *P. aeruginosa* eventually predominates from adolescence onwards (Reece *et al.*, 2017; Zhao *et al.*, 2018; Reece *et al.*, 2019). This suggests that interactions with other pathogens such as *A. fumigatus* may influence the pathogenicity of *P. aeruginosa* by altering its virulence and the host environment, to pave the way for chronic *P. aeruginosa* infection (O'Brien and Fothergill, 2017).

Analysis of the interactions between *A. fumigatus* and *P. aeruginosa* have revealed several antifungal mechanisms by which *P. aeruginosa* can outcompete *A. fumigatus* (Smith *et al.*, 2006; Mowat *et al.*, 2010; Briard *et al.*, 2015; Shirazi *et al.*, 2016; Sass *et al.*, 2018). *P. aeruginosa* isolates taken from patients with cystic fibrosis have a greater antifungal capacity than non-cystic fibrosis isolates. Non-mucoid isolates are more inhibitory than mucoid isolates, which may explain why *A. fumigatus* is detected at higher levels in older cystic fibrosis patients where chronic (non-mucoid) *P. aeruginosa* infections are more common (Bargon *et al.*, 1999; Aaron *et al.*, 2012; Ferreira *et al.*, 2015; Briard *et al.*, 2019). Many of these interaction studies have focused on the direct effects of *P. aeruginosa* on *A. fumigatus*-biofilm formation, on the effects of bacterial biosynthetic products (e.g. phenazines) on the fungal growth and development or, of fungal metabolites on *P. aeruginosa* (Briard *et al.*, 2015; Briard *et al.*, 2016; Shirazi *et al.*, 2016; Briard *et al.*, 2017; Reece *et al.*, 2018). How *A. fumigatus* shapes an

environment that may influence *P. aeruginosa* growth however, remains poorly understood.

A. fumigatus secretes a range of degradative enzymes that contribute to the ubiquity of the fungus in nature by supporting fungal growth on plant matter (de Vries and Visser, 2001; Tekaia and Latge, 2005; Wang *et al.*, 2018). Many of these biological determinants also play a role in establishing disease in humans and are associated with virulence and pathogenesis (Tekaia and Latge, 2005; Behnsen *et al.*, 2010; Wartenberg *et al.*, 2011; Paulussen *et al.*, 2017; Wang *et al.*, 2018; Vivek-Ananth *et al.*, 2018). How these enzymes directly or indirectly influence bacterial growth has not yet been investigated in detail. In this chapter, the secretome of *A. fumigatus* (i.e. the set of proteins secreted out of the cell) contained in the filtrates produced by cultures grown in a nitrate-rich and nutrient-poor medium were extracted. The effect on *P. aeruginosa* growth was also investigated. Proteomics was used to dissect the proteome of *P. aeruginosa* as a means to provide a global analysis of the pathways and biological processes activated under a set of conditions created by *A. fumigatus*.

The objective of this study was to investigate the effect of culturing *P. aeruginosa* in the presence of *A. fumigatus* culture filtrate (CF) by measuring differences in bacterial growth rate and the overall proteome of the bacteria. It was hypothesized that *A. fumigatus* creates an environment that promotes a metabolic-driven increase in *P. aeruginosa* and results in it outcompeting the fungus. Proteomics was used to analyse this environment and to characterize the contents of the *A. fumigatus* CuF in which *P. aeruginosa* growth proliferated. The molecular basis of the increased proliferation was investigated further using LFQ proteomics to characterize the proteome changes in *P. aeruginosa* when exposed to the culture filtrate of i) *A. fumigatus* alone ii) the culture filtrate of an *A. fumigatus*-*P. aeruginosa* Co-culture and iii) the culture filtrate of *P. aeruginosa* alone.

4.2 Results

4.2.1 Analysis of the effect of *A. fumigatus* culture filtrate on *P. aeruginosa* growth

To investigate the effects of the *A. fumigatus* secretome on *P. aeruginosa* growth, *A. fumigatus* culture filtrates (herein referred to as CuF) were isolated from cultures grown in Czapek-Dox media for 24, 48, 72 and 96 hours. Toxicity assays (section 2.2.5) revealed that the 24, 48 and 72-hour *A. fumigatus* CuF had a growth promoting effect on *P. aeruginosa* compared to the control, but supernatants from the 96-hour CuF had a growth inhibiting effect (Fig. 4.1A). Czapek-Dox is frequently used as a growth medium for *A. fumigatus* for the production of gliotoxin. Because of this, the levels of gliotoxin in the *A. fumigatus* CuF used for the toxicity assays here were quantified by HPLC. The highest concentration of gliotoxin (2.29 µg ±0.06/mg hyphae, $p<0.05$) was detected in the 96 hours CuF (Fig. 4.1B) and correlated with the growth inhibition of *P. aeruginosa* in Fig. 4.1A. As the 48-hour CuF produced in Czapek-Dox induced the greatest increase in growth of *P. aeruginosa*, this was chosen for further investigation.

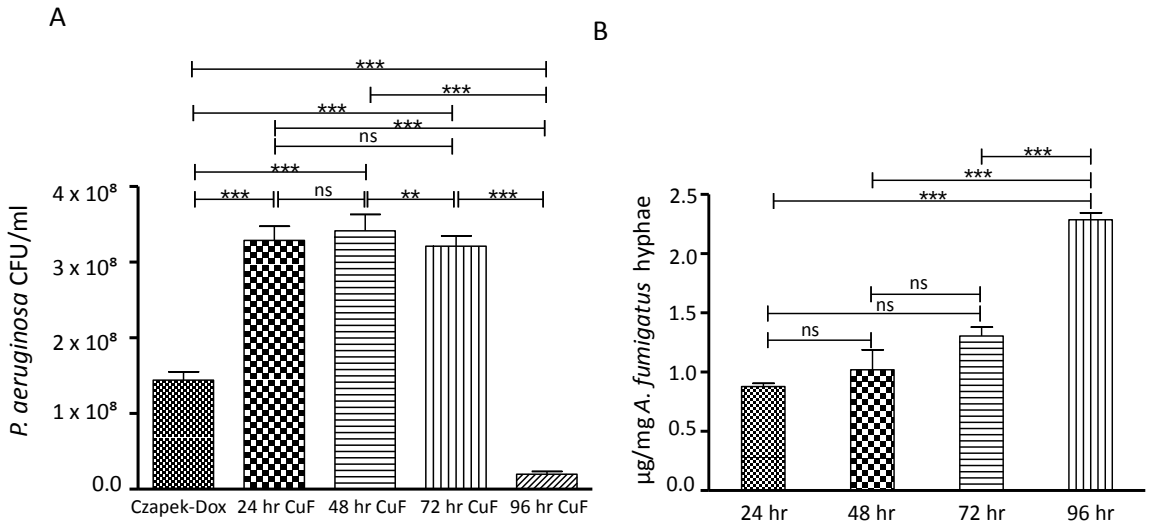

Fig. 4.1A. ***P. aeruginosa*** **growth in** ***A. fumigatus*** **culture filtrates** Change in growth of *P. aeruginosa* (OD 1 ~3 x 10^8 CFU/ml) incubated with Sterile Czapek-Dox media (control), 24-hour, 48-hour, 72-hour and 96-hour *A. fumigatus* CuF for 24-hours. Maximum growth increase was observed from bacteria exposed to the 48-hour CuF and growth inhibition was observed in bacteria incubated with 96-hour CuF. **Fig. 4.1B**. **Gliotoxin production by** ***A. fumigatus*** Gliotoxin levels were highest in *A. fumigatus* cultures grown in Czapek-Dox for 96 hours.

***: $p<0.001$ **: $p<0.01$ *: $p<0.05$ ns: not significant

To investigate whether the interactions with *P. aeruginosa* would alter the secretome of *A. fumigatus*, and to determine what, if any effects this may have on bacterial growth, *A. fumigatus* was co-cultured with *P. aeruginosa* for 24 hours (section 2.3.9), after which the microbes were separated from the medium. The culture filtrate was filter sterilized and the pH was measured (pH 4.2). *P. aeruginosa* was cultured in Czapek-Dox for 24 hours before exposure to the resulting culture filtrates (Co-culture CuF). To determine that the growth promoting effect was caused by *A. fumigatus* and not the culture medium, *P. aeruginosa* was also exposed to the culture filtrates produced by the bacteria (*P. aeruginosa* CuF) in Czapek-Dox (section 2.3.8). The effect on growth of *P. aeruginosa* when exposed to *A. fumigatus* CuF, Co-culture CuF and *P. aeruginosa* CuF was obtained by measuring the OD_{600}, where OD 1 equates to approximately 3 x 10^8 CFU/ml. The growth of *P. aeruginosa* increased by four-fold and eight-fold when cultured in Czapek-Dox supplemented with *A. fumigatus* CuF and Co-culture CuF respectively compared to that which was cultured in Czapek-Dox supplemented with *P. aeruginosa* CuF (Fig. 4.2).

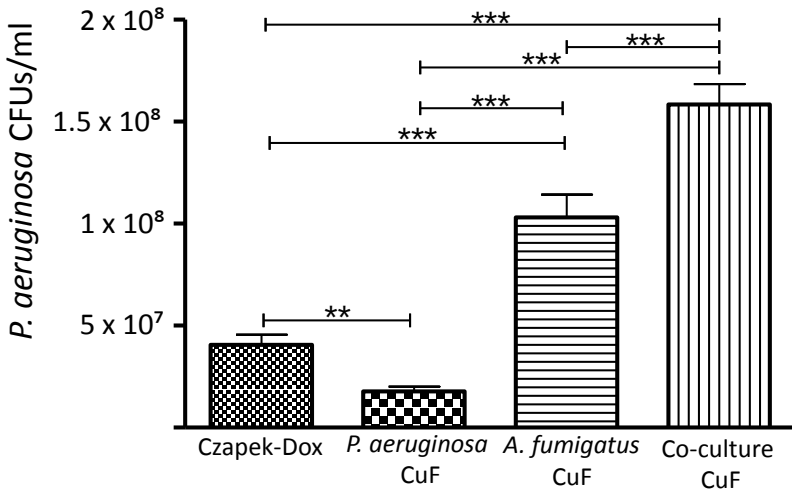

Fig. 4.2 *P. aeruginosa* growth in culture filtrates produced in Czapek-Dox Growth of *P. aeruginosa* (CFU/ml) cultured in Czapek-Dox media for 48 hours compared to growth of *P. aeruginosa* cultured in Czapek-Dox media supplemented with *P. aeruginosa* CuF, *A. fumigatus* CuF and Co-culture CuF. Change in bacterial growth is greatest where *P. aeruginosa* is cultured in Co-culture filtrate. ***: $p<0.001$ **: $p<0.01$ *: $p<0.05$ ns: not significant

To assess whether this growth-enhancing effect was media-specific, *P. aeruginosa* was cultured for 24 hours in minimal media (MM) supplemented with *P. aeruginosa* CuF and/or *A. fumigatus* CuF produced in MM. There were no significant changes in growth when the bacteria were cultured in *P. aeruginosa* CuF, *A. fumigatus* CuF and Co-culture CuF (Fig. 4.3A). *P. aeruginosa* was cultured in an amino acid-rich defined medium, synthetic cystic fibrosis medium (SCFM), supplemented with *P. aeruginosa* CuF or Co-culture CuF produced in SCFM. This medium was designed by Palmer *et al*., (2007) using the average concentration of ions, amino acids, glucose and lactate identified in sputum samples of individuals with CuF and therefore may be used to study the response of microbes to the nutrient content of CuF sputum. There was no significant difference between *P. aeruginosa* growth in Co-culture CuF and *P. aeruginosa* CuF (Fig. 4.3B), although growth was substantially greater in *P. aeruginosa* cultured for 48 hours in sterile SCFM compared to sterile Czapek-Dox or MM (Fig. 4.3B).

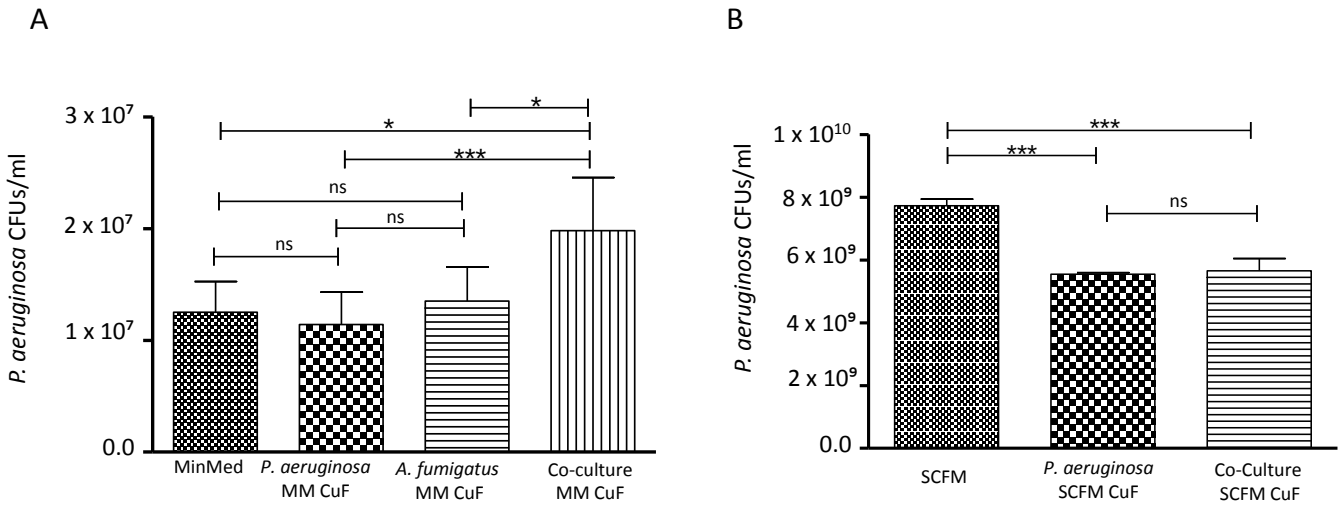

Fig. 4.3 *P. aeruginosa* growth in culture filtrates produced in minimal media and SCFM. (A) Growth of *P. aeruginosa* (CFU/ml) cultured in MM for 48 hours, compared to growth of *P. aeruginosa* cultured in *P. aeruginosa* CuF, *A. fumigatus* CuF and Co-culture produced in MM. Significant fold change ($p > 0.05$) exists between the *P. aeruginosa* cultured in minimal media for 48 hours and Co-culture CuF for 48 hours. (B) Growth of *P. aeruginosa* (CFU/ml) cultured in SCFM for 48 hours compared to growth of *P. aeruginosa* cultured in *P. aeruginosa* CuF and Co-culture CuF produced in SCFM. No significant change existed in the growth between *P. aeruginosa* cultured in *P. aeruginosa* CuF and Co-culture CuF.
***: $p<0.001$ **: $p<0.01$ *: $p<0.05$ ns: not significant

4.2.2 Proteomic analysis of *A. fumigatus* 48 hour culture filtrate

Mass spectrometry-based proteomics was performed on proteins collected from the 48 hr-*A. fumigatus* CuF in order to investigate the components that may be influencing bacterial growth. The top 25 proteins are listed in Table 1 and the full list can be found in Table A4.1. The majority of proteins detected were enzymes associated with amino acid metabolism (e.g. L-amino acid oxidase, Tripeptidyl-peptidase sed2), cell wall biosynthesis (e.g. Protein ecm33, 1,3-beta-glucanosyltransferase Bgt1, Secreted beta-glucosidase sun1), gluconeogenesis (Triosephosphate isomerase, phosphoglucomutase PgmA, Glucose-6-phosphate isomerase, oxidative stress (e.g. Peroxiredoxin, Asp f3, Superoxide dismutase) and gliotoxin production (e.g. Thioredoxin reductase gliT, Cobalamin-independent methionine synthase). A number of proteins detected were involved in sugar metabolism (e.g. Beta-fructofuranosidase, Mannitol-1-phosphate 5-dehydrogenase, Glucooligosaccharide oxidase), and several proteins were associated with virulence (Alkaline protease 2, Aspergillopepsin-1, Major allergen Asp f 2). Additionally, a number of glucanases were detected in this culture filtrate.

Table 4.1: Proteins identified in *A. fumigatus* culture filtrates. Proteins (> 3kDa) identified in the culture filtrates produced by *A. fumigatus* grown in Czapek- Dox for 48 hours. The top 25 proteins detected are listed**.**

No.	Protein Name	Score	Coverage (%)
1	L-amino acid oxidase LaoA	146.19	44.33
2	Thioredoxin reductase, putative	125.88	47.67
3	1,3-beta-glucanosyltransferase Bgt1	113.73	44.26
4	Tripeptidyl-peptidase sed2	70.44	38.54
5	Alkaline protease 1	70.10	39.45
6	Glycosyl hydrolase, putative	68.22	57.34
7	Mannosyl-oligosaccharide alpha-1,2-mannosidase 1B	62.48	39.55
8	Malate dehydrogenase	60.74	63.82
9	Uncharacterized protein	58.82	50.75
10	FAD/FMN-containing isoamyl alcohol oxidase MreA	58.60	25.39
11	Thioredoxin reductase gliT	58.02	53.59
12	Probable glycosidase crf1	51.96	46.58
13	Amidase, putative OS	51.79	27.17
14	Endonuclease/exonuclease/phosphatase	49.83	31.44
15	Formate dehydrogenase	49.25	39.23
16	FAD-dependent oxygenase	48.20	34.12
17	IgE-binding protein	48.13	29.06
18	Aspergillopepsin-1	46.92	35.19
19	Triosephosphate isomerase	46.46	44.92
20	Secreted beta-glucosidase sun1	45.68	19.81
21	Probable glucan endo-1,3-beta-glucosidase eglC	40.13	23.54
22	1,3-beta-glucanosyltransferase gel1	39.59	25.66
23	Aminopeptidase	38.20	26.23
24	Uncharacterized protein	35.63	41.78
25	Transaldolase	34.41	39.81

4.2.3 *A. fumigatus* generates an amino acid-rich environment in Czapek-Dox

Since Czapek-Dox does not contain amino acids in the original medium preparation, it was hypothesized the abundance of peptidases in the *A. fumigatus* CuF (Table 4.1 and Table A4.1) was causing elevated levels of free amino acids in the culture filtrates, thereby providing *P. aeruginosa* was additional nutrients and promoting bacterial growth. The amino acid concentration in the culture filtrates was measured by the ninhydrin assay (4.4A and C). The ninhydrin test detected an amino acid concentration of 40 µg ±2.1 /ml in the *A. fumigatus* CuF and 28 µg ±1.2 /ml in the Co-culture CuF (Fig. 4.3B). Amino acids were not detected in the *P. aeruginosa* CuF or in the *A. fumigatus* CuF produced in MM which may explain why increased rates of bacterial growth were not observed in these media (Fig. 4.4B).

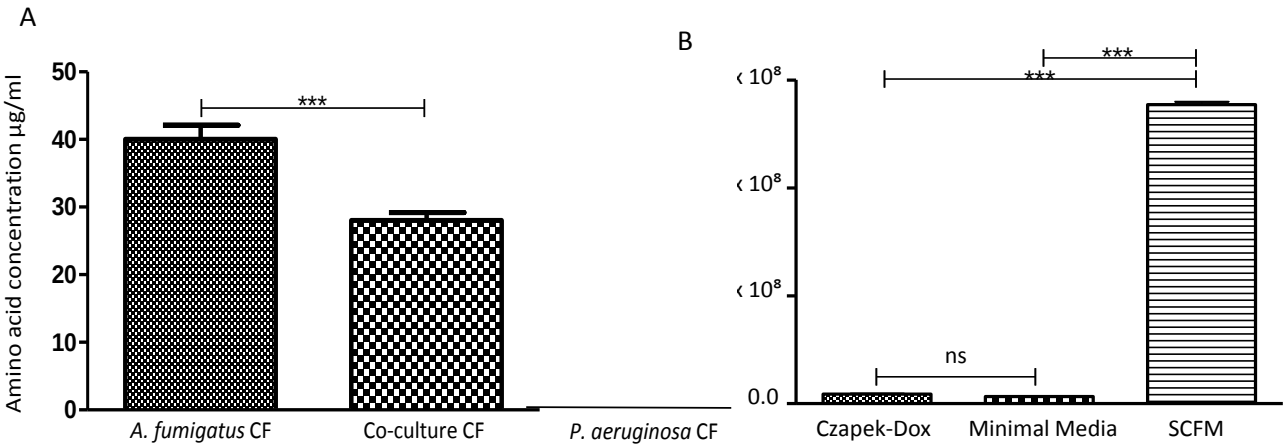

Fig. 4.4. Amino acid concentration in culture filtrates Amino acid concentration detected in 48-hour *A. fumigatus* CuF and Co-culture CuF produced in Czapek-Dox was greater in *A. fumigatus* CuF (A). Comparison of the growth between *P. aeruginosa* (OD600) cultured in (i) Czapek-Dox, MM and SCuFM for 48 hours. Maximum growth was observed in *P. aeruginosa* cultured in SCuFM (B). ***: p<0.001 **: p<0.01 *: p<0.05 ns: not significant

4.2.4 The effect of *A. fumigatus* CuF and Co-culture CuF on the proteome of *P. aeruginosa*

Label free quantitative (LFQ) proteomics was employed to examine the whole cell proteomic response of *P. aeruginosa* exposed to *P. aeruginosa* CuF, *A. fumigatus* CuF or Co-culture CuF (n = 4) and to investigate the proteins and pathways involved in regulating bacterial growth under these conditions. In total, 2317 proteins were initially identified, of which 1665 remained after filtering and processing (Table A4.2A). Of the 1665, proteins identified post-imputation, 677 proteins in the *A. fumigatus* CuF-treated group (Table A4.2B) 611 in the Co-culture CuF-treated group (Table A4.2C) were determined to be statistically significant ($p<0.05$) differentially abundant (SSDA) with a fold change of +/- 2. A principal component analysis (PCA) was performed on all filtered proteins and identified distinct proteomic differences between the groups (Fig 4.5A). Components 1 and 2 accounted for 71.3% of the total variance within the data, and all replicates resolved into their corresponding samples, with little variability between each sample. The groups exposed to *P. aeruginosa* CuF (control) displayed a clear divergence to those that were challenged with *A. fumigatus* CuF or Co-culture CuF. A distinct separation between the groups cultured in *A. fumigatus* CuF or Co-culture CuF was also observed.

Hierarchical clustering was performed on the z-scored normalised LFQ intensity values for the 1005 SSDA proteins identified (ANOVA; Benjamini Hochberg procedure, FDR cut-off value of ≤ 0.05). All four biological replicates resolved into their respective sample. Based on protein abundance profile similarities, nine protein clusters (A-I) were also resolved (Fig. 4.4B). GO and KEGG term enrichment analysis was performed on all protein clusters. Six clusters contained enriched terms (Cluster A, C, D, G-I; Table A4.3B), with each cluster having a representative process or pathway characteristic to that group (Fig. 4.5B and 4.5C). Details of all clusters are included in the Table A4.3A.

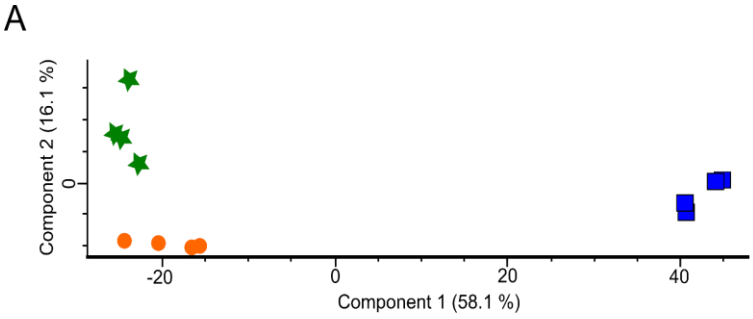

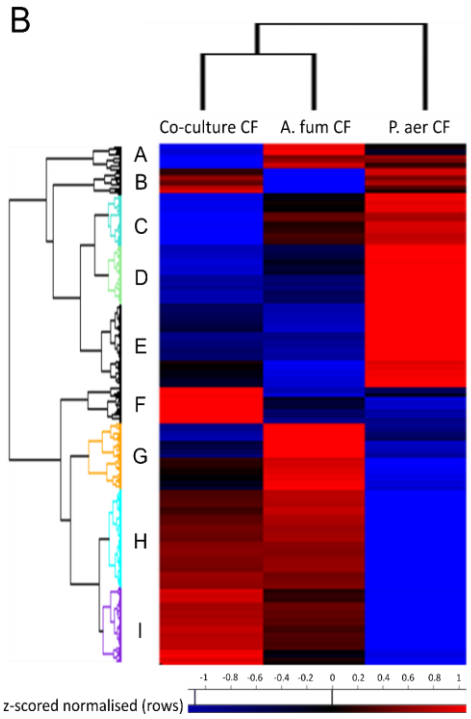

C

Cluster ID	Gene Ontology Term	P-value	Enrichment
A	Membrane	2.55E-05	4.0733
C	ABC Transporters	8.46E-07	3.9044
D	Periplasmic Space	6.47E-04	2.8202
G	Outer Membrane	8.19E-05	3.6813
H	Nucleotide Binding	2.70E-07	1.7081
I	Nitrogen compound metabolism	1.14E-07	1.6494
	Biosynthetic Process	4.30E-07	1.6754

Fig. 4.5 PCA, hierarchical clustering and enrichment analysis of *P. aeruginosa* proteins display distinct differences in groups according to type of CuF exposure. Principal component analysis (PCA) of *P. aeruginosa* exposed to Co-culture CuFs (green) *A. fumigatus* CuF (orange) and *P. aeruginosa* CuF (blue) (A). A clear distinction can be observed between each of the treated groups and the control. Clusters based on protein-abundance profile similarities were resolved by hierarchical clustering of multi-sample comparisons between the three sample groups of *P. aeruginosa* (B). Nine clusters (A-I) were resolved comprising proteins that display similar expression profiles across treatments. Of these, six clusters (A, C, D, G-I) had statistically enriched Gene Ontology (GO) and KEGG terms associated with them (Table A4.3) and the main terms are summarised for each in Fig. 4.5 C.

Enriched terms contained in the clusters in Fig. 4.5B included membrane and integral to membrane (Cluster A), ABC transporters and periplasmic space (Cluster C), periplasmic space, (Cluster D), membrane and outer membrane proteins (Cluster G), nucleotide binding (Cluster H) and transcription, cell division and amino acid biosynthesis (Cluster I).

In Cluster A, 46 proteins associated with the GOCC term, membrane, were identified. Proteins within this group were increased the most in *P. aeruginosa* cultured in *A. fumigatus* CuF compared to bacteria cultured in *P. aeruginosa* CuF and Co-culture CuF respectively. Within Cluster C, GO terms and KEGG pathway analysis resolved 99 proteins with terms associated with the periplasmic space and ABC transporters, respectively. Compared to *P. aeruginosa* cultured in *P. aeruginosa* CuF and *A. fumigatus* CuF, the abundance profile of proteins from bacteria cultured in Co-culture CuF were distinctly lower. Periplasmic proteins included in this group were associated with transport and protein folding in the periplasm. The main categories of ABC transporters observed were those involved with iron transport and phosphate and amino acid transport. In Cluster D (112 proteins), one GO enrichment term for the periplasmic space, was identified. The protein-abundance profile showed a decrease in the relative abundance of several proteins associated with the periplasmic space from bacteria cultured in *A. fumigatus* CuF and Co-culture CuF compared to the control. Periplasmic proteins in this group were involved with amino acid biosynthesis and transport.

Within Cluster G (130 proteins), seven enriched GO terms were identified, including membrane, outer membrane and external encapsulating structure part. The relative abundance of proteins associated with these terms were increased significantly in bacteria cultured in *A. fumigatus* CuF compared to Co-culture CuF or *P. aeruginosa* CuF. Proteins included in this cluster were involved with carbon metabolism, amino-acyl tRNA biosynthesis (tRNA ligases), amino acid biosynthesis, and the chemotaxis family of the two-component system.

Enriched GO and KEGG terms identified in Cluster H (192 proteins) were primarily associated with DNA replication, transcription, purine and pyrimidine metabolism and amino acid metabolism. These protein clusters included the GO terms hydrolase activity, adenylnucleotide binding, ribonucleotide binding, ATP binding. The

abundance of proteins associated with these pathways and processes were significantly greater in *P. aeruginosa* cultured in *A. fumigatus* CuF and Co-culture CuF compared to that exposed to *P. aeruginosa* CuF. Cluster I (147 proteins) contained a number of enriched terms associated with key biological processes and molecular functions involved with nitrogen metabolism, oxidoreductase activity, small molecule biosynthesis, transcription, protein folding, and cell wall formation. These pathways and processes were most increased in bacteria cultured in Co-culture CuF.

Volcano plots were produced by pairwise Student's t-tests ($p < 0.05$) to determine the differences in protein abundance between two samples and to depict the changes in pathways and processes in which those proteins are involved (Fig. 4.6A-C). SSDA protein names arising from the pair wise t-tests were inputted into the STRING and KEGG database and used to identify biological pathways and processes over-represented in a particular group. The changes in biological pathways and processes observed in the volcano plots mirror the trends in the heat map (Fig. 4.5B).

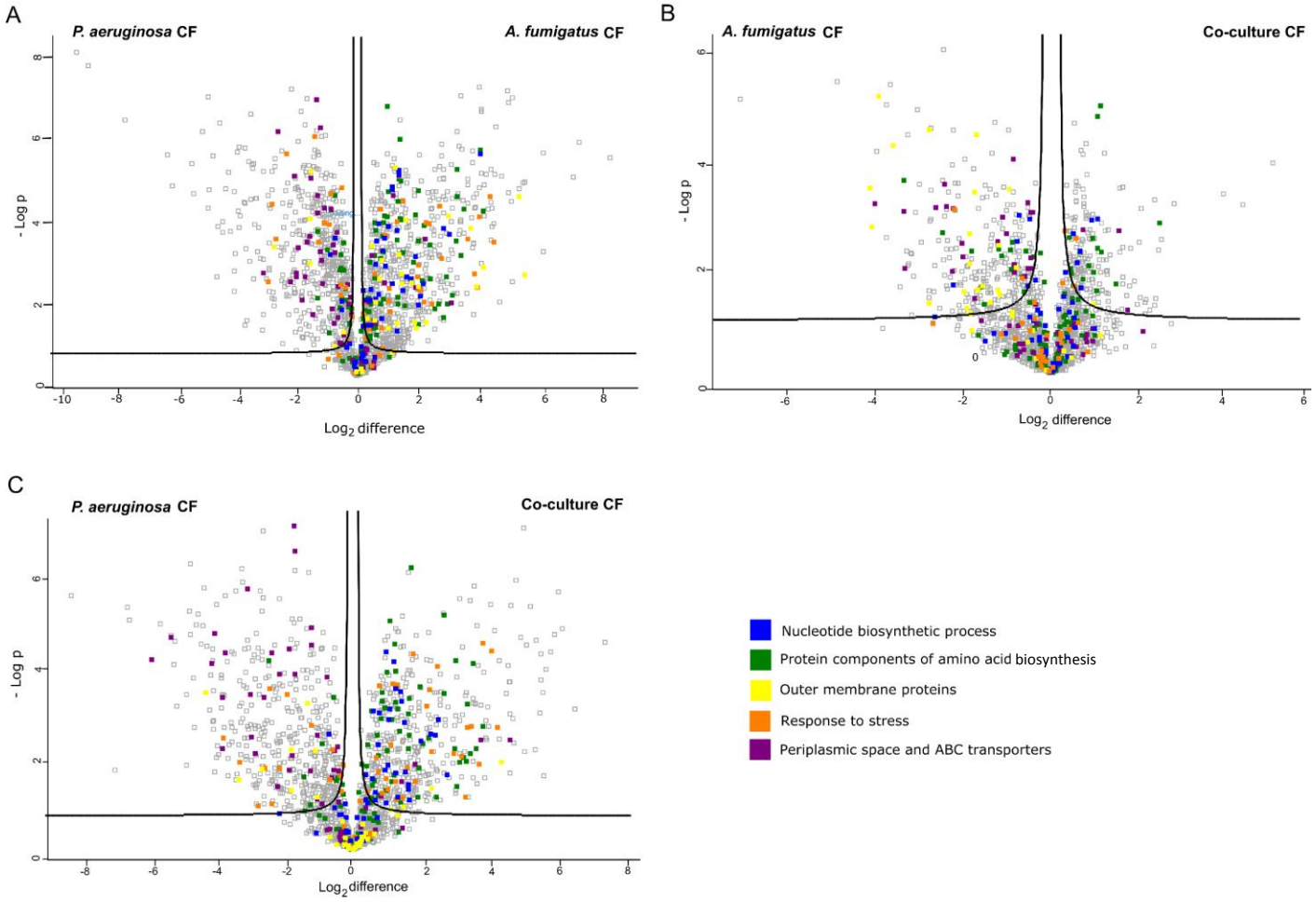

Fig. 4.6 Differential abundance of proteins detected in *P. aeruginosa* exposed to culture filtrates Volcano plots derived from pairwise comparisons between *P. aeruginosa* cultured in *A. fumigatus* CuF and *P. aeruginosa* CuF (A), Co-culture CuF and *A. fumigatus* CuF (B) and Co-culture CuF and *P. aeruginosa* CuF (C). The distribution of quantified proteins according to p value (−log10 p-value) and fold change (log_2 mean LFQ intensity difference) are shown. Proteins above the line are considered statistically significant (p-value <0.05). Protein components of amino acid (green) and nucleotide biosynthetic process (blue) and response to stress (orange) are more abundant in bacteria cultured in *A. fumigatus* CuF and Co-culture CuF than in *P. aeruginosa* CuF. The relative abundance of proteins associated with the periplasmic space and ABC transporters (purple) was decreased in bacteria cultured in *A. fumigatus* CuF and Co-culture CuF compared to *P. aeruginosa* CuF. The relative abundance of outer membrane proteins (yellow) was greater in bacteria exposed to *A. fumigatus* CuF compared to *P. aeruginosa* CuF and lower in Co-culture CuF compared to *A. fumigatus* CuF and *P. aeruginosa* CuF.

The proteomic data arising from Student's t-tests ($p < 0.05$) identified a significant increase in the relative abundance of proteins associated with cell division and cell wall formation in bacteria cultured in *A. fumigatus* CuF and Co-culture CuF, compared to bacteria exposed to *P. aeruginosa* CuF. No significant changes in these processes were observed between bacteria cultured in *A. fumigatus* CuF and Co-culture CuF. The most SSDA proteins associated with these processes are listed in Table 4.2. The relative abundance of several components from the nucleotide biosynthesis pathway was increased in bacteria cultured in *A. fumigatus* CuF and Co-culture CuF compared to that exposed to *P. aeruginosa* CuF. SSDA proteins included in this pathway are listed in Table 4.3 and are highlighted in Fig. 4.5A-C. There were no statistically significant changes in the relative abundance of proteins associated with this pathway between bacteria cultured in *A. fumigatus* CuF and Co-culture CuF. These comparisons are therefore not included in the table 4.3.

Table 4.2. Proteins associated with replication. Statistically significant (T-test, $p < 0.05$) proteins associated with cell division and cell wall biosynthesis and relative fold differences between *P. aeruginosa* cultured in *A. fumigatus* CuF and *P. aeruginosa* CuF (Af v Pa), and between Co-culture CuF and *P. aeruginosa* CuF (Cc v Pa) and between Co-culture CG and *A. fumigatus* CuF (Cc v Af).

		Fold change		
Gene	**Protein name**	**Af v Pa**	**Cc v Pa**	**Cc v Af**
ftsZ	Cell division protein FtsZ	23.1	26.7	ns
gyrB	DNA gyrase subunit B	18.7	9.77	ns
glmM	Phosphoglucosamine mutase	4.8	8.54	ns
kdsB	3-deoxy-manno-octulosonate cytidylyltransferase	1.7	1.9	ns
lpxC	UDP-3-O-acyl-N-acetylglucosamine deacetylase	3	2.8	ns
lpxD	UDP-3-O-acylglucosamine N-acyltransferase	ns	2.4	ns
murA	UDP-N-acetylglucosamine 1-carboxyvinyltransferase	1.6	2	1.23
murC	UDP-N-acetylmuramate--L-alanine ligase	ns	3.5	ns
murE	UDP-N-acetylmuramoyl-L-alanyl-D-glutamate-2,6-diaminopimelate ligase	6.4	7.5	ns
ZapE	Cell division protein ZapE	20.7	19.1	ns

Table 4.3. Proteins associated with nucleotide biosynthesis. Statistically significant (T-test, $p < 0.05$) proteins associated with nucleotide biosynthesis and relative fold differences between *P. aeruginosa* cultured in *A. fumigatus* CuF and *P. aeruginosa* CuF (Af v Pa), and between Co-culture CuF and *P. aeruginosa* CuF (Cc v Pa).

Gene	Protein name	Fold change Af v Pa	Fold change Cc v Pa
amn	AMP nucleosidase	2.8	2.4
dut	Deoxyuridine 5'-triphosphate nucleotidohydrolase	2.5	ns
folA	Dihydrofolate reductase	4.2	ns
guaA	GMP synthase	7.1	5.2
nadD	Probable nicotinate-nucleotide adenylyltransferase	4.5	ns
nrdA	Ribonucleoside-diphosphate reductase	66.9	44.2
nrdB	Ribonucleoside-diphosphate reductase subunit beta	16.1	6.7
prs	Ribose-phosphate pyrophosphokinase	2.2	2.3
purB	Adenylosuccinate lyase	8.1	5.6
purC	Phosphoribosylaminoimidazole-succinocarboxamide synthase	2.2	2
purF	Amidophosphoribosyltransferase	3.3	4.8
purL	Phosphoribosylformylglycinamidine synthase	3.7	3.1
purT	Phosphoribosylglycinamide formyltransferase 2	2.6	2.6
pyrB	Aspartate carbamoyltransferase	2	2
pyrE	Orotate phosphoribosyltransferase	2.2	1.7
pyrG	CTP synthase	3.1	3.9
pyrH	Uridylate kinase	2.4	2.4
tmk	Thymidylate kinase	4.0	3.0

Paired t-tests between the groups identified an increase in the relative abundance of SSDA proteins with the KEGG term cellular amino acid biosynthesis in bacteria exposed to *A. fumigatus* CuF and Co-culture CuF compared to *P. aeruginosa* CuF. This included the biosynthesis of valine, leucine, isoleucine, lysine, glutamine, cysteine, proline, serine and arginine (Table 4.4, Fig. 4.6A and 4.6C). There was a statistically significant change in 11 differentially expressed proteins associated with this pathway between bacteria cultured in Co-culture CuF and *A. fumigatus* CuF (Table 4.4).

Table 4.4 Proteins associated with amino acid metabolism. Statistically significant (T-test, $p < 0.05$) proteins associated with amino acid biosynthesis and relative fold differences between *P. aeruginosa* cultured in *A. fumigatus* CuF and *P. aeruginosa* CuF (Af v Pa), between Co-culture CuF and *P. aeruginosa* CuF (Cc v Pa) and between Co-culture CuF and *A. fumigatus* CuF (Cc v Af).

		Fold change		
Gene	**Protein name**	**Af v Pa**	**Cc v Af**	**Cc v Af**
leuC	3-isopropylmalate dehydratase large subunit	5.1	13.8	2.7
bauC	Putative 3-oxopropanoate dehydrogenase	5.7	11.9	ns
PA1750	Phospho-2-dehydro-3-deoxyheptonate aldolase	9.4	11.2	ns
trpE	Anthranilate synthase component 1	7.7	10.7	ns
serC	Phosphoserine aminotransferase	8.5	10.2	ns
metZ	O-succinylhomoserine sulfhydrylase	5.1	9.3	1.6
PA1752	2-dehydropantoate 2-reductase	ns	8.6	2.2
panD	Aspartate 1-decarboxylase	11.1	8.1	ns
asd	Aspartate-semialdehyde dehydrogenase	9.5	8	ns
PA0399	cystathionine beta-synthase	7	7.7	ns
leuA	2-isopropylmalate synthase	4.5	6.3	ns
proB	Glutamate 5-kinase	4	6.3	1.6
lysA	Diaminopimelate decarboxylase	2.9	4.6	ns
argH	Argininosuccinate lyase	2.8	4.1	ns
serA	D-3-phosphoglycerate dehydrogenase	2.6	3.9	ns
argA	Amino-acid acetyltransferase	ns	3.8	5.2
glnA	Glutamine synthetase	1.5	3.2	2.1
hom	Homoserine dehydrogenase	3.6	3.1	ns
PA2843	Phospho-2-dehydro-3-deoxyheptonate aldolase	2.5	3.1	ns
glyA2	Serine hydroxymethyltransferase 3	2.7	3.1	ns
hisC1	Histidinol-phosphate aminotransferase 1	4.4	3	-1.5
ilvD	Dihydroxy-acid dehydratase	ns	2.6	1.9
hisZ	ATP phosphoribosyltransferase regulatory subunit	2.5	2.5	ns
argG	Argininosuccinate synthase	2.5	2.4	ns
leuB	3-isopropylmalate dehydrogenase	2.6	2.4	ns
mtnB	Methylthioribulose-1-phosphate dehydratase	2	2.3	ns
proC	Pyrroline-5-carboxylate reductase	3.4	2.3	ns
leuD	3-isopropylmalate dehydratase small subunit	2	2.2	ns
gltB	Glutamate synthase large chain	3.7	2.2	ns
ilvI	Acetolactate synthase	2	2.1	ns
metF	Methylenetetrahydrofolate reductase	ns	2	2
lysC	Aspartokinase	2.6	2	-1.3
cysB	Transcriptional regulator CysB	-2.1	-2.7	ns
ggt	Gamma-glutamyltranspeptidase	-2.4	-5.5	-2.2
cysE	O-acetylserine synthase	-2.5	ns	ns

Table 4.5. Proteins associated with ABC transporters. Statistically significant (T-test, $p < 0.05$) proteins associated with ABC transporters and relative fold differences between *P. aeruginosa* cultured in Co-culture CuF and *P. aeruginosa* CuF (Cc v Pa) between and *A. fumigatus* CuF and *P. aeruginosa* CuF (Af v Pa).

			Fold change	
Gene	**Protein**	**Substrate**	**Cc v Pa**	**Af v Pa**
nasS/PA1786	Nitrate ABC transporter substrate-binding protein	Nitrate	23.9	8.5
PA4862	Probable ATP-binding component	Urea	13.2	4.1
metN2	Methionine import ATP-binding protein	D-Methioine	3.5	4.7
modC	Molybdenum import ATP-binding protein	Molybdate	2.7	1.4
rbsB	Binding protein component of ABC ribose transporter	Ribose	-57.7	-3.9
PA5217	Probable binding protein component of ABC iron transporter	Iron	-38.6	-4.0
PA3858	Probable amino acid-binding protein	Amino acid	-17.1	-2.9
PA4496	Probable binding protein component of ABC transporter	Dipeptide/nickel	-16.1	-3.1
PA4502	Probable binding protein component of ABC transporter	Dipeptide/nickel	-13.8	ns
PA5103	ABC transporter substrate-binding protein	Amino acid	-13.7	ns
PA4497	Probable binding protein component of ABC transporter	Peptide	-13	-3.3
braC	Branched-chain amino acid transport ATP-binding protein	Branched-chain	-8.3	-4.2
PA2338	Probable binding protein of maltose/mannitol transporter	maltose/mannitol	-7.8	-1.6
braF	Branched-chain amino acid transport ATP-binding protein	Branched-chain	-7.7	-1.7
PA2711	Probable periplasmic spermidine/putrescine-binding protein	Polyamine	-7.1	-2.2
pstS	Phosphate-binding protein PstS	Phosphate	-6	-1.3
PA3236	Probable glycine betaine-binding protein	glycine betaine	-5.1	-2.2
PA596	Probable binding protein component of ABC transporter	Amino acid	-4.6	3.9
braG	Branched-chain amino acid transport ATP-binding protein	Branched-chain	-4.4	-2.5
PA4913	Probable binding protein component of ABC transporter	Branched-chain	-3.6	-6.1
PA1342	Probable binding protein component of ABC transporter	Glutamate/Aspartate	-3.6	-2.9

PA5388	Choline ABC transporter substrate-binding protein	Choline	-3.4	-4.6
PA3931	Methionine ABC transporter substrate-binding protein	Methionine	-3.3	-1.8
PA5378	Choline ABC transporter substrate-binding protein	Choline	-3.2	-2.3
PA5317	Binding protein component of ABC dipeptide transporter	Amino Acid	-3.2	-2.1
PA1339	Amino acid ABC transporter ATP binding protein	Glutamate/Aspartate	-2.3	-4.0
PA3313	Phosphate-import protein PhnD	Phosphate	-2.3	-2.5
aotJ	Arginine/ornithine binding protein	Arginine/ornithine	-2.3	-1.7
aotP	Arginine/ornithine transport ATP-binding protein	Arginine/ornithine	-2	-2.3
PA1810	Probable binding protein component	Amino acid	-1.7	ns
cysP	Sulphate-binding protein	Sulphate	-1.5	1.4
PA5076	Probable binding protein component	Amino acid	-1.5	ns
spuD	Putrescine-binding periplasmic protein	Putrescine	-1.4	-1.6
spuE	Spermidine-binding periplasmic protein	Spermidine	-1.4	-1.3
PA2812	Probable ATP-binding component	Amino acid	-1.3	1.1

In general, there was a greater decrease in the relative abundance of proteins associated with ABC transporters in the bacteria cultured in Co-culture CuF compared to bacteria cultured in *A. fumigatus* CuF and *P. aeruginosa* CuF (Table 4.5). The majority of these proteins were substrate binding proteins and ATP binding components of ABC transporters involved with the transport of amino acids, carbohydrates and lipids. Within this group, the three proteins with the greatest decrease in relative abundance were probable amino acid binding protein (PA3858; -17.1-fold), probable binding protein component of ABC iron transporter (PA5217; -38.6-fold) and binding protein component of ABC ribose transporter (rbsB; -57.7-fold). Of the 35 ABC-transport proteins listed, four were increased in abundance. Three of these, nitrate ABC transporter substrate-binding protein (nasS;+23.9-fold), probable ATP-binding component (PA4862; +13.2-fold) and molybdenum import ATP-binding protein (modC; +2.7-fold) are associated with the import of nitrate, urea and molybdate respectively. These proteins are listed in Table 4.5.

Pairwise t-tests identified increases and decreases in the relative abundance of proteins associated with a stress response and DNA damage repair in *P. aeruginosa* cultured in *A. fumigatus* CuF and Co-culture CuF compared to bacteria cultured in *P. aeruginosa* CuF (Table 4.6). Xenobiotic reductase B (Xen B), Lon protease (lon), Alkyl hydroperoxide reductase subunit F (ahpF) and Bifunctional enzyme CysN/CysC (CysNC) showed the greatest fold-change in *P. aeruginosa* cultured in *A. fumigatus* CuF and Co-culture CuF compared to *P. aeruginosa* CuF. With the exception of Xen B, there were no changes in protein abundance between these two groups. Catalase HPII (katE), magD (magD) and cold-shock protein (CspD) had the greatest decrease in relative abundance in the bacteria cultured in *A. fumigatus* CuF and Co-culture CuF compared to *P. aeruginosa* CuF. There were no significant changes in the abundance of these proteins between *P. aeruginosa* cultured in *A. fumigatus* CuF and Co-culture CuF.

The proteomic data arising from the paired Student's t-tests ($p < 0.05$) identified a significant increase in the abundance of proteins associated with anaerobic respiration including denitrification enzymes, and a decrease in the levels of proteins associated with aerobic respiration in bacteria exposed to Co-culture CuF and *A. fumigatus* CuF compared to that exposed to *P. aeruginosa* CuF. A comparison of the proteome between bacteria cultured in Co-culture CuF and *A. fumigatus* CuF showed few significant differences in the relative abundance of proteins than when compared to bacteria cultured in *P. aeruginosa* CuF. Nonetheless, some changes in the abundance of proteins associated with these pathways were observed between these groups. Functionally annotated SSDA proteins with the greatest differential increase or decrease in abundance involved in anaerobic or aerobic respiration respectively are listed in Table 4.7.

Table 4.6 Proteins associated with a stress response. Statistically significant (T-test, $p < 0.05$) proteins associated with a stress response and DNA damage repair and relative fold differences between *P. aeruginosa* cultured in Co-culture CuF and *P. aeruginosa* CuF (Cc v Pa) between and *A. fumigatus* CuF and *P. aeruginosa* CuF (Af v Pa) and between Co-culture CuF and *A. fumigatus* CuF.

Gene	Protein	Fold change		
		Af v Pa	Cc v Pa	Cc v Af
xenB	Xenobiotic reductase B	304.4	156	-1.9
lon	Lon protease	14.2	18.6	ns
ahpF	Alkyl hydroperoxide reductase subunit F	20	16.5	ns
cysNC	Bifunctional enzyme CysN/CysC	15.4	13.8	ns
uvrB	UvrABC system protein B	15.1	12.6	ns
cysI	Sulfite reductase	12.2	10	ns
recA	Protein RecA	5.35	7.6	ns
trxB2	Thioredoxin reductase	6.5	5.5	ns
polA	DNA polymerase I	6.8	4.9	ns
ppx	Exopolyphosphatase	5.1	4.7	ns
ruvB	Holliday junction ATP-dependent DNA helicase RuvB	4.5	3.5	ns
katE	Catalase HPII	-6.3	-13.6	ns
magD	magD	-3	-12.2	ns
cspD	Cold-shock protein CspD	-7.6	-9.7	ns
msrB	Peptide methionine sulfoxide reductase	-7	-5.3	ns
SenC	SenC	ns	-5	ns
osmC	Osmotically inducible protein OsmC	-5	-4.3	ns
phoB	Phosphate regulon transcriptional regulator	ns	-3.8	ns
PA0838	Glutathione peroxidase	-2.1	-2.3	ns
gor	Glutathione reductase	-2	-1.7	ns
lexA	LexA repressor	-1.4	-1.6	ns

Table 4.7 Proteins associated with respiration. Statistically significant (T-test, $p < 0.05$) proteins associated with aerobic and anaerobic respiration and relative fold differences between *P. aeruginosa* cultured in *A. fumigatus* and *P. aeruginosa* CuF (Af v Pa) between Co-culture CuF and *P. aeruginosa* CuF (Cc v Pa) and between Co-culture CuF and *A. fumigatus* CuF (Cc v Af).

Gene	Protein	Fold change		
		Af v Pa	Cc v Pa	Cc v Af
PA5190	Probable nitroreductase	38.8	58.5	1.5
narG	Respiratory nitrate reductase alpha chain	30.3	53.8	ns
ccoO2	Cytochrome c oxidase, cbb3-type, CcoO subunit	20.53	48.5	2.4
moaB1	Molybdenum cofactor biosynthesis protein B	21.3	43.2	ns
nosZ	Nitrous-oxide reductase	20.54	39	ns
hemN	Oxygen-independent coproporphyrinogen-III oxidase	14.7	29.7	2
nirB	Assimilatory nitrite reductase large subunit	6.6	25.6	3.9
narH	Respiratory nitrate reductase beta chain	9.5	19.3	ns
nirD	Assimilatory nitrite reductase small subunit	Ns	11.2	3.9
moeA1	Molybdopterin molybdenum transferase	5.6	8.98	ns
exaB	Cytochrome c550	-447.6	-286.3	ns
exaA	Quinoprotein alcohol dehydrogenase (cytochrome c)	-13	-47.6	-3.7
PA2171	Hemerythrin-domain containing protein	-73.9	-90.5	ns
napA	Periplasmic nitrate reductase	-7	-34.8	-5
napB	Periplasmic nitrate reductase, electron transfer subunit	-9.9	-5.83	ns
bkdB	Lipoamide acyltransferase	-2.7	-24.1	-9
bkdA1	2-oxoisovalerate dehydrogenase subunit alpha	Ns	-4.9	-5.2
pdhA	Pyruvate dehydrogenase E1 component subunit alpha	-16.4	-7	-2.4
PA3415	Dihydrolipoamide acetyltransferase	-3.4	-16.4	-4.7
lpdV	Dihydrolipoyl dehydrogenase	-1.9	15.4	-8.2

Pairwise t-tests on the post-imputation dataset revealed distinct changes in the relative abundance of outer membrane proteins and efflux pumps between *P. aeruginosa* cultured in *A. fumigatus* CuF and *P. aeruginosa* CuF, Co-culture CuF and *P. aeruginosa* CuF and Co-culture CuF and *A. fumigatus* CuF. There was a clear increase in the proportion of, and the relative abundance of several SSDA outer membrane proteins in *P. aeruginosa* exposed to *A. fumigatus* CuF (Table 4.8, Fig. 4.5C).

Table 4.8 Proteins associated with OMPs. Statistically significant (T-test, $p < 0.05$) proteins associated with bacterial cell membrane and efflux, and relative fold differences between *P. aeruginosa* cultured in *A. fumigatus* and *P. aeruginosa* CuF (Af v Pa) between Co-culture CuF and *P. aeruginosa* CuF (Cc v Pa) and between Co-culture CuF and *A. fumigatus* CuF (Cc v Af).

Gene	Protein	Fold change		
		Af v Pa	Cc v Pa	Cc v Af
MexE	RND multidrug efflux membrane fusion protein	132.3	47.27	ns
oprC	Outer membrane efflux protein OprC	38.6	ns	-15.7
oprG	Outer membrane protein OprG	17.3	4.9	-3.5
oprM	Outer membrane protein OprM	15	ns	-16.3
MexF	Efflux pump membrane transporter	10.2	ns	ns
oprE	Anaerobically-induced outer membrane porin OprE	3.2	ns	-3.1
oprJ	Outer membrane protein OprJ	2.7	ns	-3.2
oprO	Porin O	2.45	ns	-2.9
opr86	Outer membrane protein assembly factor BamA	2.3	ns	ns
opmH	Channel protein TolC	2	ns	-1.9
MexC	RND multidrug efflux membrane fusion protein	1.6	ns	-3.1
oprF	Outer membrane porin F	1.2	ns	ns
oprQ	Outer membrane protein OprQ	-2.6	-23.5	-9.1
opdQ	Outer membrane porin OpdQ	-2.1	-13.7	-6.5
oprD	Porin D	-9.7	-5.6	ns
oprI	Major outer membrane lipoprotein	-6.6	-3.5	ns
oprH	PhoP/Q & low Mg2+ inducible outer membrane protein	ns	-3.5	-3.8
MexB	Multidrug resistance protein MexB	-2.28	ns	ns

4.2.5 Physical interactions between *P. aeruginosa* and *A. fumigatus*

To investigate the ability or otherwise of *P. aeruginosa* to compete with *A. fumigatus* on a solid surface, a bacterial or conidial suspension was streaked diagonally across an agar plate. The inoculum was allowed to dry for four hour prior to the next streak in the (opposite direction) to avoid dragging the spores along the path of the bacteria. The plates were incubated for 24 hours at 37°C and bacterial and fungal growth was assessed visually. To remove any potential bias that may have arisen based on the growth medium used, nutrient agar, which supports *P. aeruginosa* growth, and Sabouraud agar (SAB), which support *A. fumigatus* growth, were used. The results showed that *P. aeruginosa* grew over the spores independently of which cell suspension was applied to the surface first and of which growth media was used (Fig. 4.7A-D).

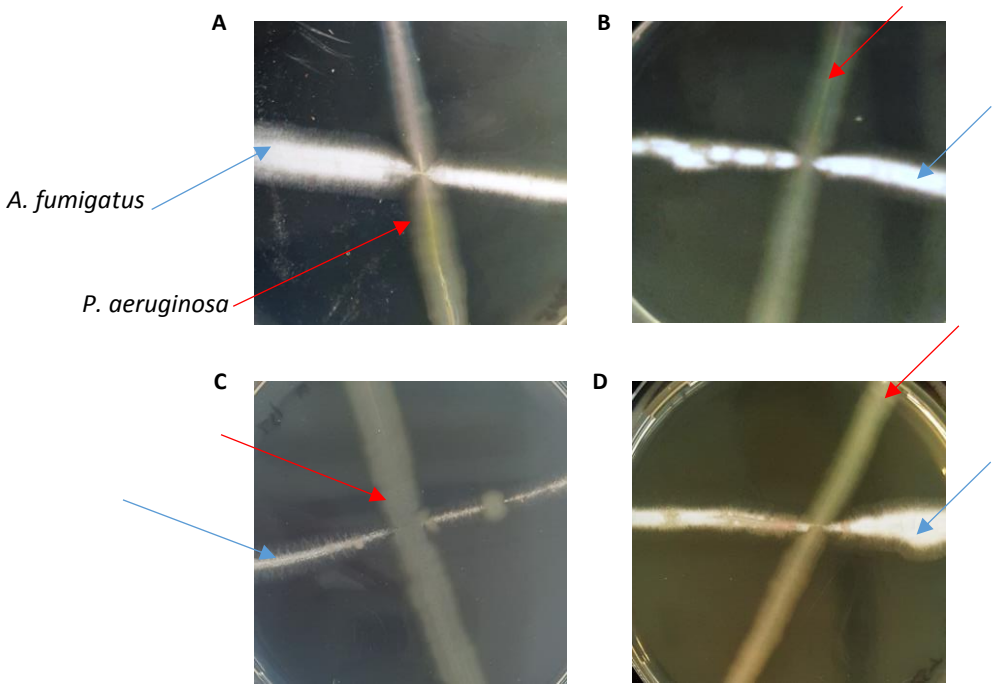

Fig. 4.7 *P. aeruginosa* vs. *A. fumigatus* X assays *P. aeruginosa* (red arrow), followed by *A. fumigatus* conidia (blue arrow) were streaked across a SAB agar plate (A) or nutrient agar (B) in an "X" shape and visualized after 24 hours. *A. fumigatus*, followed by *P. aeruginosa* was streaked across a SAB agar plate (C) or a nutrient agar plate (D) in an "X" shape and visualized after 24 hours.

The ability of *P. aeruginosa* to replicate faster than conidia may have introduced a bias to these observations. Thus, this assay was alternated somewhat to investigate the ability of *P. aeruginosa* to compete with an established culture of *A. fumigatus*. A conidial suspension was streaked horizontally across an agar plate. The inoculum was incubated for 24 hours so that the fungus could become established on the surface. A second inoculation with *P. aeruginosa* cells was performed by streaking the bacterial suspension perpendicularly to the fungus leaving a gap of about 1 cm between the fungus and the bacteria. This process was repeated with the conidial inoculum being streaked vertically and the bacterial inoculum streaked horizontally. The plate was incubated for a further 24 hours and examined visually. Visual assessment of the plate after incubation showed that

P. aeruginosa grew towards *A. fumigatus*. After a further 24 hours, the bacteria had begun to migrate through the fungus, again irrespective of what growth medium was used (Fig. 4.8A). Where the *P. aeruginosa* was streaked horizontally and *A. fumigatus*

was streaked perpendicularly, the fungus did not migrate towards the bacteria but the bacteria did begin to grow out (Fig. 4.8B).

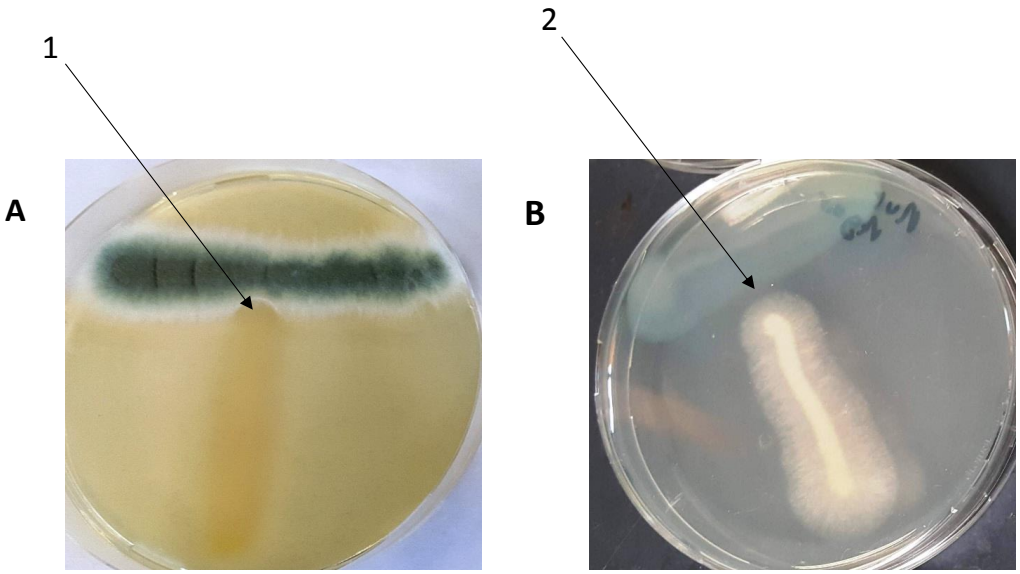

Fig. 4.8 *P. aeruginosa* vs. *A. fumigatus* T assays A "T - assay" shows *P. aeruginosa* (1) migrating through the path of *A. fumigatus* (A). *A. fumigatus* (2) did not migrate across the path of *P. aeruginosa* (B)

P. aeruginosa are mobile bacteria that use flagella for motility. A swim assay was performed to investigate the migration of *P. aeruginosa* towards *A. fumigatus* on a semi-solid surface. A drop of *A. fumigatus* conidial suspension was applied at one pole of the agar plate and incubated overnight to allow the fungus to become established. A drop of *P. aeruginosa* was applied at the other pole and the plate was incubated for a further 12 hours (Fig. 4.9A). After a further 12 hours, *P. aeruginosa* had begun to produce pyocyanin and spread towards the original focal point of *A. fumigatus* but the fungus did not spread towards the bacteria (Fig. 4.9B). The bacterial cells made contact with, and spread around the fungal colony (Fig. 4.9C). Where *A. fumigatus* was not present, *P. aeruginosa* spread throughout the plate at a slower rate as evidenced by the reduced amount of spreading over the same time-frame (Fig. 4.9D and E).

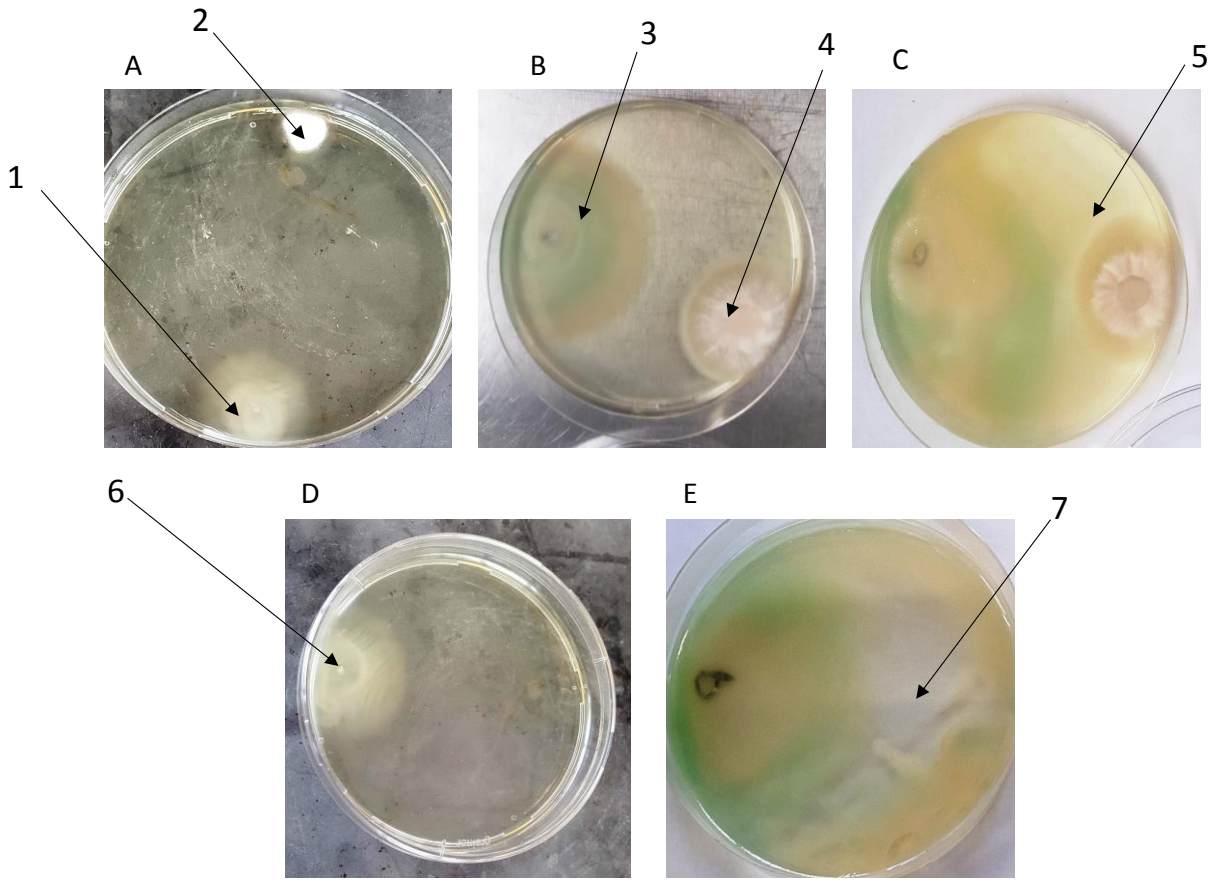

Fig. 4.9. Swim assays Swimming motility assays indicate *P. aeruginosa* (1) began to migrate towards *A. fumigatus* (2) by 12 hours post-inoculation with the bacteria (A). By 24 hours, the bacteria (3) spread closer to the fungal colony and began to produce pyocyanin (B). The *A. fumigatus* colony had grown larger and was beginning to spread out (4). By 36 hours, the bacteria (5) had surrounded the fungus. The fungal colony remained the same size (C). Bacteria (6 and 7) cultured in the absence of the *A. fumigatus* began to grow at a similar rate to A but by 36 hours growth appeared to have slowed as observed by incomplete coverage by the bacteria of the agar plate (D).

The agar plates were visualized under an inverted microscope 36 hours post-inoculation with *P. aeruginosa*. Bacterial cells were densely populated before reaching hyphal tips of *A. fumigatus* but became more dispersed as it reached the fungus (4.10A). The bacteria interacted directly with mycelia and conidia (Fig. 4.10B).

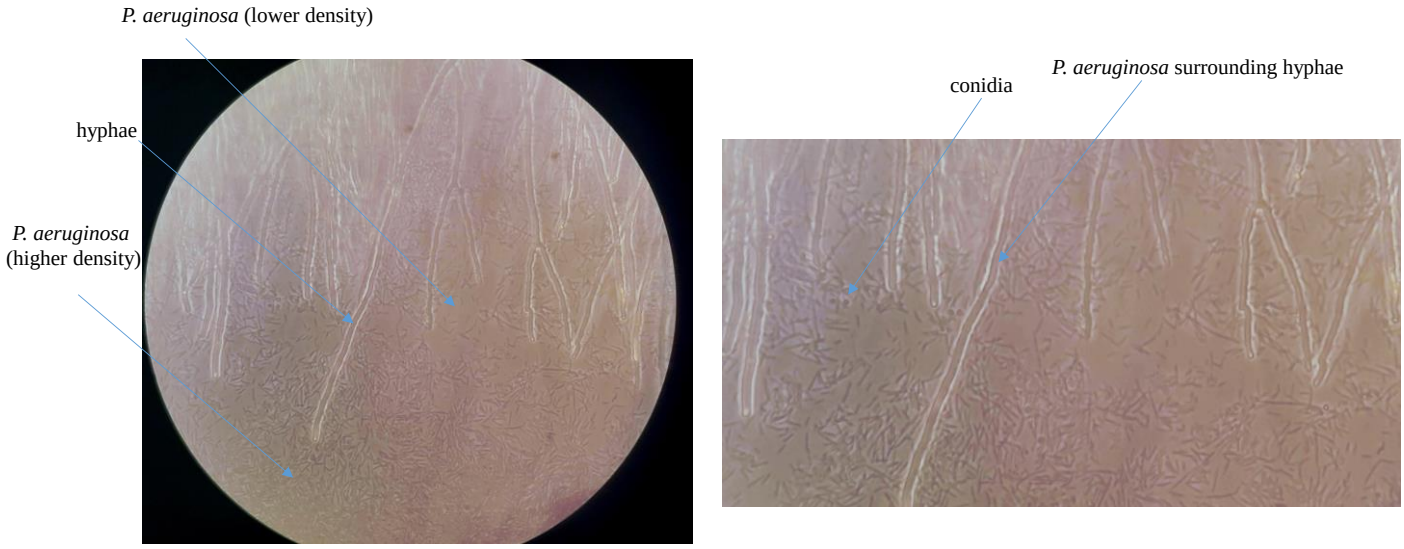

Fig. 4.10 Visualizing the interactions between *P. aeruginosa* and *A. fumigatus* by microscopy
Agar plates containing *P. aeruginosa* (36 hours-post inoculation) and *A. fumigatus* (60 hours post-inoculation). *P. aeruginosa* migrated towards *A. fumigatus* and dispersed as they reached fungal hyphae (A). Bacterial cells interact directly with conidia and hyphal strands (B). (Magnification x 40).

4.3 Discussion

The objective of the work performed in this chapter was to characterize the determinants that enable *P. aeruginosa* to predominate over *A. fumigatus* in a mixed culture. The results presented here suggest that *A. fumigatus* creates an environment that promotes the growth of *P. aeruginosa*. To meet its own nutritional needs, *A. fumigatus* secretes a range of degradative enzymes which breakdown substrates in the growth medium allowing for nutrient assimilation (Amich and Krappmann, 2012). In doing so, the fungus appears to be providing the bacteria with nutrients to which it otherwise may not have access. Thus, the findings in this chapter demonstrate a role for *A. fumigatus* in directly promoting the growth of *P. aeruginosa* by altering the composition of the environment.

The medium used for this study, Czapek-Dox, is a defined synthetic media used for the cultivation of microorganisms that can utilize sodium nitrate as the only source of nitrogen and provides a nutrient-limiting, nitrogen-rich environment. Due to the poor nutritional content, it is frequently used for inducing the production of secondary metabolites, such as fumagillin and gliotoxin (Dhingra *et al.*, 2013; Owens *et al.*, 2014). This medium alone did not promote the growth of *P. aeruginosa*. However, the culture filtrates (CuF) produced by *A. fumigatus* grown in this medium for 48-hours did induce a significant increase in bacterial growth (Fig. 4.1A). Bacterial growth was attenuated when exposed to *A. fumigatus* CuF produced after 96 hours in Czapek-Dox (Fig. 4.1A). The *A. fumigatus* secondary metabolite, gliotoxin, which has known anti-*P. aeruginosa* activity, is produced at this time-point under these conditions (Owens *et al.*, 2015; Reece *et al.*, 2019). Thus, the *A. fumigatus* CuF was analysed for gliotoxin. HPLC analysis determined that gliotoxin concentrations were highest in the 96-hours, which may explain why *P. aeruginosa* growth was inhibited at this time-point (Fig. 4.1B).

To investigate if the CuF produced by a co-culture of *A. fumigatus* and *P. aeruginosa* had a different effect on bacterial growth than that of CuF produced by *A. fumigatus*, the bacteria and fungus were co-cultured for 24 hours. *P. aeruginosa* was exposed to the resulting CuF, herein termed Co-culture CuF and the effect on growth was significantly greater than that when the bacteria was exposed to *A. fumigatus* CuF alone (Fig. 4.2).

Mass spectrometry-based proteomics was used to characterize the secretome of the 48-hour *A. fumigatus* CuF with a view to identifying the secreted proteins that may influence the growth of *P. aeruginosa* (Table 4.1; Table A4.1). A large proportion of the proteins detected were enzymes associated with peptide metabolism i.e. proteases and peptidases (Table 4.1; Table A4.1). *A. fumigatus* assimilates exogenous amino acids via membrane transporters and thus secretes a range of proteases to digest larger peptides and proteins prior to import into the cell (Farnell *et al.*, 2012). Analysis of CF sputum has shown that it contains higher concentrations of amino acids than control sputum (Barth and Pitt, 1996; Sriramulu, 2010). Synthetic cystic fibrosis medium (SCFM) contains an amino acid content comparable to that found in the sputum of CF patients (Palmer *et al.*, 2007a). In this study, the growth rate of *P. aeruginosa* was significantly greater when cultured in SCFM than that in Czapek-Dox, suggesting that the amino acid content of the culture media influences the rate of bacterial growth.

The abundance of peptide-metabolising enzymes present in the 48-hour *A. fumigatus* CuF, such as aminopeptidase and amidase, suggested high levels of amino acids in the medium (Table 4.1). This was confirmed by the ninhydrin test, a common method used to detect amino acids or peptides in a solution (Friedman, 2004). This assay detected free amino acids in the *A. fumigatus* CuF and in the Co-culture CuF (Fig. 4.4C). The reduction in levels of free amino acids in the Co-culture CuF may be indicative of amino acid consumption by *P. aeruginosa* during co-culture with *A. fumigatus* (Fig. 4.4C). Amino acids were not detected by the ninhydrin test in the *P. aeruginosa* CuF or in any culture filtrates produced in minimal media (MM). This may explain why the same rate of bacterial growth observed in *A. fumigatus* and Co-culture CuF was not observed in *P. aeruginosa* CuF or in culture filtrates produced in MM. These results indicate that *A. fumigatus* creates an environment in which *P. aeruginosa* thrive, possibly by metabolizing the media to produce substrates more easily assimilated by the bacteria. This was a media-specific effect, as the same results were not observed using culture filtrates produced in minimal media. In the cystic fibrosis lung, allergens such as Aspergillopepsin, alkaline protease, Asp f 2 and Asp f 4 proteases are major contributors to allergic responses and virulence in ABPA (Banerjee *et al.*, 1998; Knutsen *et al.*, 2004; Farnell *et al.*, 2012). Gliotoxin may also have detrimental effects to patient health (Reece *et al.*, 2018). These proteins were in the 48-hour *A. fumigatus* CuF by mass spectrometry (Table A4.1).

A label-free quantitative (LFQ) proteomics approach was utilised to investigate changes in the *P. aeruginosa* proteome that enable these bacteria to proliferate in an environment containing *A. fumigatus* secondary metabolites, degradative enzymes and limited nutrients. The increase in growth of *P. aeruginosa* cultured in *A. fumigatus* CuF and Co-culture CuF compared to *P. aeruginosa* CuF is reflected by the increase in the relative abundance of proteins associated with DNA replication (DNA gyrase subunit B and Ribonucleoside-diphosphate reductase), cell division (e.g. Cell division protein FtsZ and ZapE) and cell wall biosynthesis (Mur enzymes) (Table 4.2). There was no significant difference in the relative abundance of these proteins between bacteria cultured in *A. fumigatus* CuF and Co-culture CuF.

Nucleotide biosynthesis was increased in bacteria exposed to *A. fumigatus* CuF and Co-culture CuF (Fig. 4.6; Table 4.3). Nucleotides not only provide the precursors necessary for DNA synthesis, but also play an important role in biofilm formation and quorum sensing (Pesavento and Hengge, 2009; Kalia *et al.*, 2013; An and Ryan, 2016). The amino acid biosynthetic pathway was increased in bacteria cultured in *A. fumigatus* CuF and Co-culture CuF compared to bacteria cultured in *P. aeruginosa* CuF (Table 4.4). The enzymes responsible for the biosynthesis of amino acids are essential for bacterial growth and survival. Amino acids are required for the intracellular synthesis of quorum sensing (QS) molecules and for the biosynthesis of secondary metabolites such as phenazine-1-carboxylic acid and pyocyanin (Sriramulu, 2010; Jagmann and Philipp, 2018; Sterritt *et al.*, 2018; Defoirdt, 2019).

Despite the increased rate of bacterial growth in *A. fumigatus* CuF and Co-culture CuF, distinct changes were observed in the proteome of *P. aeruginosa* depending on the culture filtrate to which they were exposed. The relative abundance of proteins associated with ATP-binding cassette (ABC) transporters was significantly less in *P. aeruginosa* exposed to Co-culture CuF compared to bacteria exposed to *P. aeruginosa* CuF. In comparison, there was less of a decrease in the relative abundance of these proteins between bacteria cultured in *A. fumigatus* CuF and *P. aeruginosa* CuF (Fig. 4.5B; Table. 4.5). The majority of the ABC transporters decreased in the groups exposed to Co-culture CuF were importers associated with the import of nutrients such as amino acids and carbohydrates into the cell. The import of substrates is tightly regulated and the expression of ABC transporters is increased or decreased depending on the nutritional requirements of the organism (Tankana, K. J., Song, S., 2018). Differences in the relative

abundance of amino acid ABC transporters in bacteria exposed to Co-culture CuF versus *A. fumigatus* CuF and *P. aeruginosa* CuF indicate a greater need for uptake of nutrients from the environment in *P. aeruginosa* exposed to the latter and suggests tight regulation of ABC transporter-dependent import of amino acids in *P. aeruginosa* cultured in Co-culture CuF.

Interestingly, ABC transporters involved in the uptake of nitrate and molybdate were two of the four ABC transporters increased in *P. aeruginosa* exposed to Co-culture CuF compared to *P. aeruginosa* CuF. This increase in nitrate and molybdate ABC transporters indicate anaerobic growth. Molybdate is required for the formation of molybdoenzymes such as nitrate reductases, which are essential for the use of nitrates during anaerobic respiration (Iobbi-Nivol and Leimkühler, 2013), so much so that mutants for molybdate ABC transporters (ModABC) are unable to grow anaerobically and are less virulent under aerobic and anaerobic conditions (Périnet *et al.*, 2016).

The CF airways are characterized by low oxygen availability and high nitrate content due to oxygen consumption by pro-inflammatory immune cells (Jensen, 2014). The pH of CF sputum is also slightly lower than normal sputum due to impaired bicarbonate transport through defective CFTR (Ahmad *et al.*, 2019). Where normal sputum has a pH of ~ 7.2, the pH of CF sputum is ~ 6.8 (Ahmad *et al.*, 2019). The CF airway pH (pH 5.32-5.88) is also lower than that of normal airways (pH 6.1) (Tate *et al.*, 2002). The sole source of nitrogen in Czapek-Dox is sodium nitrate ($NaNO_3$) and the pH of sterile Czapek-Dox is ~6.8. The results in this chapter demonstrated that *P. aeruginosa* grew poorly in Czapek-Dox and in *P. aeruginosa* CuF (Fig. 4.2). However, an increase in the relative abundance of proteins associated with nitrogen metabolism in bacteria exposed to *A. fumigatus* CuF and Co-culture CuF suggest that *A. fumigatus* may metabolize the sodium nitrate into a form more easily assimilated by *P. aeruginosa* and may explain why *P. aeruginosa* growth proliferates in the presence of the fungus. *P. aeruginosa* is a facultative anaerobe that can perform denitrification under anaerobic conditions and in the presence of nitrate (Jensen, 2014). Additonally, *P. aeruginosa* can grow in environments with a pH as low as 4.5 (Klein *et al.*, 2009). In this study, bacterial growth was greatest in Co-culture CuF where the pH was reduced to ~ pH 5.

The reduction of nitrate to nitrite by nitrate reductases contributes to energy production more so than nitrite reduction (Berks *et al.*, 1995; Van Alst *et al.*, 2009).

Membrane nitrate reductases (NarGHI) are essential for anaerobic growth and are expressed at the expense of periplasmic nitrate reductases (NapAB) (Van Alst *et al.*, 2009). Based on the data produced here an increase in the relative abundance of NarG and NarH, and a decrease in the relative abundance of NapA and NapB in bacteria exposed to *A. fumigatus* CuF and Co-culture CuF compared to *P. aeruginosa* CuF (Table 4.7) were identified. NarG and NarH levels were highest in *P. aeruginosa* exposed to Co-culture CuF. The assimilatory nitrite reductases NirB and NirD catalyse the reduction of nitrite to ammonium (Berks *et al.*, 1995). The relative abundance of these proteins were greatest in bacteria exposed to Co-culture CuF. Taken together, these data suggest that co-incubation of *A. fumigatus* and *P. aeruginosa* create a nitrate-rich environment under which *P. aeruginosa* can adapt by upregulating the denitrification pathway.

Cystic fibrosis sputum contains levels of nitrate sufficient to support anaerobic growth of *P. aeruginosa* (Line *et al.*, 2014). Membrane nitrate reductases are essential for bacterial survival under these levels of nitrates (Palmer *et al.*, 2007; Line *et al.*, 2014). High levels of nitric oxide (resulting from denitrification) can result in nitrosative stress which *P. aeruginosa* counteracts through a variety of detoxification systems (Arai *et al.*, 2005). Among the most abundant proteins detected in *P. aeruginosa* exposed *A. fumigatus* CuF and Co-culture CuF were the RND family efflux membrane protein MexE and xenobiotic reductase (XenB) (Table 4.6 and 4.8). These proteins are induced by nitrosative stress thereby suggesting a defensive mechanism against high NO levels that occur during denitrification (Choi *et al.*, 2006; Fetar *et al.*, 2011).

The ability of *P. aeruginosa* to endure intense environmental stresses such as those found in the cystic fibrosis lung is indispensable for its success as a human pathogen. *P. aeruginosa* has a remarkable capacity to overcome stresses induced by ROS or antibiotics. The proteomic data in this study identified an increase in the relative abundance of several enzymes associated an "SOS" response, i.e. an inducible response to DNA-damage such as that caused by antibiotics (Michel, 2005). An SOS response was upregulated in bacteria exposed to *A. fumigatus* CuF and Co-culture CuF as evidenced by the number of proteins known to be increased upon DNA damage, including Lon protease and RecA (Table 4.7). Lon protease and RecA upregulate the SOS response to antibiotics such as ciprofloxacin, which target DNA (Breidenstein *et al.*, 2012). Alkyl hydroperoxide reductase protects the cell against DNA damage caused by peroxides and is associated

with detoxification of benzene derivatives and increased tolerance to zinc-containing compounds (Ochsner *et al.*, 2000; Mu *et al.*, 2013).

Changes in the relative abundance of several proteins associated with detoxification indicate similar mechanisms employed by *P. aeruginosa* to overcome the challenges associated with exposure to *A. fumigatus* CuF and Co-culture (Table 4.7). An increase in the relative abundance of thioredoxin reductase and sulfite reductase indicate a requirement to reduce redox-active disulphide bonds, for example, those formed by gliotoxin (Dolan *et al.*, 2015).

The differential abundance of outer membrane proteins (OMP) involved in *P. aeruginosa* exposed to *A. fumigatus* CuF compared to Co-culture CuF suggest different regulatory response to the contents of the two CuF (Table 4.8). OMPs regulate the influx and efflux of nutrients and potentially toxic compounds in and out of the cell. The greatest differences in the relative abundance of OMP were observed in OprC, OprG and OprM. OprC regulates the influx of copper ions into the cell (Yoneyama and Nakae, 1996; Quintana *et al.*, 2017). OprG is upregulated under anaerobic conditions and is associated with amino acid import (Mcphee *et al.*, 2009; Reddy *et al.*, 2018). OprM forms the ejection component of the MexAB-OprM efflux system and is responsible for resistance against β-lactams and quinolones, amongst others (Wang *et al.*, 2010; Horna G., López M., Guerra H., 2018). In bacteria cultured in *A. fumigatus* CuF and Co-culture CuF, the relative abundance of OprD was decreased. Downregulation of this protein has been associated with resistance to carbapenems (Farra *et al.*, 2008). An increase in the relative abundance of OMPs in bacteria exposed to *A. fumigatus* CuF indicates a greater need to expel potentially potent compounds from the bacterial cell. An increase in the relative abundance of OMPs in *P. aeruginosa* exposed to *A. fumigatus* CuF suggest a more toxic secretome than that found in the Co-culture CuF (Table 4.8). This suggests that the presence of *P. aeruginosa* during the co-culture process may have influenced anti-bacterial toxin production by *A. fumigatus* resulting in a less toxic growth medium for the bacteria.

Plate assays revealed a number of interesting results in the context of the physical interactions that occur between *P. aeruginosa* and *A. fumigatus*. *P. aeruginosa* was able to grow over and migrate through established colonies of *A. fumigatus* (Fig. 4.7 and 4.8). It is possible that proteases secreted by *P. aeruginosa* degrade *A. fumigatus* conidia,

enabling the bacteria to create a path over or through the wall of spores (Smith *et al.*, 2015).

Swim assays were performed to investigate whether *P. aeruginosa* would migrate towards *A. fumigatus*. *P. aeruginosa* had begun to migrate towards *A. fumigatus* 12 hours post-inoculation (Fig. 4.9A). The growth was not dependent on *A. fumigatus* as the same rate of growth was observed on plates where the fungus was absent (Fig. 4.9D). By 24 hours, (36 for *A. fumigatus*) both pathogens had more than doubled in size (Fig. 4.9B). By 36 hours post-inoculation, *P. aeruginosa* had covered all the space on the agar plate and surrounded the *A. fumigatus* colony which had not increased in size since 12 hours previous (Fig. 4.9C). Where *A. fumigatus* was absent, *P. aeruginosa* was slower to cover the agar. Pyocyanin production began to occur 24 hours post-inoculation as evidenced by the typical green pigment (Fig. 4.9 B, C and E). On closer inspection by microscopy, *P. aeruginosa* was making contact with the fungal hyphae and conidia by 36 hours (Fig. 4.10 A and B). Interestingly, bacterial cells were more densely packed further away from the hyphae. Closer to and surrounding the hyphae, bacterial cells were more dispersed. *P. aeruginosa* has less effect on hyphae than on conidia or germlings (Manavathu *et al.*, 2014). This may be due to the secretion of fungal metabolites such as gliotoxin (Reece *et al.*, 2018).

Onward studies are necessary to perform further analysis on the *A. fumigatus* CuF with a view to determining which factors contained within this media may be promoting the rapid growth of *P. aeruginosa*. Mutant strains of *A. fumigatus* lacking genes for certain peptidases and proteases identified in this study may be used to alter the nutrional content of the CuF. Because the pH of the environment has an influence on the secretome of *A. fumigatus* (Sriranganadane *et al.*, 2011), alterations to the pH of the growth medium may force the fungus to generate an alternative environment, which may alter bacterial growth to give different results to those detected in this study.

4.4 Conclusion

In this study, LFQ proteomics was employed to characterize the response of *P. aeruginosa* to an environment previously inhabited by *A. fumigatus* and/or *P. aeruginosa*. The culture medium chosen for this study is rich in sodium nitrates and sugars but lacks amino acids and in itself, proved unsuitable for sustaining bacterial growth. However, *A. fumigatus* altered this environment to favour the growth of, and confer fitness to *P. aeruginosa* under conditions known to exist in the cystic fibrosis airways, such as high nitrate and amino acid content. Thus, it would seem that the presence of *A. fumigatus* enhances growth of *P. aeruginosa* in co-culture. Additionally, analysis of the physical interactions that occurred between these pathogens on a solid or semi-solid surface showed that *P. aeruginosa* could outcompete *A. fumigatus* by growing over or through conidia. However, the development of hyphae somewhat halted this process. Understanding the strategies and the environmental conditions that permit *P. aeruginosa* to dominate as the primary pathogen in the cystic fibrosis lung is crucial for the development of novel therapeutic targets and for designing therapeutic programmes for patients affected by infections caused by these bacteria.

Chapter Five

Characterization of the response of *Aspergillus fumigatus* to *Pseudomonas aeruginosa*

5.1 Introduction

Many of the determinants that contribute to the success of *A. fumigatus* as a ubiquitous saprophyte, are the same factors that enable to be a successful opportunistic human pathogen (Tekaia and Latge, 2005). Among these attributes are the wide range of biosynthetic gene clusters (>30) responsible for the production of secondary metabolites that confer advantages to *A. fumigatus* in its natural habitat, including protection against UV stress, desiccation and competition with other microorganisms (Inglis *et al.*, 2013; Bignell *et al.*, 2016; Raffa and Keller, 2019). In the context of human infection, some of these secondary metabolites are involved in evading or subverting the host immune response *in vivo*. Thus, owing to their clinical relevance, *A. fumigatus* secondary metabolites and their effects on the host have been well characterized (Fallon *et al.*, 2010; Amin *et al.*, 2014; Schlam *et al.*, 2016a; Bignell *et al.*, 2016; Raffa and Keller, 2019).

From an early age, *A. fumigatus* is frequently detected in the airways of individuals with cystic fibrosis (Amin *et al.*, 2010; Reece *et al.*, 2019). Co-infection with *A. fumigatus* and *P. aeruginosa* occurs intermittently and to a lesser extent persistently, however when co-infection exists, lung function deteriorates (Reece *et al.*, 2017a; Zhao *et al.*, 2018b). Where these two pathogens have been studied in the context of co-infection, *P. aeruginosa* was shown to inhibit *A. fumigatus* growth *in vivo* and *in vitro* (Yonezawa *et al.*, 2000; Mowat *et al.*, 2010; Briard *et al.*, 2015; Ferreira *et al.*, 2015; Shirazi *et al.*, 2016; Sass *et al.*, 2018). In contrast to the findings from these direct interaction studies, indirect interaction studies have shown that the secondary metabolite, gliotoxin, isolated from *A. fumigatus* and dimethyl sulphide, a volatile organic compound derived from *P. aeruginosa*, inhibit *P. aeruginosa* growth or promote *A. fumigatus* growth respectively (Briard *et al.*, 2016; Reece *et al.*, 2018). How one pathogen impacts the metabolome of another may have serious implications for the host, as competition between microorganisms can often lead to an altered secretion profile that increases damage to host tissue (Smith *et al.*, 2015; Sass *et al.*, 2019).

Although numerous interaction studies have been performed between these pathogens, the influence of *P. aeruginosa* on the *A. fumigatus* proteome and secondary metabolite production has not been well studied to date. The objective of the study

presented in this chapter was to address this knowledge gap. The effect on *A. fumigatus* of direct and indirect interactions between the fungus and the bacteria was investigated. LFQ proteomics was employed to gain better insights into how *A. fumigatus* responds to *P. aeruginosa* and its secretome in co-culture and to elucidate the mechanisms that allow the fungus to persist or desist in the presence of the dominant bacterial pathogen.

5.3 Results

5.3.1 The effect of *P. aeruginosa* on *A. fumigatus* growth and gliotoxin production

To investigate the effect of *P. aeruginosa* on *A. fumigatus* growth, different concentrations of *P. aeruginosa* (1 ml OD 1.0, which equates to approximately 3 x 10^8 cells/ml, OD0.5 and OD0.1) were added to a 48-hour *A. fumigatus* culture grown in Czapek-Dox (100 ml). The co-culture was incubated for 24 hours after which the wet weight of the fungus was obtained (Fig. 5.1A). Gliotoxin was extracted from each group of bacterial-exposed *A. fumigatus* cultures and detected by RP-HPLC (Fig. 5.1B). The decrease in wet weight and an increase in gliotoxin production correlated with the increase in *P. aeruginosa* density levels (Fig. 5.1A and 5B). The wet weight of fungal cultures exposed to the highest concentration of *P. aeruginosa* (OD 1.0) (9.1 ±0.3 mg/ml) were 46% lower than the controls (16.7 ± 3.1 mg/ml). The levels of gliotoxin produced by *A. fumigatus* exposed to these bacterial densities was 2.82 ± 0.3 µg/mg. In contrast, gliotoxin levels produced by unexposed fungal cultures was three-fold lower (0.96 ± 0.03 µg/mg)

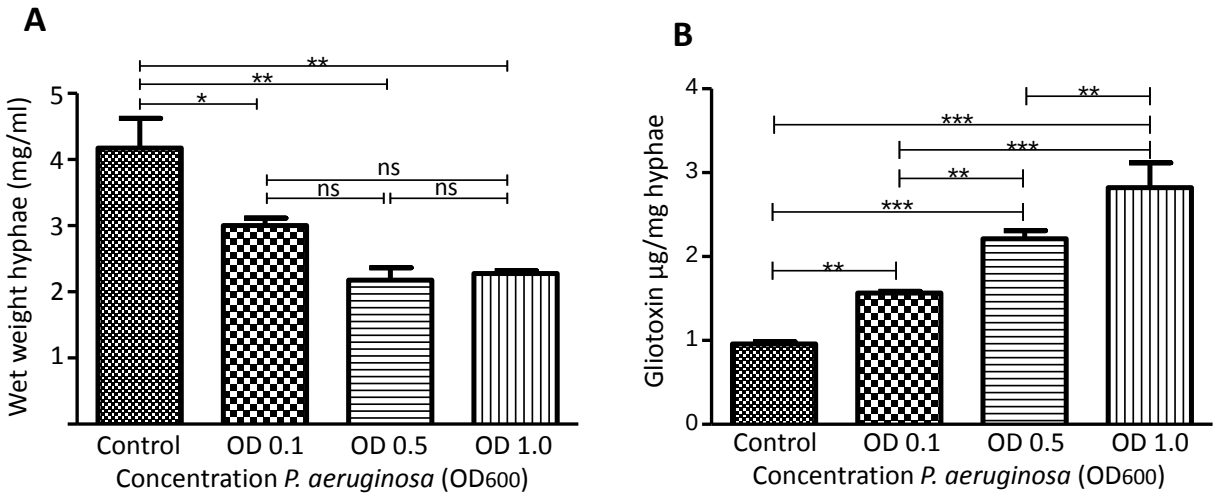

Fig. 5.1 The effect of *P. aeruginosa* on *A. fumigatus* growth and gliotoxin production. *A. fumigatus* growth decrease with increasing *P. aeruginosa* inoculum (A). *A. fumigatus* produced more gliotoxin in response to higher densities of *P. aeruginosa* (B).

To investigate the effect of the *P. aeruginosa* secretome on *A. fumigatus* growth and gliotoxin production, *A. fumigatus* conidia were cultured in Czapek-Dox (50 ml) for 24 hours. Czapek-Dox/PBS (50 ml, 1:1) was added to one group (controls), and *P. aeruginosa* culture filtrate (CuF) (50 ml) produced in a 72 –hour culture was added to the other group (treatment). The fungal cultures were incubated for 24 hours. The wet weights were measured and gliotoxin was extracted for analysis by HPLC. The wet weight of *A. fumigatus* was greater when cultured in Czapek-Dox and PBS (7.8 ±1.1 mg/ml) than when cultured in the presence of *P. aeruginosa* CuF (4.0 ± 0.65 mg/ml). In contrast, the concentration of gliotoxin was greater in fungal cultures exposed to *P. aeruginosa* CuF than the controls (2.6 ±0.5 µg/ml compared to 1.58 ± 0.22 µg/ml) (Fig. 5.2).

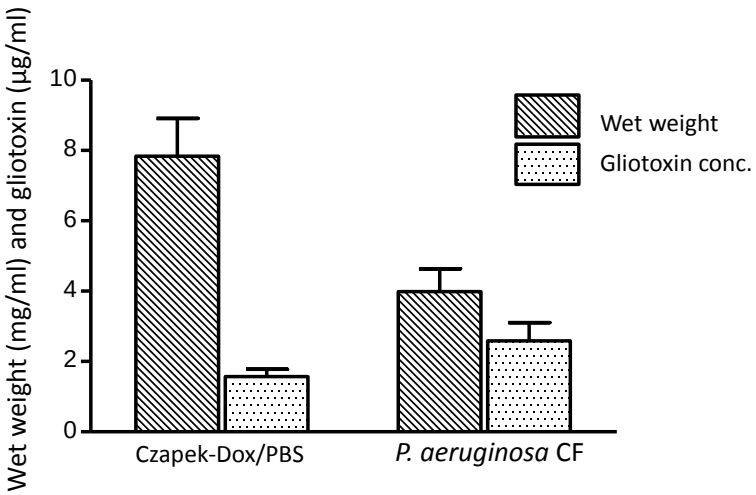

Fig. 5.2 The effect of *P. aeruginosa* CuF on *A. fumigatus* hyphal growth and gliotoxin production. In response to *P. aeruginosa* CuF *A. fumigatus* hyphal growth decreased and gliotoxin production increased in comparison to *A. fumigatus* cultured in Czapek-Dox.

To investigate the effect of *P. aeruginosa* on conidial growth and development, *P. aeruginosa* was cultured for 48 hours in Czapek-Dox and filter-sterilized to make *P. aeruginosa* CuF. The pH of this CuF was determined to be pH 8.0. The *P. aeruginosa* CuF was used as the growth medium for freshly harvested conidia. To investigate the effect of co-culture culture filtrates on fungal growth and development, *A. fumigatus* and *P. aeruginosa* were grown in Czapek-Dox for 24 hours after which the cultures were

combined and grown for a further 24 hours. The culture filtrates were filter-sterilized and the pH was determined (pH 4.2). This CuF was termed Co-culture CuF. To produce *A. fumigatus* CuF (control) *A. fumigatus* conidia were cultured in Czapek-Dox for 48 hours after which the hyphae were harvested. The culture filtrates sterilized by filtration and the pH was determined (pH 4.4). The wet weights of *A. fumigatus* hyphae that produced these culture filtrates was recorded (Fig. 5.3A). There was a 12-fold difference between the wet weight of the hyphae that produced the Co-culture CuF (0.46 ± 0.07 mg/ml) compared to that which produced the *A. fumigatus* CuF (5.6 ± 0.05 mg/ml). Conidia (5 $x10^5$/ml) were added to each of the culture filtrates (50 ml) and incubated for 24 hours. Conidia did not germinate in the flasks containing Co-culture CuF. Aliquots were removed from the Co-culture CuF and applied to MEA plates. Colonies formed after 24 hours and a total of 4.2 x 10^5 ± 0.24 x 10^5 CuFUs/ml were counted (data not shown).

This study was repeated, however the experimental designed was altered slightly to allow conidia to germinate prior to exposure to culture filtrates. Conidia were cultured in 25 ml Czapek-Dox for four hours until *A. fumigatus* germlings could be visualised. *A. fumigatus* CuF, *P. aeruginosa* CuF or and Co-culture CuF (50 ml) was added to flasks containing germinating conidia. The cultures were incubated for 24 hours. The wet weights of hyphae after exposure to the culture filtrates was measured (Fig. 5.3A). In contrast to the wet weight of hyphae obtained from the cultures having been co-cultured with *P. aeruginosa* (0.46 ± 0.07 mg/ml), *A. fumigatus* growth was greater after exposure to Co-culture CuF (7.3 ± 0.36 mg/m) and *P. aeruginosa* CuF (6.93 ± 0.25 mg/ml) compared to growth in *A. fumigatus* CuF (3.5 ± 0.21 mg/ml) (Fig. 5.3A). The workflow for this experimental design is outlined in Figure 5.4

Gliotoxin was extracted from the fungal cultures exposed to the different CuF and analysed by HPLC (Fig. 5.3B). The highest levels of gliotoxin were detected in the supernatants of the fungal cultures exposed to *A. fumigatus* CuF (2.1 ± 0.27 µg/mg hyphae). In the supernatants of fungal cultures exposed to Co-culture CuF and *P. aeruginosa* CuF, the levels of gliotoxin detected were 1.3 ± 0.26 µg/ml and 0.24 ±0.07 µg/ml respectively..

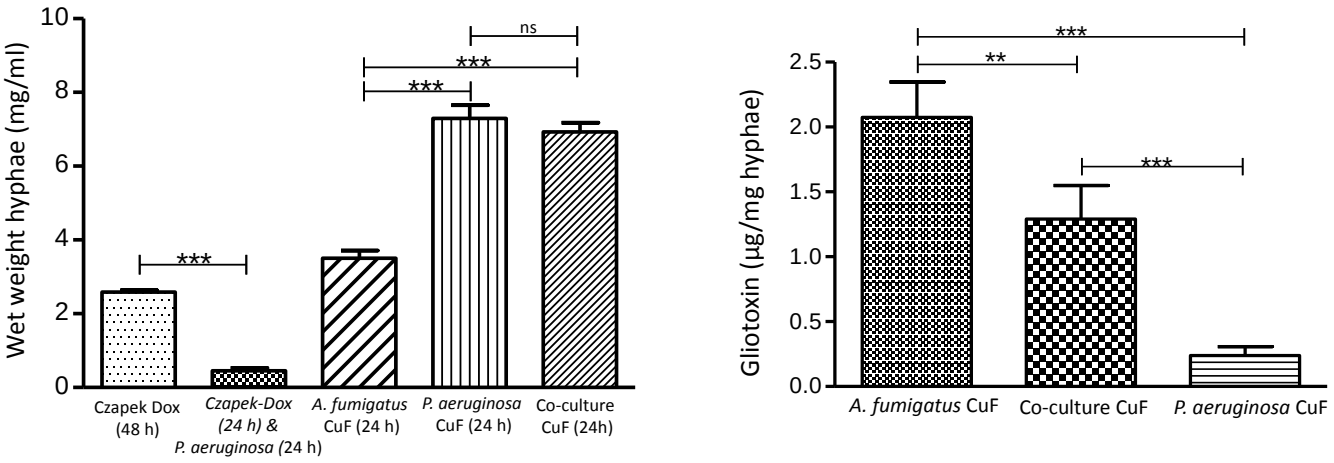

Fig. 5.3A The effect of *P. aeruginosa* and *P. aeruginosa* CuF on *A. fumigatus* growth. The wet weight of *A. fumigatus* cultured in Czapek-Dox for 48 hours was 12 times greater than the wet weight of *A. fumigatus* cultured in Czapek-Dox for 24 hours followed by co-culture with *P. aeruginosa* for 24 hours. The wet weight of *A. fumigatus* cultured for 24 hours in *A. fumigatus* CuF, *P. aeruginosa* CuF and Co-culture CuF was greater than that of *A. fumigatus* cultured in Czapek-Dox only, for 48 hours. **Fig. 5.3B The effect on gliotoxin production in *A. fumigatus* exposed to *A. fumigatus* CuF, Co-culture CuF and *P. aeruginosa* CuF.** The levels of gliotoxin production was greatest where *A. fumigatus* was cultured in *A. fumigatus* CuF and lowest when cultured in *P. aeruginosa* CuF.

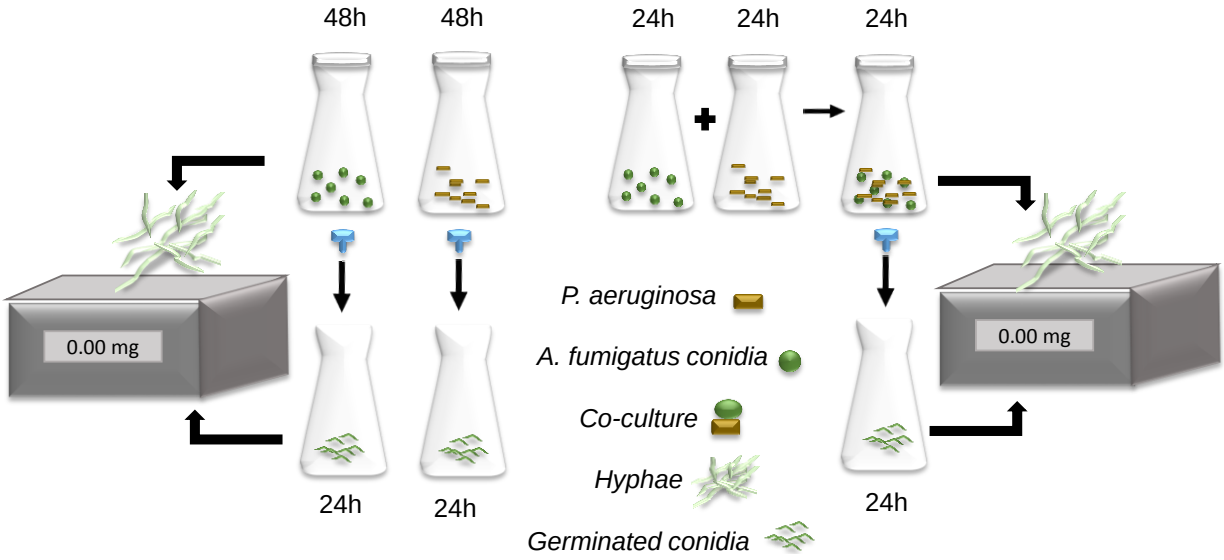

Fig. 5.4 Experimental design workflow. *A. fumigatus* conidia or *P. aeruginosa* were cultured in Czapek-Dox media 48 hours. The filtrates were filter-sterilized and the hyphae from the *A. fumigatus* culture were weighed. *A. fumigatus* and *P. aeruginosa* 24-hour cultures were co-incubated for 24 hours. The filtrates were filter-sterilized and the hyphae from the co-culture were weighed. Conidia were cultured for 4 hours until germination occured. The filter-sterilized cultured filtrates were added to the germinated conidia and incubated for 24 hours after which hyphae were weighed.

5.3.2 The proteomic response of *A. fumigatus* to *P. aeruginosa* culture filtrates

Changes to the proteome of *A. fumigatus* in response to *P. aeruginosa* were investigated by LFQ proteomics, which was performed on *A. fumigatus* exposed to *P. aeruginosa* CuF, Co-culture CuF and *A. fumigatus* CuF (control) (n = 3). In total, 3403 proteins were initially identified, of which 1291 remained after filtering and processing (Table A5.1A). Of the 1291, proteins identified post-imputation, 228 proteins in the Co-culture CuF-treated group (Table A5.1B) and 193 in the *P. aeruginosa* CuF-treated group (Table A5.1C) were determined to be statistically significant ($p<0.05$) differentially abundant (SSDA) with a fold change of +/- 1.5. A principal component analysis (PCA) was performed on all filtered proteins and identified distinct proteomic differences between the groups (Fig 5.5). Components 1 and 2 accounted for 62.2% of the total variance within the data, and all replicates resolved into their corresponding samples. The groups exposed to *A. fumigatus* CuF (control) displayed a clear divergence to those that

were challenged with *P. aeruginosa* CuF or Co-culture CuF. A distinct separation between the groups cultured in *P. aeruginosa* CuF and Co-culture CuF was also observed.

Volcano plots were produced by pairwise Student's t-tests ($p < 0.05$) to determine the differences in protein abundance between two samples and to depict the changes in pathways and processes in which those proteins are involved (Fig. 5.6A-C). SSDA protein names arising from the pair wise t-tests were inputted into the STRING and KEGG database and used to identify biological pathways and processes over-represented in a particular group.

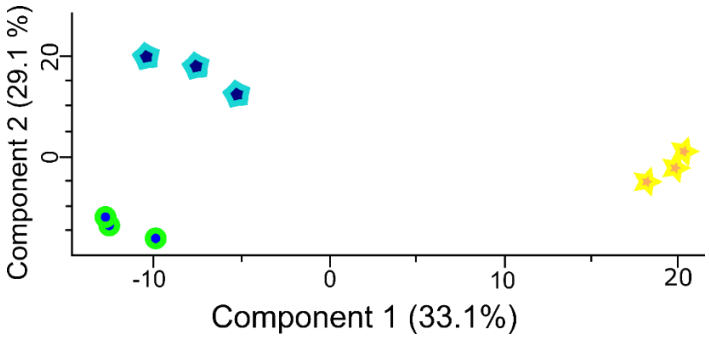

Fig. 5.5 PCA of *A. fumigatus* proteins groups Principal component analysis (PCA) of *A. fumigatus* exposed to *A. fumigatus* CuF (yellow stars) Co-culture CuFs (green circles) and *P. aeruginosa* CuF (blue hexagons). A clear distinction can be observed between each of the groups exposed to *P. aeruginosa* CuF and Co-culture CuF and the control (*A. fumigatus* CuF).

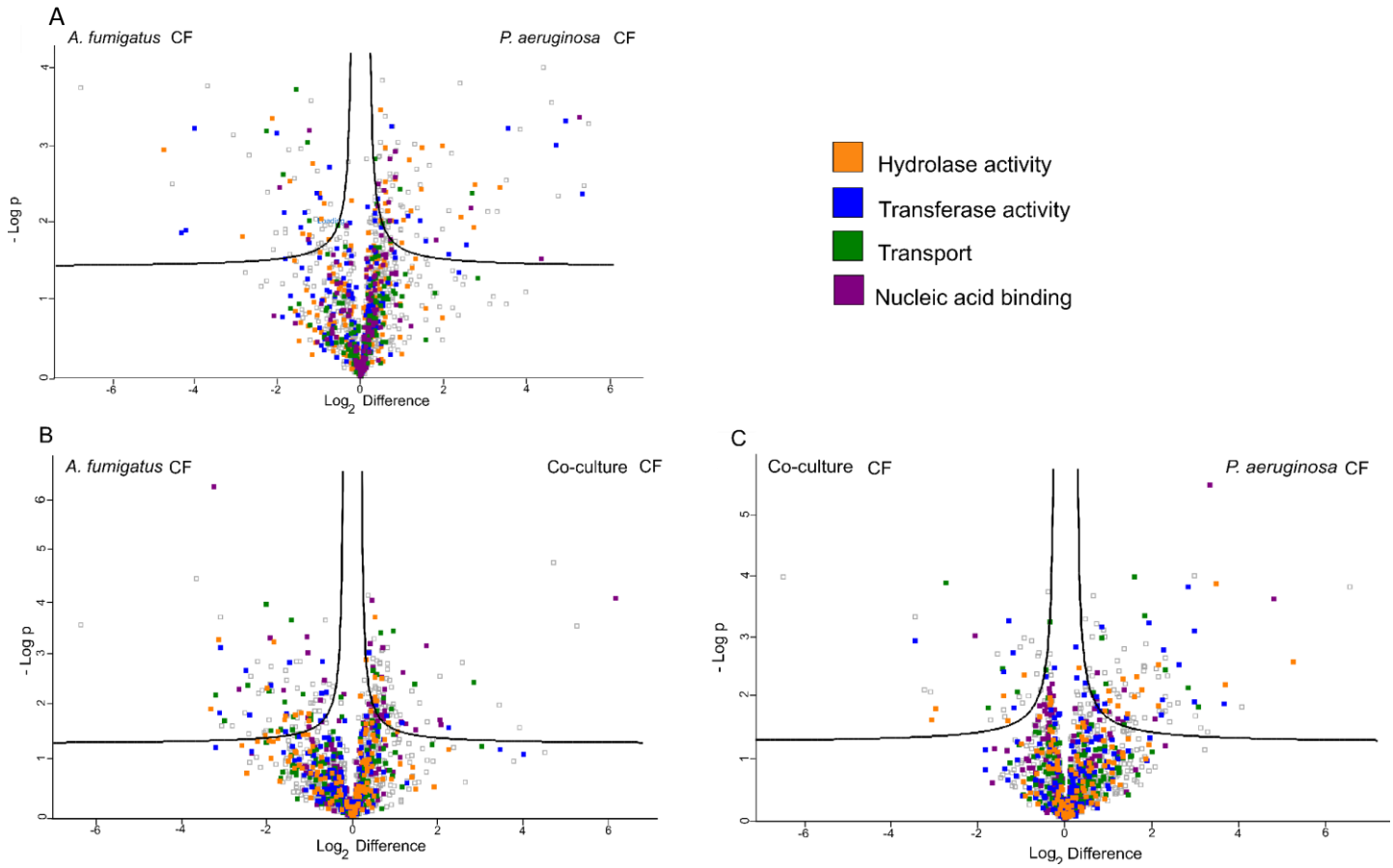

Fig 5.6 Differential abundance of proteins in the *A. fumigatus* proteome. Volcano plots derived from pairwise comparisons between *A. fumigatus* cultured in *P. aeruginosa* CuF and *A. fumigatus* CuF (A), Co-culture CuF and *A. fumigatus* CuF (B) and Co-culture CuF and *P. aeruginosa* CuF (C). The distribution of quantified proteins according to p value (−log10 p-value) and fold change (log_2 mean LFQ intensity difference) is shown. Proteins above the line are considered statistically significant (p-value <0.05). In general, protein components associated with hydrolase activity (orange) and transport (green) are more abundant in fungus cultured in *P. aeruginosa* CuF compared to *A. fumigatus* CuF and Co-culture CuF. The relative abundance of proteins associated with the transport activity (green) and transferase activity was decreased in *A. fumigatus* cultured in *P. aeruginosa* CuF and Co-culture CuF compared to *A. fumigatus* CuF.

The proteomic data arising from Student's t-tests ($p < 0.05$) identified several pathways that were most affected by fungal culture conditions. Although many of the proteins involved in such pathways were identified in both groups, significant differences in the relative abundance of these proteins were also identified, indicating distinct differences in the proteomic response of *A. fumigatus* depending on the CuF to which it was exposed. There was a significant increase in the relative abundance of proteins associated with secondary metabolite biosynthesis in *A. fumigatus* cultures exposed to *P. aeruginosa* CuF and to Co-culture CuF. The relative abundance of proteins involved in pseurotin A biosynthesis (Methyltransferase psoC and PKS-NRPS hybrid synthetase psoA), verruculogen and fumitremorgin biosynthesis (Verruculogen synthase) were increased significantly (Table 5.1; Fig. 5.10D). In contrast, the relative abundance of several proteins involved in gliotoxin biosynthesis were significantly decreased in fungal cultures exposed to *P. aeruginosa* CuF compared to *A. fumigatus* CuF and the Co-culture CuF. These included the protein products of gliF, gliG, gliN and gliT (Table 5.1).

Table 5.1 Proteins associated with secondary metabolite biosynthesis. SSDA (t-test, $p < 0.05$) proteins associated secondary metabolite biosynthesis, and relative fold differences between *A. fumigatus* cultured in Co-culture CuF and *A. fumigatus* CuF (Cc v Af), and between *P. aeruginosa* CuF and *A. fumigatus* CuF (Pa v Af).

Gene	Protein name	Fold change	
		Cc v Af	Pa v Af
AFUA_8G00550	Methyltransferase psoC	11.0	40.3
NRPS14	PKS-NRPS hybrid synthetase psoA	ns	30.6
ftmOx1	Verruculogen synthase	ns	27.3
ftmPT1	Tryprostatin B synthase	ns	5.9
AFUA_8G00440	Dual-functional monooxygenase/methyltransferase psoF	3.7	14.4
AFUA_6G09690	Glutathione S-transferase gliG	ns	-18.4
AFUA_6G09720	N-methyltransferase gliN	-9.2	-19.9
AFUA_6G09730	Cytochrome P450 monooxygenase gliF	ns	-23.3
AFUA_6G09740	Thioredoxin reductase gliT	ns	-106.6

While the majority of SSDA proteins associated with a stress-response and detoxification were increased in Co-culture CuF and *P. aeruginosa* CuF-exposed *A. fumigatus* there was a decrease in the relative abundance of several proteins involved in these pathways (Table 5.2). Changes in this pathway were most pronounced in the groups exposed to Co-culture CuF as evidenced by the frequency of changes occurring in the protein groups.

Table 5.3 lists the SSDA proteins associated with transcriptional regulation. In general, the relative abundance of proteins associated with transcriptional regulation was increased in groups exposed to Co-culture CuF and *P. aeruginosa* CuF (Table 5.3; Fig. 5.6A). Compared to *A. fumigatus* CuF, the most differentially abundant protein identified by Student's t-tests ($p < 0.05$) in *A. fumigatus* cultures exposed to Co-culture CuF or *P. aeruginosa* CuF was histone H3. Proteomic analysis detected no significant decrease of proteins associated with transcriptional regulation in fungal cultures exposed to *P. aeruginosa* CuF, however a decrease in the relative abundance of six proteins associated with this process were identified in *A. fumigatus* cultures exposed to Co-culture CuF (Table 5.3).

Student's t-tests identified 57 SSDA proteins associated with ribosomes and translation (Table A5.1B and 5.1C). Of these, the relative abundance of 13 proteins were increased and 16 proteins were decreased in *A. fumigatus* exposed to Co-culture CuF (Table A5.1B) and the relative abundance of 13 proteins was increased and 16 proteins were decreased in *A. fumigatus* exposed to *P. aeruginosa* CuF (Table A5.1C). The changes in protein abundance associated with these pathways are depicted in KEGG maps (Fig. 5.7A and B).

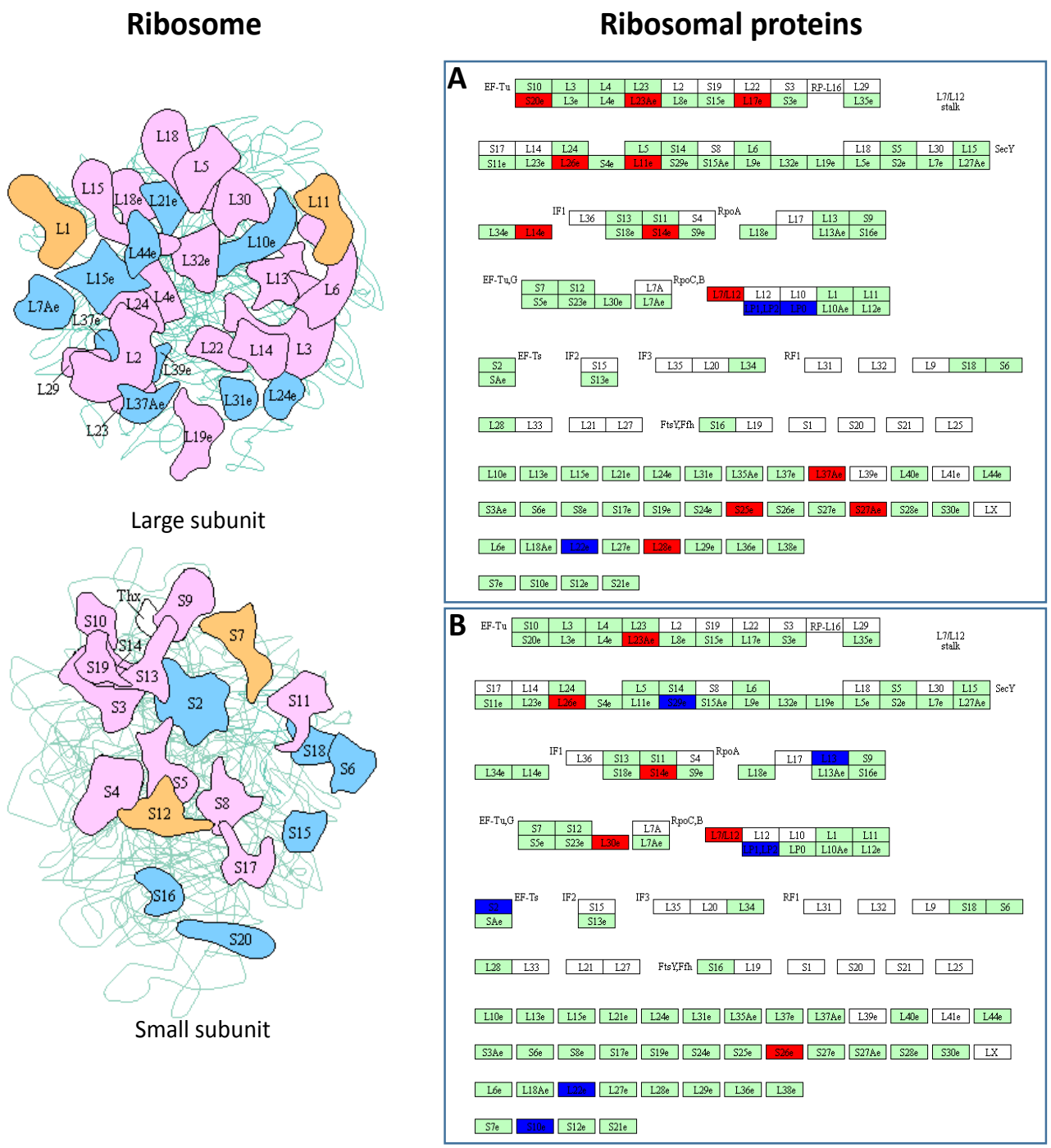

Fig. 5.7 KEGG pathway analysis depicting changes in ribosomes. The relative abundance of several SSDA proteins associated with the ribosome were increased (red) and decreased (blue) in *A. fumigatus* exposed to Co-culture CuF (A) and *P. aeruginosa* CuF (B).

Compared to the fungal cultures exposed to *A. fumigatus* CuF and Co-culture CuF, very few statistically significant changes in the relative abundance of proteins were identified in pathways associated with intracellular transport in *A. fumigatus* exposed to *P. aeruginosa* CuF (Table 5.4; Fig. 5.6). The relative abundance of several proteins involved in intracellular transport were decreased in *A. fumigatus* exposed to Co-culture CuF (Table 5.4).

The relative abundance of proteins associated with aerobic respiration was decreased while the relative abundance of proteins associated with anaerobic respiration such as nitrate reductase and nitrate/nitrite transporters were increased in *A. fumigatus* exposed to *P. aeruginosa* CuF and to a lesser extent Co-culture CuF (Table 5.5). A decrease in the relative abundance of several SSDA proteins associated with the oxidative phosphorylation (OXPHOS) pathway was observed in both groups. Proteins affected in this process are depicted in KEGG maps showing the oxidative phosphorylation pathway (Fig. 5.8). The groups exposed to *P. aeruginosa* CuF were more affected by the decreased levels of proteins involved in the OXPHOS pathway (Fig. 5.8B) than groups exposed to Co-culture CuF (Fig. 5.8A)

Table 5.2 Proteins associated with response to stress. SSDA (t-test, $p < 0.05$) proteins associated with a stress response and detoxification, and relative fold differences between *A. fumigatus* cultured in Co-culture CuF and *A. fumigatus* CuF (Cc v Af), and between *P. aeruginosa* CuF and *A. fumigatus* CuF (Pa v Af).

Gene	Protein	Fold change	
		CC v Af	Pa v Af
AFUA_5G03540	Thioredoxin reductase, putative	5.2	44.9
AFUA_5G09330	CipC-like antibiotic response protein, putative	38.1	11.4
AFUA_6G04920	Formate dehydrogenase	15.1	ns
AFUA_3G14540	Heat shock protein Hsp30/Hsp42	ns	8.4
AFUA_7G02070	AIF-like mitochondrial oxidoreductase	3.1	2.3
fes1	Hsp70 nucleotide exchange factor fes1	2.6	ns
AFUA_2G11750	Mitochondrial DnaJ chaperone (Mdj1), putative	2.1	ns
AFUA_5G04250	Homocysteine synthase CysD	2.2	2.7
AFUA_5G11430	Quinone oxidoreductase, putative	3.3	ns
mia40	Mitochondrial intermembrane space import and assembly protein 40	3.7	6.4
AFUA_3G12270	Glutathione peroxidase	ns	2.2
AFUA_6G13490	Glutamate decarboxylase	2	ns
katG	Catalase-peroxidase	2	2.5

AFUA_4G11250	Carbonic anhydrase	ns	2.6
AFUA_3G12560	Allantoicase Alc	ns	2.3
thiA	Thiamine thiazole synthase	ns	1.6
AFUA_4G03900	Peroxisomal multifunctional beta-oxidation protein	ns	1.6
AFUA_3G10190	Peroxisomal membrane anchor protein	ns	1.5
AFUA_2G04620	Hsp70 chaperone BiP/Kar2, putative	1.9	ns
AFUA_1G15050	Hsp70 family chaperone Lhs1/Orp150, putative	1.5	ns
AFUA_2G08750	Mitochondrial inner membrane nuclease Nuc1, putative	1.5	ns
AFUA_2G05500	NADH-ubiquinone oxidoreductase 18 kDa subunit	1.8	1.6
AFUA_7G01860	Heat shock protein (Sti1), putative	1.7	1.3
AFUA_1G12290	NADH-ubiquinone oxidoreductase	1.5	ns
AFUA_2G09850	Oxidoreductase, 2-nitropropane dioxygenase family, putative	1.5	ns
AFUA_7G00350	Pyr_redox_2 domain-containing protein	1.5	ns
AFUA_4G03650	Ribosome associated DnaJ chaperone Zuotin, putative	1.5	ns
AFUA_3G00730	GST N-terminal domain-containing protein	-4.3	ns
AFUA_2G03140	Peptide methionine sulfoxide reductase	-2.9	-3.0
AFUA_2G15180	Glutaredoxin domain-containing protein	-2.5	-3.0
AFUA_5G07780	Squalene monooxygenase Erg1	-2.5	ns
AFUA_6G14330	5-oxo-L-prolinase, putative	-2.3	-1.9
pim1	Lon protease homolog, mitochondrial	-2.1	ns
AFUA_1G11180	Heat shock protein/chaperonin HSP78, putative	-2.1	ns
AFUA_2G15180	Glutaredoxin domain-containing protein	-2.5	-3.0
AFUA_2G03140	Peptide methionine sulfoxide reductase	2.9	-3.0
AFUA_6G14330	5-oxo-L-prolinase, putative	2.3	-1.9
AFUA_3G01400	ABC multidrug transporter, putative	-3.4	-26.8

Table 5.3 Proteins assoictaed with transcription. SSDA (t-test, $p < 0.05$) proteins associated with transcriptional regulation, and relative fold differences between *A. fumigatus* cultured in Co-culture CuF and *A. fumigatus* CuF (Cc v Af), and between *P. aeruginosa* CuF and *A. fumigatus* CuF (Pa v Af).

Gene	Protein	Fold change	
		Cc v Af	Pa v Af
hhtA	Histone H3	72.4	39.0
htz1	Histone H2A.Z	4.2	ns
AFUA_6G02520	Eukaryotic translation initiation factor eIF-1A subunit	ns	6.4
cef1	Pre-mRNA-splicing factor cef1	ns	3.5
AFUA_1G10960	Mago nashi domain protein	ns	3.1
AFUA_2G11840	Transcriptional corepressor Cyc8, putative	ns	3
AFUA_1G14680	DNA-directed RNA polymerase subunit	2.8	3
AFUA_2G07410	Pre-mRNA splicing factor (Srp1)	2.3	1.5
AFUA_6G13330	RNA binding protein, putative	ns	2.5
AFUA_5G11390	APSES transcription factor, putative	2.0	1.8
AFUA_1G04550	HMG box protein, putative	1.5	1.8
AFUA_2G13720	DNA-directed RNA polymerase I and III subunit Rpc40, putative	2.2	2.2
AFUA_1G11190	Eukaryotic translation elongation factor 1 subunit Eef1-beta	ns	1.8
AFUA_6G10620	Nuclear pore complex subunit, putative	2.1	2.7
AFUA_5G07890	SsDNA binding protein, putative	1.7	ns
AFUA_5G13860	RNA annealing protein Yra1, putative	1.7	1.4
AFUA_2G05610	RNA binding protein Jsn1, putative	1.6	ns
AFUA_3G12290	Spliceosomal protein DIB1	4.0	2.0
AFUA_1G11190	Eukaryotic translation elongation factor 1 subunit Eef1-beta	ns	1.8
AFUA_5G02030	Cleavage and polyadenylation specific factor 5	ns	1.7
AFUA_7G05510	RSC complex subunit (RSC8	ns	1.5
rvb2	RuvB-like helicase 2	ns	1.5
AFUA_1G06190	Histone H4 arginine methyltransferase RmtA	-3.7	ns
AFUA_4G10540	Transcription regulator BDF1, putative	-2.5	ns
AFUA_1G09020	Nuclear pore complex protein (SonA), putative	-2.7	ns
AFUA_5G10770	Topisomerase II associated protein (Pat1), putative	-1.9	ns
rvb1	RuvB-like helicase 1	-1.9	ns
AFUA_7G01920	DNA-directed RNA polymerase subunit beta	-1.8	ns

Table 5.4 Proteins associated with transport. SSDA (t-test, $p < 0.05$) proteins involved with protein transport, and relative fold differences between *A. fumigatus* cultured in Co-culture CuF and *A. fumigatus* CuF (Cc v Af), and between *P. aeruginosa* CuF and *A. fumigatus* CuF (Pa v Af).

Gene	Protein name	Fold change	
		Cc v Af	Pa v Af
AFUA_2G12870	Vesicular-fusion protein sec17	8.1	ns
AFUA_2G15240	Small oligopeptide transporter, OPT family	7.2	ns
AFUA_2G03860	Plasma membrane low affinity zinc ion transporter, putative	1.9	ns
AFUA_1G04890	Translocon protein Sec61beta, putative	1.8	ns
AFUA_7G01510	SNARE domain protein	1.6	ns
AFUA_3G10740	RAB GTPase Vps21/Ypt51	1.8	1.6
AFUA_2G09830	ARF GTPase activator (Glo3)	ns	1.6
AFUA_7G01840	Membrane bound C2 domain protein (Vp115)	1.3	1.5
AFUA_1G15720	Importin beta-1 subunit	-8.0	ns
AFUA_1G04850	Dynein light chain	-5.4	ns
AFUA_1G08790	Exportin KapK	-4.0	ns
AFUA_1G09030	Coatomer subunit zeta, putative	-4.0	ns
AFUA_5G03260	Endosomal cargo receptor (Erp3), putative	-3.0	ns
AFUA_8G02840	Dynamin-like GTPase Dnm1, putative	-3.0	ns
AFUA_4G09520	SNARE protein Ykt6, putative	-2.6	ns
AFUA_1G13260	Coatomer subunit epsilon	-2.4	ns
AFUA_5G08130	Protein transport protein Sec61 alpha subunit, putative	-2.3	ns
AFUA_2G13760	Plasma membrane SNARE protein (Sec9)	-2.1	-3.5
AFUA_6G06900	Rho GTPase Rho1	ns	-2.0
AFUA_1G11730	ADP-ribosylation factor, putative	ns	-1.6

Table 5.5 Proteins associated with respiration. SSDA (t-test, $p < 0.05$) proteins associated with respiration, and relative fold differences between *A. fumigatus* cultured in Co-culture CuF and *A. fumigatus* CuF (Cc v Af), and between *P. aeruginosa* CuF and *A. fumigatus* CuF (Pa v Af).

Gene	Protein name	Fold change	
		Cc v Af	Pa v Af
AFUA_4G11390	Ubiquinol-cytochrome c reductase complex	-2.5	-6.9
AFUA_5G09680	Succinate dehydrogenase cytochrome b560 subunit	ns	-6.5
AFUA_7G02020	Uncharacterized protein	-2.8	-4.3
AFUA_6G12550	Mitochondrial carrier protein, putative	-2.2	-3.6
AFUA_5G03640	Mitochondrial export translocase Oxa1, putative	ns	-2.4
AFUA_3G06190	Cytochrome c oxidase subunit VIa, putative	ns	-1.8
AFUA_1G17470	Nitrate/nitrite transporter	ns	5.3
AFUA_1G12830	Nitrate reductase	1.8	1.6
AFUA_2G09130	NADH-ubiquinone dehydrogenase 24 kDa subunit	ns	1.5
AFUA_5G06540	NADH dehydrogenase [ubiquinone] 1 alpha subcomplex subunit	ns	1.5
AFUA_4G11250	Carbonic anhydrase	ns	2.6

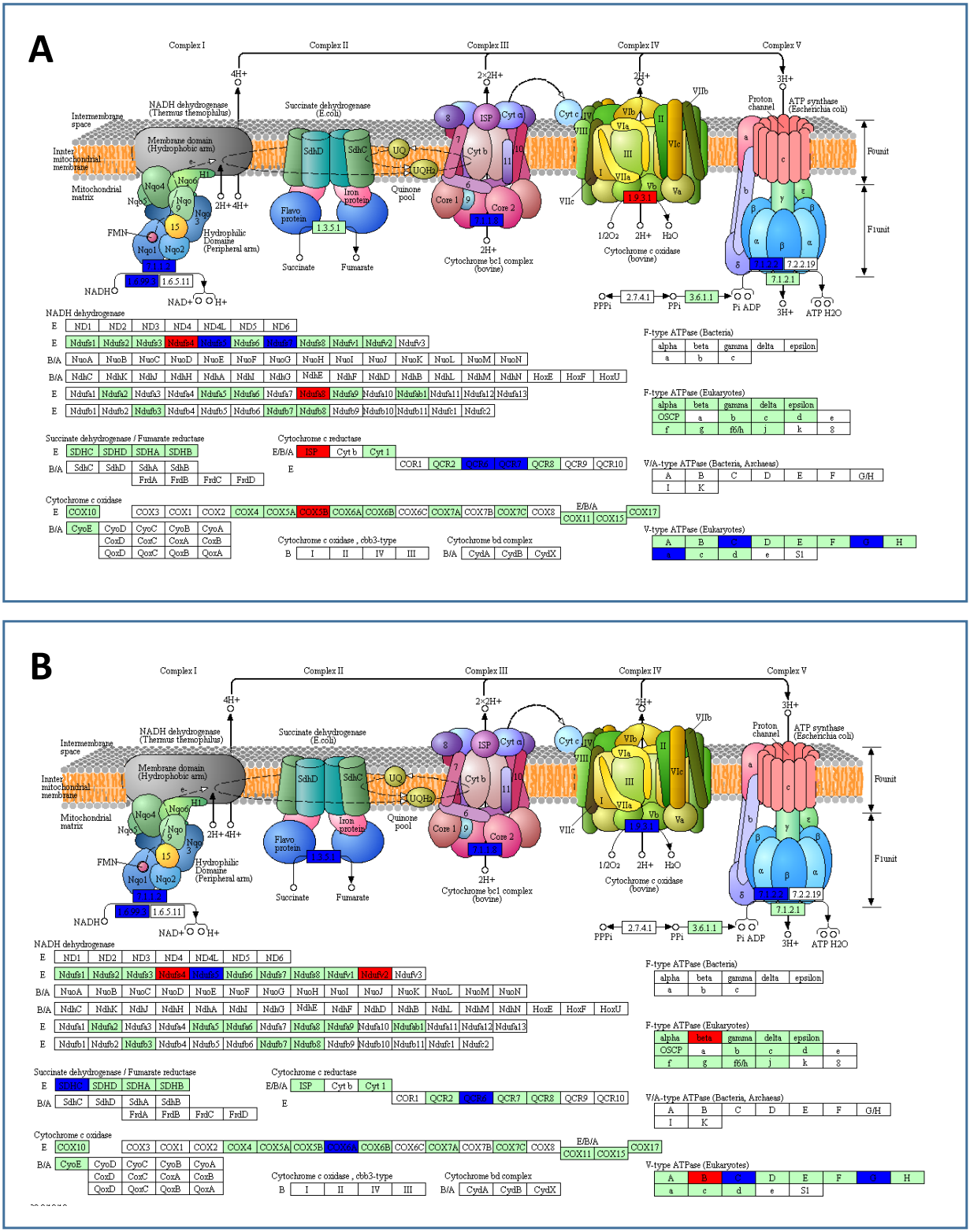

Fig. 5.8 KEGG map depicting changes in the OXPHOS pathways. The relative abundance of several SSDA proteins associated with the OXPHOS pathway were increased (red) and decreased (blue) in *A. fumigatus* exposed to Co-culture CuF (A) and *P. aeruginosa* CuF (B).

Although the relative abundance of proteins involved in cell wall biosynthesis was affected in *A. fumigatus* cultures that had been exposed to Co-culture CuF and *P. aeruginosa* CuF, there was a greater decrease in the relative abundance of proteins involved with the β-glucan biosynthetic pathway (e.g. 1,3-beta-glucan synthase catalytic subunit FksP and 1,3-beta-glucanosyltransferase Bgt1) in *A. fumigatus* exposed to Co-culture CuF (Table A5.1A and B). Similarly, a greater decrease in the relative abundance of proteins involved in proteasome-mediated degradation was observed in the group exposed to Co-culture CuF (Table A5.1A and B). These included proteins of the proteasome such as proteasome subunit beta, proteasome regulatory particle subunit (RpnI) and 26S proteasome regulatory subunit S5A.

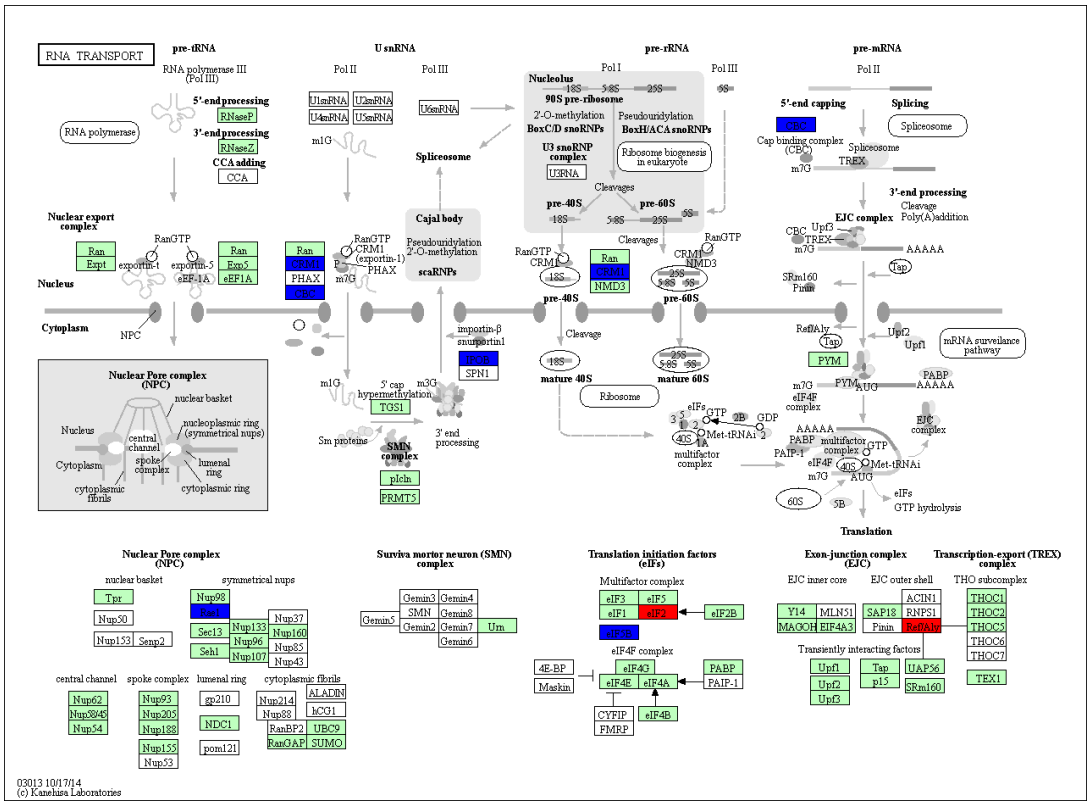

Fig. 5.9 KEGG maps depicting changes in RNA transport. The relative abundance of several SSDA proteins associated with RNA transport were decreased (blue) and few were increased (red) in *A. fumigatus* exposed to Co-culture CuF.

A *A. fumigatus* exposed to *A. fumigatus* CF

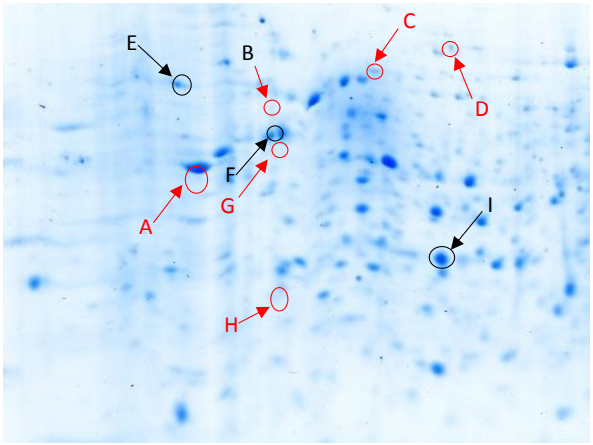

B *A. fumigatus* exposed to Co-culture CF

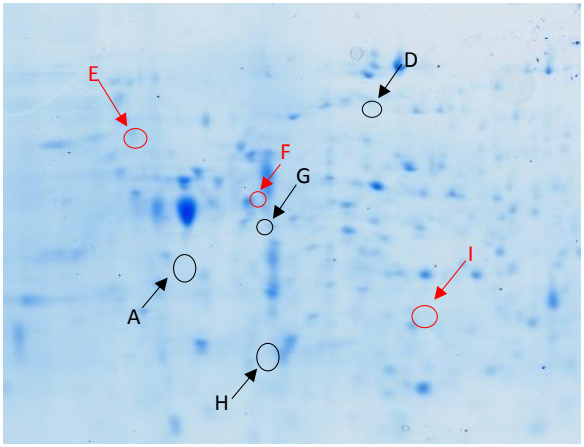

C *A. fumigatus* exposed to *P. aeruginosa* CF

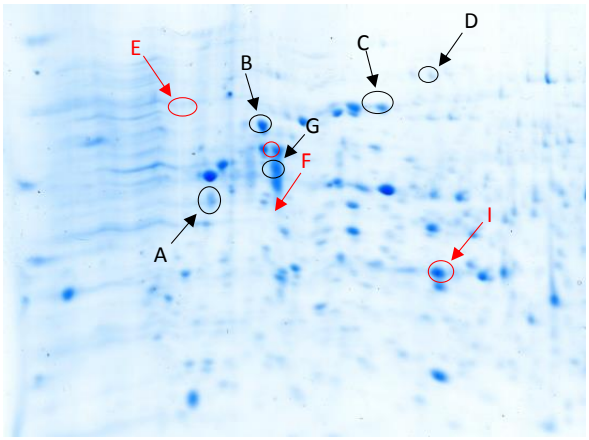

D Fold changes in proteins between different groups

ID	Protein name	Fold change Cc v Af	Fold change Pa v Af
A	ATP synthase subunit β	ns	+3.9
B	alpha-galactosidase	+1.6	+6.2
C	Heat shock protein Sti1	ns	+3.2
D	Catalase B	+5.7	ns
E	1,3-β-glucanosyltransferase gel4	-1.7	+2.7
F	Tubulin alpha chain	-4.2	-1.5
G	Major allergen Asp f2	+3.6	ns
H	Methyltransferase psoC	+4.7	ns
I	Thiamine biosynthesis protein (Nmt1)	-2.5	-1.2

Fig. 5.10 Proteins detected by 2D SDS PAGE. Proteins detected by 2D SDS PAGE in *A. fumigatus* exposed to *A. fumigatus* CuF (control) (A) were compared with proteins detected in *A. fumigatus* exposed to Co-culture CuF (B) and *P. aeruginosa* CuF (C). SSDA Protein names and fold changes ($p < 0.05$) are listed in (D.) Red and black arrows indicate a decrease and increase in the relative abundance of proteins compared to the control

5.4 Discussion

Interaction studies performed between *A. fumigatus* and *P. aeruginosa* have consistently shown that *P. aeruginosa* and its secondary metabolites inhibit *A. fumigatus* growth *in vitro* and *in vivo* (Yonezawa *et al.*, 2000; Briard *et al.*, 2015; Briard *et al.*, 2017; Briard *et al.*, 2019). While the effect of *P. aeruginosa* on *A. fumigatus* biofilm-formation and its ability to inhibit fungal growth and development is well established, the proteomic response of *A. fumigatus* to *P. aeruginosa* remains largely uncharacterized. The findings presented in this chapter contribute to the current knowledge surrounding these interactions.

P. aeruginosa exposure to 48-hour cultures of *A. fumigatus* grown in Czapek-Dox resulted in reduced fungal growth. This growth decrease was dependent on the concentration of bacteria to which *A. fumigatus* was exposed, as lower hyphal wet weights correlated with higher inocula of *P. aeruginosa* (Fig. 5.1A). In contrast, RP-HPLC detected increased levels of gliotoxin in fungal cultures exposed to higher bacterial inocula (Fig. 5.1B). Similar observations were made when 24-hour *A. fumigatus* cultures were exposed to the culture filtrates produced by *P. aeruginosa* in Czapek-Dox (Fig. 5.2).

The growth inhibiting effect of *P. aeruginosa* on *A. fumigatus* has been reported previously (Briard *et al.*, 2015; Sass *et al.*, 2018; Sass *et al.*, 2019). Rhamnolipids are a family of glycolipids produced by *P. aeruginosa* and other *Pseudomonas* species (Abalos *et al.*, 2001). Dirhamnolipids produced by *P. aeruginosa* inhibit β 1, 3-glucan synthase thereby interfering with fungal cell-wall architecture (Briard *et al.*, 2017). Other mediators of growth inhibition include pyoverdin, a bacterial siderophore that sequesters iron from the environment and the fungus and pyocyanin which disrupts the redox balance in the environment (Briard *et al.*, 2015; Sass *et al.*, 2018).

However, the effect of *P. aeruginosa* on secondary metabolite production is less well explored. The observations made during this study indicate that *P. aeruginosa* creates an environment that forces *A. fumigatus* to increase gliotoxin production. Because gliotoxin is responsible for maintaining redox homeostasis in the fungus, an increase in gliotoxin production may be indicative of bacterial-mediated induction of ROS, which is known to compromise fungal growth and survival (Briard *et al.*, 2015). Gliotoxin is a signature virulence factor of *A. fumigatus* with immunosuppressive effects on host cells

(Stanzani *et al.*, 2005; Orciuolo *et al.*, 2007; Schlam *et al.*, 2016) thus, in the context of co-infection, the propensity of *P. aeruginosa* to promote gliotoxin production in *A. fumigatus*, may have serious implications for host health.

To understand the biological pathways and processes adopted by *A. fumigatus* in response to *P. aeruginosa*, a proteomic approach was employed. *A. fumigatus* conidia were cultured in the culture filtrates produced by a) *A. fumigatus* (*A. fumigatus* CuF), b) *P. aeruginosa* (*P. aeruginosa* CuF) and c) a co-culture of *A. fumigatus* and *P. aeruginosa* (Co-culture CuF). Preliminary results showed that conidia were unable to germinate in Co-culture CuF. Conidia were not killed in this culture filtrate as when spread on agar plates, growth resumed, thus suggesting that the environment created in the co-culture was not conducive to germination.

While the inability of *A. fumigatus* to germinate in the presence of *P. aeruginosa* may have implications for its potential to become invasive, these results also highlight the capacity of conidia to withstand stress conditions imposed by *P. aeruginosa*. In the cystic fibrosis lung, *A. fumigatus* rarely becomes invasive (Massam *et al.*, 2011), although *A. fumigatus* is often cultured from the sputum samples of cystic fibrosis patients (Burgel *et al.*, 2016) suggesting that although hyphae may not form, viable spores do exist.

In order for a proteomic analysis on the effect of *P. aeruginosa* on developing hyphae to be performed, conidia were incubated for four hours in Czapek-Dox. Under optimal conditions, conidia should begin to germinate after approximately two hours (Hagiwara *et al.*, 2016). Differential gene expression is paramount for the transition from resting conidia to germinating conidia. The expression of genes associated with resting conidia include those encoding the *A. fumigatus* allergens Asp f3, Asp f13, Asp f22, Asp f27 and CatA, encoding catalase, which is responsible for enabling conidia to withstand ROS-induced stress. By contrast, the expression of the allergens Asp f1, Asp f4 and Asp f7 are associated with germinating conidia and hyphae but silent in resting conidia (Hagiwara *et al.*, 2016). Exposure to immune cells such as neutrophils also result in differential gene expression between conidia and hyphae (Sugui *et al.*, 2008). The environment in which conidia are exposed influences the programme of gene expression in developing *A. fumigatus* conidia. The changes in gene expression lead to changes in the proteomic profile which is the ultimate determinant of a phenotype and dictates the

response of the fungus to a particular environment (Vödisch *et al.*, 2011; Barker *et al.*, 2012; Briard *et al.*, 2015; Schmidt *et al.*, 2018; Raffa and Keller, 2019).

In this chapter, LFQ proteomics was employed to characterize the changes in the *A. fumigatus* proteome when exposed to the culture filtrate of i) *P. aeruginosa* alone ii) the culture filtrate of an *A. fumigatus*-*P. aeruginosa* co-culture and iii) the culture filtrate of *A. fumigatus* alone. One of the most remarkable findings in the proteomic dataset, was a significant decrease in the relative abundance of four proteins associated with the gliotoxin biosynthetic gene-cluster in *A. fumigatus* that had been exposed to *P. aeruginosa* CuF compared to *A. fumigatus* CuF or Co-culture CuF. These proteins were Glutathione S-transferase gliG (-18.4-fold), N-methyltransferase gliN (-19.9-fold), Cytochrome P450 monooxygenase gliF (-23.3-fold) and Thioredoxin reductase gliT (-106.6-fold). The only significant change in the relative abundance of proteins in this group detected in *A. fumigatus* exposed to the Co-culture CuF compared to *A. fumigatus* CuF was observed in GliN (-9.2-fold).

To investigate whether the decrease in proteins involved in gliotoxin biosynthesis resulted in decreased gliotoxin titre, gliotoxin levels in the culture filtrates from the three groups were determined by RP-HPLC. The highest level of gliotoxin was detected in the culture filtrates from *A. fumigatus* exposed to *A. fumigatus* CuF, followed by Co-culture CuF and the lowest level of gliotoxin was detected in the fungus exposed to *P. aeruginosa* CuF (Fig. 5.3B). The wet weight of *A. fumigatus* was not affected by exposure to the Co-culture CuF or the *P. aeruginosa* CuF. On the contrary and in contrast to earlier observations, an increase in growth was observed in both of these groups when compared to that, which occurred in the *A. fumigatus* CuF (Fig. 5.3A).

The wet weight of hyphae taken from the 24- hour culture that was incubated with *P. aeruginosa* and which produced the Co-culture CuF, was significantly lower than that of the fungus cultured alone in Czapek-Dox for 48 hours (Fig. 5.3A). The substantial decrease in growth observed here compared to previous experiments (Fig. 5.1) where growth was decreased less drastically, may be accounted for by the volume of bacterial suspension co-cultured with *A. fumigatus* (i.e. 1:1 ratio compared to 1 ml *P. aeruginosa* suspension in 50 ml *A. fumigatus* suspension). Furthermore, previous experiments (Fig. 5.1) used 48-hour cultures of *A. fumigatus* whereas on this occasion, *A. fumigatus* was

only grown for 24 hours prior to the addition of bacteria, thus the fungal density was lower at the time of co-culture.

Taken together, these findings suggest that 1) germination is delayed in *A. fumigatus* conidia when exposed to an environment previously occupied by *P. aeruginosa* and *A. fumigatus* in co-culture, 2) *A. fumigatus* growth is inhibited by direct interactions with *P. aeruginosa* (Fig. 5.2), 3) *P. aeruginosa* CuF has an influence gliotoxin production in *A. fumigatus* and 4) under the conditions investigated here, gliotoxin production is correlated with low wet weight of fungal hypha (Fig. 5.1 – 5.3). In essence, the effect of *P. aeruginosa* on *A. fumigatus* development and gliotoxin production is dependent upon the stage of fungal growth.

Comparisons of the *A. fumigatus* proteome in response to exposure of *P. aeruginosa* CuF and *A. fumigatus* CuF and to exposure of Co-culture CuF and *A. fumigatus* CuF revealed differential proteomic response largely mediated by changes in transcriptional regulation (Fig. 5.6, Table 5.3), ribosomal activity (Fig. 5.6), protein transport (Table 5.4), secondary metabolite production (Table 5.1) and detoxification (Table 5.2).

An increase in the relative abundance of proteins associated with the biosynthesis of *A. fumigatus* secondary metabolites pseurotin A, verruculogen, fumitremorgin b and tryprostatin B was detected in fungal cultures exposed to *P. aeruginosa* CuF (Table 5.1). The relative abundance of proteins associated with the biosynthesis of pseurotin A was increased to a lesser extent in fungal cultures exposed to Co-culture CuF, but no significant changes in the abundance of proteins associated with other secondary metabolites were detected in this group (Table 5.1). In comparison to gliotoxin, little is known about the effect of these mycotoxins on host cells. Pseurotin A is a competitive inhibitor of chitin synthase and has been reported to have cytotoxic activity against anti-cancer activities, thereby highlighting its potentially cytotoxic effect on host cells (Wenke *et al.*, 1993; Martínez-Luis *et al.*, 2012; Bladt *et al.*, 2013). Verruculogen and fumitremorgin b are known to affect the central nervous system *in vivo* and *in vitro*, verruculogen alters the electrophysiological properties of human nasal epithelial cells suggesting this metabolite may participate in fungal colonization of the airways (Tepšič *et al.*, 1997; Khoufache *et al.*, 2007). An increase in the relative abundance of proteins associated with the biosynthesis of these metabolites in *A. fumigatus* coupled with a

decrease in the relative abundance of gliotoxin biosynthetic proteins indicate that *P. aeruginosa* creates an environment that causes *A. fumigatus* to alter secondary metabolite production to adapt to the conditions created by the bacteria. This may be in part, driven by the changes in the pH of the culture filtrates produced by *P.aeruginosa* where the pH of this medium was almost twice that found in the *A. fumigatus* CuF and the Co-culture CuF. The pH of an environment is known to be a contributing factor to mycotoxin production in *Aspergillus* species including *A. fumigatus* (Calvo *et al.*, 2002; Bertuzzi *et al.*, 2014).

Upregulation of pseurotin A has been reported in *A. fumigatus* cultured under hypoxic conditions (Vödisch *et al.*, 2011). In this study an increase in the abundance of several protein groups were observed, including nitrate/nitrite transporter and nitrate reductase (Table 5.5), suggesting hypoxic conditions in the environment where *A. fumigatus* was exposed to *P. aeruginosa* CuF. Moreover, the relative abundance of several proteins associated with aerobic respiration was decreased, particularly in the fungus exposed to *P. aeruginosa* CuF.

The increases and decreases in the relative abundance of proteins associated with detoxification, DNA damage repair and oxidative stress response in *A. fumigatus* exposed to Co-culture CuF and *P. aeruginosa* CuF compared to *A. fumigatus* CuF highlights the ability of *A. fumigatus* to differentially regulate protein synthesis in response to environmental stresses imposed by competitors.

Interestingly, and perhaps reflective of fungal growth increase in the culture filtrates produced by *P. aeruginosa*, the relative abundance of many of the proteins involved in an oxidative stress response did not change drastically (Table 5.2). One exception was an increase in the relative abundance of thioredoxin reductase (TrxR). The levels of this protein increased by 44.9-fold in *A. fumigatus* exposed to *P. aeruginosa* CuF compared to *A. fumigatus* CuF. Thioredoxin reductase is a member of the thioredoxin system in *A. fumigatus* and along with thioredoxin, it is essential for fungal viability and is involved in a number of responses including neutralizing ROS, regulation of several transcription factors and mediating disulphide bond insertion into proteins as they entering the ER (Marshall *et al.*, 2019).

It is interesting to note the substantial increase in this TrxR (Table 5.2) and the contrasting decrease in GliT, another TrxR (Table 5.1). A clear disparity in the relative

abundance of numerous stress-response proteins was identified between *A. fumigatus* exposed to Co-culture CuF, *P. aeruginosa* CuF and *A. fumigatus* CuF (Table 5.2). For example, a 2.9-fold increase in methionine sulfoxide reductase was detected in fungal cultures exposed Co-culture CuF whereas the relative abundance of the same protein had decreased three-fold in *A. fumigatus* exposed to *P. aeruginosa* CuF (Table 5.2). Similar occurrences were observed in various heat shock proteins between the different groups. Changes in the abundance of proteins associated with a variety of stress responses, highlights the capacity of *A. fumigatus* to adapt proficiently in response to different environmental conditions, a property of the fungus that has been studied in detail under a combination of various environmental stresses (Albrecht *et al.*, 2010; Kurucz *et al.*, 2018).

The ability of *A. fumigatus* to adapt rapidly to changing environments is regulated by a tight programme of transcriptional regulation at the histone level. Modifications to histones have been extensively studied and have major implications in fungal growth and development (Brosch *et al.*, 2008; Palmer *et al.*, 2008). Heterochromatin and transcriptional activation states are influenced by methylation of various lysine residues on histone 3. Data analysis in this study identified histone 3 as the most differentially abundant protein associated with transcriptional regulation in *A. fumigatus* cultures exposed to Co-culture CuF and *P. aeruginosa* CuF (Table 5.3). The high levels of this protein in both groups potentially indicate significant alterations in transcriptional activity.

A characteristic of the proteomic profile of *A. fumigatus* exposed to Co-culture CuF was a general decrease in the relative abundance of proteins associated with transport and the proteasome (Table 5.4; Table A5.1B). This was reflected in the downregulation of RNA transport as depicted by KEGG (Fig. 5.9). There were fewer significant changes to proteins associated with this pathway in *A. fumigatus* exposed to *P. aeruginosa* CuF. The differential responses in protein transport between the groups of *A. fumigatus* exposed to *A. fumigatus* CuF, Co-culture CuF and *P. aeruginosa* CuF suggest the potential requirement to conserve energy or specific proteomic requirements in various parts of the cell depending on the environmental conditions.

In the CF airways, *A. fumigatus* rarely becomes invasive as germinating spores are targeted by cells of the immune system (Dagenais and Keller, 2009; Burgel *et al.*,

2016). However, conidia that germinate release antigens, proteases and other factors that induce an inflammatory response (Dagenais and Keller, 2009). Because *P. aeruginosa* is prevelant in the CF airways, it is important to understand the role of these bacteria in influencing fungal growth and development. In this study, *A. fumigatus* hyphae were allowed to develop for 24 hours prior to proteomic analysis in response to *P. aeruginosa* CuF. Onward studies should assess the impact of the *P. aeruginosa* secretome on conidial germination and the proteomic response of germinating conidia exposed to *P. aeruginosa* CuF. These studies would close the knowledge gap that exists in relation to the inetractions that occur between these pathogens and perhaps form the basis for the development of novel therapeutic targets to prevent microbial colonization of the immuncompromized airways.

5.5 Conclusion

A. fumigatus has a remarkable capacity to adapt to a range of environmental conditions in order to survive. In the cystic fibrosis airways, *A. fumigatus* rarely becomes invasive, yet the fungus is frequently cultured from the sputum of patients. The data presented in this study show that under certain environmental conditions, *A. fumigatus* conidia do not germinate but do remain viable – undoubtedly, a key feature of an opportunistic pathogen. However, once established and conidia germinate, even *P. aeruginosa* does not fully succeed in inhibiting fungal growth. The proteomic profile generated by *A. fumigatus* in response to the secretome of *P. aeruginosa* is characterized by a series of increases and decreases in the relative abundance of proteins involved in enabling the pathogen to survive under potentially challenging conditions.

Chapter Six

Characterization of a novel *Aspergillus fumigatus* compound that displays anti-bacterial activity

6.1 Introduction

Filamentous fungi are an exceptionally rich source of bioactive products, many of which are secondary metabolites, many of which have been exploited for industrial and medicinal purposes in the past century (Hoffmeister and Keller, 2007; Alberti *et al.*, 2017). Most notably, β-lactam antibiotics (penicillin and cephalosporin C) produced by *Penicillium* species have revolutionized modern medicine. Ironically, a number of filamentous fungi that cause disease are also the source of compounds that are beneficial to human health. For example, *Aspergillus terreus*, the third most common causative agent of invasive aspergillosis, and a source of food-spoiling mycotoxins, is also a producer of several pharmacologically important secondary metabolites including lovastatin (Kück *et al.*, 2014; Hachem *et al.*, 2014). Lovastatin is a polyketide derivative, also produced by *Penicillium* species, which, due to its cholesterol-lowering properties is used to treat cardiovascular disease (Seenivasan *et al.*, 2008).

Secondary metabolites originate from the products of primary metabolism. Amino acids form the building blocks for the synthesis of non-ribosomal peptide (NRP) secondary metabolites (e.g. gliotoxin, penicillin and cyclosporine), while acyl-CoAs are required for the synthesis of polyketides (e.g. lovastatin) and terpenes (e.g. terrecyclic acid) (Bladt *et al.*, 2013; Keller, 2019). The genes encoding enzymes that regulate the biosynthesis of secondary metabolites (i.e. polyketide synthases, non-ribosomal peptide synthetases, terpene synthases and terpene cyclases) are arranged in biosynthetic gene clusters (Keller, 2019;Romsdahl and Wang, 2019)

Traditionally, novel compounds with therapeutic potential have been discovered by screening individual species (Kück *et al.*, 2014). A classic example is the discovery of the immunosuppressive agent, cyclosporin A, which was discovered in a soil sample in the 1970s (Ruegger *et al.*, 1976). In light of the advances made in the area of bioinformatics there is recognition that the arsenal of secondary metabolites produced by filamentous fungi may be far greater than once perceived (Bladt *et al.*, 2013; Keller, 2019; Romsdahl and Wang, 2019). Many of the genes associated with secondary metabolite production are silent or difficult to activate under laboratory conditions (Romsdahl and Wang, 2019). However, the wealth of undiscovered bioactive molecules with potentially important medicinal properties has driven the effort to activate these silent gene clusters.

Transcriptional activation of biosynthetic gene clusters is regulated by environmental cues and is dependent on the stage of fungal development. Secondary metabolite production is crucial for fungal survival and governs its interactions (synergistic or antagonistic) with other microorganisms (Calvo *et al.*, 2002; Keller, 2019). For example, gliotoxin is essential for maintaining redox homeostasis and its secretion is induced in response to bacterial PAMPs and ROS (Gallagher *et al.*, 2012; Svahn *et al.*, 2014; Dolan *et al.*, 2015).

A. fumigatus share a similar niche with *P. aeruginosa*, both environmentally and in the cystic fibrosis airways (Briard *et al.*, 2016). The close proximity in which these pathogens exist indicate that competitive interactions exist between the two organisms. Numerous studies have identified anti-fungal secondary metabolites produced by *P. aeruginosa*, however, with the exception of gliotoxin, the anti-bacterial compounds produced by *A. fumigatus* have been less well characterized (Briard *et al.*, 2015; Briard *et al.*, 2017; Reece *et al.*, 2018; Sass *et al.*, 2018).

The ubiquitous nature of *Aspergillus* species in the environment points towards a versatile microbe that possesses a range of survival mechanisms to ensure dominance (Bignell *et al.*, 2016; Raffa and Keller, 2019). Secondary metabolite production occurs in monocultures as a mechanism of inhibiting the growth of other species, however co-cultivation of *Aspergillus* species with other filamentous fungal species induces increased secondary metabolite production (Losada *et al.*, 2009). Moreover, a shift in temperature from 30°C to 37°C favours metabolite production of some species over others. For example, *A. flavus* outcompetes *A. fumigatus* and *A. terreus* at 30°C but the roles are reversed at 37°C. The culture medium was also a factor in these studies as *A. oryzae* could outcompete *A. flavus*, typically a stronger competitor, in nutrient rich conditions (Losada *et al.*, 2009).

The "One strain-Many compounds (OSMAC) approach" was described by Zeek and colleagues (2002) as a method for investigating the production of novel secondary metabolites by varying the fermentation conditions of the organism in question (Bode *et al.*, 2002). By manipulating the growth medium, level of aeration and rate of shaking the culture flasks, the number of secondary metabolites that could be isolated from a fungal cultures substantially altered (Bode *et al.*, 2002; Scherlach and Hertweck, 2006; Bills *et al.*, 2008).

Aspergillus is a reservoir for bioactive metabolites with a range of potentially therapeutic activities (Furtado *et al.*, 2002; Losada *et al.*, 2009; Raffa and Keller, 2019). With the rapidly evolving emergence of antimicrobial resistant fungal and bacterial pathogens, the need to discover novel antibiotics is becoming more urgent. This urgency has prompted the revival of cell-based screening platforms, more commonly known as Waksman platform whereby microbes are screened for their ability to produce antimicrobial compounds (Ribeiro da Cunha *et al.*, 2019). This screening method formed the basis for the results presented in the chapter.

A. fumigatus culture filtrates were analysed for their effect on the growth of *P. aeruginosa* and a range of other bacterial pathogens. This screening method lead to the identification of a novel compound, which is believed to have anti-bacterial properties. Characterization of the compound was performed by SPE column separation, HPLC, TLC, NMR and MS/MS. LFQ proteomics was performed on *P. aeruginosa* exposed to a sub-lethal dose of the compound to investigate its effect on the bacterial proteome.

6.2 Results

6.2.1 Analysing the effect of *A. fumigatus* culture filtrates on *P. aeruginosa* growth

To investigate the effect of the *A. fumigatus* secretome on *P. aeruginosa* growth, *A. fumigatus* was cultured in; Czapek-Dox, Dulbecco's Modified Eagle Medium (DMEM) or Sabouraud Liquid Medium (SAB) for 24, 48, 72 and 96 hours. The culture filtrates (CuF) were filter sterilized and exposed to *P. aeruginosa* (100 µl CuF to 100 µl bacterial suspension, OD 0.1). Bacterial growth was measured (OD_{600}) after 24 hours. The results demonstrated differential effects on bacterial growth depending on the composition of the growth medium and the stage of fungal growth (Fig. 6.1).

Where *P. aeruginosa* was cultured in Czapek-Dox, there was an increase in growth in bacteria exposed to 24, 48 and 72-hour CuF compared to bacteria exposed to sterile Czapek-Dox, and a 12.6-fold decrease in the growth of bacteria exposed to 96-hour CuF (Fig. 6.1A). A 0.4-fold decrease in *P. aeruginosa* growth was observed in bacteria exposed to fungal CuF produced in DMEM for 48 and 72 hours compared to sterile DMEM (Fig. 6.1B). The greatest effect on bacterial growth was observed in bacteria exposed to CuF produced in SAB for 48, 72 and 96 hours. There was a 16.8 fold decrease in growth where bacteria was exposed to these *A. fumigatus* CuF produced in SAB by 72 hours (6.1C). Because the anti-bacterial effect was most pronounced in the culture filtrates produced in SAB by 72 hours, this was chosen for further analysis and characterization and is referred to herein as "72 hr SAB".

To determine whether the antimicrobial activity was an *A. fumigatus*-specific compound or if other *Aspergillus* species could produce the same antibacterial effect under these conditions, the CuF from *A. flavus* and *A. nidulans* grown in SAB for 72 hours were exposed to *P. aeruginosa* (Fig. 6.1D). The results indicate that although the other *Aspergillus* species do have anti-bacterial activity against *P. aeruginosa*, the greatest effect was observed in the CuF produced by *A. fumigatus*.

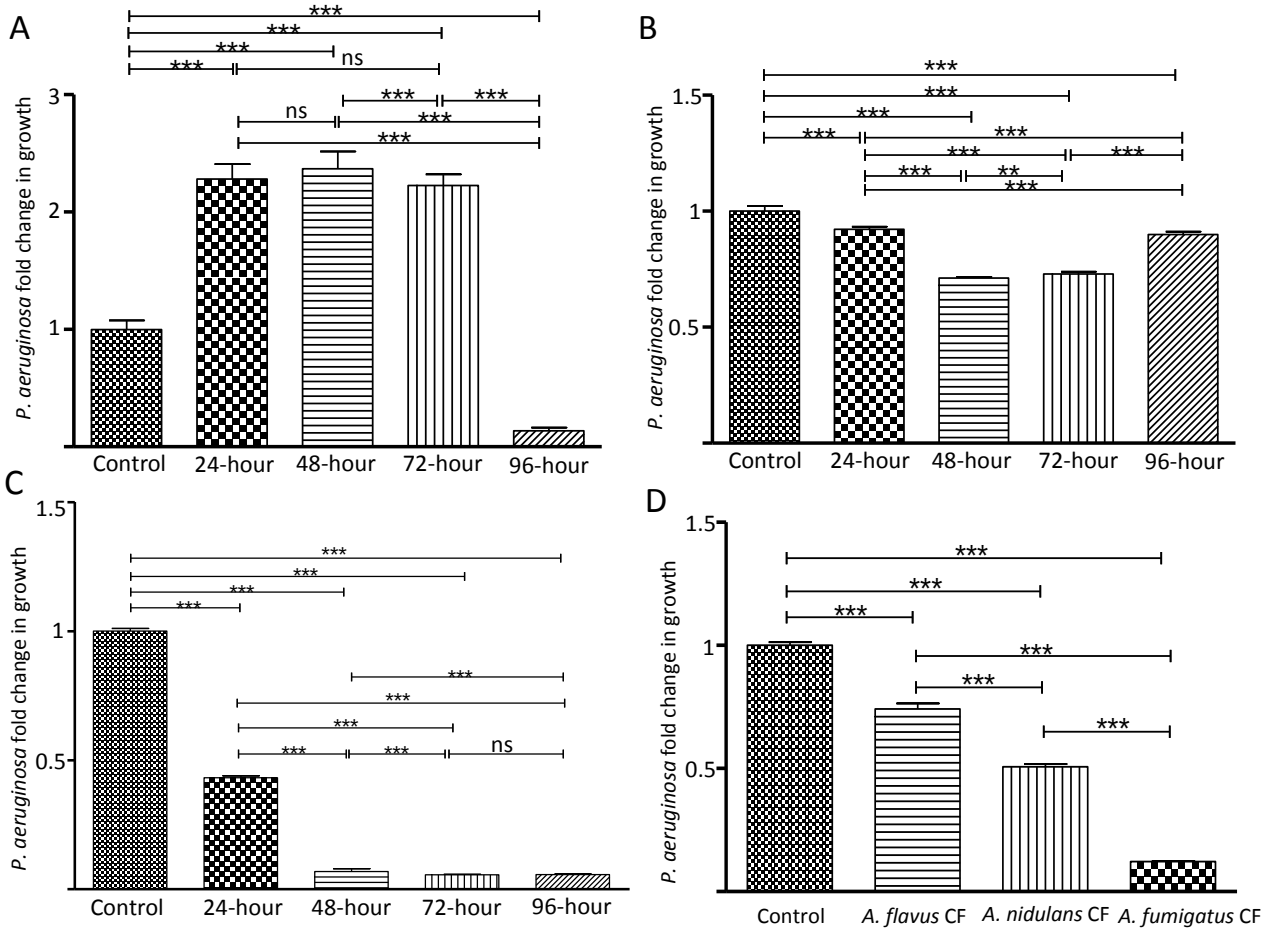

Fig 6.1 Effect of *Aspergillus sp.* culture filtrates on *P. aeruginosa* growth. The effect on *P. aeruginosa* growth of *A. fumigatus* culture filtrates produced at 24, 48, 72 and 96 hours in Czapek-Dox (A), DMEM (B) and SAB (C) compared with sterile Czapek-Dox, DMEM or SAB respectively (control). Compared to the controls, *P aeruginosa* growth (OD_{600}) was most reduced when exposed to the CuF produced in Czapek-Dox by 96 hours and when exposed to CuF produced in SAB by 48 hours, 72 hours and 96 hours. The effect of *P. aeruginosa* growth of culture filtrates produced in SAB at 72 hours by sterile SAB (control), *A. flavus*, *A. nidulans* and *A. fumigatus* (D). * $p < 0.05$ ** $p < 0.01$ *** $p < 0.001$ ns: not significant.

6.2.2 Characterization of 72 hour SAB by solid phase extraction and TLC

To determine the polarity of the compound, 72 hour SAB (20 ml) was passed through C18 Sep-Pak cartridges to isolate the polar component from the non-polar component. The retentate (2 ml) was eluted from the column with methanol and resuspended in sterile SAB (40 ml). Activity assays were performed to investigate whether the anti-bacterial properties were retained in the polar or non-polar fractions. Anti-bacterial activity was retained against *P. aeruginosa* in the polar fraction of the 72-hour SAB (Fig. 6.2A). Some activity was observed in the non-polar fraction however this may be due to partial retention of the polar compound in the non-polar fraction during the separation process. The polar fractions were collected from CuF produced at 24, 48, 72 hours and assessed for their anti-bacterial properties on *P. aeruginosa*. A decrease in the growth of *P. aeruginosa* (OD_{600}) exposed to unfractionated CuF (whole SAB) and fractionated CuF (polar SAB) from 48 and 72 hour fungal cultures compared to 24 hour CuF and sterile SAB revealed that antibacterial activity was retained in the polar fractions from the later fungal cultures. Anti-bacterial activity was not lost during the fractionation process (Fig. 6.2B).

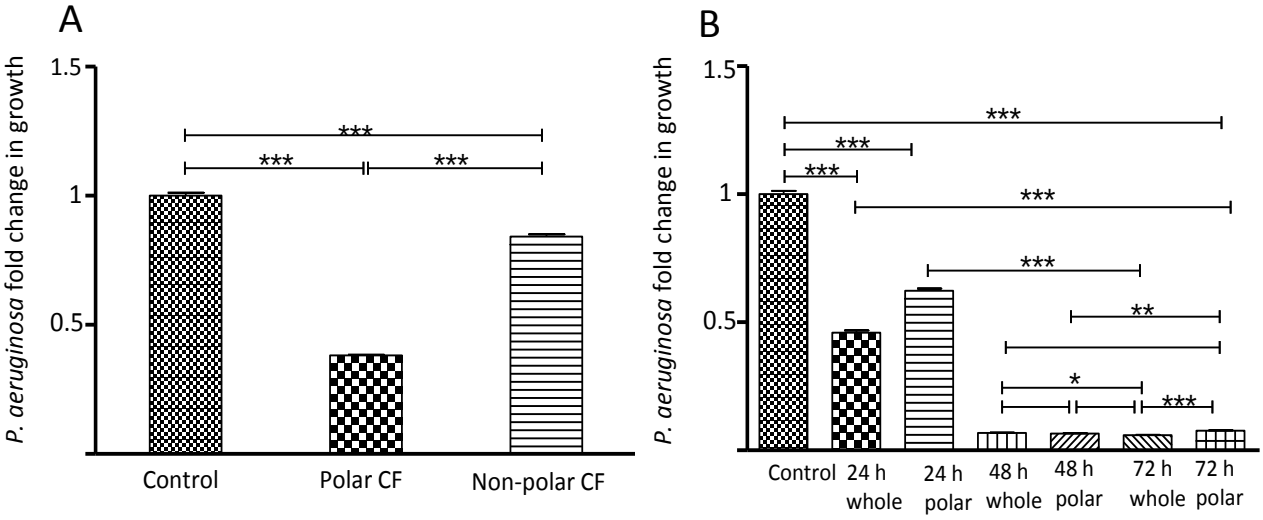

Fig. 6.2A. Antibacterial effect of polar fraction on *P. aeruginosa*. The effect on bacterial growth (OD_{600}) of the polar and non-polar fractions of CuF produced by *A. fumigatus* in SAB at 72 hours (A) showed that the antimicrobial activity was greatest in the polar fraction compared to the non-polar fraction of the CuF and sterile SAB (control). **Fig. 6.2B. Comparison of antibacterial effect of CuF produced at different time-points.** The polar fraction of the CuF produced at 24, 48 and 72 hours was compared with non-fractionated (whole) material. The antibacterial activity observed in CuF produced at 48 and 72 horus in the whole material and polar material, but less so in the CuF produced at 24 hours. * $p < 0.05$ ** $p < 0.01$ *** $p < 0.001$ ns: not significant

To investigate whether the anti-bacterial activity was caused by proteins or smaller peptides or metabolites, the polar fractions were separated by size using centrifugal column filters with a molecular cut-off weight of 3 kDa. Activity assays performed on *P. aeruginosa* revealed that the active component was retained in the lower molecular weight fraction of less than 3 kDa (Fig. 6.3).

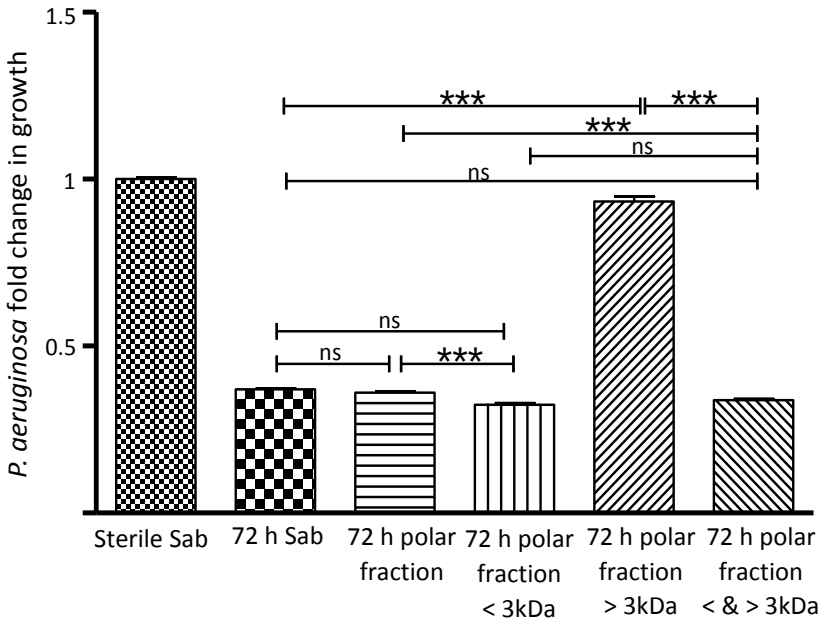

Fig. 6.3 Effect on *P. aeruginosa* growth of SAB fractions. CuF produced at 72 hours was fractionated and the tested for anti-bacterial activity on *P. aeruginosa* growth (OD_{600}). Compared to sterile SAB (polar < 3 kDa) there was activity in all fractions. The greatest level of antimicrobial activity was observed in unfractionated SAB, the polar fraction, and in the polar fraction with components > 3kDa removed. There was very little activity in the fraction containing components > 3 kDa. This activity was returned when the fraction containing components < 3 kDa were recombined with the > 3 kDa fraction. * $p < 0.05$ ** $p < 0.01$ *** $p < 0.001$ ns: not significant**.**

To investigate the activity of the (polar, < 3 kDa) SAB on other Gram-negative bacteria, a multidrug resistant (MDR) strain of *E. coli*, PEK499 was exposed to the compound for 24 hours. The compound was shown to have anti-bacterial activity against this MDR strain, with most activity observed in the 72-hour SAB (Fig. 6.4).

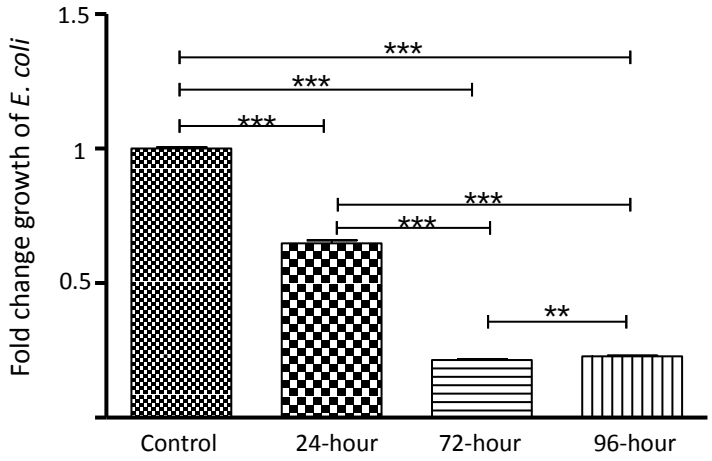

Fig. 6.4 The effect on growth of SAB on MDR *E. coli* PEK499. The polar (< 3 kDa) fractions of CuF produced by *A. fumigatus* at 72 hours in SAB had the greatest anti-bacterial effect on *E. coli* growth (OD_{600}) compared to the control (sterile SAB, polar, < 3kDa). * $p < 0.05$ ** $p < 0.01$ *** $p < 0.001$ ns: not significant

In an effort to further separate the components of the 72 hour-SAB (polar, < 3 kDa), the CuF was lyophilized to concentrate the compound, and prepared for thin layer chromatography (TLC). The solid material did not solubilize in methanol (MeOH) and instead, it was gradually dissolved in methanol and ddH_2O (1 ml, 1:1 ratio). The dissolved material (250 µl) was spotted onto TLC plates containing silica as the solid phase. The plates were placed in a mobile phase of dichloromethane (DCM) and 5 % methanol (Fig. 6.5A) or 10 % methanol (Fig. 6.5B). The plates were scanned at 254 nm (Fig. 6.5). The compound did not move from the starting point on the plate. The material was scraped off and dissolved in methanol and ddH2O (400 µl, 1:1 ratio). The scrapings were centrifuged at 14000 x *g* for 10 minutes. The supernatant was removed and was diluted in sterile SAB to give a 1/5 and 1/10 dilution. The diluted compound (50 µl) was used for an activity assay against *P. aeruginosa* (50 µl, OD_{600} 0.05). Methanol and ddH_2O (1:1 ratio) was diluted in SAB to a 1/5 and 1/10 dilution and used as a control for the activity assay. The results of this assay indicate that the anti-bacterial activity was retained in the material that did not move from the starting point of the TLC plate (Fig. 6.5C).

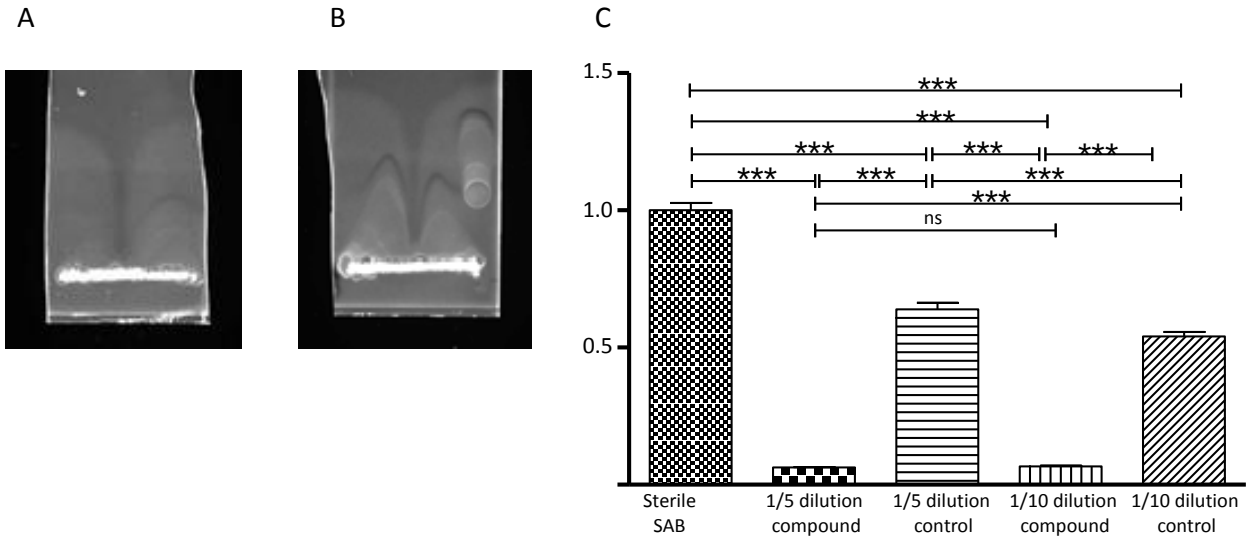

Fig. 6.5 TLC performed on 72-hour SAB. The material did not move from the starting point in DCM with 5 % MeOH **(A)** or 10 % MeOH **(B).** The material was removed from the TLC plate and diluted (1/5 and 1/10) in sterile SAB and assessed for anti-bacterial activity against *P. aeruginosa*. Both dilutions had retained activity **(C).** * $p < 0.05$ ** $p < 0.01$ *** $p < 0.001$ ns: not significant

The lyophilized 72-hour SAB was also tested for its anti-bacterial activity against other Gram-negative bacteria, *Klebsiella pneumonia* and Gram-positive bacteria, *Staphylococcus aureus.* The solid material was resuspended in ddH_2O and diluted with sterile SAB in a 1:1 ratio. The lyophilized compound had anti-bacterial activity against both bacteria compared to the control (sterile SAB) (Fig. 6.6).

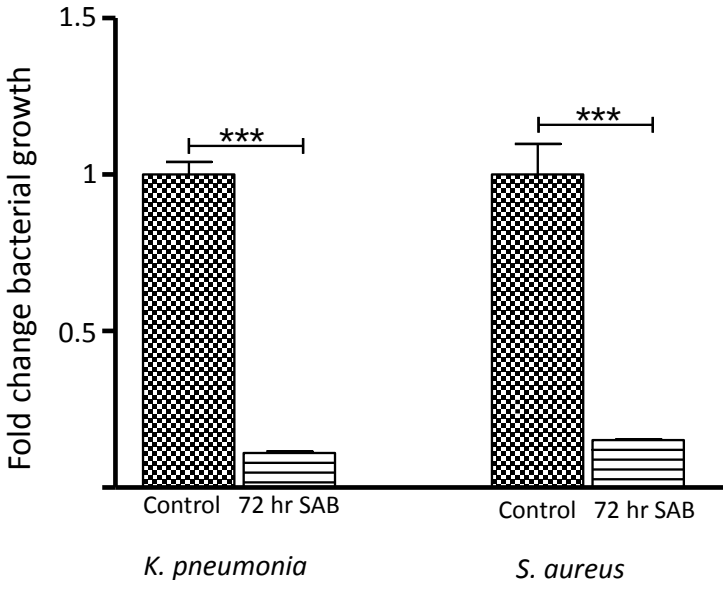

Fig. 6.6 Effect of 72 hours SAB on *K. pneumonia* and *S. aureus* growth. 72-hour lyophilized SAB was tested for anti-bacterial activity against *K. pneumonia* and *S. aureus*. The compound showed strong activity against both bacteria compared to the control. * $p < 0.05$ ** $p < 0.01$ *** $p < 0.001$ ns: not significant.

6.2.3 Analysis of the 72-hour SAB by HPLC

Lyophilized 72-hour SAB (20 ml) was dissolved in ddH_2O (1 ml) and 50 µl was loaded onto the HPLC. Fractions were collected every minute at a flow rate of 1 ml/minute. The gradient conditions were as follows: 0.01 – 10 minute: 0 % acetonitrile, 10-20 minutes: 0 % acetonitrile, 20 -25 minutes: 30 % acetonitrile and 100 % acetonitrile thereafter. The HPLC chromatographic profile (254 nm) revealed a number of peaks between 2.5 minutes and 10 minutes and between 16.5 minutes and 25 minutes over a 28-minute run time in total (Fig. 6.7).

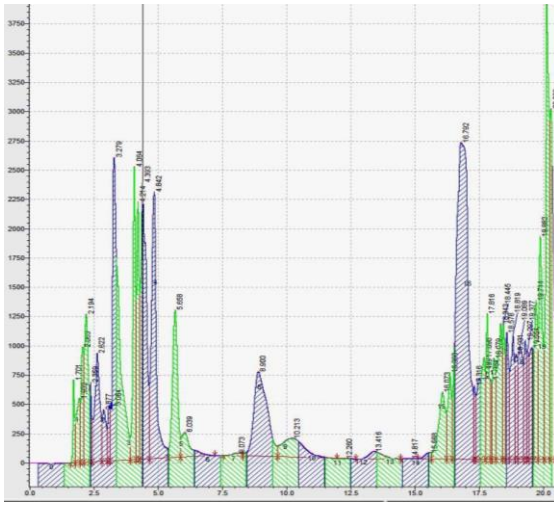

Fig. 6.7 HPLC chromatograms 72-hour SAB. Lyophilized CuF (produced at 72 hours) was resuspended in ddH_2O was loaded onto the HPLC (50 µl). Fractions were collected every minute for 20 minutes at a flow rate of 1 ml/min.

The fractions collected from the HPLC were diluted with sterile SAB (1:1) to reduce the level of TFA from in the mobile phase from 0.1 % to 0.05 % and tested for activity against *P. aeruginosa*. To ensure the antibacterial activity, the procedural control consisted of ddH_2O/0.1 % TFA diluted with sterile SAB in a 1:1 ratio. Fractions collected between 4 and 5 minutes (#5) and fractions collected between 16.5 and 17.5 minutes (#17) showed activity against *P. aeruginosa* (100 µl, OD_{600} 0.05) after 24 hours (Fig. 6.8). Because of the intrinsic polar nature of the compound, the early retention time at which the fraction with the greatest level of activity was detected, and the high level of antimicrobial activity, fraction #5 was chosen for further comprehensive analysis by NMR and mass spectrometry.

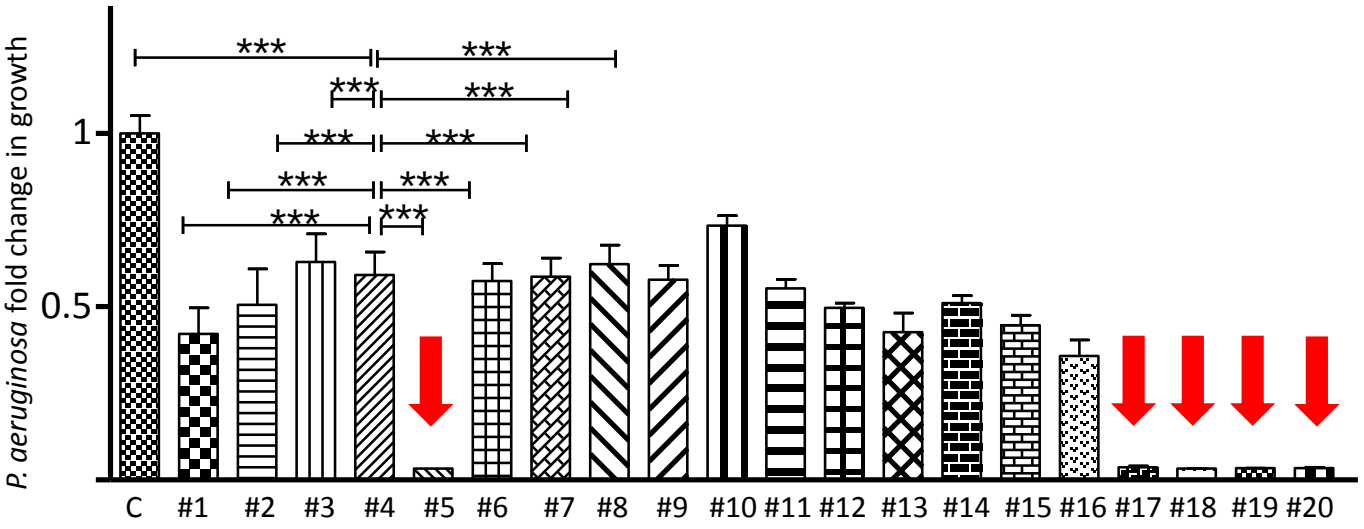

Fig. 6.8 Assessment of the anti-bacterial effect of 72-hour SAB HPLC fractions. Fractions collected from the HPLC were tested for activity against *P. aeruginosa*. Antimicrobial activity was observed in fraction #5, #17 - #20. * $p < 0.05$ ** $p < 0.01$ *** $p < 0.001$ ns: not significant.

To separate the compound by charge the 72-hour SAB (polar, < 3 kDa) was passed through cation exchange columns. The flow-through maintained activity against *P. aeruginosa*. This material (herein referred to as processed SAB) was lyophilized and resuspended in ddH_2O. Processed SAB (100 µl) was loaded onto the HPLC and run on the following gradient: 0.01-15 minutes: 0% acetonitrile: 16 to 18 minutes: 100% acetonitrile and 19 minutes to 28 minutes: 0 % acetonitrile. The flow rate was reduced to 0.5 ml/min to obtain better separation. These parameters were used for subsequent HPLC experiments in this chapter.

Fractions were collected between four minutes and 6.5 minutes (Fig. 6.9A). The fractions from each time-point were pooled together and lyophilized. Each group of fractions (20 ml lyophilized) was resuspended in ddH_2O (2 ml). The fractions were diluted in sterile SAB (1:1 ratio) and tested for activity against *P. aeruginosa*. The anti-bacterial activity was detected in fraction three, which had a retention time (RT) of 4.838, and this fraction was chosen for further analysis.

Fraction 3 (100 µl) was loaded onto the HPLC. Fractions were collected as previously described and pooled together in 20 ml aliquots prior to lyophilisation. As before, lyophilized material was resuspended in 2 ml ddH_2O and used to determine anti-bacterial activity. Activity was detected in the second fraction (RT 5.178) and this was fractionated once again by HPLC. In the final group of fractions collected, activity was detected in the second fraction (RT 5.182) (Fig. 6.9C and D). The first, second and third fractions from this group were analysed further by NMR and mass spectrometry.

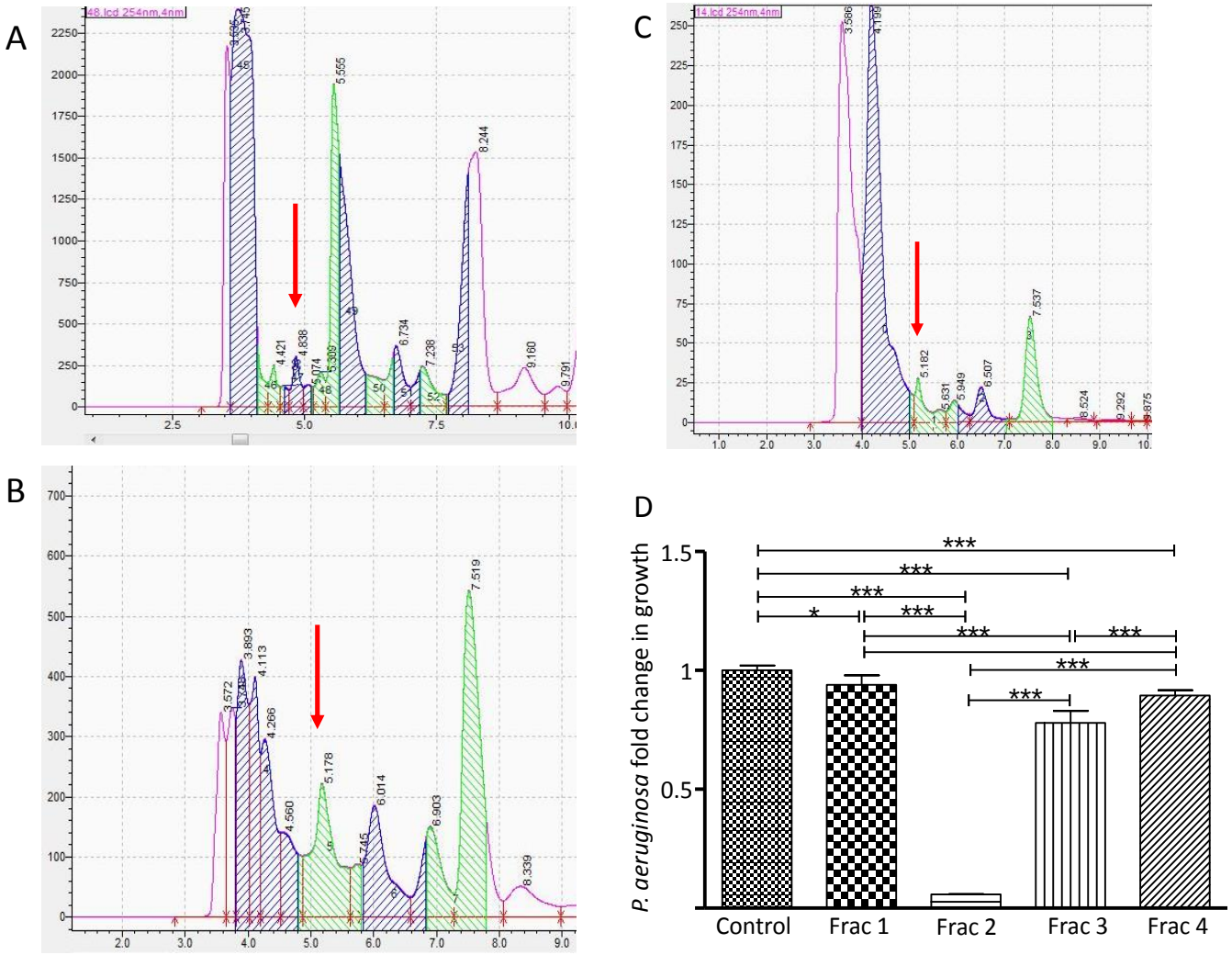

Fig. 6.9 Chromatographic profiles and anti-bacterial activity of processed SAB. Fractions were collected and tested for anti-bacterial activity. The third fraction (RT 4.838 minutes) (A) retained anti-bacterial activity and was subjected to another round of fractionation by HPLC. The second fraction (RT 5.178) (B) retained activity and was fractionated a third time. Fractions collected between five and six minutes (RT 5.182) (C) were determined to contain anti-bacterial activity (D). * $p < 0.05$ ** $p < 0.01$ *** $p < 0.001$ ns: not significant

Because initial NMR analysis revealed an abundance of free glucose (Fig. 6.10) in the fractionated samples (Sobolev *et al.*, 2003), the sequence of compound preparation for NMR was altered with a view to removing free glucose from the material. This approach involved performing the initial fractionation by HPLC prior to separating the material by SPE (Sep-Pak columns and cation exchange columns) and through centrifuge filters. The purpose of this was to avoid potentially concentrating the SAB, hence the glucose, when passing the material through the SPE columns and through the centrifuge filters. After the first round of fraction collecting, fractions were pooled together, lyophilized and tested for anti-bacterial activity. The fraction containing activity (fraction 2) was subjected to three more rounds of fractionation, lyophilisation (Fig. 6.11). The final fractions were tested for anti-bacterial activity against *P. aeruginosa* (Fig. 6.12). Fraction 1 was not tested as this has already been established not to have anti-bacterial activity. Fraction 2 showed some activity compared to the control (sterile SAB:ddH_2O/0.1 % TFA, 1:1 ratio). Fraction 3 and fraction 4 showed the greatest amount of activity (Fig. 6.12A). The anti-bacterial activity was observed in these fractions after 48 hours of incubation (Fig. 6.12B). The fractions obtained from the final (fourth) round of fractionation were analysed by NMR and mass spectrometry, however free glucose could not be completely removed from the sample (as detected by 1H NMR).

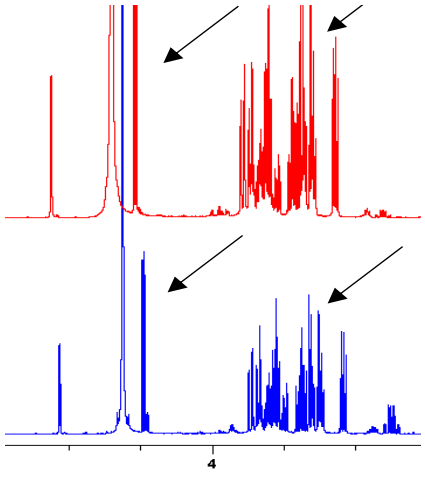

Fig. 6.10. NMR spectra of glucose detected in HPLC fractions. An abundance of glucose was detected by NMR in all fractions collected by HPLC. The black arrows point to signals that are typical of glucose. Both samples in the figure had anti-bacterial activity.

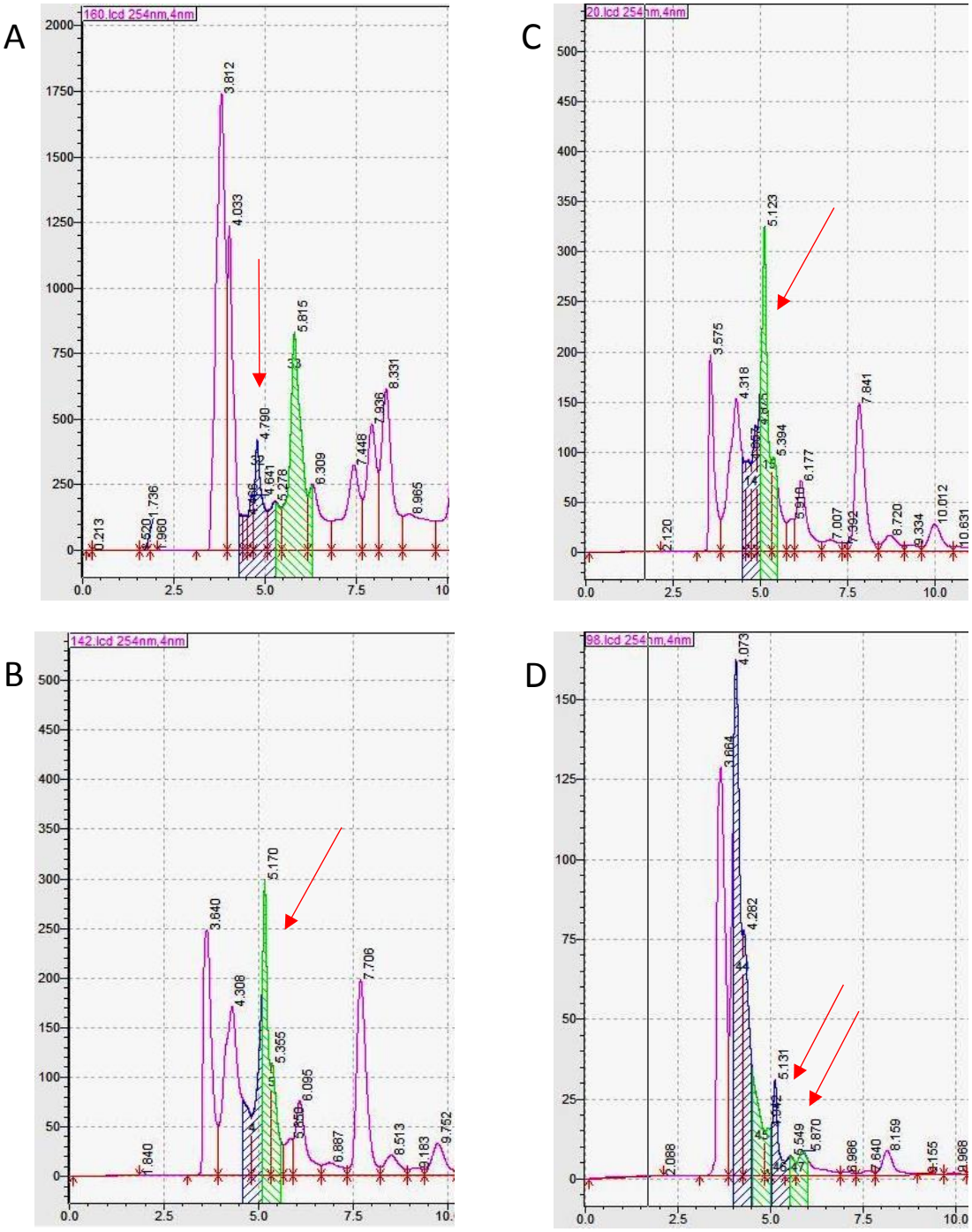

Fig. 6.11 HPLC Fractions of 72-hour SAB. Unprocessed 72-hour SAB was fractionated into two fractions. The first fraction (RT 4.790) had anti-bacterial activity (A). Fraction 1 was fractioneated into a further two fractions, the second of which (RT 5.170) had antimicrobial activity (B). Fraction 2 was fractionated into another 2 fractions (C), the second of which had anti-bacterial activity (RT 5.123). This fraction was fractionated into four fractions (D). Fraction 2 had very little anti-bacterial activity. The anti-bacterial activity was retained in the third and fourth fractions (RT 5.131, RT 5.549).

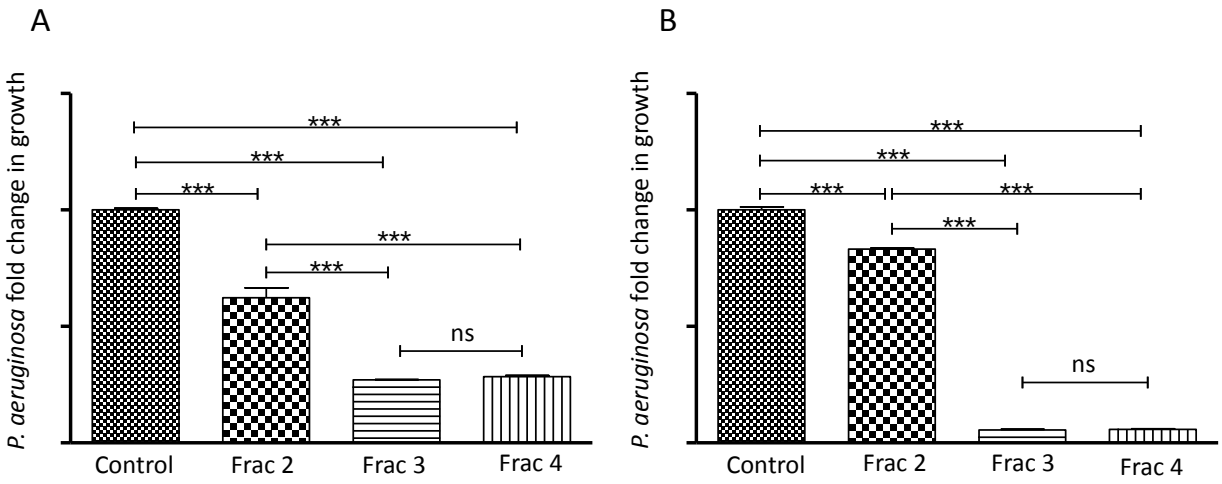

Fig 6.12 Assessing HPLC fractions of 72-hour SAB for anti-bacterial activity *P. aeruginosa* was exposed to fractions 2, 3 and 4 collected from the final (fourth) fractionation process and incubated for 24 hours (A). Fraction 3 and 4 contained the most anti-bacterial activity. Fraction 3 and 4 retained antimicrobial activity after 48 hours (B). * $p < 0.05$ ** $p < 0.01$ *** $p < 0.001$ ns: not significant

6.2.4 NMR analysis of processed SAB

A series of 1 dimensional/1D (i.e. where the x-axis corresponds to the chemical shifts in ppm/frequency and the y-axis corresponds to intensity) experiments were performed including 1H, ^{13}C NMR and 31-phosphorus NMR on fractions with and without anti-bacterial activity collected from the HPLC. Additionally, 2 dimensional/2D (i.e. where the frequency is displayed on the x-axis and y-axis) experiments including COSY, TOCSY, HSQ, HMBS and DEPT were performed on these fractions. Glucose was detected at high concentrations (Fig. 6.10 and Fig. 6.13) resulting in the overlapping of signals of the molecular determinant responsible for the anti-bacterial activity. In an effort to remove the glucose, boronic acid immobilized in solid support resin beads was attempted although this approach was unsuccessful. Thus, the analysis proceeded with the presence of glucose in the samples which resulted in only several signals in the aromatic region (6-9 ppm) and the aliphatic region (3-0 ppm) not being overlapped by glucose peaks.

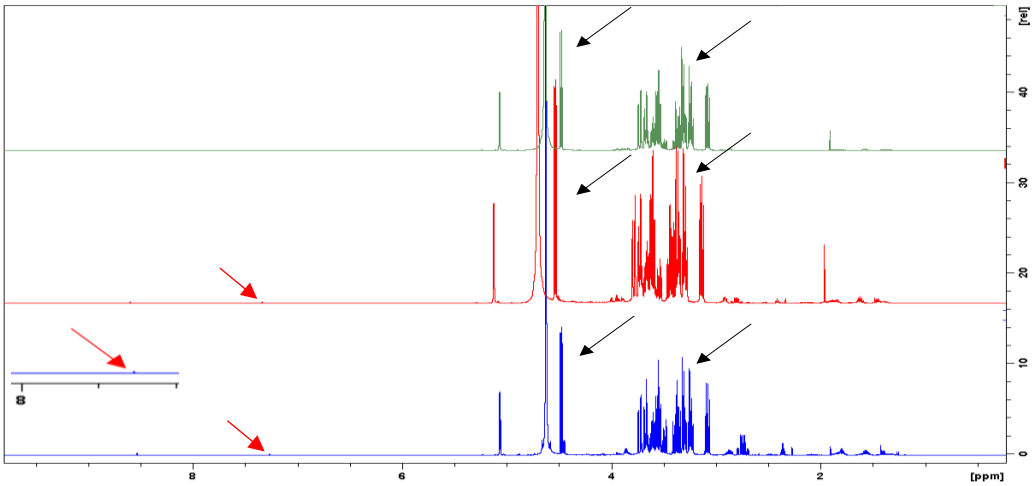

Fig. 6.13 IH NMR analysis of HPLC fractions 1H NMR of fractions collected by HPLC between 4.5 and 5.5 minutes. The first eluting fraction (blue) retained most anti-bacterial activity, the second eluting fraction (red) contained some activity and the third eluting fraction (green) contained no activity. All three fractions contained glucose as indicated by the black arrows. The red arrows point to signals that suggest double bonds, which may indicate signals other than those originating from the free glucose.

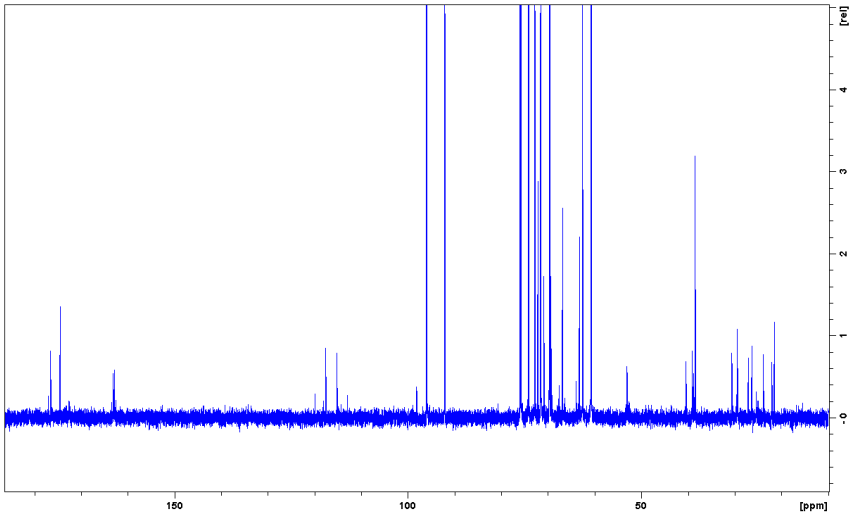

Fig. 16.14 ^{13}C NMR spectra of HPLC fraction with anti-bacterial activity ^{13}C NMR was performed on the fraction containing the highest levels of anti-bacterial activity, fraction 4. The signals at 98 ppm indicated the presence of anomeric carbons other than glucose, suggesting that the compound may be glycosylated.

^{13}C NMR spectrum of fraction 4 (Fig. 6.14) revealed signals at 177 ppm and 175 ppm, which could potentially indicate an aldehyde carbonyl or an ester. A cluster of signals, including two strong signals, at 165 ppm potentially corresponds to amide carbonyls. A cluster of signals at 120 including two strong signals, suggest that the signal at 7.5 ppm (Fig. 6.13) corresponds to double bonds. A signal at 98 ppm suggest an additional anomeric carbon other than glucose and may indicate the presence of

glycosylated products. Overall, 26 significant carbon signals (other than glucose) can be appreciated.

NMR analysis was performed on a total of four groups of fractionated samples prepared at different times from 72-hour processed SAB, which tested positive for anti-bacterial activity. Although samples were prepared at different stages over two years, they all retained the same signature characteristics (Fig. 6.15 and Fig. 6.16). These features are highlighted in the spectra arising from 1H NMR in the aromatic region and aliphatic region respectively. The final fraction (blue) which displayed the most activity from all the fractions tested (with or without activity) has the highest peaks. Peak height correlates positively with concentration thus this sample had the highest concentration of the component of the compound detected in this region of the NMR spectra. In the aromatic region of the spectra (Fig. 6.15), the signal detected at 8.5ppm is likely to be an aldehyde because the chemical shift matches with what is an aldehyde proton. While in the aromatic region, the signal detected at 7.5ppm is likely not to be caused by an aromatic residue and is possibly an alkene, which is directly bonded to electro-negative atom. Although it is detected in the range for aromatic protons, the integration for this signal is very low to account for aromatic proton. Furthermore, this signal couples with a signal in the ^{13}C NMR (Fig. 6.14), which is detected at 120 ppm, a characteristic feature of an alkene carbon.

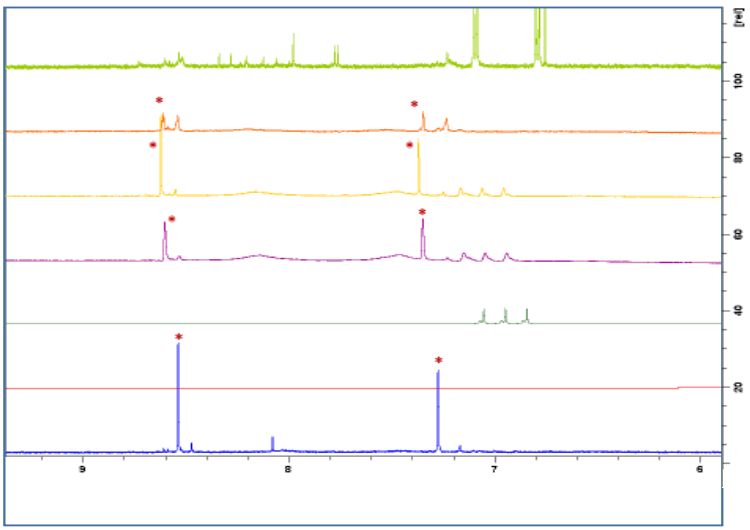

Fig. 6.15 1H NMR spectra of HPLC samples with anti-bacterial activity in the aromatic region. 1H NMR spectra of samples from all processed SAB fractions containing anti-bacterial activity. Spectra shown is in the aromatic region. Signals present in the majority of the samples are highlighted with *.

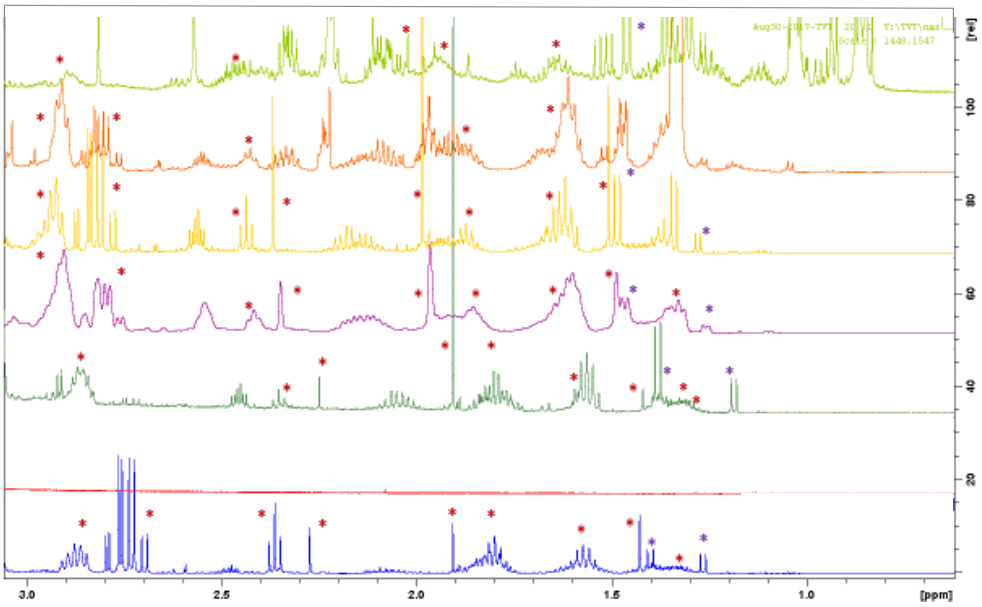

Fig. 6.16 1H NMR spectra of HPLC fraction with anti-bacterial activity in the aliphatic region. 1H NMR spectra of samples from all processed SAB fractions containing anti-bacterial activity. Spectra shown is in the aliphatic region. Signals present in the majority of the samples highlighted with *.

1H NMR performed on three samples (fraction 1, 2 and 3) obtained from HPLC-fractionated processed SAB (See Fig. 6.9C) revealed distinct differences in peaks in the aliphatic region (Fig. 6.17A) between the fractions that contained strong anti-bacterial activity (red; fraction 2) and some (i.e. less than fraction 2) anti-bacterial activity (blue; fraction 3) and no anti-bacterial activity (green; fraction 1). The spectra of the signals coming from fractions containing the most anti-bacterial activity from this group (as represented in Fig. 6.9D) have a strong peak detected in the aliphatic region (black arrow). This peak is weaker in the fraction (3) that contained less activity than fraction 2 and not visible in the fraction that contained no activity against *P. aeruginosa* (fraction 1).

An expanded 1H NMR spectra of the same three fractions showed several distinct peaks, which differed in height depending on the anti-bacterial activity (Fig. 6.17B). The middle spectra (red), represents fraction 2, which had the strongest activity against *P. aeruginosa* (Fig. 6.9D). Several peaks observed in this spectra, were lower in the spectra representing fraction 3, which had some anti-bacterial activity (blue), and not visible in the spectra representing fraction 1, which had no activity against *P. aeruginosa* (green).

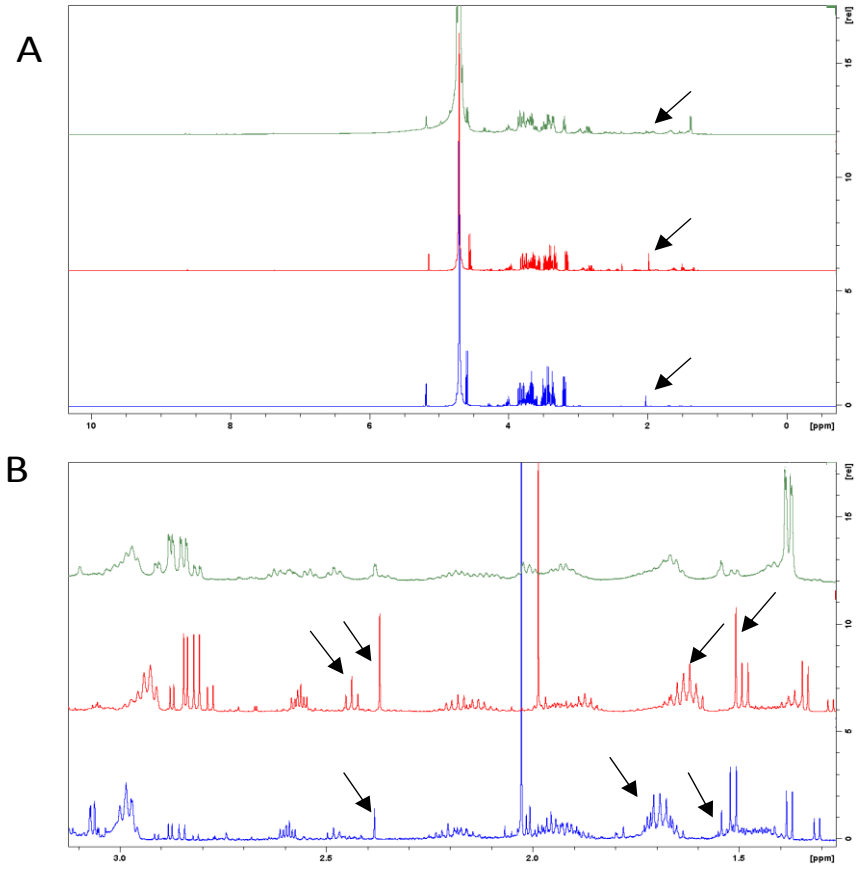

Fig. 6.17 1H NMR spectra of HPLC samples with and without anti-bacterial activity in the aliphatic region. 1H NMR spectra comparing fractions with and without anti-bacterial activity obtained from HPLC fractionations of processed SAB. Differences between the three fractions are indicated by black arrows. The middle spectra (red) represents fraction 2, which showed most anti-bacterial activity against *P. aeruginosa*. The bottom spectra (blue) represents fraction 3, which showed some anti-bacterial activity. The top spectra, representing fraction 1 (green) had no anti-bacterial activity. The main differences between the three spectra are highlighted by black arrows, which point to a peak in the aliphatic region. These peaks are highest in the spectra representing fraction 2 (red), lower in fraction 3 (blue) and not visible in fraction 1 (green).

1H NMR analysis performed on fractions collected from the final round of fractionation by HPLC (Fig. 6.11 and Figure 6.12) revealed distinct differences in peaks and peak heights between the active (red and blue; fraction 3 and 4) and non-active fractions. Similar peaks were detected in the aliphatic region of the spectra between the fraction 3 (red) and fraction 4 (blue) (Fig. 6.17A). However, several peaks were detected in fraction 4 that were not present in fraction 3 or fraction 2 (green) (Fig. 6.17B). Fraction 4 had slightly stronger anti-bacterial activity compared to fraction 3, which lasted past the 48 hours measured (as measured by observation). These peaks were not detected in the fraction that contained no anti-bacterial activity (i.e. fraction 2).

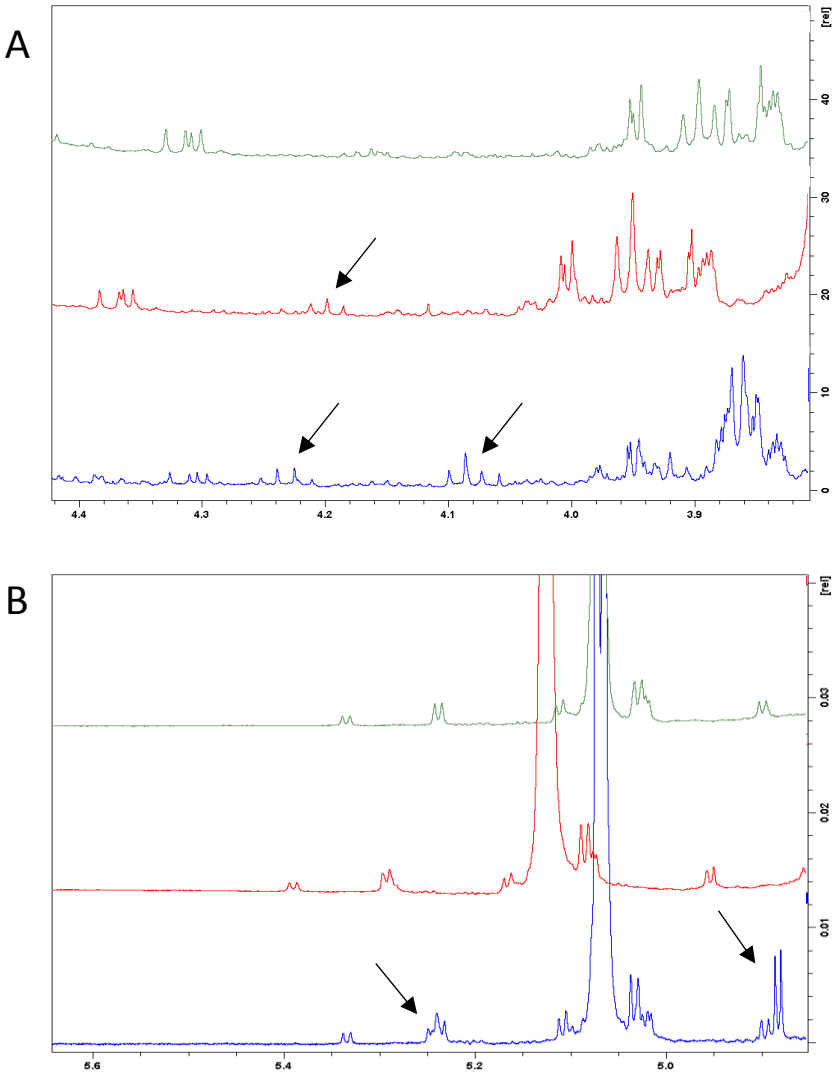

Fig. 6.18 1H NMR spectra of HPLC samples with antibacterial activity in the aromatic region. 1H NMR spectra comparing fractions with and without anti-bacterial activity (at the aliphatic region). Fractions with anti-bacterial activity, fraction 3 (red) and fraction 4 (blue) had similar peaks that were missing from fraction 2 (green) which had no anti-bacterial activity (A). The presence of these peaks are indicated with black arrows. A number of peaks present in fraction 4 were absent in fraction 3 and fraction 2 (A). A number of peaks in the alkene region of the spectra were observed in fraction 4 but not in the other fractions (B).

The final 1H NMR spectra from this group (Fig. 6.19) revealed distinct peaks in the aliphatic region belonging to fraction 4 (blue) including a quartet of doublets (~ 2.75 ppm), a singlet (~ 2.3 ppm) and a triplet (~ 2.35 ppm). The singlet may be indicative of an alanine residue and the triplet may belong to an aliphatic component of the compound. The distinctive complex splitting pattern of the quartet of doublets suggests the compound has a cyclic structure. While some of these peaks were detected in fraction 3 (red), the peak heights were much lower than that visible in fraction 4 (blue). Several of these peaks were not visible in the spectra, representing fraction 2 (green). A doublet was also detected at 1.25 ppm in fraction 4 but were completely absent from fraction 2 and fraction 3. The signals in this region correlate to amino acid side chains and suggest a glutamine or lysine residue due to the coupling pattern. This may also account for the polarity of the compound. A summary of the peaks common to the fractions with activity are included in Table 6.1.

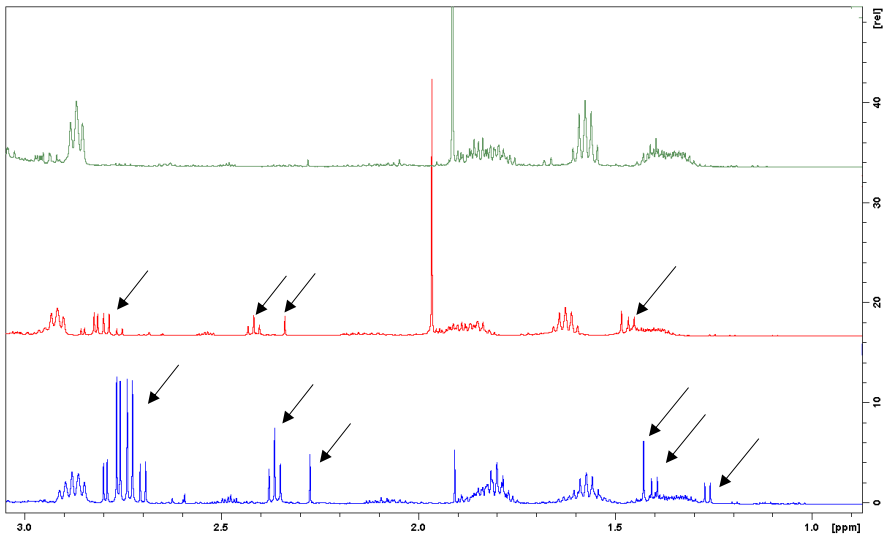

Fig. 6.19 1H NMR spectra comparing fractions with and without anti-bacterial activity in the aliphatic region. Several peaks were detected at higher levels in the spectra, representing fraction 4 (blue) than fraction 3 (red) and absent in fraction 2 (green). The peak heights of a singlet (~2.25 ppm), a triplet (~2.35 ppm) and a quartet of doubles were greater in fraction 4 than fraction 3 and absent in fraction 2.

Table 6.1 A summary of the signals detected by NMR analysis. The main signals detected, the position on the NMR spectra and some potential characteristics are described

Peak	Chemical Shift (ppm)	Multiplicity; integration	Coupling ^{13}C (ppm)	Assignation of activity
1	1.3	Doublet; weak - 0.26	18 CH	active
2	1.4	Doublet; weak - 0.26	12 CH	active
3	1.43	Singlet; weak - 0.26	28 CH	active
4	1.6 overlapping	Multiples (quintet) Multiples; strong	29 CH_2 24 CH_2	active and not active
5	1.8 overlapping	Triplet or doublet of doubles overlapping multiples; strong	20 CH_2 28 CH_2 30 CH_2	active and not active
6	2.3	Singlet; weak - 0.26	25 CH	active and not active
7	2.35	Triplet; strong	30 CH_2	active
8	2.75	Quintet; strong - 3	38 CH_2 2 CH	active
9	2.9	Quintet; strong - 2	39 CH_2	active
10	3.85	Multiples	50 CH	active and not active
11	4.5 (overlapped by H-1 Glucose)	doublet of doubles	65 CH	active and not active
12	4.8 (overlap by HOD)	Doublet; weak - 0.26	75 CH	active
13	4.9	Doublet; weak - 0.15	60 CH	active
14	7.3	Singlet; weak - 0.15	120 CH	active
15	8.5	Doublet (very small coupling constant); weak - 0.15	carbon not visible	active

6.2.5 Proteomic analysis of anti-bacterial compound

Proteomic analysis was performed on larger proteins (> 3kDa) extracted from 72-hour SAB. Proteins present in the CuF were identified using Proteome Discoverer 1.4. Peptides with minimum score of two (Xcor) were excluded from further analysis. These proteins are listed in Table A6.1. The top ten proteins with the highest score are listed in Table 6.2.

Table 6.2. Proteins detected in 72-hour SAB. Proteins (>3 kDa) extracted from 72-hour SAB were identified by mass spectrometry. The top ten proteins with the highest scores are included.

Gene	Protein name
Afu4g03490	Tripeptidyl-peptidase sed2
Afu1g11460	1,3-beta-glucanosyltransferase Bgt1
Afu1g07440	Molecular chaperone Hsp70
Afu1g17590	Phosphoesterase superfamily protein
Afu2g01170	1,3-beta-glucanosyltransferase gel1
Afu4g13770	Glycosyl hydrolase, putative
Afu3g14680	Lysophospholipase 3
Afu5g02330	Ribonuclease mitogillin
Afu5g10490	Amidase, putative
Afu7g04210	Tropomyosin, putative
Afu7g00940	Isoamyl alcohol oxidase, putative

Mass spectrometry-based analysis was performed on the same fractions collected by HPLC (Fig. 6.9C and 6.11D) that were analysed by NMR. The compound was weighed and diluted to concentrations varying from 1 – 10 µg/µl. Fractions with and without anti-bacterial activity were applied to a polar endcapped C18 column. Samples were surveyed in positive and negative mode to investigate the presence of positive or negative ions respectively. A total ion chromatogram was generated and relative intensities of candidate ions were measured against a number of base peak ions. Extracted ion chromatograms were recovered from the dataset for further analysis by fragmentation (Fig.6.20B, Fig.6.21B). Ions from fractions containing anti-bacterial activity were compared with ions from fractions containing some or no anti-bacterial activity. Additionally, ion maps were generated for each sample displaying the mass-to-charge ratio (*m/z*; y-axis) and retention time (min; x-axis) of all ions detected in the analysis (Fig. 6.20C, Fig. 6.21C). Ion maps were also generated for negative controls (no activity/blanks) to account for solvent and background ions. Following these surveys, no distinctive differences were observed between the samples. Although a number of potential candidates were considered, these will require additional research to confirm identity and activity.

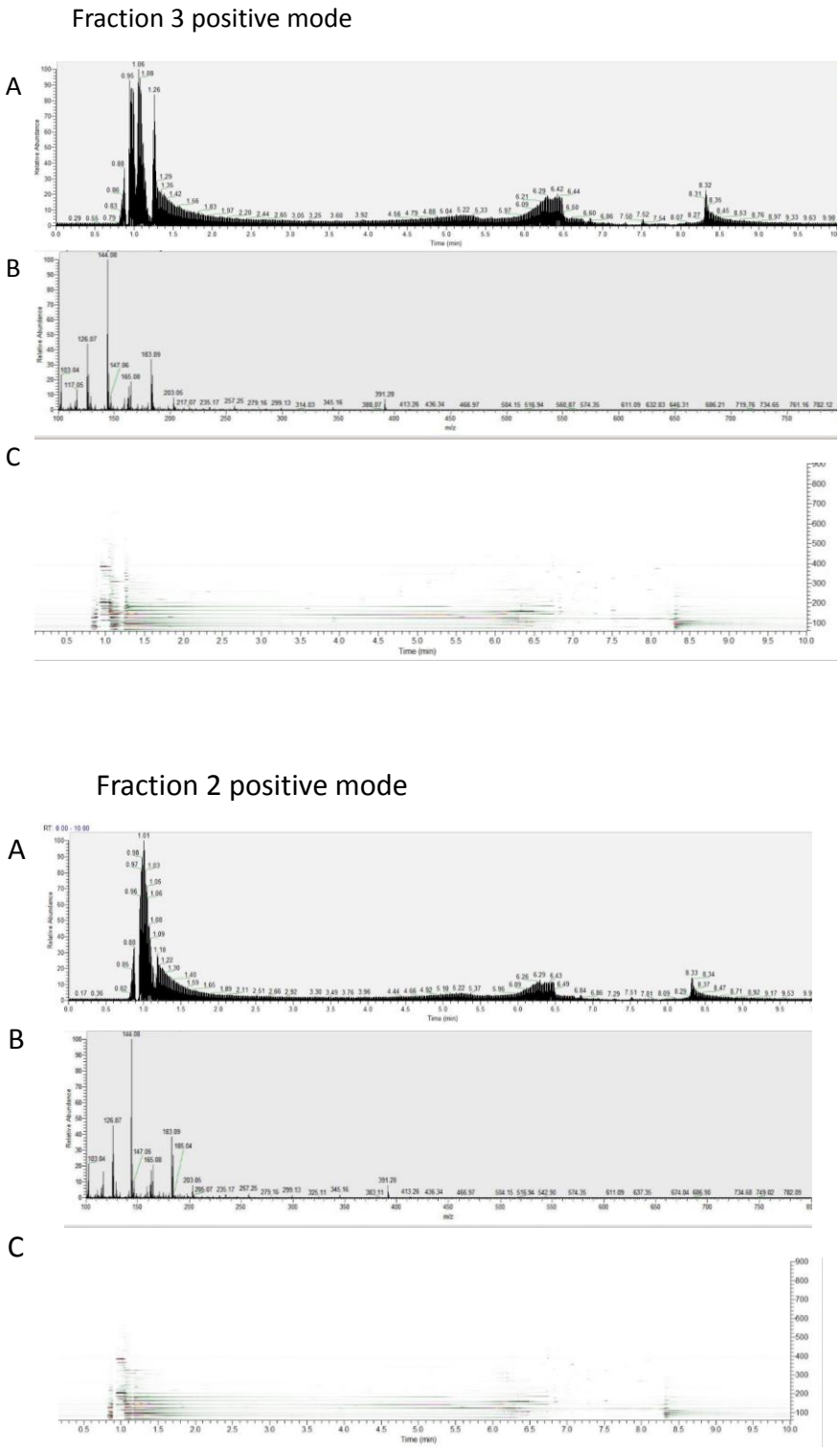

Fig. 6.20 Mass spectrometry chromatographs of fractions analysed in positive mode. Fractions with (Fraction 3) and without (Fraction 2) anti-bacterial activity were investigated by MS in positive mode (A). Ions from fractions were compared (B) and ion maps were generated (C).

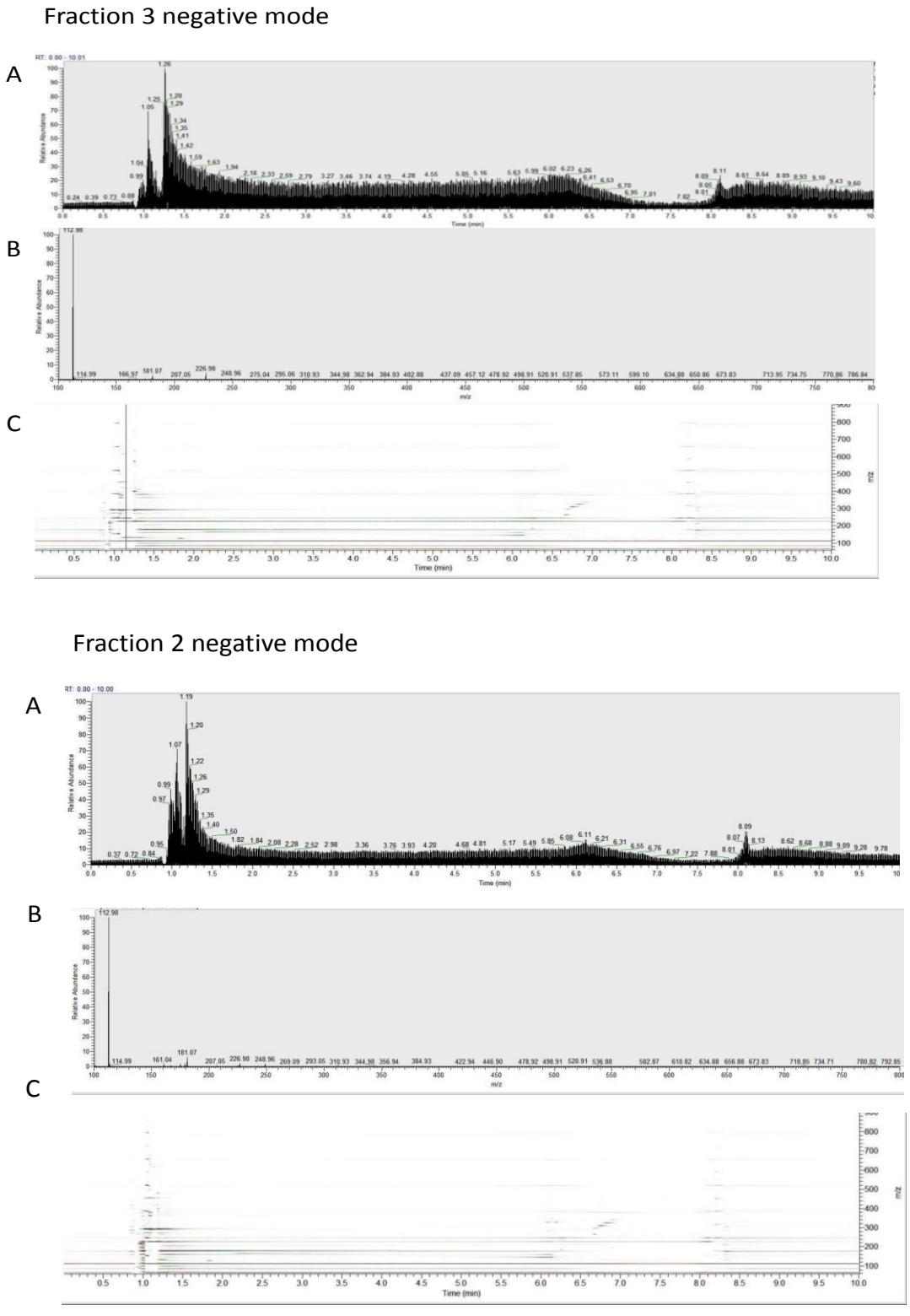

Fig. 6.21 Mass spectrometry chromatographs of fractions analysed in negative mode. Fractions with (Fraction 3) and without (Fraction 2) anti-bacterial activity were investigated by MS in negative mode (A). Ions from fractions were compared (B) and ion maps were generated (C).

6.2.6 Proteomic response of *P. aeruginosa* to sub-inhibitory concentrations of *A. fumigatus* culture filtrates produced in SAB by 72 hours.

Label free quantitative (LFQ) proteomics was employed to investigate the changes that occur in the *P. aeruginosa* proteome when exposed to the 72-hour CuF produced by *A. fumigatus* in SAB (72-hour SAB). The bacteria were exposed to neat, unprocessed 72-hour SAB (30% v/v) for 24 hours prior to protein extraction (treatment) (n = 3). Changes to the proteome were compared with bacteria exposed to sterile SAB (30% v/v) (control). In total, 2,690 proteins were initially identified and 1,952 proteins remained after filtering. Post-imputation, 321 proteins were identified as being statistically significant ($p<0.05$) and differentially abundant (relative fold change of +/- 1.5) (SSDA) (Table A6.2). A principal component analysis (PCA) was performed on all filtered proteins and identified distinct proteomic differences between the groups (Fig 6.22A). Components 1 and 2 accounted for 82.5 % of the total variance within the data, and both replicates resolved into their corresponding samples. There was a clear divergence between the groups exposed to the culture filtrate (treatment) and those unexposed (control).

Hierarchical clustering was performed on the z-scored normalised LFQ intensity values for the SSDA proteins (Fig. 6.22B). The two biological replicates resolved into their respective sample. Based on protein-abundance profile similarities, two main clusters resolved, although enrichment terms were only contained in the second cluster (black). These included the GOCC terms integral to membrane, intrinsic to membrane and membrane part, and the GOMF terms tetrapyrrole binding and heme binding (Table A6.3A and A6.3B). The relative abundance of proteins associated with this cluster was decreased in the group exposed to the *A. fumigatus* 72-hour CuF. All proteins associated with both datasets are included in Table A6.1.

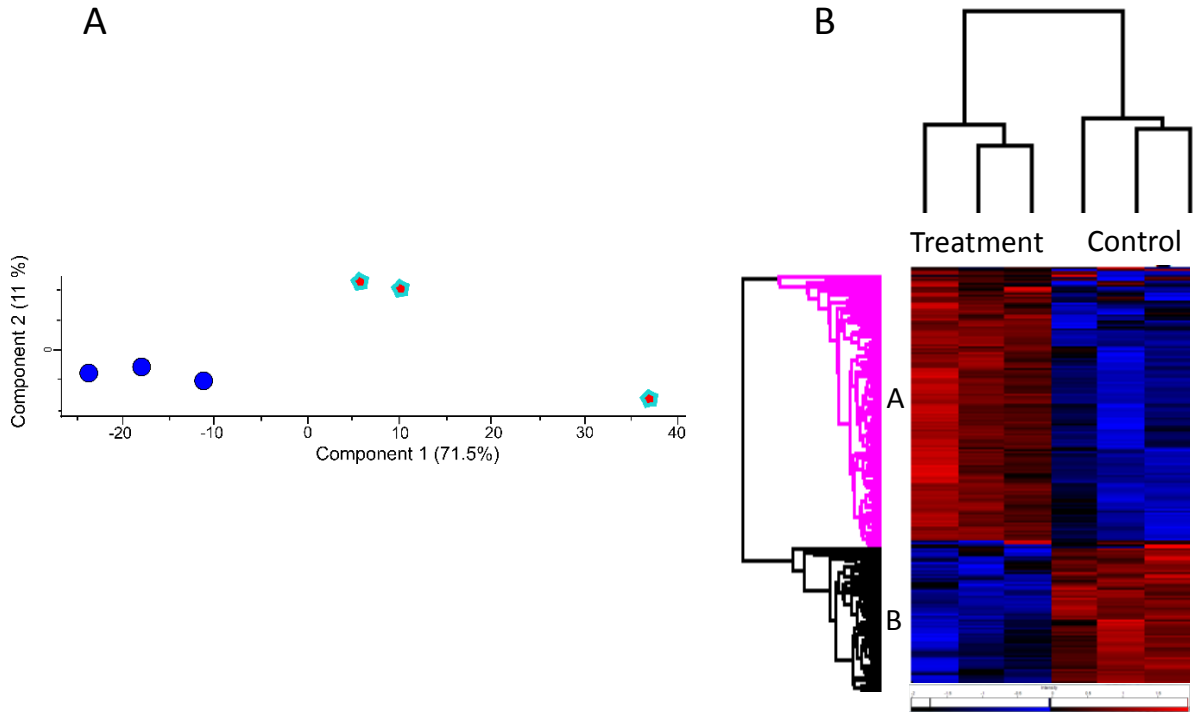

Fig. 6.22 PCA and hierarchical clustering of *P. aeruginosa* proteins. Principal component analysis (PCA) of *P. aeruginosa* exposed to *A. fumigatus* CuF (treatment) (hexagon) and sterile SAB (circles). A clear distinction can be observed between each of the groups exposed to the treatment and the control (A)**.** Clusters based on protein-abundance profile similarities were resolved by hierarchical clustering of multi-sample comparisons between the two sample groups of *P. aeruginosa* (B). Two main clusters were identified. Cluster A did not contain enrichment terms. Enrichment terms for cluster B included intrinsic to membrane and tetrapyrrole binding.

Volcano plots were produced by pairwise Student's t-tests ($p < 0.05$) to determine the differences in protein abundance between two samples and to depict the changes in pathways and processes in which those proteins are involved (Fig. 6.23). There was a general increase in the relative abundance of proteins involved in translation and a decrease in the relative abundance of proteins associated with the membrane and oxidoreductase activity.

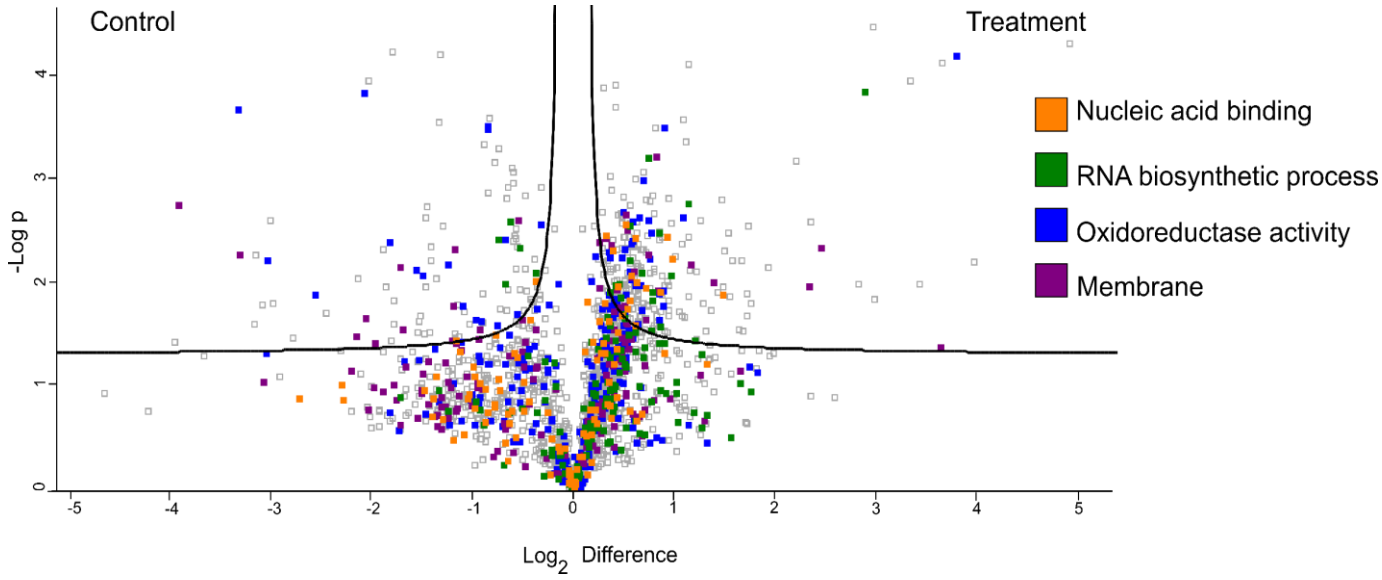

Fig. 6.23 Comparing the proteome of unexposed and 72-hour CuF-exposed *P. aeruginosa*. Volcano plots derived from pairwise comparisons between *P. aeruginosa* exposed to 72-hour *A. fumigatus* CuF produced in SAB (Treatment) and *P. aeruginosa* exposed to sterile SAB (control). The distribution of quantified proteins according to p value (−log10 p-value) and fold change (log_2 mean LFQ intensity difference) are shown. Proteins above the line are considered statistically significant (p-value <0.05). In general, the relative abundance of protein components associated with RNA biosynthetic processes (green) and nucleic acid metabolic processes (orange) was greater in bacteria exposed to the treatment than the control. The relative abundance of proteins associated with oxidoreductase activity (blue) and membrane parts (purple) was lower in bacteria exposed to the treatment than the control.

SSDA protein names arising from the pair wise t-tests were inputted into the STRING and KEGG database and used to identify biological pathways and processes over-represented in a particular group. The proteomic data arising from Student's t-tests ($p < 0.05$) identified several pathways that were most affected by bacterial culture conditions (Fig. 6.23, Fig. 6.24A, 6.24B, Table 6.3 and Table 6.4). The relative abundance of proteins associated with a stress response, the phenazine and O antigen biosynthetic pathways and phosphate transport were increased in the *P. aeruginosa* groups that had been exposed to the *A. fumigatus* CuF (Fig. 6.24A). Conversely, there was a decrease in the relative abundance of proteins associated with quorum sensing (Fig. 6.24B and Fig. 6.25), heme biosynthesis, pyochelin biosynthesis, sulphur metabolism and phenylalanine metabolism (Fig. 6.24B). A selection of SSDA proteins involved with pathways most affected by bacterial culture conditions are listed in Table 6.3 and Table 6.4.

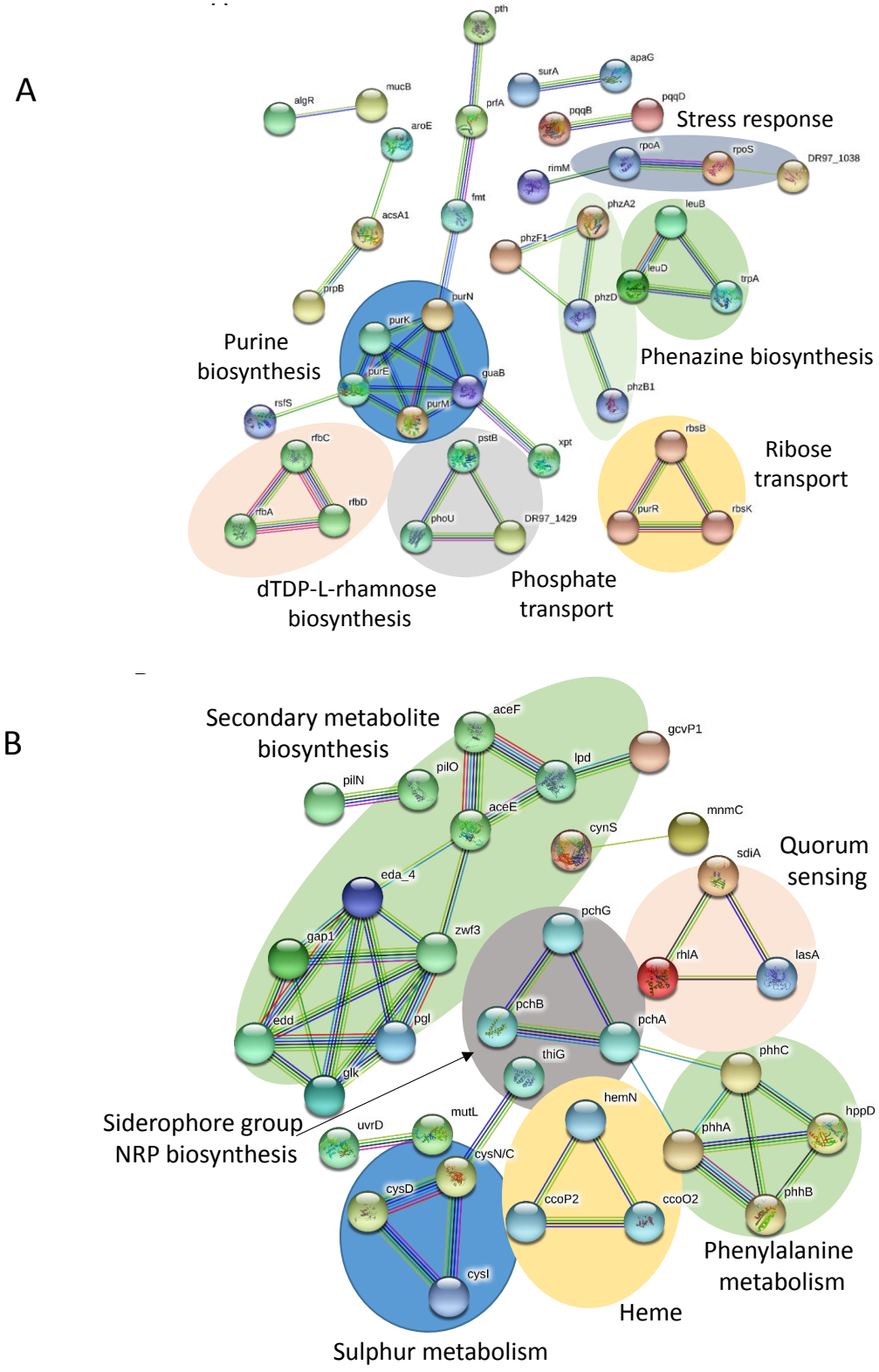

Fig. 6.24 Analysis of *P. aeruginosa* proteins by STRING. STRING was used to map known protein-protein interactions of SSDA proteins arising from Student's t-tests ($p<0.05$). Pathways associated with phenazine biosynthesis, stress response regulators, O antigen biosynthesis, phosphate and ribose transport were upregulated (A). Pathways involving pyochelin biosynthesis, heme biosynthesis, quorum sensing, and phenylalanine and sulphur metabolism were downregulated (B).

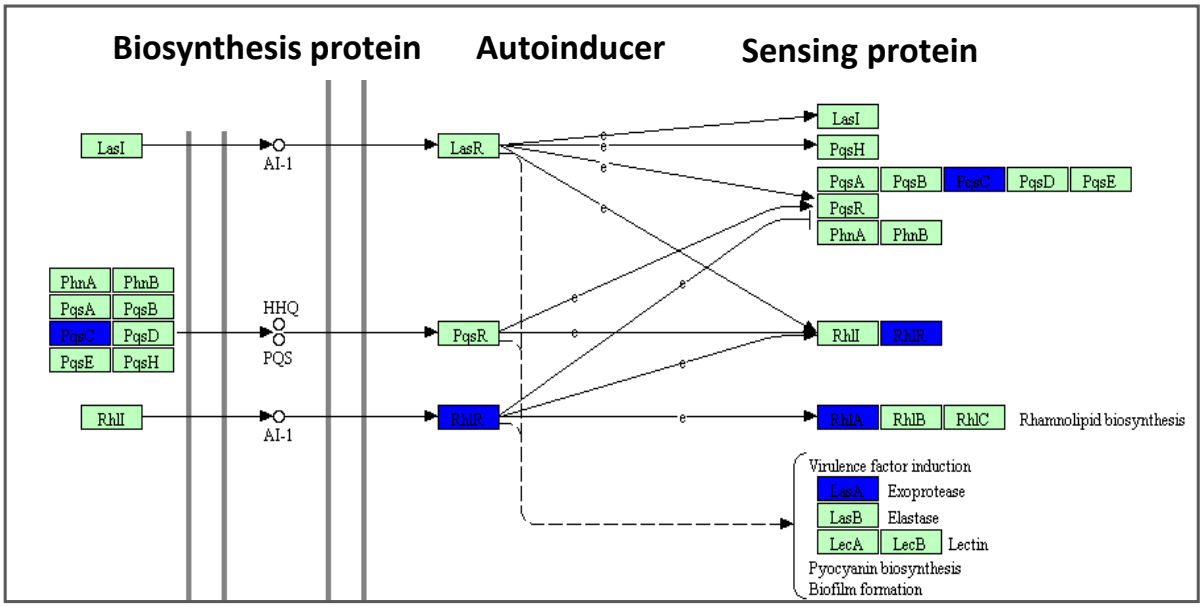

Fig. 6.25 KEGG maps depicting changes to quorum sensing pathways KEGG mapping depicts downregulation of the quorum sensing pathway in *P. aeruginosa* exposed to *A. fumigatus* CuF. SSDA proteins (blue) arising from Student's t-test involved in this pathway are highlighted.

Table 6.3 Processes affected by exposure to 72-hour SAB. SSDA proteins ($p < 0.05$) and associated categories and corresponding increases to the relative fold change in *P. aeruginosa* exposed to *A. fumigatus* 72-hour CuF produced in SAB.

Category	Gene	Protein name	Fold change
Phenazine Biosynthesis	phzA2	Phenazine biosynthesis protein PhzA2	12.6
	phzD1	Phenazine biosynthesis protein PhzD1	3.2
	phzB2	Phenazine biosynthesis protein PhzB2	2.8
Amino acid metabolism	PA0531	glutamine amidotransferase	10.2
	trpA	Tryptophan synthase alpha chain	1.9
	speE1	Polyamine aminopropyltransferase 1	1.7
	alr	Alanine racemase, biosynthetic	1.6
	proC	Pyrroline-5-carboxylate reductase	1.6
	leuB	3-isopropylmalate dehydrogenase	1.5
	cmoA	Carboxy-S-adenosyl-L-methionine synthase	1.5
	pyrC	Dihydroorotase	1.5
	PA1307	Glutamine amidotransferase type-2 domain-containing protein	1.5
	mmsB	3-hydroxyisobutyrate dehydrogenase	1.5
	aroE	Shikimate dehydrogenase (NADP(+))	1.5
Response to antibiotics	pfpI	Protease PfpI	1.9
	PA2915	Lactamase_B domain-containing protein	1.6
	algR	Positive alginate biosynthesis regulatory protein	1.7
	mucB	Sigma factor AlgU regulatory protein MucB	1.5
Response to stress	PA3628	S-formylglutathione hydrolase	2.2
	adhC	S-(hydroxymethyl)glutathione dehydrogenase	1.9
	rpoS	RNA polymerase sigma factor RpoS	1.6
	hslO	33 kDa chaperonin	1.6
	PA0361	Probable gamma-glutamyltranspeptidase	1.6
	xthA	Exodeoxyribonuclease III	1.9
	rsmA	Ribosomal RNA small subunit methyltransferase A	1.9
	tadA	tRNA-specific adenosine deaminase	1.9
	pmpR	Transcriptional regulatory protein PmpR	1.8
	purE	N5-carboxyaminoimidazole ribonucleotide mutase	1.8
Transcriptional & **translational**	sfsA	Sugar fermentation stimulation protein	1.7
	rnk	Nucleoside diphosphate kinase regulator	1.7
	xpt	Xanthine phosphoribosyltransferase	1.7

regulation	rimM	Ribosome maturation factor RimM	1.6
	guaB	Inosine-5'-monophosphate dehydrogenase	1.6
	rpoA	DNA-directed RNA polymerase subunit alpha	1.6
	rpoS	RNA polymerase sigma factor RpoS	1.6
Transcriptional & translational regulation	rsfS	Ribosomal silencing factor RsfS	1.6
	zapA	Cell division protein ZapA	1.6
	zapE	Cell division protein ZapE	1.5
	prfA	Peptide chain release factor 1	1.5

Table 6.4 Processes affected by exposure to 72-hour SAB. SSDA proteins ($p < 0.05$) and associated categories and corresponding decreases to the relative fold change in *P. aeruginosa* exposed to *A. fumigatus* 72-hour CuF produced in SAB.

Category	Gene	Protein name	Fold change
Iron binding proteins	pchA	Salicylate biosynthesis isochorismate synthase	-15.4
	pchB	Isochorismate pyruvate lyase	-8.9
	pchG	Pyochelin biosynthetic protein PchG	-8.3
	ccoN2	Cytochrome c oxidase, cbb3-type, CcoN subunit	-4.4
	ccoP2	Cbb3-type cytochrome c oxidase subunit	-3.9
	hemN	Oxygen-independent coproporphyrinogen III oxidase	-3.5
	ccoN1	Cytochrome c oxidase, cbb3-type, CcoN subunit	-2.2
	ccoO2	Cytochrome c oxidase, cbb3-type, CcoO subunit	-1.9
	kynA	Tryptophan 2,3-dioxygenase	-1.7
	pfeR	Transcriptional activator protein PfeR	-1.6
Sulphur metabolism	cysI	Sulfite reductase	-5.9
	cysNC	Bifunctional enzyme CysN/CysC	-3.5
	antC	Anthranilate dioxygenase reductase	-1.8
	cysD	Sulfate adenylyltransferase subunit 2	-1.8
	thiG	Thiazole synthase	-1.5
Quorum sensing			
	pqsC	2-heptyl-4(1H)-quinolone synthase subunit PqsC	-2.7
	pqsB	2-heptyl-4(1H)-quinolone synthase subunit PqsB	-1.5
	*pqsD	Anthraniloyl-CoA anthraniloyltransferase	-1.38
Elastase	rhlA	3-(3-hydroxydecanoyloxy)decanoate synthase	-3.7
	rhlR	Regulatory protein RhlR	-1.5
Membrane	LasA	Protease LasA	-8.0
	bamB	Outer membrane protein assembly factor BamB	-8.5

* Although pqsD did not meet the threshold for differential abundance (i.e. a fold change of +/-1.5 fold), it is included due to its association with pqsB and pqsC.

6.3 Discussion

The ubiquitous nature of *A. fumigatus* is attributed to its extensive range of enzymes, which allow it to consume nutrients from a variety of sources and compete with a vast number of other species that occupy similar niches. In this chapter, a potentially novel anti-bacterial compound produced by *A. fumigatus* in a low pH (< 5.6), nutrient rich medium, Sabouraud dextrose broth (SAB), was investigated. SAB is composed of dextrose, which provides a rich carbon source, and pancreatic digest of casein and peptic digest of animal tissue, which provides a nitrogen source for fungal growth (Hare, 2013). The anti-bacterial compound was produced specifically in this medium during the early stationary phase of *A. fumigatus* growth (between 48 and 72 hours) and not in other growth media (Fig. 6.1A-C). Moreover, the compound was not produced with the same effect by *A. nidulans* or *A. flavus* (Fig. 6.1D). Differences in the production of bioactive compounds which mediate competition between the three *Aspergillus* species have been reported (Losada *et al.*, 2009). These variations are largely regulated by environmental conditions such as nutrient availability and temperature (Bode *et al.*, 2002; Losada *et al.*, 2009).

The results presented in this chapter describe a natural bioactive compound with anti-bacterial activity against a range of pathogens including *P. aeruginosa* strain PAO1, an MDR strain of *E. coli* (PEK499), *K. pneumonia* and *S. aureus* (Fig. 6.1, Fig. 6.4, Fig. 6.6). The ability of the compound to inhibit the growth of Gram-negative and Gram-positive bacteria suggest broad-spectrum antibiotic activity.

The characterization and identification of small molecules such as anti-microbial peptides, relies on the collective analysis obtained from analytical tools such as NMR and high-resolution MS, in addition to preparative methodologies such as liquid chromatography (Xiao *et al.*, 2012). In this chapter, the physiochemical properties of the compound were investigated by accordingly. Gradual fractionation of the culture filtrates produced by *A. fumigatus* in SAB was performed with a view to isolating the bioactive agent. This process revealed an extremely polar, low molecular weight (<3 kDa) metabolite with weak light absorption at 254 nm (Fig. 6.5, 6.9C, 6.11D). However, the consistent retention time of the compound (5.0-5.2 minutes) allowed some certainty that the compound could be fractionated at this time point. The early retention time also

indicated the polar nature of the compound. This feature was exemplified by the mobile phase in which the compound was removed from the HPLC column, i.e. water with 0.1 % TFA and its inability to dissolve in methanol once lyophilised. The polarity was a key obstacle to isolating the compound by solid phase extraction (SPE) methods. Thin layer chromatography using silica plates as the stationary phase and a polar (methanol) solvent in the mobile phase did not separate the compound (Fig. 6.5). As many SPE methods are silica-based (Huck and Bonn, 2000), this posed a further challenge in terms of separating and concentrating the product based on cation or anion exchange due to the difficulties associated with separating the compound from the silica resin. However, the polarity of the compound allowed for the separation of polar from non-polar fractions using C18 Sep-Pak columns as the non-polar component was contained in the column while the polar flow through could be collected. Further separation was obtained using cation exchange C18 columns, and although the level of ion exchange was unpredictable, these columns were relied upon as an extra "cleaning" step as opposed to ion separation specifically, and provided better separation on the HPLC column.

Such was the potency of the compound that several fractionation steps by SPE and HPLC did not remove the activity from the compound. However, while several fractionation steps were performed on the HPLC to remove non-polar and other contaminants, one of the main challenges faced with isolating the active compound was the inherent presence of glucose contained within the samples. This raised some difficulties during NMR analysis as the signals from the compound were masked by more prominent glucose signals (Fig. 6.13). Because glucose is a polar compound, glucose removal from the compound by SPE was not an option. Boronic acids are known to have affinity for sugar residues (Wu *et al.*, 2013; Awino *et al.*, 2016). As such, removal of glucose residues was attempted using boronic acids immobilized in solid supported resin beads at various pH. However, this approach was unsuccessful in removing the excess sugar from the samples and NMR analysis proceeded in the presence of sugar.

Comparative analysis by 1H NMR revealed several distinct features that were evident in the fractions containing anti-bacterial activity, that were less visible in fractions that had some activity and undetectable in the fractions that had no activity. For example, fractions isolated from processed SAB and collected by HPLC showed most anti-bacterial activity in fraction 2, less in fraction 3 and none in fraction 1 (Fig. 6.9D). Analysis by 1H NMR on these fractions (Fig. 6.16), revealed distinct peaks in the aliphatic region of the

spectra (0-3 ppm) in fraction 2. Although weaker, these signals were detected in fraction 3, and absent in fraction 1. As peak height is indicative of concentration, this suggests that the peaks observed here belong to the structure that formulates the compound. This was somewhat unexpected because aliphatic molecules tend to be hydrophobic and thus contradict the strength of hydrophilicity of this compound. However, as anti-microbial peptides tend to be amphipathic (similar proportion of polar and non-polar amino acids), these findings may account for the non-polar determinant (Jiménez *et al.*, 2018).

Several peaks that were unique to the biologically active fractions were detected between 4.05 ppm and 5.2 ppm on the 1H NMR spectra (Fig. 6.18A and Fig. 6.18B) However as this is the region where glucose is detected, it was difficult to ascertain with clarity, what these peaks represent. A complex splitting pattern revealed a quartet of doublets (Fig. 6.19), a triplet and a singlet, in the aliphatic region of the spectra representing the fractions with the greatest amount of antimicrobial activity. These signals were weaker in the fraction containing slightly less activity but detectable nonetheless. In contrast, these signals were absent in the fraction containing no activity (Fig. 6.19). This complex splitting pattern is indicative of a cyclic (ring-like) structure. Due to the coupling pattern, the aliphatic signals in this region are indicative of polar amino acid side groups and suggest the presence lysine or glutamine. This would account, in part, for the water solubility of the compound. Finally, 13 C NMR indicated towards an anomeric carbon other than glucose (Fig. 6.14). This suggests the presence of a glycosylated residue and may explain in part, the presence of excess glucose signals in the sample (Fig. 6.13). Moreover, this may explain the hydrophilic nature of the compound.

To investigate the identity of the compound further, LC/MS was performed in positive and negative mode on several fractions with and without anti-bacterial activity (Fig. 6.20 and Fig. 6.21). Comparisons were made between the total ion chromatograms generated from the different fractions. A range of concentrations (1- 10 µg/ml) were analysed by LC/MS although significant differences between the fractions were not detected. Several potentially interesting ions potential were analysed by MS/MS. Ion maps of the various fractions were generated and compared against each other (Fig. 6.20C and Fig. 6.21C). However, these analyses did not yield definitive results. Given the high concentrations of the compound that was analysed by mass spectrometry, it was expected that major differences would be observed between fractions, as was in the NMR analysis. One possible explanation for this is that the bioactive compound is not charged. Mass

spectrometry measures the mass of charged particles and as such, only ions are detected (El-Aneed *et al.*, 2009). Thus, a neutral compound is not suitable for analysis with this approach. To overcome this obstacle, a charge can be applied to the sample by chemical derivatization with charged groups (Krusemark *et al.*, 2009). However, this requires some prior knowledge of the compound structure.

Analysis of the larger fractions (> 3 kDa) of the 72-hour *A. fumigatus* CuF by MS revealed an abundance of enzymes involved in fungal cell wall biosynthesis and integrity and in the breakdown and assimilation of nutrients (Table A6.1). A group of enzymes including peptidases and phosphatases involved in protein degradation and catalytic activity respectively, at low pH were detected (e.g. Tripeptidyl-peptidase sed2 and sed4, acid phosphatase). This highlights a role for environmentally controlled enzymes in the fungus, which has implications for the type of anti-bacterial compounds produced (Losada *et al.*, 2009). Acyl-CoA binding protein was also detected in this dataset and, given its role in NRP synthesis (Bloudoff and Schmeing, 2017), this may be indicative of the type of anti-bacterial compound under investigation.

Analysis of the bacterial proteome in response to sub-lethal or sub-inhibitory levels of antibiotics provides invaluable information as to how bacteria respond to, and acquire resistance to antibiotics (Pérez-Llarena and Bou, 2016; Jones-Dias *et al.*, 2017; Hashemi *et al.*, 2019; Opoku-Temeng *et al.*, 2019). Moreover, this approach may be employed to assess the antibiotic mode of action (Bandow *et al.*, 2003; Lok *et al.*, 2006).

In this study, a label-free quantitative (LFQ) proteomics approach was employed to examine the proteomic response of *P. aeruginosa* to exposure of the *A. fumigatus* anti-bacterial compound and to investigate its mode of action against the bacteria. The response of *P. aeruginosa* to sub-inhibitory levels of the CuF was characterized, in part, by an increase in the relative abundance of LPS-producing enzymes, rhamnolipids, stress response proteins and phenazine biosynthetic proteins and upregulation of translation (Fig. 6.24A; Table 6.3). In contrast, there was a distinct decrease in the relative abundance of proteins associated with the membrane, quorum-sensing (QS) regulation, iron binding proteins, siderophores biosynthesis and sulphur metabolism (Fig. 6.22B, Fig. 6.24B and Fig. 6.25, Table 4). Despite its exposure to a relatively low concentration of *A. fumigatus* CuF (i.e. 30 % v/v compared to 50 % v/ used for toxicity assays), a clear antibiotic-mediated effect was observed in the bacterial proteome (Fig. 6.19).

A classic bacterial response to antibiotics is the upregulation of pathways and processes associated with LPS production and alterations to membrane transport proteins (Ghai and Ghai, 2018). Here, a decrease in the relative abundance of several membrane proteins was observed in the dataset, including protein-export membrane protein SecG, outer membrane porin OprE and Na(+)-translocating NADH-quinone reductase (decreased by 2.3-, 1.87- and 2.2-fold respectively). In contrast the relative abundance of proteins associated with O-antigen biosynthesis, Glucose-1-phosphate thymidylyltransferase, dTDP-4-dehydrorhamnose 3,5-epimerase and dTDP-4-dehydrorhamnose reductase (encoded by rmlA, rmlC and rmlD respectively) was increased between 1.7- and 1.74-fold (. O-antigen forms part of the LPS out membrane structure of Gram-negative bacteria. The increase in LPS biosynthesis is a well-established mechanism for maintaining antibiotic resistance by decreasing the permeability of the cell membrane to antibiotics (Delcour, 2009; Hashemi *et al.*, 2019; Sharp *et al.*, 2019). These proteins are also involved in rhamnolipid production, the synthesis of which is increased under iron-limiting conditions (Guerra-Santos *et al.*, 1986; Ochsner and Reiser, 1995). Rhamnolipids are important regulators of cell motility, cell-cell interactions and biofilm formation and possess intrinsic anti-microbial activity (Dusane *et al.*, 2010).

The phenazine biosynthetic pathway was significantly increased in bacteria exposed to the *A. fumigatus* CuF (Fig. 6.24A). A notable fold-increase in several proteins involved in this pathway was detected, including Phenazine biosynthesis protein PhzA2 (12.6-fold), PhzD1 (3.2-fold) and PhzB2 (2.8-fold), and glutamine amidotransferase (10.2-fold) (Table 6.3). The latter protein is responsible for supplying ammonia that is used to convert chorismate into aminodeoxyisochorismate which is used in the biosynthesis of phenazines (Culbertson and Toney, 2013). Phenazines (e.g. pyocyanin) are redox active pigments that regulate bacterial redox homeostasis, affect metabolic pathways and gene expression and promote resistance against antibiotics in bacterial biofilms (Price-Whelan *et al.*, 2007; Schiessl *et al.*, 2019). Phenazine biosynthesis is induced in nutrient-depleted environments, such as iron limitations (Nguyen *et al.*, 2015), and is deployed as an antimicrobial during competitive interactions with other species such as *A. fumigatus* (Briard *et al.*, 2015).

The RNA polymerase sigma factor, encoded by RpoS, orchestrates the transcription of genes associated with environmental stress response (Lu *et al.*, 2018).

This protein and DNA-directed RNA polymerase subunit alpha, encoded by RpoA were increased along with several other ribosome-associated proteins, transcriptional and translational regulators and antibiotic-degrading enzymes, suggesting the upregulation of a stress response to antibiotic exposure (Fig. 6.24A; Table 6.3). An RpoS-dependent small regulatory RNA, RgsA is a transcriptional inhibitor of AcpP1, the gene encoding acyl carrier protein 1 (Lu *et al.*, 2018). The dataset here revealed a decrease in the relative abundance of acyl carrier protein. In the context of QS, this may be important because acyl carrier proteins are involved in the synthesis of QS molecules, N-acylhomoserine lactones (C4-HSL, 3-oxo-C12-HSL), *Pseudomonas* quinolone signal (PQS) and rhamnolipids.

This finding was in line with the observation in the dataset, of the decrease in the relative abundance of proteins associated with the QS pathway in bacteria exposed to the *A. fumigatus* CuF (Fig. 6.24B, Fig. 6.25, Table 6.4). Specifically, there was a decrease in the relative abundance of 2-heptyl-4(1H)-quinolone synthase subunit PqsC (encoded by PqsC, decreased by 2.7-fold), 2-heptyl-4(1H)-quinolone synthase subunit PqsB (encoded by pqsB, decreased by 1.5-fold), anthraniloyl-CoA anthraniloyltransferase (encoded by pqsD, decreased by 1.38-fold), and 3-(3-hydroxydecanoyloxy) decanoate synthase (encoded by rhlA, decreased by 3.7-fold). Pqs proteins are required for the biosynthesis of the PQS signalling pathway (Gallagher *et al.*, 2002) which utilizes the alkylquinolone signals, 2-heptyl-4(1H)-quinolone and 2-heptyl-3-hydroxy-4(1H)-quinolone, to regulate biofilm formation and the biosynthesis of phenazines, rhamnolipids and siderophores (Heeb *et al.*, 2011). PQS also functions as an iron chelator (Tettmann *et al.*, 2016; Lin *et al.*, 2018). Interestingly, the relative abundance of phenazine and rhamnolipid biosynthetic proteins were increased in bacteria exposed to *A. fumigatus* CuF, despite a decrease in the levels of proteins associated with the QS pathways that regulate the induction of genes encoding these proteins. This highlights the ability of these pathways and process to function independently of each other (Farrow *et al.*, 2015).

Because phenazine biosynthesis is regulated in part, by limited iron availability, an increase in the relative abundance of proteins associated with phenazine biosynthesis may be explained by a decrease in the relative abundance of proteins associated with the synthesis of pyochelin, a *P. aeruginosa* siderophore (Fig. 6.24B; Table 6.4). Pyochelin is also involved in chelating copper and zinc, and thus provides a valuable mechanisms of nutrient acquisition for the cell (Brandel *et al.*, 2012). LFQ proteomics revealed a

significant decrease in the relative abundance of proteins involved in pyochelin biosynthesis in bacteria exposed to the *A. fumigatus* CuF, including salicylate biosynthesis isochorismate synthase (encoded by pchA, decreased by 15.4-fold), isochorismate pyruvate lyase (encoded by pchB, decreased by 8.9-fold), and pyochelin biosynthetic protein PchG (encoded by pchG, decreased by 8.3-fold). PchA is the first enzyme in salicylate formation, and this pathway ultimately concludes with the production of pyochelin (Gaille *et al.*, 2003). The reduced levels of this protein in bacteria exposed to *A. fumigatus* CuF may indicate reduced levels of pyochelin (Gaille *et al.*, 2003). The relative abundance of several other iron-binding proteins was significantly decreased in bacteria exposed to *A. fumigatus* CuF (Table 6.4). These proteins included iron-binding oxidases, sulphite reductase and the PfeR (decreased by 1.6-fold), which regulates expression of ferric enterobactin,, another *P. aeruginosa* siderophore (Dean *et al.*, 1996; Moynié *et al.*, 2019). Proteins associated with the third *P. aeruginosa* siderophore, pyoverdin were not identified in this dataset.

It is well established that *P. aeruginosa* differentially regulates its iron-uptake systems depending on the environmental conditions to which it is exposed. Although a more efficient uptake system, pyoverdin is more metabolically expensive. In contrast, pyochelin is a less efficient system for iron uptake but is also (metabolically) less costly (Dumas *et al.*, 2013). Pyochelin-deficient *P. aeruginosa*, expressing pyoverdin only, grows better under iron-limiting conditions than pyoverdin-deficient strains expressing pyochelin only. On the other hand, pyoverdin-deficient strains producing pyochelin only, grew better under moderate iron limitations than pyochelin-deficient strains expressing pyoverdin only (Dumas *et al.*, 2013). This indicates that *P. aeruginosa* balances iron-acquisition mechanisms with the energy costs for producing these siderophores.

Taken together, these results show a decrease in the relative abundance of several iron-acquisition proteins and in increase in the relative abundance of proteins induced by iron limitations. This suggests that the mechanism of action employed by the *A. fumigatus* CuF may be characterized by its ability to limit iron availability for the bacteria, which consequently induces a metabolically expensive stress response and inhibits bacterial growth. *A. fumigatus* produce siderophores that protect the fungus against the anti-fungal activity of *P. aeruginosa* (Sass *et al.*, 2019). Thus, the proteomic response of the bacteria to the CuF may hold clues as to the mechanism of action and the identity of the antibacterial compound. Further studies using siderophore-deficient strains of *A.*

fumigatus will be invaluable in determining whether siderophores are responsible for the antibacterial effect observed in theis CuF.

Downregulation of QS pathways also point towards the possibility that the antibacterial compound possesses activity that inhibits QS. QS inhibitors are small molecules with the ability to interfere with QS-mediated gene expression (Padder *et al.*, 2018). QS inhibitors have been described in a number of fungal species, the classic example being the *Penicillium* species (Rasmussen *et al.*, 2005). Given the close proximity in which *A. fumigatus* and *P. aeruginosa* reside in the environment and in the cystic fibrosis airways, it is not outside the realms of possibility that *A. fumigatus* possess mechanisms beyond our knowledge, with which to subdue bacterial growth.

6.4 Conclusion

NMR is an invaluable tool for elucidating peptide structures. Coupled with mass spectrometry, this technology plays a major role in anti-microbial peptide discovery and design. However, as is evident from the results presented in this chapter, separation of the compound from the original source prior to and for the purpose of analysis is imperative for successful identification. The success of peptide identification is also governed in many ways, by the physiochemical properties that characterize a particular compound. Here, the separation of a compound with potent broad-spectrum anti-bacterial was contained in a complex liquid filtrate obtained from a fungal culture. A number of obstacles prevented complete characterization of the compound within the limitations of this research. 1) Compound identity by NMR was obstructed by the intrinsic abundance of free glucose, which masked a number of potentially important signals required for structural characterization. 2) The polarity of the compound made it difficult to analyse by traditional HPLC and mass spectrometry methods, which require the use of non-polar solvents. 3) Compound identification by MS/MS methods was not possible without altering the charge of the compound, which appeared to be neutral. 4) Altering the charge by the addition of a chemical adduct requires knowledge of specific residues contained within the compound. Nevertheless, even within these limitations, informative data was obtained with collective analysis by HPLC, mass spectrometry and NMR. Further in-depth analysis by NMR including additional 2D experiments including COSY and TOCSY should be performed to account for the observed multiplicities. This may provide vital information regarding the characteristics of functional groups that may be amenable to chemical modification (e.g. acetylation). The potential for chemical derivatization may reintroduce mass spectrometry as an option for investigating the identity of this compound and overcome the problems arising from analysis of neutral compounds.

LFQ proteomics was employed to investigate changes to the proteome of *P. aeruginosa* when exposed to the antibacterial agent contained in the culture filtrates of *A. fumigatus*. The proteomic data arising from this approach provided informative clues as to the mechanism of action used by the compound to inhibit bacterial growth. Iron-dependent processes and QS pathways were processes most affected by exposure to the fungal culture filtrates.

Chapter 7

General Discussion

7.1 General Discussion

By definition, polymicrobial communities are a collection of microbial species that co-exist in a particular habitat (Peters *et al.*, 2012). Arising from co-habitation, interspecies interactions occur and these interactions shape the landscape of the environment in which the microbial communities reside (Murray *et al.*, 2014). When that environment exists in humans, such interactions can influence the health status of an individual. In the context of infectious disease, polymicrobial interactions can be synergistic, whereby the combined effect of multiple microbial species is worse than that where individual species act alone (Murray *et al.*, 2014). On the other hand, antagonistic interactions arise due to competition, and occur when one species suppresses the other (Gabrilska and Rumbaugh, 2015). The mechanisms employed by microbes as a consequence of these interactions is very often detrimental to host health (Peters *et al.*, 2012). Inter-species interactions may influence microbial pathogenesis by altering microbial virulence factors, and ergo, disease progression. Thus, an understanding of how polymicrobial communities, interact with each other and with the host is important when deciding appropriate therapeutic strategies (Peters *et al.*, 2012; Yang *et al.*, 2015).

The cystic fibrosis airways are characterized by chronic infection caused by a multitude of microbial species, and thus represent an excellent model for elucidating the interactions that occur between these species and the outcomes arising from these interactions, both for the host and for the pathogens involved (Filkins and O'Toole, 2015; Darch *et al.*, 2017). Traditionally, chronic CF infections were associated with a limited number of pathogens, which included *Haemophilia influenzae, Staphylococcus aureus*, *Pseudomonas aeruginosa* and *Burkholderia cepacia*. With the advent of culture-independent techniques, there came an appreciation of the diverse nature of the microbial community that exists in the CF airways (Harrison, 2007; Filkins *et al.*, 2012). Nonetheless, with each annual report published by international CF registries, *P. aeruginosa* is consistently identified as the most common pathogen isolated from the CF airways of patients after their first decade of life (Cystic Fibrosis Trust, 2014; CF Registry of Ireland 2017 Annual Report, 2017; Cystic Fibrosis Foundation, 2018). Coupled with this, *Aspergillus fumigatus* is the most common fungal pathogen that is isolated from CF sputum samples (Sudfeld *et al.*, 2010; Reece *et al.*, 2017b).

While the impact on the CF airways by bacterial pathogens, such as *S. aureus, P. aeruginosa* and *B. cepacia* is well established, less is known about the participation of fungal pathogens in disease progression (Govan and Deretic, 1996; Lyczak *et al.*, 2002; Leclair and Hogan, 2010; Williams *et al.*, 2016b; Delfino *et al.*, 2019). However, a greater acknowledgment for the role of fungal pathogens in CF pathogenesis is beginning to emerge and the impact these microbes have on influencing disease progression is the focus of many studies (Williams *et al.*, 2016b; King *et al.*, 2016a).

A. fumigatus is frequently isolated from the lungs of CF patients, yet despite its propensity to cause disease in immunocompromised individuals, this pathogen is succeeded by *P. aeruginosa* as the primary pathogens in the CF airways and persistent infection with *P. aeruginosa* is associated with higher rates of mortality (Ratjen and Döring, 2003; Crull *et al.*, 2016). However, co-colonization by *A. fumigatus* and *P. aeruginosa* is associated with a greater decline in lung function and higher rates of pulmonary exacerbations than colonization by either pathogen alone (Reece *et al.*, 2017). Interestingly, *A. fumigatus* has been reported as the only fungal pathogen associated with an increased risk for *P. aeruginosa* infection to occur (Hector *et al.*, 2016). What drives pulmonary exacerbation when the two pathogens are present, remains to be fully elucidated (Williams *et al.*, 2016; Briard *et al.*, 2019). The purpose of this thesis was to close that knowledge gap by providing valuable insights into the molecular mechanisms that mediate the interactions between *A. fumigatus* and *P. aeruginosa*.

Advances in high-throughput proteomics and associated computational tools, have made this approach a widely accepted method for studying pathogen-host and pathogen-pathogen interactions (Graham *et al.*, 2007; Kamath *et al.*, 2015; Yang *et al.*, 2015; Jean Beltran *et al.*, 2017). However, the complexity that underpins these interactions poses several challenges, such as isolating individual species after a period of co-incubation, or finding a suitable medium that does not unintentionally support the growth of one species over the other (Gabrilska and Rumbaugh, 2015). The experimental design applied to the co-infection studies described in Chapter 3, 4 and 5 of this thesis aimed to address some of these challenges with a view to gaining a better understanding as to the dynamics that occur between *A. fumigatus* and *P. aeruginosa* and, in the context of infection, how the interactions between these pathogens affect the host. In essence, three main questions formed the basis for the first three results Chapters in this thesis:

1) What is the response of the host to co-infection and how does this compare when it is infected with only one pathogen?

2) What are the molecular mechanisms that enable *P. aeruginosa* to become a more prolific pathogen in the presence of *A. fumigatus*?

3) What are the molecular mechanisms that enable these two pathogens to co-exist in the same habitat?

LFQ proteomics was employed to discover the answers to these questions. With this approach, it was possible to delineate how one organism responds to the presence of another by investigating the changes that occur in the proteome of that organism.

In Chapter 3, the alveolar epithelial cell line, A549, was employed to investigate the host cellular proteomic response to exposure with *A. fumigatus* or *P. aeruginosa* alone and compare this with the response to exposure with both pathogens. The decision to take this approach arose from clinical studies which report that co-infection with both pathogens results in poorer lung function than infection with either one (Amin *et al.*, 2010; Reece *et al.*, 2017). LFQ proteomics was employed to investigate changes in the proteome of A549 cells that had been exposed to either *A. fumigatus* or *P. aeruginosa* for 12 hours and to compare these changes, with those occurring due to co-exposure with both pathogens for 12 hours. Some cellular responses were common to infection caused by either pathogen, including an increase in oxidative stress and immune system responses, and a decrease in translation and structural integrity. Other responses appeared to be pathogen-specific. For example, proteins associated with processing in the ER increased in cells exposed to *P. aeruginosa* compared to *A. fumigatus*-exposed cells and unexposed cells. These results demonstrate that some host cellular responses to different pathogens are distinct from others and are indicative of how a pathogen might initiate infection by inducing particular host responses (Bertuzzi *et al.*, 2019).

A feature of bacterial infection, which was not observed in cells exposed to *A. fumigatus* was the loss of integrity in A549 cells after exposure to *P. aeruginosa*. The morphology of the cells changed from a flat, cobblestone shape, to smaller, rounded shaped cells in cells that had been exposed to bacteria for 12 hours. This morphology is characteristic of cells undergoing oxidative stress (Smit-de Vries *et al.*, 2007) and the absence of such a morphology in cells exposed to *A. fumigatus* suggest the levels of oxidative stress induced by the fungal pathogen are less than that of *P. aeruginosa*. As a

human pathogen, *A. fumigatus* is known to subvert the host recognition response through a molecular mechanism controlled by DHN-melanin, a pigment that coats the conidial wall (Amin *et al.*, 2014; Heinekamp *et al.*, 2015). Conidia that enter A549 cells can avoid degradation by acidic compartments in the host cell allowing time for conidia to germinate (Wasylnka and Moore, 2002; Wasylnka, 2003). Thus, although after 12 hours A549 cells looked relatively "unstressed" compared to *P. aeruginosa*-exposed cells, the proteomic analysis of these cells told a different story characterized by alterations to ribosome activity, mitochondrial activity, and components of the immune response.

In reality, pulmonary epithelial cells are subject to exposure by multiple pathogens. Due to difficulties in obtaining information from multi-species interactions, the whole cell proteomic response of A549 cells to exposure by more than one pathogen has not been characterized. To address this knowledge gap, LFQ proteomics was performed on A549 cells that had been co-exposed to *A. fumigatus* and *P. aeruginosa* for 12 hours with a view to comparing this response with that of the response to the individual challenges. Preliminary experiments revealed that the replication of *P. aeruginosa* increased exponentially in the presence of *A. fumigatus.* Consequently, a hypothesis was generated that *A. fumigatus* promotes the growth of *P. aeruginosa.* This hypothesis was subsequently validated. To investigate this further, an alternative approach was chosen, whereby A549 cells were exposed to *A. fumigatus* for eight hours, followed by *P. aeruginosa* for a further four hours. To determine specifically how a sequential infection differs from an individual one, comparative LFQ analysis was conducted on A549 cells exposed to *A. fumigatus* or *P. aeruginosa* or sequential exposure to both pathogens. The results revealed distinct changes to the host-cell proteome in response to either or both pathogens. Key signatures of infection were retained amongst all pathogen-exposed groups, including changes in mitochondrial activity and energy output. However, by comparison to cells challenged with *A. fumigatus* or *P. aeruginosa*, the response of sequentially exposed A549 cells was characterized by a decrease in the relative abundance of proteins associated with endocytosis, phagosomes and lysosomes. These findings indicate that A549 cells responded to infection with either *A. fumigatus* or *P. aeruginosa* by initiating a pathway of phagocytosis and pathogen degradation but sequentially challenged cells were unable to upregulate a similar process of pathogen elimination. The sequence of pathogen exposure suggests that *A. fumigatus* render A549 cells unable to internalize bacteria, thereby providing an environment in which *P.*

aeruginosa can proliferate. The ability of *A. fumigatus* conidia to interfere with pathogen up-take and processing by a variety of human cells is well established (Bertout *et al.*, 2002; Aimanianda *et al.*, 2009; Thywißen *et al.*, 2011; Amin *et al.*, 2014). Thus, an inability to clear microbial infection by phagocytosis and reduced intracellular degradative abilities could be detrimental to the host and favour pathogen survival and proliferation. This research provided novel insights into the whole-cell proteomic response of A549 cells to *A. fumigatus* and *P. aeruginosa*, and highlights distinct differences in the proteome following sequential exposure to both pathogens, which may explain why *P. aeruginosa* can predominate.

In Chapter 4, question two was addressed, i.e. what are the molecular mechanisms that enable *P. aeruginosa* to become a more prolific pathogen in the presence of *A. fumigatus*? In an effort to characterize the proteomic response of *P. aeruginosa* to exposure by *A. fumigatus* culture filtrates, the ability of *P. aeruginosa* to proliferate rapidly in what is classically a nutrient-poor liquid medium was analyzed. Czapek-Dox is traditionally used to drive *A. fumigatus* into secondary metabolite production, particularly the production of gliotoxin (Gardiner and Howlett, 2005; Thrane *et al.*, 2007; Dolan *et al.*, 2014; Owens *et al.*, 2014; Johns *et al.*, 2017). The observations made in this Chapter were in agreement with findings from other studies; gliotoxin inhibits the growth of *P. aeruginosa* (Reece *et al.*, 2018). However, exposure of *P. aeruginosa* to *A. fumigatus* culture filtrates produced prior to high levels of gliotoxin production (i.e. between 48 and 72 hours), revealed increased rates of bacterial growth compared to the growth of bacteria in sterile Czapek-Dox medium. Mass spectrometry-based proteomic analysis of the *A. fumigatus* culture filtrate (*A. fumigatus* CuF) produced at 48 hours identified an abundance of peptidases and proteases in the medium, suggesting an increase in the levels of amino acids resulting from enzymatic degradation. Indeed, a hallmark of the *A. fumigatus* secretome is the abundance of degradative enzymes, which facilitate the acquisition of nutrients from a range of different substrates thereby ensuring ubiquity in a vast range of environments (de Vries and Visser, 2001; Dagenais and Keller, 2009; Sharma Ghimire *et al.*, 2016). The hypothesis that *A. fumigatus* created an environment characterized by an abundance of amino acids on which *P. aeruginosa* could thrive, was supported by the ninhydrin assay, a method commonly used for the detection of amino acids (Friedman, 2004) which demonstrated increased mounts of free amino acids.

The objective of this Chapter was in part, to characterize the proteomic response of *P. aeruginosa* to interactions with *A. fumigatus*. However, as highlighted previously, the need to separate multiple species in order to analyse the effect on one is a major obstacle for delineating polymicrobial interactions (Darch *et al.*, 2017). To overcome this challenge, *A. fumigatus* and *P. aeruginosa* were co-cultured to create a culture filtrate (CuF) containing the secretome of both organisms generated while in the presence of each other. Interestingly, compared to bacteria exposed to the culture filtrate produced in its own culture, the Co-culture CuF promoted the growth of *P. aeruginosa* more than that produced by *A. fumigatus* alone. A prominent feature of the response detected in the proteomic comparison between bacteria exposed to its own (*P. aeruginosa*) CuF and Co-culture CuF, was a decrease in the relative abundance of several ABC transporters involved with the cellular import and export of nutrients. This response is perhaps indicative of the nutrient levels available to *P. aeruginosa* when exposed to a medium processed by *A. fumigatus*. Conversely, this comparison indicates that *P. aeruginosa* does not have the same enzymatic capacity as *A. fumigatus* to degrade and to extract nutrients from Czapek-Dox. Thus, to survive, it must increase the number and abundance of transporters required to import nutrients from the nutrient-deprived environment into the cell. This highlights the ability of *P. aeruginosa* to exploit the environment created by *A. fumigatus*, which enables the bacteria to outcompete the fungus under these conditions.

LFQ proteomics performed on *P. aeruginosa* revealed a bacterial response to *A. fumigatus* CuF and Co-culture CuF in-line with that produced under anaerobic conditions. Coupled with the growth increased observed in the bacteria when exposed to *A. fumigatus* CuF and Co-culture CuF, this was interesting, particular in the context of cystic fibrosis, a disease characterized by a nitrate-rich, amino acid rich, anaerobic environment (Barth and Pitt, 1996; Palmer *et al.*, 2007b; Line *et al.*, 2014).

Investigations into the physical interactions of *A. fumigatus* and *P. aeruginosa* on a solid surface highlighted the ability of *P. aeruginosa* to compete with *A. fumigatus* and images of the bacteria growing through an established line of fungal spores, suggest *P. aeruginosa* has the molecular capability to inhibit fungal growth when in direct competition with conidiophores. However, on a semi-solid surface, *P. aeruginosa* migrated towards the fungal colonies that had formed hyphae in the agar. It is possible that the breakdown of nutrients by *A. fumigatus* mycelia in the semi-sold agar used for these swim assays, may promote the chemotaxis of *P. aeruginosa* towards the hyphae. *A.*

fumigatus adopts a foraging response in a nutrient-poor environment, which involves the extension of hyphae to identify a nutrient source (Richie and Askew, 2008). Thus, in the process of creating nutrients for itself, the fungus may also be providing a more easily assimilated source of nutrients for the bacteria. Polymicrobial interactions between the fungal mycelia and bacteria extracted from soil, have identified mycelial exudates as growth promoters of bacteria, including *Pseudomonas* species (Toljander *et al*., 2007). Interestingly, the bacterial density appeared to become reduced the closer *P. aeruginosa* came to the hyphae. *P. aeruginosa* is thought to inhibit conidial growth and alter, but not inhibit hyphal growth, possibly due to the production of secondary metabolites such a fumagillin and gliotoxin by *A. fumigatus* hyphae (Mowat *et al.*, 2010; Manavathu *et al*., 2014; Briard *et al.*, 2017).

In Chapter 5, the response of *A. fumigatus* to exposure to *P. aeruginosa* and *P. aeruginosa* culture filtrates (CuF) was investigated with respect to gliotoxin production and alterations to the proteome. Inoculation of 48-hour *A. fumigatus* cultures with varying densities of *P. aeruginosa* cells resulted in an inverse correlation between hyphal mass (measured as wet weight) and gliotoxin production. A similar outcome was observed when *A. fumigatus* cultures were exposed to the culture filtrate of *P. aeruginosa* grown in Czapek-Dox for 72 hours. These results suggest what has previously been demonstrated, that *P. aeruginosa* affects the growth of *A. fumigatus* hyphae (Briard *et al*., 2017). Moreover, *P. aeruginosa* induces oxidative stress to which *A. fumigatus* responds by producing gliotoxin, a redox active metabolite employed by the fungus to neutralize reactive oxygen species (Briard *et al.*, 2015; Dolan *et al.*, 2015). However, secondary metabolite production comes at the expense of growth, which, explains why hyphal growth was reduced in cultures containing high levels of gliotoxin (Ruiz *et al.*, 2010).

Barring complications, individuals with cystic fibrosis are not affected by invasive aspergillosis, suggesting that invasive hyphae do not form in the cystic fibrosis airways (Reece *et al.*, 2017; Schwarz *et al.*, 2018). Nevertheless, the fungus is frequently isolated from cystic fibrosis sputum. Thus, it may be more appropriate when, characterizing the interactions between *A. fumigatus* and *P. aeruginosa* in the context of cystic fibrosis, to investigate the effect on conidial or germling growth rather than fully developed hyphae, which are more characteristic of invasive aspergillosis. With this in mind, *A. fumigatus* conidia were cultured in the culture filtrate produced by *P. aeruginosa* in Czapek-Dox and in the Co-culture CuF. However, the conidia did not germinate in the culture filtrates.

Interestingly, the conidia were not killed and spores retrieved from the cultures grew when cultivated on agar plates. Thus, it is possible that in these conditions, *A. fumigatus* conidia remain dormant until such a time that is appropriate to resume growth (Sugui *et al.*, 2014).

To overcome this, conidia were allowed to germinate before they were exposed to *P. aeruginosa* CuF and Co-culture CuF. With this approach the effect of *P. aeruginosa* on the early stages of *A. fumigatus* growth could be investigated. Growth was not affected and gliotoxin concentrations were not increased relative to the control. Together, these finding suggested that the response of *A. fumigatus* to *P. aeruginosa* CuF is dependent on the stage of fungal growth. LFQ proteomic analysis supported the findings that gliotoxin production was decreased in the *A. fumigatus* cultures that had been exposed to Co-culture CuF. The relative abundance of four proteins out of the 12 encoded by genes associated with the gliotoxin gene cluster was decreased (Kwon-Chung and Sugui, 2009). Unsurprisingly perhaps, given the function of gliotoxin, the levels of proteins involved with oxidative phosphorylation was lowered in cultures exposed to Co-culture CuF.

Interestingly however, the relative abundance of proteins associated with the biosynthesis of other secondary metabolites including pseurotin A, verruculogen and fumitremorgin were increased in cultures exposed to *P. aeruginosa* CuF but not significantly in Co-culture CuF. In general, alterations to the proteome of *A. fumigatus* cultured in *A. fumigatus* CuF differed quite significantly between the fungal cultures exposed to *P. aeruginosa* CuF and Co-culture CuF, particularly in terms of secondary metabolite production and intracellular transport. These findings indicate the complexity of the *A. fumigatus* proteome and its ability to adapt to different conditions to ensure its survival.

In the final results Chapter, the identity of a potentially novel *A. fumigatus* compound, with significant anti-bacterial activity was investigated. The discovery of this compound arose from traditional screening methods, similar to those employed by Selman Waksman and his students in the 1940s, from which came the discovery of streptomycin (Valiquette and Laupland, 2015). *A. fumigatus* was cultured in several types of media and the resulting culture filtrates were applied to 96-well plates containing *P. aeruginosa*. The results presented clear inhibition of bacterial growth where exposed to the culture filtrate from an *A. fumigatus* culture grown to early stationary phase (48-72

hours) in a nutrient rich, complex media, Sabouraud dextrose broth. Sabouraud dextrose broth was formulated specifically for the growth of certain fungi that can grow well in a low pH environment. The low pH was initially intended to prevent bacterial contamination (pre-antibiotic era) (Hare, 2013). It is characterized as a complex, or undefined media based on the formulation, which includes peptone and pancreatic digests of casein and peptic digest of animal tissue as the nitrogen source, and glucose or dextrose as the carbon source (Hare, 2013).

In general, antimicrobial compounds are associated with secondary metabolism, which begins to occur in the latter stages of the stationary phase when the nutritional content of the environment becomes depleted (Ruiz et al., 2010). It was interesting then, to discover an antibiotic produced during the early stationary phase of fungal growth, in a nutrient rich environment.

With the level of anti-bacterial activity contained within the culture filtrates, one could assume that the compound was gliotoxin however activity assay performed with fractions of the culture filtrate collected from the HPLC excluded gliotoxin as a possibility and instead revealed a highly polar fraction as the compound with activity. The extreme polar nature of the compound posed challenges for obtaining separation using non-polar solvents and solvents which some would consider suitable for separating polar compounds (e.g. ethyl acetate or methanol) (Cepas *et al.*, 2019). However, separation could be obtained using a variety of silica-based solid phase extraction (SPE) columns, which allowed the non-polar fraction to be retained and the polar fraction to flow through the SPE column. With each round of separation by HPLC, contaminants surrounding the active fraction became less abundant. However, one contaminant that could not be removed was free glucose. The abundance of glucose is probably not surprising given the high concentration of the product in the starting material. Removing the glucose from the sample proved quite difficult, given the extremely polar nature of glucose and the compound. Alterations to the fraction method did remove some glucose making the compound more amenable to NMR analysis, although its presence hindered analysis of the compound in a large region of the NMR spectra.

NMR is an invaluable tool for elucidating the structure of anti-microbial peptides (Daletos *et al.*, 2017) and provided valuable information about the possible structure of this compound. Possibly the most standout feature observed was the quartet of doublets

in the aliphatic region of the spectra, which may potentially represent a cyclic feature of the compound. The number of peaks in the aliphatic region indicate an aliphatic component of the compound. This contradicts the evidence that shows the polar nature of the compound. However this is not uncommon as naturally occurring antimicrobial compounds tend to be amphipathic molecules containing a hydrophilic region and hydrophobic region which interact with the bacterial membranes leading to perturbation and sometimes internalization and targeting of intracellular compartments (Jiménez *et al.*, 2018).

Combined with NMR, mass spectrometry is useful for sequence analysis of antimicrobial compounds (Stegemann and Hoffmann, 2008). Unlike the NMR, analysis of the compound did not reveal any significant changes between the fractions with or without antimicrobial activity. Furthermore, in contrast to NMR, where milligrams of material are necessary for analysis, mass spectrometry requires far smaller amounts of material (i.e. micrograms or nanograms). Thus, given the high concentration of sample that was analysed by mass spectrometry, with few differences in the results, it is possible that the compound is uncharged. In general, antimicrobial peptides are charged (Jiménez *et al.*, 2018), however, the net charge of the compound may be neutral in this case. Because mass spectrometry works on the principle that the mass of charged particles are measured, only ions are detected (El-Aneed et al., 2009). However, chemical derivatization of compounds, i.e. the addition of a charged molecule, can be used to overcome this obstacle. Some prior knowledge of the compound structure must be obtained before this can occur (Krusemark *et al.*, 2009).

Knowledge of the compound structure may be derived in part, by understanding how the compound affects the target microbe. The approach employed here focused on investigating the effect of the compound on *P. aeruginosa*. Although the compound did show activity against other bacteria including clinical strains of *K. pneumonia* and *S. aureus* and an MDR strain of *E. coli*, *P. aeruginosa* was chosen for further investigation because of its close relationship with *A. fumigatus*. What these activity assays on the other bacteria did show however, was that the compound has broad spectrum activity, a useful feature to have in an antibiotic during the initial stages of treatment when the causative agent of the infection is unknown (Kollef, 2008).

LFQ proteomics performed on *P. aeruginosa* exposed to the compound contained in the culture filtrate produced by *A. fumigatus* revealed significant changes to the bacterial proteome. A decrease in the relative abundance of proteins encoded by genes regulating the biosynthesis of pyochelin siderophores and other iron-binding proteins provide some indication that the compound influences iron availability for the bacteria. Iron is an important nutrient for microbial survival and sequestration of this compound from the environment is known to inhibit growth and is a common strategy used by a host to fight infection (Parrow *et al.*, 2013). Such is the importance of iron in the ability of *P. aeruginosa* to sustain infection in the cystic fibrosis airways, limiting iron availability is a potential therapeutic strategy for treating these infections (Smith *et al.*, 2013a).

A decrease in the relative abundance of proteins associated with quorum sensing suggested this may play a role in the antimicrobial activity of the compound. Interfering with bacterial cell-cell signalling by targeting quorum-sensing mechanisms is a potential therapeutic target for antibiotics (Hirakawa and Tomita, 2013). It is uncertain as to whether or not these antibiotics are bacteriocidal or bacteriostatic. Preliminary results indicate that the compound has bacteriostatic effects rather than being bacteriocidal, although further studies are needed to establish this. The ability to quantify the concentration of the compound will allow for assays that determine the minimum inhibitory concentration (MIC). While it is preferable that antibiotics possess bacteriocidal activity, bacteriostatic agents have a major role to play in the treatment of infection and they may function successfully as part of combined therapy by reducing bacterial load, modulating virulence and reducing tolerance against antibiotics (Pankey and Sabath, 2004; Hirakawa and Tomita, 2013).

An increase in the relative abundance of redox active proteins encoded by phenazine biosynthetic genes and stress response regulators such as RNA polymerase sigma factor, indicate the environmental stress conditions forced on *P. aeruginosa* by this compound. Phenazines also play a role in reducing insoluble Fe III to ferrous iron (Fe II) (Wang *et al.*, 2011) and thus the significant increase in the phenazine biosynthetic pathway may not only be indicative of the redox status of the environment but also of the levels of iron availability. These findings may provide some clues as to the mechanism of action.

7.2 Concluding Remarks

For a long time, bacteria were thought to be the main causes of infections associated with the cystic fibrosis airways while fungal pathogens were given less attention (Williams *et al.*, 2016). Although frequently isolated from the CF lung, *A. fumigatus* causes disease in the form of ABPA in a relatively small cohort of CF patients (1-15 %) (Stevens *et al.*, 2003b). However, where *A. fumigatus* co-exists with *P. aeruginosa*, lung function declines (Amin *et al.*, 2010; Reece *et al.*, 2017). The findings presented in this thesis suggest that rather than just being a bystander, *A. fumigatus* may facilitate the pathogenesis of *P. aeruginosa* by altering the nutrient content of the environment and debilitating the phagocytic abilities of host cells. The discovery-driven approach afforded by LFQ proteomics provided an invaluable, un-biased level of information as to the molecular mechanisms of the host response to multiple pathogens and the pathogen response another pathogenic species.

There is an irony in the concept that microorganisms, which have the potential to cause disease, can also synthesise products to treat disease. Fortuitously for humans, these bioactive products can be harvested and harnessed for their many health benefits, including their anti-microbial properties. However, the difficulties arising from isolating and purifying natural products has encouraged a movement away from traditional antibacterial-discovery methods. As we face an era of antimicrobial resistance, the necessity to identify novel antimicrobial agents will encourage the return to traditional methods of discovery. Combined with the advances in NMR, mass spectrometry and associated computational tools, the opportunity to discover and develop novel antimicrobials using traditional techniques has never been more accessible. Moreover, as our understanding of how microbial communities evolve and adapt to interact with each other and with the host, the therapeutic strategies we employ to combat infectious disease will also require adaptation and evolution.

To that end, future work surrounding the identification of the anti-bacterial compound should involve further structural analysis by NMR with a view to derivatizing the compound and performing additional investigations by mass spectrometry so that the structure and identity may be elucidated. The culture filtrates produced in SAB by a selection of *A. fumigatus* mutants should be screened for anti-bacterial activity.

Identifying the gene cluster that may be responsible for generating the compound, whether intracellularly or extracellularly, may provide some indications as the type of compound in question. *In vitro* studies to assess the cytotoxicity of the compound on a mammalian cell line should be considered and the anti-bacterial effect on a range of bacteria in the presence of a mammalian cell line should be performed. Additional LFQ proteomic-based analysis on *P. aeruginosa* using varying concentrations of the purified compounds would be beneficial so that the mode of action can be investigated further. Using proteomic data as a guide, bacteria carrying mutations may be employed for further analysis as to the target of the anti-bacterial compound.

Chapter 8

Bibliography

Aaron, S.D., Vandemheen, K.L., Freitag, A., Pedder, L., Cameron, W., Lavoie, A., *et al.* (2012) Treatment of *Aspergillus fumigatus* in Patients with Cystic Fibrosis: A Randomized, Placebo-Controlled Pilot Study. *PLoS One* **7**: e36077.

Abalos, A., Pinazo, A., Infante, M.R., Casals, M., García, F., and Manresa, A. (2001) Physicochemical and Antimicrobial Properties of New Rhamnolipids Produced by *Pseudomonas aeruginosa* AT10 from Soybean Oil Refinery Wastes. *Langmuir* **17**: 1367–1371.

Abbott, A. (1999) A post-genomic challenge: learning to read patterns of protein synthesis. *Nature* **402**: 715–720.

Agarwal, N., Shrestha, P., and Chokhani, R. (2014) Allergic BronchoPulmonary Aspergillosis in Nepal. *JNMA J Nepal Med Assoc* **52**: 1020–1023.

Agarwal, R., Maskey, D., Aggarwal, A.N., Saikia, B., Garg, M., Gupta, D., and Chakrabarti, A. (2013) Diagnostic Performance of Various Tests and Criteria Employed in Allergic Bronchopulmonary Aspergillosis: A Latent Class Analysis. *PLoS One* **8**: e61105.

Ahmad, S., Gilmore, R.C., Alexis, N.E., and Tarran, R. (2019) SPLUNC1 Loses Its Antimicrobial Activity in Acidic Cystic Fibrosis Airway Secretions. *Am J Respir Crit Care Med* **200**: 633–636.

Ailiyaer, Y., Wang, X., Zhang, Y., Li, C., Li, T., Qi, Q., and Li, Y. (2018) A Prospective Trial of Nebulized Amikacin in the Treatment of Bronchiectasis Exacerbation. *Respiration* **95**: 327–333.

Aimanianda, V., Bayry, J., Bozza, S., Kniemeyer, O., Perruccio, K., Elluru, S.R., *et al.* (2009) Surface hydrophobin prevents immune recognition of airborne fungal spores. *Nature* **460**: 1117–1121.

Akasaka, T., Tanaka, M., Yamaguchi, A., and Sato, K. (2001) Type II Topoisomerase Mutations in Fluoroquinolone-Resistant Clinical Strains of *Pseudomonas aeruginosa* Isolated in 1998 and 1999: Role of Target Enzyme in Mechanism of Fluoroquinolone Resistance. *Antimicrob Agents Chemother* **45**: 2263 LP – 2268.

Akoumianaki, T., Kyrmizi, I., Valsecchi, I., Gresnigt, M.S., Samonis, G., Drakos, E., *et al.* (2016) *Aspergillus* Cell Wall Melanin Blocks LC3-Associated Phagocytosis to Promote Pathogenicity. *Cell Host Microbe* **19**: 79–90.

Alberti, F., Foster, G.D., and Bailey, A.M. (2017) Natural products from filamentous fungi and production by heterologous expression. *Appl Microbiol Biotechnol* **101**: 493–500.

Albrecht, D., Guthke, R., Brakhage, A.A., and Kniemeyer, O. (2010) Integrative analysis of the heat shock response in *Aspergillus fumigatus*. *BMC Genomics* **11**: 32.

Allard, J.B., Poynter, M.E., Marr, K.A., Cohn, L., Rincon, M., and Whittaker, L.A. (2006) *Aspergillus fumigatus* Generates an Enhanced Th2-Biased Immune Response in Mice with Defective Cystic Fibrosis Transmembrane Conductance Regulator. *J Immunol* **177**: 5186 LP – 5194.

Alst, N.E. Van, Sherrill, L.A., Iglewski, B.H., and Haidaris, C.G. (2009) Compensatory periplasmic nitrate reductase activity supports anaerobic growth of *Pseudomonas aeruginosa* PAO1 in the absence of membrane nitrate reductase. *Can J Microbiol* **55**: 1133–1144.

Alves, V. (2014) Translational regulation triggered by fungal pathogens: still a mystery. *OA Mol Cell Biol* **1**: 2–5.

Amich, J., and Krappmann, S. (2012) Deciphering metabolic traits of the fungal pathogen *Aspergillus fumigatus*: redundancy vs. essentiality. *Front Microbiol* **3**: 414.

Amin, R., Dupuis, A., Aaron, S.D., and Ratjen, F. (2010) The effect of chronic infection with *Aspergillus fumigatus* on lung function and hospitalization in patients with cystic fibrosis. *Chest* **137**: 171–176.

Amin, S., Thywissen, A., Heinekamp, T., Saluz, H.P., and Brakhage, A.A. (2014) Melanin dependent survival of *Apergillus fumigatus* conidia in lung epithelial cells. *Int J Med Microbiol* **304**: 626–636.

Amitani, R., Taylor, G., Elezis, E.N., Llewellyn-Jones, C., Mitchell, J., Kuze, F., *et al.* (1995) Purification and characterization of factors produced by *Aspergillus fumigatus* which affect human ciliated respiratory epithelium. *Infect Immun* **63**: 3266 LP – 3271

An, S.-Q., and Ryan, R.P. (2016) Combating chronic bacterial infections by manipulating cyclic nucleotide-regulated biofilm formation. *Future Med Chem* **8**: 949–961.

Angus, A.A., Lee, A.A., Augustin, D.K., Lee, E.J., Evans, D.J., and Fleiszig, S.M.J. (2008) *Pseudomonas aeruginosa* induces membrane blebs in epithelial cells, which are utilized as a niche for intracellular replication and motility. *Infect Immun* **76**: 1992–2001.

Arai, H., Hayashi, M., Kuroi, A., Ishii, M., and Igarashi, Y. (2005) Transcriptional Regulation of the Flavohemoglobin Gene for Aerobic Nitric Oxide Detoxification by the Second Nitric Oxide-Responsive Regulator of *Pseudomonas aeruginosa*. *J Bacteriol* **187:** 3960-8.

Araújo, D., Shteinberg, M., Aliberti, S., Goeminne, P.C., Hill, A.T., Fardon, T.C., *et al.* (2018) The independent contribution of *Pseudomonas aeruginosa* infection to long-term clinical outcomes in bronchiectasis. *Eur Respir J* **51:** 1701953.

Arlehamn, C.S.L., and Evans, T.J. (2011) *Pseudomonas aeruginosa* pilin activates the inflammasome. *Cell Microbiol* **13**: 388–401.

Ashida, H., Kim, M., Schmidt-Supprian, M., Ma, A., Ogawa, M., and Sasakawa, C. (2010) A bacterial E3 ubiquitin ligase IpaH9.8 targets NEMO/IKKgamma to dampen the host NF-kappaB-mediated inflammatory response. *Nat Cell Biol* **12**: 66–69.

Aslam, B., Wang, W., Arshad, M.I., Khurshid, M., Muzammil, S., Rasool, M.H., *et al.* (2018) Antibiotic resistance: a rundown of a global crisis. *Infect Drug Resist* **11**: 1645–1658.

Athanazio, R. (2012) Airway disease: similarities and differences between asthma, COPD and bronchiectasis. *Clinics (Sao Paulo)* **67**: 1335–1343.

Awino, J.K., Gunasekara, R.W., and Zhao, Y. (2016) Selective Recognition of d-Aldohexoses in Water by Boronic Acid-Functionalized, Molecularly Imprinted Cross-Linked Micelles. *J Am Chem Soc* **138**: 9759–9762.

Baker, S.J., Payne, D.J., Rappuoli, R., and Gregorio, E. De (2018) Technologies to address antimicrobial resistance. *Proc Natl Acad Sci* **115**: 12887 LP – 12895.

Baldan, R., Cigana, C., Testa, F., Bianconi, I., Simone, M. De, Pellin, D., *et al.* (2014) Adaptation of *Pseudomonas aeruginosa* in cystic fibrosis airways influences virulence of *Staphylococcus aureus* in vitro and murine models of co-infection. *PLoS One* **9**.

Balloy, V., and Chignard, M. (2009) The innate immune response to *Aspergillus fumigatus*. *Microbes Infect* **11**: 919–927.

Balloy, V., Sallenave, J.M., Wu, Y., Touqui, L., Latgé, J.P., Si-Tahar, M., and Chignard, M. (2008) *Aspergillus fumigatus*-induced interleukin-8 synthesis by respiratory epithelial cells is controlled by the phosphatidylinositol 3-kinase, p38 MAPK, and ERK1/2 pathways and not by the toll-like receptor-MyD88 pathway. *J Biol Chem* **283**: 30513–30521.

Balsamo, R., Lanata, L., and Egan, C.G. (2010) Mucoactive drugs. *Eur Respir Rev* **19**: 127 LP – 133.

Bandara, H.M.H.N., Yau, J.Y.Y., Watt, R.M., Jin, L.J., and Samaranayake, L.P. (2010) *Pseudomonas aeruginosa* inhibits in-vitro Candida biofilm development. *BMC Microbiol* **10**: 125.

Bandow, J.E., Brötz, H., Leichert, L.I.O., Labischinski, H., and Hecker, M. (2003) Proteomic Approach to Understanding Antibiotic Action. *Antimicrob Agents Chemother* **47**: 948 LP – 955.

Banerjee, B., Greenberger, P.A., Fink, J.N., and Kurup, V.P. (1998) Immunological characterization of Asp f 2, a major allergen from *Aspergillus fumigatus* associated with allergic bronchopulmonary aspergillosis. *Infect Immun* **66**: 5175–5182.

Banks, C.J., and Andersen, J.L. (2019) Mechanisms of SOD1 regulation by post-translational modifications. *Redox Biol* **26**: 101270.

Bargon, J., Dauletbaev, N., Köhler, B., Wolf, M., Posselt, H.-G., and Wagner, T.O.F. (1999) Prophylactic antibiotic therapy is associated with an increased prevalence of Aspergillus colonization in adult cystic fibrosis patients. *Respir Med* **93**: 835–838.

Barker, B.M., Kroll, K., Vödisch, M., Mazurie, A., Kniemeyer, O., and Cramer, R.A. (2012) Transcriptomic and proteomic analyses of the *Aspergillus fumigatus* hypoxia response using an oxygen-controlled fermenter. *BMC Genomics* **13**: 62.

Barth, A.L., and Pitt, T.L. (1996) The high amino-acid content of sputum from cystic fibrosis patients promotes growth of auxotrophic *Pseudomonas aeruginosa*. *J Med Microbiol* **45**: 110–119.

Barth, A.L., and Pltt, T.L. (1996) The high amino-acid content of sputum from cystic fibrosis patients promotes growth of auxotrophic Pseudornonas aeruginosa. *J Med Microbiol* **45**: 110–119.

Bassetti, M., Vena, A., Croxatto, A., Righi, E., and Guery, B. (2018a) How to manage *Pseudomonas aeruginosa* infections. *Drugs Context* **7**: 212527.

Bassetti, M., Vena, A., Russo, A., Croxatto, A., Calandra, T., and Guery, B. (2018b) Rational approach in the management of *Pseudomonas aeruginosa* infections. *Curr Opin Infect Dis* **31:** 578-586.

Beaudoin, T., Yau, Y.C.W., Stapleton, P.J., Gong, Y., Wang, P.W., Guttman, D.S., and Waters, V. (2017) *Staphylococcus aureus* interaction with *Pseudomonas aeruginosa* biofilm enhances tobramycin resistance. *NPJ biofilms microbiomes* **3**: 25.

Beaumont, P.E., McHugh, B., Gwyer Findlay, E., Mackellar, A., Mackenzie, K.J., Gallo, R.L., *et al.* (2014) Cathelicidin Host Defence Peptide Augments Clearance of Pulmonary *Pseudomonas aeruginosa* Infection by Its Influence on Neutrophil Function In Vivo. *PLoS One* **9**: e99029.

Behnsen, J., Lessing, F., Schindler, S., Wartenberg, D., Jacobsen, I.D., Thoen, M., *et al.* (2010) Secreted *Aspergillus fumigatus* protease Alp1 degrades human complement proteins C3, C4, and C5. *Infect Immun* **78**: 3585–3594.

Beisswenger, C., Hess, C., and Bals, R. (2012) *Aspergillus fumigatus* conidia induce interferon-β signalling in respiratory epithelial cells. *Eur Respir J* **39**: 411 LP – 418.

Bellanger, A.-P., Millon, L., Khoufache, K., Rivollet, D., Bieche, I., Laurendeau, I., *et al.* (2009) *Aspergillus fumigatus* germ tube growth and not conidia ingestion induces expression of inflammatory mediator genes in the human lung epithelial cell line A549. *J Med Microbiol* **58**: 174–179.

Ben-Ami, R., Lewis, R.E., Leventakos, K., and Kontoyiannis, D.P. (2009) *Aspergillus fumigatus* inhibits angiogenesis through the production of gliotoxin and other secondary metabolites. *Blood* **114**: 5393–5399.

Bentzmann, S. de, and Plésiat, P. (2011) The *Pseudomonas aeruginosa* opportunistic pathogen and human infections. *Environ Microbiol* **13**: 1655–1665.

Bergeron, A.C., Seman, B.G., Hammond, J.H., Archambault, L.S., Hogan, D.A., and Wheeler, R.T. (2017) *Candida albicans* and *Pseudomonas aeruginosa* Interact To Enhance Virulence of Mucosal Infection in Transparent Zebrafish. *Infect Immun* **85**: e00475-17.

Bergin, D., Reeves, E.P., Renwick, J., Wientjes, F.B., and Kavanagh, K. (2005) Superoxide production in Galleria mellonella hemocytes: identification of proteins homologous to the NADPH oxidase complex of human neutrophils. *Infect Immun* **73**: 4161–4170.

Berkova, N., Lair-Fulleringer, S., Féménia, F., Huet, D., Wagner, M.C., Gorna, K., *et al.* (2006) *Aspergillus fumigatus* conidia inhibit tumour necrosis factor- or staurosporine-induced apoptosis in epithelial cells. *Int Immunol* **18**: 139–150.

Berks, B.C., Ferguson, S.J., Moir, J.W.B., and Richardson, D.J. (1995) Enzymes and associated electron transport systems that catalyse the respiratory reduction of nitrogen oxides and oxyanions. *Biochim Biophys Acta* **1232:** 97-173.

Berrazeg, M., Jeannot, K., Ntsogo Enguéné, V.Y., Broutin, I., Loeffert, S., Fournier, D., and Plésiat, P. (2015) Mutations in β-Lactamase AmpC Increase Resistance of *Pseudomonas aeruginosa* Isolates to Antipseudomonal Cephalosporins. *Antimicrob Agents Chemother* **59**: 6248 LP – 6255.

Bertelli, C., and Greub, G. (2013) Rapid bacterial genome sequencing: methods and applications in clinical microbiology. *Clin Microbiol Infect* **19**: 803–813.

Bertout, S., Badoc, C., Mallié, M., Giaimis, J., and Bastide, J.M. (2002) Spore diffusate isolated from some strains of *Aspergillus fumigatus* inhibits phagocytosis by murine alveolar macrophages. *FEMS Immunol Med Microbiol* **33**: 101–106.

Bertuzzi, M., Hayes, G., Icheoku, U., Rhijn, N. van, Denning, D., Osherov, N., and Bignell, E. (2018a) Anti-Aspergillus Activities of the Respiratory Epithelium in Health and Disease. *J Fungi* **4**: 8.

Bertuzzi, M., Hayes, G.E., and Bignell, E.M. (2019) Microbial uptake by the respiratory epithelium: outcomes for host and pathogen. *FEMS Microbiol Rev* **43**: 145–161.

Bertuzzi, M., Schrettl, M., Alcazar-Fuoli, L., Cairns, T.C., Munoz, A., Walker, L.A., *et al.* (2014) The pH-responsive PacC transcription factor of *Aspergillus fumigatus* governs epithelial entry and tissue invasion during pulmonary aspergillosis. *PLoS Pathog* **10**: e1004413.

Bignell, E., Cairns, T.C., Throckmorton, K., Nierman, W.C., and Keller, N.P. (2016) Secondary metabolite arsenal of an opportunistic pathogenic fungus. *Philos Trans R Soc B Biol Sci* **371**: 20160023.

Bignell, E., Negrete-Urtasun, S., Calcagno, A.M., Haynes, K., Arst Jr, H.N., and Rogers, T. (2005) The Aspergillus pH-responsive transcription factor PacC regulates virulence. *Mol Microbiol* **55**: 1072–1084.

Bills, G.F., Platas, G., Fillola, A., Jiménez, M.R., Collado, J., Vicente, F., *et al.* (2008) Enhancement of antibiotic and secondary metabolite detection from filamentous fungi by growth on nutritional arrays. *J Appl Microbiol* **104**: 1644–1658.

Bilton, D. (2008) Update on non-cystic fibrosis bronchiectasis. *Curr Opin Pulm Med* **14:** 595-9.

Bilton, D., Bellon, G., Charlton, B., Cooper, P., Boeck, K. De, Flume, P.A., *et al.* (2013) Pooled analysis of two large randomised phase III inhaled mannitol studies in cystic fibrosis. *J Cyst Fibros* **12**: 367–376.

Bladt, T.T., Frisvad, J.C., Knudsen, P.B., and Larsen, T.O. (2013) Anticancer and antifungal compounds from Aspergillus, Penicillium and other filamentous fungi. *Molecules* **18**: 11338–11376.

Blohmke, C.J., Mayer, M.L., Tang, A.C., Hirschfeld, A.F., Fjell, C.D., Sze, M.A., *et al.* (2012) Atypical Activation of the Unfolded Protein Response in Cystic Fibrosis Airway Cells Contributes to p38 MAPK-Mediated Innate Immune Responses. *J Immunol* **189**: 5467–5475.

Bloudoff, K., and Schmeing, T.M. (2017) Structural and functional aspects of the nonribosomal peptide synthetase condensation domain superfamily: discovery, dissection and diversity. *Biochim Biophys Acta - Proteins Proteomics* **1865**: 1587–1604.

Bode, H.B., Bethe, B., Höfs, R., and Zeeck, A. (2002) Big Effects from Small Changes: Possible Ways to Explore Nature's Chemical Diversity. *ChemBioChem* **3**: 619–627.

Boeck, K. De, and Amaral, M.D. (2016) Progress in therapies for cystic fibrosis. *Lancet Respir Med* **4**: 662–674.

Bomberger, J.M., Ely, K.H., Bangia, N., Ye, S., Green, K.A., Green, W.R., *et al.* (2014) *Pseudomonas aeruginosa* Cif protein enhances the ubiquitination and proteasomal degradation of the transporter associated with antigen processing (TAP) and reduces major histocompatibility complex (MHC) class I antigen presentation. *J Biol Chem* **289**: 152–162.

Bomberger, J.M., Ye, S., MacEachran, D.P., Koeppen, K., Barnaby, R.L., O'Toole, G.A., and Stanton, B.A. (2011) A *Pseudomonas aeruginosa* toxin that hijacks the host ubiquitin proteolytic system. *PLoS Pathog* **7**.

Bompadre, S.G., Li, M., and Hwang, T.-C. (2008) Mechanism of G551D-CFTR (cystic fibrosis transmembrane conductance regulator) potentiation by a high affinity ATP analog. *J Biol Chem* **283**: 5364–5369.

Bottazzi, B., Doni, A., Garlanda, C., and Mantovani, A. (2010) An Integrated View of Humoral Innate Immunity: Pentraxins as a Paradigm. *Annu Rev Immunol* **28**: 157–183.

Bouzani, M., Ok, M., McCormick, A., Ebel, F., Kurzai, O., Morton, C.O., *et al.* (2011) Human NK Cells Display Important Antifungal Activity against *Aspergillus fumigatus* Which Is Directly Mediated by IFN-γ Release. *J Immunol* **187**: 1369 LP – 1376.

Bozza, S., Gaziano, R., Spreca, A., Bacci, A., Montagnoli, C., Francesco, P. di, and Romani, L. (2002) Dendritic Cells Transport Conidia and Hyphae of *Aspergillus fumigatus* from the Airways to the Draining Lymph Nodes and Initiate Disparate Th Responses to the Fungus. *J Immunol* **168**: 1362 LP – 1371.

Brandel, J., Humbert, N., Elhabiri, M., Schalk, I.J., Mislin, G.L.A., and Albrecht-Gary, A.-M. (2012) Pyochelin, a siderophore of *Pseudomonas aeruginosa*: physicochemical characterization of the iron(III), copper(II) and zinc(II) complexes. *Dalton Trans* **41**: 2820–2834.

Breidenstein, E.B.M., Janot, L., Strehmel, J., Fernandez, L., Taylor, P.K., Kukavica-ibrulj, I., *et al.* (2012) The Lon Protease Is Essential for Full Virulence in *Pseudomonas aeruginosa*. *PLoS One* **7**: e49123.

Breidenstein, E.B.M., la Fuente-Núñez, C. de, and Hancock, R.E.W. (2011) *Pseudomonas aeruginosa*: All roads lead to resistance. *Trends Microbiol* **19**: 419–426.

Breuker, K., Jin, M., Han, X., Jiang, H., and McLafferty, F.W. (2008) Top-down identification and characterization of biomolecules by mass spectrometry. *J Am Soc Mass Spectrom* **19**: 1045–1053.

Briard, B., Bomme, P., Lechner, B.E., Mislin, G.L.A., Lair, V., Prévost, M.C., *et al.* (2015) *Pseudomonas aeruginosa* manipulates redox and iron homeostasis of its microbiota partner *Aspergillus fumigatus* via phenazines. *Sci Rep* **5**: 8220.

Briard, B., Heddergott, C., and Latgé, J.P. (2016) Volatile compounds emitted by *Pseudomonas aeruginosa* stimulate growth of the fungal pathogen *Aspergillus fumigatus*. *MBio* **7**: 1–5.

Briard, B., Mislin, G.L.A., Latgé, J.-P., and Beauvais, A. (2019) Interactions between *Aspergillus fumigatus* and Pulmonary Bacteria: Current State of the Field, New Data, and Future Perspective. *J fungi (Basel)* **5**: 48.

Briard, B., Rasoldier, V., Bomme, P., ElAouad, N., Guerreiro, C., Chassagne, P., *et al.* (2017) Dirhamnolipids secreted from *Pseudomonas aeruginosa* modify fungal susceptibility of *Aspergillus fumigatus* by inhibiting beta1,3 glucan synthase activity. *ISME J* **11**: 1578–1591.

Brosch, G., Loidl, P., and Graessle, S. (2008) Histone modifications and chromatin dynamics: a focus on filamentous fungi. *FEMS Microbiol Rev* **32**: 409–439.

Brown, G.D., and Gordon, S. (2001) A new receptor for β-glucans. *Nature* **413**: 36–37.

Bucior, I., Pielage, J.F., and Engel, J.N. (2012) *Pseudomonas aeruginosa* Pili and Flagella Mediate Distinct Binding and Signaling Events at the Apical and Basolateral Surface of Airway Epithelium. *PLOS Pathog* **8**: e1002616.

Burgel, P.-R., Paugam, A., Hubert, D., and Martin, C. (2016) *Aspergillus fumigatus* in the cystic fibrosis lung: pros and cons of azole therapy. *Infect Drug Resist* **9**: 229–238.

Burrows, L.L. (2012) *Pseudomonas aeruginosa* Twitching Motility: Type IV Pili in Action. *Annu Rev Microbiol* **66**: 493–520.

Burstein, D., Satanower, S., Simovitch, M., Belnik, Y., Zehavi, M., Yerushalmi, G., *et al.* (2015) Novel Type III Effectors in *Pseudomonas aeruginosa*. *MBio* **6**: e00161-15.

Byrne, A.J., Mathie, S.A., Gregory, L.G., and Lloyd, C.M. (2015) Pulmonary macrophages: key players in the innate defence of the airways. *Thorax* **70**: 1189 LP – 1196.

Caldwell, C.C., Chen, Y., Goetzmann, H.S., Hao, Y., Borchers, M.T., Hassett, D.J., *et al.* (2009) *Pseudomonas aeruginosa* exotoxin pyocyanin causes cystic fibrosis airway pathogenesis. *Am J Pathol* **175**: 2473–2488.

Caldwell, R.A., Boucher, R.C., and Stutts, M.J. (2005) Neutrophil elastase activates near-silent epithelial Na+ channels and increases airway epithelial Na+ transport. *Am J Physiol Lung Cell Mol Physiol* **288**: L813-9.

Calvo, A.M., Wilson, R.A., Bok, J.W., and Keller, N.P. (2002) Relationship between secondary metabolism and fungal development. *Microbiol Mol Biol Rev* **66**: 447–459.

Cambau, E., Perani, E., Dib, C., Petinon, C., Trias, J., and Jarlier, V. (1995) Role of mutations in DNA gyrase genes in ciprofloxacin resistance of *Pseudomonas aeruginosa* susceptible or resistant to imipenem. *Antimicrob Agents Chemother* **39**: 2248 LP – 2252.

Caminati, M., Pham, D. Le, Bagnasco, D., and Canonica, G.W. (2018) Type 2 immunity in asthma. *World Allergy Organ J* **11**: 13.

Cao, Y., Huang, Y., Xu, K., Liu, Y., Li, X., Xu, Y., *et al.* (2017) Differential responses of innate immunity triggered by different subtypes of influenza a viruses in human and avian hosts. *BMC Med Genomics* **10**: 70.

Carreto-Binaghi, L.E., Aliouat, E.M., and Taylor, M.L. (2016) Surfactant proteins, SP-A and SP-D, in respiratory fungal infections: their role in the inflammatory response. *Respir Res* **17**: 66.

Carrion, S. de J., Leal Jr, S.M., Ghannoum, M.A., Aimanianda, V., Latgé, J.-P., and Pearlman, E. (2013) The RodA hydrophobin on *Aspergillus fumigatus* spores masks dectin-1- and dectin-2-dependent responses and enhances fungal survival in vivo. *J Immunol* **191**: 2581–2588.

Carterson, A.J., Höner zu Bentrup, K., Ott, C.M., Clarke, M.S., Pierson, D.L., Vanderburg, C.R., *et al.* (2005a) A549 lung epithelial cells grown as three-dimensional aggregates: alternative tissue culture model for *Pseudomonas aeruginosa* pathogenesis. *Infect Immun* **73**: 1129–40.

Carterson, A.J., Höner zu Bentrup, K., Ott, C.M., Clarke, M.S., Pierson, D.L., Vanderburg, C.R., *et al.* (2005b) A549 Lung Epithelial Cells Grown as Three-Dimensional Aggregates: Alternative Tissue Culture Model for *Pseudomonas aeruginosa* Pathogenesis. *Infect Immun* **73**: 1129 LP – 1140.

Castanheira, M., Davis, A.P., Mendes, R.E., Serio, A.W., Krause, K.M., and Flamm, R.K. (2018) In Vitro Activity of Plazomicin against Gram-Negative and Gram-Positive Isolates Collected from U.S. Hospitals and Comparative Activities of Aminoglycosides against Carbapenem-Resistant Enterobacteriaceae and Isolates Carrying Carbapenemase Genes. *Antimicrob Agents Chemother* **62**: e00313-18.

Celli, J., and Tsolis, R.M. (2015) Bacteria , the ER and the Unfolded Protein Response : Friends or. *Nat Rev Microbiol* **13**: 71–82.

Cepas, V., López, Y., Gabasa, Y., Martins, B.C., Ferreira, D.J., Correia, J.M., *et al.* (2019) Inhibition of Bacterial and Fungal Biofilm Formation by 675 Extracts from Microalgae and Cyanobacteria. *Antibiot* **8:** 77.

CF Registry, Ireland 2007 Annual Report (2007). cfri.ie

CF Registry of Ireland 2017 Annual Report (2017). cfri.ie

Chabi, M.L., Goracci, A., Roche, N., Paugam, A., Lupo, A., and Revel, M.P. (2015) Pulmonary aspergillosis. *Diagn Interv Imaging* **96**: 435–442.

Chai, Y.-H., and Xu, J.-F. (2020) How does *Pseudomonas aeruginosa* affect the progression of bronchiectasis? *Clin Microbiol Infect* **26**: 313–318.

Chalmers, J.D., Aliberti, S., and Blasi, F. (2015) Management of bronchiectasis in adults. *Eur Respir J* **45**: 1446 LP – 1462.

Chandorkar, P., Posch, W., Zaderer, V., Blatzer, M., Steger, M., Ammann, C.G., *et al.* (2017) Fast-track development of an in vitro 3D lung/immune cell model to study Aspergillus infections. *Sci Rep* **7**: 11644.

Chang, Y.C., Tsai, H.-F., Karos, M., and Kwon-Chung, K.J. (2004) THTA, a thermotolerance gene of *Aspergillus fumigatus*. *Fungal Genet Biol* **41**: 888–896.

Chaudhary, N., and Marr, K.A. (2011) Impact of *Aspergillus fumigatus* in allergic airway diseases. *Clin Transl Allergy* **1**: 4.

Chauhan, K., Kalam, H., Dutt, R., and Kumar, D. (2019) RNA Splicing: A New Paradigm in Host–Pathogen Interactions. *J Mol Biol* **431**: 1565–1575.

Chen, A.I., Dolben, E.F., Okegbe, C., Harty, C.E., Golub, Y., Thao, S., *et al.* (2014) *Candida albicans* Ethanol Stimulates *Pseudomonas aeruginosa* WspR-Controlled Biofilm Formation as Part of a Cyclic Relationship Involving Phenazines. *PLOS Pathog* **10**: e1004480.

Chen, F., Zhang, C., Jia, X., Wang, S., Wang, J., Chen, Y., *et al.* (2015) Transcriptome Profiles of Human Lung Epithelial Cells A549 Interacting with *Aspergillus fumigatus* by RNA-Seq. *PLoS One* **10**: e0135720.

Cheung, D.O., Halsey, K., and Speert, D.P. (2000) Role of pulmonary alveolar macrophages in defense of the lung against *Pseudomonas aeruginosa*. *Infect Immun* **68**: 4585–4592.

Chi, E., Mehl, T., Nunn, D., and Lory, S. (1991) Interaction of *Pseudomonas aeruginosa* with A549 pneumocyte cells. *Infect Immun* **59**: 822–828.

Chmiel, J.F., Aksamit, T.R., Chotirmall, S.H., Dasenbrook, E.C., Elborn, J.S., LiPuma, J.J., *et al.* (2014) Antibiotic management of lung infections in cystic fibrosis. I. The microbiome, methicillin-resistant *Staphylococcus aureus*, gram-negative bacteria, and multiple infections. *Ann Am Thorac Soc* **11**: 1120–1129.

Choi, P.S., Naal, Z., Moore, C., Casado-rivera, E., Abrun, H.D., Helmann, J.D., and Shapleigh, J.P. (2006) Assessing the Impact of Denitrifier-Produced Nitric Oxide on Other Bacteria. *App Enivron Microbiol* **72**: 2200–2205.

Cigana, C., Lorè, N.I., Bernardini, M.L., and Bragonzi, A. (2011) Dampening Host Sensing and Avoiding Recognition in *Pseudomonas aeruginosa* Pneumonia. *J Biomed Biotechnol* **2011**: 1–10.

Coates, A.R.M., and Hu, Y. (2007) Novel approaches to developing new antibiotics for bacterial infections. *Br J Pharmacol* **152**: 1147–1154.

Coburn, B., Wang, P.W., Caballero, J.D., Clark, S.T., Brahma, V., Donaldson, S., *et al.* (2015) Lung microbiota across age and disease stage in cystic fibrosis. *Sci Rep* **5**: 10241.

Cole, A.M., Dewan, P., and Ganz, T. (1999) Innate Antimicrobial Activity of Nasal Secretions. *Infect Immun* **67**: 3267 LP – 3275.

Colemeadow, J., Joyce, H., and Turcanu, V. (2016) Precise treatment of cystic fibrosis – current treatments and perspectives for using CRISPR. *Expert Rev Precis Med Drug Dev* **1**: 169–180.

Cooney, A.L., McCray Jr, P.B., and Sinn, P.L. (2018) Cystic Fibrosis Gene Therapy: Looking Back, Looking Forward. *Genes (Basel)* **9**: 538.

Coutinho, H.D.M., Falcão-Silva, V.S., and Gonçalves, G.F. (2008) Pulmonary bacterial pathogens in cystic fibrosis patients and antibiotic therapy: a tool for the health workers. *Int Arch Med* **1**: 24.

Cozens, A.L., Yezzi, M.J., Kunzelmann, K., Ohrui, T., Chin, L., Eng, K., *et al.* (1994) CFTR expression and chloride secretion in polarized immortal human bronchial epithelial cells. *Am J Respir Cell Mol Biol* **10**: 38–47.

Croft, C.A., Culibrk, L., Moore, M.M., and Tebbutt, S.J. (2016) Interactions of *Aspergillus fumigatus* conidia with airway epithelial cells: A critical review. *Front Microbiol* **7**: 1–15.

Crull, M.R., Ramos, K.J., Caldwell, E., Mayer-Hamblett, N., Aitken, M.L., and Goss, C.H. (2016) Change in *Pseudomonas aeruginosa* prevalence in cystic fibrosis adults over time. *BMC Pulm Med* **16**: 176.

Culbertson, J.E., and Toney, M.D. (2013) Expression and characterization of PhzE from *P. aeruginosa* PAO1: aminodeoxyisochorismate synthase involved in pyocyanin and phenazine-1-carboxylate production. *Biochim Biophys Acta - Proteins Proteomics* **1834**: 240–246.

Curran, C.S., Bolig, T., and Torabi-Parizi, P. (2017) Mechanisms and Targeted Therapies for *Pseudomonas aeruginosa* Lung Infection. *Am J Respir Crit Care Med* **197**: 708–727.

UK Cystic Fibrosis Registry Annual data report 2017, Cystic Fibrosis Trust.

Dacheux, D., Attree, I., Schneider, C., and Toussaint, B. (1999) Cell death of human polymorphonuclear neutrophils induced by a *Pseudomonas aeruginosa* cystic fibrosis isolate requires a functional type III secretion system. *Infect Immun* **67**: 6164–6167.

Dagenais, T.R.T., and Keller, N.P. (2009) Pathogenesis of *Aspergillus fumigatus* in invasive aspergillosis. *Clin Microbiol Rev* **22**: 447–465.

Daletos, G., Ancheeva, E., Orfali, R.S., Wray, V., and Proksch, P. (2017) Structure Elucidation of Antibiotics by Nmr Spectroscopy. *Methods Mol Biol* **1520**: 63–83.

Daly, P., and Kavanagh, K. (2001) Pulmonary aspergillosis: Clinical presentation, diagnosis and therapy. *Br J Biomed Sci* **58**: 197–205.

Daly, P., Verhaegen, S., Clynes, M., and Kavanagh, K. (1999) Culture filtrates of *Aspergillus fumigatus* induce different modes of cell death in human cancer cell lines. *Mycopathologia* **146**: 67–74.

Darch, S.E., Ibberson, C.B., and Whiteley, M. (2017) Evolution of Bacterial "Frenemies." *MBio* **8**: e00675-17.

David, J., Bell, R.E., and Clark, G.C. (2015) Mechanisms of Disease: Host-Pathogen Interactions between *Burkholderia* Species and Lung Epithelial Cells. *Front Cell Infect Microbiol* **5**: 80.

Dean, C.R., Neshat, S., and Poole, K. (1996) PfeR, an enterobactin-responsive activator of ferric enterobactin receptor gene expression in *Pseudomonas aeruginosa*. *J Bacteriol* **178**: 5361–5369.

Debono, M., Barnhart, M., Carrell, C.B., Hoffmann, J.A., Occolowitz, J.L., Abbott, B.J., *et al.* (1987) A21978C, a complex of new acidic peptide antibiotics: isolation, chemistry, and mass spectral structure elucidation. *J Antibiot (Tokyo)* **40**: 761–777.

Defoirdt, T. (2019) Amino acid – derived quorum sensing molecules controlling the virulence of vibrios (and beyond). *PLoS Pathog* **15**: 1–8.

Delcour, A.H. (2009) Outer membrane permeability and antibiotic resistance. *Biochim Biophys Acta* **1794**: 808–816.

Delfino, E., Puente, F. Del, Briano, F., Sepulcri, C., and Giacobbe, D.R. (2019) Respiratory Fungal Diseases in Adult Patients With Cystic Fibrosis. *Clin Med Insights Circ Respir Pulm Med* **13**: 1179548419849939.

Deng, Q., and Barbieri, J.T. (2008) Modulation of host cell endocytosis by the type III cytotoxin, pseudomonas ExoS. *Traffic* **9**: 1948–1957.

Denning, D.W. (1998) Invasive aspergillosis. *Clin Infect Dis* **26**: 781–785.

Denning, G.M., Iyer, S.S., Reszka, K.J., O'Malley, Y., Rasmussen, G.T., and Britigan, B.E. (2003) Phenazine-1-carboxylic acid, a secondary metabolite of *Pseudomonas aeruginosa*, alters expression of immunomodulatory proteins by human airway epithelial cells. *Am J Physiol Lung Cell Mol Physiol* **285**: L584-92.

Dhingra, S., Lind, A.L., Lin, H.C., Tang, Y., Rokas, A., and Calvo, A.M. (2013) The Fumagillin Gene Cluster, an Example of Hundreds of Genes under veA Control in *Aspergillus fumigatus*. *PLoS One* **8**: 1–16.

Dickson, R.P., Erb-Downward, J.R., Martinez, F.J., and Huffnagle, G.B. (2016) The Microbiome and the Respiratory Tract. *Annu Rev Physiol* **78**: 481–504.

Dittrich, A.S., Kühbandner, I., Gehrig, S., Rickert-Zacharias, V., Twigg, M., Wege, S., *et al.* (2018) Elastase activity on sputum neutrophils correlates with severity of lung disease in cystic fibrosis. *Eur Respir J* **51**.

Dolan, S.K., O'Keeffe, G., Jones, G.W., and Doyle, S. (2015) Resistance is not futile: gliotoxin biosynthesis, functionality and utility. *Trends Microbiol* **23**: 419–428.

Dolan, S.K., Owens, R.A., O'Keeffe, G., Hammel, S., Fitzpatrick, D.A., Jones, G.W., and Doyle, S. (2014) Regulation of Nonribosomal Peptide Synthesis: bis-Thiomethylation Attenuates Gliotoxin Biosynthesis in *Aspergillus fumigatus*. *Chem Biol* **21**: 999–1012.

Downey, D.G., Bell, S.C., and Elborn, J.S. (2009) Neutrophils in cystic fibrosis. *Thorax* **64**: 81 LP – 88.

Duan, K., Dammel, C., Stein, J., Rabin, H., and Surette, M.G. (2003) Modulation of *Pseudomonas aeruginosa* gene expression by host microflora through interspecies communication. *Mol Microbiol* **50**: 1477–1491.

Dubourdeau, M., Athman, R., Balloy, V., Philippe, B., Sengmanivong, L., Chignard, M., *et al.* (2006) Interaction of *Aspergillus fumigatus* with the alveolar macrophage. *Med Mycol* **44**: S213–S217.

Dumas, Z., Ross-Gillespie, A., and Kümmerli, R. (2013) Switching between apparently redundant iron-uptake mechanisms benefits bacteria in changeable environments. *Proc Biol Sci* **280**: 20131055.

Dunbar, T.L., Yan, Z., Balla, K.M., Smelkinson, M.G., and Troemel, E.R. (2012) C. elegans Detects Pathogen-Induced Translational Inhibition to Activate Immune Signaling. *Cell Host Microbe* **11**: 375–386.

Dusane, D.H., Zinjarde, S.S., Venugopalan, V.P., McLean, R.J.C., Weber, M.M., and Rahman, P.K.S.M. (2010) Quorum sensing: implications on rhamnolipid biosurfactant production. *Biotechnol Genet Eng Rev* **27**: 159–184.

Eisenman, H.C., and Casadevall, A. (2012) Synthesis and assembly of fungal melanin. *Appl Microbiol Biotechnol* **93**: 931–940.

Eisenreich, W., Heesemann, J., Rudel, T., and Goebel, W. (2013) Metabolic host responses to infection by intracellular bacterial pathogens. *Front Cell Infect Microbiol* **3**: 1–22.

Eisenreich, W., Rudel, T., Heesemann, J., and Goebel, W. (2017) To Eat and to Be Eaten: Mutual Metabolic Adaptations of Immune Cells and Intracellular Bacterial Pathogens upon Infection. *Front Cell Infect Microbiol* **7**: 1–26.

El-Aneed, A., Cohen, A., and Banoub, J. (2009) Mass Spectrometry, Review of the Basics: Electrospray, MALDI, and Commonly Used Mass Analyzers. *Appl Spectrosc Rev* **44**: 210–230.

Eljaaly, K., Alharbi, A., Alshehri, S., Ortwine, J.K., and Pogue, J.M. (2019) Plazomicin: A Novel Aminoglycoside for the Treatment of Resistant Gram-Negative Bacterial Infections. *Drugs* **79**: 243–269.

Endo, Y., Matsushita, M., and Fujita, T. (2011) The role of ficolins in the lectin pathway of innate immunity. *Int J Biochem Cell Biol* **43**: 705–712.

Escoll, P., Mondino, S., Rolando, M., and Buchrieser, C. (2015) Targeting of host organelles by pathogenic bacteria: a sophisticated subversion strategy. *Nat Rev Microbiol* **14**: 5.

Esposito, A., Pompilio, A., Bettua, C., Crocetta, V., Giacobazzi, E., Fiscarelli, E., *et al.* (2017) Evolution of *Stenotrophomonas maltophilia* in Cystic Fibrosis Lung over Chronic Infection: A Genomic and Phenotypic Population Study. *Front Microbiol* **8**: 1590.

Everaerts, S., Lagrou, K., Dubbeldam, A., Lorent, N., Vermeersch, K., Hoeyveld, E. Van, *et al.* (2017) Sensitization to *Aspergillus fumigatus* as a risk factor for bronchiectasis in COPD. *Int J Chron Obstruct Pulmon Dis* **12**: 2629–2638.

Everaerts, S., Lagrou, K., Vermeersch, K., Dupont, L.J., Vanaudenaerde, B.M., and Janssens, W. (2018) *Aspergillus fumigatus* Detection and Risk Factors in Patients with COPD-Bronchiectasis Overlap. *Int J Mol Sci* **19**: 523.

Fahy, J. V (2015) Type 2 inflammation in asthma--present in most, absent in many. *Nat Rev Immunol* **15**: 57–65.

Fallon, J.P., Reeves, E.P., and Kavanagh, K. (2010) Inhibition of neutrophil function following exposure to the *Aspergillus fumigatus* toxin fumagillin. *J Med Microbiol* **59**: 625–633.

Farnell, E., Rousseau, K., Thornton, D.J., Bowyer, P., and Herrick, S.E. (2012) Expression and secretion of *Aspergillus fumigatus* proteases are regulated in response to different protein substrates. *Fungal Biol* **116**: 1003–1012.

Faro-Trindade, I., Willment, J.A., Kerrigan, A.M., Redelinghuys, P., Hadebe, S., Reid, D.M., *et al.* (2012) Characterisation of innate fungal recognition in the lung. *PLoS One* **7**: e35675.

Farra, A., Islam, S., Str, A., Mikael, S., and Wretlind, B. (2008) Role of outer membrane protein OprD and penicillin-binding proteins in resistance of *Pseudomonas aeruginosa* to imipenem and meropenem. *Int J Antimicrob Ag* **31**: 427–433.

Farrell, P.M., Joffe, S., Foley, L., Canny, G.J., Mayne, P., and Rosenberg, M. (2007) Diagnosis of cystic fibrosis in the Republic of Ireland: Epidemiology and costs. *Ir Med J* **100**.

Farrow, J.M. 3rd, Hudson, L.L., Wells, G., Coleman, J.P., and Pesci, E.C. (2015) CysB Negatively Affects the Transcription of pqsR and Pseudomonas Quinolone Signal Production in *Pseudomonas aeruginosa*. *J Bacteriol* **197**: 1988–2002.

Féménia, F., Huet, D., Lair-Fulleringer, S., Wagner, M.C., Sarfati, J., Shingarova, L., *et al.* (2009) Effects of Conidia of Various *Aspergillus* Species on Apoptosis of Human Pneumocytes and Bronchial Epithelial Cells. *Mycopathologia* **167**: 249.

Ferreira, J.A.G., Penner, J.C., Moss, R.B., Haagensen, J.A.J., Clemons, K. V, Spormann, A.M., *et al.* (2015) Inhibition of *Aspergillus fumigatus* and Its Biofilm by *Pseudomonas aeruginosa* Is Dependent on the Source, Phenotype and Growth Conditions of the Bacterium. *PLoS One* **10**: e0134692.

Fetar, H., Gilmour, C., Klinoski, R., Daigle, D.M., Dean, C.R., and Poole, K. (2011) mexEF-oprN Multidrug Efflux Operon of *Pseudomonas aeruginosa* : Regulation by the MexT Activator in Response to Nitrosative Stress and Chloramphenicol **55**: 508–514.

Cystic Fibrosis Foundation Patient Registry 2017 Annual Data Report. https://www.cff.org/Research/Researcher-Resources/Patient-Registry/2017-Patient-Registry-Annual-Data-Report.pdf.

Filkins, L.M., Graber, J.A., Olson, D.G., Dolben, E.L., Lynd, L.R., Bhuju, S., and O'Toole, G.A. (2015) Coculture of *Staphylococcus aureusPseudomonas aeruginosa*S. aureus towards Fermentative Metabolism and Reduced Viability in a Cystic Fibrosis Model. *J Bacteriol* **197**: 2252 LP – 2264.

Filkins, L.M., Hampton, T.H., Gifford, A.H., Gross, M.J., Hogan, D.A., Sogin, M.L., *et al.* (2012) Prevalence of streptococci and

increased polymicrobial diversity associated with cystic fibrosis patient stability. *J Bacteriol* **194**: 4709–4717.

Filkins, L.M., and O'Toole, G.A. (2015) Cystic Fibrosis Lung Infections: Polymicrobial, Complex, and Hard to Treat. *PLOS Pathog* **11**: e1005258.

Finck-Barbançon, V., Goranson, J., Zhu, L., Sawa, T., Wiener-Kronish, J.P., Fleiszig, S.M.J., *et al.* (1997) ExoU expression by *Pseudomonas aeruginosa* correlates with acute cytotoxicity and epithelial injury. *Mol Microbiol* **25**: 547–557.

Floyd, M., Winn, M., Cullen, C., Sil, P., Chassaing, B., Yoo, D., *et al.* (2016) Swimming Motility Mediates the Formation of Neutrophil Extracellular Traps Induced by Flagellated *Pseudomonas aeruginosa*. *PLOS Pathog* **12**: e1005987.

Fontana, M.F., Banga, S., Barry, K.C., Shen, X., Tan, Y., Luo, Z.-Q., and Vance, R.E. (2011) Secreted Bacterial Effectors That Inhibit Host Protein Synthesis Are Critical for Induction of the Innate Immune Response to Virulent *Legionella pneumophila*. *PLOS Pathog* **7**: e1001289.

Fontana, M.F., Shin, S., and Vance, R.E. (2012) Activation of Host Mitogen-Activated Protein Kinases by Secreted *Legionella pneumophila* Effectors That Inhibit Host Protein Translation. *Infect Immun* **80**: 3570 LP – 3575.

Frese, S., Schaper, M., Kuster, J.-R., Miescher, D., Jaattela, M., Buehler, T., and Schmid, R.A. (2003) Cell death induced by down-regulation of heat shock protein 70 in lung cancer cell lines is p53-independent and does not require DNA cleavage. *J Thorac Cardiovasc Surg* **126**: 748–754.

Friedman, M. (2004) Applications of the ninhydrin reaction for analysis of amino acids, peptides, and proteins to agricultural and biomedical sciences. *J Agric Food Chem* **52**: 385–406.

Fugère, A., Lalonde Séguin, D., Mitchell, G., Déziel, E., Dekimpe, V., Cantin, A.M., *et al.* (2014) Interspecific Small Molecule Interactions between Clinical Isolates of *Pseudomonas aeruginosa* and *Staphylococcus aureus* from Adult Cystic Fibrosis Patients. *PLoS One* **9**: e86705.

Furtado, N.A.J.C., Said, S., Ito, I.Y., and Bastos, J.K. (2002) The antimicrobial activity of *Aspergillus fumigatus* is enhanced by a pool of bacteria. *Microbiol Res* **157**: 207–211.

Gabrilska, R.A., and Rumbaugh, K.P. (2015) Biofilm models of polymicrobial infection. *Future Microbiol* **10**: 1997–2015.

Gafa, V., Lande, R., Gagliardi, M.C., Severa, M., Giacomini, E., Remoli, M.E., *et al.* (2006) Human dendritic cells following *Aspergillus fumigatus* infection express the CCR7 receptor and a differential pattern of interleukin-12 (IL-12), IL-23, and IL-27 cytokines, which lead to a Th1 response. *Infect Immun* **74**: 1480–1489.

Gaille, C., Reimmann, C., and Haas, D. (2003) Isochorismate synthase (PchA), the first and rate-limiting enzyme in salicylate biosynthesis of *Pseudomonas aeruginosa*. *J Biol Chem* **278**: 16893–16898.

Gallagher, L., Owens, R.A., Dolan, S.K., O'Keeffe, G., Schrettl, M., Kavanagh, K., *et al.* (2012) The *Aspergillus fumigatus* Protein GliK Protects against Oxidative Stress and Is Essential for Gliotoxin Biosynthesis. *Eukaryot Cell* **11**: 1226 LP – 1238.

Gallagher, L.A., McKnight, S.L., Kuznetsova, M.S., Pesci, E.C., and Manoil, C. (2002) Functions required for extracellular quinolone signaling by *Pseudomonas aeruginosa*. *J Bacteriol* **184**: 6472–6480.

Gallego, M., Pomares, X., Espasa, M., Castañer, E., Solé, M., Suárez, D., *et al.* (2014) *Pseudomonas aeruginosa* isolates in severe chronic obstructive pulmonary disease: characterization and risk factors. *BMC Pulm Med* **14**: 103.

Galluzzi, L., Kepp, O., and Kroemer, G. (2012) Mitochondria: Master regulators of danger signalling. *Nat Rev Mol Cell Biol* **13**: 780–788.

Gardiner, D.M., and Howlett, B.J. (2005) Bioinformatic and expression analysis of the putative gliotoxin biosynthetic gene cluster of *Aspergillus fumigatus*. *FEMS Microbiol Lett* **248**: 241–248.

Garlanda, C., Hirsch, E., Bozza, S., Salustri, A., Acetis, M. De, Nota, R., *et al.* (2002) Non-redundant role of the long pentraxin PTX3 in anti-fungal innate immune response. *Nature* **420**: 182–186.

Garlanda, C., Jaillon, S., Doni, A., Bottazzi, B., and Mantovani, A. (2016) PTX3, a humoral pattern recognition molecule at the interface between microbe and matrix recognition. *Curr Opin Immunol* **38**: 39–44.

Garrity-Ryan, L., Kazmierczak, B., Kowal, R., Comolli, J., Hauser, A., and Engel, J.N. (2000) The Arginine Finger Domain of ExoT Contributes to Actin Cytoskeleton Disruption and Inhibition of Internalization *Pseudomonas aeruginosa* by Epithelial Cells and Macrophages. *Infect Immun* **68**: 7100 LP – 7113.

Gars, M. Le, Descamps, D., Roussel, D., Saussereau, E., Guillot, L., Ruffin, M., *et al.* (2013) Neutrophil elastase degrades cystic fibrosis transmembrane conductance regulator via calpains and disables channel function in vitro and in vivo. *Am J Respir Crit Care Med* **187**: 170–179.

Gellatly, S.L., and Hancock, R.E.W. (2013) *Pseudomonas aeruginosa* : new insights into pathogenesis and host defenses . *Pathog Dis* **67**: 159–173.

Genster, N., Præstekjær Cramer, E., Rosbjerg, A., Pilely, K., Cowland, J.B., and Garred, P. (2016) Ficolins Promote Fungal Clearance in vivo and Modulate the Inflammatory Cytokine Response in Host Defense against *Aspergillus fumigatus*. *J Innate Immun* **8**: 579–588.

Ghai, I., and Ghai, S. (2018) Understanding antibiotic resistance via outer membrane permeability. *Infect Drug Resist* **11**: 523–530.

Ghosh, S., Hoselton, S.A., and Schuh, J.M. (2015) Allergic Inflammation in *Aspergillus fumigatus*-Induced Fungal Asthma. *Curr Allergy Asthma Rep* **15**: 59.

Gibbs, K., and Holzman, I.R. (2012) Endotracheal tube: friend or foe? Bacteria, the endotracheal tube, and the impact of colonization and infection. *Semin Perinatol* **36**: 454–461.

Giddey, A.D., Kock, E. de, Nakedi, K.C., Garnett, S., Nel, A.J.M., Soares, N.C., and Blackburn, J.M. (2017) A temporal proteome dynamics study reveals the molecular basis of induced phenotypic resistance in Mycobacterium smegmatis at sub-lethal rifampicin concentrations. *Sci Rep* **7**: 43858.

Goldberg, J.B., and Pier, G.B. (2000) The role of the CFTR in susceptibility to *Pseudomonas aeruginosa* infections in cystic fibrosis. *Trends Microbiol* **8**: 514–520.

Golovkine, G., Faudry, E., Bouillot, S., Elsen, S., Attrée, I., and Huber, P. (2016) *Pseudomonas aeruginosa* Transmigrates at Epithelial Cell-Cell Junctions, Exploiting Sites of Cell Division and Senescent Cell Extrusion. *PLOS Pathog* **12**: e1005377.

Goodman, A.L., Kulasekara, B., Rietsch, A., Boyd, D., Smith, R.S., and Lory, S. (2004) A signaling network reciprocally regulates genes associated with acute infection and chronic persistence in *Pseudomonas aeruginosa*. *Dev Cell* **7**: 745–754.

Gould, K. (2016) Antibiotics: from prehistory to the present day. *J Antimicrob Chemother* **71**: 572–575.

Govan, J.R., and Deretic, V. (1996) Microbial pathogenesis in cystic fibrosis: mucoid *Pseudomonas aeruginosa* and Burkholderia cepacia. *Microbiol Rev* **60**: 539–74.

Goyal, S., Castrillón-Betancur, J.C., Klaile, E., and Slevogt, H. (2018) The Interaction of Human Pathogenic Fungi With C-Type Lectin Receptors. *Front Immunol* **9**: 1261.

Graham, R.L., Graham, C., and McMullan, G. (2007) Microbial proteomics: a mass spectrometry primer for biologists. *Microb Cell Fact* **6**: 26.

Graves, P.R., and Haystead, T.A.J. (2002) Molecular biologist's guide to proteomics. *Microbiol Mol Biol Rev* **66**: 39–63.

Greenberg, E.P. (2000) Pump up the versatility. *Nature* **406**: 947–948.

Griffith, E.C., Su, Z., Niwayama, S., Ramsay, C.A., Chang, Y.H., and Liu, J.O. (1998) Molecular recognition of angiogenesis inhibitors fumagillin and ovalicin by methionine aminopeptidase 2. *Proc Natl Acad Sci* **95**: 15183–15188.

Guerra-Santos, L.H., Käppeli, O., and Fiechter, A. (1986) Dependence of *Pseudomonas aeruginosa* continous culture biosurfactant production on nutritional and environmental factors. *Appl Microbiol Biotechnol* **24**: 443–448.

Guillon, A., Fouquenet, D., Morello, E., Henry, C., Georgeault, S., Si-Tahar, M., and Hervé, V. (2018) Treatment of *Pseudomonas aeruginosa* Biofilm Present in Endotracheal Tubes by Poly-1-Lysine. *Antimicrob Agents Chemother* **62**: e00564-18.

Gundry, R.L., White, M.Y., Murray, C.I., Kane, L.A., Fu, Q., Stanley, B.A., and Eyk, J.E. Van (2010) Preparation of Proteins and Peptides for Mass Spectrometry Analysis in a Bottom-Up Proteomics Workflow. *Curr Protoc Mol Biol* **10:** 10.25.

Gurbuxani, S., Schmitt, E., Cande, C., Parcellier, A., Hammann, A., Daugas, E., *et al.* (2003) Heat shock protein 70 binding inhibits the nuclear import of apoptosis-inducing factor. *Oncogene* **22**: 6669–6678.

Guruceaga, X., Ezpeleta, G., Mayayo, E., Sueiro-Olivares, M., Abad-Diaz-De-Cerio, A., Aguirre Urízar, J.M., *et al.* (2018) A possible role for fumagillin in cellular damage during host infection by *Aspergillus fumigatus*. *Virulence* **9**: 1548–1561.

Guttenplan, S.B., and Kearns, D.B. (2013) Regulation of flagellar motility during biofilm formation. *FEMS Microbiol Rev* **37**: 849–871.

Hachem, R., Gomes, M.Z.R., Helou, G. El, Zakhem, A. El, Kassis, C., Ramos, E., *et al.* (2014) Invasive aspergillosis caused by *Aspergillus terreus*: an emerging opportunistic infection with poor outcome independent of azole therapy. *J Antimicrob Chemother* **69**: 3148–3155.

Hagiwara, D., Takahashi, H., Kusuya, Y., Kawamoto, S., Kamei, K., and Gonoi, T. (2016) Comparative transcriptome analysis revealing dormant conidia and germination associated genes in *Aspergillus* species: an essential role for AtfA in conidial dormancy. *BMC Genomics* **17**: 358.

Hahn, I., Klaus, A., Janze, A.-K., Steinwede, K., Ding, N., Bohling, J., *et al.* (2011) Cathepsin G and Neutrophil Elastase Play Critical and Nonredundant Roles in Lung-Protective Immunity against Streptococcus pneumoniae in Mice. *Infect Immun* **79**: 4893 LP – 4901.

Hall-Stoodley, L., Nistico, L., Sambanthamoorthy, K., Dice, B., Nguyen, D., Mershon, W.J., *et al.* (2008) Characterization of biofilm matrix, degradation by DNase treatment and evidence of capsule downregulation in *Streptococcus pneumoniae* clinical isolates. *BMC Microbiol* **8**: 173.

Hall, S., McDermott, C., Anoopkumar-Dukie, S., McFarland, A.J., Forbes, A., Perkins, A. V, *et al.* (2016) Cellular Effects of Pyocyanin, a Secreted Virulence Factor of *Pseudomonas aeruginosa*. *Toxins (Basel)* **8**.

Hamed, K., and Debonnett, L. (2017) Tobramycin inhalation powder for the treatment of pulmonary *Pseudomonas aeruginosa* infection in patients with cystic fibrosis: a review based on clinical evidence. *Ther Adv Respir Dis* **11**: 193–209.

Hamon, Y., Jaillon, S., Person, C., Ginies, J.-L., Garo, E., Bottazzi, B., *et al.* (2013) Proteolytic cleavage of the long pentraxin PTX3 in the airways of cystic fibrosis patients. *Innate Immun* **19**: 611–622.

Haq, I.J., Gray, M.A., Garnett, J.P., Ward, C., and Brodlie, M. (2016) Airway surface liquid homeostasis in cystic fibrosis: pathophysiology and therapeutic targets. *Thorax* **71**: 284–287.

Hare, J.M. (2013) Sabouraud Agar for Fungal Growth BT - Laboratory Protocols in Fungal Biology: Current Methods in Fungal Biology. In Gupta, V.K., Tuohy, M.G., Ayyachamy, M., Turner, K.M., and O'Donovan, A. (eds). Springer New York, New York, NY. pp. 211–216.

Harriott, M.M., and Noverr, M.C. (2011) Importance of Candida-bacterial polymicrobial biofilms in disease. *Trends Microbiol* **19**: 557–563.

Harrison, F. (2007) Microbial ecology of the cystic fibrosis lung. *Microbiology* **153**: 917–923.

Hartl, D. (2009) Immunological mechanisms behind the cystic fibrosis-ABPA link. *Med Mycol* **47**: S183–S191.

Hartl, D., Griese, M., Kappler, M., Zissel, G., Reinhardt, D., Rebhan, C., *et al.* (2006) Pulmonary T(H)2 response in *Pseudomonas aeruginosa*-infected patients with cystic fibrosis. *J Allergy Clin Immunol* **117**: 204–211.

Hartl, D., Latzin, P., Hordijk, P., Marcos, V., Rudolph, C., Woischnik, M., *et al.* (2007) Cleavage of CXCR1 on neutrophils disables bacterial killing in cystic fibrosis lung disease. *Nat Med* **13**: 1423–1430.

Hashemi, M.M., Holden, B.S., Coburn, J., Taylor, M.F., Weber, S., Hilton, B., *et al.* (2019) Proteomic Analysis of Resistance of Gram-Negative Bacteria to Chlorhexidine and Impacts on Susceptibility to Colistin, Antimicrobial Peptides, and Ceragenins. *Front Microbiol* **10**: 210.

Hatori, Y., and Lutsenko, S. (2016) The Role of Copper Chaperone Atox1 in Coupling Redox Homeostasis to Intracellular Copper Distribution. *Antioxidants (Basel)* **5**: 25.

Hauser, A.R. (2009) The type III secretion system of *Pseudomonas aeruginosa*: infection by injection. *Nat Rev Microbiol* **7**: 654–665.

Hawdon, N.A., Aval, P.S., Barnes, R.J., Gravelle, S.K., Rosengren, J., Khan, S., *et al.* (2010) Cellular responses of A549 alveolar epithelial cells to serially collected *Pseudomonas aeruginosa* from cystic fibrosis patients at different stages of pulmonary infection. *FEMS Immunol Med Microbiol* **59**: 207–220.

He, Y., Hara, H., and Núñez, G. (2016) Mechanism and Regulation of NLRP3 Inflammasome Activation. *Trends Biochem Sci* **41**: 1012–1021.

Hector, A., Kirn, T., Ralhan, A., Graepler-Mainka, U., Berenbrinker, S., Riethmueller, J., *et al.* (2016) Microbial colonization and lung function in adolescents with cystic fibrosis. *J Cyst Fibros* **15**: 340–349.

Heeb, S., Fletcher, M.P., Chhabra, S.R., Diggle, S.P., Williams, P., and Cámara, M. (2011) Quinolones: from antibiotics to autoinducers. *FEMS Microbiol Rev* **35**: 247–274.

Heinekamp, T., Schmidt, H., Lapp, K., Pähtz, V., Shopova, I., Köster-Eiserfunke, N., *et al.* (2015) Interference of *Aspergillus fumigatus* with the immune response. *Semin Immunopathol* **37**: 141–152.

Heinekamp, T., Thywißen, A., Macheleidt, J., Keller, S., Valiante, V., and Brakhage, A.A. (2013) *Aspergillus fumigatus* melanins: interference with the host endocytosis pathway and impact on virulence. *Front Microbiol* **3**: 440.

Henke, M.O., and Ratjen, F. (2007) Mucolytics in cystic fibrosis. *Paediatr Respir Rev* **8**: 24–29.

Herrmann, J., Lukežič, T., Kling, A., Baumann, S., Hüttel, S., Petković, H., and Müller, R. (2016) Strategies for the Discovery and Development of New Antibiotics from Natural Products: Three Case Studies. How to Overcome the Antibiotic Crisis: Facts, Challenges, Technologies and Future Perspectives. Stadler, M., and Dersch, P. (eds). Springer International Publishing, Cham. pp. 339–363.

Herschend, J., Damholt, Z.B. V, Marquard, A.M., Svensson, B., Sørensen, S.J., Hägglund, P., and Burmølle, M. (2017) A meta-proteomics approach to study the interspecies interactions affecting microbial biofilm development in a model community. *Sci Rep* **7**: 16483.

Hibbing, M.E., Fuqua, C., Parsek, M.R., and Peterson, S.B. (2010) Bacterial competition: surviving and thriving in the microbial jungle. *Nat Rev Microbiol* **8**: 15–25.

Hirakawa, H., and Tomita, H. (2013) Interference of bacterial cell-to-cell communication: a new concept of antimicrobial chemotherapy breaks antibiotic resistance. *Front Microbiol* **4**: 114.

Hirche, T.O., Benabid, R., Deslee, G., Gangloff, S., Achilefu, S., Guenounou, M., *et al.* (2008) Neutrophil Elastase Mediates Innate Host Protection against *Pseudomonas aeruginosa J Immunol* **181**: 4945 LP – 4954.

Hodges, C.A., and Conlon, R.A. (2019) Delivering on the promise of gene editing for cystic fibrosis. *Genes Dis* **6**: 97–108.

Hoffman, L.R., Kulasekara, H.D., Emerson, J., Houston, L.S., Burns, J.L., Ramsey, B.W., and Miller, S.I. (2009) *Pseudomonas aeruginosa* lasR mutants are associated with cystic fibrosis lung disease progression. *J Cyst Fibros* **8**: 66–70.

Hoffmeister, D., and Keller, N.P. (2007) Natural products of filamentous fungi: enzymes, genes, and their regulation. *Nat Prod Rep* **24**: 393–416.

Hogardt, M., and Heesemann, J. (2010) Adaptation of *Pseudomonas aeruginosa* during persistence in the cystic fibrosis lung. *Int J Med Microbiol* **300**: 557–562.

Holcombe, L.J., McAlester, G., Munro, C.A., Enjalbert, B., Brown, A.J.P., Gow, N.A.R., *et al.* (2010) *Pseudomonas aeruginosa* secreted factors impair biofilm development in *Candida albicans*. *Microbiology* **156**: 1476–1486.

Hope, W.W., Walsh, T.J., and Denning, D.W. (2005) The invasive and saprophytic syndromes due to *Aspergillus spp*. *Med Mycol* **43**: S207–S238.

Horna G., López M., Guerra H., S.Y. and R.J. (2018) Interplay between MexAB-OprM and MexEF-OprN in clinical isolates of *Pseudomonas aeruginosa*. *Sci Rep* **8**: 16463.

Howell, H.A., Logan, L.K., and Hauser, A.R. (2013) Type III Secretion of ExoU Is Critical during Early *Pseudomonas aeruginosa* Pneumonia. *MBio* **4**: e00032-13.

Hsieh, S.-H., Kurzai, O., and Brock, M. (2017) Persistence within dendritic cells marks an antifungal evasion and dissemination strategy of *Aspergillus terreus*. *Sci Rep* **7**: 10590.

Huck, C.W., and Bonn, G.K. (2000) Recent developments in polymer-based sorbents for solid-phase extraction. *J Chromatogr A* **885**: 51–72.

Huerta, A., Soler, N., Esperatti, M., Guerrero, M., Menendez, R., Gimeno, A., *et al.* (2014) Importance of *Aspergillus spp.* isolation in Acute exacerbations of severe COPD: prevalence, factors and follow-up: the FUNGI-COPD study. *Respir Res* **15**: 17.

Hunter, R.C., Klepac-Ceraj, V., Lorenzi, M.M., Grotzinger, H., Martin, T.R., and Newman, D.K. (2012) Phenazine content in the cystic fibrosis respiratory tract negatively correlates with lung function and microbial complexity. *Am J Respir Cell Mol Biol* **47**: 738–745.

Hurley, M.N. (2018) *Staphylococcus aureus* in cystic fibrosis: problem bug or an innocent bystander? *Breathe (Sheff)* **14**: 87–90.

Ibrahim-Granet, O., Philippe, B., Boleti, H., Boisvieux-Ulrich, E., Grenet, D., Stern, M., and Latge, J.P. (2003) Phagocytosis and intracellular fate of *Aspergillus fumigatus* conidia in alveolar macrophages. *Infect Immun* **71**: 891–903.

Ichikawa, J.K., Norris, A., Bangera, M.G., Geiss, G.K., & van 't Wout, A.B. van, Bumgarner, R.E., and Lory, S. (2000) Interaction of *Pseudomonas aeruginosa* with epithelial cells: Identification of differentially regulated genes by expression microarray analysis of human cDNAs. *Proc Natl Acad Sci* **97**: 9659 LP – 9664.

Inglis, D.O., Binkley, J., Skrzypek, M.S., Arnaud, M.B., Cerqueira, G.C., Shah, P., *et al.* (2013) Comprehensive annotation of secondary metabolite biosynthetic genes and gene clusters of *Aspergillus nidulans, A. fumigatus, A. niger* and *A. oryzae*. *BMC Microbiol* **13**: 91.

Iobbi-Nivol, C., and Leimkühler, S. (2013) Molybdenum enzymes, their maturation and molybdenum cofactor biosynthesis in *Escherichia coli*. *Biochim Biophys Acta* **1827**: 1086–1101.

Ivanov, A. V., Bartosch, B., and Isaguliants, M.G. (2017) Oxidative Stress in Infection and Consequent Disease. *Oxid Med Cell Longev* **2017**: 1–3.

Jackson, M.P., and Hewitt, E.W. (2016) Cellular proteostasis: degradation of misfolded proteins by lysosomes. *Essays Biochem* **60**: 173–180.

Jagmann, N., and Philipp, B. (2018) SpoT-Mediated Regulation and Amino Acid Prototrophy Are Essential for Pyocyanin Production During Parasitic Growth of *Pseudomonas aeruginosa* in a Co-culture Model System With *Aeromonas hydrophila*. *Front Microbiol* **9**: 761.

Jahn, B., Langfelder, K., Schneider, U., Schindel, C., and Brakhage, A.A. (2002) PKSP-dependent reduction of phagolysosome fusion and intracellular kill of *Aspergillus fumigatus* conidia by human monocyte-derived macrophages. *Cell Microbiol* **4**: 793–803.

Jaillon, S., Peri, G., Delneste, Y., Fremaux, I., Doni, A., Moalli, F., *et al.* (2007) The humoral pattern recognition receptor PTX3 is stored in neutrophil granules and localizes in extracellular traps. *J Exp Med* **204**: 793–804.

Jain, M., Ramirez, D., Seshadri, R., Cullina, J.F., Powers, C.A., Schulert, G.S., *et al.* (2004) Type III secretion phenotypes of *Pseudomonas aeruginosa* strains change during infection of individuals with cystic fibrosis. *J Clin Microbiol* **42**: 5229–5237.

Janahi, I.A., Rehman, A., and Al-Naimi, A.R. (2017) Allergic bronchopulmonary aspergillosis in patients with cystic fibrosis. *Ann Thorac Med* **12**: 74–82.

Jean Beltran, P.M., Federspiel, J.D., Sheng, X., and Cristea, I.M. (2017) Proteomics and integrative omic approaches for understanding host-pathogen interactions and infectious diseases. *Mol Syst Biol* **13**: 922.

Jensen, L.J., Kuhn, M., Stark, M., Chaffron, S., Creevey, C., Muller, J., *et al.* (2009) STRING 8 - A global view on proteins and their functional interactions in 630 organisms. *Nucleic Acids Res* **37**: 412–416.

Jensen, P.Ø. (2014) Physiological levels of nitrate support anoxic growth by denitrification of *Pseudomonas aeruginosa* at growth rates reported in cystic fibrosis lungs and sputum. **5**: 1–11.

Jensen, P.Ø., Bjarnsholt, T., Phipps, R., Rasmussen, T.B., Calum, H., Christoffersen, L., *et al.* (2007) Rapid necrotic killing of polymorphonuclear leukocytes is caused by quorum-sensing-controlled production of rhamnolipid by *Pseudomonas aeruginosa*. *Microbiology* **153**: 1329–1338.

Jeong, J.S., Kim, S.R., and Lee, Y.C. (2018) Can Controlling Endoplasmic Reticulum Dysfunction Treat Allergic Inflammation in Severe Asthma With Fungal Sensitization? *Allergy Asthma Immunol Res* **10**: 106–120.

Jesaitis, A.J., Franklin, M.J., Berglund, D., Sasaki, M., Lord, C.I., Bleazard, J.B., *et al.* (2003) Compromised host defense on *Pseudomonas aeruginosa* biofilms: characterization of neutrophil and biofilm interactions. *J Immunol* **171**: 4329–4339.

Jiang, F., Wang, X., Wang, B., Chen, L., Zhao, Z., Waterfield, N.R., *et al.* (2016) The *Pseudomonas aeruginosa* Type VI Secretion PGAP1-like Effector Induces Host Autophagy by Activating Endoplasmic Reticulum Stress. *Cell Rep* **16**: 1502–1509.

Jiménez, A., García, P., la Puente, S. de, Madrona, A., Camarasa, M.J., Pérez-Pérez, M.-J., *et al.* (2018) A Novel Class of Cationic and Non-Peptidic Small Molecules as Hits for the Development of Antimicrobial Agents. *Molecules* **23**: 1513.

Johns, A., Scharf, D.H., Gsaller, F., Schmidt, H., Heinekamp, T., Straßburger, M., *et al.* (2017) A Nonredundant Phosphopantetheinyl Transferase, PptA, Is a Novel Antifungal Target That Directs Secondary Metabolite, Siderophore, and Lysine Biosynthesis in *Aspergillus fumigatus* and Is Critical for Pathogenicity. *MBio* **8**: e01504-16.

Jones-Dias, D., Carvalho, A.S., Moura, I.B., Manageiro, V., Igrejas, G., Caniça, M., and Matthiesen, R. (2017) Quantitative proteome analysis of an antibiotic resistant *Escherichia coli* exposed to tetracycline reveals multiple affected metabolic and peptidoglycan processes. *J Proteomics* **156**: 20–28.

Jundi, K., and Greene, C.M. (2015) Transcription of Interleukin-8: How Altered Regulation Can Affect Cystic Fibrosis Lung Disease. *Biomolecules* **5**: 1386–1398.

Kalam, H., Fontana, M.F., and Kumar, D. (2017) Alternate splicing of transcripts shape macrophage response to Mycobacterium tuberculosis infection. *PLOS Pathog* **13**: e1006236.

Kalia, D., Merey, G., Nakayama, S., Zheng, Y., Zhou, J., Luo, Y., *et al.* (2013) Nucleotide, c-di-GMP, c-di-AMP, cGMP, cAMP, (p)ppGpp signaling in bacteria and implications in pathogenesis. *Chem Soc Rev* **42**: 305–341.

Kamath, K.S., Kumar, S.S., Kaur, J., Venkatakrishnan, V., Paulsen, I.T., Nevalainen, H., and Molloy, M.P. (2015) Proteomics of hosts and pathogens in cystic fibrosis. *Proteomics Clin Appl* **9**: 134–146.

Kanekura, K., Nishimoto, I., Aiso, S., and Matsuoka, M. (2006) Characterization of amyotrophic lateral sclerosis-linked P56S mutation of vesicle-associated membrane protein-associated protein B (VAPB/ALS8). *J Biol Chem* **281**: 30223–30233.

Kasperkovitz, P. V, Cardenas, M.L., and Vyas, J.M. (2010) TLR9 is actively recruited to *Aspergillus fumigatus* phagosomes and requires the N-terminal proteolytic cleavage domain for proper intracellular trafficking. *J Immunol* **185**: 7614–7622.

Kaur, G., and Dufour, J.M. (2012) Cell lines: Valuable tools or useless artifacts. *Spermatogenesis* **2**: 1–5.

Kaur, J., Pethani, B.P., Kumar, S., Kim, M., Sunna, A., Kautto, L., *et al.* (2015) *Pseudomonas aeruginosa* inhibits the growth of *Scedosporium aurantiacum*, an opportunistic fungal pathogen isolated from the lungs of cystic fibrosis patients. *Front Microbiol* **6**: 866.

Keller, N.P. (2019) Fungal secondary metabolism: regulation, function and drug discovery. *Nat Rev Microbiol* **17**: 167–180.

Kelly, E., Greene, C.M., and McElvaney, N.G. (2008) Targeting neutrophil elastase in cystic fibrosis. *Expert Opin Ther Targets* **12**: 145–157.

Ketko, A.K., Lin, C., Moore, B.B., and LeVine, A.M. (2013) Surfactant Protein A Binds Flagellin Enhancing Phagocytosis and IL-1β Production. *PLoS One* **8**: e82680.

Khoufache, K., Puel, O., Loiseau, N., Delaforge, M., Rivollet, D., Coste, A., *et al.* (2007) Verruculogen associated with *Aspergillus fumigatus* hyphae and conidia modifies the electrophysiological properties of human nasal epithelial cells. *BMC Microbiol* **7**: 5.

Kim, J.-T., Kim, K.D., Song, E.Y., Lee, H.G., Kim, J.W., Kim, J.W., *et al.* (2006) Apoptosis-inducing factor (AIF) inhibits protein synthesis by interacting with the eukaryotic translation initiation factor 3 subunit p44 (eIF3g). *FEBS Lett* **580**: 6375–6383.

Kim, S., Joe, Y., Park, S.-U., Jeong, S.O., Kim, J.-K., Park, S.H., *et al.* (2018) Induction of endoplasmic reticulum stress under endotoxin tolerance increases inflammatory responses and decreases *Pseudomonas aeruginosa* pneumonia. *J Leukoc Biol* **104**: 1003–1012.

King, J., Brunel, S.F., and Warris, A. (2016a) Aspergillus infections in cystic fibrosis. *J Infect* **72 Suppl**: S50-5.

King, J., Henriet, S.S. V, and Warris, A. (2016b) Aspergillosis in Chronic Granulomatous Disease. *J fungi (Basel, Switzerland)* **2**: 15.

Klein, S., Lorenzo, C., Hoffmann, S., Walther, J.M., Storbeck, S., Piekarski, T., *et al.* (2009) Adaptation of *Pseudomonas aeruginosa* to various conditions includes tRNA-dependent formation of alanyl-phosphatidylglycerol. *Mol Microbiol* **71**: 551–565.

Knapp, E.A., Fink, A.K., Goss, C.H., Sewall, A., Ostrenga, J., Dowd, C., *et al.* (2016) The Cystic Fibrosis Foundation Patient Registry. Design and Methods of a National Observational Disease Registry. *Ann Am Thorac Soc* **13**: 1173–1179.

Knowles, M.R., and Boucher, R.C. (2002) Mucus clearance as a primary innate defense mechanism for mammalian airways. *J Clin Invest* **109**: 571–577.

Knutsen, A.P., Hutcheson, P.S., Slavin, R.G., and Kurup, V.P. (2004) IgE antibody to *Aspergillus fumigatus* recombinant allergens in cystic fibrosis patients with allergic bronchopulmonary aspergillosis. *Allergy* **59**: 198–203.

Knutsen, A.P., and Slavin, R.G. (2011) Allergic bronchopulmonary aspergillosis in asthma and cystic fibrosis. *Clin Dev Immunol* 843763.

Koch, C. (2002) Early infection and progression of cystic fibrosis lung disease. *Pediatr Pulmonol* **34**: 232–236.

Kogan, T. V, Jadoun, J., Mittelman, L., Hirschberg, K., and Osherov, N. (2004) Involvement of Secreted *Aspergillus fumigatus* Proteases in Disruption of the Actin Fiber Cytoskeleton and Loss of Focal Adhesion Sites in Infected A549 Lung Pneumocytes. *J Infect Dis* **189**: 1965–1973.

Koh, A.Y., Priebe, G.P., Ray, C., Rooijen, N. Van, and Pier, G.B. (2009) Inescapable Need for Neutrophils as Mediators of Cellular Innate Immunity to Acute *Pseudomonas aeruginosa* Pneumonia. *Infect Immun* **77**: 5300 LP – 5310.

Kollef, M.H. (2008) Broad-Spectrum Antimicrobials and the Treatment of Serious Bacterial Infections: Getting It Right Up Front. *Clin Infect Dis* **47**: S3–S13.

Koo, S.H. (2015) Overexpression of Efflux Pump in Multiresistant *Pseudomonas aeruginosa*: How You Will Discover and Treat It? *Infect Chemother* **47**: 142–144.

Korgaonkar, A., Trivedi, U., Rumbaugh, K.P., and Whiteley, M. (2013) Community surveillance enhances *Pseudomonas aeruginosa* virulence during polymicrobial infection. *Proc Natl Acad Sci U S A* **110**: 1059–1064.

Kosmidis, C., and Denning, D.W. (2015) The clinical spectrum of pulmonary aspergillosis. *Postgrad Med J* **91**: 403–410.

Kraemer, R., Delosea, N., Ballinari, P., Gallati, S., and Crameri, R. (2006) Effect of allergic bronchopulmonary aspergillosis on lung function in children with cystic fibrosis. *Am J Respir Crit Care Med* **174**: 1211–1220.

Krall, R., Sun, J., Pederson, K.J., and Barbieri, J.T. (2002) In vivo Rho GTPase-activating protein activity of *Pseudomonas aeruginosa* cytotoxin Exos. *Infect Immun* **70**: 360–367.

Kroll, M., Arenzana-Seisdedos, F., Bachelerie, F., Thomas, D., Friguet, B., and Conconi, M. (1999) The secondary fungal metabolite gliotoxin targets proteolytic activities of the proteasome. *Chem Biol* **6**: 689–698.

Krusemark, C.J., Frey, B.L., Belshaw, P.J., and Smith, L.M. (2009) Modifying the charge state distribution of proteins in electrospray ionization mass spectrometry by chemical derivatization. *J Am Soc Mass Spectrom* **20**: 1617–1625.

Kuang, Z., Hao, Y., Hwang, S., Zhang, S., Kim, E., Akinbi, H.T., *et al*. (2011a) The *Pseudomonas aeruginosa* flagellum confers resistance to pulmonary surfactant protein-A by impacting the production of exoproteases through quorum-sensing. *Mol Microbiol* **79**: 1220–1235.

Kuang, Z., Hao, Y., Walling, B.E., Jeffries, J.L., Ohman, D.E., and Lau, G.W. (2011b) *Pseudomonas aeruginosa* Elastase Provides an Escape from Phagocytosis by Degrading the Pulmonary Surfactant Protein-A. *PLoS One* **6**: e27091.

Kück, U., Bloemendal, S., and Teichert, I. (2014) Putting fungi to work: harvesting a cornucopia of drugs, toxins, and antibiotics. *PLoS Pathog* **10**: e1003950–e1003950.

Kurucz, V., Krüger, T., Antal, K., Dietl, A.-M., Haas, H., Pócsi, I., *et al.* (2018) Additional oxidative stress reroutes the global response of *Aspergillus fumigatus* to iron depletion. *BMC Genomics* **19**: 357.

Kwon-Chung, K.J., and Sugui, J.A. (2009) What do we know about the role of gliotoxin in the pathobiology of *Aspergillus fumigatus*? *Med Mycol* **47 Suppl 1**: S97–S103.

Labby, K.J., and Garneau-Tsodikova, S. (2013) Strategies to overcome the action of aminoglycoside-modifying enzymes for treating resistant bacterial infections. *Future Med Chem* **5**: 1285–1309.

Lapaquette, P., Guzzo, J., Bretillon, L., and Bringer, M.-A. (2015) Cellular and Molecular Connections between Autophagy and Inflammation. *Mediators Inflamm* **2015**: 398483.

Latgé, J.P. (1999) *Aspergillus fumigatus* and Aspergillosis. **12**: 310–350.

Lavoie, E.G., Wangdi, T., and Kazmierczak, B.I. (2011) Innate immune responses to *Pseudomonas aeruginosa* infection. *Microbes Infect* **13**: 1133–1145.

Leão, R.S., Pereira, R.H. V, Folescu, T.W., Albano, R.M., Santos, E.A., Junior, L.G.C., and Marques, E.A. (2011) KPC-2 Carbapenemase-producing Klebsiella pneumoniae isolates from patients with Cystic Fibrosis. *J Cyst Fibros* **10**: 140–142.

Leclair, L.W., and Hogan, D.A. (2010) Mixed bacterial-fungal infections in the CF respiratory tract. *Med Mycol* **48**: 125–132.

Lee, J.A., Uhlik, M.T., Moxham, C.M., Tomandl, D., and Sall, D.J. (2012) Modern Phenotypic Drug Discovery Is a Viable, Neoclassic Pharma Strategy. *J Med Chem* **55**: 4527–4538.

Lee, K.S., Jeong, J.S., Kim, S.R., Cho, S.H., Kolliputi, N., Ko, Y.H., *et al.* (2016) Phosphoinositide 3-kinase-delta regulates fungus-induced allergic lung inflammation through endoplasmic reticulum stress. *Thorax* **71**: 52–63.

Li, H., Luo, Y.-F., Williams, B.J., Blackwell, T.S., and Xie, C.-M. (2012a) Structure and function of OprD protein in *Pseudomonas aeruginosa*: from antibiotic resistance to novel therapies. *Int J Med Microbiol* **302**: 63–68.

Li, J., Chai, Q.Y., and Liu, C.H. (2016) The ubiquitin system: A critical regulator of innate immunity and pathogen-host interactions. *Cell Mol Immunol* **13**: 560–576.

Li, Z., Adams, R.M., Chourey, K., Hurst, G.B., Hettich, R.L., and Pan, C. (2012b) Systematic Comparison of Label-Free, Metabolic Labeling, and Isobaric Chemical Labeling for Quantitative Proteomics on LTQ Orbitrap Velos. *J Proteome Res* **11**: 1582–1590.

Li, Z., Tao, L., Zhang, J., Zhang, H., and Qu, J.-M. (2012c) Role of NOD2 in regulating the immune response to *Aspergillus fumigatus*. *Inflamm Res* **61**: 643–648.

Lieber, M., Smith, B., Szakal, A., Nelson-Rees, W., and Todaro, G. (1976) A continuous tumor-cell line from a human lung carcinoma with properties of type II alveolar epithelial cells. *Int J cancer* **17**: 62–70.

Limoli, D.H., Whitfield, G.B., Kitao, T., Ivey, M.L., Davis, M.R., Grahl, N., *et al.* (2017) *Pseudomonas aeruginosa* Alginate Overproduction Promotes Coexistence with *Staphylococcus aureus* in a Model of Cystic Fibrosis Respiratory Infection. *MBio* **8**: e00186-17.

Limoli, D.H., Yang, J., Khansaheb, M.K., Helfman, B., Peng, L., Stecenko, A.A., and Goldberg, J.B. (2016) *Staphylococcus aureus* and *Pseudomonas aeruginosa* co-infection is associated with cystic fibrosis-related diabetes and poor clinical outcomes. *Eur J Clin Microbiol Infect Dis* **35**: 947–953.

Lin, D., Tabb, D.L., and Yates, J.R. 3rd (2003) Large-scale protein identification using mass spectrometry. *Biochim Biophys Acta* **1646**: 1–10.

Lin, J., Cheng, J., Wang, Y., and Shen, X. (2018) The Pseudomonas Quinolone Signal (PQS): Not Just for Quorum Sensing Anymore. *Front Cell Infect Microbiol* **8**: 230.

Line, L., Alhede, M., Kolpen, M., Kühl, M., Ciofu, O., Bjarnsholt, T., *et al.* (2014) Physiological levels of nitrate support anoxic growth by denitrification of *Pseudomonas aeruginosa* at growth rates reported in cystic fibrosis lungs and sputum. *Front Microbiol* **5**: 554.

Lippolis, R., and Angelis, M. De (2016) Proteomics and Human Diseases. *J Proteomics Bioinform* **09**.

LiPuma, J.J. (2010) The Changing Microbial Epidemiology in Cystic Fibrosis. *Clin Microbiol Rev* **23**: 299 LP – 323.

Liu, W., Chen, Y., Lu, G., Sun, L., and Si, J. (2011) Down-regulation of HSP70 sensitizes gastric epithelial cells to apoptosis and growth retardation triggered by *H. pylori*. *BMC Gastroenterol* **11**: 146.

Liu, X., Shao, K., and Sun, T. (2013) SIRT1 regulates the human alveolar epithelial A549 cell apoptosis induced by *Pseudomonas aeruginosa* lipopolysaccharide. *Cell Physiol Biochem* **31**: 92–101.

Lok, C.-N., Ho, C.-M., Chen, R., He, Q.-Y., Yu, W.-Y., Sun, H., *et al.* (2006) Proteomic analysis of the mode of antibacterial action of silver nanoparticles. *J Proteome Res* **5**: 916–924.

Lopes-Pacheco, M. (2020) CFTR Modulators: The Changing Face of Cystic Fibrosis in the Era of Precision Medicine. *Front Pharmacol* **10**: 1662.

López-Boado, Y.S., Espinola, M., Bahr, S., and Belaaouaj, A. (2004) Neutrophil Serine Proteinases Cleave Bacterial Flagellin, Abrogating Its Host Response-Inducing Activity. *J Immunol* **172**: 509 LP – 515.

Lopez-Medina, E., Fan, D., Coughlin, L.A., Ho, E.X., Lamont, I.L., Reimmann, C., *et al.* (2015) *Candida albicans* Inhibits *Pseudomonas aeruginosa* Virulence through Suppression of Pyochelin and Pyoverdine Biosynthesis. *PLOS Pathog* **11**: e1005129.

Losada, L., Ajayi, O., Frisvad, J.C., Yu, J., and Nierman, W.C. (2009) Effect of competition on the production and activity of secondary metabolites in *Aspergillus* species. *Med Mycol* **47**: S88–S96.

Lovewell, R.R., Hayes, S.M., O'Toole, G.A., and Berwin, B. (2014a) *Pseudomonas aeruginosa* flagellar motility activates the phagocyte PI3K/Akt pathway to induce phagocytic engulfment. *Am J Physiol Lung Cell Mol Physiol* **306**: L698–L707.

Lovewell, R.R., Patankar, Y.R., and Berwin, B. (2014b) Mechanisms of phagocytosis and host clearance of *Pseudomonas aeruginosa*. *Am J Physiol Lung Cell Mol Physiol* **306**: L591–L603.

Lu, P., Wang, Y., Hu, Y., and Chen, S. (2018) RgsA, an RpoS-dependent sRNA, negatively regulates rpoS expression in *Pseudomonas aeruginosa*. *Microbiology* **164**: 716–724.

Lyczak, J.B., Cannon, C.L., and Pier, G.B. (2000) Establishment of *Pseudomonas aeruginosa* infection: lessons from a versatile opportunist. *Microbes Infect* **2**: 1051–1060.

Lyczak, J.B., Cannon, C.L., and Pier, G.B. (2002) Lung Infections Associated with Cystic Fibrosis. *Clin Microbiol Rev* **15**: 194 LP – 222.

Ma, Y.J., Doni, A., Hummelshoj, T., Honore, C., Bastone, A., Mantovani, A., *et al.* (2009) Synergy between ficolin-2 and pentraxin 3 boosts innate immune recognition and complement deposition. *J Biol Chem* **284**: 28263–28275.

Maculins, T., Fiskin, E., Bhogaraju, S., and Dikic, I. (2016) Bacteria-host relationship: Ubiquitin ligases as weapons of invasion. *Cell Res* **26**: 499–510.

Madan, T., Kishore, U., Shah, A., Eggleton, P., Strong, P., Wang, J.Y., *et al.* (1997) Lung surfactant proteins A and D can inhibit specific IgE binding to the allergens of *Aspergillus fumigatus* and block allergen-induced histamine release from human basophils. *Clin Exp Immunol* **110**: 241–249.

Madan, T., Kishore, U., Singh, M., Strong, P., Clark, H., Hussain, E.M., *et al.* (2001) Surfactant proteins A and D protect mice against pulmonary hypersensitivity induced by *Aspergillus fumigatus* antigens and allergens. *J Clin Invest* **107**: 467–475.

Maguire, R., Kunc, M., Hyrsl, P., and Kavanagh, K. (2017) Analysis of the acute response of *Galleria mellonella* larvae to potassium nitrate. *Comp Biochem Physiol C Toxicol Pharmacol* **195**: 44–51.

Mahenthiralingam, E., Campbell, M.E., and Speert, D.P. (1994) Nonmotility and phagocytic resistance of *Pseudomonas aeruginosa* isolates from chronically colonized patients with cystic fibrosis. *Infect Immun* **62**: 596 LP – 605.

Máiz, L., Nieto, R., Cantón, R., Gómez G de la Pedrosa, E., and Martinez-García, M.Á. (2018) Fungi in Bronchiectasis: A Concise Review. *Int J Mol Sci* **19**: 142.

Malet, J.K., Impens, F., Carvalho, F., Hamon, M.A., Cossart, P., and Ribet, D. (2018) Rapid Remodeling of the Host Epithelial Cell Proteome by the Listeriolysin O (LLO) Pore-forming Toxin. *Mol Cell Proteomics* **17**: 1627–1636.

Maliniak, M.L., Stecenko, A.A., and McCarty, N.A. (2016) A longitudinal analysis of chronic MRSA and *Pseudomonas aeruginosa* co-infection in cystic fibrosis: A single-center study. *J Cyst Fibros* **15**: 350–356.

Managò, A., Becker, K.A., Carpinteiro, A., Wilker, B., Soddemann, M., Seitz, A.P., *et al.* (2015). *Pseudomonas aeruginosa* Pyocyanin Induces Neutrophil Death via Mitochondrial Reactive Oxygen Species and Mitochondrial Acid Sphingomyelinase. *Antioxid Redox Signal* **22**: 1097–1110.

Manavathu, E.K., Vager, D.L., and Vazquez, J.A. (2014) Development and antimicrobial susceptibility studies of in vitro monomicrobial and polymicrobial biofilm models with *Aspergillus fumigatus* and *Pseudomonas aeruginosa*. *BMC Microbiol* **14**: 53.

Manicone, A.M., Birkland, T.P., Lin, M., Betsuyaku, T., Rooijen, N. van, Lohi, J., *et al.* (2009) Epilysin (MMP-28) Restrains Early Macrophage Recruitment in *Pseudomonas aeruginosa* Pneumonia. *J Immunol* **182**: 3866 LP – 3876.

Mao, P., Wu, S., Li, J., Fu, W., He, W., Liu, X., *et al.* (2015) Human alveolar epithelial type II cells in primary culture. *Physiol Rep* **3**: e12288.

Mariencheck, W.I., Alcorn, J.F., Palmer, S.M., and Wright, J.R. (2003) *Pseudomonas aeruginosa* elastase degrades surfactant proteins A and D. *Am J Respir Cell Mol Biol* **28**: 528–537.

Marshall, A.C., Kidd, S.E., Lamont-Friedrich, S.J., Arentz, G., Hoffmann, P., Coad, B.R., and Bruning, J.B. (2019) Structure, Mechanism, and Inhibition of *Aspergillus fumigatus* Thioredoxin Reductase. *Antimicrob Agents Chemother* **63**: e02281-18.

Martínez-Luis, S., Cherigo, L., Arnold, E., Spadafora, C., Gerwick, W.H., and Cubilla-Rios, L. (2012) Antiparasitic and Anticancer Constituents of the Endophytic Fungus *Aspergillus sp*. strain F1544. *Nat Prod Commun* **7**: 165-8.

Martinon, F., Burns, K., and Tschopp, J. (2002) The Inflammasome: A Molecular Platform Triggering Activation of Inflammatory Caspases and Processing of proIL-β. *Mol Cell* **10**: 417–426.

Martins, M. de F., Honório-Ferreira, A., Martins, P., and Gonçalves, C.A. (2019) Presence of sialic acids in bronchioloalveolar cells and identification and quantification of N-acetylneuraminic and N-glycolylneuraminic acids in the lung. *Acta Histochem* **121**: 712–717.

Marvig, R.L., Sommer, L.M., Molin, S., and Johansen, H.K. (2014) Convergent evolution and adaptation of *Pseudomonas aeruginosa* within patients with cystic fibrosis. *Nat Genet* **47**: 57.

Mashburn, L.M., Jett, A.M., Akins, D.R., and Whiteley, M. (2005) *Staphylococcus aureus* serves as an iron source for *Pseudomonas aeruginosa* during *in vivo* coculture. *J Bacteriol* **187**: 554–566.

Mason, R.J. (2006) Biology of alveolar type II cells. *Respirology* **11**: S12–S15.

Massam, J., Bitnun, A., Solomon, M., Somers, G.R., Guerguerian, A.-M., Wylick, R. van, and Waters, V. (2011) Invasive aspergillosis in cystic fibrosis: a fatal case in an adolescent and review of the literature. *Pediatr Infect Dis J* **30**: 178–180.

Mauch, R.M., Jensen, P.O., Moser, C., Levy, C.E., and Hoiby, N. (2018) Mechanisms of humoral immune response against *Pseudomonas aeruginosa* biofilm infection in cystic fibrosis. *J Cyst Fibros* **17**: 143–152.

Mavrodi, D. V, Bonsall, R.F., Delaney, S.M., Soule, M.J., Phillips, G., and Thomashow, L.S. (2001) Functional Analysis of Genes for Biosynthesis of Pyocyanin and Phenazine-1-Carboxamide from *Pseudomonas aeruginosa* PAO1. *J Bacteriol* **183**: 6454–6465.

May, R.C., and Machesky, L.M. (2001) Phagocytosis and the actin cytoskeleton. *J Cell Sci* **114**: 1061–1077.

McClean, S., and Callaghan, M. (2009) *Burkholderia cepacia* complex: epithelial cell-pathogen confrontations and potential for therapeutic intervention. *J Med Microbiol* **58**: 1–12.

McDonnell, M.J., Jary, H.R., Perry, A., MacFarlane, J.G., Hester, K.L.M., Small, T., *et al.* (2015) Non cystic fibrosis bronchiectasis: A longitudinal retrospective observational cohort study of *Pseudomonas* persistence and resistance. *Respir Med* **109**: 716–726.

McElroy, M.C., and Kasper, M. (2004) The use of alveolar epithelial type I cell-selective markers to investigate lung injury and repair. *Eur Respir J* **24**: 664 LP – 673.

McEwan, D.L., Kirienko, N.V., and Ausubel, F.M. (2012) Host Translational Inhibition by *Pseudomonas aeruginosa* Exotoxin A Triggers an Immune Response in *Caenorhabditis elegans*. *Cell Host Microbe* **11**: 364–374.

McIsaac, S.M., Stadnyk, A.W., and Lin, T.-J. (2012) Toll-like receptors in the host defense against *Pseudomonas aeruginosa* respiratory infection and cystic fibrosis. *J Leukoc Biol* **92**: 977–985.

Mcphee, J.B., Tamber, S., Bains, M., Maier, E., Gellatly, S., Lo, A., and Hancock, R.E.W. (2009) The major outer membrane protein OprG of *Pseudomonas aeruginosa* contributes to cytotoxicity and forms an anaerobically regulated cation-selective channel. *FEMS Microbiol Lett* **296**: 241–7.

McShane, P.J., Naureckas, E.T., Tino, G., and Strek, M.E. (2013) Non–Cystic Fibrosis Bronchiectasis. *Am J Respir Crit Care Med* **188**: 647–656.

Meier, A., Kirschning, C.J., Nikolaus, T., Wagner, H., Heesemann, J., and Ebel, F. (2003) Toll-like receptor (TLR) 2 and TLR4 are essential for Aspergillus-induced activation of murine macrophages. *Cell Microbiol* **5**: 561–570.

Meissner, F., and Mann, M. (2014) Quantitative shotgun proteomics: Considerations for a high-quality workflow in immunology. *Nat Immunol* **15**: 112–117.

Miao, E.A., Mao, D.P., Yudkovsky, N., Bonneau, R., Lorang, C.G., Warren, S.E., *et al.* (2010) Innate immune detection of the type III secretion apparatus through the NLRC4 inflammasome. *Proc Natl Acad Sci* **107**: 3076–3080.

Michel, B. (2005) After 30 years of study, the bacterial SOS response still surprises us. *PLoS Biol* **3**: e255–e255.

Mircescu, M.M., Lipuma, L., Rooijen, N. van, Pamer, E.G., and Hohl, T.M. (2009) Essential role for neutrophils but not alveolar macrophages at early time points following *Aspergillus fumigatus* infection. *J Infect Dis* **200**: 647–656.

Moalli, F., Doni, A., Deban, L., Zelante, T., Zagarella, S., Bottazzi, B., *et al.* (2010) Role of complement and Fc{gamma} receptors in the protective activity of the long pentraxin PTX3 against *Aspergillus fumigatus*. *Blood* **116**: 5170–5180.

Mohr, I., and Sonenberg, N. (2012) Host translation at the nexus of infection and immunity. *Cell Host Microbe* **12**: 470–483.

Moradali, M.F., Ghods, S., and Rehm, B.H.A. (2017) *Pseudomonas aeruginosa* Lifestyle : A Paradigm for Adaptation , Survival , and Persistence. *Front Cell Infect Microbiol* **7**: 39.

Morales, D.K., Grahl, N., Okegbe, C., Dietrich, L.E.P., Jacobs, N.J., and Hogan, D.A. (2013) Control of *Candida albicans* metabolism and biofilm formation by *Pseudomonas aeruginosa* phenazines. *MBio* **4**: e00526.

Moser, C., Jensen, P.O., Kobayashi, O., Hougen, H.P., Song, Z., Rygaard, J., *et al.* (2002) Improved outcome of chronic *Pseudomonas aeruginosa* lung infection is associated with induction of a Th1-dominated cytokine response. *Clin Exp Immunol* **127**: 206–213.

Moss, R.B. (2015) Fungi in cystic fibrosis and non-cystic fibrosis bronchiectasis. *Semin Respir Crit Care Med* **36**: 207–216.

Moss, R.B., Hsu, Y.-P., Sullivan, M.M., and Lewiston, N.J. (1986) Altered Antibody Isotype in Cystic Fibrosis. Possible Role in Opsonic Deficiency. *Pediatr Res* **20**: 453–459.

Mowat, E., Rajendran, R., Williams, C., McCulloch, E., Jones, B., Lang, S., and Ramage, G. (2010) *Pseudomonas aeruginosa* and their small diffusible extracellular molecules inhibit *Aspergillus fumigatus* biofilm formation. *FEMS Microbiol Lett* **313**: 96–102.

Moynié, L., Milenkovic, S., Mislin, G.L.A., Gasser, V., Malloci, G., Baco, E., *et al.* (2019) The complex of ferric-enterobactin with its transporter from *Pseudomonas aeruginosa* suggests a two-site model. *Nat Commun* **10**: 3673.

Mu, S., Cierniak, P., and Ju, M. (2013) Insights into Mechanisms and Proteomic Characterisation of *Pseudomonas aeruginosa* Adaptation to a Novel Antimicrobial Substance. *PLoS One* **8**: e66862.

Munday, D.C., Emmott, E., Surtees, R., Lardeau, C.-H., Wu, W., Duprex, W.P., *et al.* (2010) Quantitative Proteomic Analysis of A549 Cells Infected with Human Respiratory Syncytial Virus. *Mol Cell Proteomics* **9**: 2438 LP – 2459.

Murdock, B.J., Shreiner, A.B., McDonald, R.A., Osterholzer, J.J., White, E.S., Toews, G.B., and Huffnagle, G.B. (2011) Coevolution of TH_1, TH_2 and TH_{17} Responses during Repeated Pulmonary Exposure to *Aspergillus fumigatus* Conidia. *Infect Immun* **79**: 125 LP – 135.

Murphy, T.F., Brauer, A.L., Eschberger, K., Lobbins, P., Grove, L., Cai, X., and Sethi, S. (2008) *Pseudomonas aeruginosa* in chronic obstructive pulmonary disease. *Am J Respir Crit Care Med* **177**: 853–860.

Murray, J.L., Connell, J.L., Stacy, A., Turner, K.H., and Whiteley, M. (2014) Mechanisms of synergy in polymicrobial infections. *J Microbiol* **52**: 188–199.

Mytilineou, C., Kramer, B.C., and Yabut, J.A. (2002) Glutathione depletion and oxidative stress. *Park Relat Disord* **8**: 385–387.

Nevitt, S.J., Thornton, J., Murray, C.S., and Dwyer, T. (2018) Inhaled mannitol for cystic fibrosis. *Cochrane database Syst Rev* **2**: CD008649–CD008649.

Newman, D.J., and Cragg, G.M. (2012) Natural products as sources of new drugs over the 30 years from 1981 to 2010. *J Nat Prod* **75**: 311–335.

Nguyen, A.T., Jones, J.W., Ruge, M.A., Kane, M.A., and Oglesby-Sherrouse, A.G. (2015) Iron Depletion Enhances Production of Antimicrobials by *Pseudomonas aeruginosa*. *J Bacteriol* **197**: 2265–2275.

Nguyen, A.T., and Oglesby-sherrouse, A.G. (2016) Interactions between *Pseudomonas aeruginosa* and *Staphylococcus aureus* during co-cultivations and polymicrobial infections. *Appl Microbiol Biotechnol* 6141–6148.

Nogueira, M.F., Pereira, L., Jenull, S., Kuchler, K., and Lion, T. (2019) Klebsiella pneumoniae prevents spore germination and hyphal development of *Aspergillus* species. *Sci Rep* **9**: 218.

Nomura, K., Obata, K., Keira, T., Miyata, R., Hirakawa, S., Takano, K., *et al.* (2014) *Pseudomonas aeruginosa* elastase causes transient disruption of tight junctions and downregulation of PAR-2 in human nasal epithelial cells. *Respir Res* **15**: 21.

O'Brien, S., and Fothergill, J.L. (2017) The role of multispecies social interactions in shaping *Pseudomonas aeruginosa* pathogenicity in the cystic fibrosis lung. *FEMS Microbiol Lett* **364**.

O'Sullivan, B.P., and Freedman, S.D. (2009) Cystic fibrosis. *Lancet* **373**: 1891–1904.

Ochsner, U.A., and Reiser, J. (1995) Autoinducer-mediated regulation of rhamnolipid biosurfactant synthesis in *Pseudomonas aeruginosa*. *Proc Natl Acad Sci* **92**: 6424–6428.

Ochsner, U.A., Vasil, M.L., Alsabbagh, E., Parvatiyar, K., and Hassett, D.J. (2000) Role of the *Pseudomonas aeruginosa* oxyR-recG Operon in Oxidative Stress Defense and DNA Repair: OxyR-Dependent Regulation of katB-ankB, ahpB, and ahpC-ahpF. *J Bacteriol* **182**: 4533 LP – 4544.

Oglesby, A.G., Farrow, J.M. 3rd, Lee, J.-H., Tomaras, A.P., Greenberg, E.P., Pesci, E.C., and Vasil, M.L. (2008) The influence of iron on *Pseudomonas aeruginosa* physiology: a regulatory link between iron and quorum sensing. *J Biol Chem* **283**: 15558–15567.

Opoku-Temeng, C., Onyedibe, K.I., Aryal, U.K., and Sintim, H.O. (2019) Proteomic analysis of bacterial response to a 4-hydroxybenzylidene indolinone compound, which re-sensitizes bacteria to traditional antibiotics. *J Proteomics* **202**: 103368.

Orazi, G., and O'Toole, G.A. (2017) *Pseudomonas aeruginosa* Alters *Staphylococcus aureus* Sensitivity to Vancomycin in a Biofilm Model of Cystic Fibrosis Infection. *MBio* **8**: e00873-17.

Orciuolo, E., Stanzani, M., Canestraro, M., Galimberti, S., Carulli, G., Lewis, R., *et al.* (2007) Effects of *Aspergillus fumigatus* gliotoxin and methylprednisolone on human neutrophils: implications for the pathogenesis of invasive aspergillosis. *J Leukoc Biol* **82**: 839–848.

Osherov, N. (2012) Interaction of the pathogenic mold *Aspergillus fumigatus* with lung epithelial cells . *Front Microbiol* **3**: 346.

Ott, M., Gogvadze, V., Orrenius, S., and Zhivotovsky, B. (2007) Mitochondria, oxidative stress and cell death. *Apoptosis* **12**: 913–922.

Otter, J.A., Yezli, S., and French, G.L. (2014) The Role of Contaminated Surfaces in the Transmission of Nosocomial Pathogens - Use of Biocidal Surfaces for Reduction of Healthcare Acquired Infections. Borkow, G. (ed.). Springer International Publishing, Cham. pp. 27–58.

Owens, R.A., Hammel, S., Sheridan, K.J., Jones, G.W., and Doyle, S. (2014) A proteomic approach to investigating gene cluster expression and secondary metabolite functionality in *Aspergillus fumigatus*. *PLoS One* **9**: e106942.

Owens, R.A., O'Keeffe, G., Smith, E.B., Dolan, S.K., Hammel, S., Sheridan, K.J., *et al.* (2015) Interplay between Gliotoxin Resistance, Secretion, and the Methyl/Methionine Cycle in *Aspergillus fumigatus*. *Eukaryot Cell* **14**: 941 LP – 957.

Padder, S.A., Prasad, R., and Shah, A.H. (2018) Quorum sensing: A less known mode of communication among fungi. *Microbiol Res* **210**: 51–58.

Painter, R.G., Valentine, V.G., Lanson Nicholas A., Leidal, K., Zhang, Q., Lombard, G., *et al.* (2006) CFTR Expression in Human Neutrophils and the Phagolysosomal Chlorination Defect in Cystic Fibrosis. *Biochemistry* **45**: 10260–10269.

Pal, A.K., Gajjar, D.U., and Vasavada, A.R. (2013) DOPA and DHN pathway orchestrate melanin synthesis in *Aspergillus* species. *Med Mycol* **52**: 10–18.

Palmer, J.M., Perrin, R.M., Dagenais, T.R.T., and Keller, N.P. (2008) H3K9 Methylation Regulates Growth and Development in *Aspergillus fumigatus*. *Eukaryot Cell* **7**: 2052 LP – 2060.

Palmer, K.L., Aye, L.M., and Whiteley, M. (2007a) Nutritional cues control *Pseudomonas aeruginosa* multicellular behavior in cystic fibrosis sputum. *J Bacteriol* **189**: 8079–8087.

Palmer, K.L., Brown, S.A., Whiteley, M., Al, P.E.T., and Acteriol, J.B. (2007b) Membrane-Bound Nitrate Reductase Is Required for Anaerobic Growth in Cystic Fibrosis Sputum. *J Bacteriol* **189**: 4449–4455.

Pang, Z., Raudonis, R., Glick, B.R., Lin, T.-J., and Cheng, Z. (2019) Antibiotic resistance in *Pseudomonas aeruginosa*: mechanisms and alternative therapeutic strategies. *Biotechnol Adv* **37**: 177–192.

Pankey, G.A., and Sabath, L.D. (2004) Clinical Relevance of Bacteriostatic versus Bactericidal Mechanisms of Action in the Treatment of Gram-Positive Bacterial Infections. *Clin Infect Dis* **38**: 864–870.

Pardo, J., Urban, C., Galvez, E.M., Ekert, P.G., Müller, U., Kwon-Chung, J., *et al.* (2006) The mitochondrial protein Bak is pivotal for gliotoxin-induced apoptosis and a critical host factor of *Aspergillus fumigatus* virulence in mice. *J Cell Biol* **174**: 509–519.

Park, S.J., Hughes, M.A., Burdick, M., Strieter, R.M., and Mehrad, B. (2009) Early NK cell-derived IFN-{gamma} is essential to host defense in neutropenic invasive aspergillosis. *J Immunol* **182**: 4306–4312.

Parkins, M.D., Sibley, C.D., Surette, M.G., and Rabin, H.R. (2008) The Streptococcus milleri group--an unrecognized cause of disease in cystic fibrosis: a case series and literature review. *Pediatr Pulmonol* **43**: 490–497.

Parkins, M.D., Somayaji, R., and Waters, V.J. (2018) Epidemiology, Biology, and Impact of Clonal *Pseudomonas aeruginosa* Infections in Cystic Fibrosis. *Clin Microbiol Rev* **31**: e00019-18.

Parkos, C.A. (2016) Neutrophil-Epithelial Interactions: A Double-Edged Sword. *Am J Pathol* **186**: 1404–1416.

Parrow, N.L., Fleming, R.E., and Minnick, M.F. (2013) Sequestration and scavenging of iron in infection. *Infect Immun* **81**: 3503–3514.

Parsek, M.R., and Greenberg, E.P. (2005) Sociomicrobiology: the connections between quorum sensing and biofilms. *Trends Microbiol* **13**: 27–33.

Patterson, K., and Strek, M.E. (2010) Allergic Bronchopulmonary Aspergillosis. *Proc Am Thorac Soc* **7**: 237–244.

Paugam, A., Baixench, M.-T., Demazes-Dufeu, N., Burgel, P.-R., Sauter, E., Kanaan, R., *et al.* (2010) Characteristics and consequences of airway colonization by filamentous fungi in 201 adult patients with cystic fibrosis in France. *Med Mycol* **48**: S32–S36.

Paulussen, C., Hallsworth, J.E., Álvarez-Pérez, S., Nierman, W.C., Hamill, P.G., Blain, D., *et al.* (2017) Ecology of aspergillosis: insights into the pathogenic potency of *Aspergillus fumigatus* and some other *Aspergillus* species. *Microb Biotechnol* **10**: 296–322.

Pedersen, S.S., Espersen, F., Høiby, N., and Jensen, T. (1990) Immunoglobulin A and immunoglobulin G antibody responses to alginates from *Pseudomonas aeruginosa* in patients with cystic fibrosis. *J Clin Microbiol* **28**: 747 LP – 755.

Pérez-Llarena, F.J., and Bou, G. (2016) Proteomics As a Tool for Studying Bacterial Virulence and Antimicrobial Resistance. *Front Microbiol* **7**: 410.

Périnet, S., Jeukens, J., Ibrulj, I.K., Ouellet, M.M., Charette, S.J., and Levesque, R.C. (2016) Molybdate transporter ModABC is important for *Pseudomonas aeruginosa* chronic lung infection. *BMC Res Notes* **9**: 1–9.

Pesavento, C., and Hengge, R. (2009) Bacterial nucleotide-based second messengers. *Curr Opin Microbiol* **12**: 170–176.

Peters, B.M., Jabra-rizk, M.A., Costerton, J.W., and Shirtliff, M.E. (2012) Polymicrobial Interactions : Impact on Pathogenesis and Human Disease. *Clin Microbiol Rev* **25:** 193–213.

Pezzulo, A.A., Starner, T.D., Scheetz, T.E., Traver, G.L., Tilley, A.E., Harvey, B.-G., *et al.* (2011) The air-liquid interface and use of primary cell cultures are important to recapitulate the transcriptional profile of in vivo airway epithelia. *Am J Physiol Lung Cell Mol Physiol* **300**: L25–L31.

Pezzulo, A.A., Tang, X.X., Hoegger, M.J., Abou Alaiwa, M.H., Ramachandran, S., Moninger, T.O., *et al.* (2012) Reduced airway surface pH impairs bacterial killing in the porcine cystic fibrosis lung. *Nature* **487**: 109–113.

Philippe, B., Ibrahim-Granet, O., Prévost, M.C., Gougerot-Pocidalo, M.A., Sanchez Perez, M., Meeren, A. Van der, and Latgé, J.P. (2003) Killing of *Aspergillus fumigatus* by alveolar macrophages is mediated by reactive oxidant intermediates. *Infect Immun* **71**: 3034–3042.

Pihet, M., Carrere, J., Cimon, B., Chabasse, D., Delhaes, L., Symoens, F., and Bouchara, J.-P. (2009) Occurrence and relevance of filamentous fungi in respiratory secretions of patients with cystic fibrosis--a review. *Med Mycol* **47**: 387–397.

Pillich, H., Loose, M., Zimmer, K.P., and Chakraborty, T. (2012) Activation of the unfolded protein response by Listeria monocytogenes. *Cell Microbiol* **14**: 949–964.

Polanec, J., Patzer, J., Grzybowski, J., Strukelj, M., and P Pavelic, Z. (1997) Amount and avidity of IgG antibodies to *Pseudomonas aeruginosa* exotoxin A antigen in cystic fibrosis patients. *Pathol Oncol Res* **3**: 26.

Pollack, M. (1983) The role of exotoxin A in *Pseudomonas* disease and immunity. *Rev Infect Dis* **5 Suppl 5**: S979-84.

Price-Whelan, A., Dietrich, L.E.P., and Newman, D.K. (2006) Rethinking "secondary" metabolism: physiological roles for phenazine antibiotics. *Nat Chem Biol* **2**: 71–78.

Price-Whelan, A., Dietrich, L.E.P., and Newman, D.K. (2007) Pyocyanin Alters Redox Homeostasis and Carbon Flux through Central Metabolic Pathways in *Pseudomonas aeruginosa* PA14. *J Bacteriol* **189**: 6372 LP – 6381.

Price, C.E., Brown, D.G., Limoli, D.H., Phelan, V. V, and O'Toole, G.A. (2019) Exogenous alginate protects *Staphylococcus aureus* from killing by *Pseudomonas aeruginosa*. *J Bacteriol* **202**: e00559-19.

Qu, Z., Gao, F., Li, L., Zhang, Y., Jiang, Y., Yu, L., *et al.* (2017) Label-Free Quantitative Proteomic Analysis of Differentially Expressed Membrane Proteins of Pulmonary Alveolar Macrophages Infected with Highly Pathogenic Porcine Reproductive and Respiratory Syndrome Virus and Its Attenuated Strain. *Proteomics* **17**: 1700101.

Quijano, C., Trujillo, M., Castro, L., and Trostchansky, A. (2016) Interplay between oxidant species and energy metabolism. *Redox Biol* **8**: 28–42.

Quintana, J., Novoa-aponte, L., and Argüello, J.M. (2017) Copper Homeostasis Networks in the bacterium *Pseudomonas aeruginosa*. *J Biol Chem* **292**: 15691–15704.

Rada, B., and Leto, T.L. (2013) Pyocyanin effects on respiratory epithelium: relevance in *Pseudomonas aeruginosa* airway infections. *Trends Microbiol* **21**: 73–81.

Raffa, N., and Keller, N.P. (2019) A call to arms: Mustering secondary metabolites for success and survival of an opportunistic pathogen. *PLOS Pathog* **15**: e1007606.

Ramírez-Estrada, S., Borgatta, B., and Rello, J. (2016) *Pseudomonas aeruginosa* ventilator-associated pneumonia management. *Infect Drug Resist* **9**: 7–18.

Ramirez-Ortiz, Z.G., Specht, C.A., Wang, J.P., Lee, C.K., Bartholomeu, D.C., Gazzinelli, R.T., and Levitz, S.M. (2008) Toll-Like Receptor 9-Dependent Immune Activation by Unmethylated CpG Motifs in *Aspergillus fumigatus* DNA. *Infect Immun* **76**: 2123 LP – 2129.

Ramírez Granillo, A., Canales, M.G.M., Espíndola, M.E.S., Martínez Rivera, M.A., Lucio, V.M.B. de, and Tovar, A.V.R. (2015) Antibiosis interaction of *Staphylococccus aureus* on *Aspergillus fumigatus* assessed in vitro by mixed biofilm formation. *BMC*

Microbiol **15**: 33.

Ramsey, B.W., Downey, G.P., and Goss, C.H. (2019) Update in Cystic Fibrosis 2018. *Am J Respir Crit Care Med* **199**: 1188–1194.

Rangel, S.M., Diaz, M.H., Knoten, C.A., Zhang, A., and Hauser, A.R. (2015) The Role of ExoS in Dissemination of *Pseudomonas aeruginosa* during Pneumonia. *PLoS Pathog* **11**: e1004945–e1004945.

Raoust, E., Balloy, V., Garcia-Verdugo, I., Touqui, L., Ramphal, R., and Chignard, M. (2009) *Pseudomonas aeruginosa* LPS or flagellin are sufficient to activate TLR-dependent signaling in murine alveolar macrophages and airway epithelial cells. *PLoS One* **4**: e7259–e7259.

Rasmussen, T.B., Skindersoe, M.E., Bjarnsholt, T., Phipps, R.K., Christensen, K.B., Jensen, P.O., *et al.* (2005) Identity and effects of quorum-sensing inhibitors produced by Penicillium species. *Microbiology* **151**: 1325–1340.

Ratjen, F., and Döring, G. (2003) Cystic fibrosis. *Lancet* **361**: 681–689.

Ratner, D., and Mueller, C. (2012) Immune Responses in Cystic Fibrosis. *Am J Respir Cell Mol Biol* **46**: 715–722.

Reddy, R., Gari, S., Seelheim, P., Marsh, B., Kiessling, V., Creutz, C.E., and Tamm, L.K. (2018) Quaternary structure of the small amino acid transporter OprG from *Pseudomonas aeruginosa*. *J Biol Chem* 1–23.

Reece, E., Doyle, S., Greally, P., Renwick, J., and McClean, S. (2018) *Aspergillus fumigatus* inhibits *Pseudomonas aeruginosa* in co-culture: Implications of a mutually antagonistic relationship on virulence and inflammation in the CF airway. *Front Microbiol* **9**: 1–14.

Reece, E., McClean, S., Greally, P., and Renwick, J. (2019) The prevalence of *Aspergillus fumigatus* in early cystic fibrosis disease is underestimated by culture-based diagnostic methods. *J Microbiol Methods* **164**: 105683.

Reece, E., Segurado, R., Jackson, A., McClean, S., Renwick, J., and Greally, P. (2017a) Co-colonisation with *Aspergillus fumigatus* and *Pseudomonas aeruginosa* is associated with poorer health in cystic fibrosis patients: An Irish registry analysis. *BMC Pulm Med* **17**: 1–8.

Reece, E., Segurado, R., Jackson, A., McClean, S., Renwick, J., and Greally, P. (2017b) Co-colonisation with *Aspergillus fumigatus* and *Pseudomonas aeruginosa* is associated with poorer health in cystic fibrosis patients: an Irish registry analysis. *BMC Pulm Med* **17**: 70.

Reeves, E.P., Molloy, K., Pohl, K., and McElvaney, N.G. (2012) Hypertonic saline in treatment of pulmonary disease in cystic fibrosis. *ScientificWorldJournal* **2012**: 465230.

Rella, A., Yang, M.W., Gruber, J., Montagna, M.T., Luberto, C., Zhang, Y.-M., and Poeta, M. Del (2012) *Pseudomonas aeruginosa* inhibits the growth of *Cryptococcus* species. *Mycopathologia* **173**: 451–461.

Ribeiro da Cunha, B., Fonseca, P.L., and Calado, R.C.C. (2019) Antibiotic Discovery: Where Have We Come from, Where Do We Go? *Antibiot* **8:** 45.

Richie, D.L., and Askew, D.S. (2008) Autophagy: A role in metal ion homeostasis? *Autophagy* **4**: 115–117.

Riol-Blanco, L., Sánchez-Sánchez, N., Torres, A., Tejedor, A., Narumiya, S., Corbí, A.L., *et al.* (2005) The Chemokine Receptor CCR7 Activates in Dendritic Cells Two Signaling Modules That Independently Regulate Chemotaxis and Migratory Speed. *J Immunol* **174**: 4070 LP – 4080.

Rogers, G.B., Bruce, K.D., Martin, M.L., Burr, L.D., and Serisier, D.J. (2014) The effect of long-term macrolide treatment on respiratory microbiota composition in non-cystic fibrosis bronchiectasis: an analysis from the randomised, double-blind, placebo-controlled BLESS trial. *Lancet Respir Med* **2**: 988–996.

Rogers, G.B., Hart, C.A., Mason, J.R., Hughes, M., Walshaw, M.J., and Bruce, K.D. (2003) Bacterial diversity in cases of lung infection in cystic fibrosis patients: 16S ribosomal DNA (rDNA) length heterogeneity PCR and 16S rDNA terminal restriction fragment length polymorphism profiling. *J Clin Microbiol* **41**: 3548–3558.

Rogers, G.B., Hoffman, L.R., Carroll, M.P., and Bruce, K.D. (2013) Interpreting infective microbiota: the importance of an ecological perspective. *Trends Microbiol* **21**: 271–276.

Rommens, J.M., Iannuzzi, M.C., Kerem, B., Mitchell, L., Melmer, G., Dean, M., *et al.* (1989). Identification of the Cystic Fibrosis Gene : Chromosome Walking and Jumping. *Science* **245:** 1059-65.

Romsdahl, J., and Wang, C.C.C. (2019) Recent advances in the genome mining of Aspergillus secondary metabolites (covering 2012–2018). *Medchemcomm* **10**: 840–866.

Ron, D., and Walter, P. (2007) Signal integration in the endoplasmic reticulum unfolded protein response. *Nat Rev Mol Cell Biol* **8**: 519–529.

Rosales, C., Lowell, C.A., Schnoor, M., and Uribe-Querol, E. (2017) Neutrophils: Their Role in Innate and Adaptive Immunity 2017. *J Immunol Res* **2017**: 9748345.

Rosowski, E.E., Raffa, N., Knox, B.P., Golenberg, N., Keller, N.P., and Huttenlocher, A. (2018) Macrophages inhibit *Aspergillus fumigatus* germination and neutrophil-mediated fungal killing. *PLOS Pathog* **14**: e1007229.

Ruegger, A., Kuhn, M., Lichti, H., Loosli, H.R., Huguenin, R., Quiquerez, C., and Wartburg, A. von (1976) Cyclosporin A, a Peptide Metabolite from *Trichoderma polysporum* with a remarkable immunosuppressive activity. *Helv Chim Acta* **59**: 1075–1092.

Ruiz, B., Chávez, A., Forero, A., García-Huante, Y., Romero, A., Sánchez, M., *et al.* (2010) Production of microbial secondary metabolites: Regulation by the carbon source. *Crit Rev Microbiol* **36**: 146–167.

Saïd-Sadier, N., Padilla, E., Langsley, G., and Ojcius, D.M. (2010) *Aspergillus fumigatus* Stimulates the NLRP3 Inflammasome through a Pathway Requiring ROS Production and the Syk Tyrosine Kinase. *PLoS One* **5**: e10008.

Salsgiver, E.L., Fink, A.K., Knapp, E.A., Lipuma, J.J., Olivier, K.N., Marshall, B.C., and Saiman, L. (2016) Changing Epidemiology of the Respiratory Bacteriology of Patients With Cystic Fibrosis. *Chest* **149**: 390–400.

Sass, G., Ansari, S.R., Dietl, A.M., Déziel, E., Haas, H., and Stevens, D.A. (2019) Intermicrobial interaction: *Aspergillus fumigatus* siderophores protect against competition by *Pseudomonas aeruginosa*. *PLoS One* **14**: e0216085.

Sass, G., Nazik, H., Penner, J., Shah, H., Ansari, S.R., Clemons, K., *et al.* (2018) Studies of *Pseudomonas aeruginosa* Mutants Indicate Pyoverdine as the Central Factor in Inhibition of *Aspergillus fumigatus* Biofilm. *J Bacteriol* **200**: 1–24.

Scharf, D.H., Brakhage, A.A., and Mukherjee, P.K. (2016) Gliotoxin – bane or boon? *Environ Microbiol* **18**: 1096–1109.

Scherlach, K., and Hertweck, C. (2006) Discovery of aspoquinolones A–D, prenylated quinoline-2-one alkaloids from *Aspergillus nidulans*, motivated by genome mining. *Org Biomol Chem* **4**: 3517–3520.

Schiessl, K.T., Hu, F., Jo, J., Nazia, S.Z., Wang, B., Price-Whelan, A., *et al.* (2019) Phenazine production promotes antibiotic tolerance and metabolic heterogeneity in *Pseudomonas aeruginosa* biofilms. *Nat Commun* **10**: 762.

Schlam, D., Canton, J., Carreño, M., Kopinski, H., Freeman, S.A., and Grinstein, S. (2016a) Gliotoxin Suppresses Macrophage Immune Function by Subverting. *MBio* **7**: 1–15.

Schlam, D., Canton, J., Carreño, M., Kopinski, H., Freeman, S.A., Grinstein, S., and Fairn, G.D. (2016b) Gliotoxin Suppresses Macrophage Immune Function by Subverting Phosphatidylinositol 3,4,5-Trisphosphate Homeostasis. *MBio* **7**: e02242–e02242.

Schmidt, H., Vlaic, S., Kruger, T., Schmidt, F., Balkenhol, J., Dandekar, T., *et al.* (2018) Proteomics of *Aspergillus fumigatus* Conidia-containing Phagolysosomes Identifies Processes Governing Immune Evasion. *Mol Cell Proteomics* **17**: 1084–1096.

Schrettl, M., Carberry, S., Kavanagh, K., Haas, H., Jones, G.W., O'Brien, J., *et al.* (2010) Self-protection against gliotoxin-a component of the gliotoxin biosynthetic cluster, GliT, completely protects *Aspergillus fumigatus* against exogenous gliotoxin. *PLoS Pathog* **6**: e1000952–e1000952.

Schuster, M., Joseph Sexton, D., Diggle, S.P., and Peter Greenberg, E. (2013) Acyl-Homoserine Lactone Quorum Sensing: From Evolution to Application. *Annu Rev Microbiol* **67**: 43–63.

Schwarz, C., Brandt, C., Whitaker, P., Sutharsan, S., Skopnik, H., Gartner, S., *et al.* (2018) Invasive Pulmonary Fungal Infections in Cystic Fibrosis. *Mycopathologia* **183**: 33–43.

Scott, J.E., Li, K., Filkins, L.M., Zhu, B., Kuchma, S.L., Schwartzman, J.D., and O'Toole, G.A. (2019) *Pseudomonas aeruginosa* Can Inhibit Growth of Streptococcal Species via Siderophore Production. *J Bacteriol* **201**: e00014-19.

Seenivasan, A., Subhagar, S., Aravindan, R., and Viruthagiri, T. (2008) Microbial production and biomedical applications of lovastatin. *Indian J Pharm Sci* **70**: 701–709.

Seimon, T.A., Kim, M.J., Blumenthal, A., Koo, J., Ehrt, S., Wainwright, H., *et al.* (2010) Induction of ER stress in macrophages of tuberculosis granulomas. *PLoS One* **5**: 1–12.

Sermet-Gaudelus, I. (2013) Ivacaftor treatment in patients with cystic fibrosis and the G551D-CFTR mutation. *Eur Respir Rev* **22**: 66 LP – 71.

Serrano-Gómez, D., Antonio Leal, J., and Corbí, A.L. (2005) DC-SIGN mediates the binding of *Aspergillus fumigatus* and keratinophylic fungi by human dendritic cells. *Immunobiology* **210**: 175–183.

Shanks, K.K., Guang, W., Kim, K.C., and Lillehoj, E.P. (2010) Interleukin-8 production by human airway epithelial cells in response to *Pseudomonas aeruginosa* clinical isolates expressing type a or type b flagellins. *Clin Vaccine Immunol* **17**: 1196–1202.

Sharma Ghimire, P., Ouyang, H., Wang, Q., Luo, Y., Shi, B., Yang, J., *et al.* (2016) Insight into Enzymatic Degradation of Corn, Wheat, and Soybean Cell Wall Cellulose Using Quantitative Secretome Analysis of *Aspergillus fumigatus*. *J Proteome Res* **15**: 4387–4402.

Sharon, H., Amar, D., Levdansky, E., Mircus, G., Shadkchan, Y., Shamir, R., and Osherov, N. (2011) PrtT-regulated proteins secreted by *Aspergillus fumigatus* activate MAPK signaling in exposed A549 lung cells leading to necrotic cell death. *PLoS One* **6**.

Sharon, Hoffman, Emerson, J., Mcnamara, L.R., De, E., Gibson, R.L., Ramsey, B.W., and Miller, S.I. (2006) Selection for *Staphylococcus aureus* small-colony variants due to growth in the presence of *Pseudomonas aeruginosa*. *Proc Natl Acad Sci* **103:**19890-5.

Sharp, C., Boinett, C., Cain, A., Housden, N.G., Kumar, S., Turner, K., *et al.* (2019) O-Antigen-Dependent Colicin Insensitivity of Uropathogenic *Escherichia coli*. *J Bacteriol* **201**: e00545-18.

Shende, R., Wong, S.S.W., Rapole, S., Beau, R., Ibrahim-Granet, O., Monod, M., *et al.* (2018) *Aspergillus fumigatus* conidial metalloprotease Mep1p cleaves host complement proteins. *J Biol Chem* **293**: 15538–15555.

Shevchenko, A., Tomas, H., Havliš, J., Olsen, J. V., and Mann, M. (2007) In-gel digestion for mass spectrometric characterization of proteins and proteomes. *Nat Protoc* **1**: 2856–2860.

Shirazi, F., Ferreira, J.A.G., Stevens, D.A., Clemons, K. V., and Kontoyiannis, D.P. (2016) Biofilm filtrates of *Pseudomonas aeruginosa* strains isolated from cystic fibrosis patients inhibit preformed *Aspergillus fumigatus* biofilms via apoptosis. *PLoS One* **11**: e0150155.

Shlezinger, N., Irmer, H., Dhingra, S., Beattie, S.R., Cramer, R.A., Braus, G.H., *et al.* (2017) Sterilizing immunity in the lung relies on targeting fungal apoptosis-like programmed cell death. *Science* **357**: 1037–1041 .

Shopova, I.A., Belyaev, I., Dasari, P., Jahreis, S., Stroe, M.C., Cseresnyés, Z., *et al.* (2019) Human neutrophils produce antifungal extracellular vesicles against *Aspergillus fumigatus*. *MBio* **11:** e00596-20.

Short, F.L., Murdoch, S.L., and Ryan, R.P. (2014) Polybacterial human disease: the ills of social networking. *Trends Microbiol* **22**: 508–516.

Silver, L.L. (2011) Challenges of antibacterial discovery. *Clin Microbiol Rev* **24**: 71–109.

Sin, N., Meng, L., Wang, M.Q.W., Wen, J.J., Bornmann, W.G., and Crews, C.M. (1997) The anti-angiogenic agent fumagillin covalently binds and inhibits the methionine aminopeptidase, MetAP-2. *Proc Natl Acad Sci* **94**: 6099–6103.

Singh, P.K., Parsek, M.R., Greenberg, E.P., and Welsh, M.J. (2002) A component of innate immunity prevents bacterial biofilm development. *Nature* **417**: 552–555.

Smit-de Vries, M.P., Toorn, M. van der, Bischoff, R., and Kauffman, H.F. (2007) Resistance of quiescent and proliferating airway epithelial cells to H_2O_2 challenge. *Eur Respir J* **29**: 633 LP – 642.

Smith, D.J., Lamont, I.L., Anderson, G.J., and Reid, D.W. (2013a) Targeting iron uptake to control *Pseudomonas aeruginosa* infections in cystic fibrosis. *Eur Respir J* **42**: 1723 LP – 1736.

Smith, E.E., Buckley, D.G., Wu, Z., Saenphimmachak, C., Hoffman, L.R., D\textquoterightArgenio, D.A., *et al.* (2006) Genetic adaptation by *Pseudomonas aeruginosa* to the airways of cystic fibrosis patients. *Proc Natl Acad Sci* **103**: 8487–8492.

Smith, J.A., Khan, M., Magnani, D.D., Harms, J.S., Durward, M., Radhakrishnan, G.K., *et al.* (2013b) *Brucella* Induces an Unfolded Protein Response via TcpB That Supports Intracellular Replication in Macrophages. *PLoS Pathog* **9**: 1–12.

Smith, K., Rajendran, R., Kerr, S., Lappin, D.F., Mackay, W.G., Williams, C., and Ramage, G. (2015) *Aspergillus fumigatus* enhances elastase production in *Pseudomonas aeruginosa* co-cultures. *Med Mycol* **53**: 645–655.

Smith, L.M., Kelleher, N.L., and Proteomics, C. for T.D. (2013c) Proteoform: a single term describing protein complexity. *Nat Methods* **10**: 186–187.

Smith, W.D., Bardin, E., Cameron, L., Edmondson, C.L., Farrant, K. V, Martin, I., *et al.* (2017) Current and future therapies for *Pseudomonas aeruginosa* infection in patients with cystic fibrosis. *FEMS Microbiol Lett* **364**.

Smits, H.H., Beelen, A.J. van, Hessle, C., Westland, R., Jong, E. de, Soeteman, E., *et al.* (2004) Commensal Gram-negative bacteria prime human dendritic cells for enhanced IL-23 and IL-27 expression and enhanced Th1 development. *Eur J Immunol* **34**: 1371–1380.

So, J.-S. (2018) Roles of Endoplasmic Reticulum Stress in Immune Responses. *Mol Cells* **41**: 705–716.

Sobolev, A.P., Segre, A., and Lamanna, R. (2003) Proton high-field NMR study of tomato juice. *Magn Reson Chem* **41**: 237–245.

Sonawane, A., Jyot, J., During, R., and Ramphal, R. (2006) Neutrophil Elastase, an Innate Immunity Effector Molecule, Represses Flagellin Transcription in *Pseudomonas aeruginosa*. *Infect Immun* **74**: 6682 LP – 6689.

Soyza, A. De, and Aliberti, S. (2016) Bronchiectasis and Aspergillus: How are they linked? *Med Mycol* **55**: 69–81.

Sriramulu, D.D. (2010) Amino Acids Enhance Adaptive Behaviour of *Pseudomonas aeruginosa* in the Cystic Fibrosis Lung Environment. *Microbiol Insights* **3**: 17–26.

Sriranganadane, D., Reichard, U., Salamin, K., Fratti, M., Jousson, O., Waridel, P., *et al.* (2011) Secreted glutamic protease rescues aspartic protease Pep deficiency in *Aspergillus fumigatus* during growth in acidic protein medium. *Microbiology* **157**: 1541–1550.

Stanzani, M., Orciuolo, E., Lewis, R., Kontoyiannis, D.P., Martins, S.L.R., John, L.S. St., and Komanduri, K. V (2005) *Aspergillus fumigatus* suppresses the human cellular immune response via gliotoxin-mediated apoptosis of monocytes. *Blood* **105**: 2258–2265.

Stappers, M.H.T., Clark, A.E., Aimanianda, V., Bidula, S., Reid, D.M., Asamaphan, P., *et al.* (2018) Recognition of DHN-melanin by a C-type lectin receptor is required for immunity to *Aspergillus*. *Nature* **555**: 382—386.

Starr, A.E., Deeke, S.A., Li, L., Zhang, X., Daoud, R., Ryan, J., *et al.* (2018) Proteomic and Metaproteomic Approaches to Understand Host–Microbe Interactions. *Anal Chem* **90**: 86–109.

Stegemann, C., and Hoffmann, R. (2008) Sequence analysis of antimicrobial peptides by tandem mass spectrometry. *Methods Mol Biol* **494**: 31–46.

Stephens-Romero, S.D., Mednick, A.J., and Feldmesser, M. (2005) The pathogenesis of fatal outcome in murine pulmonary aspergillosis depends on the neutrophil depletion strategy. *Infect Immun* **73**: 114–125.

Sterritt, O.W., Lang, E.J.M., Kessans, S.A., Ryan, T.M., Demeler, B., Jameson, G.B., and Parker, E.J. (2018) Structural and functional characterisation of the entry point to pyocyanin biosynthesis in *Pseudomonas aeruginosa* defines a new 3-deoxy-d-arabino-heptulosonate 7-phosphate synthase subclass. *Biosci Rep* **38**: BSR20181605.

Stevens, D.A. (2006) Th1/Th2 in aspergillosis. *Med Mycol* **44**: S229–S235.

Stevens, D.A., Moss, R.B., Kurup, V.P., Knutsen, A.P., Greenberger, P., Judson, M.A., *et al.* (2003a) Allergic Bronchopulmonary Aspergillosis in Cystic Fibrosis—State of the Art: Cystic Fibrosis Foundation Consensus Conference. *Clin Infect Dis* **37**: S225–S264.

Stevens, D.A., Moss, R.B., Kurup, V.P., Knutsen, A.P., Greenberger, P., Judson, M.A., *et al.* (2003b) Allergic bronchopulmonary aspergillosis in cystic fibrosis--state of the art: Cystic Fibrosis Foundation Consensus Conference. *Clin Infect Dis* **37**: S225-64.

Stintzi, A., Evans, K., Meyer, J.M., and Poole, K. (1998) Quorum-sensing and siderophore biosynthesis in *Pseudomonas aeruginosa*: lasR/lasI mutants exhibit reduced pyoverdine biosynthesis. *FEMS Microbiol Lett* **166**: 341–345.

Stover, C.K., Pham, X.Q., Erwin, A.L., Mizoguchi, S.D., Warrener, P., Hickey, M.J., *et al.* (2000) Complete genome sequence of *Pseudomonas aeruginosa* PAO1, an opportunistic pathogen. *Nature* **406**: 959–964.

Stutts, M.J., Canessa, C.M., Olsen, J.C., Hamrick, M., Cohn, J.A., Rossier, B.C., and Boucher, R.C. (1995) CFTR as a cAMP-dependent regulator of sodium channels. *Science* **269**: 847–850.

Sudfeld, C.R., Dasenbrook, E.C., Merz, W.G., Carroll, K.C., and Boyle, M.P. (2010) Prevalence and risk factors for recovery of filamentous fungi in individuals with cystic fibrosis. *J Cyst Fibros* **9**: 110–116.

Sugui, J.A., Kim, H.S., Zarember, K.A., Chang, Y.C., Gallin, J.I., Nierman, W.C., and Kwon-Chung, K.J. (2008) Genes Differentially Expressed in Conidia and Hyphae of *Aspergillus fumigatus* upon Exposure to Human Neutrophils. *PLoS One* **3**: e2655.

Sugui, J.A., Kwon-Chung, K.J., Juvvadi, P.R., Latgé, J.-P., and Steinbach, W.J. (2014) *Aspergillus fumigatus* and related species. *Cold Spring Harb Perspect Med* **5**: a019786–a019786.

Sugui, J.A., Pardo, J., Chang, Y.C., Zarember, K.A., Nardone, G., Galvez, E.M., *et al.* (2007) Gliotoxin is a virulence factor of *Aspergillus fumigatus*: gliP deletion attenuates virulence in mice immunosuppressed with hydrocortisone. *Eukaryot Cell* **6**: 1562–1569.

Sun, H., Xu, X.-Y., Shao, H.-T., Su, X., Wu, X.-D., Wang, Q., and Shi, Y. (2013) Dectin-2 is predominately macrophage restricted and exhibits conspicuous expression during *Aspergillus fumigatus* invasion in human lung. *Cell Immunol* **284**: 60–67 Surette, M.G. (2014) The cystic fibrosis lung microbiome. *Ann Am Thorac Soc* **11**: 61–65.

Surmann, K., Michalik, S., Hildebrandt, P., Gierok, P., Depke, M., Brinkmann, L., *et al.* (2014) Comparative proteome analysis reveals conserved and specific adaptation patterns of *Staphylococcus aureus* after internalization by different types of human non-professional phagocytic host cells. *Front Microbiol* **5**: 392.

Surmann, K., Simon, M., Hildebrandt, P., Pförtner, H., Michalik, S., Dhople, V.M., *et al.* (2016) Proteome data from a host-pathogen interaction study with *Staphylococcus aureus* and human lung epithelial cells. *Data Br* **7**: 1031–1037

Surmann, K., Simon, M., Hildebrandt, P., Pförtner, H., Michalik, S., Stentzel, S., *et al.* (2015) A proteomic perspective of the interplay of *Staphylococcus aureus* and human alveolar epithelial cells during infection. *J Proteomics* **128**: 203–217.

Sutterwala, F.S., Mijares, L.A., Li, L., Ogura, Y., Kazmierczak, B.I., and Flavell, R.A. (2007) Immune recognition of *Pseudomonas aeruginosa* mediated by the IPAF/NLRC4 inflammasome. *J Exp Med* **204**: 3235 LP – 3245.

Svahn, K.S., Göransson, U., Chryssanthou, E., Olsen, B., Sjölin, J., and Strömstedt, A.A. (2014) Induction of gliotoxin secretion in *Aspergillus fumigatus* by bacteria-associated molecules. *PLoS One* **9**: e93685–e93685.

Tanaka, R.J., Boon, N.J., Vrcelj, K., Nguyen, A., Vinci, C., Armstrong-James, D., and Bignell, E. (2015) In silico modeling of spore inhalation reveals fungal persistence following low dose exposure. *Sci Rep* **5**: 13958.

Tang, A.C., Turvey, S.E., Alves, M.P., Regamey, N., Tümmler, B., and Hartl, D. (2014) Current concepts: host–pathogen interactions in cystic fibrosis airways disease. *Eur Respir Rev* **23**: 320 LP – 332.

Tankana, K. J., Song, S., M. (2018) Selective substrate uptake: The role of ATP-binding cassette (ABC) importers in pathogenesis. *Biochim Biophys Acta* **1860**: 868–877.

Tanner, N.T., and Judson, M.A. (2008) Diagnosis and treatment of allergic bronchopulmonary aspergillosis. *Curr Fungal Infect Rep* **2**: 199.

Tate, S., MacGregor, G., Davis, M., Innes, J.A., and Greening, A.P. (2002) Airways in cystic fibrosis are acidified: detection by exhaled breath condensate. *Thorax* **57**: 926 LP – 929.

Tekaia, F., and Latge, J.-P. (2005) *Aspergillus fumigatus*: saprophyte or pathogen? *Curr Opin Microbiol* **8**: 385–392.

Tepšič, K., Gunde-Cimerman, N., and Frisvad, J.C. (1997) Growth and mycotoxin production by *Aspergillus fumigatus* strains isolated from a saltern. *FEMS Microbiol Lett* **157**: 9–12.

Tettmann, B., Niewerth, C., Kirschhöfer, F., Neidig, A., Dötsch, A., Brenner-Weiss, G., *et al.* (2016) Enzyme-Mediated Quenching of the Pseudomonas Quinolone Signal (PQS) Promotes Biofilm Formation of *Pseudomonas aeruginosa* by Increasing Iron Availability. *Front Microbiol* **7**: 1978.

Thomas, C.G., and Spyrou, G. (2009) ERdj5 sensitizes neuroblastoma cells to endoplasmic reticulum stress-induced apoptosis. *J Biol Chem* **284**: 6282–6290.

Thrane, U., Anderson, B., Frisvad, J.C., and Smedsgaard, J. (2007) The exo-metabolome in filamentous fungi. *Metabolomics: A Powerful Tool in Systems Biology.* Nielsen, J., and Jewett, M.C. (eds). Springer Berlin Heidelberg, Berlin, Heidelberg. pp. 235–252.

Thywißen, A., Heinekamp, T., Dahse, H.-M., Schmaler-Ripcke, J., Nietsche, S., Zipfel, P., and Brakhage, A. (2011) Conidial Dihydroxynaphthalene Melanin of the Human Pathogenic Fungus *Aspergillus fumigatus* Interferes with the Host Endocytosis Pathway . *Front Microbiol* **2**: 96.

Tilley, A.E., Walters, M.S., Shaykhiev, R., and Crystal, R.G. (2015) Cilia dysfunction in lung disease. *Annu Rev Physiol* **77**: 379–406.

Toby, T.K., Fornelli, L., and Kelleher, N.L. (2016) Progress in Top-Down Proteomics and the Analysis of Proteoforms. *Annu Rev Anal Chem (Palo Alto Calif)* **9**: 499–519.

Tognon, M., Köhler, T., Luscher, A., and Delden, C. Van (2019) Transcriptional profiling of *Pseudomonas aeruginosa* and *Staphylococcus aureus* during *in vitro* co-culture. 1–15.

Toljander, J.F., Lindahl, B.D., Paul, L.R., Elfstrand, M., and Finlay, R.D. (2007) Influence of arbuscular mycorrhizal mycelial exudates on soil bacterial growth and community structure. *FEMS Microbiol Ecol* **61**: 295–304.

Tomiotto-Pellissier, F., Cataneo, A.H.D., Orsini, T.M., Thomazelli, A.P.F.D.S., Dalevedo, G.A., Oliveira, A.G. de, *et al.* (2016) *Galleria mellonella* hemocytes: A novel phagocytic assay for *Leishmania* (Viannia) *braziliensis. J Microbiol Methods* **131**: 45–50.

Trojanek, J.B., Cobos-Correa, A., Diemer, S., Kormann, M., Schubert, S.C., Zhou-Suckow, Z., *et al.* (2014) Airway mucus obstruction triggers macrophage activation and matrix metalloproteinase 12-dependent emphysema. *Am J Respir Cell Mol Biol* **51**: 709–720.

Tsai, H.-F., Chang, Y.C., Washburn, R.G., Wheeler, M.H., and Kwon-Chung, K.J. (1998) The Developmentally Regulated alb1 Gene of *Aspergillus fumigatus*: Its Role in Modulation of Conidial Morphology and Virulence. *J Bacteriol* **180**: 3031 LP – 3038.

Tsai, H.F., Washburn, R.G., Chang, Y.C., and Kwon-Chung, K.J. (1997) *Aspergillus fumigatus* arp1 modulates conidial pigmentation and complement deposition. *Mol Microbiol* **26**: 175–183.

Tsuchiya, K., Nakajima, S., Hosojima, S., Thi Nguyen, D., Hattori, T., Manh Le, T., *et al.* (2019) Caspase-1 initiates apoptosis in the absence of gasdermin D. *Nat Commun* **10**: 2091.

Tsunawaki, S., Yoshida, L.S., Nishida, S., Kobayashi, T., and Shimoyama, T. (2004) Fungal Metabolite Gliotoxin Inhibits Assembly of the Human Respiratory Burst NADPH Oxidase. *Infect Immun* **72**: 3373 LP – 3382.

Twigg, M.S., Brockbank, S., Lowry, P., Fitzgerald, S.P., Taggart, C., and Weldon, S. (2015) The Role of Serine Proteases and Antiproteases in the Cystic Fibrosis Lung. *Mediators Inflamm* **2015**: 11–13.

Uemura, A., Oku, M., Mori, K., and Yoshida, H. (2009) Unconventional splicing of XBP1 mRNA occurs in the cytoplasm during the mammalian unfolded protein response. *J Cell Sci* **122**: 2877–2886.

Uribe-Quero, E., and Rosales, C. (2017) Control of phagocytosis by microbial pathogens. *Front Immunol* **8**: 1–23.

Valiquette, L., and Laupland, K.B. (2015) Digging for new solutions. *Can J Infect Dis Med Microbiol* **26**: 289–290.

van ‘t Wout, E.F.A., Schadewijk, A., Boxtel, R. van, Dalton, L.E., Clarke, H.J., Tommassen, J., et al. (2015) Virulence Factors of Pseudomonas aeruginosa Induce Both the Unfolded Protein and Integrated Stress Responses in Airway Epithelial Cells. PLOS Pathog 11: e1004946.

Vankeerberghen, A., Cuppens, H., and Cassiman, J.J. (2002) The cystic fibrosis transmembrane conductance regulator: An intriguing protein with pleiotropic functions. *J Cyst Fibros* **1**: 13–29.

Vareechon, C., Zmina, S.E., Karmakar, M., Pearlman, E., and Rietsch, A. (2017) *Pseudomonas aeruginosa* Effector ExoS Inhibits ROS Production in Human Neutrophils. *Cell Host Microbe* **21**: 611-61.e5.

Veeranki, S., Duan, X., Panchanathan, R., Liu, H., and Choubey, D. (2011) IFI16 Protein Mediates the Anti-inflammatory Actions of the Type-I Interferons through Suppression of Activation of Caspase-1 by Inflammasomes. *PLoS One* **6**: e27040.

Verkman, A.S., Song, Y., and Thiagarajah, J.R. (2003) Role of airway surface liquid and submucosal glands in cystic fibrosis lung disease. *Am J Physiol Cell Physiol* **284**: C2-15.

Vivek-Ananth, R.P., Mohanraj, K., Vandanashree, M., Jhingran, A., Craig, J.P., and Samal, A. (2018) Comparative systems analysis of the secretome of the opportunistic pathogen *Aspergillus fumigatus* and other *Aspergillus* species. *Sci Rep* **8**: 6617.

Vödisch, M., Scherlach, K., Winkler, R., Hertweck, C., Braun, H.-P., Roth, M., *et al.* (2011) Analysis of the *Aspergillus fumigatus* proteome reveals metabolic changes and the activation of the pseurotin A biosynthesis gene cluster in response to hypoxia. *J Proteome Res* **10**: 2508–2524.

Vos, J.B., Sterkenburg, M.A. van, Rabe, K.F., Schalkwijk, J., Hiemstra, P.S., and Datson, N.A. (2005) Transcriptional response of bronchial epithelial cells to *Pseudomonas aeruginosa*: identification of early mediators of host defense. *Physiol Genomics* **21**: 324–336.

Vries, R.P. de, and Visser, J. (2001) Aspergillus Enzymes Involved in Degradation of Plant Cell Wall Polysaccharides. *Microbiol Mol Biol Rev* **65**: 497 LP – 522.

Wagner, C.J., Schultz, C., and Mall, M.A. (2016) Neutrophil elastase and matrix metalloproteinase 12 in cystic fibrosis lung disease. *Mol Cell Pediatr* **3**: 0–6.

Wan, Q., Kuang, E., Dong, W., Zhou, S., Xu, H., Qi, Y., and Liu, Y. (2007) Reticulon 3 mediates Bcl-2 accumulation in mitochondria in response to endoplasmic reticulum stress. *Apoptosis* **12**: 319–328.

Wang, D., Zhang, L., Zou, H., and Wang, L. (2018) Secretome profiling reveals temperature-dependent growth of *Aspergillus fumigatus*. *Sci China Life Sci* **61**: 578–592.

Wang, H., Meng, J., Jia, M., He, G., Yu, J., Wang, R., *et al.* (2010) oprM as a new target for reversion of multidrug resistance in *Pseudomonas aeruginosa* by antisense phosphorothioate oligodeoxynucleotides. *FEMS Immunol Med Mycol* **60**: 1–8.

Wang, J., Dong, Y., Zhou, T., Liu, X., Deng, Y., Wang, C., *et al.* (2013) *Pseudomonas aeruginosa* Cytotoxicity Is Attenuated at High Cell Density and Associated with the Accumulation of Phenylacetic Acid. *PLoS One* **8**: e60187 https://doi.org/10.1371/journal.pone.0060187.

Wang, Y., Wilks, J.C., Danhorn, T., Ramos, I., Croal, L., and Newman, D.K. (2011) Phenazine-1-carboxylic acid promotes bacterial biofilm development via ferrous iron acquisition. *J Bacteriol* **193**: 3606–3617.

Ward, C.L., Omura, S., and Kopito, R.R. (1995) Degradation of CFTR by the ubiquitin-proteasome pathway. *Cell* **83**: 121–127.

Wark, P., Gibson, P.G., and Wilson, A. (2004) Azoles for allergic bronchopulmonary aspergillosis associated with asthma. *Cochrane Database Syst Rev*.

Wark, P.A.B., Hensley, M.J., Saltos, N., Boyle, M.J., Toneguzzi, R.C., Epid, G.D.C., *et al.* (2003) Anti-inflammatory effect of itraconazole in stable allergic bronchopulmonary aspergillosis: a randomized controlled trial. *J Allergy Clin Immunol* **111**: 952–957.

Wartenberg, D., Lapp, K., Jacobsen, I.D., Dahse, H.-M., Kniemeyer, O., Heinekamp, T., and Brakhage, A.A. (2011) Secretome analysis of *Aspergillus fumigatus* reveals Asp-hemolysin as a major secreted protein. *Int J Med Microbiol* **301**: 602–611.

Wasylnka, J.A. (2003) *Aspergillus fumigatus* conidia survive and germinate in acidic organelles of A549 epithelial cells. *J Cell Sci* **116**: 1579–1587.

Wasylnka, J.A., Hissen, A.H.T., Wan, A.N.C., and Moore, M.M. (2005) Intracellular and extracellular growth of *Aspergillus fumigatus*. *Med Mycol* **43** Suppl 1: S27-30.

Wasylnka, J.A., and Moore, M.M. (2002) Uptake of *Aspergillus fumigatus* conidia by phagocytic and nonphagocytic cells in vitro: Quantitation using strains expressing green fluorescent protein. *Infect Immun* **70**: 3156–3163.

Wenke, J., Anke, H., and Sterner, O. (1993) Pseurotin A and 8-O-Demethylpseurotin A from *Aspergillus fumigatus* and Their Inhibitory Activities on Chitin Synthase. *Biosci Biotechnol Biochem* **57**: 961–964.

Weycker, D., Hansen, G.L., and Seifer, F.D. (2017) Prevalence and incidence of noncystic fibrosis bronchiectasis among US adults in 2013. *Chron Respir Dis* **14**: 377–384.

Whitsett, J.A., and Alenghat, T. (2015) Respiratory epithelial cells orchestrate pulmonary innate immunity. *Nat Immunol* **16**: 27–35.

Wilkins, M.R., Sanchez, J.-C., Gooley, A.A., Appel, R.D., Humphery-Smith, I., Hochstrasser, D.F., and Williams, K.L. (1996) Progress with Proteome Projects: Why all Proteins Expressed by a Genome Should be Identified and How To Do It. *Biotechnol Genet Eng Rev* **13**: 19–50.

Williams, B.J., Dehnbostel, J., and Blackwell, T.S. (2010) *Pseudomonas aeruginosa*: Host defence in lung diseases. *Respirology* **15**: 1037–1056.

Williams, C., Ranjendran, R., and Ramage, G. (2016a) Pathogenesis of Fungal Infections in Cystic Fibrosis. *Curr Fungal Infect Rep* **10**: 163–169.

Williams, C., Ranjendran, R., and Ramage, G. (2016b) Pathogenesis of Fungal Infections in Cystic Fibrosis. *Curr Fungal Infect Rep* **10**: 163–169.

Winstanley, C., O'Brien, S., and Brockhurst, M.A. (2016) *Pseudomonas aeruginosa* Evolutionary Adaptation and Diversification in Cystic Fibrosis Chronic Lung Infections. *Trends Microbiol* **24**: 327–337.

Wohlleben, W., Mast, Y., Stegmann, E., and Ziemert, N. (2016) Antibiotic drug discovery. *Microb Biotechnol* **9**: 541–548.

Wojnarowski, C., Frischer, T., Hofbauer, E., Grabner, C., Mosgoeller, W., Eichler, I., and Ziesche, R. (1999) Cytokine expression in bronchial biopsies of cystic fibrosis patients with and without acute exacerbation. *Eur Respir J* **14**: 1136 LP – 1144.

Wolfgang, M.C., Jyot, J., Goodman, A.L., Ramphal, R., and Lory, S. (2004) *Pseudomonas aeruginosa* regulates flagellin expression as part of a global response to airway fluid from cystic fibrosis patients. *Proc Natl Acad Sci* **101**: 6664–6668.

Wolfgang, M.C., Lee, V.T., Gilmore, M.E., and Lory, S. (2003) Coordinate Regulation of Bacterial Virulence Genes by a Novel Adenylate Cyclase-Dependent Signaling Pathway. *Dev Cell* **4**: 253–263.

Wu, X., Li, Z., Chen, X.-X., Fossey, J.S., James, T.D., and Jiang, Y.-B. (2013) Selective sensing of saccharides using simple boronic acids and their aggregates. *Chem Soc Rev* **42**: 8032–8048.

Xiao, J.F., Zhou, B., and Ressom, H.W. (2012) Metabolite identification and quantitation in LC-MS/MS-based metabolomics. *Trends Analyt Chem* **32**: 1–14 https://www.ncbi.nlm.nih.gov/pubmed/22345829.

Yan, Z., McCray Jr, P.B., and Engelhardt, J.F. (2019) Advances in gene therapy for cystic fibrosis lung disease. *Hum Mol Genet* **28**: R88–R94.

Yang, C., and Montgomery, M. (2018) Dornase alfa for cystic fibrosis. *Cochrane database Syst Rev* **9**: CD001127.

Yang, D., Chen, Q., Schmidt, A.P., Anderson, G.M., Wang, J.M., Wooters, J., *et al*. (2000) LL-37, the neutrophil granule- and epithelial cell-derived cathelicidin, utilizes formyl peptide receptor-like 1 (FPRL1) as a receptor to chemoattract human peripheral blood neutrophils, monocytes, and T cells. *J Exp Med* **192**: 1069–1074.

Yang, J., Lee, K.-M., Park, S., Cho, Y., Lee, E., Park, J.-H., *et al*. (2017) Bacterial Secretant from *Pseudomonas aeruginosa* Dampens Inflammasome Activation in a Quorum Sensing-Dependent Manner. *Front Immunol* **8**: 333.

Yang, Y., Hu, M., Yu, K., Zeng, X., and Liu, X. (2015) Mass spectrometry-based proteomic approaches to study pathogenic bacteria-host interactions. *Protein Cell* **6**: 265–274.

Yemm, E.W., Cocking, E.C., and Ricketts, R.E. (1955) The determination of amino-acids with ninhydrin. *Analyst* **80**: 209–214.

Yoneyama, H., and Nakae, T. (1996) Protein C (OprC) of the outer membrane of *Pseudomonas aeruginosa* is a copper-regulated channel protein. *Microbiology* **142**: 2137–2144.

Yonezawa, M., Sugiyama, H., Kizawa, K., Hori, R., Mitsuyama, J., Araki, H., *et al.* (2000) A new model of pulmonary superinfection with *Aspergillus fumigatus* and *Pseudomonas aeruginosa* in mice. *J Infect Chemother* **6**: 155–161.

Yoshimura, K., Nakamura, H., Trapnell, B.C., Chu, C.S., Dalemans, W., Pavirani, A., *et al.* (1991) Expression of the cystic fibrosis transmembrane conductance regulator gene in cells of non-epithelial origin. *Nucleic Acids Res* **19**: 5417–5423

Zarember, K.A., Sugui, J.A., Chang, Y.C., Kwon-Chung, K.J., and Gallin, J.I. (2007) Human polymorphonuclear leukocytes inhibit *Aspergillus fumigatus* conidial growth by lactoferrin-mediated iron depletion. *J Immunol* **178**: 6367–6373.

Zeitlin, P.L., Lu, L., Rhim, J., Cutting, G., Stetten, G., Kieffer, K.A., *et al.* (1991) A cystic fibrosis bronchial epithelial cell line: immortalization by adeno-12-SV40 infection. *Am J Respir Cell Mol Biol* **4**: 313–319.

Zemanick, E.T., Wagner, B.D., Robertson, C.E., Ahrens, R.C., Chmiel, J.F., Clancy, J.P., *et al.* (2017) Airway microbiota across age and disease spectrum in cystic fibrosis. *Eur Respir J* **50**: 1–13

Zhang, K., and Kaufman, R.J. (2008) From endoplasmic-reticulum stress to the inflammatory response. *Nature* **454**: 455–462.

Zhang, S., McCormack, F.X., Levesque, R.C., O'Toole, G.A., and Lau, G.W. (2007) The Flagellum of *Pseudomonas aeruginosa* Is Required for Resistance to Clearance by Surfactant Protein A. *PLoS One* **2**: e564.

Zhang, Z., Liu, R., Noordhoek, J.A., and Kauffman, H.F. (2005a) Interaction of airway epithelial cells (A549) with spores and mycelium of *Aspergillus fumigatus*. *J Infect* **51**: 375–382.

Zhang, Z., Louboutin, J.-P., Weiner, D.J., Goldberg, J.B., and Wilson, J.M. (2005b) Human airway epithelial cells sense *Pseudomonas aeruginosa* infection via recognition of flagellin by Toll-like receptor 5. *Infect Immun* **73**: 7151–7160

Zhao, J., Cheng, W., He, X., and Liu, Y. (2018a) The co-colonization prevalence of *Pseudomonas aeruginosa* and *Aspergillus fumigatus* in cystic fibrosis: A systematic review and meta-analysis. *Microb Pathog* **125**: 122–128.

Zhao, J., Cheng, W., He, X., and Liu, Y. (2018b) The co-colonization prevalence of *Pseudomonas aeruginosa* and *Aspergillus fumigatus* in cystic fibrosis: A systematic review and meta-analysis. *Microb Pathog* **125**: 122–128.

Zhao, J., and Yu, W. (2018) Interaction between *Pseudomonas aeruginosa* and *Aspergillus fumigatus* in cystic fibrosis. .

Zhao, K., Li, W., Li, J., Ma, T., Wang, K., Yuan, Y., *et al*. (2019) TesG is a type I secretion effector of *Pseudomonas aeruginosa* that suppresses the host immune response during chronic infection. *Nat Microbiol* **4**: 459–469 http://dx.doi.org/10.1038/s41564-018-0322-4.

Zhou, H., Monack, D.M., Kayagaki, N., Wertz, I., Yin, J., Wolf, B., and Dixit, V.M. (2005) Yersinia virulence factor YopJ acts as a deubiquitinase to inhibit NF-kappa B activation. *J Exp Med* **202**: 1327–1332.

Zhu, Z., Homer, R.J., Wang, Z., Chen, Q., Geba, G.P., Wang, J., *et al.* (1999) Pulmonary expression of interleukin-13 causes inflammation, mucus hypersecretion, subepithelial fibrosis, physiologic abnormalities, and eotaxin production. *J Clin Invest* **103**: 779–788.

Chapter 9

Appendix

Supplementary datasets can be accessed with the link provided:

https://maynoothuniversity-my.sharepoint.com/:f:/r/personal/anatte_margalit_2012_mumail_ie/Documents/Supplementary%20datasets?csf=1&web=1&e=BAd1rG

Chapter 3

Table A3.1A	All Proteins identified in A549 cells exposed to *A. fumigatus* or *P. aeruginosa*
Table A3.1B	SSDA proteins identified in *A. fumigatus*-exposed A549 cells
Table A3.1C	SSDA proteins identified in *A. P. aeruginosa*-exposed A549 cells
Table A3.2A	List of proteins arising from hierarchical clustering
Table A3.2B	Details of clusters and enrichment terms
Table A3.3A	All Proteins identified in A549 cells exposed to *A. fumigatus* or *P. aeruginosa*
Table A3.3B	SSDA proteins identified in *A. fumigatus*-exposed A549 cells
Table A3.3C	SSDA proteins identified in *P. aeruginosa*-exposed A549 cells
Table A3.3D	SSDA proteins identified in sequentially exposed A549 cells
Table A3.4A	List of proteins arising from hierarchical clustering
Table A3.4B	Details of clusters and enrichment terms

Chapter 4

Table A4.1	Proteins identified in *A. fumigatus* culture filtrates
Table A4.2	All Proteins identified in *P. aeruginosa* exposed to culture filtrates
Table A4.2B	SSDA proteins identified in *P. aeruginosa* exposed to *A. fumigatus* CuF
Table A4.2C	SSDA proteins identified in *P. aeruginosa* exposed to Co-culutre CF
Table A4.3A	List of proteins arising from hierarchical clustering
Table A4.3B	Details of clusters and enrichment terms

Chapter 5

Table A5.1A	All Proteins identified in *A. fumigatus* exposed to culture filtrates
Table A5.1B	SSDA proteins identified in *A. fumigatus* exposed to *P. aeruginosa* CuF
Table A5.1C	SSDA proteins identified in *A. fumigatus* exposed to Co-culture CuF

Chapter 6

Table A6.1	Proteins (> 3 kDa) present in *A. fumigatus* culture filtrates produced in SAB
Table A6.2	SSDA proteins identified in *P. aeruginosa* exposed to *A. fumigatus* CuF
Table A6.3B	List of proteins arising from hierarchical clustering
Table A6.3B	Details of clusters and enrichment terms